

The Results of the PEP'93 Intercomparison of Reference Cell Calibrations and Newer Technology Performance Measurements: Final Report

C.R. Osterwald (*National Renewable Energy Laboratory, Golden, Colorado*), **S. Anevsky** (*All-Union Research Institute for Optophysical Measurements, Moscow, Russia*), **A.K. Barua** (*Indian Association for the Cultivation of Science, Calcutta, India*), **K. Bücher** (*Fraunhofer-Institut für Solare Energiesysteme, Freiburg, Germany*), **P. Chauduri** (*Indian Association for the Cultivation of Science, Calcutta, India*), **J. Dubard** (*Laboratoire Central des Industries Electriques, Fontenay-aux-Roses, France*), **K. Emery** (*National Renewable Energy Laboratory, Golden, Colorado*), **D. King** and **B. Hansen** (*Sandia National Laboratories, Albuquerque, New Mexico*), **J. Metzdorf** (*Physikalisch-Technische Bundesanstalt, Braunschweig, Germany*), **F. Nagamine** (*Japan Quality Assurance Organization, Tokyo, Japan*), **R. Shimokawa** (*Electrotechnical Laboratory, Ibaraki, Japan*), **Y.X. Wang** (*Tianjin Institute of Power Sources, Tianjin, China*), **T. Wittchen** (*Physikalisch-Technische Bundesanstalt, Braunschweig, Germany*), **W. Zaaiman** (*European Solar Test Installation, Ispra, Italy*), **A. Zastrow** (*Fraunhofer-Institut für Solare Energiesysteme, Freiburg, Germany*), and **J. Zhang** (*National Institute of Metrology, Beijing, China*)



National Renewable Energy Laboratory
1617 Cole Boulevard
Golden, Colorado 80401-3393
A national laboratory of
the U.S. Department of Energy
Managed by Midwest Research Institute
for the U.S. Department of Energy
under Contract No. DE-AC36-83CH10093

The Results of the PEP'93 Intercomparison of Reference Cell Calibrations and Newer Technology Performance Measurements: Final Report

C.R. Osterwald (*National Renewable Energy Laboratory, Golden, Colorado*), **S. Anevsky** (*All-Union Research Institute for Optophysical Measurements, Moscow, Russia*), **A.K. Barua** (*Indian Association for the Cultivation of Science, Calcutta, India*), **K. Bücher** (*Fraunhofer-Institut für Solare Energiesysteme, Freiburg, Germany*), **P. Chauduri** (*Indian Association for the Cultivation of Science, Calcutta, India*), **J. Dubard** (*Laboratoire Central des Industries Electriques, Fontenay-aux-Roses, France*), **K. Emery** (*National Renewable Energy Laboratory, Golden, Colorado*), **D. King** and **B. Hansen** (*Sandia National Laboratories, Albuquerque, New Mexico*), **J. Metzdorf** (*Physikalisch-Technische Bundesanstalt, Braunschweig, Germany*), **F. Nagamine** (*Japan Quality Assurance Organization, Tokyo, Japan*), **R. Shimokawa** (*Electrotechnical Laboratory, Ibaraki, Japan*), **Y.X. Wang** (*Tianjin Institute of Power Sources, Tianjin, China*), **T. Wittchen** (*Physikalisch-Technische Bundesanstalt, Braunschweig, Germany*), **W. Zaaiman** (*European Solar Test Installation, Ispra, Italy*), **A. Zastrow** (*Fraunhofer-Institut für Solare Energiesysteme, Freiburg, Germany*), and **J. Zhang** (*National Institute of Metrology, Beijing, China*)



National Renewable Energy Laboratory
1617 Cole Boulevard
Golden, Colorado 80401-3393
A national laboratory of
the U.S. Department of Energy
Managed by Midwest Research Institute
for the U.S. Department of Energy
under Contract No. DE-AC36-83CH10093

Prepared under Task No. PV706101

March 1998

This publication was reproduced from the best available camera-ready copy submitted by the subcontractor and received no editorial review at NREL.

NOTICE

This report was prepared as an account of work sponsored by an agency of the United States government. Neither the United States government nor any agency thereof, nor any of their employees, makes any warranty, express or implied, or assumes any legal liability or responsibility for the accuracy, completeness, or usefulness of any information, apparatus, product, or process disclosed, or represents that its use would not infringe privately owned rights. Reference herein to any specific commercial product, process, or service by trade name, trademark, manufacturer, or otherwise does not necessarily constitute or imply its endorsement, recommendation, or favoring by the United States government or any agency thereof. The views and opinions of authors expressed herein do not necessarily state or reflect those of the United States government or any agency thereof.

Available to DOE and DOE contractors from:
Office of Scientific and Technical Information (OSTI)
P.O. Box 62
Oak Ridge, TN 37831
Prices available by calling (423) 576-8401

Available to the public from:
National Technical Information Service (NTIS)
U.S. Department of Commerce
5285 Port Royal Road
Springfield, VA 22161
(703) 487-4650



The Results of the PEP'93 Intercomparison of Reference Cell Calibrations and Newer Technology Performance Measurements: Final Report

C.R. Osterwald, National Renewable Energy Laboratory, Golden, Colorado, USA
S. Anevsky, All-Union Research Institute for Optophysical Measurements, Moscow, Russia
A.K. Barua, Indian Association for the Cultivation of Science, Calcutta, India
K. Bücher, Fraunhofer-Institut für Solare Energiesysteme, Freiburg, Germany
P. Chaudhuri, Indian Association for the Cultivation of Science, Calcutta, India
J. Dubard, Laboratoire Central des Industries Electriques, Fontenay-aux-Roses, France
K. Emery, National Renewable Energy Laboratory, Golden, Colorado, USA
D. King, Sandia National Laboratories, Albuquerque, New Mexico, USA
B. Hansen, Sandia National Laboratories, Albuquerque, New Mexico, USA
J. Metzdorf, Physikalisch-Technische Bundesanstalt, Braunschweig, Germany
F. Nagamine, Japan Quality Assurance Organization, Tokyo, Japan
R. Shimokawa, Electrotechnical Laboratory, Ibaraki, Japan
Y.X. Wang, Tianjin Institute of Power Sources, Tianjin, China
T. Wittchen, Physikalisch-Technische Bundesanstalt, Braunschweig, Germany
W. Zaaiman, European Solar Test Installation, Ispra, Italy
A. Zastrow, Fraunhofer-Institut für Solare Energiesysteme, Freiburg, Germany
J. Zhang, National Institute of Metrology, Beijing, China

Abstract

This report presents the results of an international intercomparison of photovoltaic (PV) performance measurements and calibrations that took place from 1993 to 1997. The intercomparison, which was organized and operated by a group of representatives from national PV measurement laboratories, was accomplished by circulating two sample sets. One set, consisting of 20 silicon reference cells, was intended to form the basis of an international PV reference scale. A qualification procedure applied to the calibration results gave average calibration numbers with an overall standard deviation of less than 2% for the entire set. The second sample set was assembled from a wide range of newer technologies that present unique problems for PV measurements. As might be expected, these results showed much greater differences among the laboratories. Methods were then identified that should be used to measure such devices, along with problems to avoid. The report concludes with recommendations for future intercomparisons.

Acknowledgment

This work was supported by the U.S. Department of Energy under contract no. DE-AC3683CH10093.

Table of Contents

1.	General	1-1
1.1	Introduction	1-1
1.2	Organization and Objectives	1-1
1.3	History of the Intercomparison	1-3
2.	World Photovoltaic Scale Sample Set	2-1
2.1	Sample Set	2-1
2.2	Protocol	2-6
2.3	Circulation History	2-6
2.4	Calibration Methods	2-7
2.4.1	SNL (S)	2-7
2.4.2	NREL (A)	2-8
2.4.3	VNIIOFI (C)	2-8
2.4.4	JQA/ETL (C)	2-9
2.4.5	LCIE (R)	2-9
2.4.6	PTB (D)	2-9
2.4.7	NIM (D)	2-10
2.4.8	TIPS (C)	2-10
2.4.9	ESTI (S)	2-11
2.4.10	IACS (S)	2-11
2.4.11	ISE (S)	2-11
2.5	Pre- and Post-Circulation Measurements	2-11
2.6	Data Analysis and Selection Procedures	2-14
2.7	Results	2-16
2.7.1	Reported Short-Circuit Currents	2-16
2.7.2	Reported I_{sc} Temperature Coefficients	2-16
2.7.3	Reported Total Uncertainties	2-16
2.7.4	Spectral Responsivity	2-18
2.8	WPVS Analysis and Calibration Values	2-18
2.8.1	Short-Circuit Currents	2-18
2.8.2	I_{sc} Temperature Coefficients	2-28
2.8.3	Spectral Responsivity	2-29
2.9	Discussion	2-56
2.9.1	Results	2-56
2.9.2	Future Calibrations and Maintenance of the WPVS	2-62
2.9.3	Traceability	2-65
2.9.4	Recommendations	2-66

3.	Newer Technology Series Sample Set	3-1
3.1	Sample Set	3-1
3.2	Protocol	3-6
3.3	Circulation History	3-6
3.4	Measurement Methods and Reported Anomalies	3-6
3.4.1	NREL	3-7
3.4.2	LCIE	3-7
3.4.3	JQA/ETL	3-7
3.4.4	SNL	3-7
3.4.5	ESTI	3-8
3.4.6	ISE	3-8
3.4.7	PTB	3-8
3.4.8	USPL	3-8
3.4.9	TIPS	3-8
3.4.10	IACS	3-9
3.4.11	NREL	3-9
3.5	Data Analysis Procedures	3-9
3.6	Reported Results	3-10
3.6.1	Open-Circuit Voltage	3-10
3.6.2	Short-Circuit Current	3-11
3.6.3	Fill Factor	3-12
3.6.4	Maximum Power	3-13
3.6.5	Spectral Responsivity	3-14
3.6.6	Device Area	3-14
3.7	Discussion	3-14
3.7.1	II-VI Thin-Film Devices	3-14
3.7.2	Amorphous Silicon Thin-Film Devices	3-37
3.7.3	Non-Silicon Spectral Responsivity Devices	3-38
3.7.4	Large Area Devices	3-38
3.7.5	GaAs Concentrator Module	3-39
3.8	Conclusions	3-64
3.9	Recommendations	3-65
4.	General Recommendations	4-1
4.1	Objectives	4-1
4.2	Organization	4-1
4.3	Pitfalls	4-1
4.4	Data Submission	4-2
5.	References	5-1

Appendix 1	WPVS Reference Cell Package Design	A1-1
A1.1	Physical Reference Cell Package	A1-1
A1.2	Solar Cell	A1-4
A1.3	Window	A1-4
A1.4	Encapsulation	A1-4
A1.5	Temperature Sensors	A1-5
A1.6	Electrical Connections	A1-5
Appendix 2	WPVS Reference Cell Acceptance Test Procedure	A2-1
A2.1	Physical and Dimensional Verification	A2-1
A2.2	Visual Inspection	A2-1
A2.3	Light I-V at STC Measurement	A2-1
A2.4	Transient Photocurrent Test	A2-3
A2.5	Dark I-V Measurement	A2-3
A2.6	Temperature Sensor Integrity Test	A2-3
A2.7	Light Soak	A2-4
A2.8	Light Instability Test	A2-4
Appendix 3	Individual WPVS Calibration Reports	A3-1
	930216-1	A3-2
	930216-2	A3-4
	930417-1	A3-6
	930417-2	A3-8
	93308	A3-10
	93309	A3-12
	NIM 9351	A3-14
	NIM 9352	A3-16
	PX102C	A3-18
	PX201C	A3-20
	PTB RS-58	A3-22
	PTB RS-67	A3-24
	PTB RS-68	A3-26
	PTB RS-69	A3-28
	PTB RS-78	A3-30
	TDB 9303	A3-32
	TDC 9305	A3-34
	Y09	A3-36
	Y45	A3-38
	Y124	A3-40

Appendix 4	Minutes of the PEP'93 Participants Meetings	A4-1
A4.1	Minutes of the First Participants Meeting, October 1992	A4-1
A4.2	Minutes of the Second Participants Meeting, May 1993	A4-5
A4.3	Minutes of the Third Participants Meeting, December 1994	A4-7
A4.4	Minutes of the Final Participants Meeting, March 1996	A4-9
Appendix 5	Acronyms, Abbreviations, and Symbols	A5-1

List of Figures

Figure 2-1. NREL reference cell 930216-2	2-2
Figure 2-2. LCIE reference cell 930417-2	2-3
Figure 2-3. JQA/ETL reference cell 93309	2-3
Figure 2-4. NIM reference cell NIM 9351	2-3
Figure 2-5. TIPS reference cell TDC 9305	2-3
Figure 2-6. ESTI reference cell PX102C	2-4
Figure 2-7. ISE reference cell PTB RS-68	2-4
Figure 2-8. SNL reference cell Y09	2-4
Figure 2-9. Reference spectral mismatch factor parameter spectra	2-15
Figure 2-10. Laboratories ranked according to WPVS calibration values	2-20
Figures 2-11 – 2-13.	
I_{sc} results normalized by WPVS calibration values	2-21– 2-23
Figure 2-14. I_{sc} results from WPVS accepted laboratories normalized by calibration values	2-23
Figures 2-15 – 2-25.	
WPVS I_{sc} scatter plots	2-25 – 2-28
Figures 2-26 – 2-45.	
WPVS area-normalized spectral responsivity and deviation plots	2-32 – 2-51
Figures 2-46 – 2-50.	
Accepted WPVS average spectral responsivity	2-52 – 2-54
Figures 2-51 – 2-55.	
Integrated PTB SR data as a function of light bias	2-54 – 2-55
Figures 2-56 – 2-58.	
Normalized reference spectral mismatch parameters	2-57 – 2-59
Figure 3-1. ESTI sensor ESTI 2	3-2
Figure 3-2. CuIn(Ga)Se ₂ cell S31	3-3
Figure 3-3. CdTe cell 9321	3-3
Figure 3-4. a-Si two-junction tandem cell 9312	3-3
Figure 3-5. a-Si bi-cell 9306.....	3-3
Figure 3-6. 10×10 cm Si cell TIPS 2	3-3
Figure 3-7. Low-pass filtered Si cell PTB RS-44	3-4
Figure 3-8. High-pass filtered Si cell PTB RS-64	3-4
Figure 3-9. GaAs cell SNL003	3-4
Figure 3-10. GaAs 1000× concentrator module	3-5
Figure 3-11. 10×10 cm Si cell in module package LCIE 1	3-5

Figures 3-12 – 3-15.	
Normalized I-V parameter data for the II-VI thin-film cells	3-15 – 3-17
Figures 3-16 – 3-19.	
Normalized I-V parameter data for the a-Si cells	3-19 – 3-21
Figures 3-20 – 3-23.	
Normalized I-V parameter data for the non-silicon responsivity cells	3-23 – 3-25
Figures 3-24 – 3-27.	
Normalized I-V parameter data for the large-area devices	3-27 – 3-29
Figures 3-28 – 3-31.	
Normalized I-V parameter data for the GaAs concentrator module	3-31 – 3-33
Figure 3-32. Normalized V_{oc} standard deviations	3-35
Figure 3-33. Normalized I_{sc} standard deviations	3-35
Figure 3-34. Normalized FF standard deviations	3-36
Figure 3-35. Normalized P_{max} standard deviations	3-36
Figures 3-36 – 3-59.	
NT series area-normalized spectral responsivity and deviation plots	3-40 – 3-63
Figure A1-1 WPVS reference cell package design	A1-2
Figure A1-2 WPVS reference cell package temperature control block	A1-3
Figure A1-3 WPVS reference cell package wiring diagram	A1-6
Figure A2-1 WPVS reference cell acceptance test flow diagram	A2-2

List of Tables

Table 2-1.	WPVS sample set	2-2
Table 2-2.	WPVS sample set circulation history	2-6
Table 2-3.	WPVS calibration methods	2-7
Table 2-4.	Pre- and post-circulation illuminated I-V characteristic differences	2-12
Table 2-5.	Pre- and post-circulation dark I-V characteristic differences	2-13
Table 2-6.	Post-circulation illuminated and dark I-V characteristics	2-13
Table 2-7.	Reported WPVS short-circuit current results	2-16
Table 2-8.	WPVS I_{sc} temperature coefficients	2-17
Table 2-9.	Estimated U_{95} total uncertainty for WPVS calibrations	2-17
Table 2-10.	Cell-averaged WPVS short-circuit currents	2-18
Table 2-11.	Cell-averaged WPVS short-circuit currents for four accepted laboratories	2-19
Table 2-12.	Normalized WPVS short-circuit current results	2-20
Table 2-13.	Normalized WPVS I_{sc} data averaged by laboratory	2-25
Table 2-14.	WPVS mean temperature coefficients	2-28
Table 2-15.	Reference spectral mismatch for WPVS SR data	2-30
Table 2-16.	Normalized reference spectral mismatch averaged by laboratory	2-31
Table 2-17.	Total measurement uncertainty U_{95} calculated from WPVS results	2-62
Table 2-18.	Traceability of WPVS calibrations	2-65
Table 3-1.	NT series sample set	3-1
Table 3-2.	NT series sample set circulation history	3-6
Table 3-3.	Reported NT series open-circuit voltages	3-10
Table 3-4.	Reported NT series short-circuit currents	3-11
Table 3-5.	Reported NT series fill factors	3-12
Table 3-6.	Reported NT series maximum powers	3-13
Table 3-7.	Reported NT series device areas	3-14

1. General

1.1 Introduction

Under the auspices of the seven-nation Photovoltaic Energy Project (PEP), an international round robin of reference cell calibrations and performance measurements of Newer Technology (NT) PV devices was initiated in 1993. The round robin was preceded by two other PEP-sponsored projects in 1984 [1] and 1987 [2]. Initially, the PEP'93 intercomparison functioned identically to the previous round robins, where representatives from the participant laboratories formed an "expert group" of the PEP. After the start of the intercomparison, however, the PEP was officially disbanded, and the expert group continued to operate independently. Twelve laboratories from eight nations participated in the intercomparison, which required four years to complete.

1.2 Organization and Objectives

Organization of the intercomparison was initiated informally in 1992 by participants from the PEP'87, and resulted in the National Renewable Energy Laboratory (NREL) agreeing to act as the organizing agent for the program. Carl Osterwald of NREL was assigned the task of coordinating the intercomparison. The blindness of the intercomparison was preserved because the coordinator did not participate in any of NREL's measurements.

The program was designed on the basis of the recommendations of the PEP'87, which are summarized here [2]:

- Frequent intercomparisons are desirable.
- Other non-silicon technologies should be evaluated.
- Narrowband spectral responsivities, especially amorphous silicon, should be evaluated.
- Differences in fill factor (FF) and open-circuit voltage (V_{oc}) should be evaluated.
- Secondary outdoor calibrations of modules should be evaluated.
- Round robins should be held every four years, with one year breaks.
- A single primary calibration procedure should not be adopted by the International Electrotechnical Commission (IEC).
- The total uncertainty (U_{95})¹ of primary calibrations should be $\leq \pm 2\%$.
- Primary calibrations should be based on a group of at least three radiometric standards, i.e. detectors or lamps.
- Linear reference cells are desirable.
- Primary reference cell package designs should consider cell area, case size, temperature sensors, and thermal mass.

¹ See references [3] and [4] for definitions of measurement uncertainty and U_{95} .

The year selected as the start of the intercomparison, 1993, came from the recommendation to hold formal international PV measurement round robins every four years. With these considerations in mind, the first meeting of the participants was held during the 11th European Photovoltaic Solar Energy Conference and Exhibition in Montreux, Switzerland, on 12-15 October 1992 (the minutes and attendees of all meetings are provided in Appendix 4). At this meeting, the objectives, sample set, participants, protocol, and schedule for the intercomparison were discussed and established.

The objectives of the intercomparison were threefold: (1) establish the World PV Scale (WPVS) by comparing primary reference cell calibrations traceable to national metrology programs, (2) identify problems with emerging technology measurements and propose recommendations for suitable measurement procedures to be considered by standardization organizations, and (3) recommend methods of qualifying calibration data in publications.

In a major change from the previous intercomparisons, laboratories from countries outside of the seven-nation PEP (Japan, Germany, Italy, France, United Kingdom, Canada, and the United States) were invited to participate. The additional nations were Spain, Russia, India, and China. Because of the increased number of potential participants and the time required for sample circulation, it was decided to circulate two independent sample sets simultaneously. The first sample set consisted of monocrystalline silicon 2×2 cm packaged reference cells for the WPVS, and the second set, the NT series, contained various types of PV devices intended for finding problems with performance measurements of non-silicon technologies. These types were: European Solar Test Installation (ESTI) sensor, CuIn(Ga)Se₂, CdTe, a-Si bi-cell (two-cell minimodule), low-pass (300-800 nm) filtered Si, high-pass (600-1200 nm) filtered Si, GaAs, large area Si, a-Si two-terminal tandem, and a two-cell GaAs concentrator module with fixed optics.

In order to complete the sample circulation within two years, it was necessary to allow each participant only two months to complete all measurements and ship the samples to the next laboratory. Following the first meeting of the participants, the proposed organization and schedule was reviewed at the 10th PEP Coordination Meeting in Freiburg, Germany, 20-21 October 1992, and some modifications were made. The Coordination Committee of the PEP requested that the NT series set be circulated in two rounds, with the first round among laboratories represented on the Coordination Committee. The first round would be conducted as fast as possible, with eight weeks per laboratory as an absolute upper limit. Preliminary results from the fast first round would be made available as soon as possible. Following the first round, the NT set would then be circulated among the other laboratories that wished to participate. The Coordination Committee also requested that participants send a copy of the intercomparison invitation to their respective national standardization organizations.

1.3 History of the Intercomparison

The intercomparison began with a formal invitation to participate sent by NREL to laboratories identified earlier as possible participants. The invitation included checklists for preferred and unacceptable months of the year to have the sample sets. An initial circulation schedule was developed from the responses and collection of the sample sets began in February 1993. The initial schedule had a date of 1 July 1995 for completion of circulation of both sample sets. The laboratories that agreed to participate were:

All-Union Research Institute for Optophysical Measurements (VNIIOFI), Moscow, Russia
Electrotechnical Laboratory (ETL), Ibaraki, Japan
European Solar Test Installation (ESTI), Ispra, Italy
Fraunhofer-Institut für Solare Energiesysteme (ISE), Freiburg, Germany
Indian Association of the Cultivation of Science (IACS), Calcutta, India
Japan Quality Assurance Organization (JQA), Tokyo, Japan²
Laboratoire Central des Industries Electriques (LCIE), Fontenay-aux-Roses, France
National Institute of Metrology (NIM), Beijing, China
National Renewable Energy Laboratory (NREL), Golden, Colorado, USA
Physikalisch-Technische Bundesanstalt (PTB), Braunschweig, Germany
Sandia National Laboratories (SNL), Albuquerque, New Mexico, USA
Tianjin Institute of Power Sources (TIPS), Tianjin, China
Udhaya Semiconductors (P) Ltd. (USPL), Coimatore, India

A second meeting of the participants was held prior to the initiation of sample circulation on 12 May 1993 at the 23rd Institute of Electrical and Electronics Engineers (IEEE) PV Specialists Conference (PVSC) in Louisville, Kentucky, USA. The data reporting requirements and the initial schedule were amended at this time. Sample circulation began in July 1993 after pre-circulation measurements were made at NREL. The WPVS sample set was packaged and shipped by SNL to the second participant following SNL's calibrations, and, similarly, the NT series sample set was packaged and shipped by NREL.

To fulfill the requirement set by the PEP Coordination Committee for a fast first round of the NT series, a third meeting of the participants was held on 8 December 1994 at the 1st World Conference on PV Energy Conversion in Waikoloa, Hawaii, USA. Data from the first six laboratories reporting measurements on the NT series samples were discussed at this meeting. This arrangement of providing results prior to the conclusion of sample circulation was problematic because of

² At the start of the intercomparison, JQA was called JMI, Japan Machinery and Metals Inspection Institute.

questions regarding the blindness of later participants who were able to see data before they measured the samples. Fortunately, this case applied to only one laboratory, and the representative from this laboratory, IACS, agreed to not show the results to personnel making measurements. Because by this time the PEP had disbanded, the expert group did not feel obligated to comply with the fast first round requirement and decided to not disseminate any results that might compromise the integrity of the intercomparison. Thus, the early NT results were not provided to anyone outside of the meeting attendees.

The date and location for a final meeting of the participants was determined at the third meeting, and the final meeting was held on 4-8 March 1996 at NREL. This date was a projection of when sample circulation was likely to be completed (the WPVS was four months behind schedule by the time of the Hawaii meeting, and the NT series two months late), and also was chosen considering the timing of future PV conferences at which the results could potentially be published. This conference turned out to be the 25th IEEE PVSC, which was held the week of 13-17 May 1996. It was intended that all samples be returned to NREL by the time of the meeting for post-circulation measurements. It was planned that NREL would return the samples to their respective owning laboratories during the meeting, but circumstances prevented completion of sample circulation by this time. In spite of this, all but two laboratories provided measurement data prior to the meeting. From the very involved discussions of the data that resulted, valuable conclusions were made and a paper of the results was presented at the 25th IEEE PVSC [5]. The results in this paper were normalized so that the integrity of the intercomparison was uncompromised, and the raw data compilations discussed at the meeting were not seen by the last participants until they submitted their results. In keeping with convention established by prior PEP round robins, data sets were not identified with owning laboratories in the PVSC paper.

Space restrictions prevented publication of the details of the WPVS proposal in the 25th IEEE PVSC, so excerpts of the material in Appendices 1 and 2 were published at the 26th IEEE PVSC, 29 September through 3 October, 1997 [6].

Sample circulation began on schedule in July 1993, but the goal of two years for completion of the intercomparison was not met because of delays in shipping and communication. Circulation of the WPVS sample set was completed in August 1996, and the NT series finished in May 1997, two full years late (see Sections 2.3 and 3.3).

2. World Photovoltaic Scale Sample Set

2.1 Sample Set

Each participant was asked to supply one or two packaged, monocrystalline silicon reference cells. The cells had to be packaged in accordance with IEC 60904-2, Sec. 9.3, which states [7]:

9.3 *Single cell package*

If a single cell package is used, the following recommendations are made:

9.3.1 The field of view should be at least 160°.

9.3.2 All surfaces in the package within the cell's field of view should be non-reflective, with an absorption of at least 0.95 in the cell's wavelength response band.

9.3.3 The material used for bonding the cell to the holder should not be degraded electrically and optically. Its physical characteristics should remain stable over the entire period of intended use.

9.3.4 The use of a protective window is recommended. If the cell is to be calibrated or used in total sunlight, the space between the window and the cell should be filled with a stable, transparent encapsulant. The refractive index of the encapsulant shall be similar (within 10%) to that of the window to minimize errors due to the internal reflection of light at high angles of incidence. The transparency, continuity and adhesion of the encapsulant should not be adversely affected by ultraviolet light and operational temperatures.

The WPVS cells can be divided into several general categories. ESTI (PX201C), NREL, and LCIE submitted cells manufactured by PRC Krochmann GmbH in Germany [8], and the ISE, VNIIOFI, and PTB cells were all made by PTB. These cells are based on an older PTB design that was used for a national intercomparison [9] (note, however, that the NREL and LCIE cells are of two different PRC designs—see Figs. 2-1 and 2-2). The “Y” cells (SNL and IACS) are of a design by the NASA-Lewis Research Center in Cleveland, Ohio, that has been widely used in the United States for many years [10]. Although the connectors and temperature sensors differ, the NIM are physically very similar to the standard Japanese design to which the JQA/ETL cells were made [11]. Finally, the TIPS cells are of a unique design, and the other ESTI cell (PX102C) was manufactured by Stella. Table 2-1 lists the WPVS sample set, and Figs. 2-1 through 2-8 illustrate the different designs used.

Several of these cells have provisions for active cooling. The JQA/ETL and NIM cells are equipped with tubing connections for water cooling, and the LCIE cells from PRC Krochmann have thermoelectric coolers underneath the solar cells. All the other cells rely on mounting to a temperature-controlled plate, which means that a small thermal mass between the solar cell and the back of the package is advantageous.

The different reference cell designs presented a formidable logistical challenge to the participating laboratories. Ten different plug and cable connection schemes, and seven different

Table 2-1. WPVS sample set (all cells are 2×2 cm Si)

Organization	Cell ID	Temperature Sensor
ESTI	PX102C PX201C	LM 35 integrated circuit AD590 integrated circuit
NREL	930216-1 930216-2	Pt 100Ω Resistance Temperature Detector (RTD)
JQA/ETL	93308 93309	T-type thermocouple
LCIE	930417-1 930417-2	LM 35 integrated circuit
IACS	Y124	J-type thermocouple
TIPS ³	TDB 9303 TDC 9305	Pt 46Ω RTD
NIM	NIM 9351 NIM 9352	Thermistor
ISE	PTB RS-67 PTB RS-68	Pt 100Ω RTD
VNIOFI	PTB RS-78	Pt 100Ω RTD
PTB	PTB RS-58 PTB RS-69	Pt 100Ω RTD
SNL	Y09 Y45	J-type thermocouple

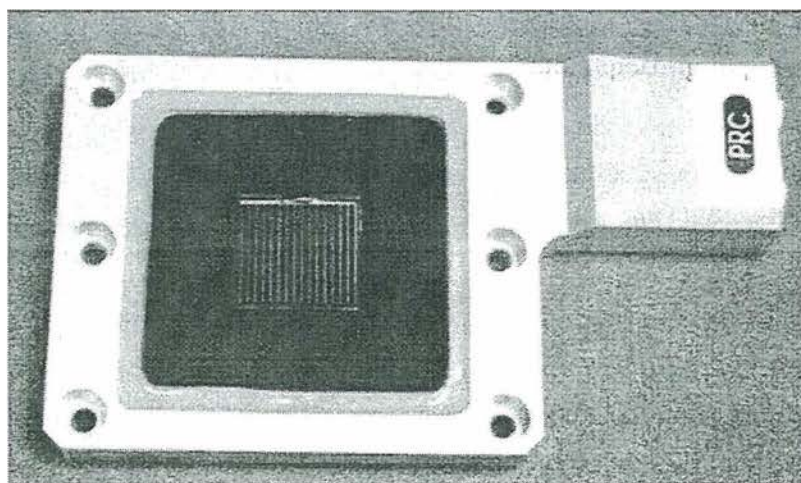


Figure 2-1. NREL reference cell 930216-2, manufactured by PRC Krochmann

³ Note that the TIPS cells appeared to be labeled IDB 9303 and IDC 9305, but the data submitted by TIPS referred to them as TDB 9303 and TDC 9305. In this report, we use the TIPS designations for these cells.

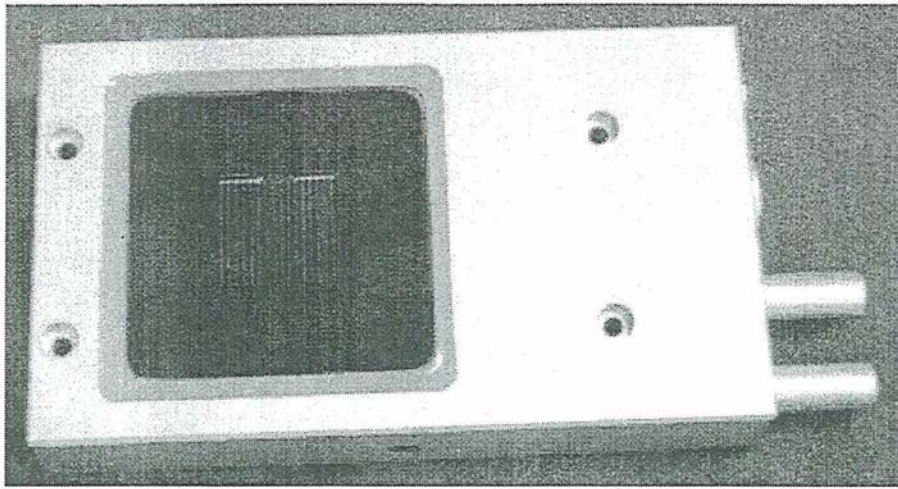


Figure 2-2. LCIE reference cell 930417-2, manufactured by PRC Krochmann

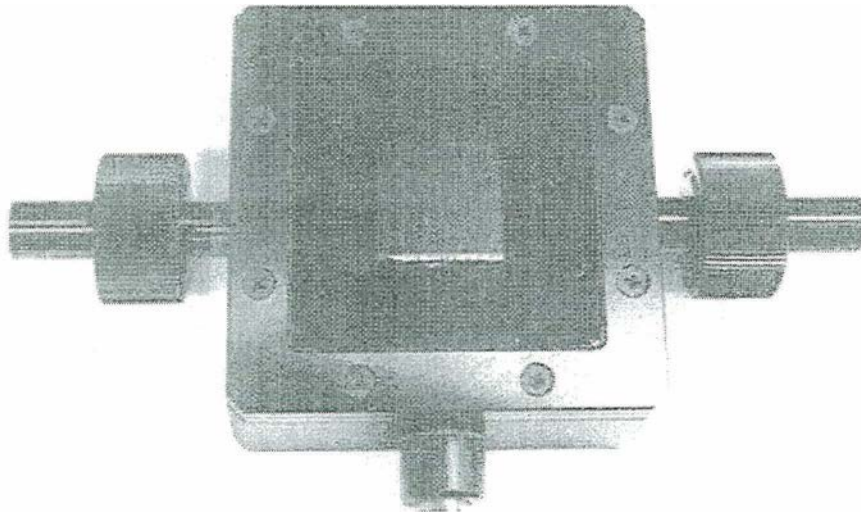


Figure 2-3. JQA/ETL reference cell 93309

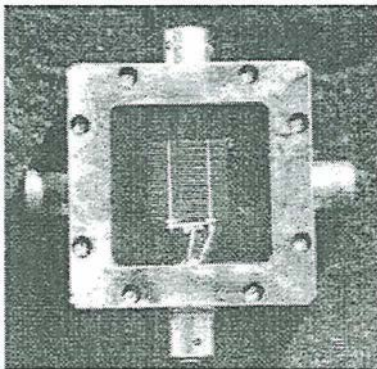


Figure 2-4. NIM reference cell NIM 9351

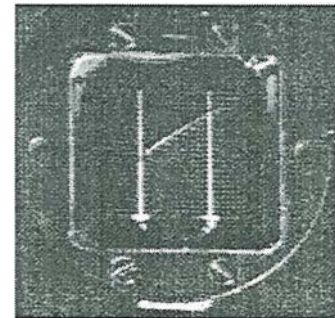


Figure 2-5. TIPS reference cell TDC 9305.
The window crack is visible.

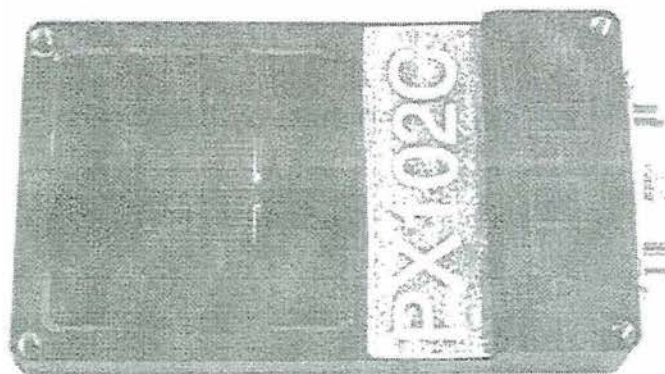


Figure 2-6. ESTI reference cell PX102C, manufactured by Stella

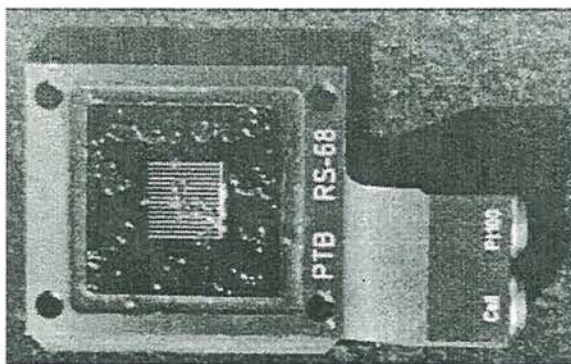


Figure 2-7. ISE reference cell PTB RS-68, manufactured by PTB
Bubbles in the encapsulation are clearly visible.

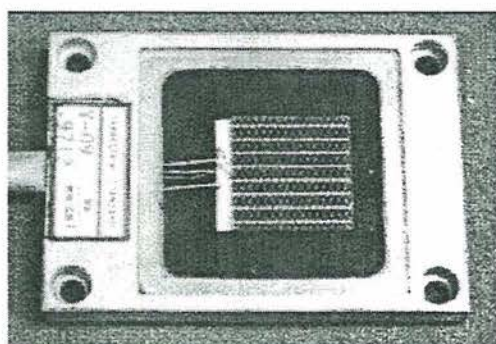


Figure 2-8. SNL reference cell Y09, manufactured by NASA-Lewis Research Center

temperature sensors (with nine different connections) were used. The various physical designs also made optical alignments problematic in measurement systems that may have been intended for only a single reference cell design.

Several problems or technical issues with these cells were uncovered before and during the WPVS circulation. Y124 has internal reflections that causes the I_{sc} to be lower when only the solar cell is illuminated, as opposed to when the entire front window is illuminated. Therefore, it does not meet the requirements of IEC 60904-2. The PTB design, the Japanese design, the “Y” cells, and the ESTI cells all had one side of the solar cell shorted to the metal package, which can cause problems when several cells are measured simultaneously. Cells 93308 and PTB RS-67 had high-resistance or unstable internal connections that caused measurement problems for several participants. The connections to 93308 were repaired on March 3, 1994 at JQA. However, no problems were found with the connections to PTB RS-67 when checked in September 1997—the reported problems may have involved cables or external connections. Unstable contacts to the temperature sensor were also a problem with NIM 9352. Three cells, PTB RS-68, PTB RS-69, and TDC 9305, sustained cracked windows during circulation (Fig. 2-5 illustrates the crack in TDC 9305). The window of PTB RS-68 was repaired in June 1994 at PTB.

Y45 and Y124 replaced two cells that were found to have severe contact problems which could have prevented calibration of these cells. The substitution was done at SNL after the pre-circulation characterization at NREL.

Bubbles in the encapsulation of the PTB cells began appearing after the cells were shipped from PTB to NREL in May 1993. These bubbles are clearly visible in the photograph of PTB RS-68 (Fig. 2-7). The bubbles were due to the pressure sensitivity of a special silicone rubber, Wacker Silgel 612, that was used to encapsulate the PTB cells according to a special recommendation. Silgel 612 is softer than Silgel 601, which was used in older PTB cells [9] (Silgel 612 is no longer in use).

Six cells—93308, 93309, NIM 9351, NIM 9352, PX102C and PX201C—had non-permanent identification labels on the reference cell packages that became difficult to read by the end of the sample circulation period.

The TIPS cells, TDB 9303 and TDC 9305, had connectors that were thicker than the cell package. This caused the connectors to extend below the bottom surfaces of the packages and complicated obtaining good thermal contact to the cells.

At the conclusion of the post-circulation measurements, it was noted that TDB 9303 appeared to have developed an internal short. It was not known if this fault could be repaired.

2.2 Protocol

The protocol for the WPVS sample set called for the participants to calibrate the WPVS reference cells at Standard Test Conditions (STC, defined in reference [12]) using their best calibration methods, which are traceable to national radiometric standards. Additionally, the participants were to report the I_{sc} , the relative spectral responsivity (SR), the estimated total uncertainty (expressed as U_{95}), and optionally, the temperature coefficient of I_{sc} . A description of the calibration methods used was also required. Each laboratory was allowed two months to complete all measurements and ship the cells to the next participant. Although not required, it was highly recommended that results be submitted to the coordinator on disks or via electronic mail to avoid errors when transcribing data from paper. This also saved time because the data did not have to be retyped. Of the eleven participating laboratories, only two did not submit results electronically.

2.3 Circulation History

Table 2-2 documents the circulation history of the WPVS sample set.

Before the circulation period began, the reference cells were collected at NREL, and a series of pre-circulation measurements was performed, so that any changes in the cells might be detected after completion of the intercomparison (see Section 2.5). The cells were then shipped to the first scheduled participant, SNL, who obtained and outfitted the plastic shipping crate that was used throughout the intercomparison. SNL also photographed eleven of the cells at this time. Two cells were substituted at this time to replace two other cells that were found to be inadequate during the pre-circulation measurements.

The original schedule called for ISE to receive the cells after LCIE, and the last participant was to be USPL. Shipping problems within Russia caused the samples to be delayed after VNIIOFI

Table 2-2. WPVS sample set circulation history

Laboratory	Time Period
SNL	July – August 1993
NREL	September – October 1993
VNIIOFI	November 1993 – February 1994
JQA/ETL	March 1994
LCIE	April – May 1994
PTB	June – July 1994
NIM	August – October 1994
TIPS	November 1994 – January 1995
ESTI	February – April 1995
IACS	May 1995 – February 1996
ISE	March – August 1996

finished its calibrations, and almost halted the intercomparison. The schedule was resumed when representatives of JQA traveled to Moscow and hand-carried the sample set to Japan. JQA was able to complete the measurements in four weeks, but the net delay still prevented ISE from having the cells at the original time (May-June 1994). Because of internal scheduling problems, ISE was unable to perform the measurements during the June-July 1994 time period and had to be rescheduled as the final participant.

As a result of shipping and communications problems in India, the coordinator decided that the samples should not proceed to USPL after IACS finished. USPL had held the NT series samples for more than one year, and another long delay was unacceptable. IACS was also unable to ship the WPVS cells on schedule because of problems with obtaining customs clearances, which caused the samples to remain there for nine months. The extreme delays resulted in ISE receiving the cells in March 1996. Because of this, it was decided at the final meeting of the participants to allow ISE as much time as needed to obtain its calibrations.

Following return of the samples to NREL in August 1996, the pre-circulation measurements were repeated.

2.4 Calibration Methods

Different methods were used by the participating laboratories to calibrate the WPVS reference cells. A list of these methods, along with designation letter codes, is given in Table 2-3. The letter codes are similar to those used in reference [2]. Each of the actual procedures used by the participants is summarized below.

Table 2-3. WPVS calibration methods

Designation	Method
A	Outdoor primary calibration against a cavity radiometer
C	Indoor primary with absolute spectral irradiance
D	Differential spectral responsivity with variable bias light
R	Absolute spectral responsivity
S	Secondary calibration against a primary reference cell

2.4.1 SNL (S)

SNL's calibrations were obtained with a solar simulator against a primary reference cell calibrated by NREL, and also calibrated against a standard irradiance lamp at the National Institute for Standards and Technology (NIST). A grating monochromator system was used to measure the spectral responsivities, which were used to correct the calibrations for spectral mismatch.

2.4.2 NREL (A)

The NREL primary calibration procedures are documented in reference [13], and summarized here.

Spectral responsivities of all samples were measured using a Xe arc lamp and narrow bandwidth (~10 nm full width at half maximum [FWHM]) interference filters. Each cell was biased with a tungsten-halogen lamp with a dichroic reflector to produce a current approximately equal to its calibrated I_{sc} . The filtered light intensity was measured with a pyroelectric detector and the calibration further refined using a reference solar cell of known spectral response. The data were used to compute the spectral correction factors for each cell.

The I_{sc} generated by a Spectrolab X25 solar simulator (set with a silicon reference cell with no spectral corrections) was measured at a number of cell temperatures. Fitting a straight line to the data produced the temperature coefficient.

Each cell's I_{sc} was measured under natural sunlight simultaneously with the total and spectral irradiances. Four reference cell's short circuit currents could be measured simultaneously with active biasing to zero volts. Collimating tubes limited the cells' fields of view to 5.00°. The total irradiance was measured with an absolute cavity radiometer (5.00° field of view) that was directly traceable to the World Radiometric Reference. A Li-Cor LI-1800 spectroradiometer (also with a 5.00° field of view) measured the spectral irradiance between 350 and 1100 nm, and an atmospheric transmittance model then used this spectral information to compute the spectral irradiance from 305 to 4045 nm. Each spectral irradiance measurement required approximately 30 s. During this time, approximately 30 I_{sc} and total irradiance readings were collected with temperature data to form a single data point. Rejection criteria were applied to each data point. After temperature corrections were applied to each data point using the temperature coefficients, a spectral correction was made to each data point using the calculated spectral irradiance. The calibration values were then obtained by averaging. The data reported represents measurements from at least three days for most cells, two days for three cells, and one day for one cell whose intermittent instability rendered it impossible to measure on other days.

2.4.3 VNIIOFI (C)

VNIIOFI's calibrations were performed in a solar simulator using absolute spectral irradiance and relative SR measurements. The spectral measurements were traceable to the Russian national standard of spectral density of irradiance in the range 0.25-25.0 μm . The measured short-circuit currents were corrected with the same method as used by JQA/ETL (see Section 2.4.4).

2.4.4 JQA/ETL (C)

The JQA/ETL calibrations employed the Japanese solar simulator method [14]. The SR both with and without white bias light were measured at a cell temperature of 25°C. Next, the I_{sc} was measured in a steady-state Xe solar simulator, again at a cell temperature of 25°C. A spectro-radiometer, calibrated against a standard irradiance lamp traceable to the Commission Internationale de l'Eclairage (CIE) scale, measured the absolute spectral irradiance of the solar simulator. Using the spectral irradiance and the SR with white bias light, the calibrated I_{sc} was computed by multiplying the measured short-circuit currents (I_{scm}) by the ratio of two integrals of the SR (R_λ) against the global reference spectral irradiance ($E_{o\lambda}$) and the measured simulator spectral irradiance ($E_{m\lambda}$):

$$I_{sc} = I_{scm} \frac{\int E_{o\lambda} \cdot R_\lambda \cdot d\lambda}{\int E_{m\lambda} \cdot R_\lambda \cdot d\lambda}$$

Using the calibrated I_{sc} , the I-V curve was then measured in a pulsed solar simulator that had a better match to the global reference spectrum.

Temperature coefficients of six of the WPVS cells were determined using the following procedure. The test cell and a calibrated reference cell were placed in a pulsed Class A solar simulator and the cell temperatures measured. The reference cell temperature was controlled to 25°C, and the test cell's temperature was controlled from 15° to 55°C in approximately 10°C steps. The I-V curve of the test cell was measured at each temperature. From a plot of I_{sc} and V_{oc} and a least squares curve fit, the temperature coefficients α and β were calculated.

2.4.5 LCIE (R)

The calibrations performed by LCIE used the absolute SR measured over the spectral range of 350 to 1200 nm and a wavelength step of 25 nm, integrated with the global reference spectral irradiance to obtain the calibrated I_{sc} . The spectral line width was 10 nm. A bias light level of 3 W/m² and a cell temperature of 25°C were used.

2.4.6 PTB (D)

PTB's differential spectral responsivity (DSR) calibrations are described in detail in reference [15] and summarized below. The PTB method uses a quantity called the responsivity, s , which is defined as the ratio of short-circuit current to total irradiance, and therefore has units of A·m²/W. DSR is similarly defined by $\tilde{s}(\lambda) = \Delta I_{sc} / \Delta E_\lambda$, where ΔI_{sc} is the current produced by the chopped monochromatic irradiance ΔE_λ . Notice that \tilde{s} has different units from those of spectral responsivity,

R_λ , which is defined as the ratio of the monochromatic short-circuit current *density* to total irradiance, and thus has units of A/W. Except for the discussion of the PTB method in this section, we use SR to indicate R_λ throughout the remainder of this report.

A dual-beam optical arrangement was used to measure the relative spectral responsivity of the test cell at a series of discrete operating points that were set with a steady-state bias light at levels of $\sim 1 \text{ W/m}^2$ to $\sim 2000 \text{ W/m}^2$. The monochromatic light irradiance behind a double grating monochromator was measured with a PTB standard detector not exposed to the bias light. Using a uniform quartz halogen light source, 10-nm FWHM filters, and a PTB absolute standard detector, absolute spectral responsivity was measured at five discrete wavelengths (436.8, 548.5, 651.9, 744.5, and 858.0 nm) and used to scale the relative spectral responsivities. The DSR curves were then integrated with the global reference spectrum to obtain the responsivity as a function of the dc short-circuit current determined by the bias light.

With the range of responsivity measurements, a cell can be seen to be either linear, or have a DSR that varies with the operating point. If a cell is linear, the calibrated responsivity was simply the mean value of all the responsivities. For the case of a nonlinear cell, an iterative integration was used to obtain the calibrated responsivity.

2.4.7 NIM (D)

The NIM calibration method is similar to the PTB DSR method. A prism/grating monochromator system was used to measure the absolute SR against standard detectors. The standard detectors used by NIM were intercompared in China. Absolute SR was measured both with and without 1000 W/m^2 bias light.

2.4.8 TIPS (C)

TIPS also used absolute spectral irradiance relative SR measurements for reference cell calibrations. Relative SR was determined with a double-grating monochromator (5-nm bandwidth and 10-nm wavelength steps) against a spectral standard calibrated by the National Metrology Institute of Australia (NMI). These values were then scaled to absolute SR using the I_{sc} of the cell produced by a standard irradiance lamp, traceable to NIM. The calibrated I_{sc} was computed using the correction factor in Section 2.4.4, except that the spectral irradiance of the solar simulator was replaced with the spectral irradiance of the standard lamp.

2.4.9 ESTI (S)

ESTI used a secondary calibration against a calibrated reference cell. Each cell was measured in two different pulsed solar simulators (a Pasan and a Spectrolab), and spectral response was measured using the Pasan simulator and interference filters. Following correction for spectral mismatch, the two values were averaged to obtain the calibrated I_{sc} .

2.4.10 IACS (S)

The IACS secondary calibration procedures used a reference cell calibrated by NREL in a two-source (Xe and tungsten-halogen) Wacom solar simulator. Spectral irradiance of the simulator was measured against a calibrated photodiode using an Oriel 0.25 m monochromator. After the SR was measured with a 1000 W/m² halogen lamp bias light, the spectral mismatch parameter was calculated.

2.4.11 ISE (S)

ISE's calibrations were obtained with a modified 1600 W AEG Wedel Xe solar simulator against a primary reference cell calibrated by PTB. Spectral responsivities were measured with an interference filter monochromator system using both quartz halogen and Xe illumination. The reference detector was a solar cell calibrated by PTB. Spectral mismatch was used to correct the calibration values for spectral error.

2.5 Pre- and Post-Circulation Measurements

In order to characterize the WPVS cells as much as possible and to detect device changes that may have occurred, a number of measurements were performed at NREL before and after the sample circulation period. These measurements included 1000 W/m² current-voltage characterization under a Spectrolab X-25 steady-state Xe solar simulator (irradiance level set against a silicon reference cell without spectral mismatch corrections), followed by forward and reverse dark current-voltage measurements, all at 25°C.

From the light I-V data the open-circuit voltage, fill factor, maximum power, and slope at short-circuit current were obtained. Analysis of the dark I-V data gave the saturation current and diode quality factors for two forward regions, the series resistance (from far-forward bias), and the shunt resistance (from reverse bias). Following return to NREL, the area of each cell was determined from the coordinates of the cell corners measured using an optical microscope and an X-Y translation stage. Also at this time, the series resistances were measured by the two irradiance

method [16]. Table 2-4 contains the comparison pre- and post-circulation light I-V measurements; Table 2-5 lists the dark I-V comparison. Note that Y45 and Y124 are missing from these tables because these cells were added after the initial characterization at NREL was completed (see Section 2.1).

Examination of these tables shows very few differences that are greater than can be expected from normal experimental repeatability. Three cells showed open-circuit voltages higher for the post-circulation measurements. These are almost certainly caused by temperature differences of about 1°–2°C. The only detectable degradation here is the fill factor of PTB RS-69, the cover glass of which was replaced at PTB during the circulation. It is likely that the degradation occurred when the glass was broken or replaced because a fill factor of 0.764 was measured initially by NREL, 0.769 by JQA, 0.746 by ESTI, and finally 0.742 again at NREL.

Table 2-6 lists the illuminated and the dark I-V characteristics that were measured at NREL following completion of sample circulation.

Table 2-4. Differences between post- and pre-circulation illuminated I-V characteristics

ID	ΔV_{oc} (mV)	ΔI_{sc} (mA)	ΔFF	ΔP_{max} (mW)	$\Delta dI/dV$ (S)
930216-1	4.4	0.8	0.0042	1.1	0.23
930216-2	6.1	0.3	0.0016	0.9	-0.12
930417-1	23.3	0.3	0.0088	3.0	-0.60
930417-2	20.2	0.7	0.0068	2.7	0.59
93308	4.7	-2.7	-0.0013	-0.7	1.34
93309	6.5	-2.5	-0.0016	-0.5	0.11
NIM 9351	8.4	-7.5	0.0042	-2.0	-0.28
NIM 9352	8.5	-3.4	0.0101	-0.1	0.41
PX102C	7.9	1.8	-0.0017	1.2	-0.03
PX201C	4.1	0.8	0.0019	0.9	-0.62
PTB RS-58	8.5	0.7	0.0062	1.5	0.82
PTB RS-67	6.7	-3.0	0.0029	-0.5	0.07
PTB RS-68	5.5	-2.0	0.0037	-0.1	-0.04
PTB RS-69	4.6	-0.9	-0.0217	-1.6	0.00
PTB RS-78	6.8	-0.7	0.0085	0.9	-0.18
TDB 9303	8.2	0.9	0.0002	1.3	0.49
TDC 9305	16.6	-0.4	0.0047	1.7	0.98
Y09	7.2	0.9	0.0037	1.1	0.84
Y45					
Y124					

Table 2-5. Differences between post- and pre-circulation dark I-V characteristics

ID	ΔR_s (Ω)	ΔR_{sh} (k Ω)	ΔI_{o1} (A)	Δn_1	ΔI_{o2} (A)	Δn_2
930216-1	-0.06	13.80	-4.447E-11	-0.005	1.532E-6	0.162
930216-2	0.01	10.24	1.633E-9	0.004	-1.818E-5	-0.216
930417-1	0.00	4.80	-3.418E-9	-0.007	4.013E-6	0.132
930417-2	-0.15	0.36	-2.257E-9	-0.007	9.092E-6	0.231
93308	-0.03	-19.10	6.029E-10	0.024	8.077E-6	0.664
93309	-0.06	-40.70	1.870E-9	0.070	1.659E-5	0.992
NIM 9351	0.04	16.50	-1.854E-8	-0.040	-2.402E-8	0.055
NIM 9352	-0.01	8.98	-1.613E-8	-0.062	-5.843E-6	-0.386
PX102C	0.01	0.06	4.891E-9	0.000	5.519E-5	0.207
PX201C	0.03	309.90	-2.057E-10	-0.023	-2.768E-7	0.043
PTB RS-58	-0.04	7.80	-9.518E-8	-0.032	-2.978E-6	-0.219
PTB RS-67	-0.05	4.69	-1.232E-7	-0.185	-5.318E-6	-0.006
PTB RS-68	-0.04	17.50	-4.027E-9	-0.022	-2.784E-7	0.032
PTB RS-69	-0.04	-2.37	1.798E-8	0.068	6.258E-5	0.926
PTB RS-78	-0.04	11.00	-2.823E-8	-0.072	-5.555E-6	-0.044
TDB 9303	0.03	3.50	1.583E-9	0.022	6.406E-7	0.126
TDC 9305	-0.08	7.20	-1.329E-10	0.001	2.827E-7	0.161
Y09	-0.08	0.49	-2.299E-10	-0.013	-2.220E-6	-0.054
Y45						
Y124						

Table 2-6. Post-circulation illuminated and dark I-V characteristics measured at NREL

ID	V_{oc} (V)	FF	P_{max} (mW)	dI/dV (mS)	R_s (Ω)	R_{sh} (k Ω)	I_{o1} (A)	n_1	I_{o2} (A)	n_2
930216-1	0.599	0.779	56.6	-0.45	0.14	36.3	4.37E-9	1.39	1.44E-5	3.40
930216-2	0.598	0.753	54.7	-0.50	0.28	19.8	3.91E-8	1.61	5.73E-5	4.24
930417-1	0.602	0.761	57.1	-0.57	0.15	16.7	1.94E-8	1.52	4.59E-5	3.92
930417-2	0.598	0.759	55.7	-0.30	0.15	6.6	2.48E-8	1.53	3.69E-5	3.72
93308	0.546	0.788	53.1	-0.12	0.14	44.5	1.69E-9	1.20	1.25E-5	3.87
93309	0.547	0.778	52.4	-0.22	0.15	10.4	2.98E-9	1.24	2.08E-5	4.09
NIM 9351	0.549	0.735	47.7	-0.29	0.42	65.6	3.50E-8	1.48	1.82E-6	2.32
NIM 9352	0.591	0.763	53.0	-0.46	0.25	18.8	1.64E-8	1.50	1.56E-6	2.52
PX102C	0.581	0.674	45.0	-3.19	0.28	1.8	7.61E-7	1.94	3.30E-4	4.62
PX201C	0.600	0.794	57.9	-0.13	0.18	421.9	5.51E-10	1.23	1.29E-6	2.64
PTB RS-58	0.596	0.731	55.0	0.14	0.22	23.6	3.47E-7	1.86	3.85E-6	2.36
PTB RS-67	0.602	0.745	55.2	-0.47	0.22	12.7	3.18E-8	1.58	1.07E-4	4.44
PTB RS-68	0.603	0.769	57.0	-0.23	0.23	41.0	1.49E-8	1.51	6.54E-6	2.92
PTB RS-69	0.601	0.742	55.4	-0.79	0.21	6.1	3.60E-8	1.59	7.38E-5	4.06
PTB RS-78	0.597	0.759	52.5	-0.42	0.22	21.4	2.87E-8	1.56	2.02E-5	3.46
TDB 9303	0.592	0.776	61.3	0.11	0.12	55.0	6.58E-9	1.39	2.26E-6	2.75
TDC 9305	0.547	0.785	52.8	-0.24	0.12	114.2	1.63E-9	1.19	1.53E-6	2.48
Y09	0.594	0.782	42.3	0.20	0.07	5.4	1.25E-9	1.28	3.02E-5	4.01
Y45	0.602	0.735	55.7	-0.31	0.10	10.3	3.28E-8	1.56	2.22E-5	3.10
Y124	0.570	0.742	45.4	-0.36	0.37	4.4	2.22E-8	1.50	4.52E-5	5.03

2.6 Data Analysis and Selection Procedures

A major problem that confronted the participants was how to qualify the results and obtain the calibration values of the WPVS reference cells so that the goal of a $\pm 2\%$ total uncertainty might be achieved. Secondary to this problem was how to analyze the results so the participating laboratories might use them to locate any errors. At the final participants meeting, the following procedure to qualify and analyze the results was adopted:

- Normalize the I_{sc} results by the averages of each cell.
- Exclude secondary calibrations from the WPVS averages.
- Exclude laboratories with 50% or more data points outside of $\pm 2\%$ of cell averages.
- Renormalize I_{sc} results by cell averages from qualified laboratories.
- Remove outliers outside of $\pm 2\%$.
- Average remaining data points to obtain WPVS calibration values for each cell.
- Calculate standard deviations for each cell.
- Renormalize all data by WPVS calibration values and plot as bar charts.
- Take every combination of each laboratory's normalized data as X-Y data pairs and plot.
- Normalize reported SR data by area over 400–1050 nm range and plot for each cell.
- Select qualified laboratories for average WPVS SR.
- Average selected SR and scale by WPVS I_{sc} .
- Plot WPVS SR.
- Calculate and plot deviation of reported SR from WPVS average.
- Calculate reference spectral mismatch, normalize by cell average, and plot.

The SR normalization was performed on each cell individually as described below. First, the data from every laboratory were combined. Wavelength units were converted to nm and responsivity units from quantum efficiency, if necessary. Next, each reported measurement was sampled at 2 nm wavelength intervals over the 400–1050 nm range using linear interpolation. These sampled responsivities are denoted by $s_{\lambda i}$ (i refers to individual laboratories). The area, A_i , of each measurement was then calculated using numerical integration. From the area, a normalization factor was obtained:

$$F_i = A_i / (1050 - 400)$$

The dimensionless average SR was then computed using:

$$R_{\lambda} = \sum (s_{\lambda i} / F_i) / n$$

Note that R_λ was obtained using only those laboratories selected for inclusion in the WPVS SR average. The deviation from the WPVS average for every measurement could then be obtained using:

$$\Delta_\lambda = (s_{\lambda i} / F_i) - R_\lambda$$

An iterative process was used to qualify laboratories for the WPVS SR average. The average was calculated initially using the measurements from all the laboratories, and the area-normalized SR and SR deviation plotted. Using these plots, a visual examination showed laboratories that had problems with SR measurements and were subsequently excluded from the average.

In order to obtain an indication of the magnitude of the differences caused by errors in the SR measurements, each SR curve was used to calculate a spectral mismatch factor against a reference cell SR, a 4500K blackbody spectral irradiance, and high-wavelength resolution solar spectral irradiance. These curves, shown in Fig. 2-9, were chosen using several criteria. The reference cell curve represents a wide-bandgap device with a high quantum efficiency and smooth cutoffs (the curve was synthesized and is not an actual device). A wide bandgap prevents throwing away data from spectral regions where the test cells respond. The solar spectrum is a direct normal spectral irradiance that was generated by an atmospheric transmittance model and was selected because it contains a large number of wavelength points. Finally, a blackbody spectrum was used because it is a smooth curve and therefore should not bias the calculation. 4500K was chosen because it gave a value close to unity, but not so close as to make differences difficult to resolve.

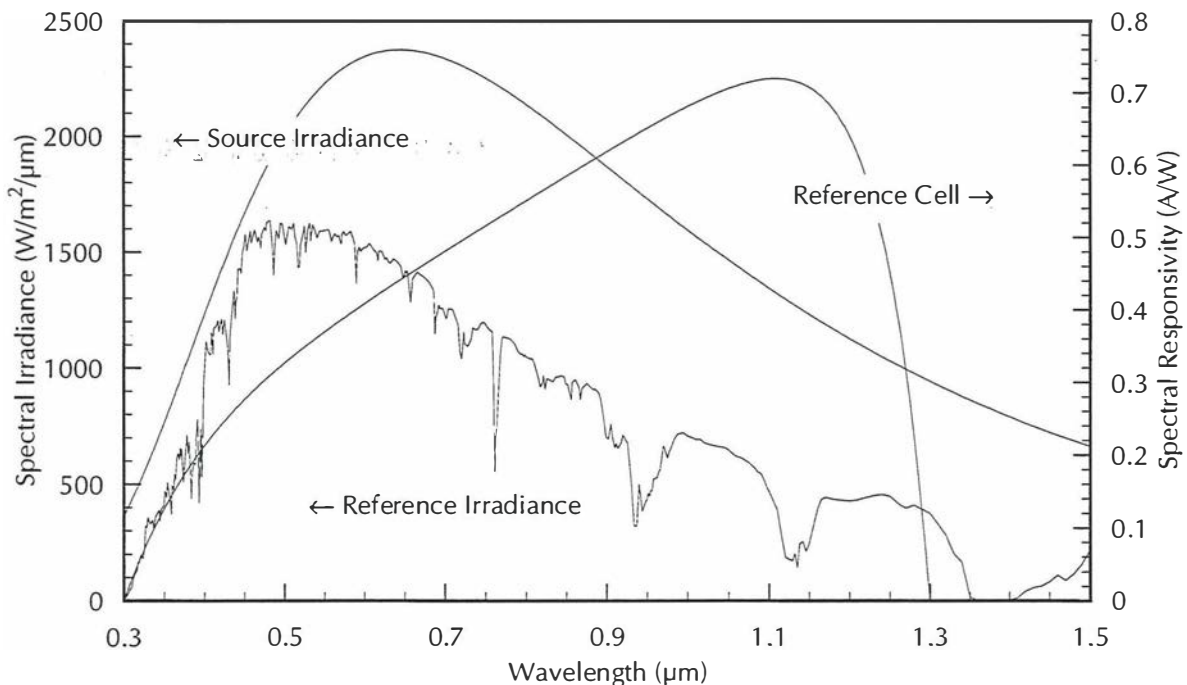


Figure 2-9. Reference spectral mismatch factor parameter spectra

2.7 Results

2.7.1 Reported Short-Circuit Currents

Table 2-7 lists the short-circuit current values reported by the participating laboratories.

2.7.2 Reported I_{sc} Temperature Coefficients

Table 2-8 gives the temperature coefficients reported for the WPVS reference cells. Because laboratories used different units, all values were converted to ppm/°C to allow direct comparisons.

2.7.3 Reported Total Uncertainties

With the exceptions of IACS and ISE, most of the laboratories gave an estimate of their total uncertainty for the WPVS calibrations, which are listed in Table 2-9.

Table 2-7. Reported short-circuit current results for the WPVS reference cells (mA). The columns are in order of circulation.

ID	SNL	NREL	VNIIOFI	JQA/ETL	LCIE	PTB	NIM	TIPS	ESTI	IACS	ISE
930216-1	121.7	122.9	126.4	124.1	118.5	121.98	113.7	124.17	128	123.7	120.3
930216-2	122.2	123.2	124.2	124.4	119.4	121.99	114.5	124.27	128	123.9	120.8
930417-1	124.1	124.1	129.3	125.8	120.0	123.61	115.0	126.45	130	125.6	122.7
930417-2	121.8	122.2	117.2	123.9	119.2	121.45	112.1	124.87	128	123.6	120.9
93308	124.5	126.5	132.5	126.1	119.3	125.32	120.5	127.52	132	127.0	123.5
93309	124.8	126.7	132.8	125.9	119.9	125.15	116.4	127.78	132	127.5	123.7
NIM 9351	125.6	122.1	126.5	120.9	115.4	119.59	106.9	121.59	125	121.6	118.0
NIM 9352	121.7	120.8	125.7	120.3	112.8	118.46	111.0	121.10	123	121.1	118.0
PX102C	116.2	116.2	120.4	117.5	113.2	116.09	90.4	118.40	122	117.9	113.8
PX201C	122.2	122.5	124.7	123.9	120.4	122.04	118.3	124.71	127	124.2	120.7
PTB RS-58	125.6	126.1	124.9	126.7	119.3	124.80	115.7	128.82	132	126.8	125.6
PTB RS-67	125.9	125.4	123.7	126.2	119.8	123.91	112.9	127.10	129	124.8	122.4
PTB RS-68	124.9	125.1	128.2	126.0	119.0	123.57	117.3	127.69	130	124.9	122.3
PTB RS-69	125.4	125.6	127.6	126.1		123.44	110.7	127.60	130	124.9	123.7
PTB RS-78	117.4	117.3	115.1	117.7	110.3	115.80	107.1	119.19	122	117.4	115.2
TDB 9303	133.8	133.8	137.7	136.5	131.1	133.24	129.2	137.16	140	135.7	134.0
TDC 9305	124.5	124.3	122.9	126.4	120.6	123.48	117.1	126.23	130	123.8	122.9
Y09	93.34	93.4	97.55	94.08	90.7	93.26	88.4	94.35	98	94.2	90.9
Y45	127.1	126.5	125.6	126.8	125.4	126.93	117.5	129.86	136	128.3	124.6
Y124	108.8	107.9	110.8	111.3	108.5	109.12	91.9	105.32	113	111.3	106.9

Table 2-8. Converted I_{sc} temperature coefficients (ppm/°C)

ID	SNL	NREL	JQA/ETL	TIPS	ESTI	ISE
930216-1	600	443	403	560	250	480
930216-2	527	416		580	250	600
930417-1	416	485		480	31	470
930417-2	421	434	404	500	188	480
93308	594	757		470	303	670
93309	619	767	537	490	273	480
NIM 9351	466	473		590	480	470
NIM 9352	368	395		460	325	470
PX102C	494	654		580	230	560
PX201C	426	453	403	540	283	430
PTB RS-58	567	574		560	303	790
PTB RS-67	547	537		510	93	
PTB RS-68	603	591		560	185	
PTB RS-69	551	570		610	308	610
PTB RS-78	590	545		570	230	560
TDB 9303	558	542	457	520	343	470
TDC 9305	586	466		580	338	470
Y09	606	609	564	650	286	710
Y45	605	903		670	271	680
Y124	466	487		540	265	300

Table 2-9. Estimated U_{95} total uncertainty for WPVS calibrations (%)

ID	SNL	NREL	VNIIOFI	JQA/ETL	LCIE	PTB	NIM	TIPS	ESTI	ISE
930216-1	1.5	1.0	3.9	1.4	2.6	1.0	1.6	2.7	1.2	1.5
930216-2	1.5	1.0	3.9	1.4	2.6	1.0	1.6	2.7	1.2	1.5
930417-1	1.5	1.0	3.9	1.4	2.6	1.0	1.6	2.7	1.2	1.5
930417-2	1.5	1.0	3.9	1.4	2.6	1.0	1.6	2.7	1.2	1.5
93308	1.5	1.0	3.9	1.4	2.6	1.0	1.6	2.7	1.2	1.5
93309	1.5	1.0	3.9	1.4	2.6	1.0	1.6	2.7	1.2	1.5
NIM 9351	1.5	1.2	3.9	1.4	2.6	1.0	1.6	2.7	1.2	1.5
NIM 9352	1.5	2.3	3.9	1.4	2.6	1.0	1.6	2.7	1.2	1.5
PX102C	1.5	1.0	3.9	1.4	2.6	1.0	1.6	2.7	1.2	1.5
PX201C	1.5	1.0	3.9	1.4	2.6	1.0	1.6	2.7	1.2	1.5
PTB RS-58	1.5	1.4	3.9	1.4	2.6	1.0	1.6	2.7	1.2	1.5
PTB RS-67	1.5	1.0	3.9	1.4	2.6	1.0	1.6	2.7	1.2	1.5
PTB RS-68	1.5	1.0	3.9	1.4	2.6	1.0	1.6	2.7	1.2	1.5
PTB RS-69	1.5	1.0	3.9	1.4	2.6	1.0	1.6	2.7	1.2	1.5
PTB RS-78	1.5	1.0	3.9	1.4	2.6	1.0	1.6	2.7	1.2	1.5
TDB 9303	1.5	1.0	3.9	1.4	2.6	1.0	1.6	2.7	1.2	1.5
TDC 9305	1.5	1.0	3.9	1.4	2.6	1.0	1.6	2.7	1.2	1.5
Y09	1.5	1.2	3.9	1.4	2.6	1.0	1.6	2.7	1.2	1.5
Y45	1.5	1.0	3.9	1.4	2.6	1.0	1.6	2.7	1.2	1.5
Y124	1.5	1.1	3.9	1.4	2.6	1.0	1.6	2.7	1.2	1.5

2.7.4 Spectral Responsivity

The spectral responsivity results submitted by the participants are not tabulated in this report, but are available on the companion CD-ROM.

2.8 WPVS Analysis and Calibration Values

2.8.1 Short-Circuit Currents

Averaging the rows of Table 2-7 and normalizing by these factors results in Table 2-10. Using the criteria from Section 2.6 above, SNL, ESTI, IACS, and ISE are excluded from the WPVS average because they are secondary calibrations, and VNIIOFI, LCIE, and NIM are excluded because of the number of points that exceed 1.00 ± 0.02 . Using only the data from the accepted laboratories, the normalization was repeated with the results shown in Table 2-11.

Table 2-10. Cell average-normalized WPVS short-circuit currents (dimensionless). Laboratories marked with a ‡ are secondary calibrations, and the bottom row shows the number of measurements that exceed 1.00 ± 0.02 for that laboratory.

ID	SNL‡	NREL	VNIIOFI	JQA/ETL	LCIE	PTB	NIM	TIPS	ESTI‡	IACS‡	ISE‡
930216-1	0.9950	1.0048	1.0334	1.0146	0.9688	0.9973	0.9296	1.0152	1.0465	1.0113	0.9835
930216-2	0.9980	1.0062	1.0144	1.0160	0.9752	0.9963	0.9351	1.0149	1.0454	1.0119	0.9866
930417-1	0.9989	0.9989	1.0407	1.0125	0.9659	0.9949	0.9256	1.0178	1.0463	1.0109	0.9876
930417-2	1.0034	1.0067	0.9655	1.0207	0.9820	1.0005	0.9235	1.0287	1.0545	1.0183	0.9960
93308	0.9890	1.0049	1.0525	1.0017	0.9477	0.9955	0.9572	1.0130	1.0486	1.0089	0.9811
93309	0.9929	1.0080	1.0565	1.0016	0.9539	0.9957	0.9261	1.0166	1.0502	1.0144	0.9841
NIM 9351	1.0442	1.0151	1.0516	1.0051	0.9594	0.9942	0.8887	1.0108	1.0392	1.0109	0.9810
NIM 9352	1.0188	1.0113	1.0523	1.0071	0.9443	0.9917	0.9293	1.0138	1.0297	1.0138	0.9879
PX102C	1.0128	1.0128	1.0494	1.0241	0.9866	1.0118	0.7879	1.0319	1.0633	1.0276	0.9918
PX201C	0.9952	0.9977	1.0156	1.0091	0.9806	0.9939	0.9635	1.0157	1.0343	1.0115	0.9830
PTB RS-58	1.0038	1.0078	0.9982	1.0126	0.9535	0.9974	0.9247	1.0296	1.0550	1.0134	1.0038
PTB RS-67	1.0175	1.0134	0.9997	1.0199	0.9682	1.0014	0.9124	1.0272	1.0425	1.0086	0.9892
PTB RS-68	1.0036	1.0052	1.0301	1.0124	0.9562	0.9929	0.9425	1.0260	1.0446	1.0036	0.9827
PTB RS-69	1.0072	1.0088	1.0249	1.0128		0.9915	0.8891	1.0249	1.0441	1.0032	0.9935
PTB RS-78	1.0133	1.0124	0.9934	1.0159	0.9520	0.9995	0.9244	1.0287	1.0530	1.0133	0.9943
TDB 9303	0.9930	0.9930	1.0219	1.0130	0.9729	0.9888	0.9588	1.0179	1.0390	1.0071	0.9945
TDC 9305	1.0054	1.0037	0.9924	1.0207	0.9739	0.9971	0.9456	1.0193	1.0498	0.9997	0.9924
Y09	0.9986	0.9992	1.0436	1.0065	0.9704	0.9977	0.9457	1.0094	1.0485	1.0078	0.9725
Y45	1.0025	0.9978	0.9907	1.0002	0.9891	1.0012	0.9268	1.0243	1.0727	1.0120	0.9828
Y124	1.0101	1.0017	1.0287	1.0333	1.0073	1.0131	0.8532	0.9778	1.0491	1.0333	0.9925
		0	13	3	15	0	20	9			

Table 2-11. Cell average-normalized WPVS short-circuit currents for the four accepted laboratories (dimensionless). Underlined data points exceeded 1.00 ± 0.02 and were excluded as outliers. The last two columns give the mean (mA) and standard deviation (%) of the accepted calibration data, and therefore constitute the WPVS calibrations. The average standard deviation is 1.05%.

ID	NREL	JQA/ETL	PTB	TIPS	Mean (mA)	Std. dev. (%)
930216-1	0.9969	1.0066	0.9894	1.0072	123.29	0.85
930216-2	0.9979	1.0076	0.9881	1.0065	123.47	0.91
930417-1	0.9929	1.0065	0.9890	1.0117	124.99	1.08
930417-2	0.9926	1.0065	0.9866	1.0143	123.11	1.27
93308	1.0011	0.9979	0.9918	1.0092	126.36	0.72
93309	1.0025	0.9962	0.9902	1.0111	126.38	0.89
NIM 9351	1.0087	0.9988	0.9880	1.0045	121.05	0.90
NIM 9352	1.0053	1.0011	0.9858	1.0078	120.17	0.98
PX102C	0.9928	1.0039	0.9918	1.0116	117.05	0.94
PX201C	0.9936	1.0050	0.9899	1.0115	123.29	1.00
PTB RS-58	0.9960	1.0008	0.9857	1.0175	126.61	1.32
PTB RS-67	0.9980	1.0044	0.9861	1.0115	125.65	1.08
PTB RS-68	0.9961	1.0033	0.9839	1.0167	125.59	1.37
PTB RS-69	0.9993	1.0033	0.9821	1.0152	125.69	1.37
PTB RS-78	0.9983	1.0017	0.9856	1.0144	117.50	1.19
TDB 9303	0.9898	1.0098	0.9857	1.0147	135.18	1.44
TDC 9305	0.9936	1.0104	0.9870	1.0090	125.10	1.15
Y09	0.9960	1.0033	0.9945	1.0062	93.77	0.56
Y45	0.9920	0.9943	0.9954	1.0183	127.52	1.23
Y124	0.9953	<u>1.0267</u>	1.0065	<u>0.9715</u>	108.51	0.80

Renormalizing the reported I_{sc} data by the WPVS calibration values and bar charting versus cells produced Table 2-12 and Figs. 2-11 through 2-13. The normalized I_{sc} data for each laboratory can then be averaged to rank the laboratories against the WPVS average (Table 2-13). The rankings are plotted in Fig. 2-10, along with the total uncertainties reported by the participants (Table 2-9) as error bars. As a means to view the WPVS as a whole, the data from the accepted laboratories used for the qualified average are normalized and plotted in Fig. 2-14 (the outliers were not removed from this plot).

Table 2-12. Normalized (by WPVS calibration values) I_{sc} data

ID	SNL	NREL	VNIIOFI	JQA/ETL	LCIE	PTB	NIM	TIPS	ESTI	IACS	ISE
930216-1	0.9871	0.9969	1.0252	1.0066	0.9612	0.9894	0.9222	1.0072	1.0382	1.0033	0.9758
930216-2	0.9898	0.9979	1.0060	1.0076	0.9671	0.9881	0.9274	1.0065	1.0367	1.0035	0.9784
930417-1	0.9929	0.9929	1.0345	1.0065	0.9601	0.9890	0.9201	1.0117	1.0401	1.0049	0.9817
930417-2	0.9894	0.9926	0.9520	1.0065	0.9683	0.9866	0.9106	1.0143	1.0398	1.0040	0.9821
93308	0.9853	1.0011	1.0486	0.9979	0.9441	0.9918	0.9536	1.0092	1.0446	1.0051	0.9774
93309	0.9875	1.0025	1.0508	0.9962	0.9487	0.9902	0.9210	1.0111	1.0444	1.0088	0.9788
NIM 9351	1.0376	1.0087	1.0451	0.9988	0.9534	0.9880	0.8831	1.0045	1.0327	1.0046	0.9748
NIM 9352	1.0128	1.0053	1.0461	1.0011	0.9387	0.9858	0.9237	1.0078	1.0236	1.0078	0.9820
PX102C	0.9928	0.9928	1.0286	1.0039	0.9671	0.9918	0.7723	1.0116	1.0423	1.0073	0.9723
PX201C	0.9912	0.9936	1.0115	1.0050	0.9766	0.9899	0.9595	1.0115	1.0301	1.0074	0.9790
PTB RS-58	0.9921	0.9960	0.9865	1.0008	0.9423	0.9857	0.9139	1.0175	1.0426	1.0015	0.9921
PTB RS-67	1.0020	0.9980	0.9845	1.0044	0.9534	0.9861	0.8985	1.0115	1.0266	0.9932	0.9741
PTB RS-68	0.9945	0.9961	1.0208	1.0033	0.9475	0.9839	0.9340	1.0167	1.0351	0.9945	0.9738
PTB RS-69	0.9977	0.9993	1.0152	1.0033		0.9821	0.8808	1.0152	1.0343	0.9938	0.9842
PTB RS-78	0.9992	0.9983	0.9796	1.0017	0.9387	0.9856	0.9115	1.0144	1.0383	0.9992	0.9804
TDB 9303	0.9898	0.9898	1.0187	1.0098	0.9699	0.9857	0.9558	1.0147	1.0357	1.0039	0.9913
TDC 9305	0.9952	0.9936	0.9824	1.0104	0.9640	0.9870	0.9360	1.0090	1.0391	0.9896	0.9824
Y09	0.9954	0.9960	1.0403	1.0033	0.9672	0.9945	0.9427	1.0062	1.0451	1.0046	0.9694
Y45	0.9967	0.9920	0.9849	0.9943	0.9834	0.9954	0.9214	1.0183	1.0665	1.0061	0.9771
Y124	1.0027	0.9944	1.0211	1.0257	0.9999	1.0056	0.8469	0.9706	1.0414	1.0257	0.9852

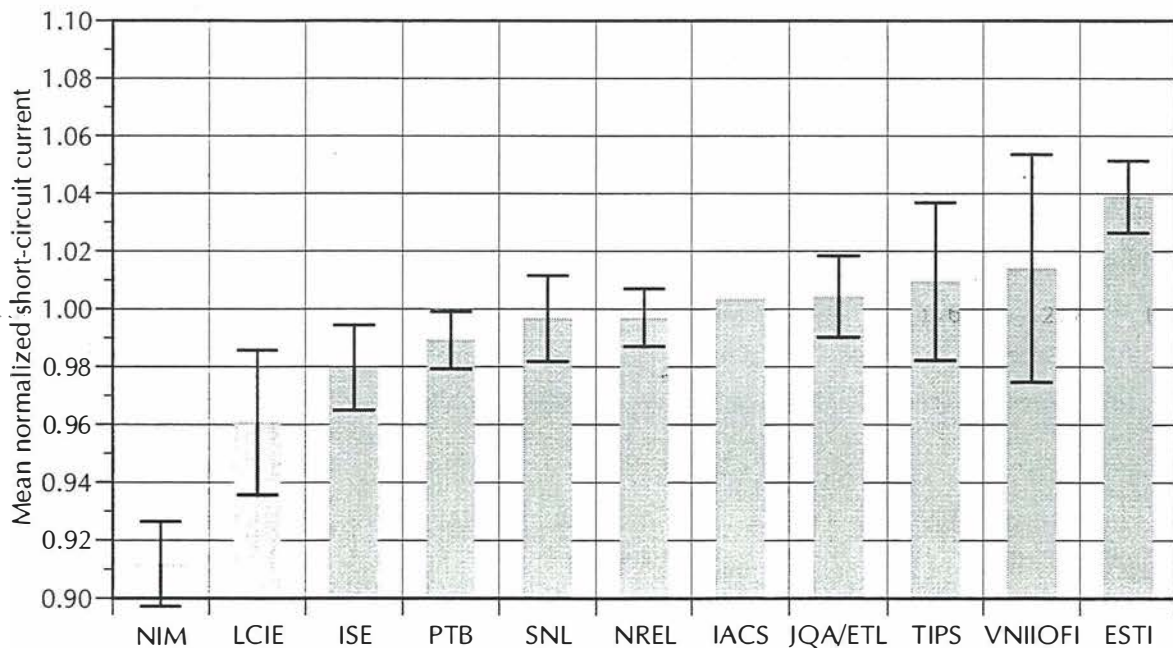


Figure 2-10. Laboratories ranked according to WPVS calibration values. The error bars are the total uncertainties reported by the laboratories (see Table 2-9).

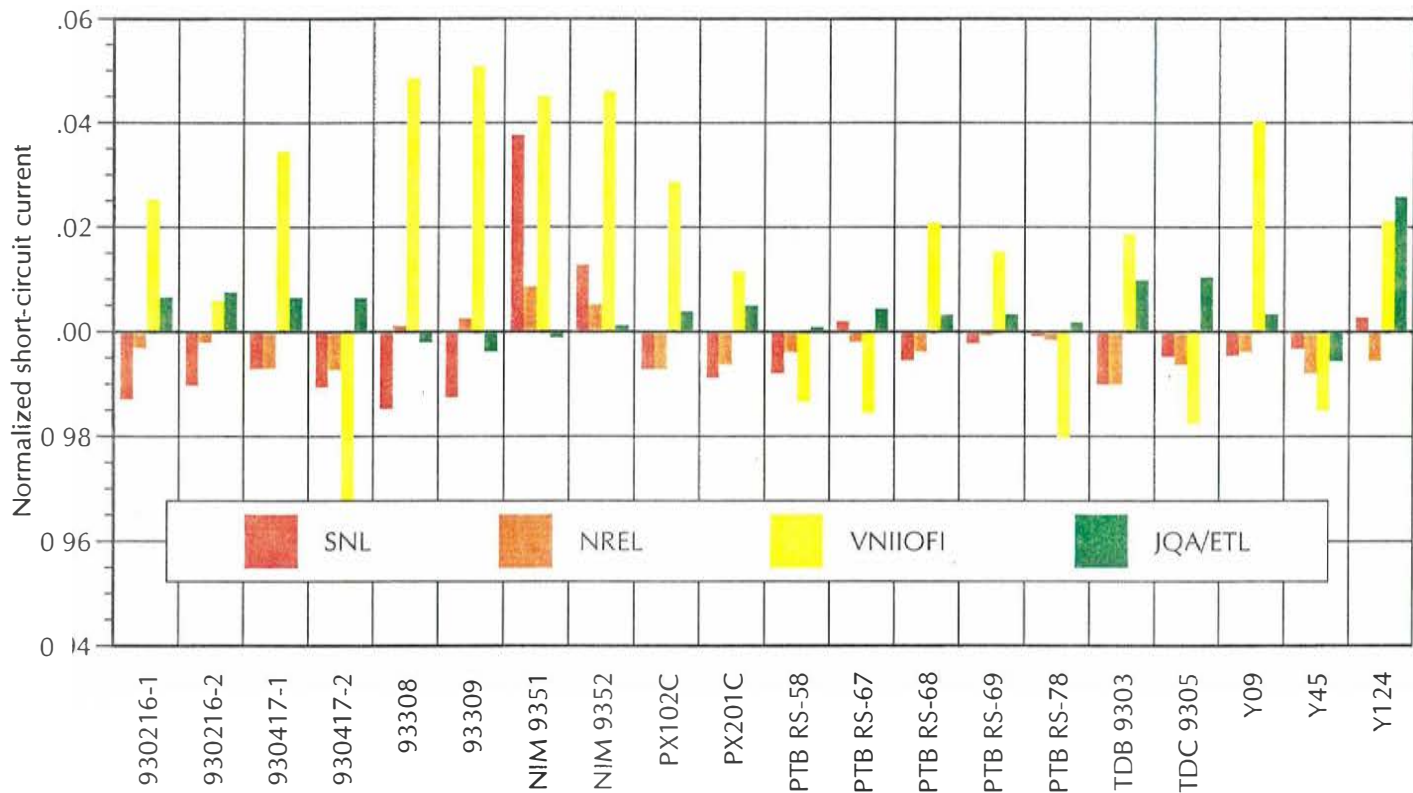


Figure 2-11. I_{sc} results normalized by WPVS calibration values (part 1)

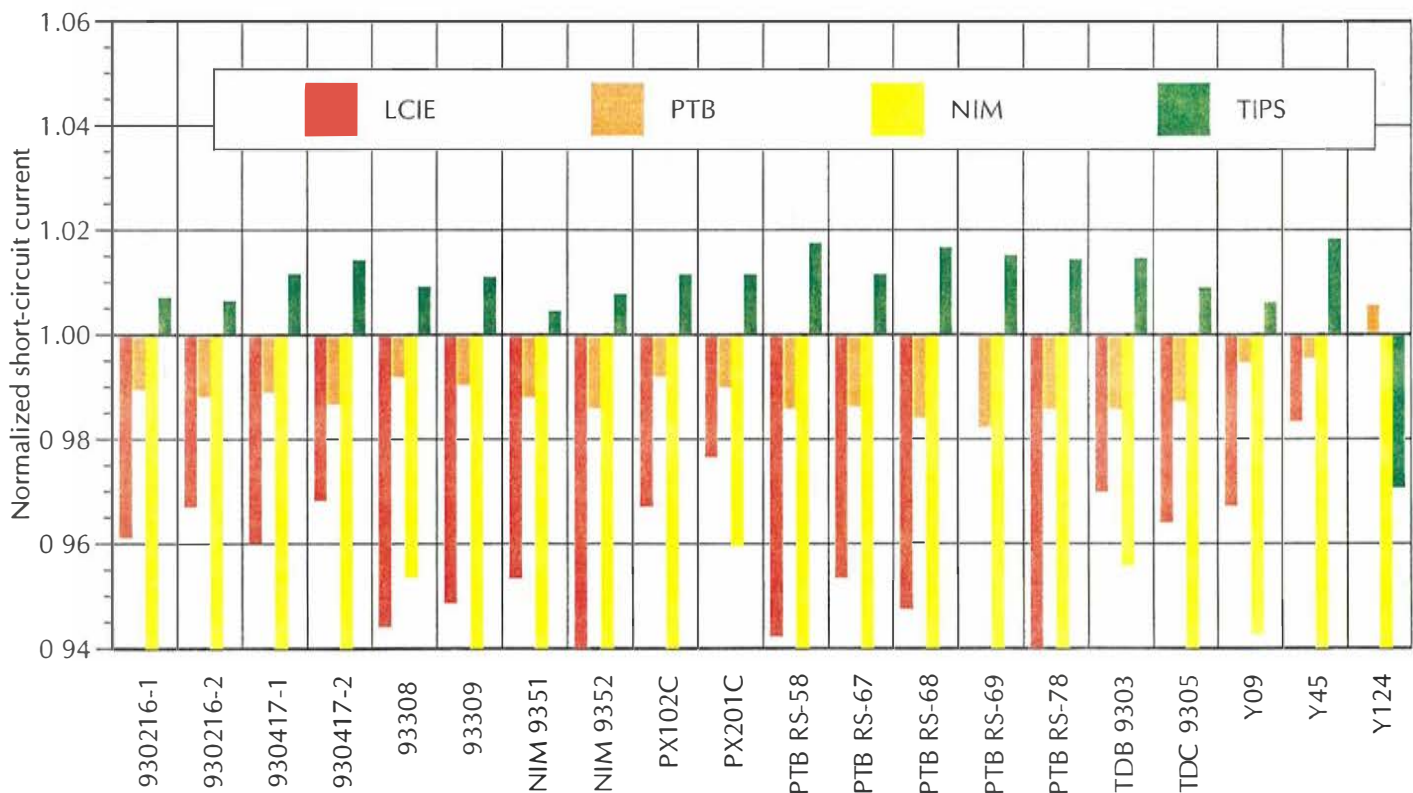


Figure 2-12. I_{sc} results normalized by WPVS calibration values (part 2)

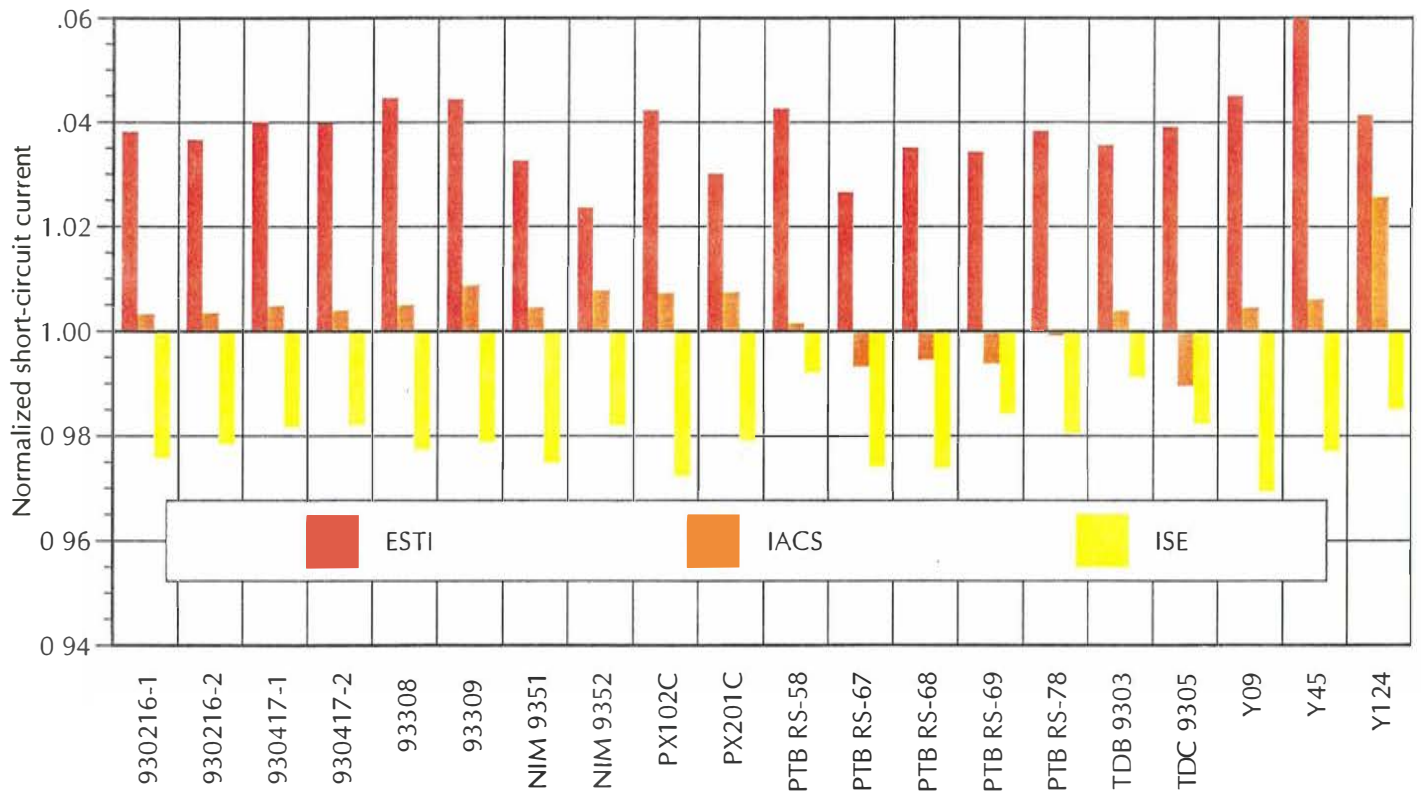


Figure 2-13. I_{sc} results normalized by WPVS calibration values (part 3)

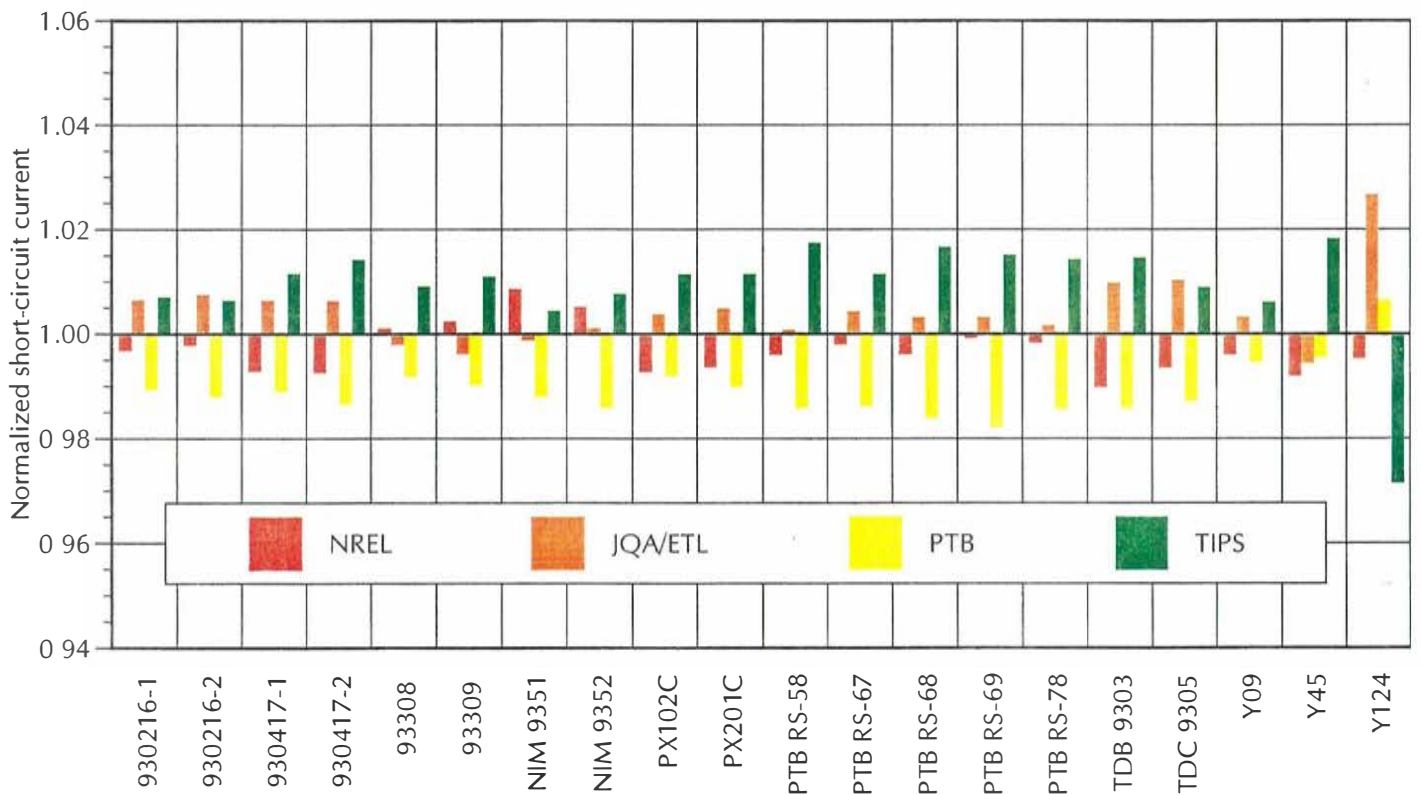


Figure 2-14. I_{sc} results from the WPVS accepted laboratories normalized by the final calibration values.

Table 2-13. Normalized (by WPVS calibration values) I_{sc} data averaged by laboratory. The second row is the standard deviation (%).

SNL	NREL	VNIIOFI	JQA/ETL	LCIE	PTB	NIM	TIPS	ESTI	IACS	ISE
0.9966	0.9969	1.0141	1.0043	0.9606	0.9891	0.9118	1.0095	1.0389	1.0034	0.9796
1.16	0.47	2.74	0.65	1.66	0.52	4.66	0.99	0.84	0.75	0.59

As a final method of viewing the I_{sc} results, the renormalized data were then processed in the following way. Every combination of each laboratory's data was taken two at a time to produce a set of X-Y pairs. Thus, for 20 cells, there are 190 different X-Y pairs ($C(20,2) = 190$). These pairs were then graphed as scatter plots for each laboratory and are shown in Fig. 2-15 through 2-25. Several features of these scatter plots can be noted. The size of the groupings is proportional to the laboratory standard deviations in Table 2-13, and the positions along the diagonal line are equivalent to the laboratory rankings. Outliers from the main groupings are very easy to observe and are seen as horizontal or vertical lines of points. SNL's data (Fig. 2-15) shows two distinct outliers for the NIM cells, and several laboratories (JQA/ETL, LCIE, PTB, TIPS, and IACS) show the cell Y124 as an outlier. Note that the NIM data (Fig. 2-21) has several cell averages below 0.88 that do not show on the plot.

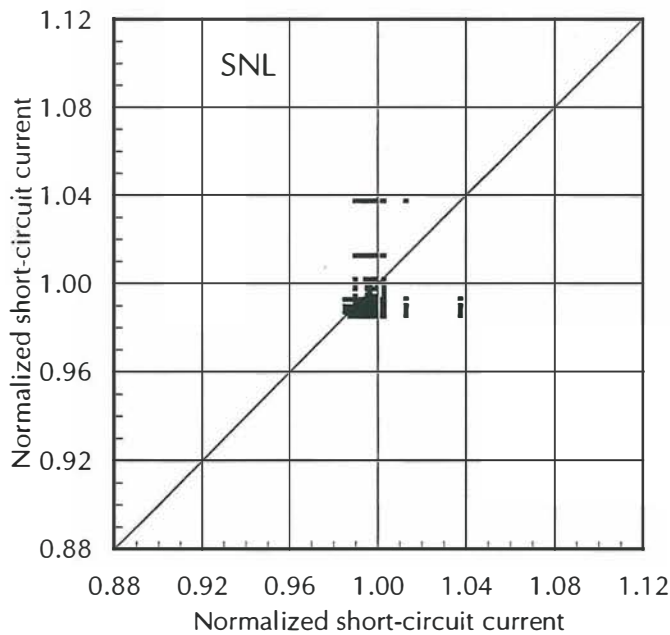


Figure 2-15. I_{sc} scatter plot for SNL

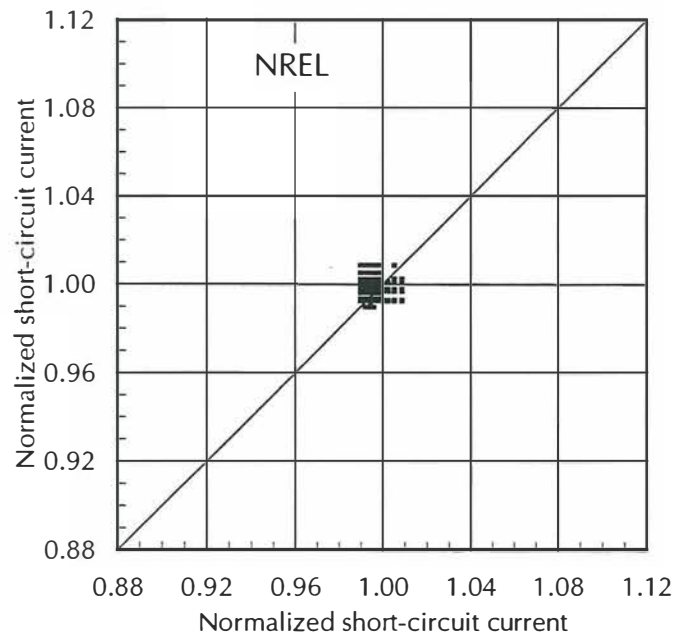


Figure 2-16. I_{sc} scatter plot for NREL

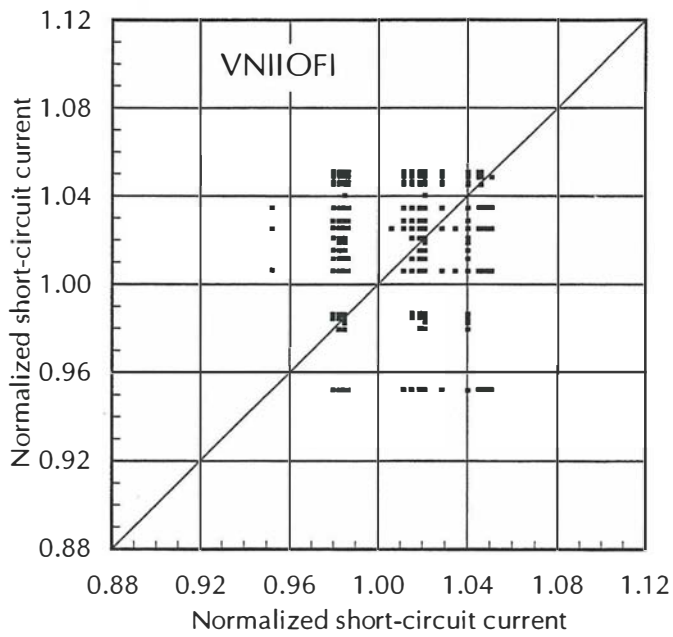


Figure 2-17. I_{sc} scatter plot for VNIIOFI

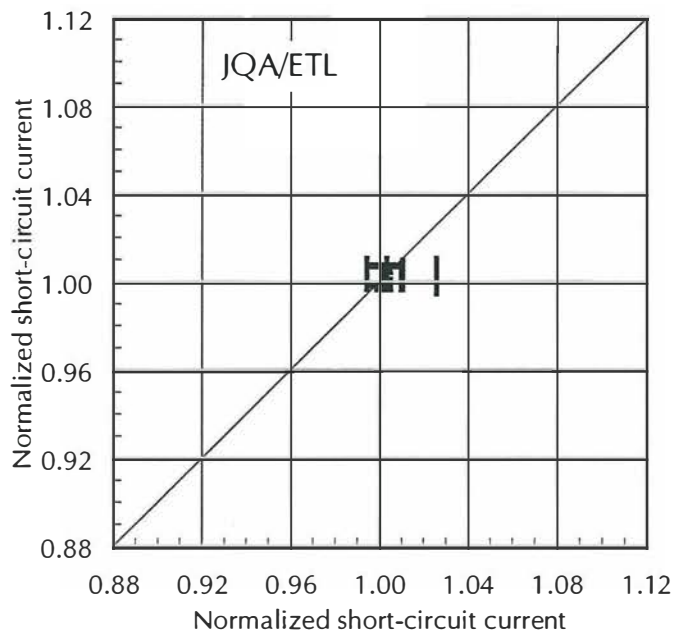


Figure 2-18. I_{sc} scatter plot for JQA/ETL

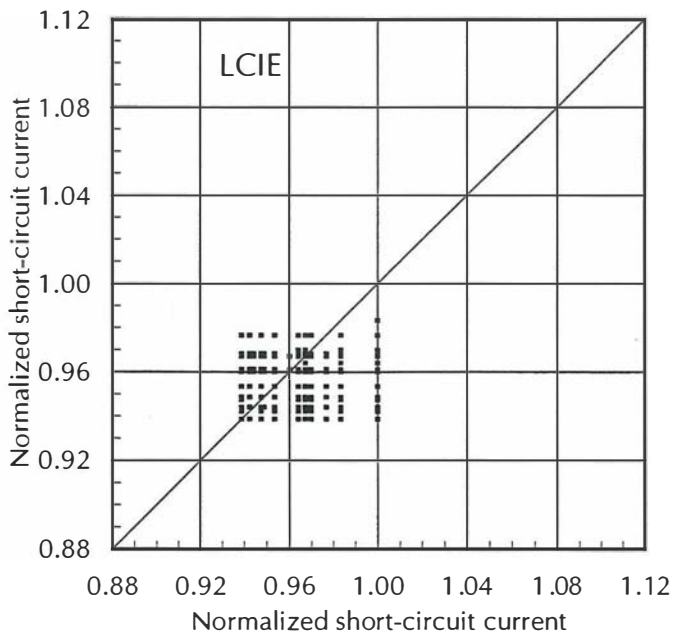


Figure 2-19. I_{sc} scatter plot for LCIE

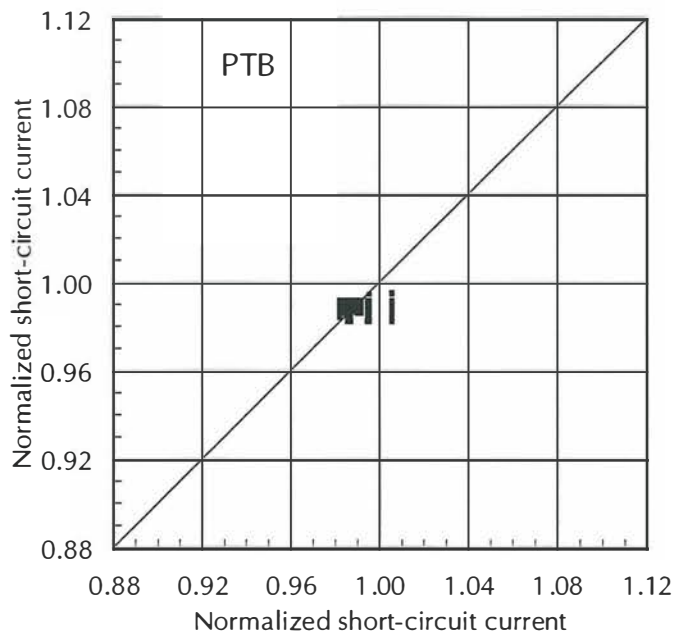


Figure 2-20. I_{sc} scatter plot for PTB

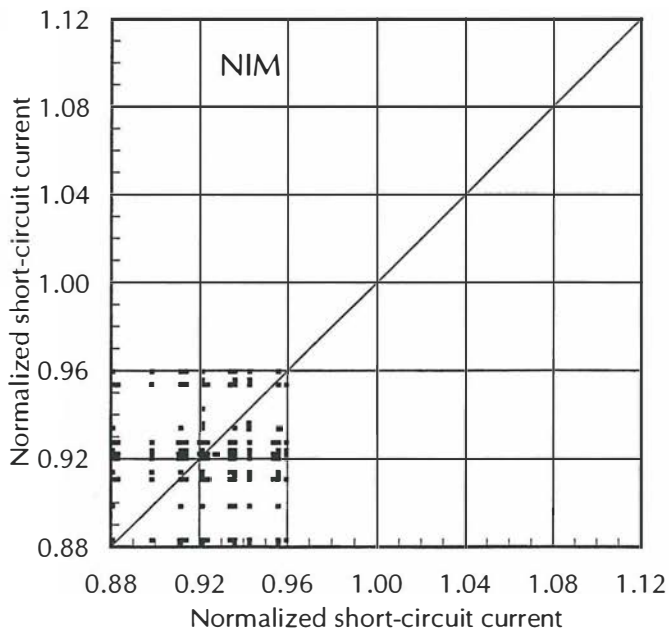


Figure 2-21. I_{sc} scatter plot for NIM

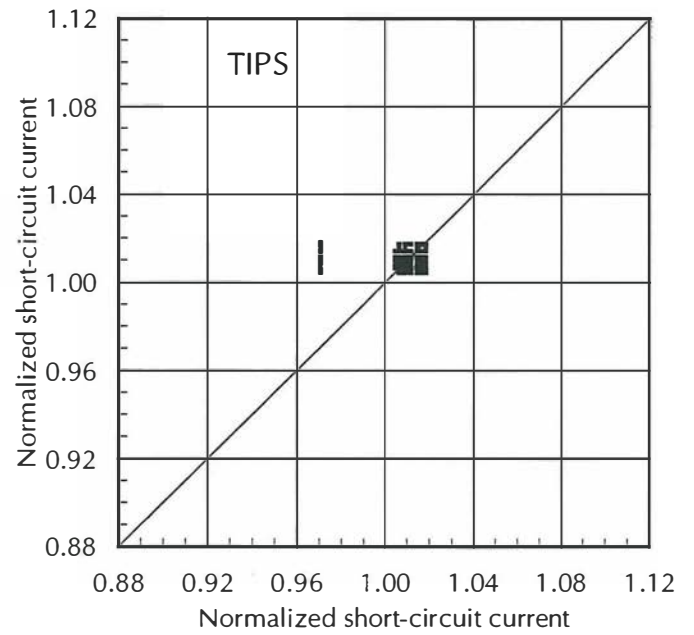


Figure 2-22. I_{sc} scatter plot for TIPS

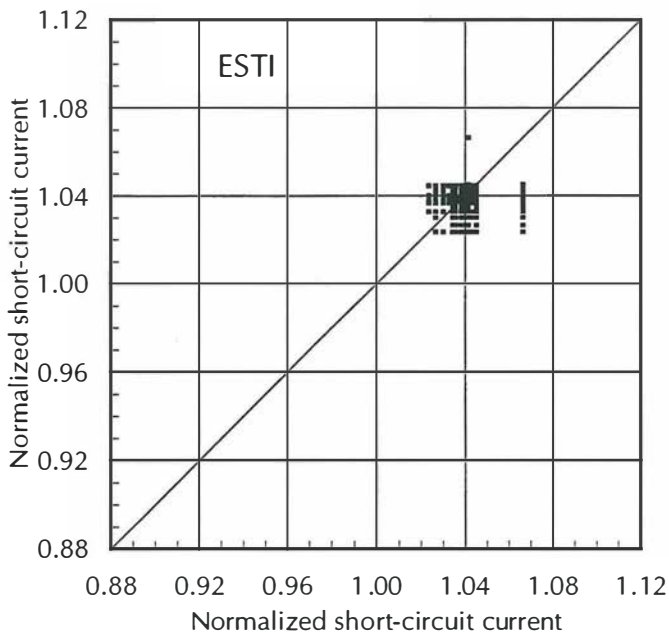


Figure 2-23. I_{sc} scatter plot for ESTI

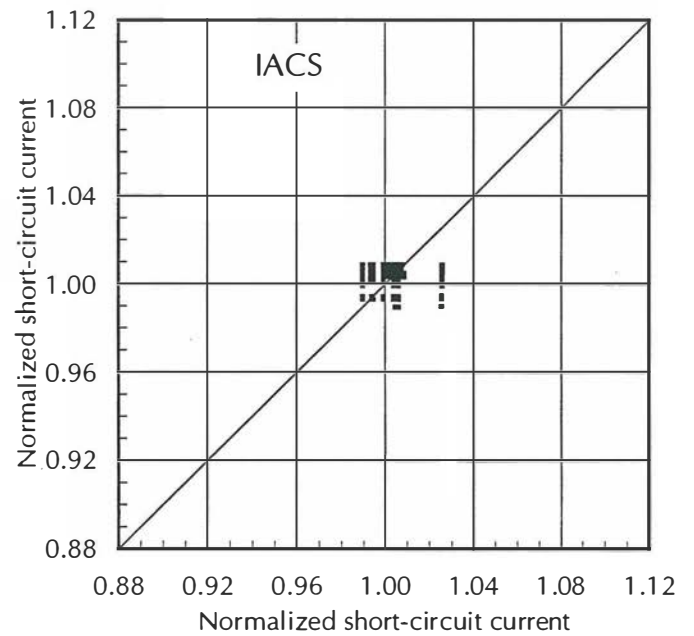


Figure 2-24. I_{sc} scatter plot for IACS

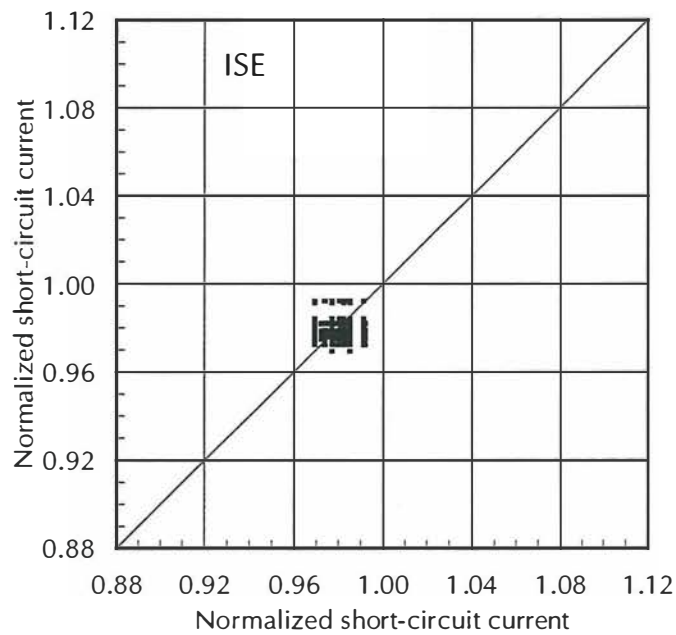


Figure 2-25. I_{sc} scatter plot for ISE

2.8.2 I_{sc} Temperature Coefficients

Table 2-14 lists the mean and standard deviation of the I_{sc} temperature coefficients contained in Table 2-8. Note the large values of the standard deviations, typically about 20–30%.

Table 2-14. WPVS mean temperature coefficients (ppm/°C)

ID	α (ppm/°C)	Std. Dev. (%)
930216-1	456	27
930216-2	475	30
930417-1	376	52
930417-2	404	28
93308	559	32
93309	528	31
NIM 9351	496	11
NIM 9352	404	15
PX102C	504	32
PX201C	423	20
PTB RS-58	559	31
PTB RS-67	422	52
PTB RS-68	485	41
PTB RS-69	530	24
PTB RS-78	499	30
TDB 9303	482	16
TDC 9305	488	21
Y09	571	26
Y45	626	29
Y124	412	29

2.8.3 Spectral Responsivity

The spectral responsivity data (available on the companion CD-ROM) were analyzed using the procedures detailed in Section 2.6 above, and Figs. 2-26 through 2-45 show the area-normalized SR for each WPVS cell along with deviations from the averages. The most visible features of these plots are the IACS data, all of which show an abnormal peak at 980 nm. This is obviously a measurement system problem, and was later determined to have been caused by a faulty Si photodiode calibration.

Measurement system problems are much more visible in the deviation plots than in the area-normalized plots. Note that if a laboratory's data were high in a certain spectral region, the area averaging caused the other regions to be lower than the average. The NREL data are characterized by large swings in the infrared region above 750 nm, which were caused by a combination of the thin-film interference filter monochromator and the Xe arc lamp in this system. Similar effects are visible in the ESTI data, which were obtained using interference filters with the Xe pulsed simulators. The TIPS data all have an anomalously high region about 100 nm wide centered at 900 nm. VNIIOFI's data seem to have an error that causes the shape to be high at shorter wavelengths and low at longer wavelengths (see Fig. 2-31), and LCIE's data occasionally show a similar problem that is opposite in direction (see Fig. 2-34). Both the SNL and the NREL data for cell NIM 9351 show a higher response below 500 nm (Fig. 2-32). ISE's data tend to agree with the average, although the deviation curves also show undulations typical of interference filter monochromators.

Using the iterative process, the SNL, JQA/ETL, and PTB data were selected for the WPVS SR average, with the exception of SNL's data for the NIM cells. The qualified SR data, scaled to the WPVS average short-circuit currents in Table 2-8, are tabulated in Appendix 3 and plotted in Figs. 2-46 through 2-50.

Several individual cells show greater deviations, including 93308, NIM 9351, PX201C, TDB 9303, Y09, and Y45. Although it is not possible to determine the cause differences without a detailed analysis of each measurement system, some of these may be due to nonlinearities with bias light level. To document the degree of nonlinearities inherent in the WPVS cells, the linearity data obtained by PTB with the differential spectral responsivity method are shown in Figs. 2-51 through 2-55. These plots show the DSR data, obtained at bias light levels spanning two orders of magnitude, integrated with the global reference spectral irradiance and peak-normalized. Most of the cells show less than 0.5% nonlinearity, and the maximum nonlinearity is a bit less than 2%. The nonlinearities are an increasing responsivity with increasing bias level, centered at a wavelength of about 900 nm (not shown). It is therefore difficult to attribute the deviations seen to differences in bias light level.

Table 2-15. Reference spectral mismatch (see text) for the WPVS SR data. The last column is the calculation performed using the WPVS qualified SR results.

ID	SNL	NREL	VNIIOFI	JQA/ETL	LCIE	PTB	NIM	TIPS	ESTI	IACS	ISE	WPVS SR
9302161	0.9180	0.9080	0.9079	0.9155	0.9206	0.9139	0.9214	0.9075	0.9127	0.9534	0.9180	0.9157
9302162	0.9188	0.9090	0.9102	0.9161	0.9226	0.9143	0.9220	0.9078	0.9130	0.9539	0.9233	0.9163
9304171	0.9198	0.9183	0.9085	0.9176	0.9229	0.9154	0.9221	0.9089	0.9152	0.9571	0.9193	0.9175
9304172	0.9209	0.9177	0.9082	0.9179	0.9264	0.9161	0.9240	0.9093	0.9152	0.9577	0.9193	0.9182
93308	0.9023	0.8974	0.8936	0.9007	0.9005	0.8980	0.9079	0.8909	0.8956	0.9417	0.9030	0.9002
93309	0.9017	0.8980	0.8835	0.9009	0.9039	0.8975	0.9054	0.8912	0.8959	0.9414	0.9022	0.9000
NIM 9351	0.9043	0.9038	0.8960	0.9119	0.9078	0.9069	0.9146	0.9002	0.9086	0.9495	0.9121	0.9094
NIM 9352	0.9389	0.9382	0.9285	0.9425	0.9393	0.9395	0.9491	0.9333	0.9384	0.9822	0.9426	0.9410
PX102C	0.9162	0.9129	0.9022	0.9126	0.9344	0.9103	0.9146	0.9039	0.9097	0.9614	0.9140	0.9130
PX201C	0.9140	0.9018	0.8905	0.9112	0.9192	0.9094	0.9156	0.9033	0.9081	0.9543	0.9140	0.9115
PTB RS-58	0.9093	0.9004	0.8996	0.9072	0.9020	0.9051	0.9099	0.8975	0.9044	0.9527	0.9064	0.9070
PTB RS-67	0.9090	0.9010	0.8919	0.9073	0.9041	0.9053	0.9122	0.8982	0.9050	0.9517	0.9081	0.9070
PTB RS-68	0.9079	0.8997	0.8950	0.9060	0.8998	0.9039	0.9089	0.8948	0.9023	0.9483	0.9066	0.9057
PTB RS-69	0.9074	0.8970	0.8944	0.9054		0.9033	0.9101	0.8943	0.9012	0.9491	0.9062	0.9052
PTB RS-78	0.9053	0.8953	0.8952	0.9035	0.8985	0.9010	0.9077	0.8939	0.9002	0.9483	0.9031	0.9032
TDB 9303	0.9220	0.9210	0.9061	0.9198	0.9212	0.9174	0.9307	0.9087	0.9140	0.9432	0.9182	0.9196
TDC 9305	0.9042	0.9042	0.8955	0.9029	0.9026	0.8998	0.9067	0.8919	0.8974	0.9665	0.9042	0.9022
Y09	0.9230	0.9188	0.9129	0.9222	0.9432	0.9193	0.9252	0.9109	0.9203	0.9591	0.9222	0.9214
Y45	0.9149	0.9130	0.9161	0.9132	0.9238	0.9139	0.9183	0.9071	0.9117	0.9571	0.9133	0.9137
Y124	0.9387	0.9325	0.9297	0.9357	0.9446	0.9328	0.9404	0.9248	0.9333	0.9734	0.9378	0.9356

Reference spectral mismatch calculations, as described above in Section 2-6, are presented in Table 2-15. Normalization of these calculations by the last column of Table 2-15 and plotting as bar charts produced Figs. 2-56 through 2-58. Table 2-16 shows the mean and standard deviations by laboratory of the normalized reference spectral mismatch. This table shows that the effects of SR errors on calibration results are very small for methods that do not require absolute SR, which includes methods A, C, and S (see Table 2-2).

Table 2-16. Normalized reference spectral mismatch averaged by laboratory. The second row is the standard deviation (%).

SNL	NREL	VNIIOFI	JQA/ETL	LCIE	PTB	NIM	TIPS	ESTI	IACS	ISE
1.002	0.996	0.989	1.000	1.005	0.998	1.006	0.990	0.997	1.046	1.002
0.21	0.40	0.54	0.08	0.86	0.07	0.22	0.13	0.13	0.79	0.19

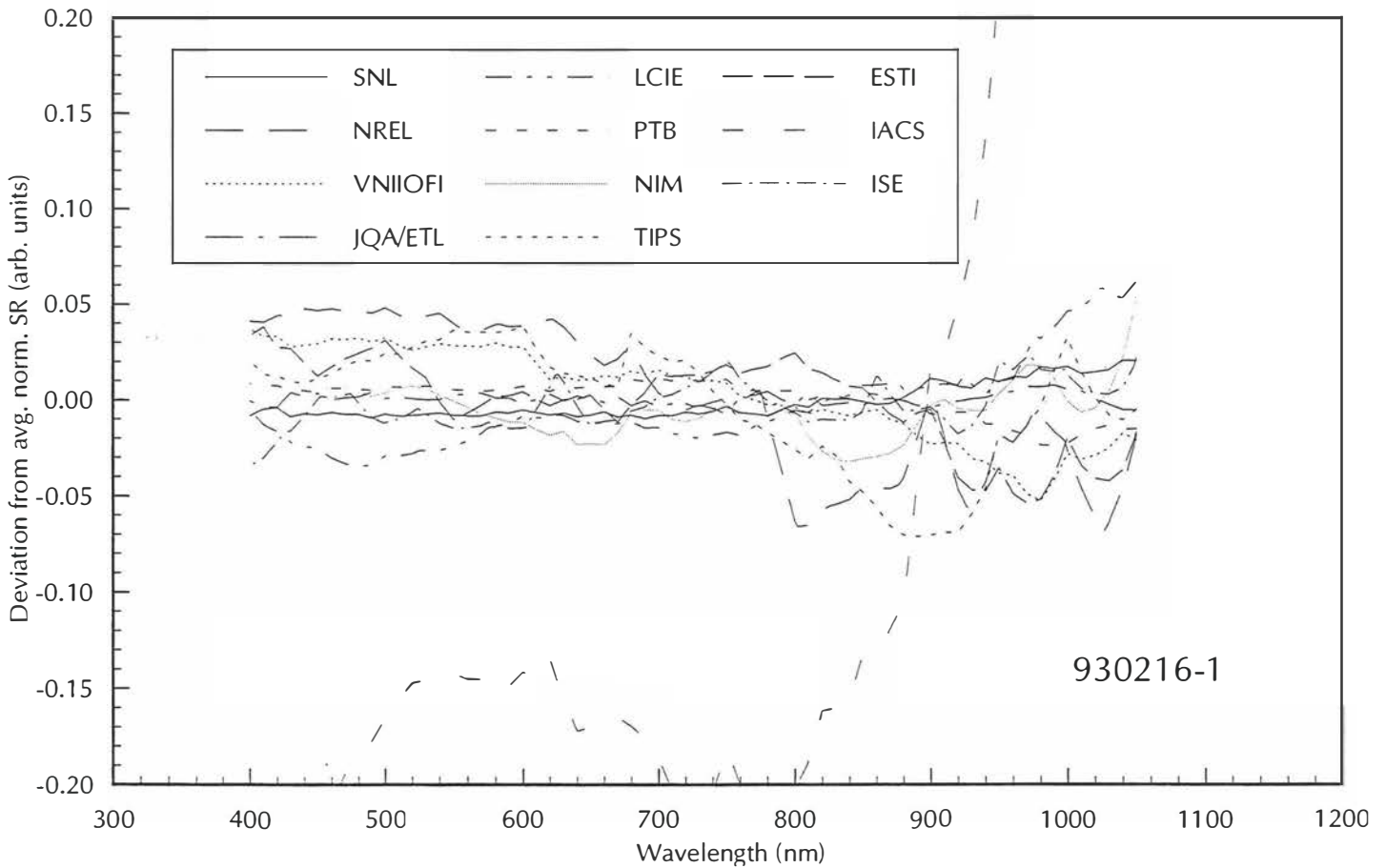
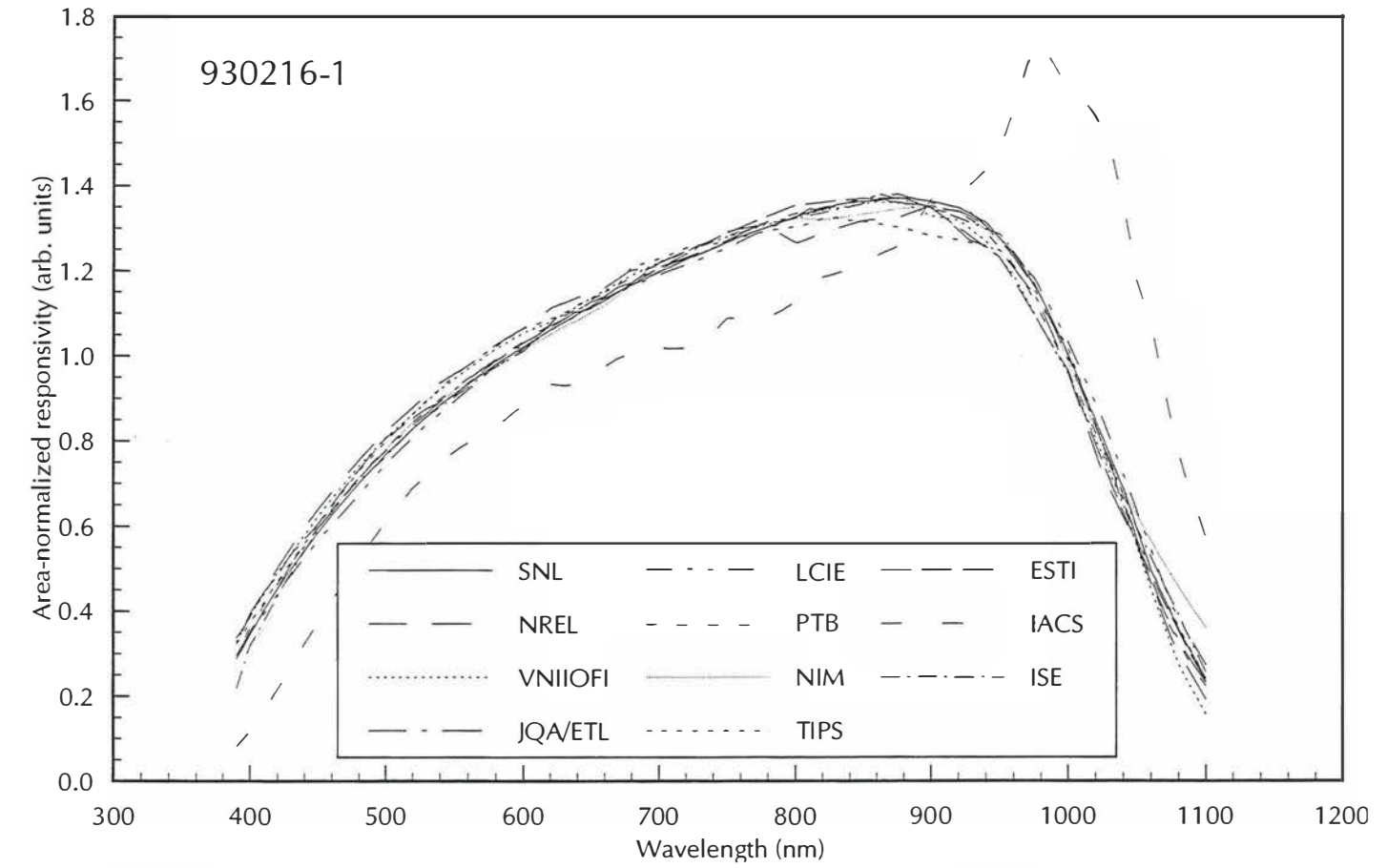


Figure 2-26. Area-normalized spectral responsivity and deviation from WPVS SR for 930216-1

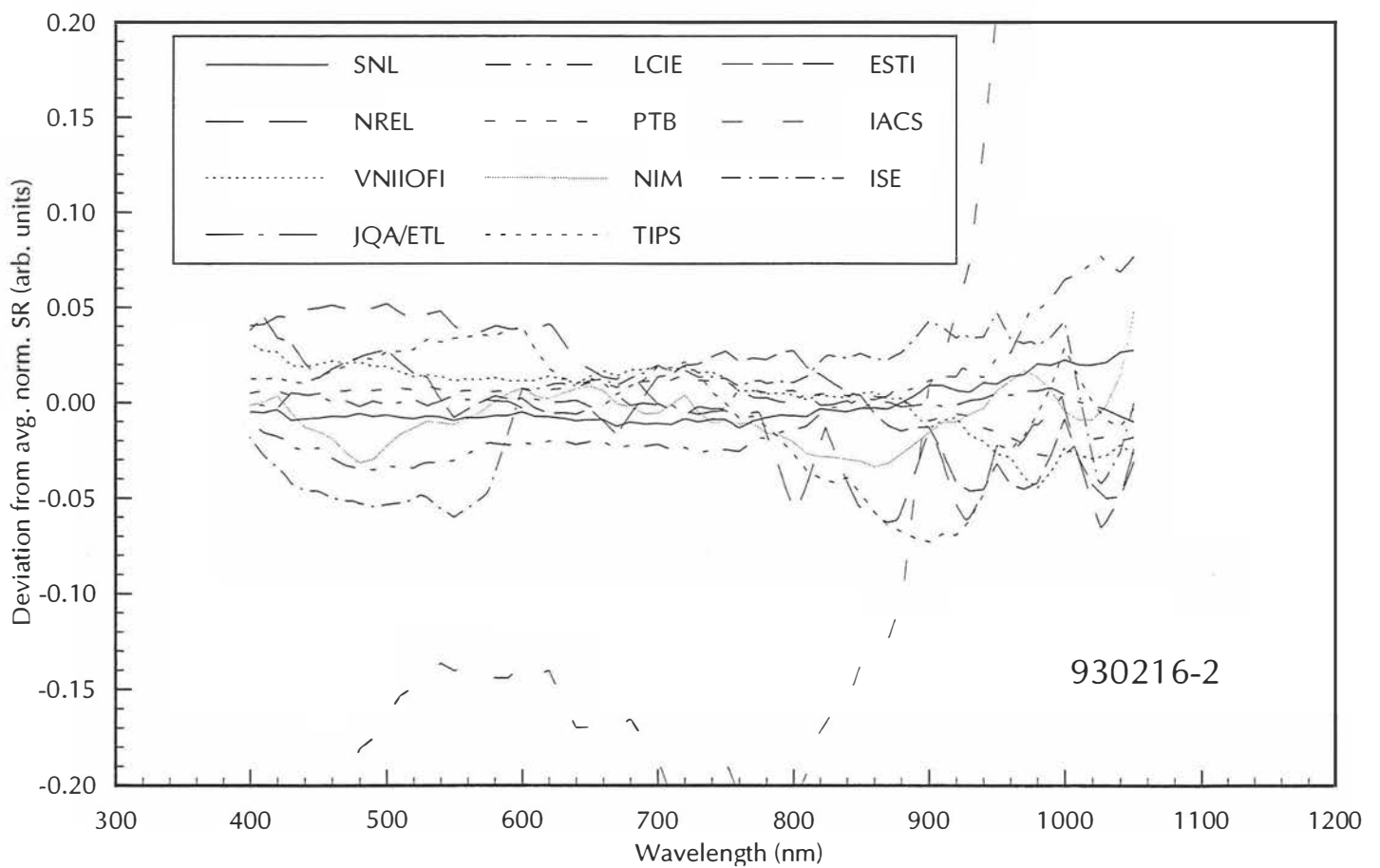
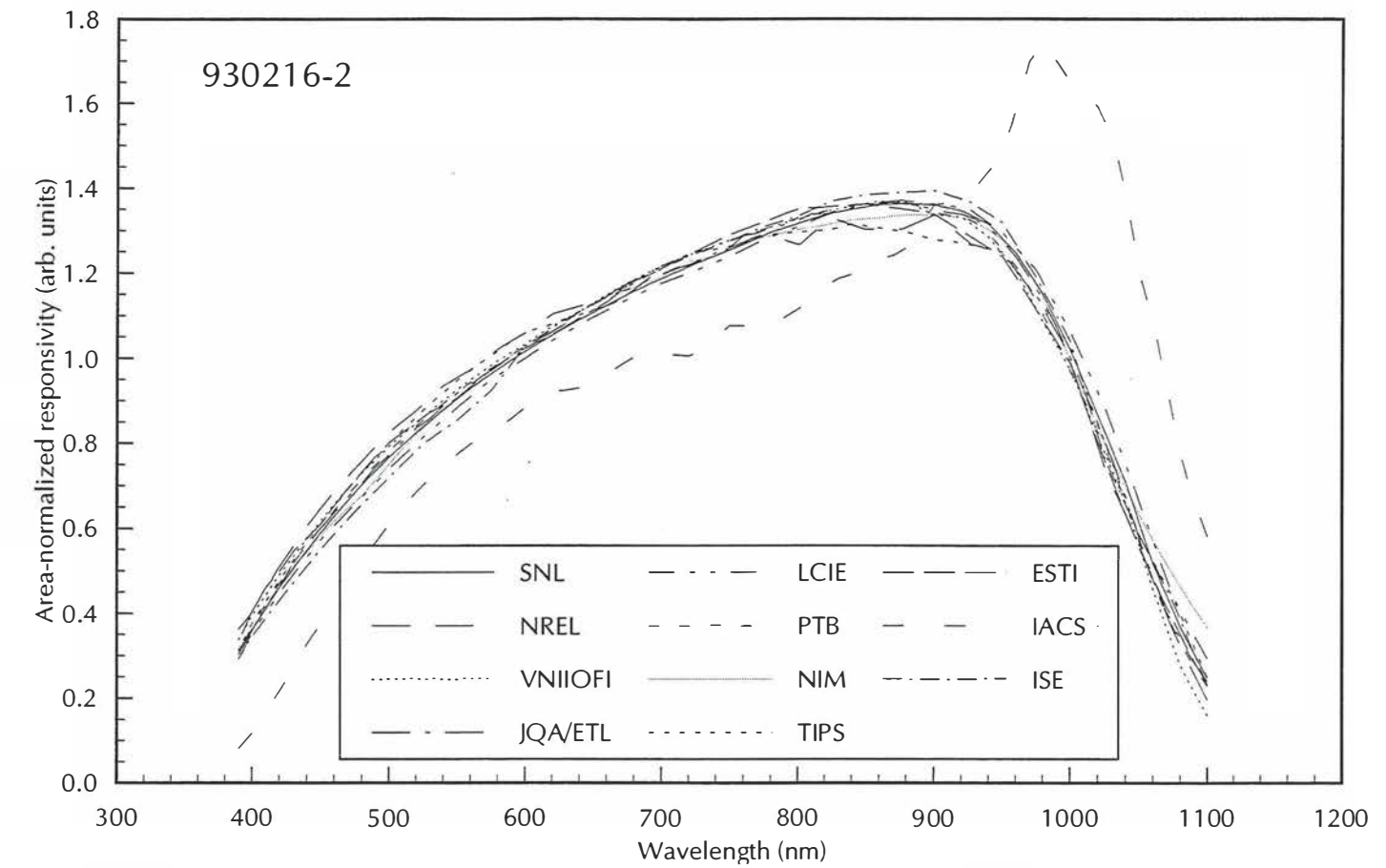


Figure 2-27. Area-normalized spectral responsivity and deviation from WPVS SR for 930216-2

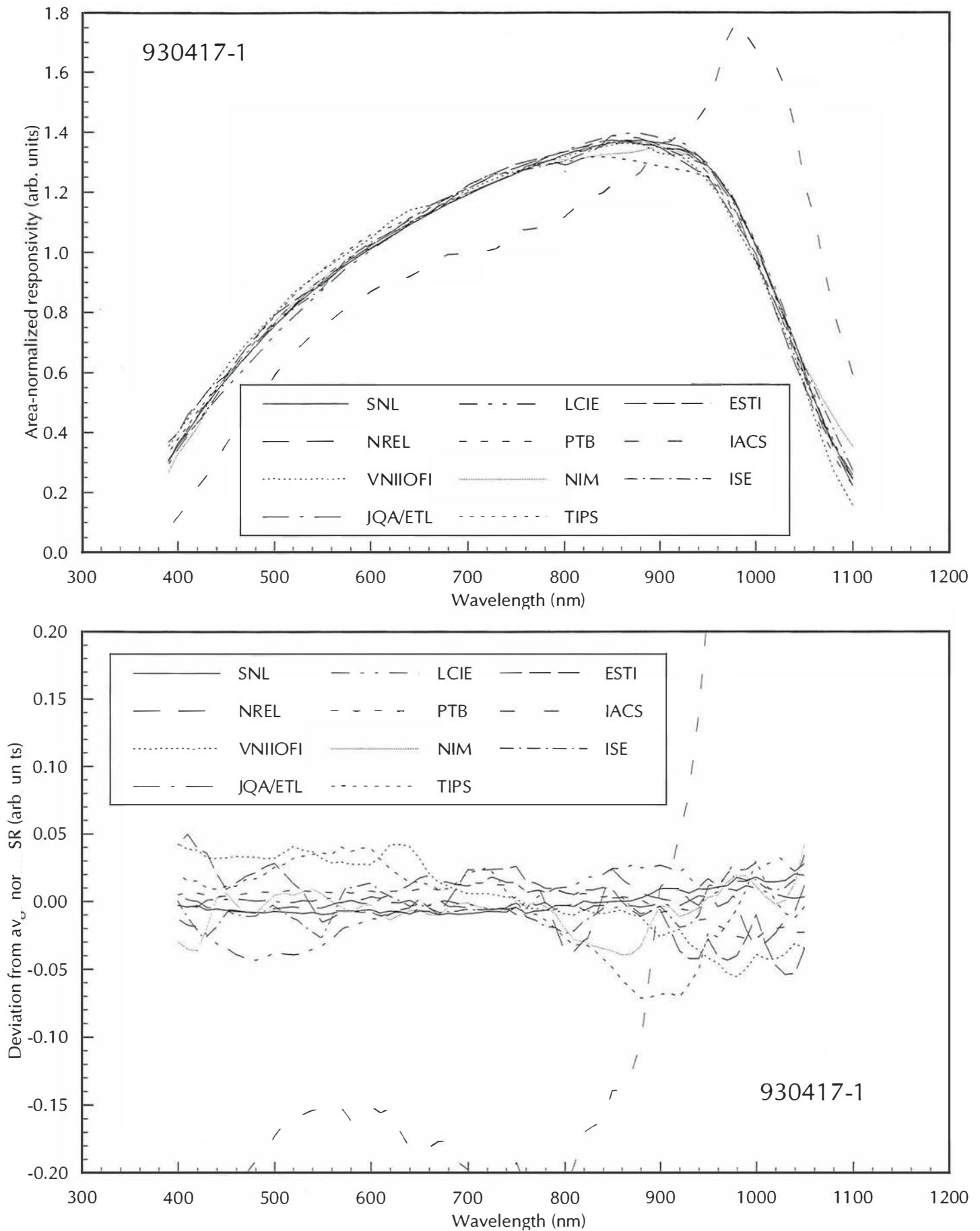


Figure 2-28. Area-normalized spectral responsivity and deviation from WPVS SR for 930417-1

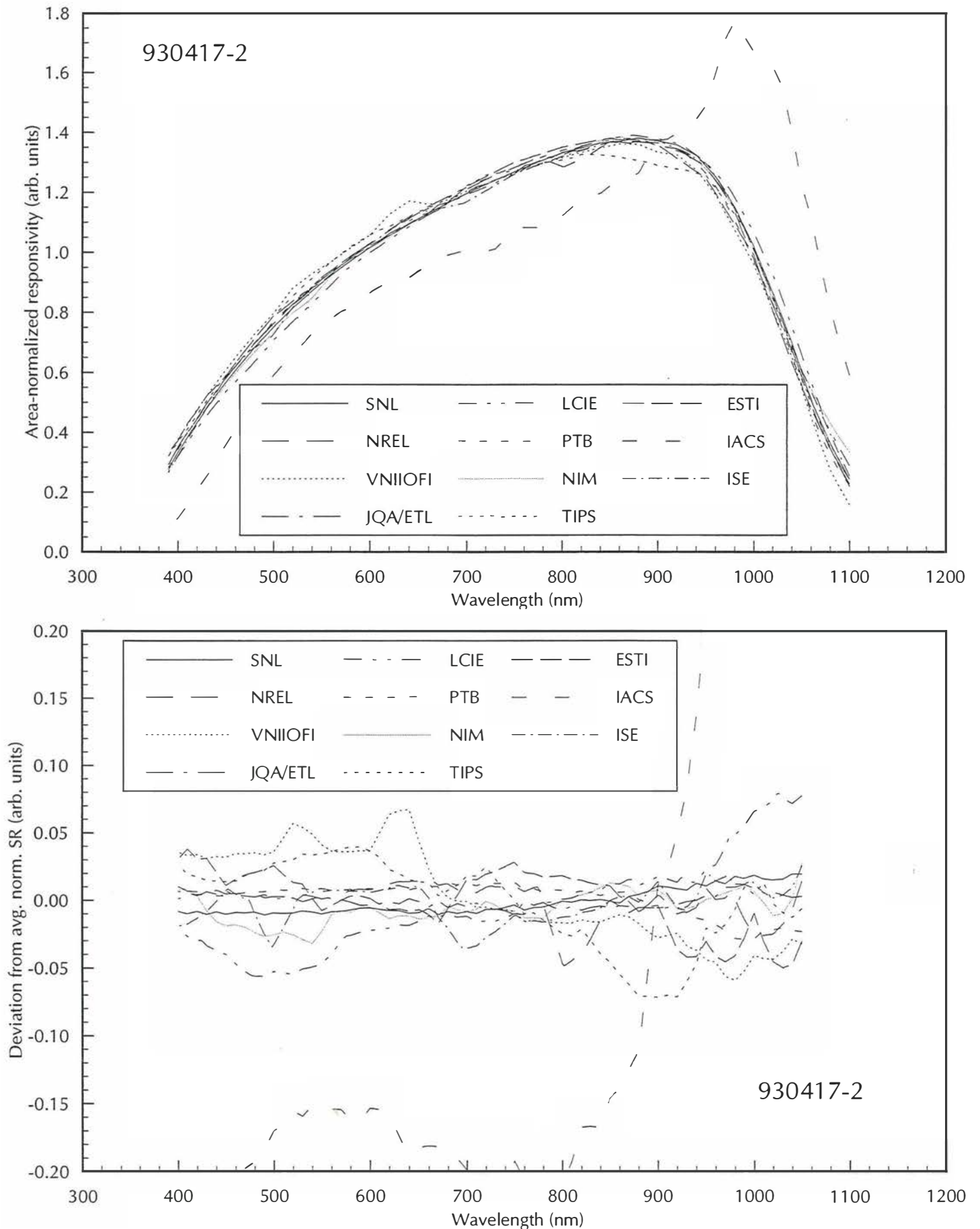


Figure 2-29. Area-normalized spectral responsivity and deviation from WPVS SR for 930417-2

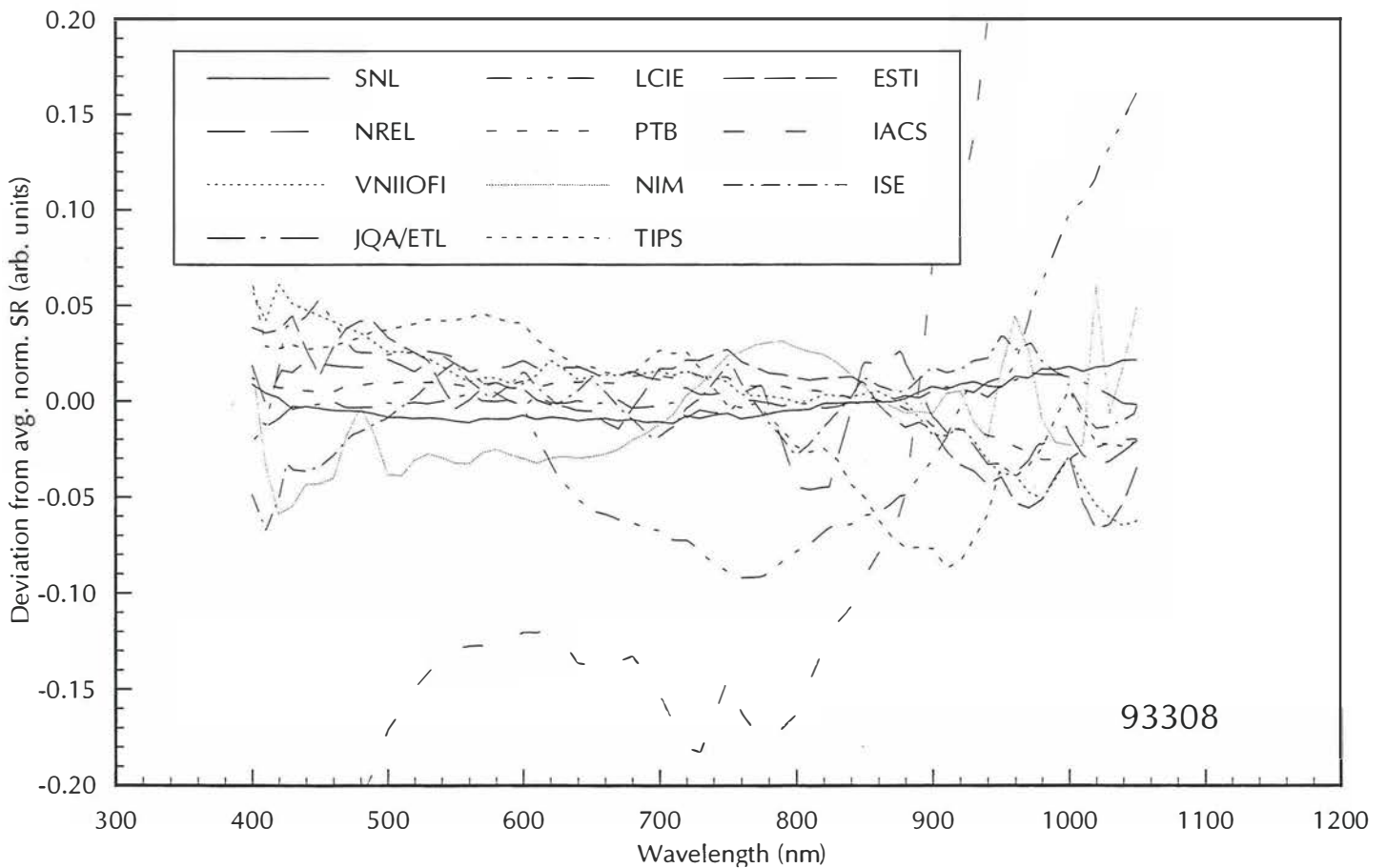
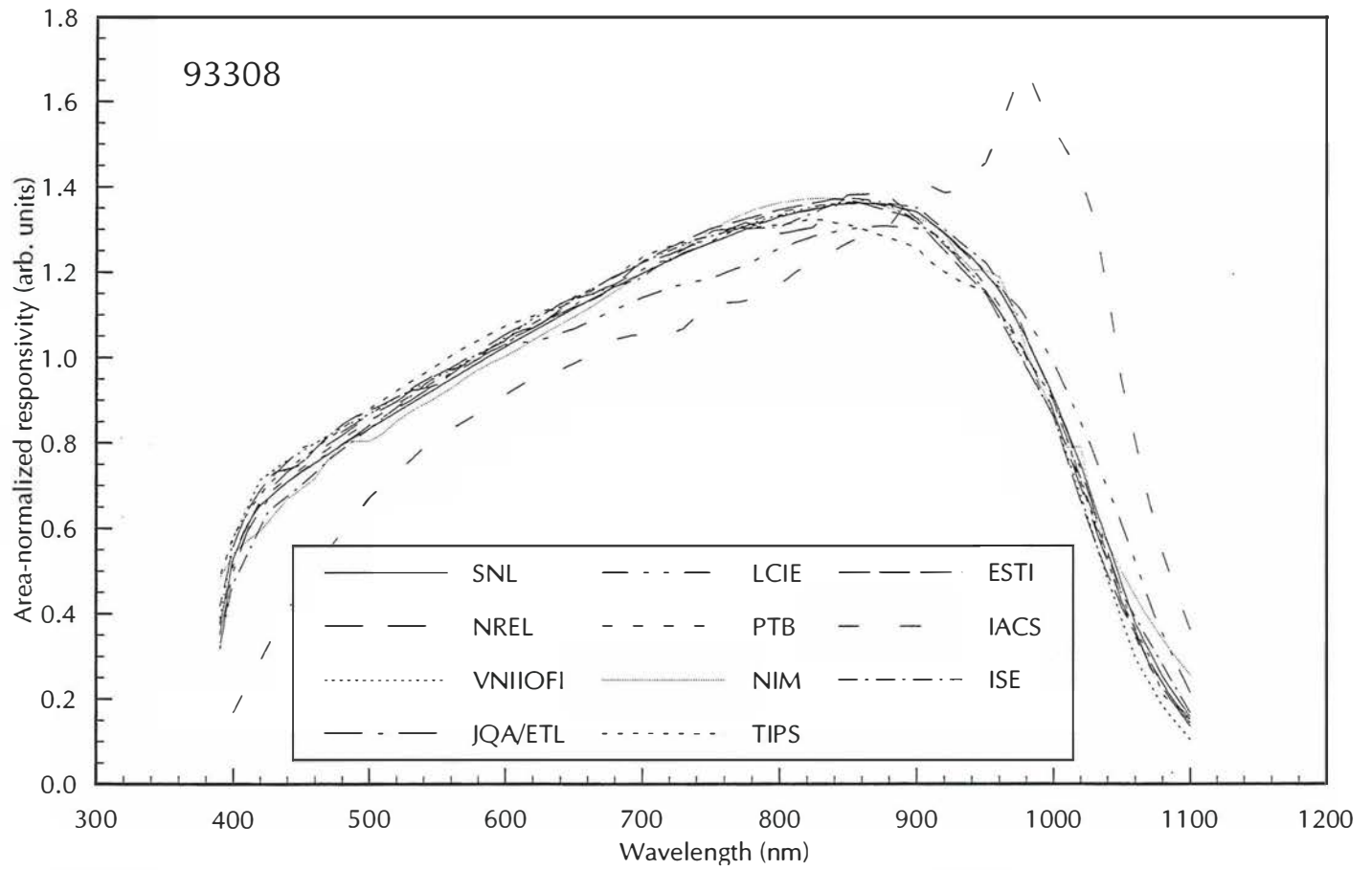


Figure 2-30. Area-normalized spectral responsivity and deviation from WPVS SR for 93308

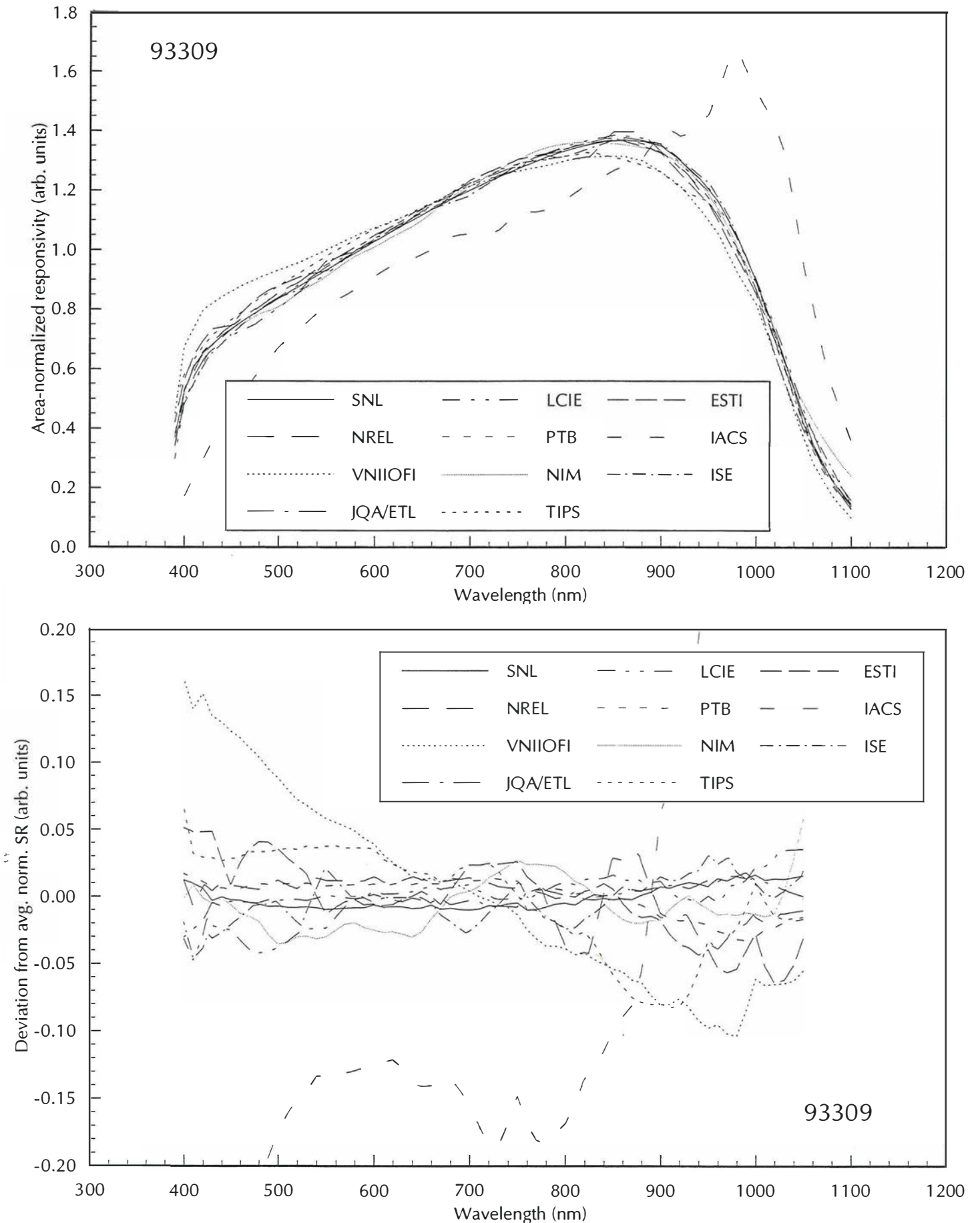


Figure 2-31. Area-normalized spectral responsivity and deviation from WPVS SR for 93309

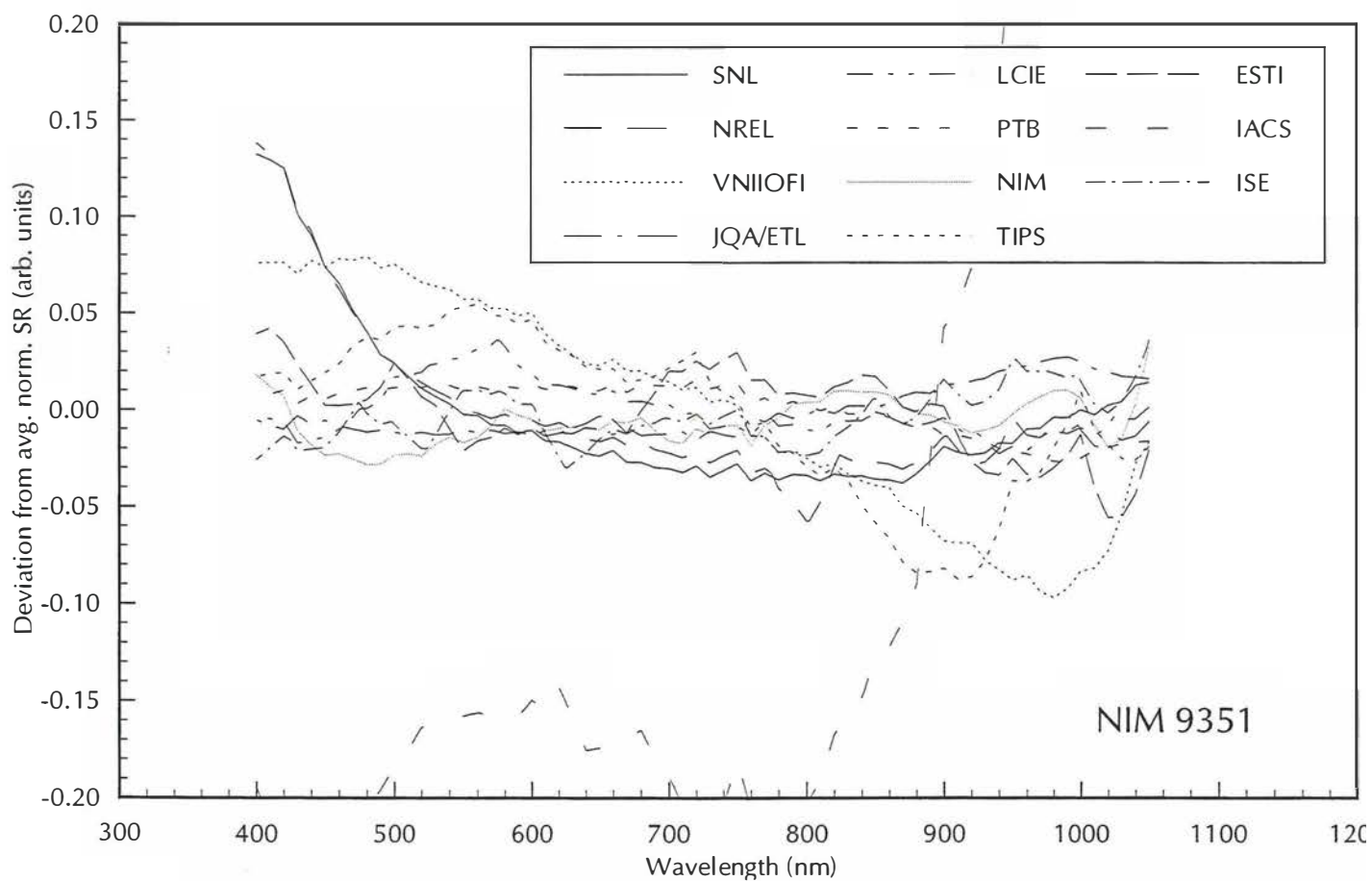
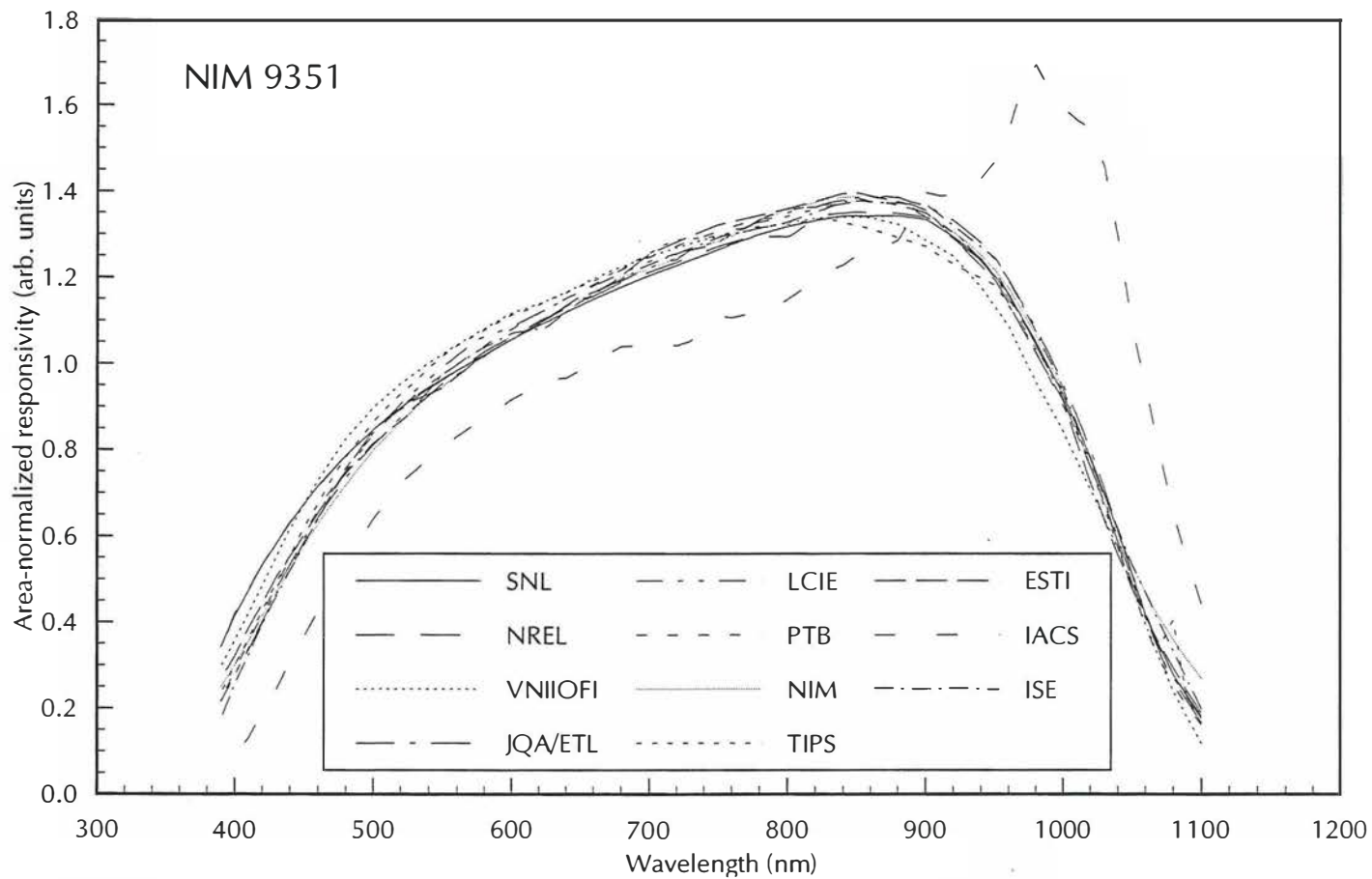


Figure 2-32. Area-normalized spectral responsivity and deviation from WPVS SR for NIM 9351

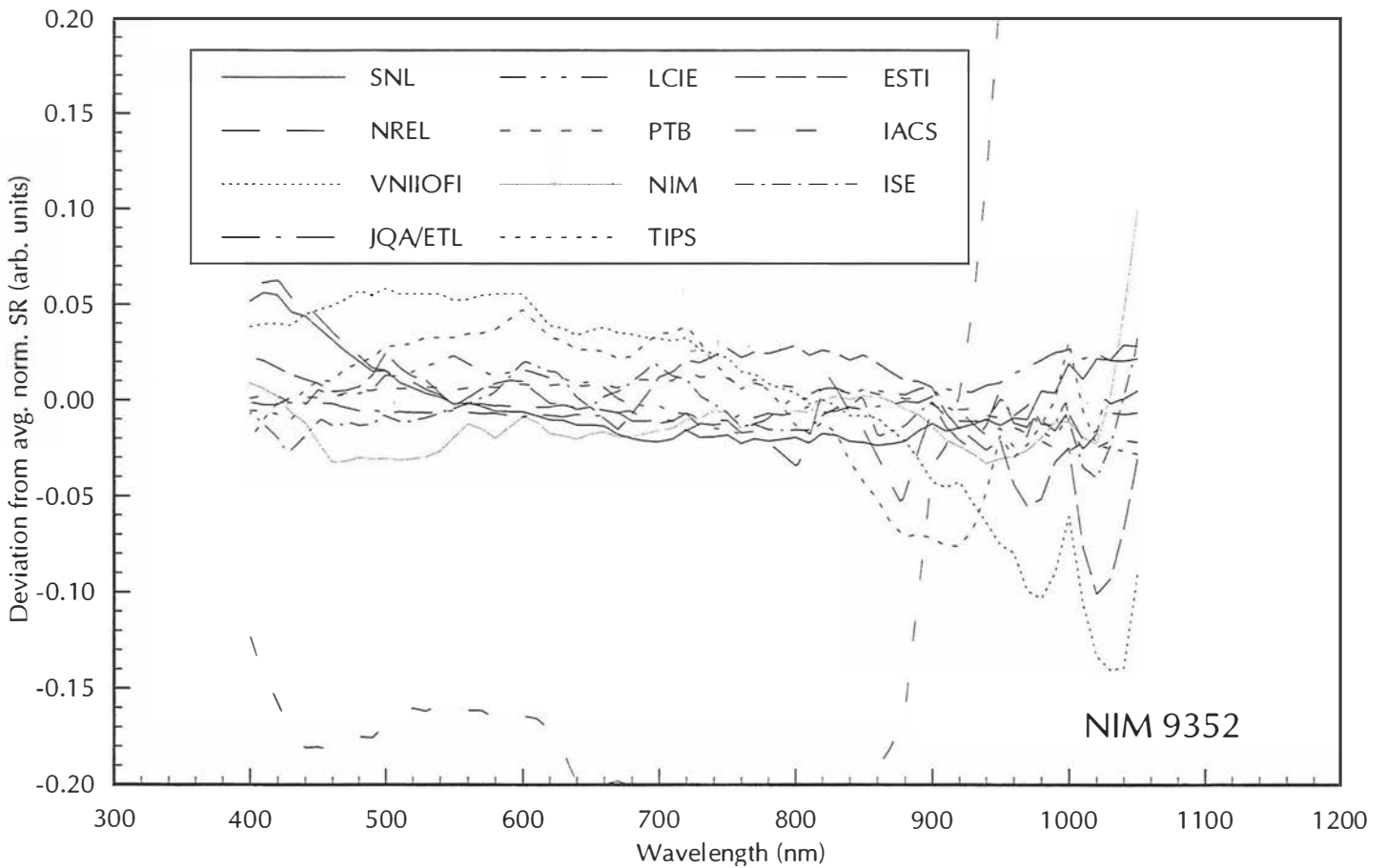
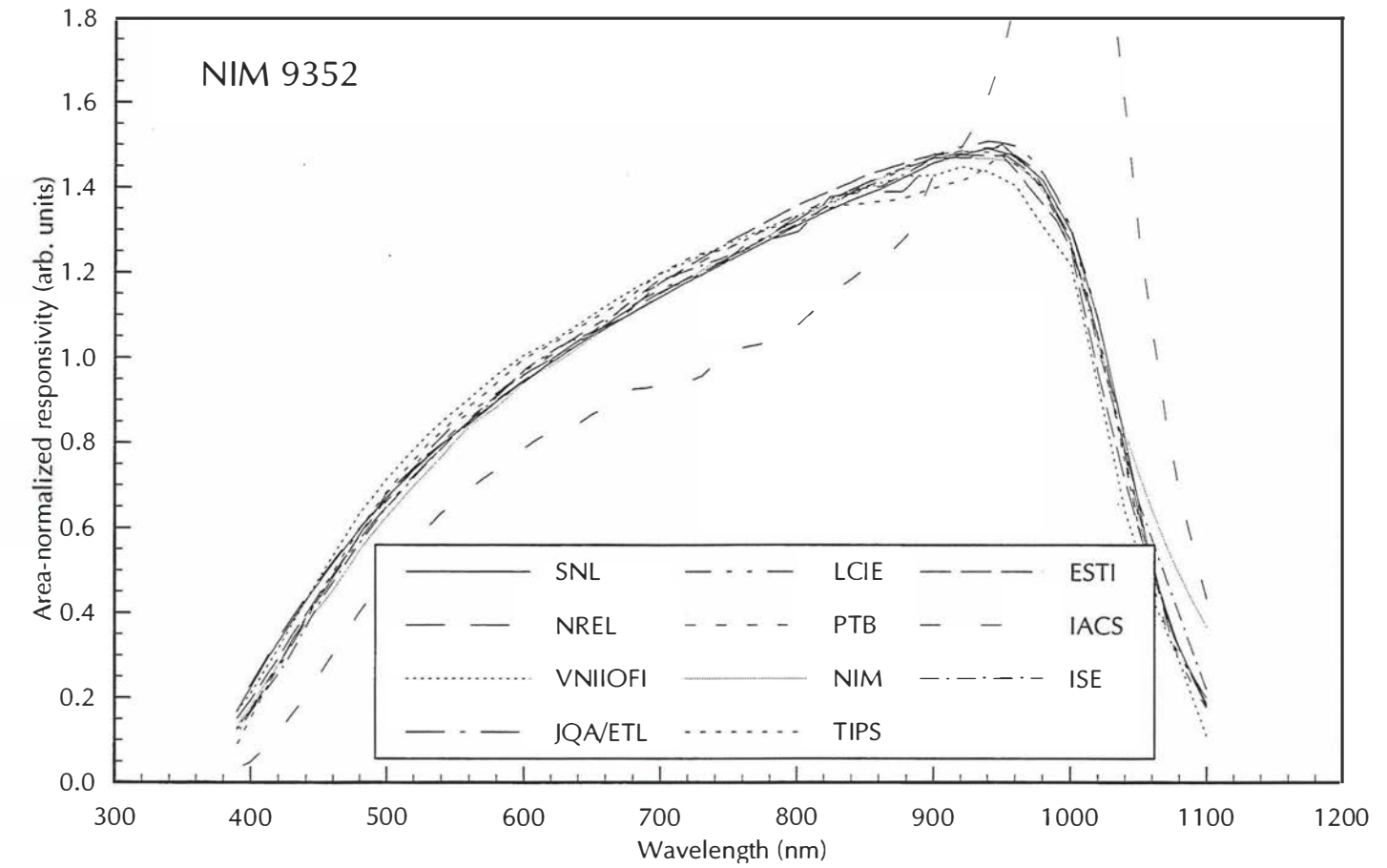


Figure 2-33. Area-normalized spectral responsivity and deviation from WPVS SR for NIM 9352

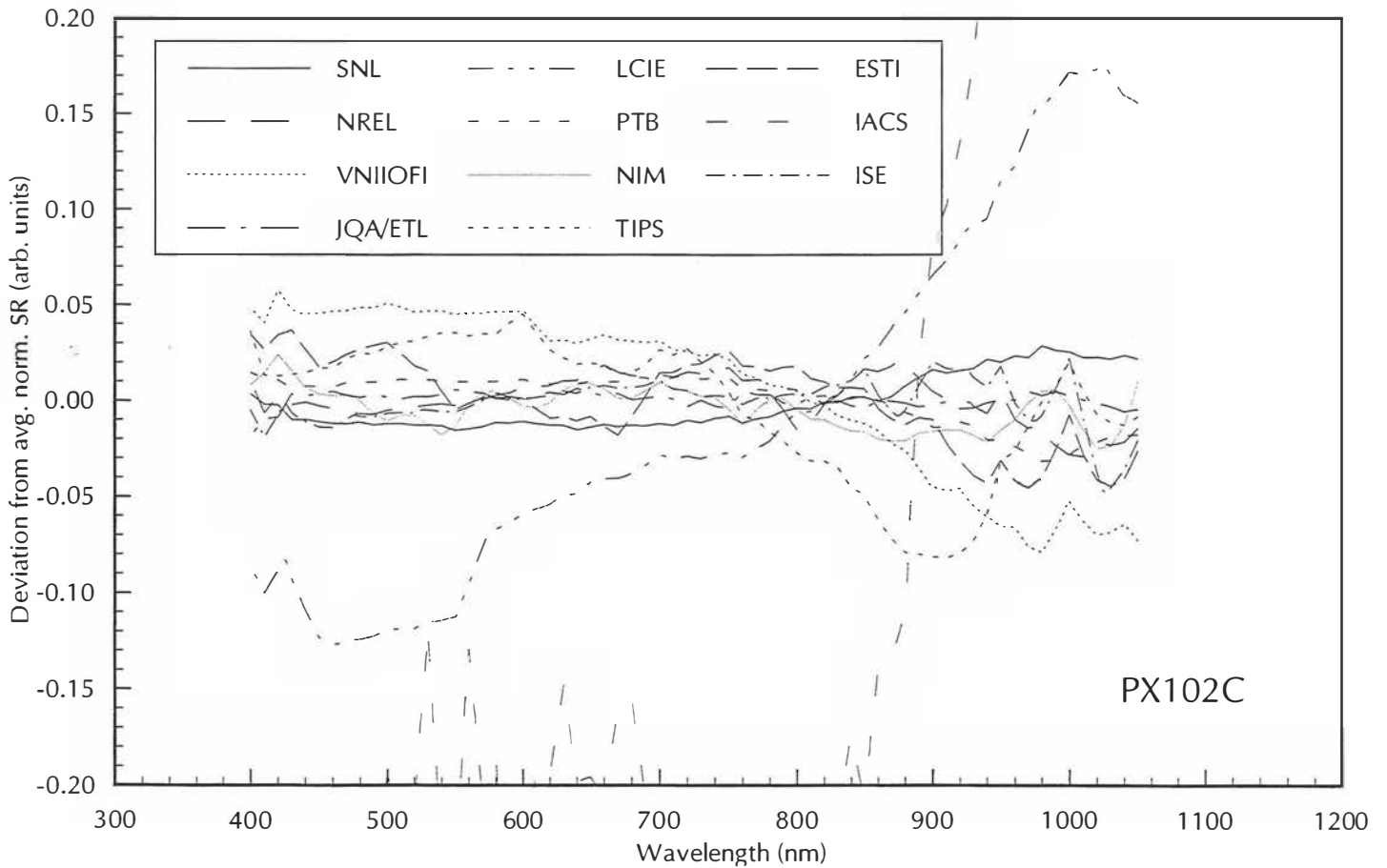
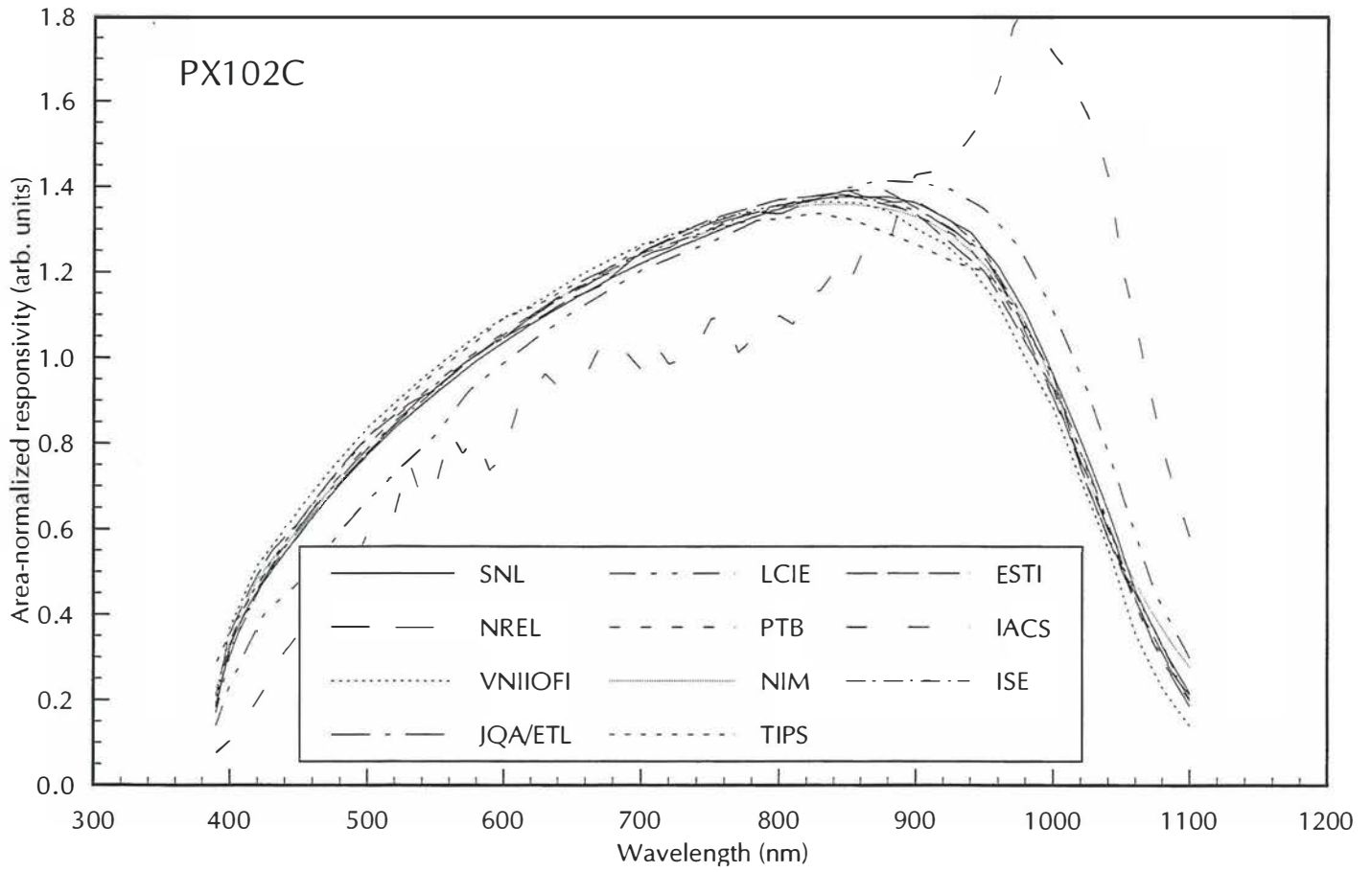


Figure 2-34. Area-normalized spectral responsivity and deviation from WPVS SR for PX102C

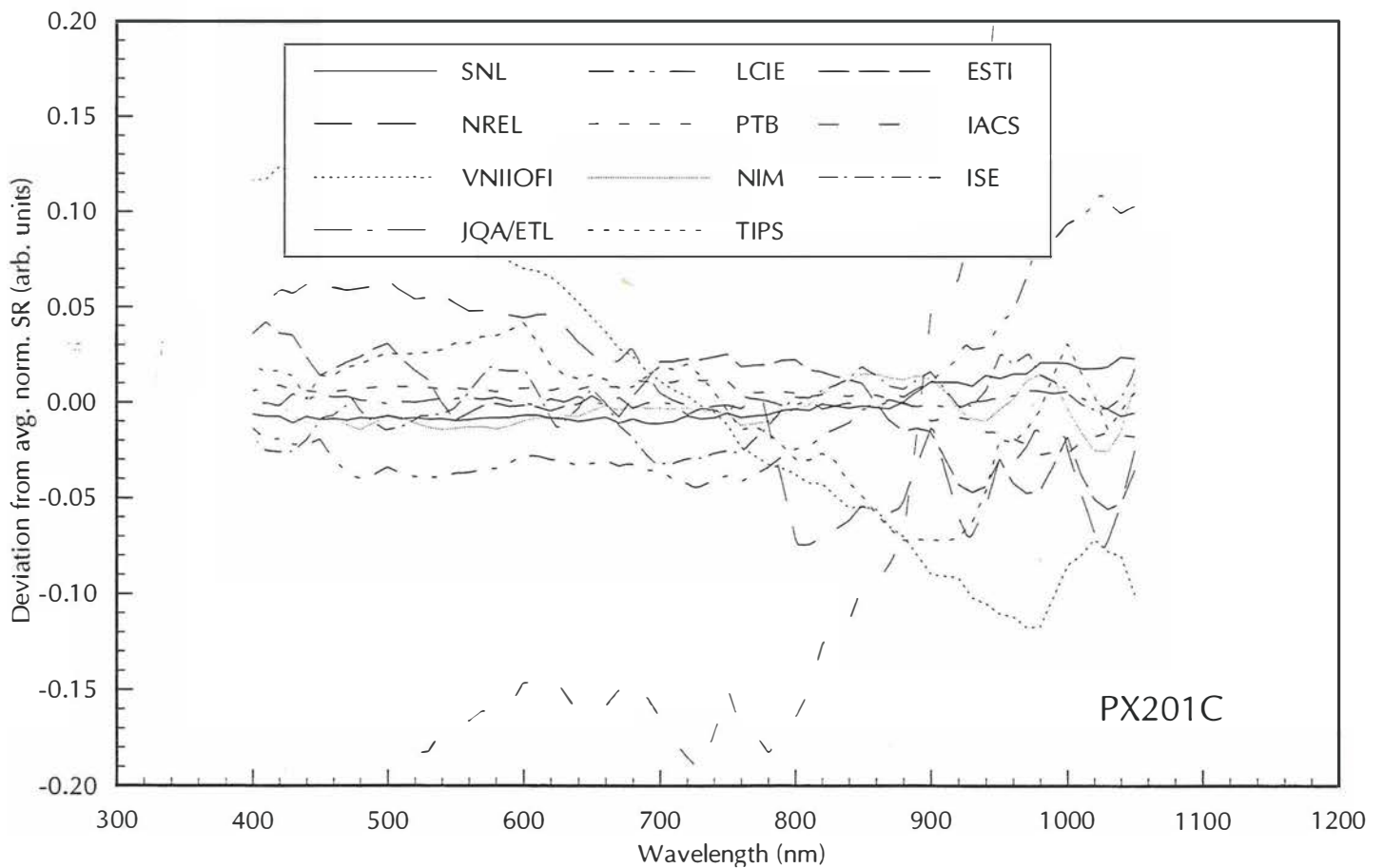
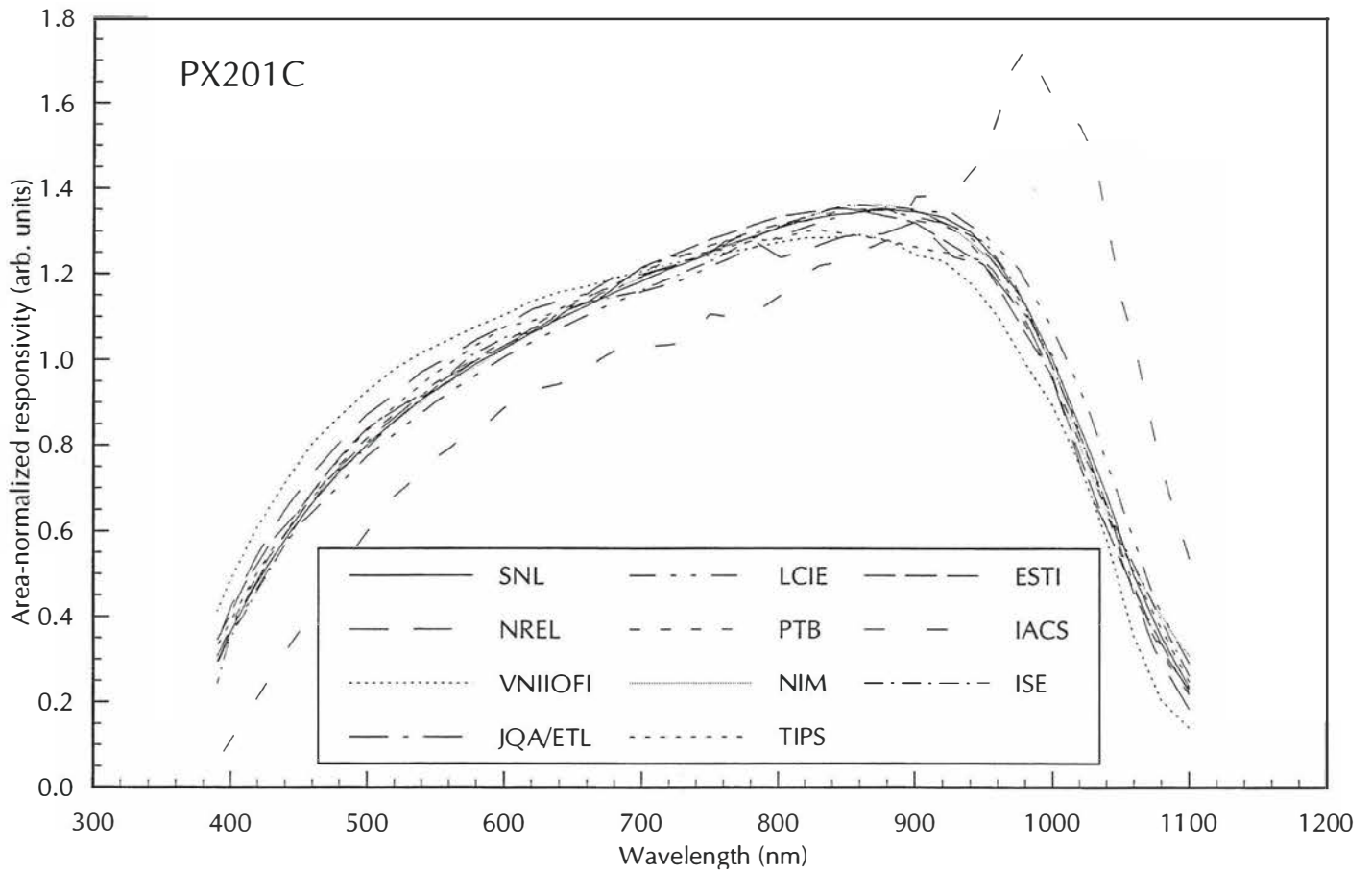


Figure 2-35. Area-normalized spectral responsivity and deviation from WPVS SR for PX201C

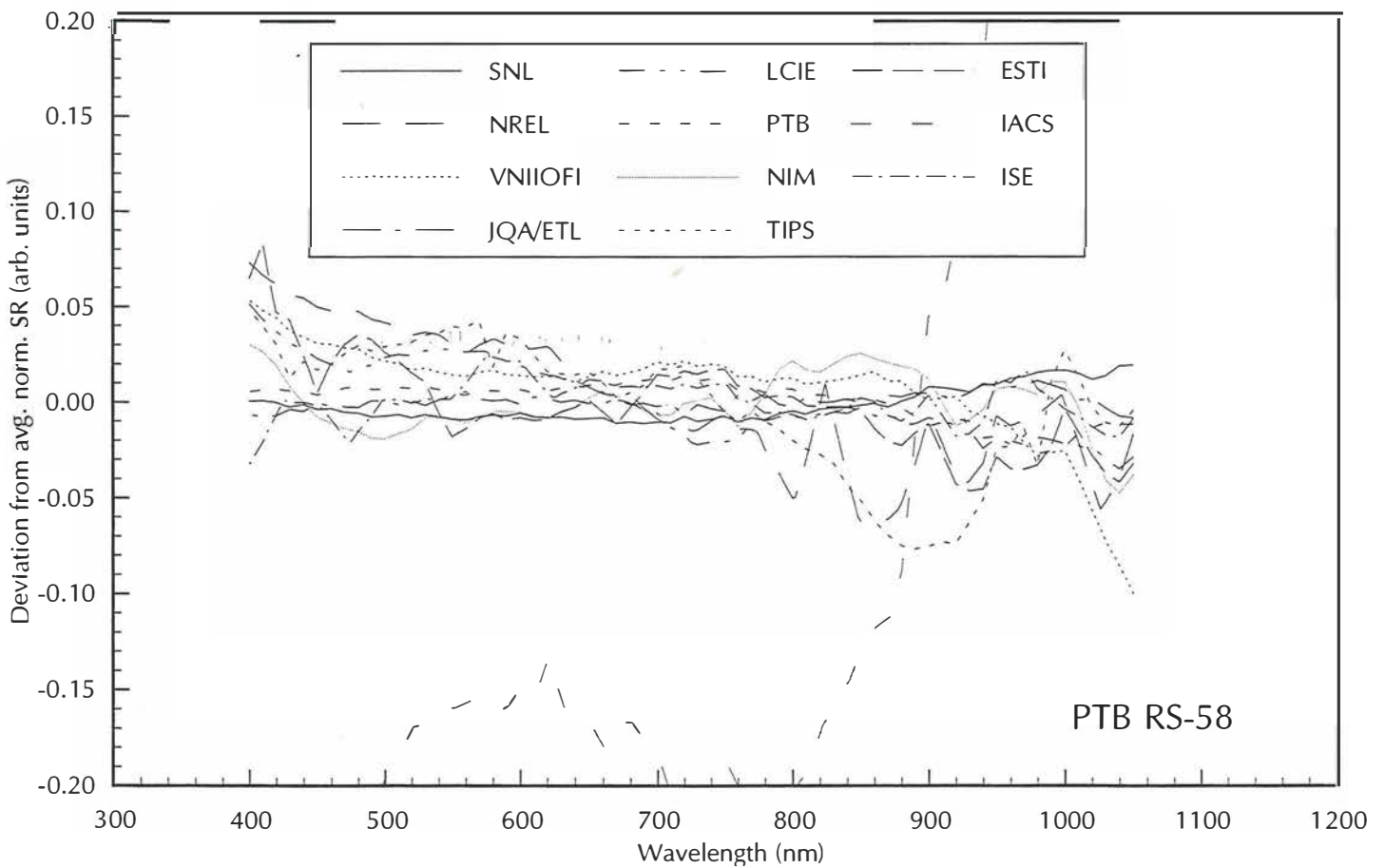
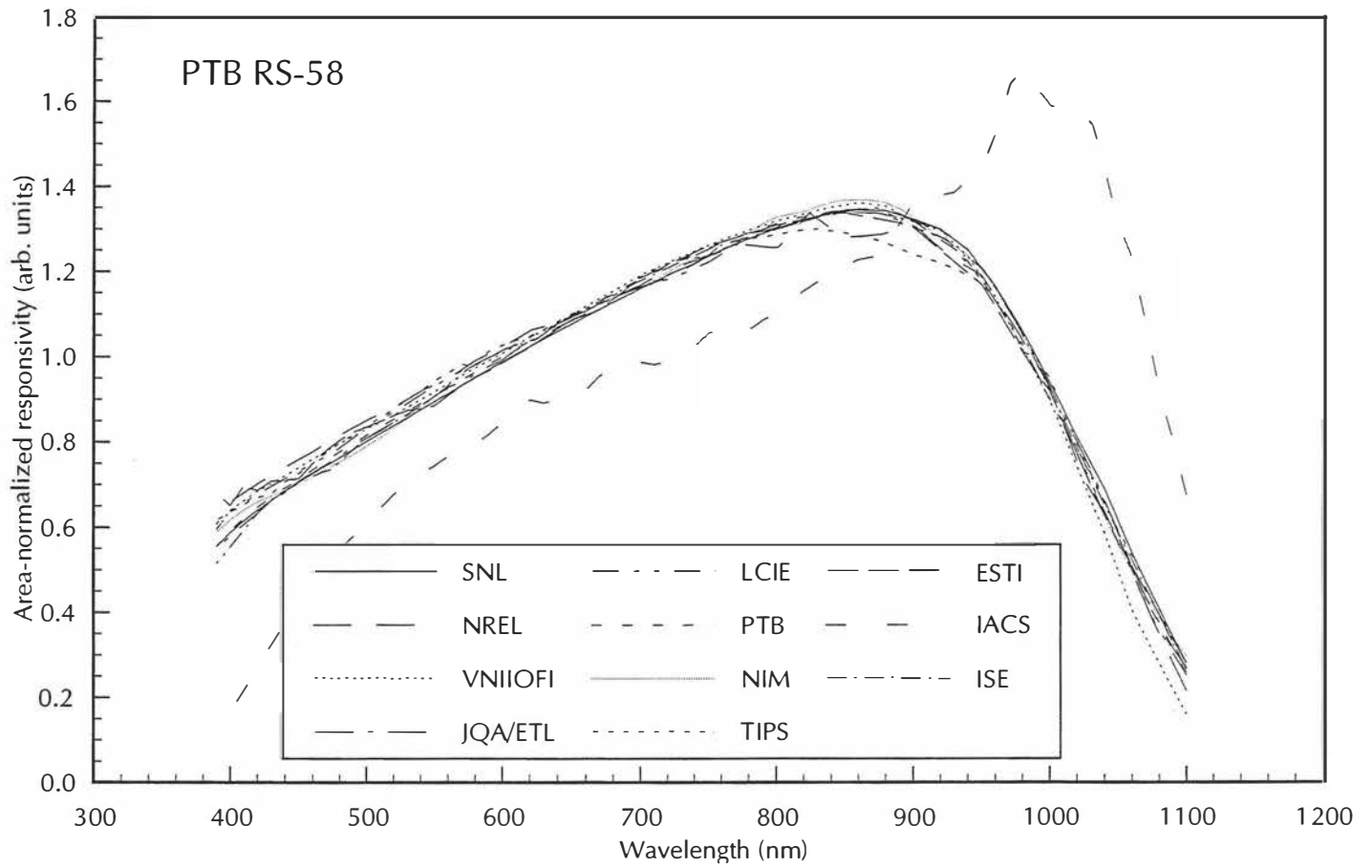


Figure 2-36. Area-normalized spectral responsivity and deviation from WPVS SR for PTB RS-58

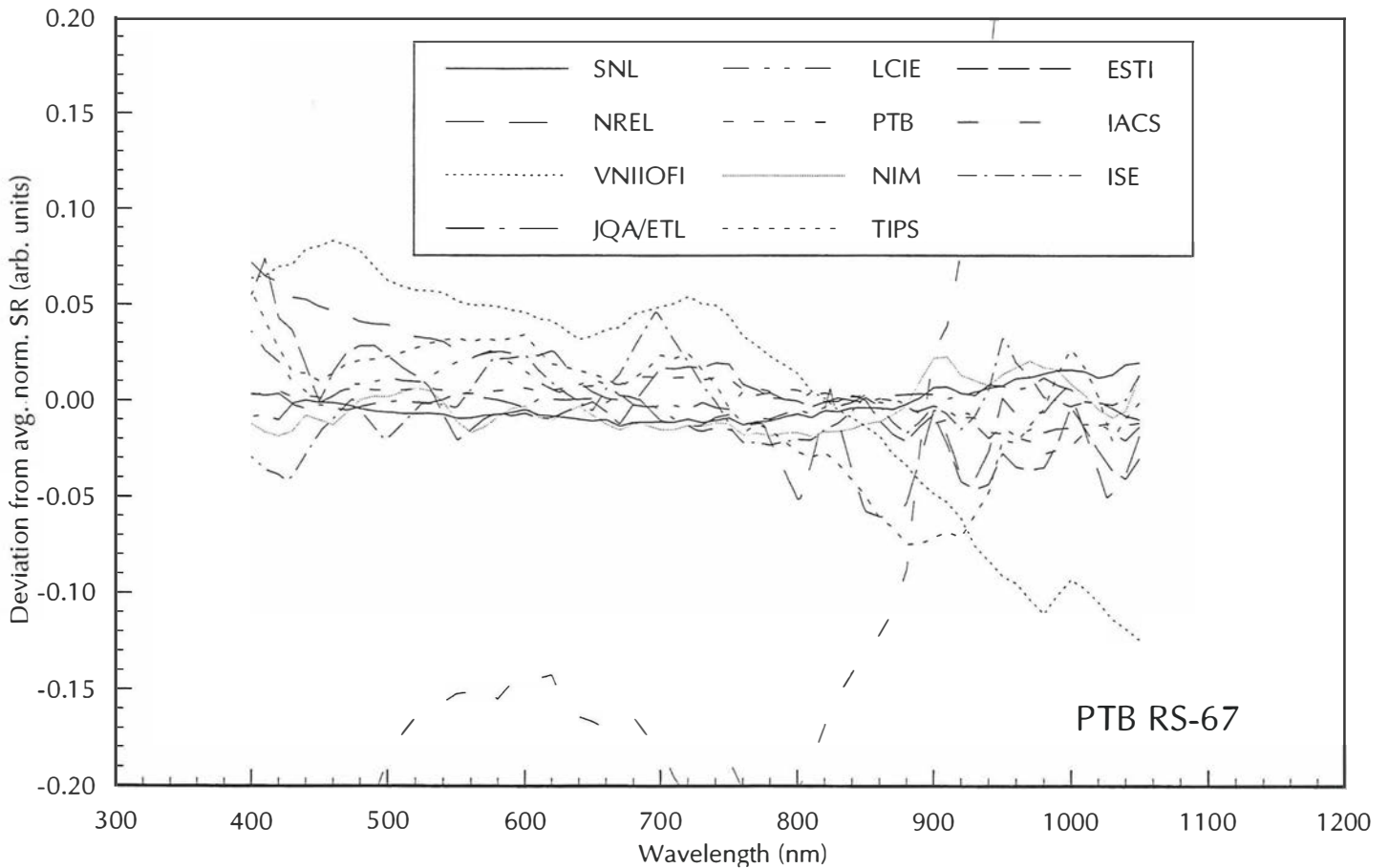
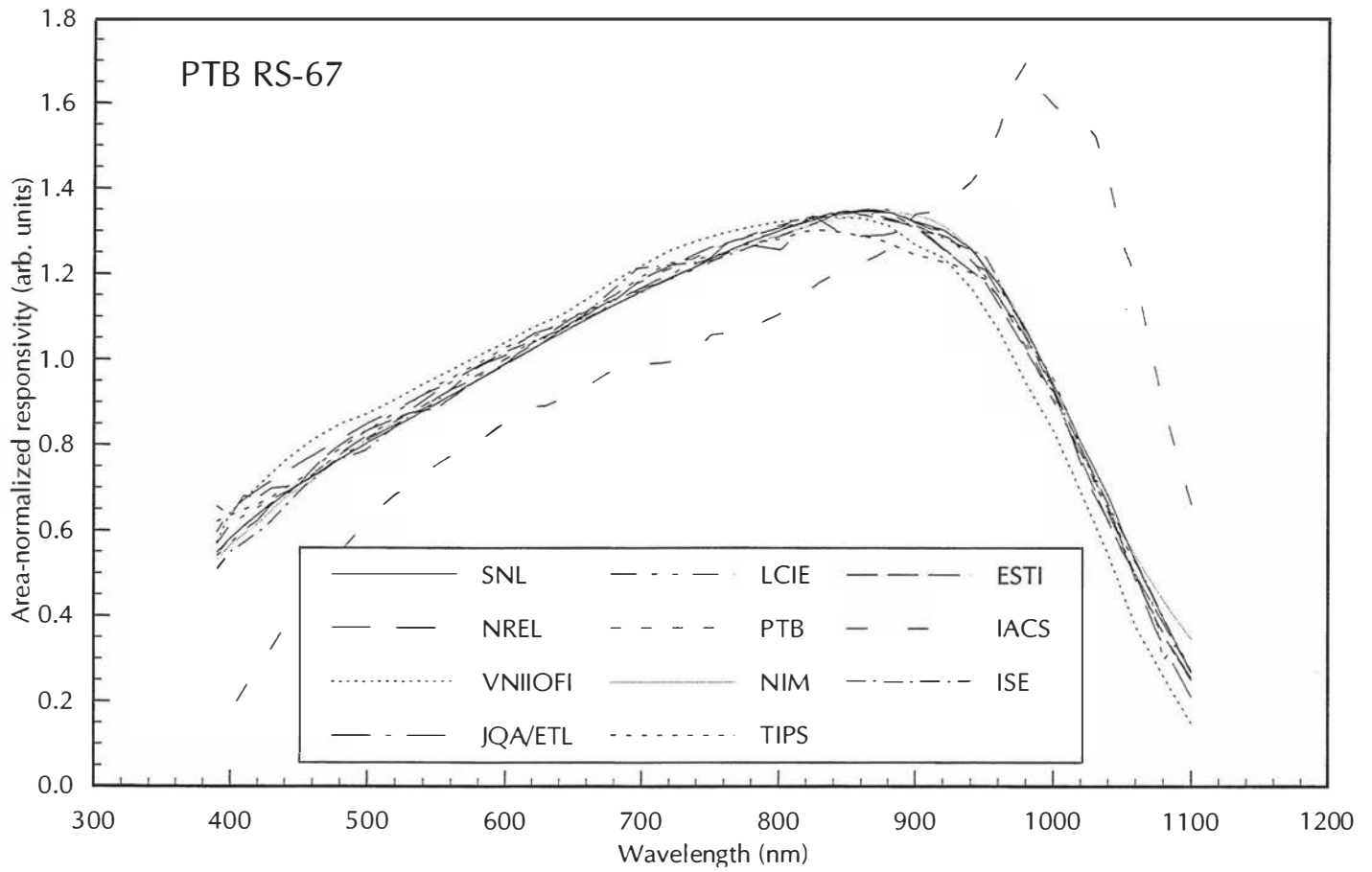


Figure 2-37. Area-normalized spectral responsivity and deviation from WPVS SR for PTB RS-67

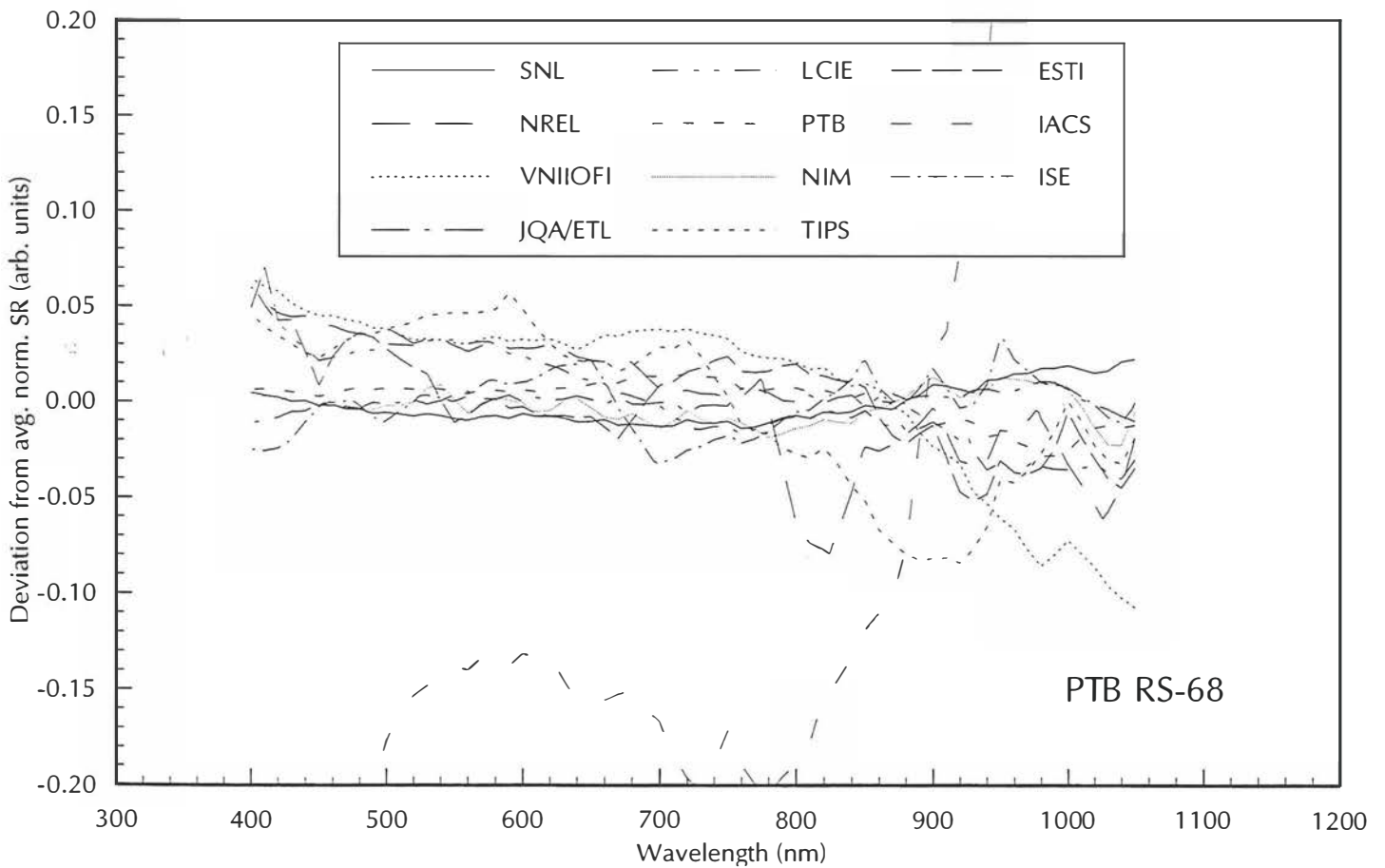
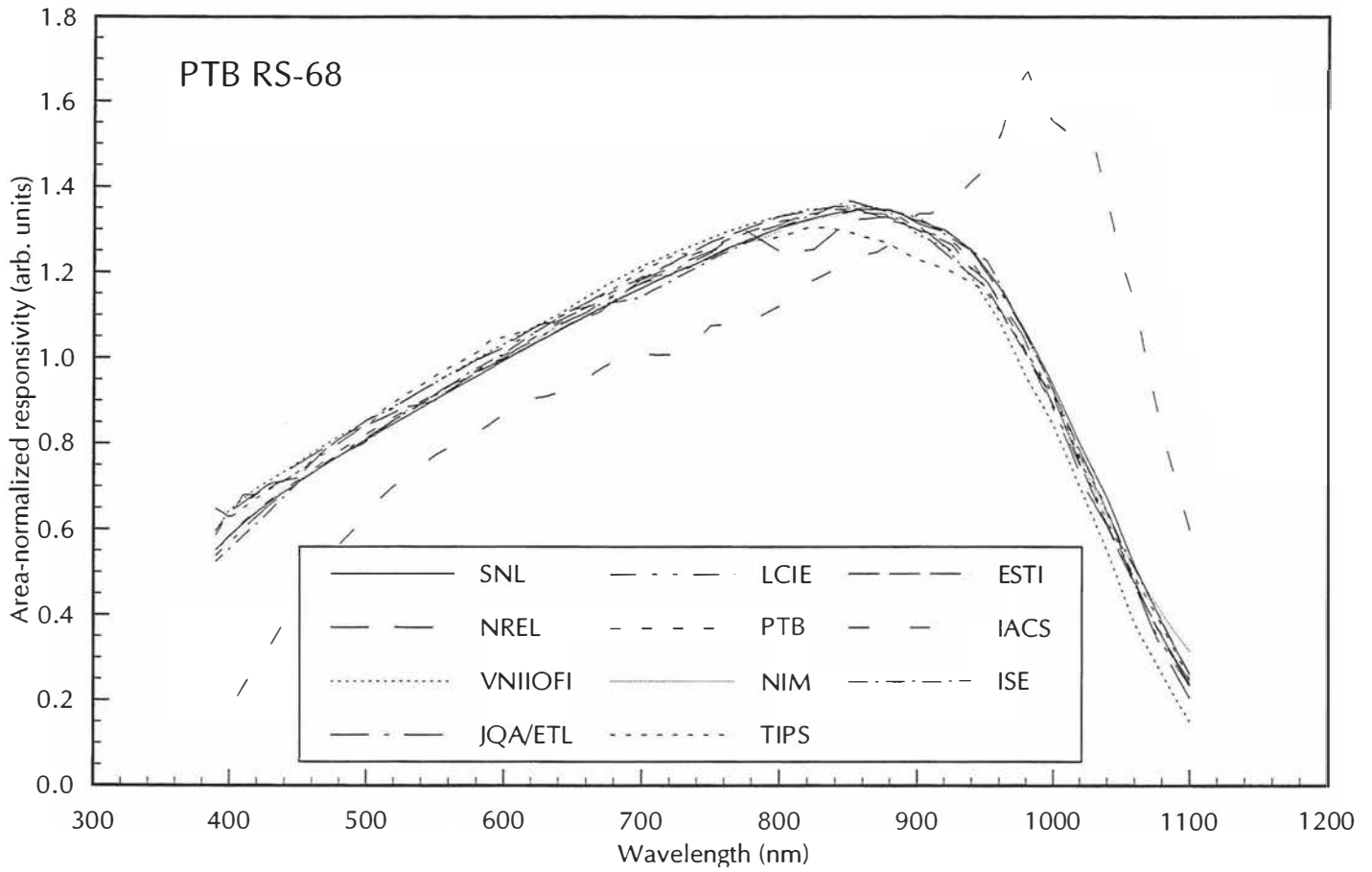


Figure 2-38. Area-normalized spectral responsivity and deviation from WPVS SR for PTB RS-68

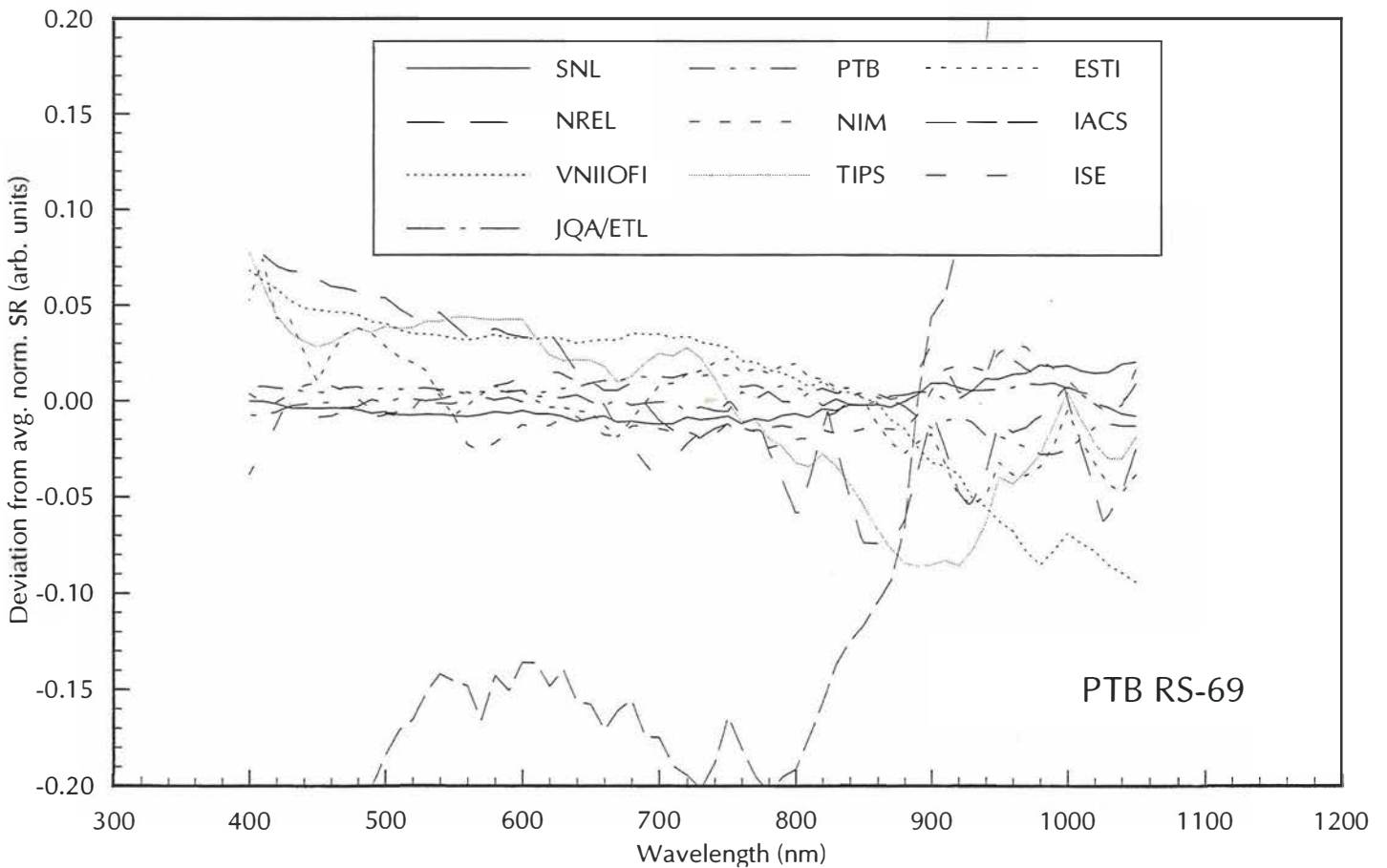
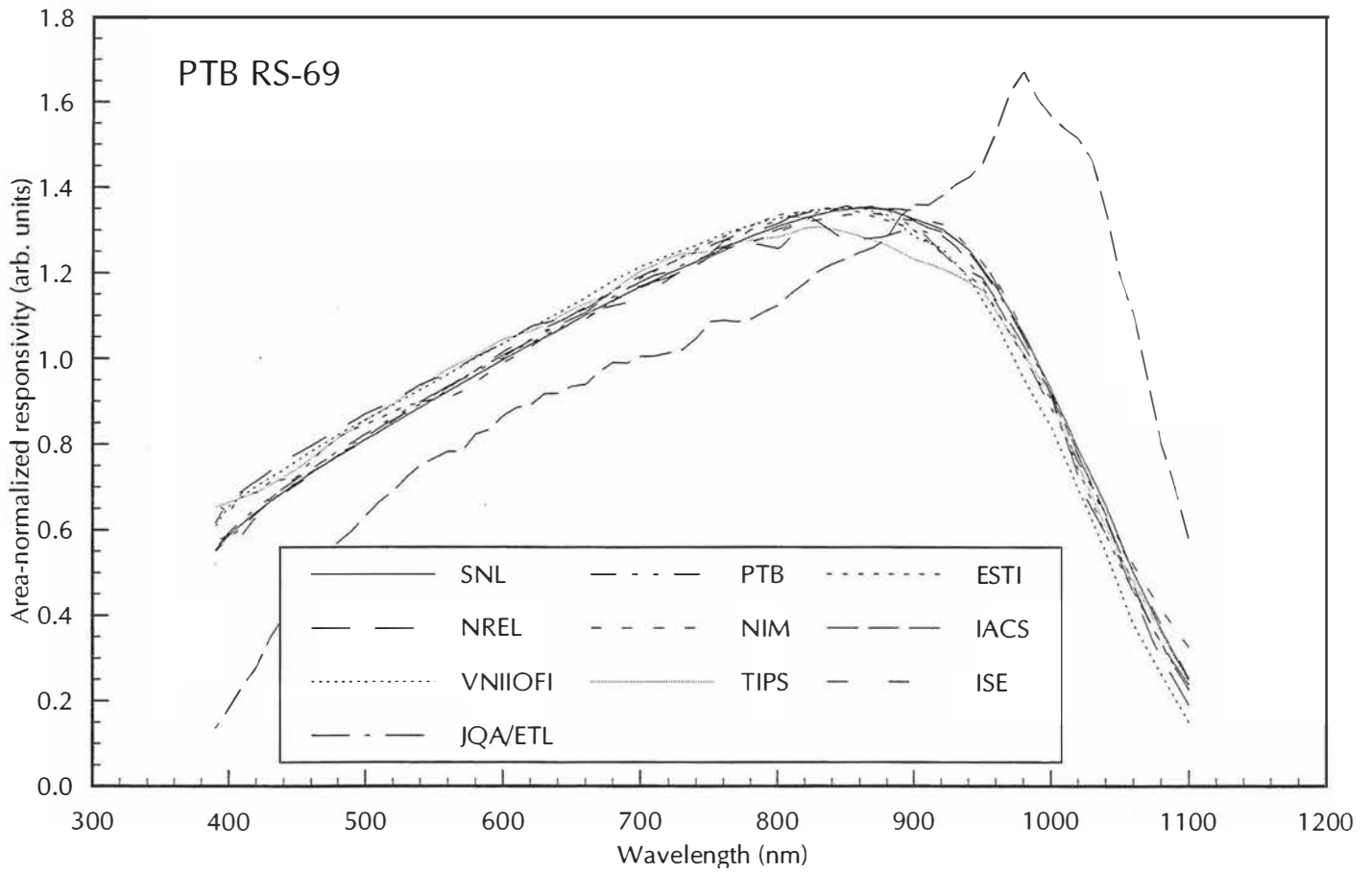


Figure 2-39. Area-normalized spectral responsivity and deviation from WPVS SR for PTB RS-69

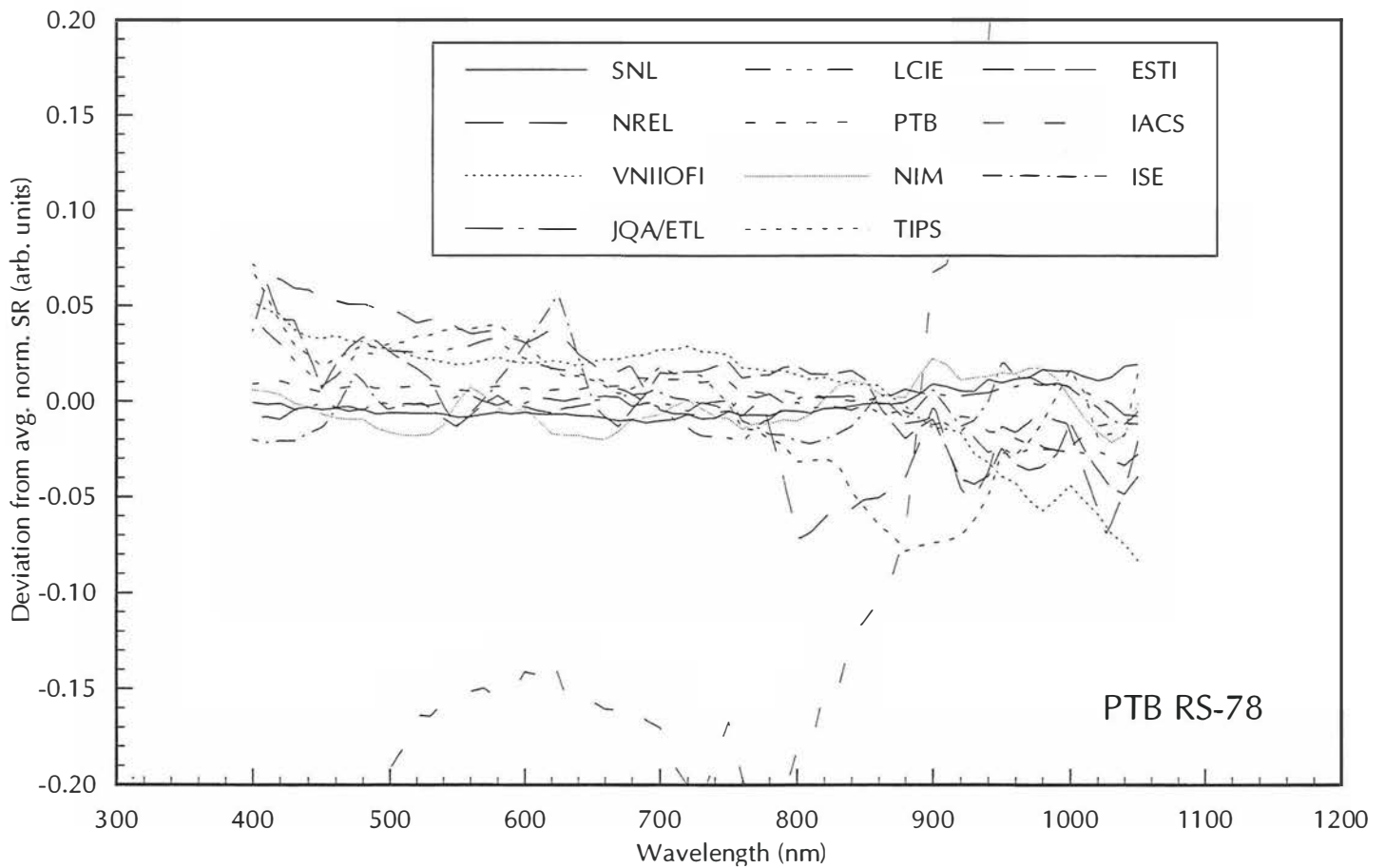
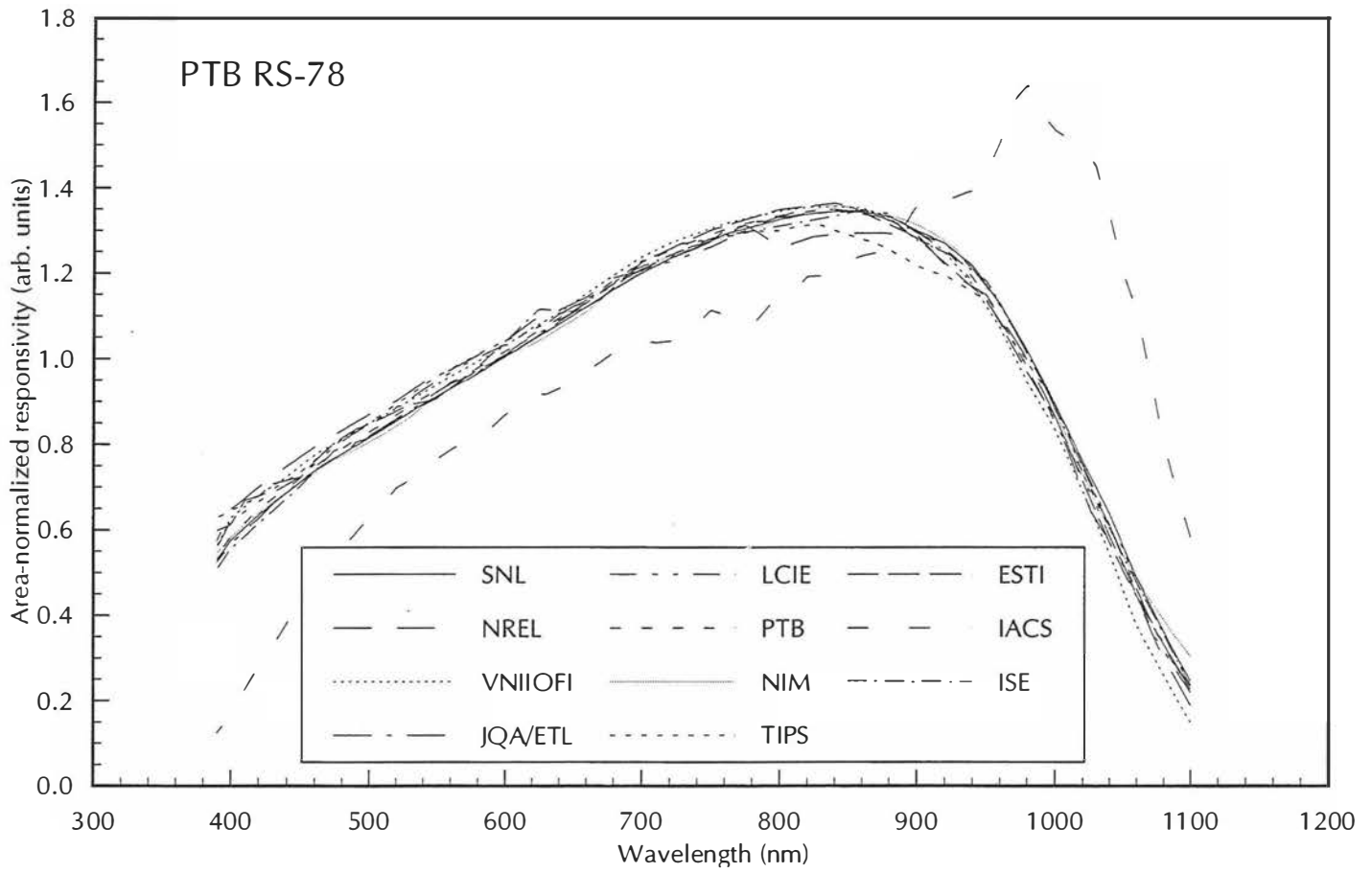


Figure 2-40. Area-normalized spectral responsivity and deviation from WPVS SR for PTB RS-78

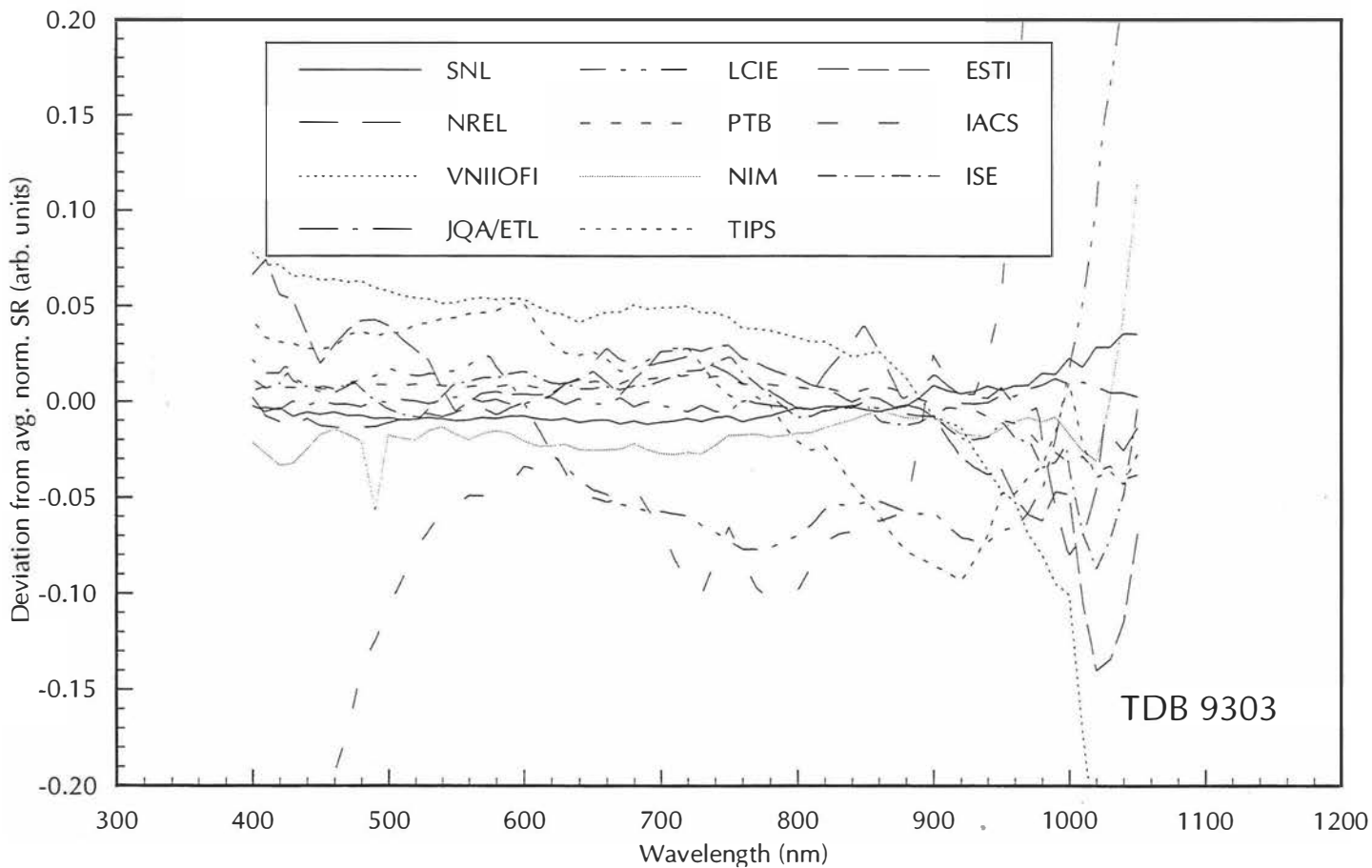
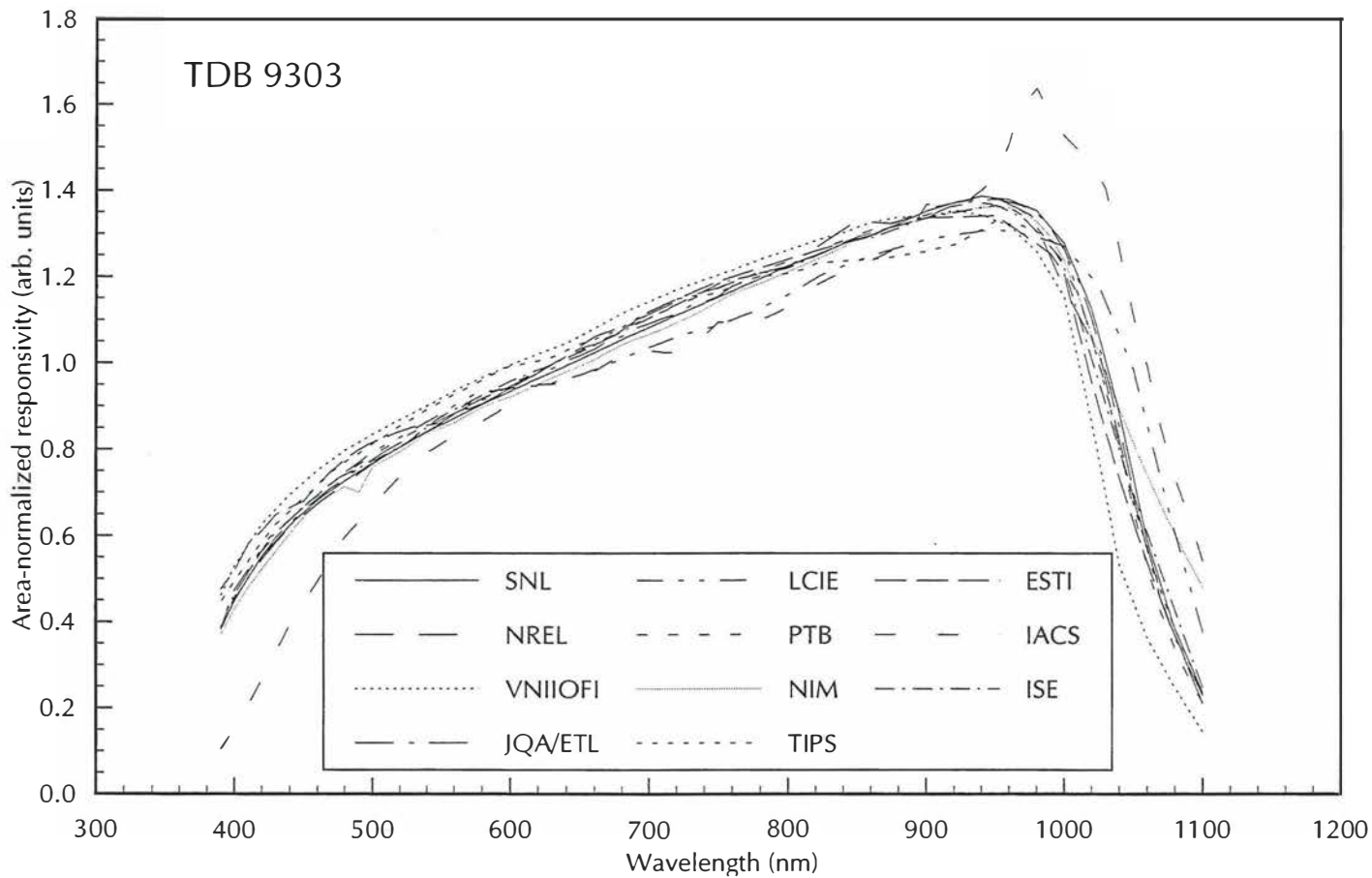


Figure 2-41. Area-normalized spectral responsivity and deviation from WPVS SR for TDB 9303

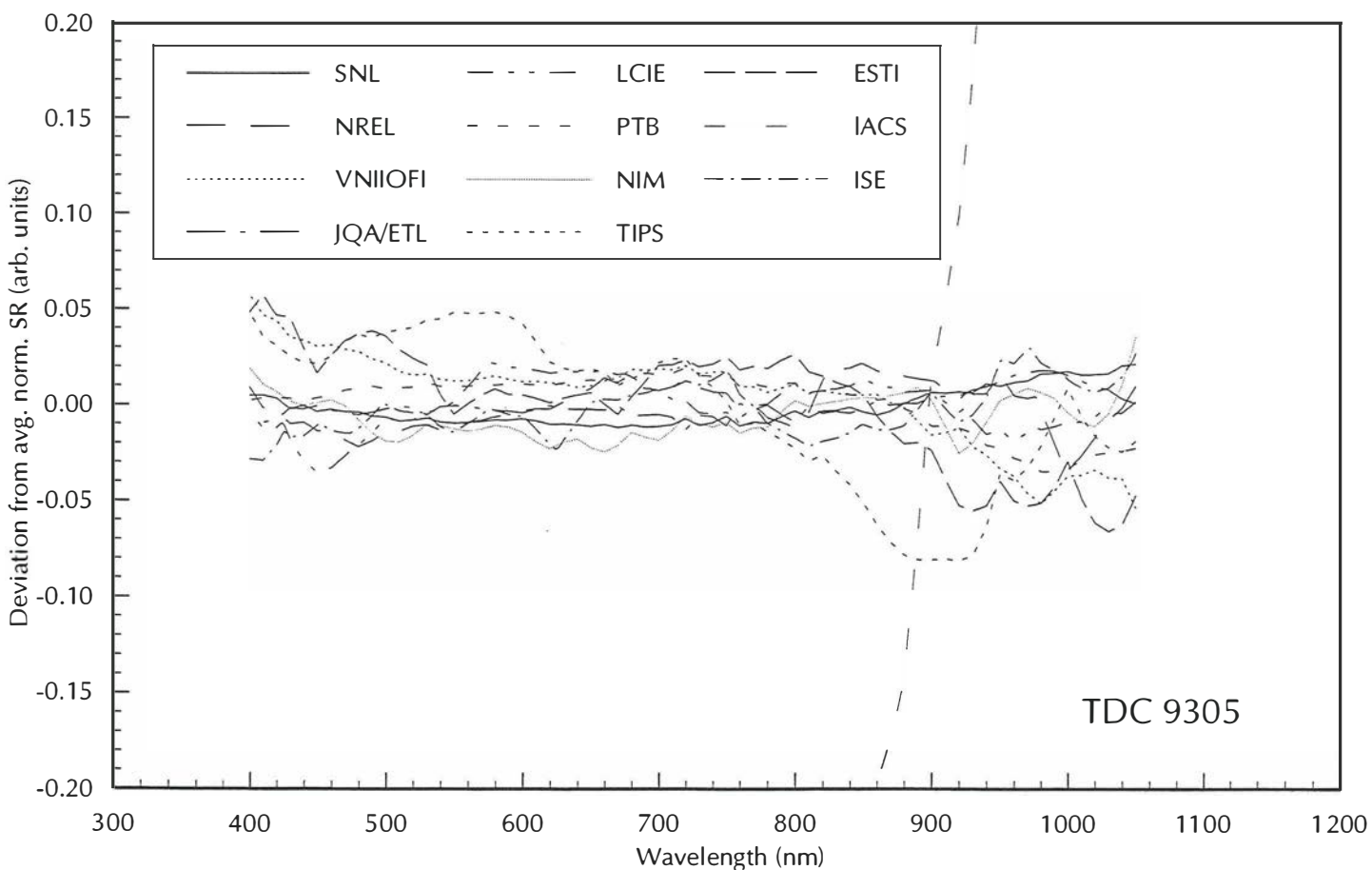
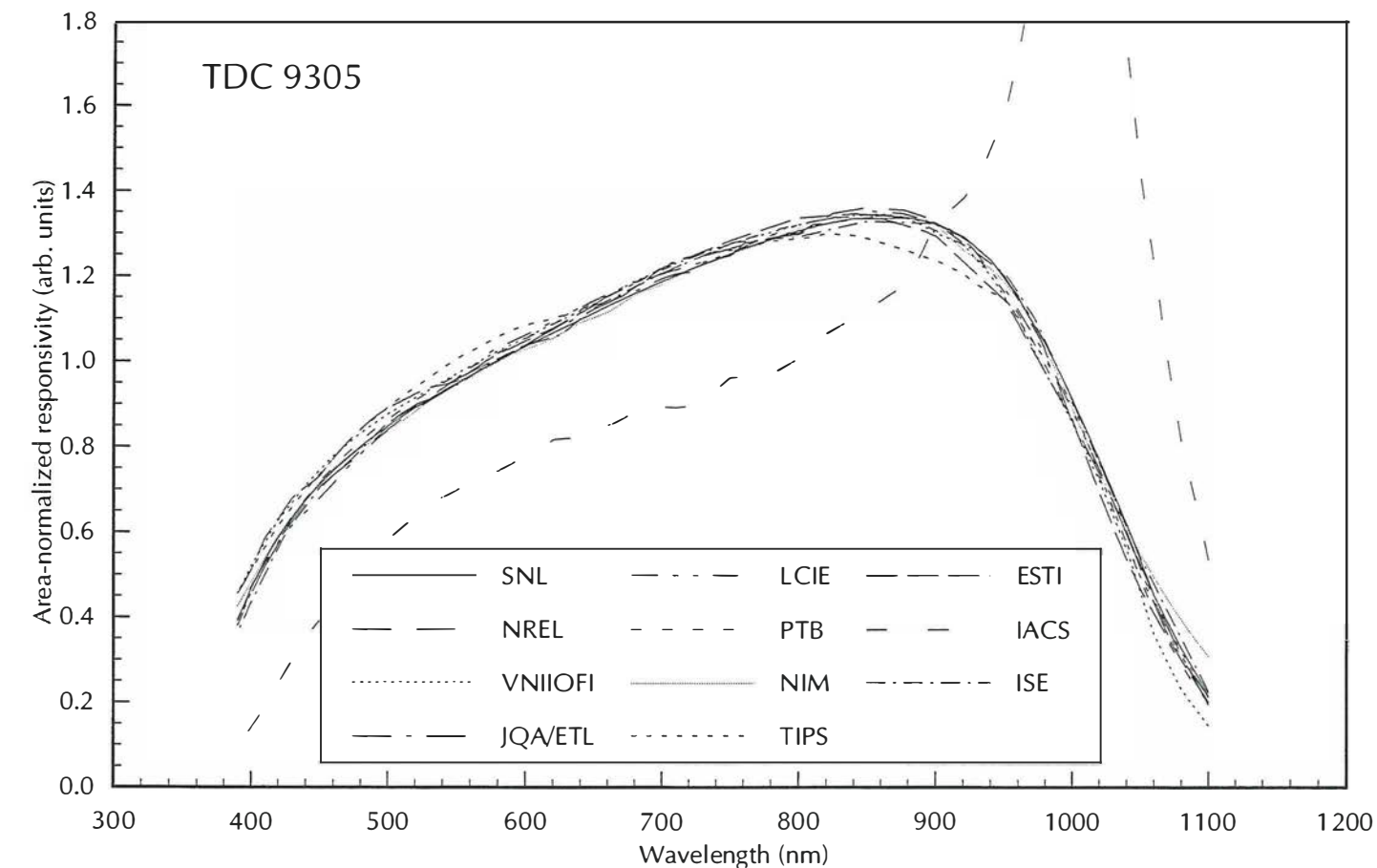


Figure 2-42. Area-normalized spectral responsivity and deviation from WPVS SR for TDC 9305

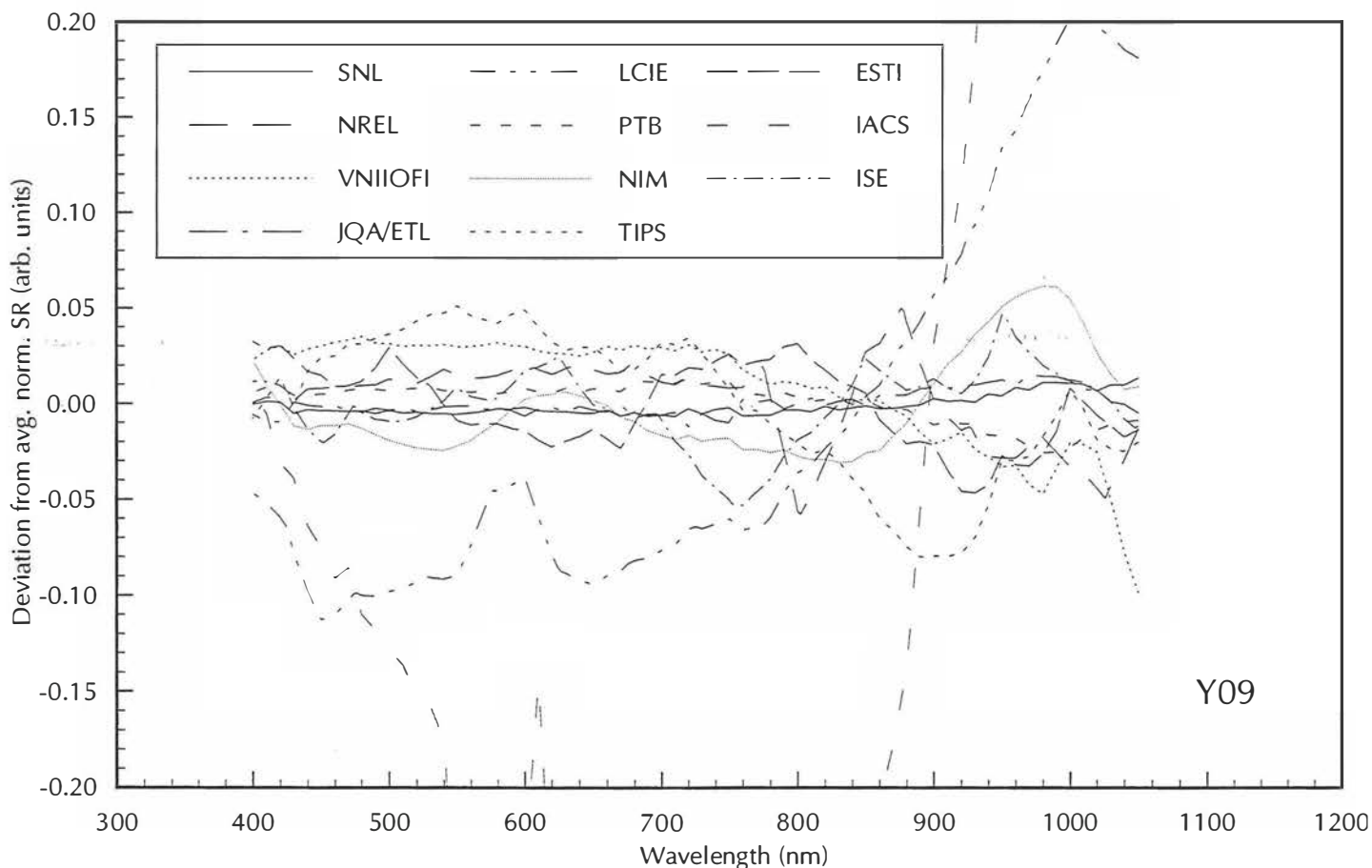
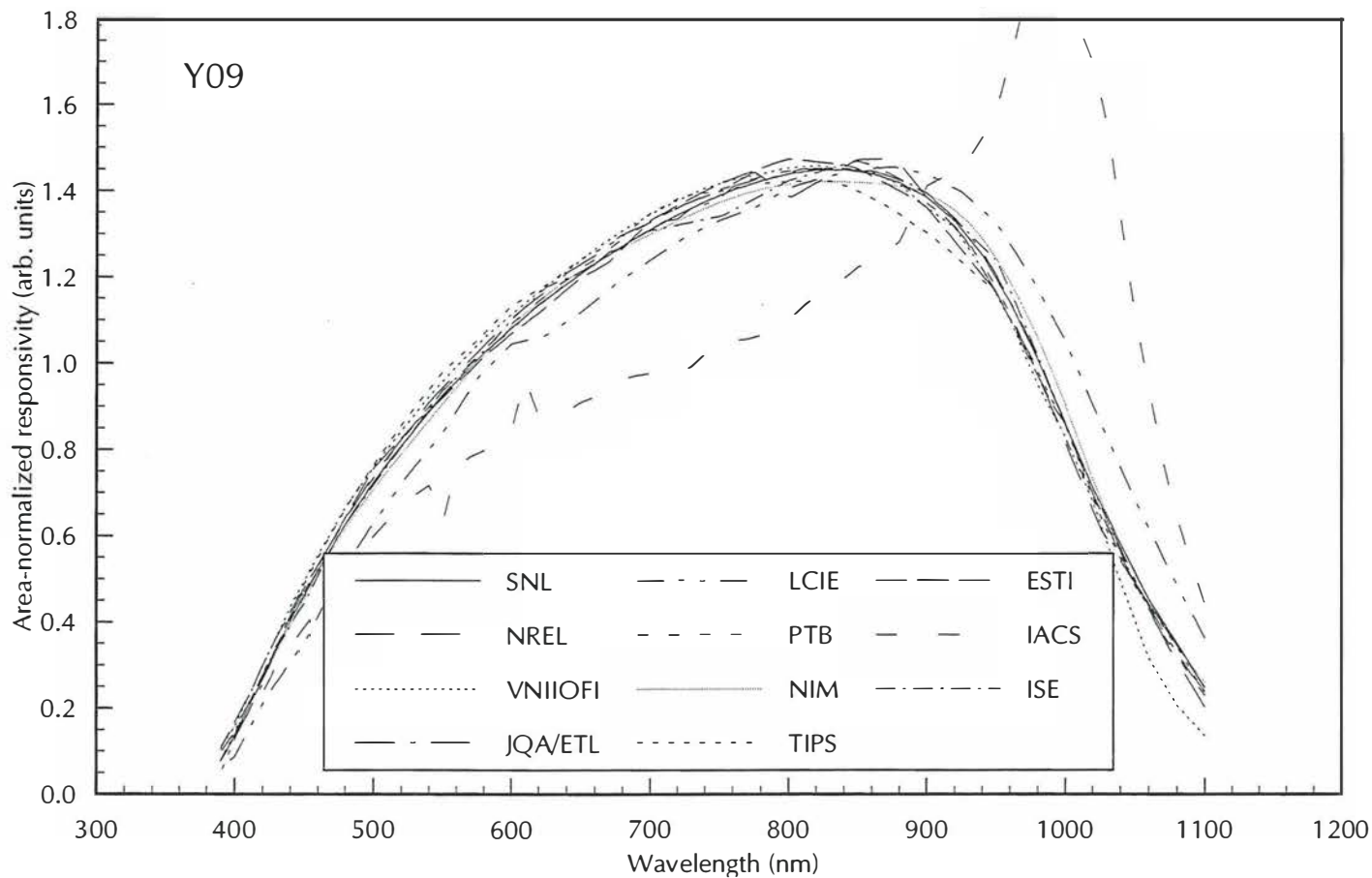


Figure 2-43. Area-normalized spectral responsivity and deviation from WPVS SR for Y09

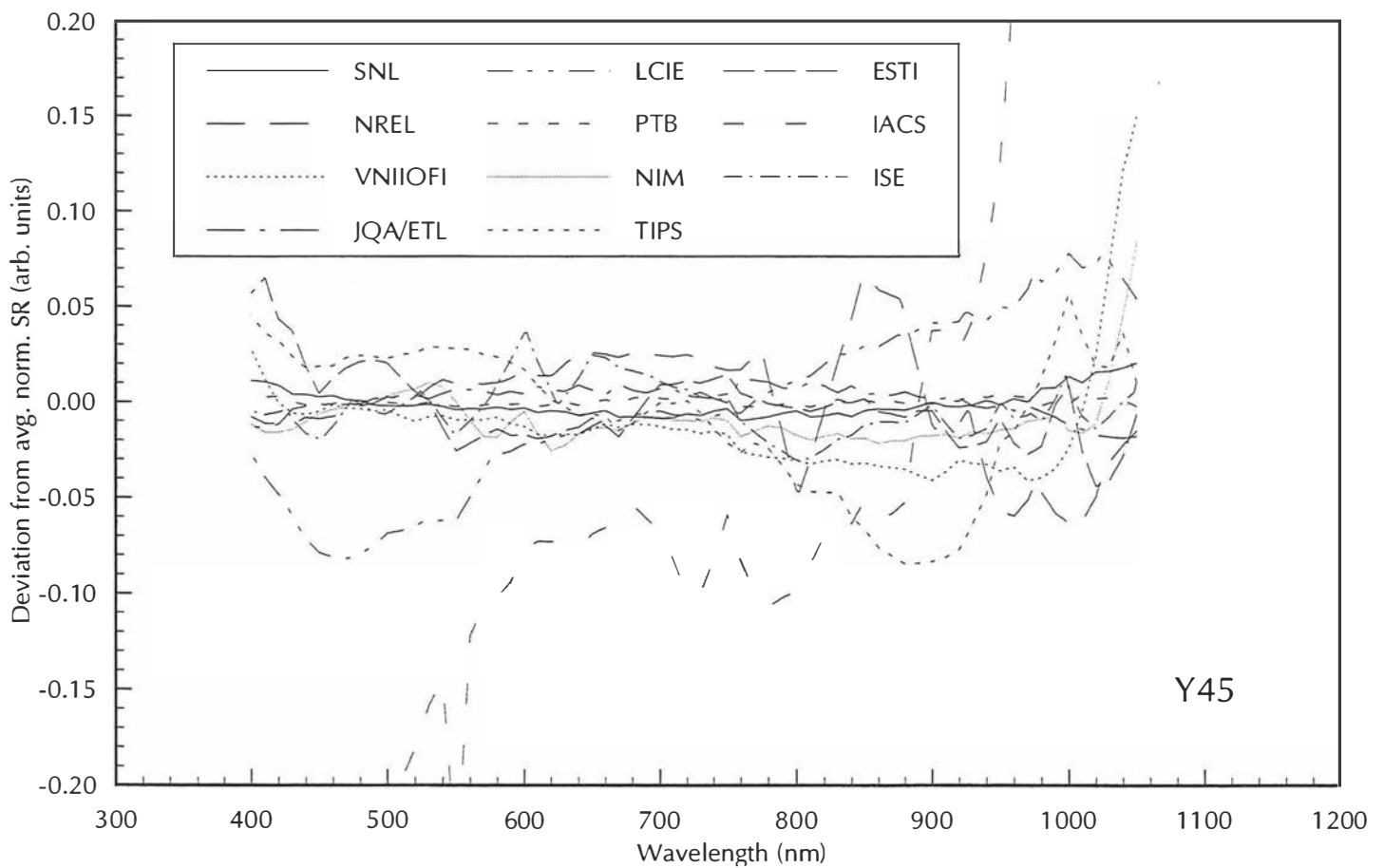
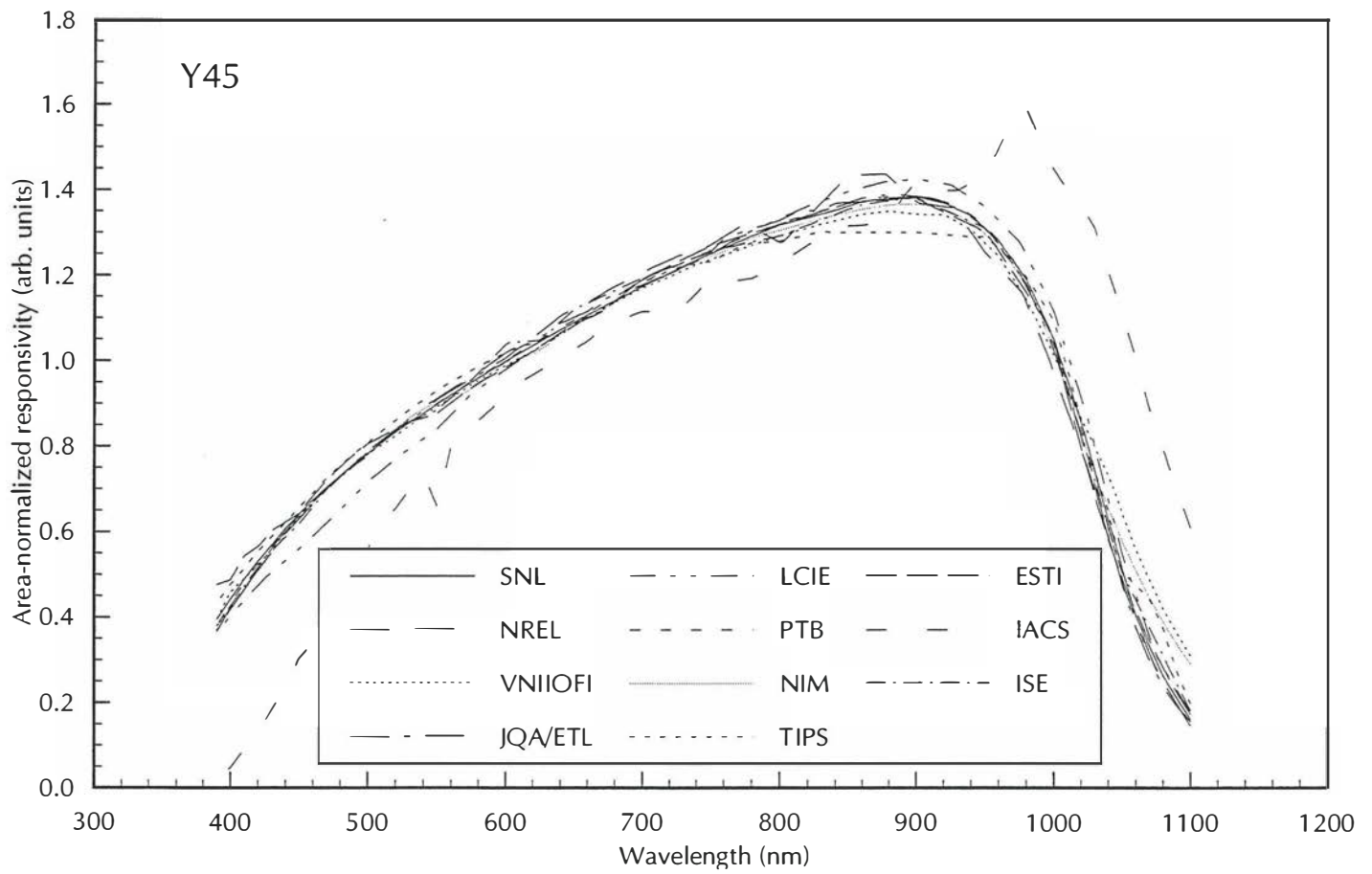


Figure 2-44. Area-normalized spectral responsivity and deviation from WPVS SR for Y45

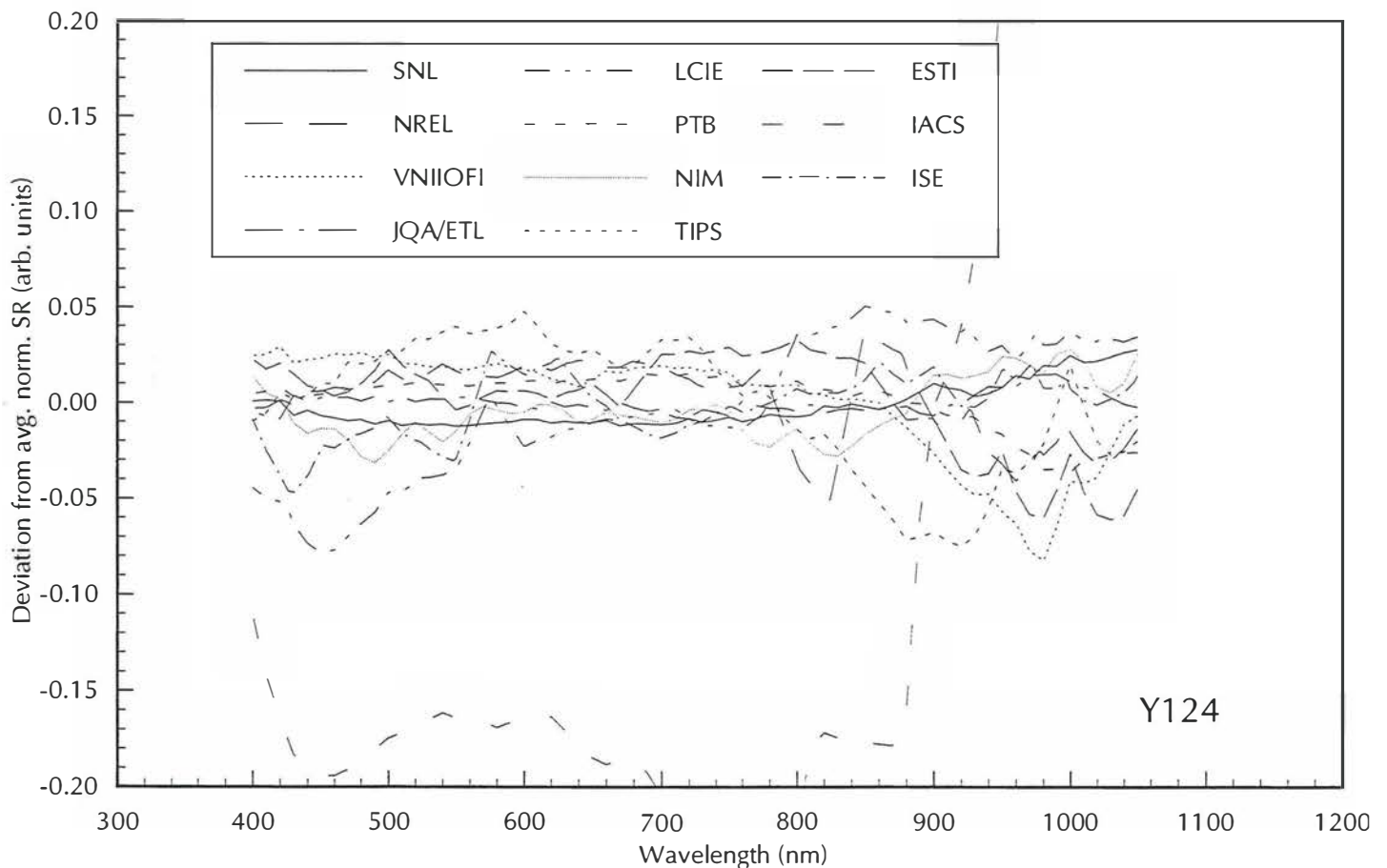
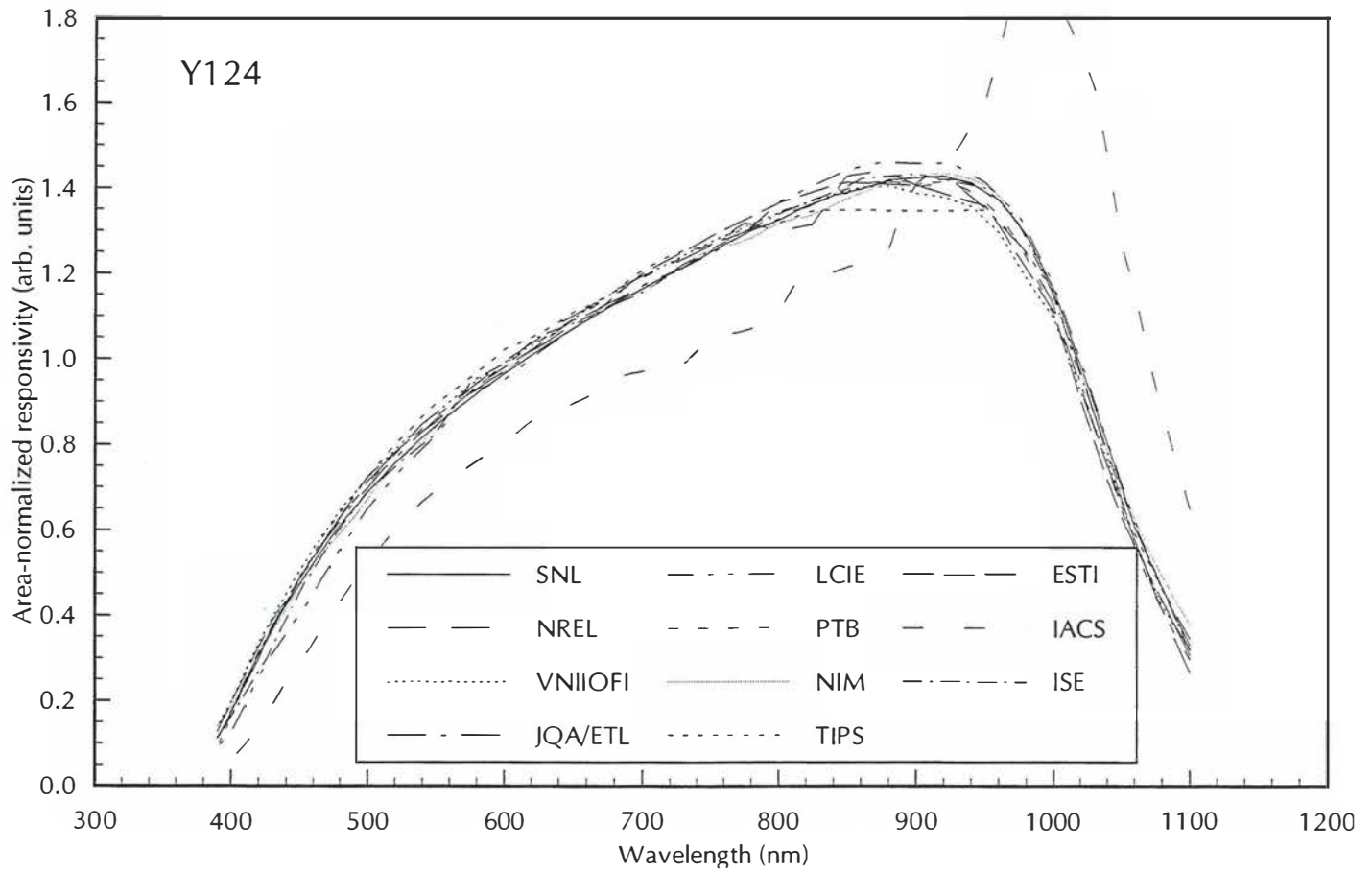


Figure 2-45. Area-normalized spectral responsivity and deviation from WPVS SR for Y124

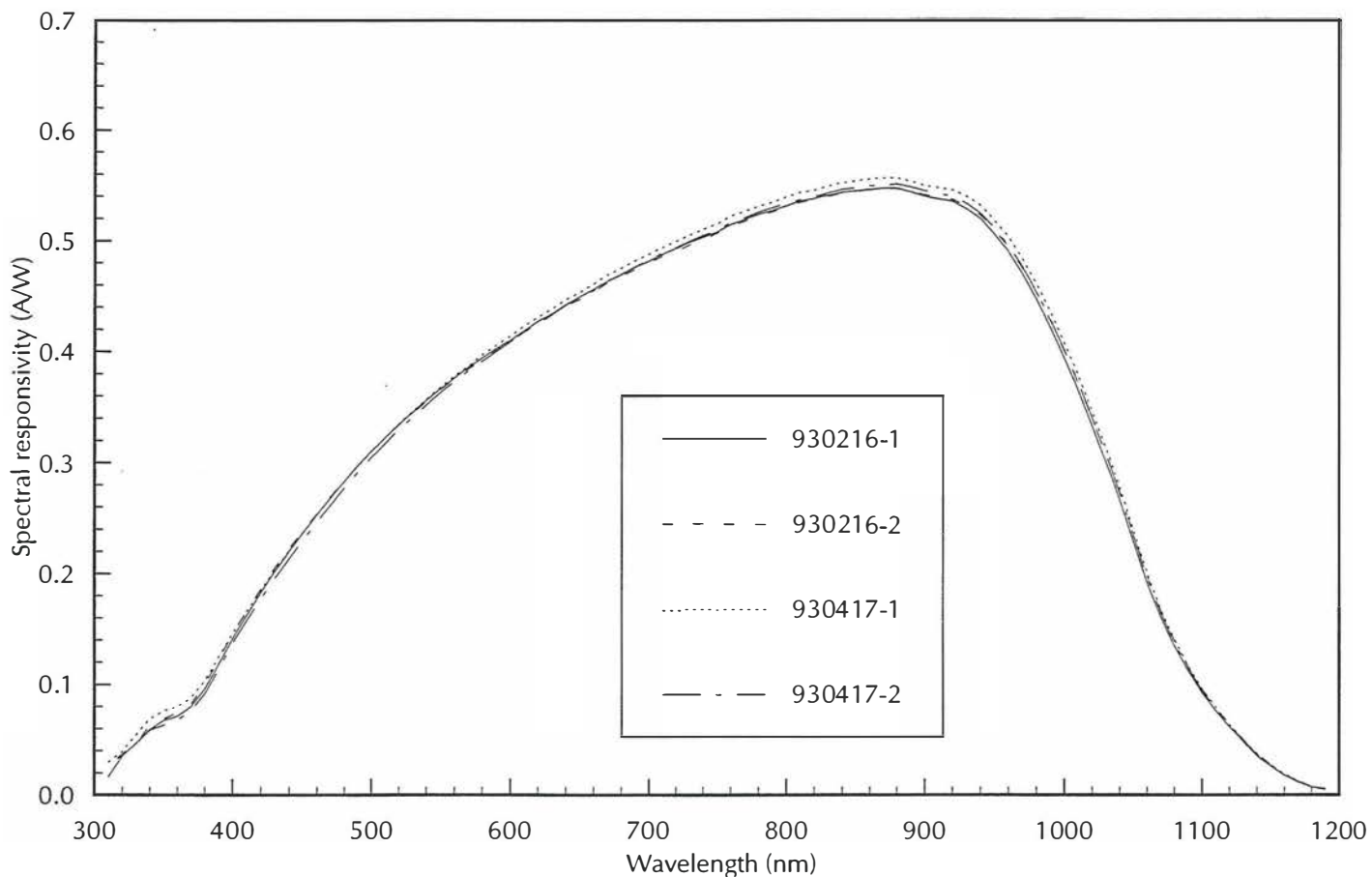


Figure 2-46. Accepted WPVS average spectral responsivity (part 1)

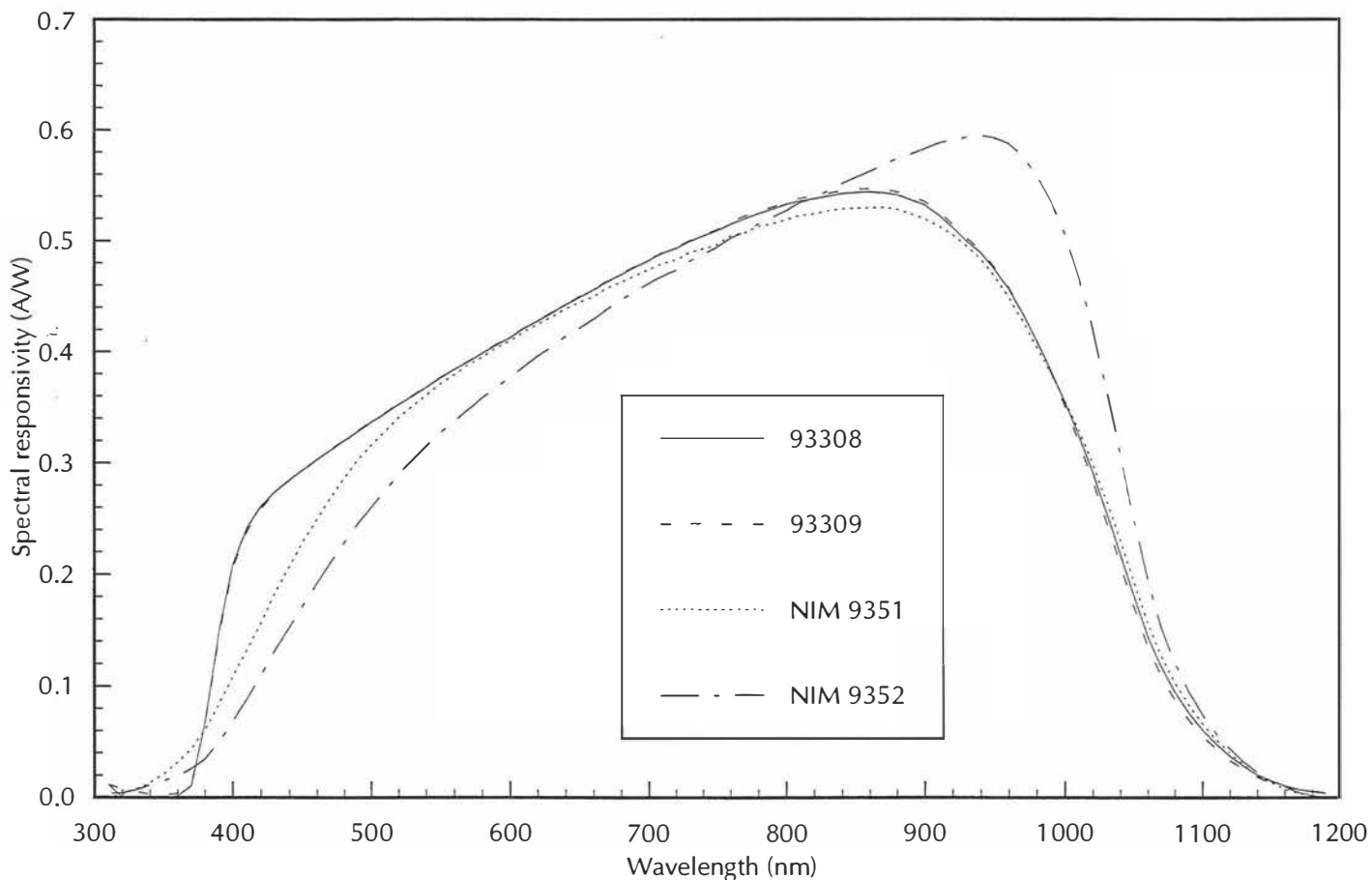


Figure 2-47. Accepted WPVS average spectral responsivity (part 2)

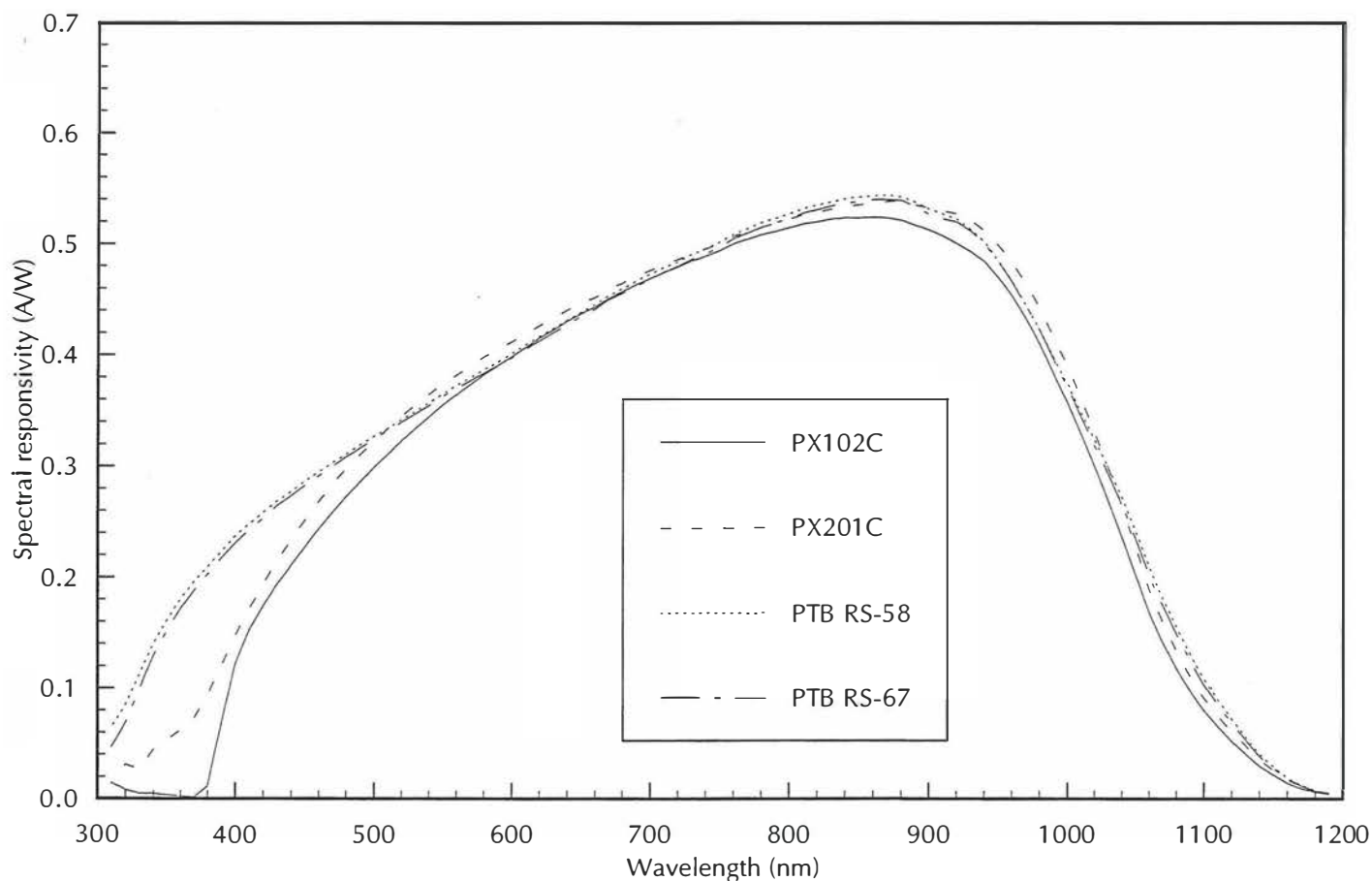


Figure 2-48. Accepted WPVS average spectral responsivity (part 3)

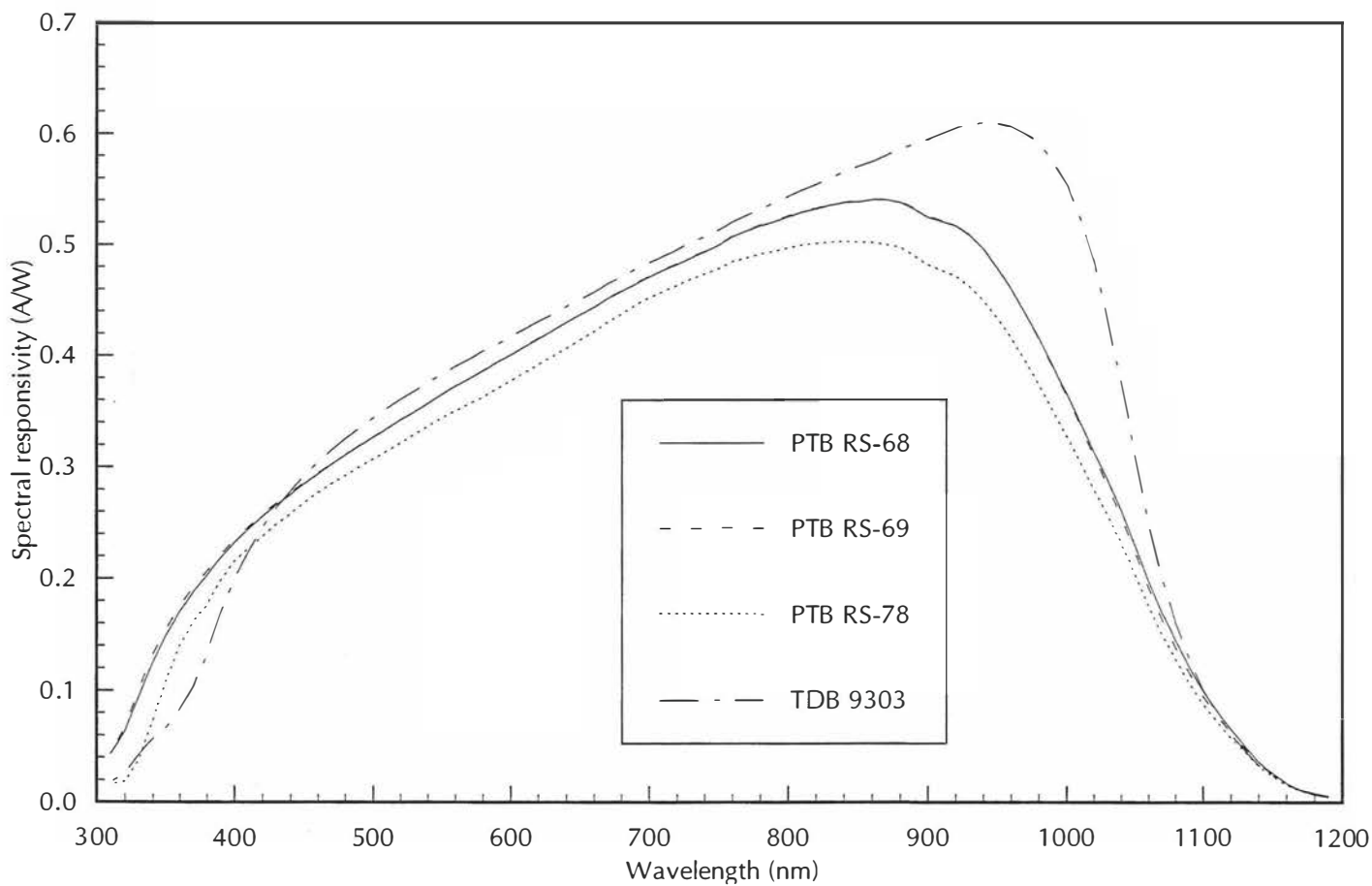


Figure 2-49. Accepted WPVS average spectral responsivity (part 4)

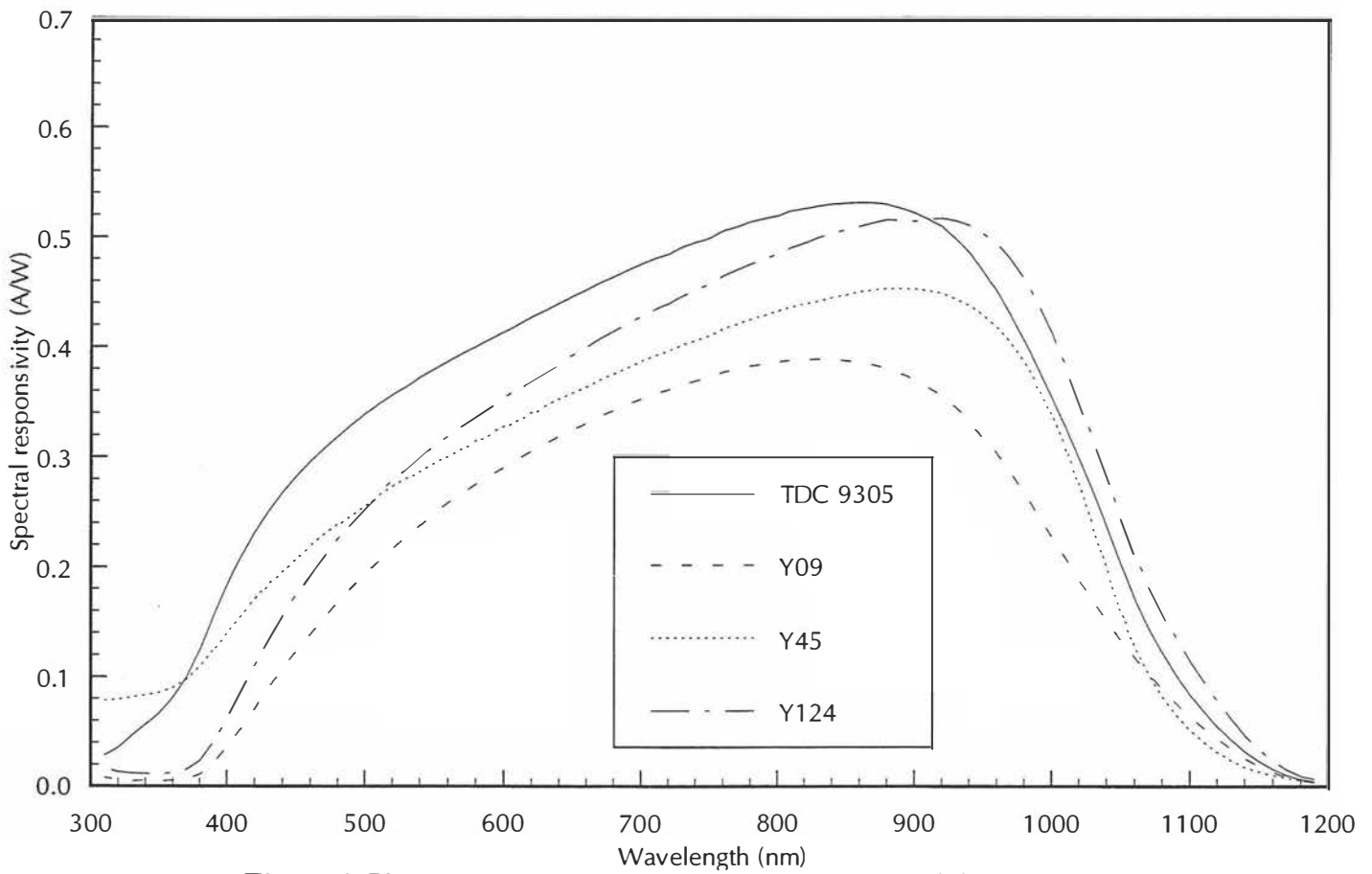


Figure 2-50. Accepted WPVS average spectral responsivity (part 5)

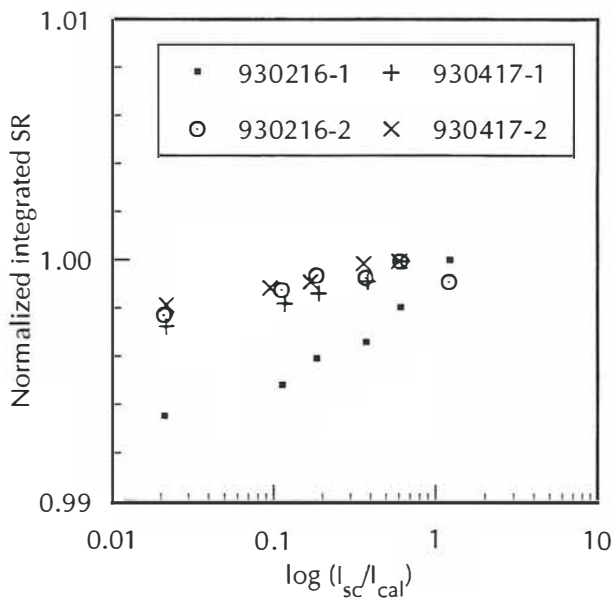


Figure 2-51. Integrated PTB SR data as a function of light bias (part 1)

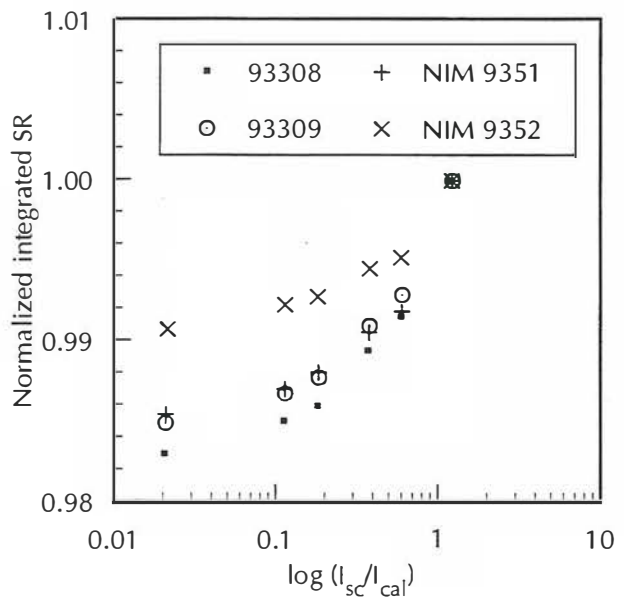


Figure 2-52. Integrated PTB SR data as a function of light bias (part 2)

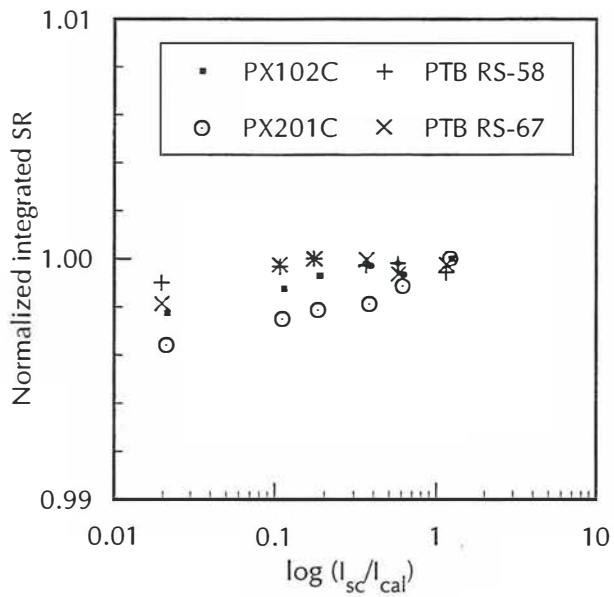


Figure 2-53. Integrated PTB SR data as a function of light bias (part 3)

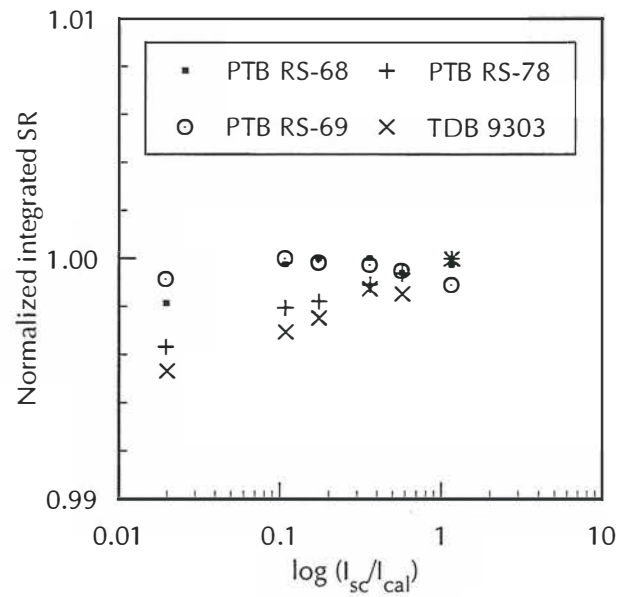


Figure 2-54. Integrated PTB SR data as a function of light bias (part 4)

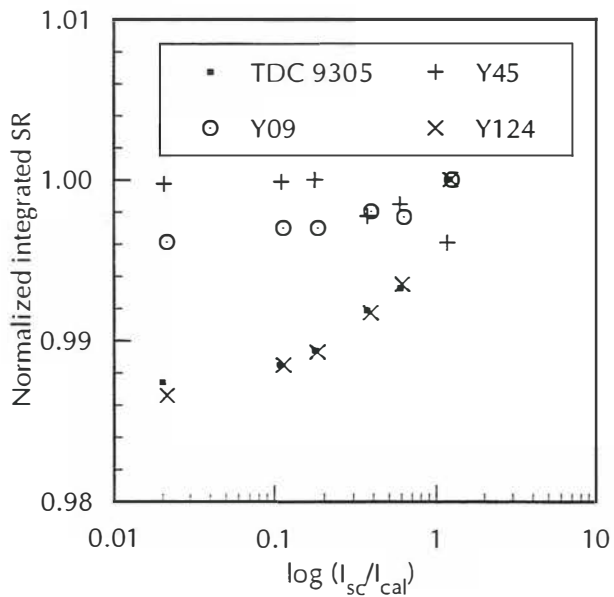


Figure 2-55. Integrated PTB SR data as a function of light bias (part 5)

2.9 Discussion

2.9.1 Results

The most significant result of the WPVS intercomparison is that for the first time, national laboratories from across the globe have agreed on the calibration values for a set of terrestrial PV reference cells. After analysis and qualification, the calibration values from four laboratories (PTB, JQA/ETL, TIPS, and NREL) were within $\pm 1\%$.

Examination of the WPVS results from the individual laboratories reveals many interesting points. Looking at the ranking bar chart (Fig. 2-10), the lowest laboratory average is seen to be NIM. The scatter plot of the NIM data (Fig. 2-21) shows the largest deviations of any laboratory (including one point for PX102C that, at 0.77, falls outside of the graph limits). This is also seen in the laboratory standard deviation for NIM of 4.7% (Table 2-13). Therefore, the NIM calibrations have repeatability problems that are much greater than the reported total uncertainty of 1.6% (Table 2-9). Table 2-16 shows that the low calibration values cannot be explained by spectral responsivity shape errors. Therefore, the NIM results were most likely caused by faulty detector calibration or use.

The LCIE results are also anomalously low. Scatter is moderately high as seen in Fig. 2-19, with one cell, Y124, away from the main grouping. LCIE's spectral responsivity measurements were made with a low light bias, 3 W/m², which corresponds to an I_{bias} to I_{cal} ratio of 0.03. Spectral responsivity nonlinearity is therefore a bias error for the LCIE results. As an attempt to quantify this error, the normalized calibration values from Table 2-12 were divided by the low bias values in Figs. 2-51 through 2-55. Averaging these results shifted LCIE from 0.961 (Table 2-13) to 0.966. The standard deviation reduced slightly from 1.66% to 1.58%. Thus, bias light level can account for only part of the low values of the LCIE calibrations. Spectral responsivity shape does not explain the differences (Table 2-16), so again the cause is likely due to detector calibration or use.

Secondary calibration values obtained by ISE are 2% below the WPVS average, with only a small amount of scatter (Fig. 2-25). ISE used reference cells calibrated by PTB, and ISE's results are therefore close (1% lower) to those of PTB (Fig. 2-10). These differences are not explained by spectral responsivity shape.

PTB's results and repeatability are seen to be quite good, with the laboratory average just 1% below the WPVS average and the lowest laboratory standard deviation. The scatter diagram (Fig. 2-20) shows Y124 separated from the main grouping. These results are undoubtedly the result of the careful detector calibrations and spectral responsivity measurements employed by PTB. PTB's detector calibrations are traceable to the Système International (SI) radiometric scale through

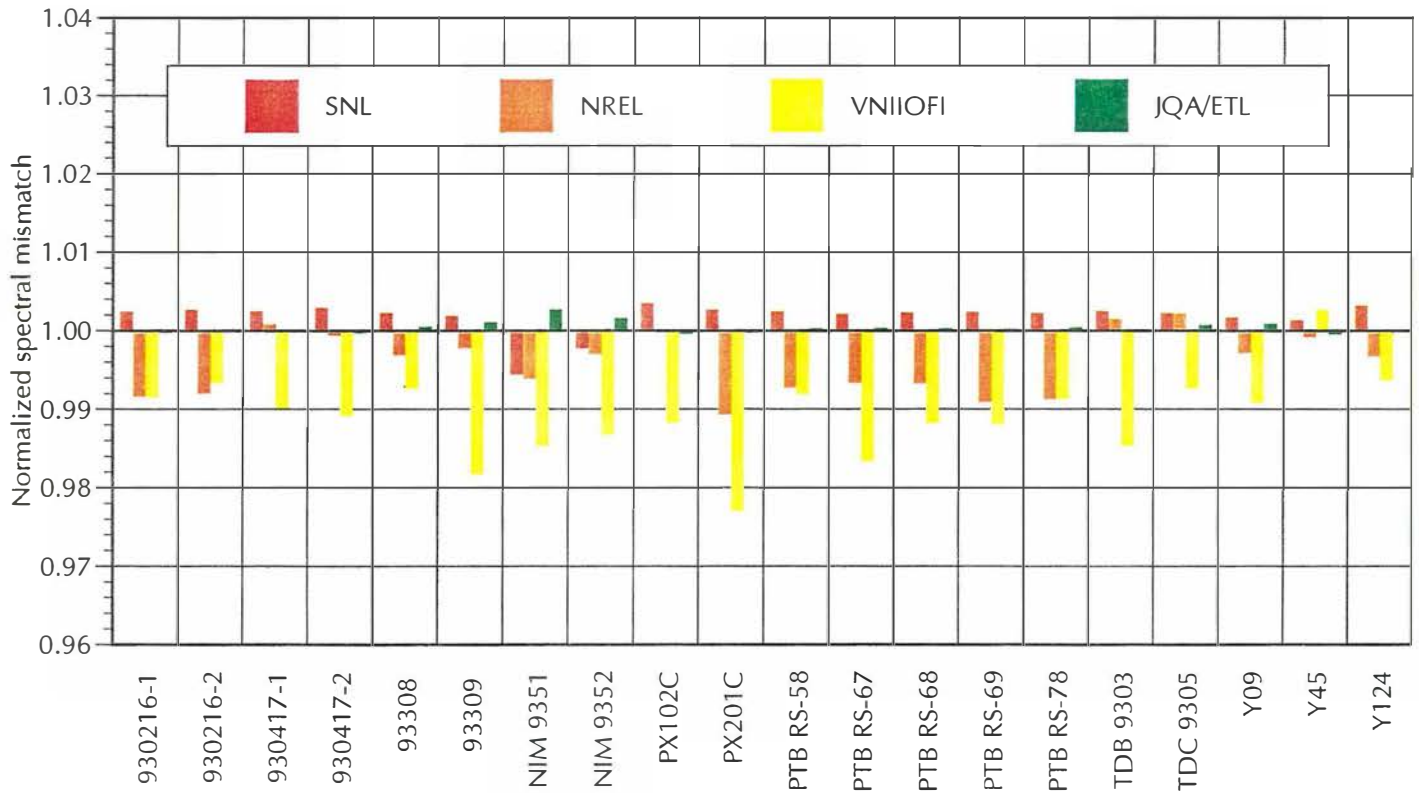


Figure 2-56. Reference spectral mismatch parameters normalized by the mismatch parameters calculated using the accepted WPVS spectral responsivity (part 1)

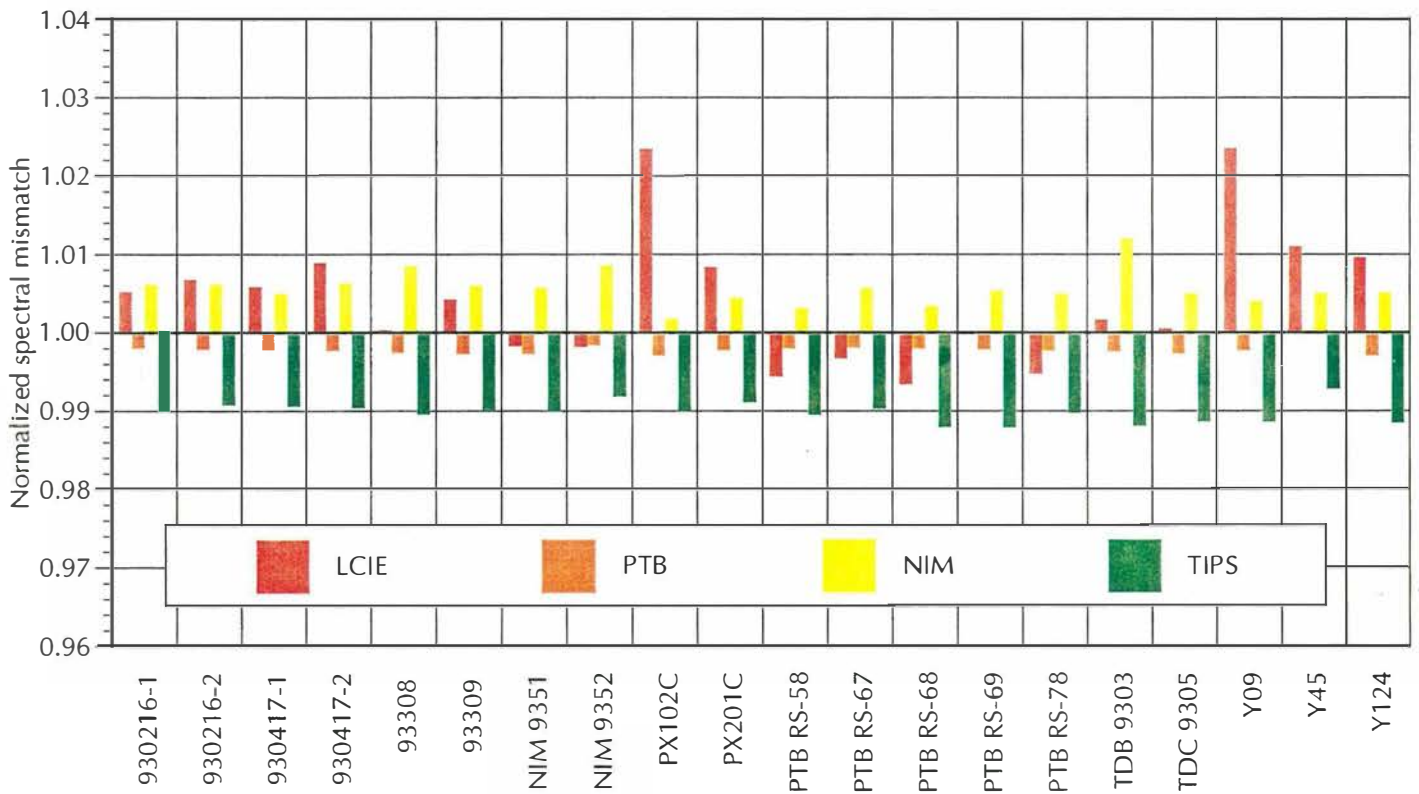


Figure 2-57. Reference spectral mismatch parameters normalized by the mismatch parameters calculated using the accepted WPVS spectral responsivity (part 2)

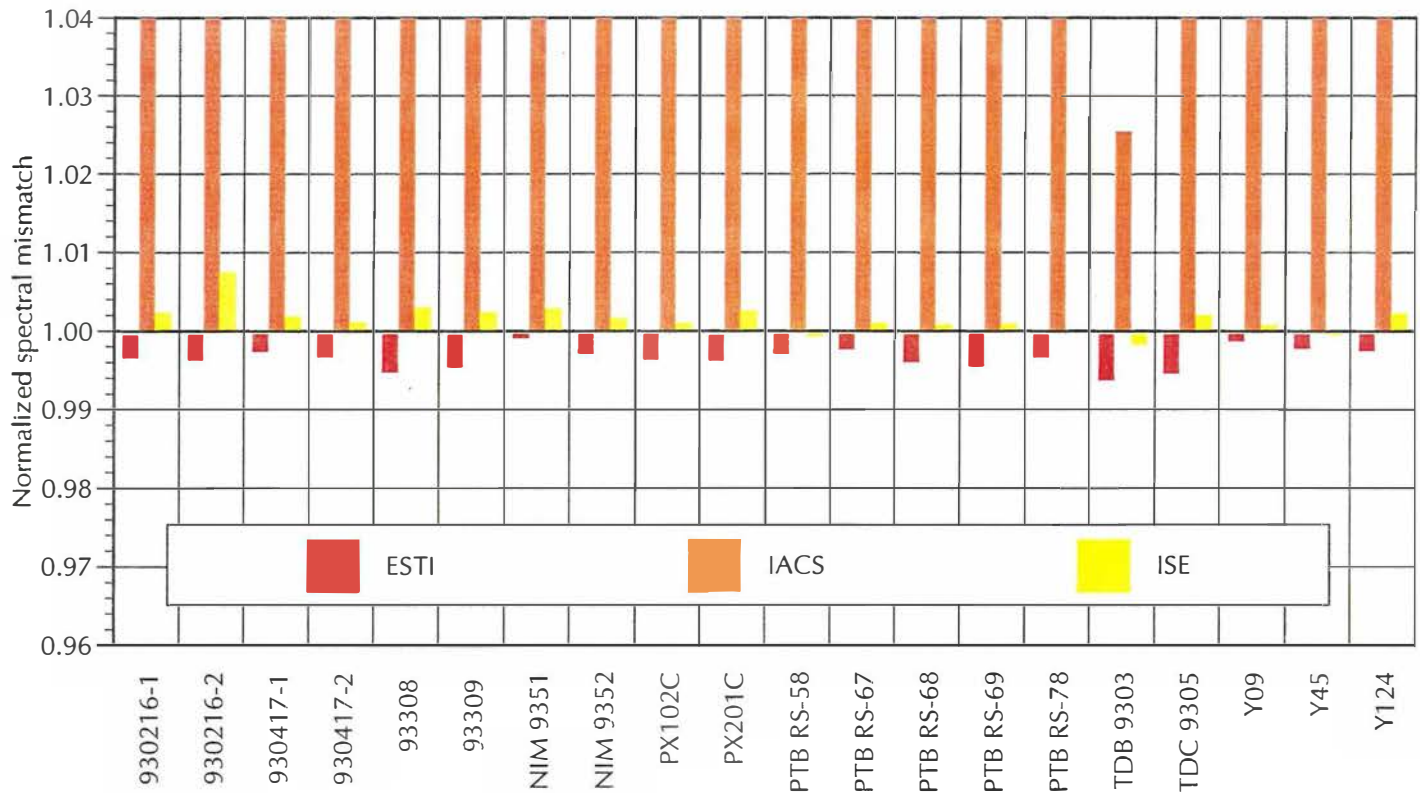


Figure 2-58. Reference spectral mismatch parameters normalized by the mismatch parameters calculated using the accepted WPVS spectral responsivity (part 3)

cryogenic radiometers. The repeatability of the PTB spectral responsivity measurements is very good, as seen by the lowest laboratory standard deviation of the reference spectral mismatch calculations (Table 2-16).

The SNL data are very close to the WPVS average, and the scatter diagram (Fig. 2-15) shows a small main grouping with two cells, NIM 9351 and NIM 9352, outside. A problem with the spectral responsivity measurements for these two cells is a possible cause. The spectral responsivity deviation plots for NIM 9351 and NIM 9352 show the SNL data to be high in the shorter wavelength regions (Figs. 2-32 and 2-33). SNL used a primary reference cell calibrated against a NIST standard irradiance lamp. This cell also received a primary calibration at NREL, and SNL's data are very close to NREL's.

NREL's primary calibrations are just 0.3% below the overall average, and the scatter diagram is small with no outliers (Fig. 2-16). These results are obtained even though NREL's spectral irradiance measurements, made using a Xe arc lamp with narrowband interference filters, are somewhat noisy (see Figs. 2-26 through 2-45).

The IACS secondary calibrations, using a reference cell calibrated by NREL, are close to the WPVS average, in spite of the errors caused by the faulty detector calibration (see Section 2.8.3 and Table 2-16). The scatter diagram (Fig. 2-24) shows good repeatability with one cell away from the main group, Y124.

Primary calibration results from JQA/ETL using the absolute spectral irradiance calibration show very good repeatability (Fig. 2-18), with Y124 as an outlier, and an average just 0.4% above the WPVS average. TIPS, which uses a similar calibration procedure, also shows excellent repeatability (Fig. 2-22). Note that Y124 is again away from the main group, but in the opposite direction (lower) than other laboratories where Y124 appeared as an outlier.

VNIIOFI also employs the absolute spectral irradiance calibration, and the VNIIOFI laboratory average is 1.4% above the WPVS average. The scatter plot (Fig. 2-17) shows a low repeatability. However, the repeatability is consistent with the reported total uncertainty (Table 2-9) of 3.9% (the standard deviation was 2.7%).

ESTI's secondary calibrations are seen to be somewhat high, 3.9% above the overall average. The scatter (Fig. 2-23), however, is good with the exception of the data for Y45, which are higher than the main grouping. The large bias error was later found to be due to an incorrect calibration for the reference cell used for the ESTI WPVS measurements.

If the results from Table 2-13 are assumed to be bias and precision indexes, it is possible to calculate U_{95} for each laboratory using the following equation:

$$U_{95} = \sqrt{(100 \cdot (1 - \bar{I}_{sc}))^2 + (t_{95} \cdot \sigma_{sc})^2}$$

For 20 degrees of freedom and 95% confidence, t_{95} is 2.086. Applying this equation to Table 2-13 gives the uncertainty values in Table 2-17. It should be noted that this bias error assumption is artificial and not strictly correct because the WPVS average is not a true value and could change in the future.

Table 2-17. Total measurement uncertainty U_{95} calculated assuming the laboratory deviation from the WPVS average is bias index and the laboratory standard deviation is precision (%).

SNL	NREL	VNIIOFI	JQA/ETL	LCIE	PTB	NIM	TIPS	ESTI	IACS	ISE
2.45	1.04	5.89	1.43	5.25	1.54	13.14	2.27	4.26	1.61	2.39

2.9.2 Future Calibrations and Maintenance of the WPVS

A major discussion topic during the final meeting of the participants (see Section A4.4) was how future WPVS calibrations should be conducted. The discussion was prompted by concerns that the time required to circulate the reference cells is excessive (circulation of the PEP'93 took 38 months), and the possibility that all the cells could be lost at once. Also, it was seen that provisions for adding new cells to WPVS group are needed. With these considerations in mind, the following proposal for future WPVS calibrations was developed.

First, laboratories traceable to the WPVS will have exactly two WPVS cells. This provision will limit the number of cells that have to be recalibrated. Circulation will be replaced with single-laboratory calibration events every 18 to 24 months. The recalibration events will be held at one of the laboratories selected for the WPVS final average on a rotating basis. Each traceable laboratory will carry or send one of the two WPVS cells to the calibration laboratory, which will perform the calibration using the same method that was used for the PEP'93. Representatives from the traceable laboratories are encouraged to observe the calibrations, if possible. A laboratory that does not provide a cell and previous calibration data will no longer be considered traceable to the WPVS. Following the calibration event, a meeting of the laboratories traceable to the WPVS will be held to determine the WPVS values using a qualified running average. Although representatives of traceable laboratories would not be required to carry cells to the calibration event and attend the subsequent meeting, attendance is important and encouraged so that all inputs can be discussed and weighed.

A method for adding new cells to the WPVS group is required because of damage to or attrition of the current group. In addition, two laboratories currently have only one WPVS cell. The method selected requires new cells to be calibrated by at least three of the final WPVS average laboratories prior to a recalibration event. Following this informal circulation, new cells can then be carried to the next calibration event. At a followup meeting all data for new cells will be considered, and new WPVS calibration values will be determined.

The time and complexity required for calibrations can be reduced if a single standardized package is adopted. Also, loss of cells resulting from common flaws can be minimized by requiring cells to pass an inspection and an acceptance test procedure. The wide variety of package designs and connector schemes that are currently used in the 20 cells of the WPVS group (see Section 2-1) caused logistical problems for the calibration laboratories, which had to contend with mounting, unmounting, connecting, and disconnecting the cells in a reasonable amount of time. These factors led the representatives at the final participants meeting to develop recommendations for a standard WPVS reference cell package.

All of the package designs currently used were discussed and considered, including the standard Japanese design [11], the American package [10], the Chinese packages, and the PRC Krochmann designs, represented by the LCIE, NREL, and ESTI cells. The strengths and weaknesses of all these designs were weighed, along with the needs of the WPVS, and the following design goals were developed:

- Thermal mass of package minimized
- Any active cooling provisions detachable
- Meet IEC 60904-2 specification (see Section 2-1)
- Height ≤ 15 mm
- Detachable cables using female connectors on package side
- Standardized mounting holes
- Silicone or EVA encapsulation
- Durable, smooth front window
- Standardized temperature sensor
- Solar cell electrically isolated from package

Several participants felt that a single standardized temperature sensor should be used. Considerations of existing facilities, however, made this goal impossible. A compromise was reached whereby two different temperature sensors would be used, a T-type copper-constantan thermocouple soldered to the front of the solar cell, plus a thin-film platinum RTD at the back of the solar cell. Having two temperature sensors increases reliability because the loss of one does not render the

reference cell completely useless, and a sensor on each side of the cell enables the determination of the temperature gradient between the front and back, if necessary. The detachable cabling goal was achieved by specifying Lemo series 0S 10 mm round socket connectors., which can have thermocouple alloy contacts in addition to normal electrical contacts [21].

The inspection and acceptance tests were designed to uncover common flaws that can render a reference cell useless, and to document parameters that may be used to detect damage or degradation at a later date. Most of the common flaws were observed in the current WPVS group, and the flawed cells will have to be replaced with new ones in the future. Thus, a great deal of time and expense can be saved if defects are discovered prior to calibration. The list of flaws includes, but is not limited to, the following:

- Internal reflections
- Poor I-V characteristics
- Encapsulant flaws such as bubbles or delamination
- Intermittent or broken electrical contacts
- Electrical and optical instabilities
- Illegible identification markings
- Broken or scratched window

The complete specifications, design, and acceptance test procedures are contained in Appendices 1 and 2. These are identical to those developed at the final participants meeting, with a few exceptions. First, the package recommendations are replaced with drawings of the new JQA design (Figs. A1-1, A1-2, and A1-3). Second, the limit for the slope of the I-V curve at I_{sc} was reduced from 25 mS to 5 mS. The original limit was calculated on the basis of a maximum 1% error in the measured I_{sc} at a cell voltage of 50 mV. Examination of the values for the current WPVS cells (see Table 2-6), shows that typical values are much lower, around 0.4 mS, and the maximum was 3 mS. There is, then, no reason not to have a tighter limit. Third, the fill factor limit was raised from 60% to 65% because a good-quality monocrystalline silicon cell has a fill factor greater than 70%, with typical values about 74–76%. Finally, the original 15-pin D-subminiature connector specification was changed to three Lemo 10 mm circular connectors because of concerns about contact reliability and manufacturing costs.

Finally, a procedure is needed for adding laboratories to the original four that contributed to the current WPVS average. One feature of the WPVS portion of the PEP'93 was the fairly high number of samples, 20, which allowed statistically significant conclusions to be made. The results would have been much harder to interpret if, for example, the number of samples was only six. Similar information should be obtained about new laboratories, and this can only be accomplished

through round-robin circulation of a similar number of samples. Because circulation of the WPVS group will no longer take place, a different set of reference cells is needed. This set could be used for solely this purpose, and could also function as a proficiency test for the laboratories already accepted for WPVS calibrations. Proficiency testing would serve to increase confidence in the WPVS.

To minimize the chances of thermal damage, storage temperatures for WPVS reference cells should be restricted to a range from -10° to +40°C, and from +10° to +50°C for operating temperatures.

2.9.3 Traceability

Because the WPVS is an average of calibrations performed by national laboratories, the total uncertainty of the average is very dependent on the traceability of the individual calibrations to measurement standards, and, ultimately, to the SI system of units. This is especially important because the International Bureau of Weights and Measures (BIPM) adopted a resolution at the 20th Conference Generale des Poids et Mesures, October 1995, that agencies

“responsible for studies of Earth resources, the environment, human well-being and related issues ensure that measurements made within their programmes are in terms of well-characterized SI units so that they are reliable in the long term, are comparable worldwide, and are linked to other areas of science and technology through the world’s measurement system established and maintained under the Convention du Metre.”

This resolution is certainly applicable to photovoltaics, so the WPVS should be traceable to SI units only. Photovoltaic calibrations involve both electrical (current and voltage) and radiometric (radiant power) measurements. Electrical traceability is normally achieved through calibration of instrumentation to SI transfer standards, but radiometric traceability is not as easily attained, and radiometric measurements in general are much more difficult to perform. Table 2-18 summarizes the radiometric traceability of the WPVS calibrations, as reported by the laboratories. Some of the apparent disparity of traceability has been relieved by a recent comparison of the SI radiometric scale against the WRR. The comparison showed that the WRR is very close to the SI radiometric scale, at $-0.0005 \pm 0.026\%$, as realized by cryogenic radiometers [18].

Table 2-18. Traceability of WPVS calibrations

Laboratory	Instrument	Traceability
JQA/ETL	Spectroradiometer	CIE
NREL	Absolute cavity radiometer	WRR
PTB	Standard diode detectors	SI radiometric scale through cryogenic radiometers
TIPS	Standard irradiance lamp	NIM

2.9.4 Recommendations

Several recommendations concerning the WPVS have been made, and are summarized below:

- Round-robin circulation of the WPVS group will not be used for recalibration.
- As means of proficiency testing, laboratories will continue intercomparisons of a separate set of reference cells.
- Recalibrations of the WPVS group will be performed at single laboratories at intervals of 1.5–2 years.
- The present WPVS reference cell group should be replaced with cells of the new design.
- New cells will have to pass an acceptance test prior to calibration.

In many respects the WPVS process may actually be more advantageous than a single IEC primary reference cell calibration standard. Assuming the calibrations are traceable to SI units, each laboratory is free to use whatever method best suits its capabilities, and the comparison with other laboratories helps increase confidence in the quality of the measurements. Also, the process provides a goal for laboratories not currently part of the WPVS average that are attempting to improve their calibrations.

For these reasons, it is recommended that IEC Technical Committee 82 (TC-82) consider developing a standard for the WPVS process. In conjunction with this, it is also recommended that TC-82 consider the new reference cell package design and acceptance test for standardization. This will help disseminate the information beyond the limited circulation of this report and facilitate acceptance of the design.

It is desirable that reference cells manufactured according to the new WPVS design will become commercially available in the near future.

3. Newer Technology Series Sample Set

3.1 Sample Set

During the organizational meeting in Montreux, Switzerland, the participants developed a list of PV device types that should be included in the NT series. The invitation to participate included a request for volunteers to supply devices from the list. A tentative sample set was developed from the responses, and a call for samples was then issued. NREL assembled the final sample set from the devices that were subsequently received. The sample set is listed in Table 3-1, and representative photographs appear in Figs. 3-1 through 3-11.

Most of these devices were small (about 2×2 cm) cells in a reference cell-style package, with some notable exceptions. The ESTI sensors consisted of a 10×10 cm silicon cell cut into two pieces,

Table 3-1. NT series sample set

Organization	Cell ID	Type
ESTI	ESTI 1 ESTI 2	ESTI sensor
NREL	S11 S31	CuIn(Ga)Se ₂
JQA/ETL	9321 9324 9312 9313 9306 9307	CdTe a-Si two-junction tandem a-Si bi-cell
IACS	DT 1 DT 2	a-Si two-junction tandem
TIPS	TIPS 1 TIPS 2	10×10 cm bare Si
PTB	PTB RS-41 PTB RS-44 PTB RS-64 PTB RS-74	Low-pass Si (2mm KG3 filter) High-pass Si (2mm RG670 filter)
SNL	SNL003 SNL-04 Cell #1 Cell #2	GaAs GaAs concentrator module
LCIE	LCIE 1 LCIE 2	Single 10×10 cm Si cell in module package

and laminated side-by-side in a package. One cell was connected across a 20 mΩ load, and the other brought out through the integral cable, for a total of four wires. The ESTI sensors are intended to measure module temperature using the V_{oc} of one cell, and total irradiance through the I_{sc} of the other cell.

The a-Si bi-cells were two 1×2 cm a-Si cells connected in series on a single quartz superstrate, and the tandems were dual-junction a-Si cells. Colored glass filters were used to modify the spectral response of the PTB silicon cells. These gave a responsivity wavelength range of about 300–800 nm for the low-pass cells, and about 600–1200 nm for the high-pass cells.

The concentrator module had optics that focused light onto two 5-mm round GaAs cells that could be connected in series, or measured separately. Spectral responsivity data for the GaAs concentrators were provided for the intercomparison.

The large-area silicon cells all had contacts wired to outside connectors, but the TIPS cells had four contact terminals intended for four-wire Kelvin connections, and the LCIE devices (which were in actuality small modules) had two-wire terminals.

During the early rounds of sample circulation, the contacts to the IACS a-Si tandem cells (DT 1 and DT 2) were found to be unstable so that the cells could not be used in the intercomparison. For this reason, no data from these cells are reported here.

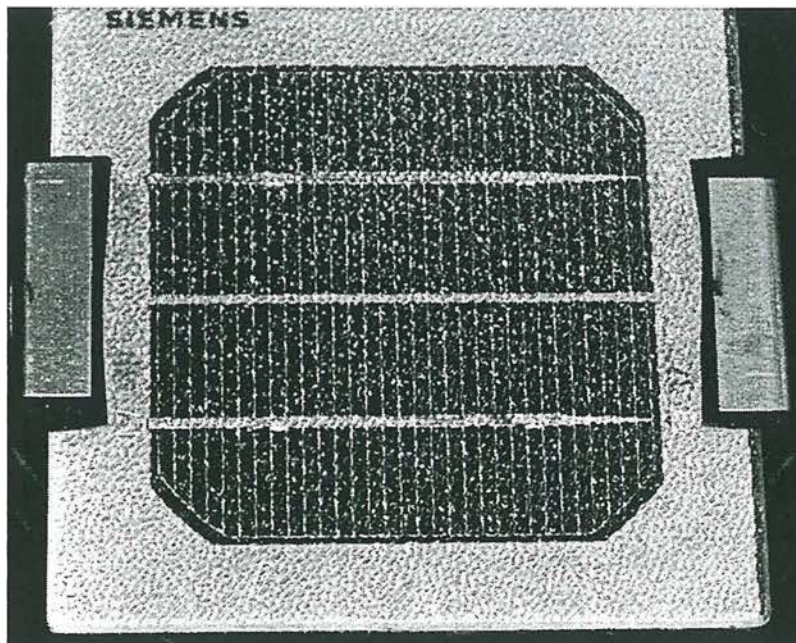


Figure 3-1. ESTI sensor ESTI 2

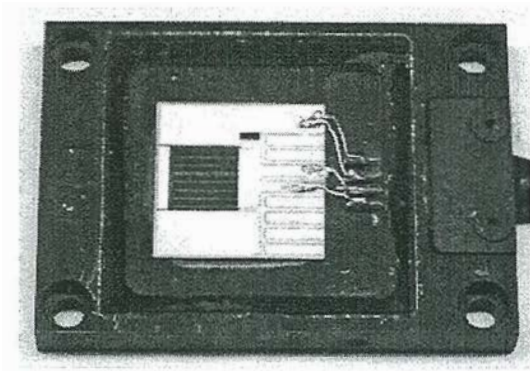


Figure 3-2. CuIn(Ga)Se₂ cell S31

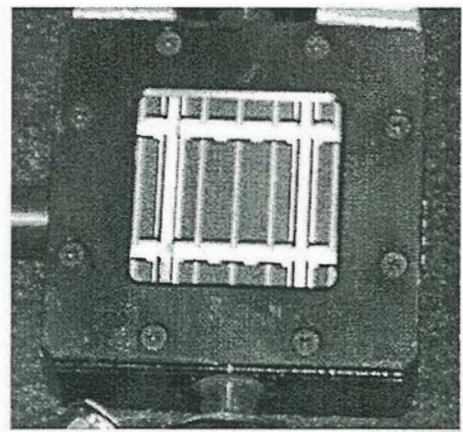


Figure 3-3. CdTe cell 9321

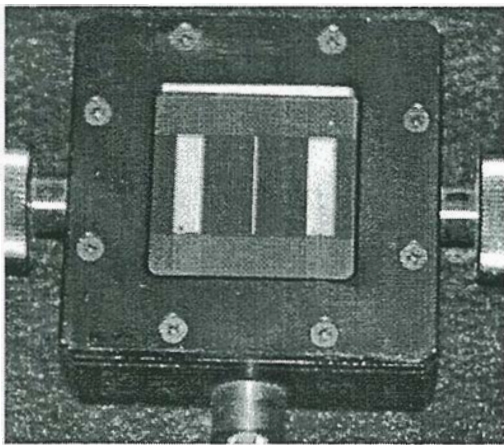


Figure 3-4. a-Si two-junction tandem cell 9312

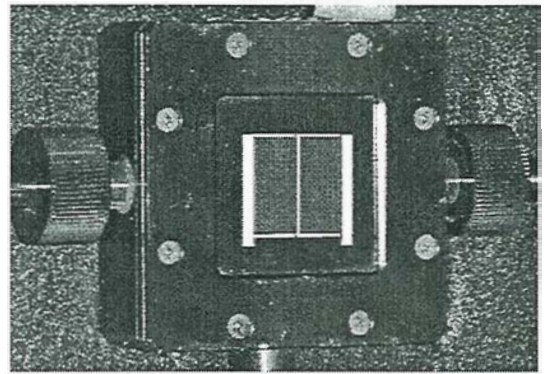


Figure 3-5. a-Si bi-cell 9306

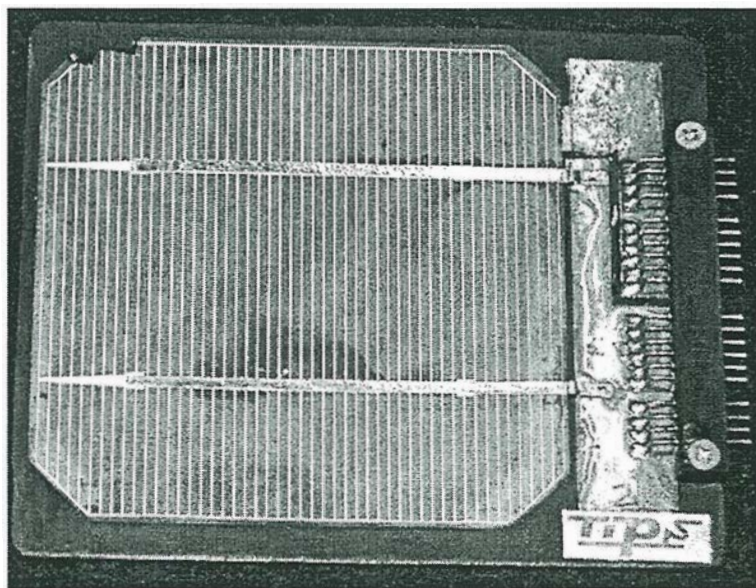


Figure 3-6. 10×10 cm Si cell TIPS 2

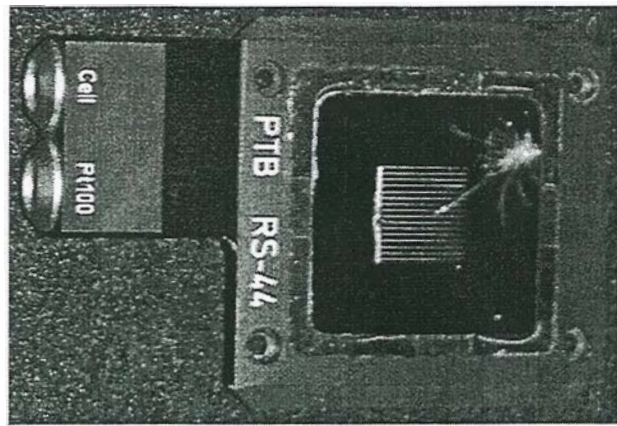


Figure 3-7. Low-pass filtered Si cell PTB RS-44. The cracked filter is visible.

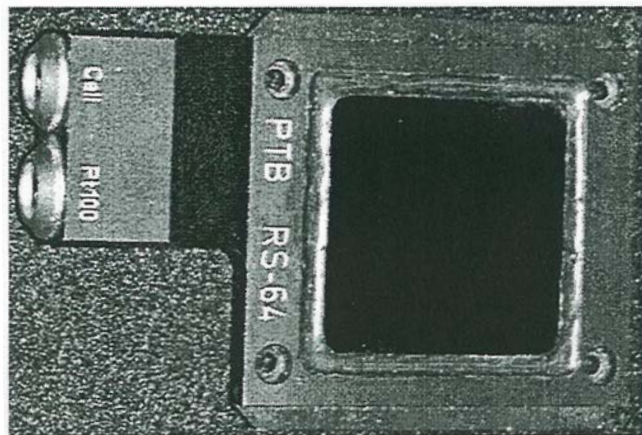


Figure 3-8. High-pass filtered Si cell PTB RS-64

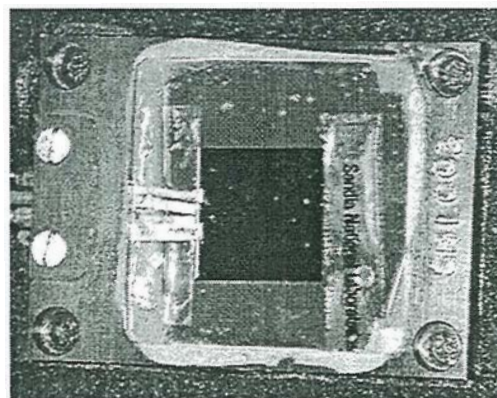


Figure 3-9. GaAs cell SNL003

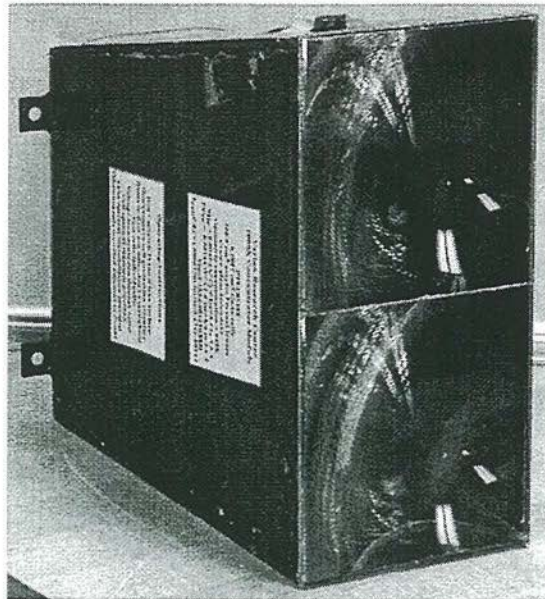


Figure 3-10. GaAs 1000× concentrator module

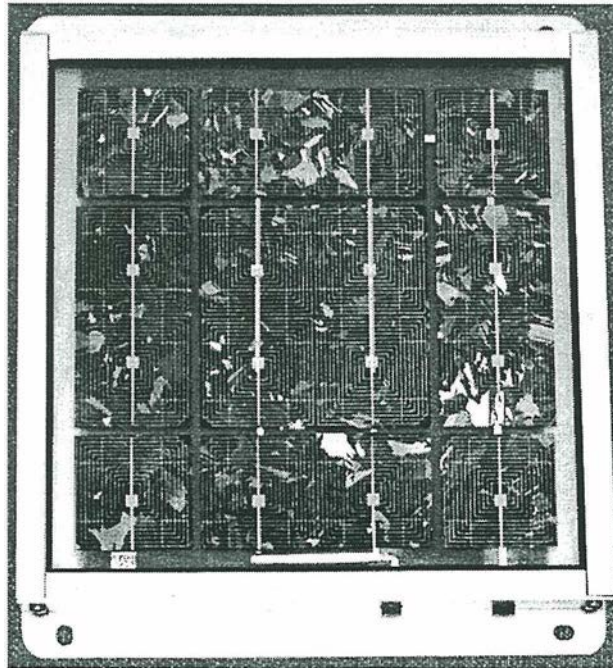


Figure 3-11. 10×10 cm Si cell in module package LCIE 1

3.2 Protocol

Except for necessary information about contacts and connectors, no restrictions or guidance on the methods used to measure the device performance were given in the protocol for the NT series. Because the objective was to identify measurement problems, participants were free to measure the samples with whatever procedures they chose. In addition, participants could elect to not measure individual samples if the required procedures or equipment were beyond their capabilities. Requirements for reporting results included the I-V parameters (V_{oc} , I_{sc} , P_{max} , FF), efficiency, and the device area, plus descriptions of measurement methods and how device areas were determined. All parameters had to be corrected to STC, as defined in IEC 60904-3 [12]. Although not required, most laboratories provided SR data.

3.3 Circulation History

The circulation history of the NT series samples is documented in Table 3-2. Because the organizing agent (NREL) was the first laboratory to measure the samples, NREL's measurements were used as the pre-circulation baseline. Following the return of the sample set, NREL repeated its measurements, which then served as the post-circulation comparison as well as another data set. It should be noted that NIM and VNIIOFI both elected to not participate in the NT series circulation.

Table 3-2. NT series sample set circulation history

Laboratory	Time Period
NREL	July – August 1993
LCIE	September – October 1993
JQA/ETL	November – December 1993
SNL	January – February 1994
ESTI	March – April 1994
ISE	May – June 1994
PTB	July – August 1994
USPL	September 1994 – August 1995
TIPS	September – November 1995
IACS	December 1995 – November 1996
NREL	December 1996 – May 1997

3.4 Measurement Methods and Reported Anomalies

The participating laboratories used a number of different measurement procedures for the NT series sample set. These procedures reflected not only the capabilities of the participants but the diverse nature of the newer technology devices.

3.4.1 NREL

With the exception of the GaAs concentrator module, all of NREL's data were obtained using a Spectrolab X-25 xenon solar simulator. The irradiance of the simulator was set using primary reference cells that were selected to match the spectral responsivity range of the test cells as much as possible. A monocrystalline silicon reference was used for the Si, high-pass filtered Si, and CuIn(Ga)Se₂ cells, a GaAs reference for the CdTe and GaAs cells, and a filtered Si reference for the a-Si bi cells and the low-pass filtered Si cells. Spectral mismatch corrections were applied to the reference cell calibration constants to account for spectral differences. NREL's spectral responsivity measurements were described previously (see Section 2.4.2). For the concentrator module, an outdoor calibration procedure very similar to that used for the WPVS was employed (also in Section 2.4.2); however, I-V curve data were not reported. For the a-Si tandem cells, colored light biasing was used to obtain the spectral responsivity of the top and bottom cells independently. Two reference cells were used to adjust both the total irradiance and the spectral irradiance of the solar simulator for the tandem cells—one reference cell for the top junction and the other for the bottom junction.

3.4.2 LCIE

LCIE used the same short-circuit current calibration procedures for the NT series samples that were previously described (see Section 2.4.5) for the WPVS cells. LCIE reported data for only the crystalline silicon devices and did not measure I-V curves.

3.4.3 JQA/ETL

Single junction devices were measured with the solar simulator method previously described (see Section 2.4.4). The multijunction spectral responsivities were measured using colored light biasing (Hoya O56 and B390 colored glass filters). Reference cells with suitable filters to match the tandem cells were selected and then calibrated with the solar simulator method. These reference cells were then used to adjust the total and spectral irradiance of an adjustable supplementary-light solar simulator [19]. The concentrator module was measured in a Class A pulsed solar simulator against a GaAs reference cell, with the ambient room temperature at 25°C. Temperature corrections were not applied to the I-V data.

3.4.4 SNL

SNL used methods similar to those of the WPVS cells for the NT series (see Section 2.4.1). Colored light biasing was used to measure the spectral responsivities of the tandem cell junctions independently. I-V data for the tandem cells could not be obtained because the voltage of the cells

exceeded the limits of the measurement system. SNL measured the concentrator module as a single device with the cells connected in series; the reported open-circuit voltages and areas were divided by two for comparison purposes.

3.4.5 ESTI

Identical procedures to those outlined above (see Section 2.4.9) were used for the NT series. The concentrator module was aligned to the pulsed solar simulator beam with a small laser pointing to the simulator. ESTI did not report I-V curve data for the ESTI sensors, but reported the irradiance and temperature calibrations instead. Spectral responsivities were measured on only one device of each of the sample pairs.

3.4.6 ISE

ISE used a single source simulator for the single junction cells, a multiple source simulator for a-Si tandem cells, and outdoor measurements for the ESTI sensors and concentrator modules. All of these used spectral mismatch corrections, although ISE did not report spectral responsivity data.

ISE noted that light soaking affected the CdTe and CuIn(Ga)Se₂ I-V data; results were obtained after 20 min of 1000 W/m² soaking. A decreasing FF was observed in the a-Si bi cells. The reported data were from the initial measurements.

3.4.7 PTB

Differential spectral responsivity calibrations (see Section 2.4.6) were also used for the NT series. Following the I_{sc} calibrations, I-V curves were obtained. PTB did not report data for the concentrator module, nor for CuIn(Ga)Se₂ cell S31 because of the very low open-circuit voltage observed (< 70mV). Prior to arrival at PTB, S31 had obviously degraded or become defective.

3.4.8 USPL

USPL did not report any results for the PEP'93 Intercomparison.

3.4.9 TIPS

Most of the I-V data reported by TIPS were obtained under a Xe solar simulator with the irradiance level set against a reference cell. A filtered Si cell was used for the a-Si devices, a GaAs reference for the GaAs cells, and crystalline Si reference cells for the large-area LCIE devices and

the ESTI sensors. The high- and low-pass Si cells and the CdTe cells were calibrated with the procedure described above (see Section 2.4.8) because similar reference cells were not available. TIPS did not report spectral responsivity data, and did not report I-V data on the concentrator module, the TIPS large-area cells, nor the CuIn(Ga)Se₂ cells.

3.4.10 IACS

IACS used identical procedures to measure the NT series that were described previously (see Section 2.4.10). I-V data were not reported for the large-area devices, the ESTI sensors, the concentrator module, nor for CuIn(Ga)Se₂ cell S31.

3.4.11 NREL

Following the return of the samples, NREL repeated the measurements made at the beginning of the NT series circulation. Spectral responsivities were remeasured only on cells that were suspected of having changed during sample circulation. Complete I-V data for the concentrator module were reported, although the cell temperatures were 55°–60°C.

Remeasurements of the ESTI sensors and the LCIE modules showed that NREL's initial measurements appeared to have been made at temperatures well above 25°C.

NREL noted in December 1996 that PTB RS-41 and PTB RS-44 both had cracks in the filters over the solar cells. The cracks started at the same location at a single point on the edge of the filter and progressed inward. PTB RS-41 had just a single crack about 5 mm long, but PTB RS-44 had a network of cracks, one of which extended over the solar cell (see Fig. 3-7).

3.5 Data Analysis Procedures

At the final meeting of the participants, attendees discussed how the NT series measurement results should be presented and made the following recommendations. First, the reported V_{oc} , I_{sc} , FF, and P_{max} results should be normalized by the average value for each device, with obvious outliers excluded from the device averages. An obvious outlier was defined as a normalized result that exceeded 1.00 ± 0.10 of the average for all reporting laboratories. Efficiency should not be analyzed because only four laboratories actually measured the device areas (see Section 3.6.6). Reported SR data should be area-normalized and the deviations from the averages calculated using the same procedure as the WPVS data (see Section 2.6). The deviations were not calculated as the differences from a qualified average, as was the case for the WPVS data; rather, the deviations were from an overall average of all the SR data available for each device.

3.6 Reported Results

3.6.1 Open-Circuit Voltage

Table 3-3 contains the open-circuit voltage data reported by the laboratories, and Figs. 3-12, 3-16, 3-20, 3-24, and 3-28 show the same data normalized by the device averages. These data are summarized in Fig. 3-32, which shows the standard deviations of the normalized open-circuit voltages for each of the device types.

Table 3-3. Reported device open-circuit voltages (V). The columns are in order of circulation.

ID	NREL	JQA/ETL	SNL	ESTI	ISE	PTB	TIPS	IACS	NREL
CuIn(Ga)Se ₂ S11	0.464	0.432	0.436	0.435	0.446	0.431		0.400	0.409
CuIn(Ga)Se ₂ S31	0.471	0.438	0.438	0.435	0.407				0.121
CdTe 9321	0.711	0.718	0.724	0.715	0.717	0.726	0.729	0.730	0.735
CdTe 9324	0.722	0.725	0.730	0.726	0.727	0.731	0.724	0.730	0.731
a-Si bi-cell 9306	1.754	1.758	1.744	1.761	1.763	1.740	1.758	1.760	1.740
a-Si bi-cell 9307	1.649	1.656	1.641	1.651	1.653	1.639	1.681	1.660	1.654
a-Si tand. 9312	3.432	3.476	3.410	3.422	3.470	3.465	3.477	3.430	3.474
a-Si tand. 9313	3.404	3.449	3.400	3.423	3.448	3.458	3.499	3.430	3.479
LP Si PTB RS-41	0.575	0.579	0.575	0.574	0.579	0.573	0.580	0.580	0.574
LP Si PTB RS-44	0.574	0.579	0.576	0.578	0.579	0.577	0.579	0.580	0.574
HP Si PTB RS-64	0.575	0.583	0.585	0.582	0.582	0.584	0.578	0.580	0.574
HP Si PTB RS-74	0.576	0.584	0.585	0.583	0.583	0.582	0.581	0.580	0.576
GaAs SNL003	1.000	1.007	1.005	1.008	1.003	0.998	0.996	1.010	1.000
GaAs SNL-04	1.003	1.010	1.008	1.008	1.005	1.003	0.997	1.010	1.005
10×10 Si TIPS 1	0.567	0.570	0.569	0.573	0.574	0.556			0.568
10×10 Si TIPS 2	0.575	0.581	0.579	0.582	0.582	0.567			0.577
ESTI sensor 1	0.559	0.587	0.562	0.590	0.579	0.580	0.584		0.579
ESTI sensor 2	0.562	0.589	0.578	0.590	0.567	0.578	0.597		0.580
Module LCIE 1	0.541	0.591	0.591	0.592	0.595	0.551	0.599		0.593
Module LCIE 2	0.545	0.592	0.591	0.592	0.595	0.551	0.586		0.598
GaAs Conc. 1		1.182	1.195	1.190	1.184				1.131
GaAs Conc. 2		1.180	1.195	1.190	1.185				1.130

3.6.2 Short-Circuit Current

Table 3-4 contains the short-circuit current data reported by the laboratories, and Figs. 3-13, 3-17, 3-21, 3-25, and 3-29 show the same data normalized by the device averages. These data are summarized in Fig. 3-33, which shows the standard deviations of the normalized short-circuit currents for each of the device types.

Table 3-4. Reported device short-circuit currents (mA). The columns are in order of circulation.

ID	NREL	LCIE	JQA/ETL	SNL	ESTI	ISE	PTB	TIPS	IACS	NREL
CuIn(Ga)Se ₂ S11	32.40		33.03	33.39	33.37	32.38	32.93		31.60	32.38
CuIn(Ga)Se ₂ S31	32.37		31.84	31.70	32.74	30.67				18.13
CdTe 9321	51.82		54.83	53.95	57.25	53.11	54.80	54.83	54.00	56.55
CdTe 9324	56.41		55.88	55.47	59.39	55.03	57.36	56.74	55.75	58.91
a-Si bi-cell 9306	26.39		25.25	25.67	26.42	25.14	24.99	26.59	27.50	26.34
a-Si bi-cell 9307	26.75		25.44	25.83	25.78	25.24	25.53	26.29	27.62	26.20
a-Si tand. 9312	13.91		13.78	13.56	12.08	13.54	14.14	12.94	14.65	14.04
a-Si tand. 9313	13.95		13.76	13.11	13.22	13.78	14.13	12.97	14.75	14.18
LP Si PTB RS-41	74.85	72.00	72.57	72.39	73.56	71.12	72.42	71.81	72.50	73.68
LP Si PTB RS-44	72.05	65.00	69.91	69.72	70.32	68.48	69.45	69.24	70.00	70.35
HP Si PTB RS-64	66.52	70.00	69.82	67.89	71.38	68.65	67.97	70.68	67.70	69.21
HP Si PTB RS-74	66.15	70.00	69.57	67.64	71.22	68.50	67.93	70.82	68.00	69.37
GaAs SNL003	106.80		106.10	106.71	109.03	103.00	105.03	105.70	100.50	107.90
GaAs SNL-04	74.02		74.02	74.20	75.51	72.60	73.16	73.20	70.50	74.28
10×10 Si TIPS 1	2750	2550	2771	2769	2866	2880	2725			2754
10×10 Si TIPS 2	2617	2440	2647	2642	2704	2689	2603			2576
ESTI sensor 1	1466	1490	1484	1017		1462	1516	1386		1465
ESTI sensor 2	1473	1480	1487	1021		1470	1510	1386		1471
Module LCIE 1	2747	2580	2796	2760	2795	2728	2792	2713		2747
Module LCIE 2	2740	2460	2777	2757	2772	2725	2729	2688		2740
GaAs Conc. 1	3870		3558	3800	3954	3254				3046
GaAs Conc. 2	3830		3533	3800	3901	3261				2620

3.6.3 Fill Factor

Table 3-5 contains the FF data reported by the laboratories, and Figs. 3-14, 3-18, 3-22, 3-26, and 3-30 show the same data normalized by the device averages. These data are summarized in Fig. 3-34, which shows the standard deviations of the normalized fill factors for each of the device types.

Table 3-5. Reported device fill factors. The columns are in order of circulation.

ID	NREL	JQA/ETL	SNL	ESTI	ISE	PTB	TIPS	IACS	NREL
CuIn(Ga)Se ₂ S11	0.590	0.554	0.561	0.535	0.584	0.325		0.497	0.504
CuIn(Ga)Se ₂ S31	0.647	0.540	0.536	0.541	0.418				0.251
CdTe 9321	0.518	0.527	0.522	0.530	0.533	0.521	0.531	0.530	0.534
CdTe 9324	0.545	0.543	0.539	0.545	0.546	0.539	0.546	0.531	0.548
a-Si bi-cell 9306	0.602	0.610	0.618	0.610	0.611	0.602	0.622	0.614	0.622
a-Si bi-cell 9307	0.606	0.610	0.614	0.627	0.604	0.586	0.624	0.613	0.618
a-Si tand. 9312	0.625	0.549		0.598	0.553	0.594	0.566	0.553	0.558
a-Si tand. 9313	0.652	0.657		0.732	0.665	0.714	0.692	0.670	0.680
LP Si PTB RS-41	0.770	0.767	0.760	0.769	0.766	0.769	0.786	0.743	0.771
LP Si PTB RS-44	0.789	0.788	0.787	0.790	0.788	0.788	0.803	0.763	0.787
HP Si PTB RS-64	0.734	0.735	0.740	0.704	0.733	0.736	0.744	0.721	0.735
HP Si PTB RS-74	0.755	0.753	0.757	0.770	0.752	0.754	0.768	0.737	0.756
GaAs SNL003	0.795	0.787	0.792	0.812	0.797	0.793	0.798	0.778	0.794
GaAs SNL-04	0.644	0.636	0.635	0.649	0.644	0.644	0.649	0.635	0.648
10×10 Si TIPS 1	0.638	0.640	0.636	0.634	0.641	0.635			0.599
10×10 Si TIPS 2	0.667	0.669	0.666	0.664	0.670	0.668			0.640
ESTI sensor 1	0.321	0.335	0.416		0.316	0.325	0.348		0.319
ESTI sensor 2	0.321	0.335	0.428		0.319	0.321	0.366		0.323
Module LCIE 1	0.523	0.648	0.655	0.653	0.653	0.634	0.632		0.628
Module LCIE 2	0.523	0.649	0.657	0.591	0.648	0.636	0.616		0.619
GaAs Conc. 1		0.808	0.830	0.816	0.831				0.820
GaAs Conc. 2		0.833	0.830	0.843	0.844				0.842

3.6.4 Maximum Power

Table 3-6 contains the maximum power data reported by the laboratories, and Figs. 3-15, 3-19, 3-23, 3-27, and 3-31 show the same data normalized by the device averages. These data are summarized in Fig. 3-35, which shows the standard deviations of the normalized maximum powers for each of the device types. Note that SNL did not report maximum power for the NT series devices; the data in Table 3-6 were calculated from the reported efficiency and device area.

Table 3-6. Reported device maximum powers (mW). The columns are in order of circulation.

ID	NREL	JQA/ETL	SNL	ESTI	ISE	PTB	TIPS	IACS	NREL
CuIn(Ga)Se2 S11	8.86	7.91	8.17	7.78	8.43	7.76		6.28	6.68
CuIn(Ga)Se2 S31	9.87	7.53	7.44	7.71	5.21				0.55
CdTe 9321	20.73	20.72	20.37	21.71	20.27	20.74	21.24	20.88	22.21
CdTe 9324	22.20	22.01	21.83	23.52	21.84	22.63	22.40	21.60	23.58
a-Si bi-cell 9306	27.88	27.07	27.70	28.39	27.10	26.16	29.08	29.70	28.50
a-Si bi-cell 9307	26.73	25.72	26.05	26.69	25.19	24.50	27.56	28.13	26.76
a-Si tand. 9312	29.82	26.29		24.73	25.98	29.11	25.44	27.81	27.24
a-Si tand. 9313	30.94	31.19		33.15	31.60	34.89	31.40	33.89	33.53
LP Si PTB RS-41	33.12	32.23	31.63	32.43	31.54	31.94	32.76	31.01	32.62
LP Si PTB RS-44	32.61	31.90	31.63	32.09	31.23	31.55	32.00	30.96	31.86
HP Si PTB RS-64	28.09	29.95	29.34	29.26	29.27	29.22	30.48	28.32	29.24
HP Si PTB RS-74	28.76	30.56	29.95	31.95	30.03	29.79	31.60	29.06	30.17
GaAs SNL003	84.90	84.08	85.01	89.25	83.74	83.14	84.08	78.95	85.67
GaAs SNL-04	47.76	47.55	47.49	49.40	47.28	47.21	47.32	45.24	48.42
10×10 Si TIPS 1	983	1011	1002	1042	1012	962			936
10×10 Si TIPS 2	995	1028	1018	1045	1020	985			951
ESTI sensor 1	263	292	237		267	286	282		271
ESTI sensor 2	266	294	252		266	280	303		275
Module LCIE 1	778	1071	1071	1080	1060	975	1028		1024
Module LCIE 2	781	1067	1067	970	1051	956	962		1015
GaAs Conc. 1		3396	3751	3840	3202				2859
GaAs Conc. 2		3473	3751	3912	3261				2521

3.6.5 Spectral Responsivity

The spectral responsivity data (available on the companion CD-ROM) were analyzed according to Section 3.5. Note that the IACS SR data were excluded from the averages used to calculate the spectral deviations.

3.6.6 Device Area

Table 3-7 contains the areas of the NT devices reported by the participating laboratories. Note that PTB and TIPS gave estimates of the areas, while LCIE and IACS did not report any areas.

3.7 Discussion

3.7.1 II-VI Thin-Film Devices

Figs. 3-12 through 3-15 show the reported results for the II-VI thin-film devices normalized by the device averages. Note that LCIE did not measure these devices. The most striking features are the large variations for the CuIn(Ga)Se₂ devices. Comparison of the initial and final data reported by NREL shows that the V_{oc} of both devices degraded, especially S31 (0.471 to 0.121 V). S31 had a

Table 3-7. NT series reported device areas (mm²)

ID	NREL	JQA/ETL	SNL	ESTI	ISE	PTB	TIPS
S11	9.96	11.0	9.84	11.6	9.89	10	
S31	9.96	11.0	9.84	11.7	9.90		
9321	49.97	40.0	39.02	40.0	39.68	40	40
9324	51.81	40.0	38.98	40.0	39.73	40	40
9306	44.70	40.0	40.55	40.0	40.90	40	40
9307	45.20	40.0	40.32	40.0	40.68	40	40
9312	39.91	40.0	39.66	40.0	40.00	40	40
9313	39.97	40.0	39.59	40.0	40.01	40	40
PTB RS-41	41.68	40.0	41.29	44.1	41.70	40	40
PTB RS-44	41.36	40.0	41.46	44.1	41.80	40	40
PTB RS-64	41.52	40.0	39.59	44.1	39.99	40	40
PTB RS-74	41.52	40.0	39.56	44.1	39.89	40	40
SNL003	41.11	40.0	40.83	44.1	41.23	40	40
SNL-04	41.28	40.0	40.73	44.1	41.22	40	40
TIPS 1	972.8	975.4	965.1	976	969.9	980	
TIPS 2	967.2	975.4	963.6	976	969.2	980	
ESTI 1	994.2	487.0	484.6	486	487.9	490	500
ESTI 2	985.0	487.0	484.6	486	487.7	490	500
LCIE 1	1011	1020	1014.0	1000	1021	1000	1000
LCIE 2	1011	1020	1020.0	1000	1025	1000	1000
Conc. 1	2045	1909	1905.0	2000	1909		
Conc. 2	2016	1909	1905.0	2000	1909		

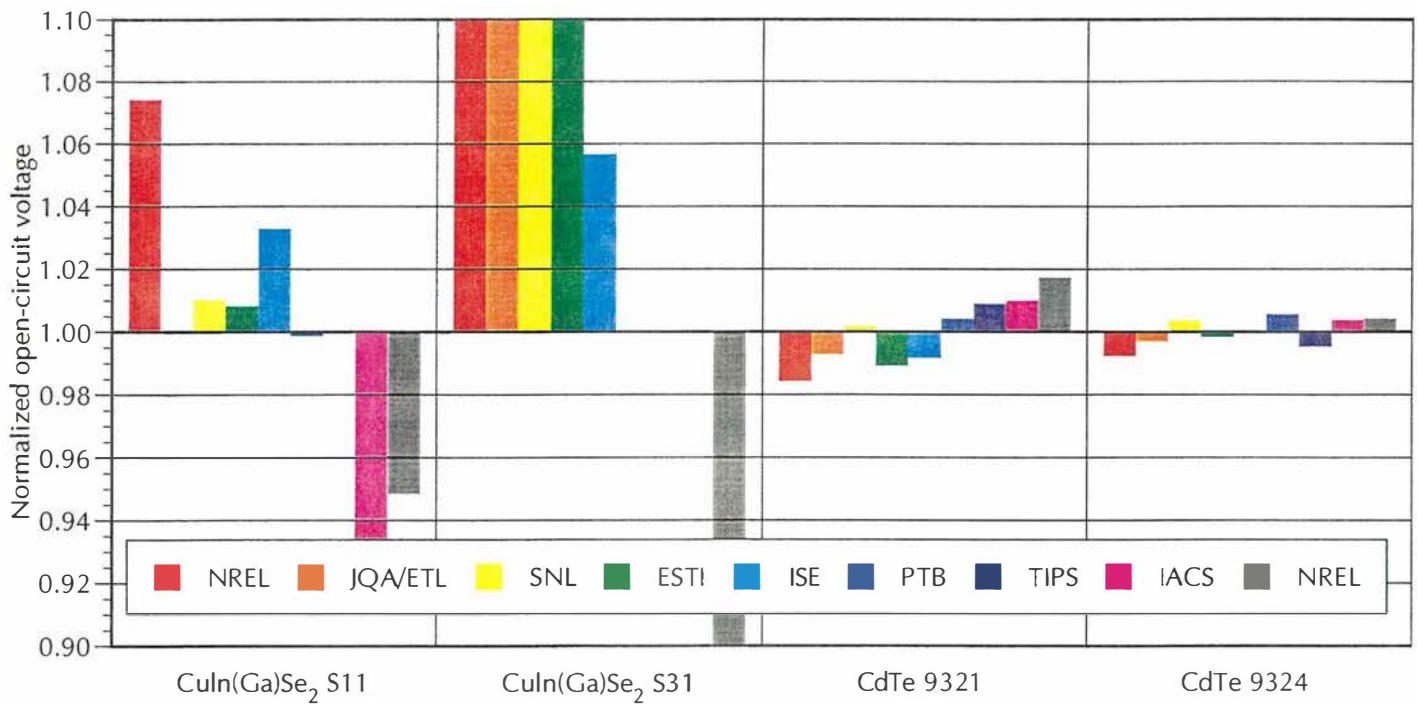


Figure 3-12. Reported open-circuit voltage data for the NT series II-VI thin-film cells normalized by the device averages. The laboratory bars for each device are in order of circulation.

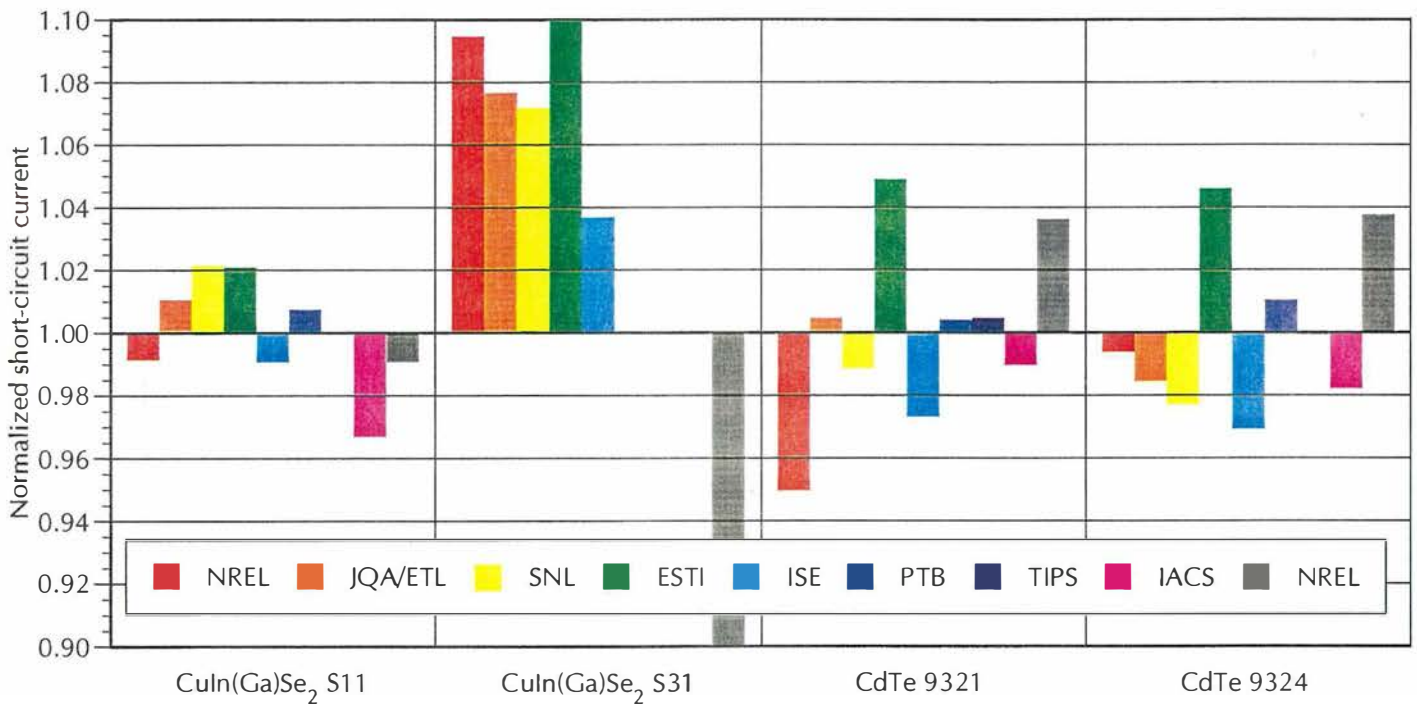


Figure 3-13. Reported short-circuit current data for the NT series II-VI thin-film cells normalized by the device averages. The laboratory bars for each device are in order of circulation.

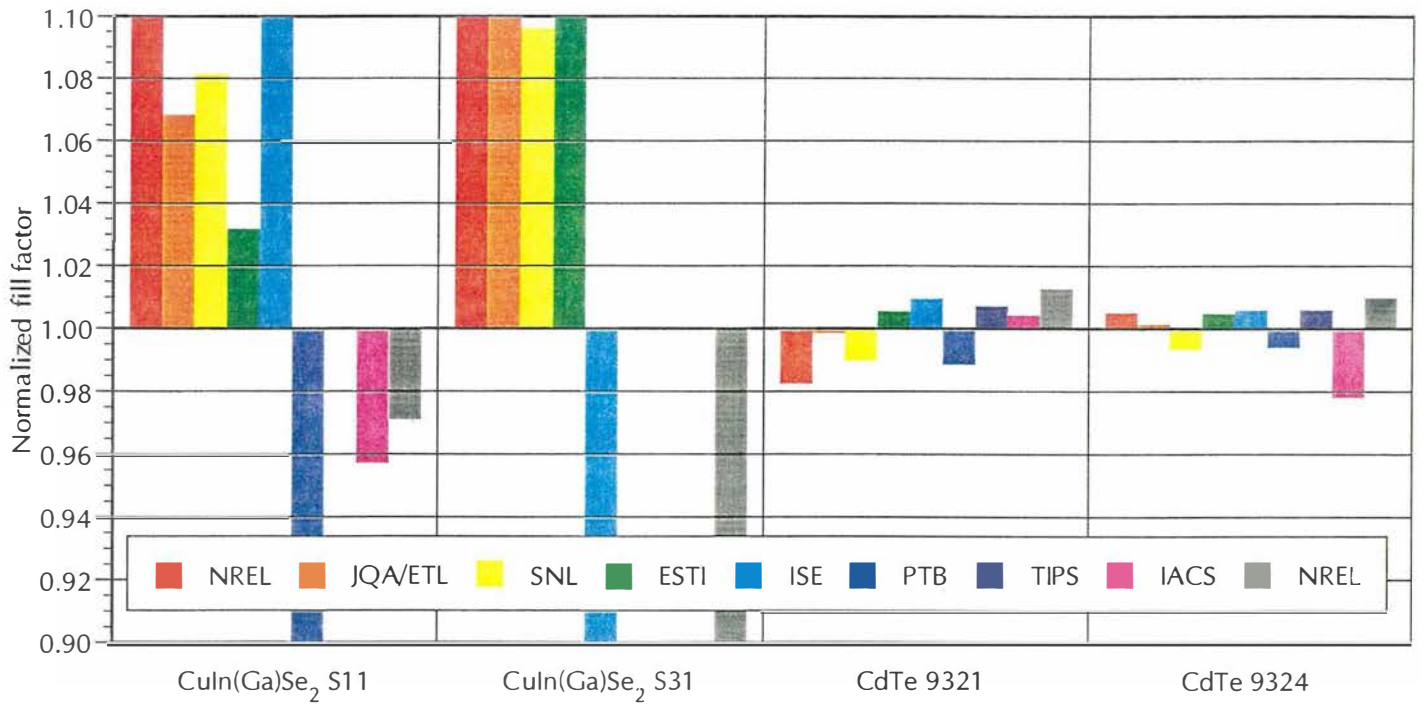


Figure 3-14. Reported FF data for the NT series II-VI thin-film cells normalized by the device averages. The laboratory bars for each device are in order of circulation.

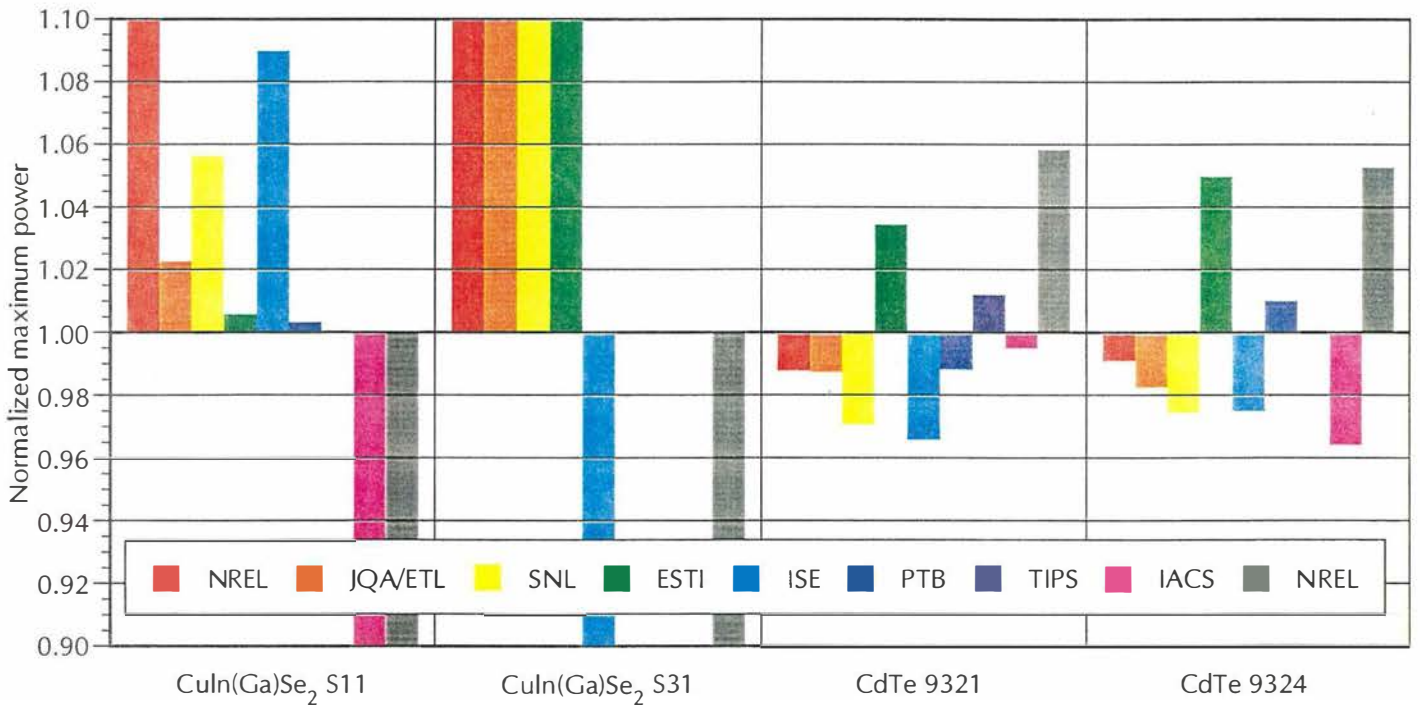


Figure 3-15. Reported maximum power data for the NT series II-VI thin-film cells normalized by the device averages. The laboratory bars for each device are in order of circulation.

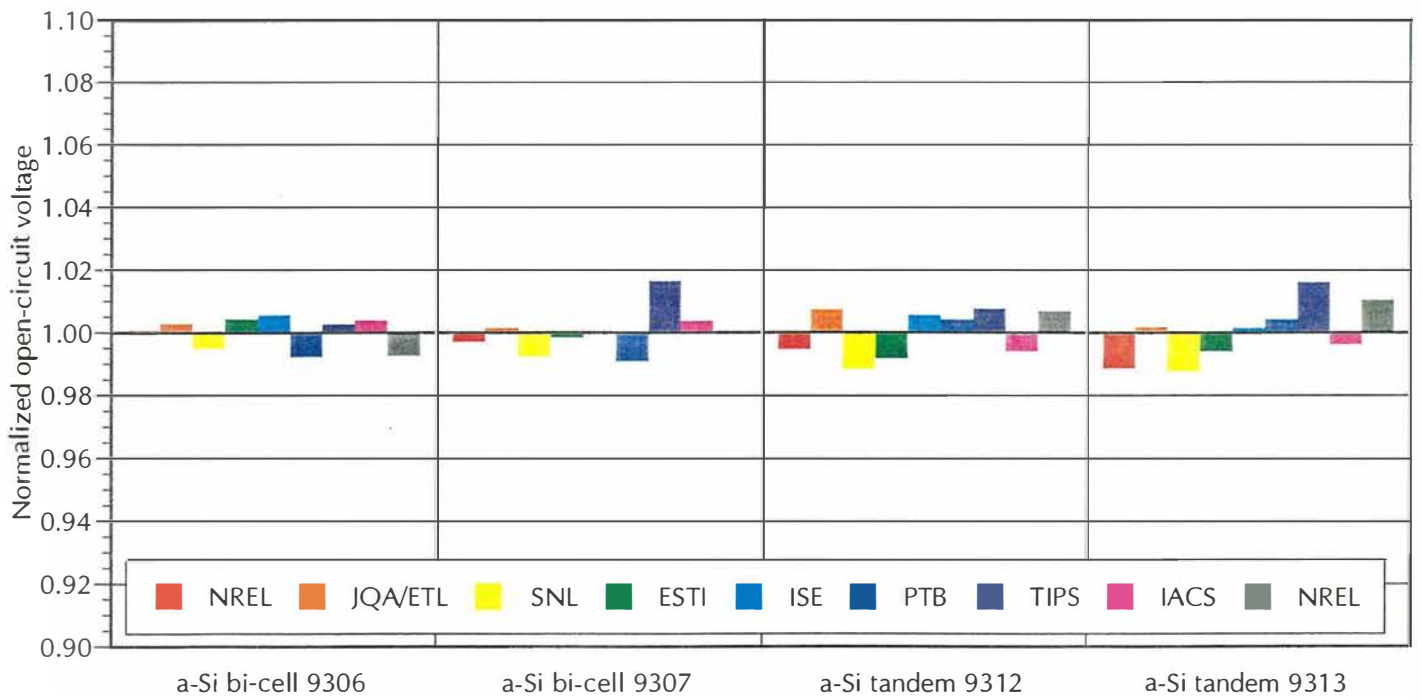


Figure 3-16. Reported open-circuit voltage data for the NT series a-Si cells normalized by the device averages. The laboratory bars for each device are in order of circulation.

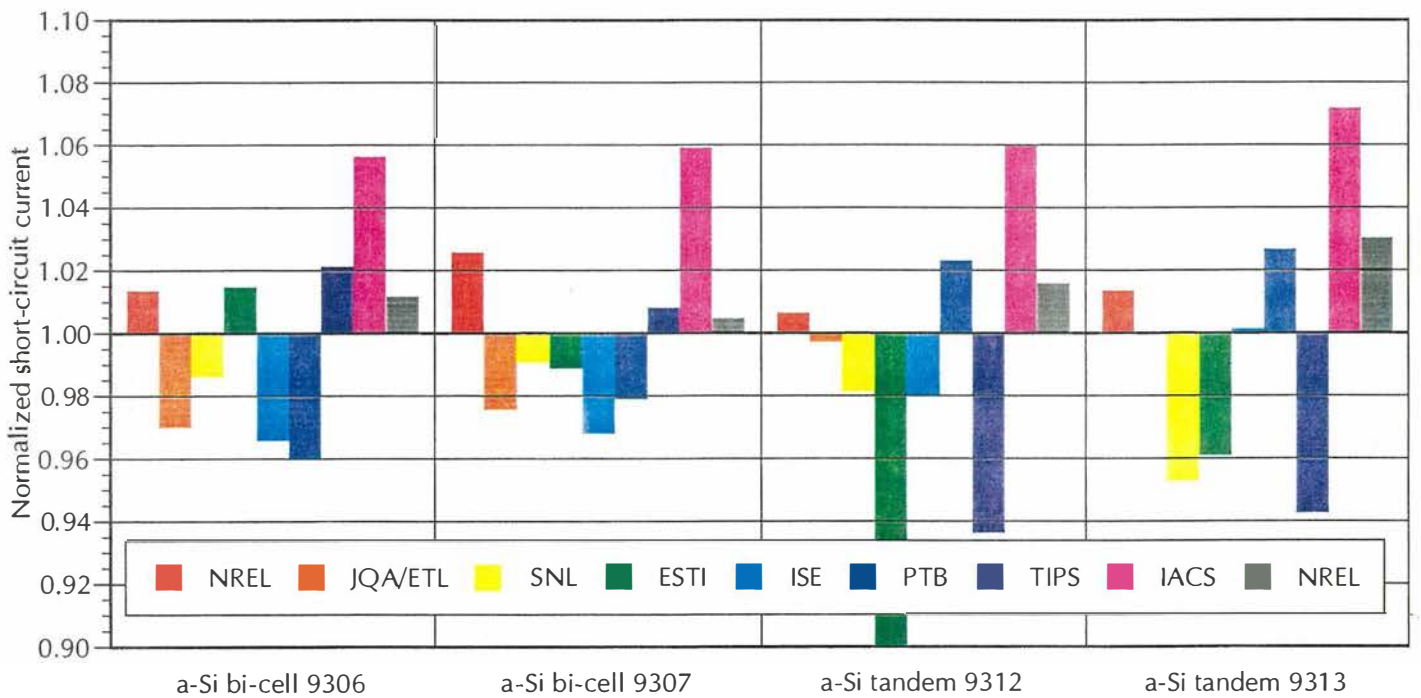


Figure 3-17. Reported short-circuit current data for the NT series a-Si cells normalized by the device averages. The laboratory bars for each device are in order of circulation.

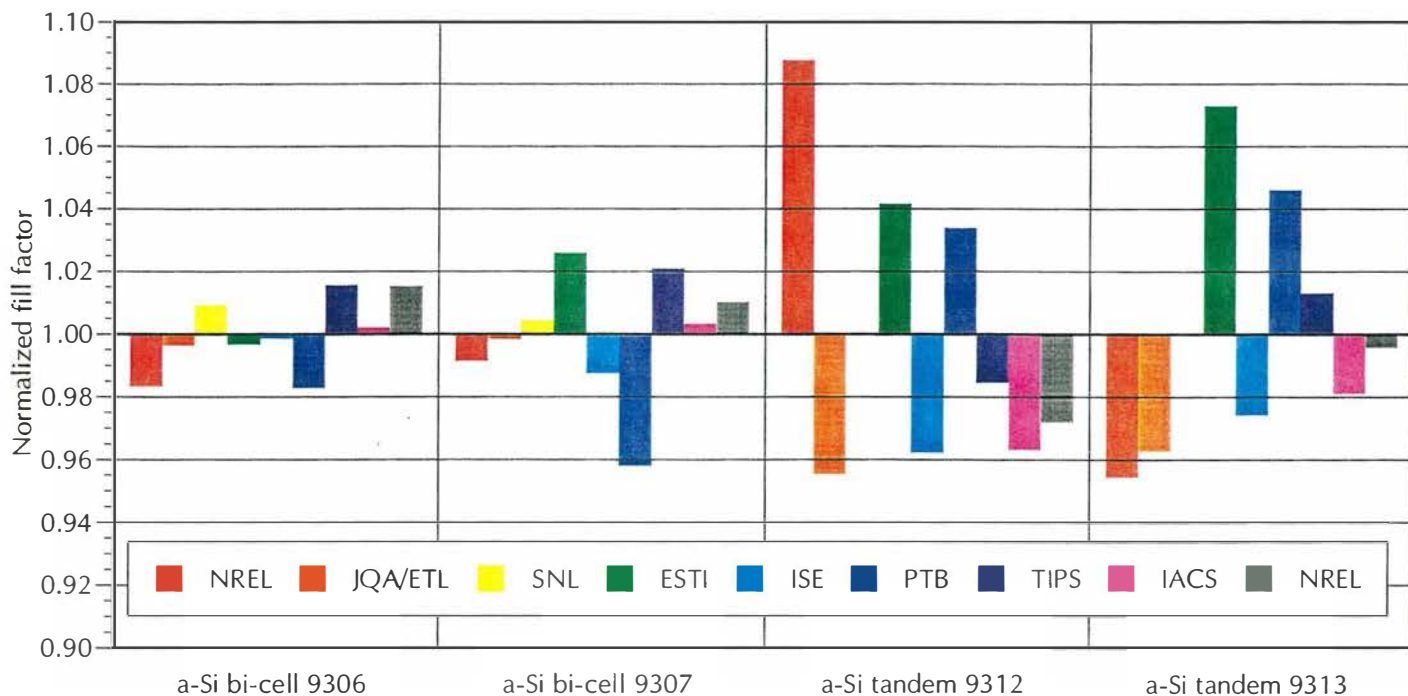


Figure 3-18. Reported FF data for the NT series a-Si cells normalized by the device averages. The laboratory bars for each device are in order of circulation.

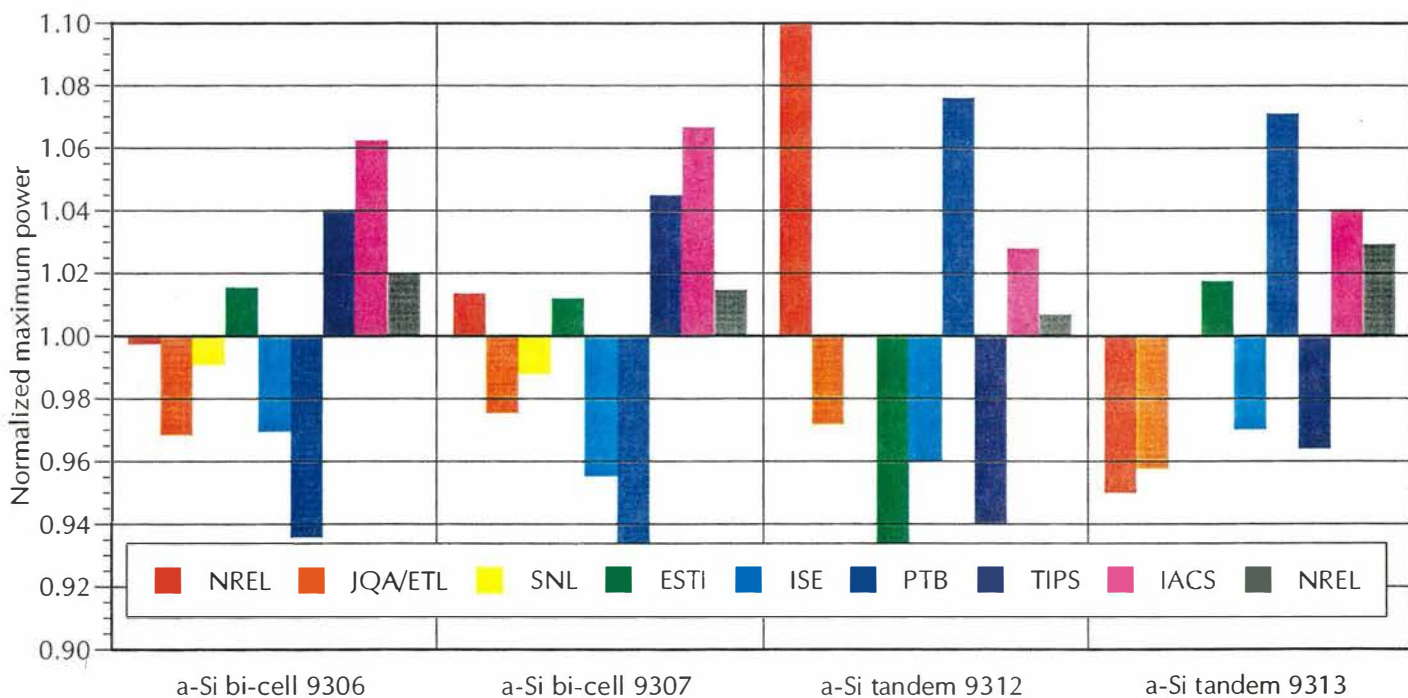


Figure 3-19. Reported maximum power data for the NT series a-Si cells normalized by the device averages. The laboratory bars for each device are in order of circulation.

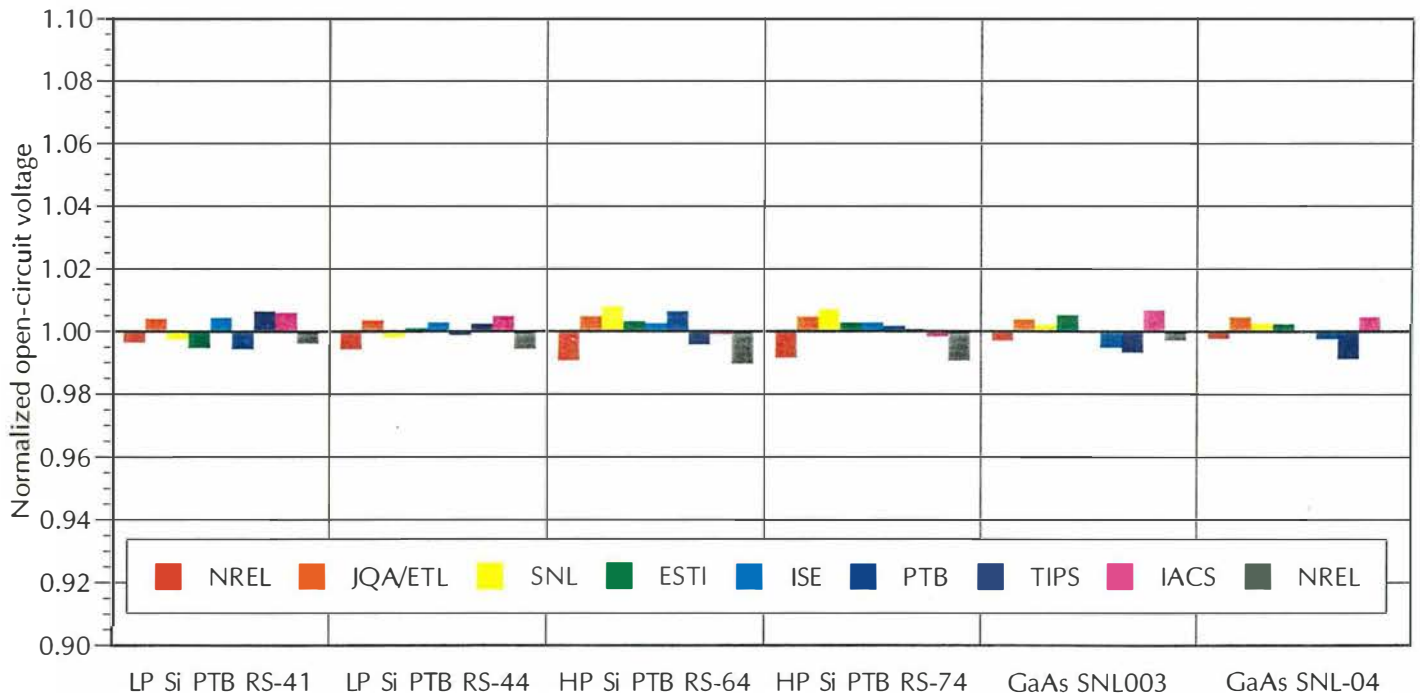


Figure 3-20. Reported open-circuit voltage data for the NT series non-silicon SR cells normalized by the device averages. The laboratory bars for each device are in order of circulation.

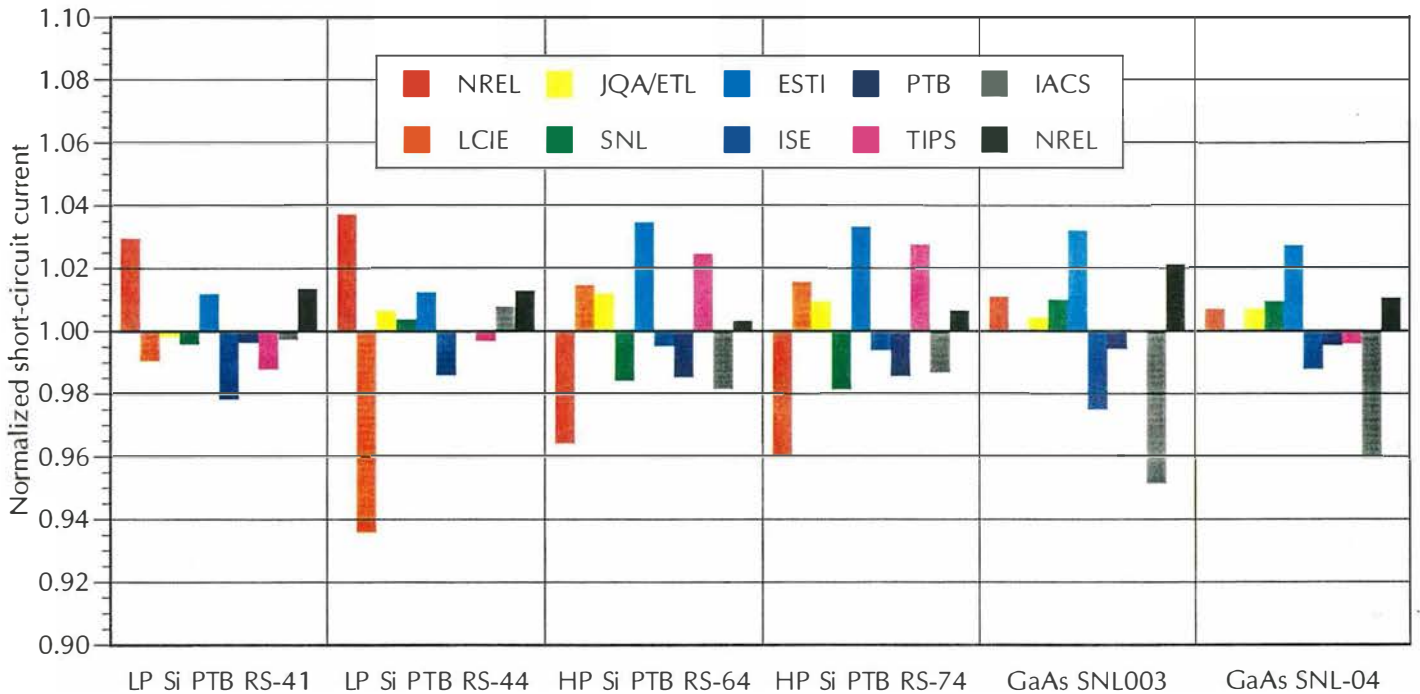


Figure 3-21. Reported short-circuit current data for the NT series non-silicon SR cells normalized by the device averages. The laboratory bars for each device are in order of circulation.

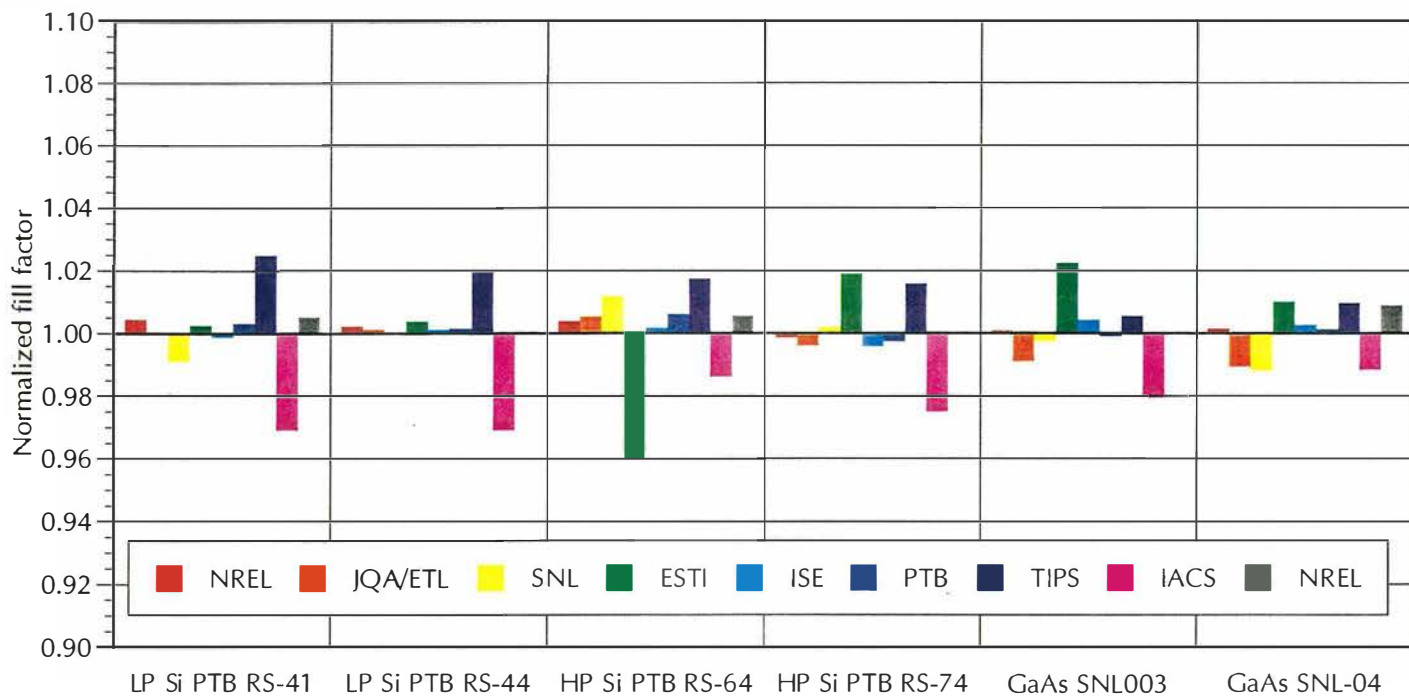


Figure 3-22. Reported FF data for the NT series non-silicon SR cells normalized by the device averages. The laboratory bars for each device are in order of circulation.

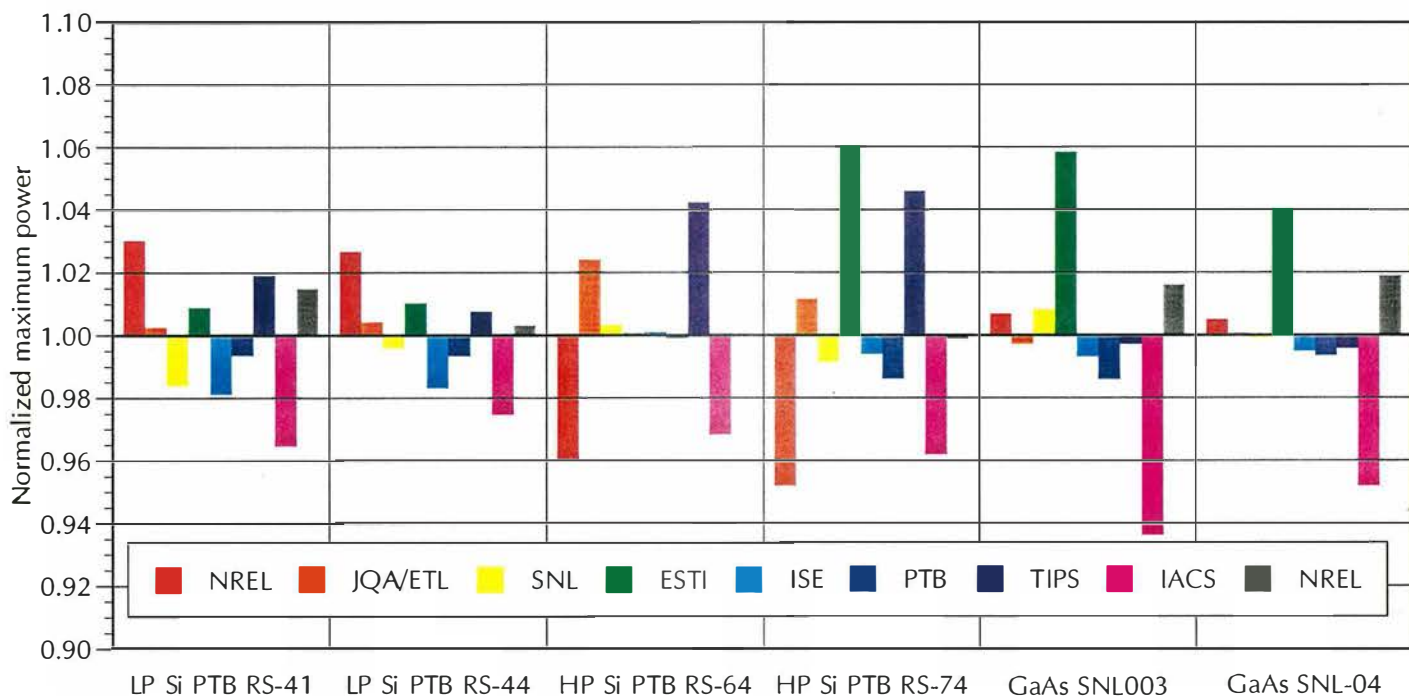


Figure 3-23. Reported maximum power data for the NT series non-silicon SR cells normalized by the device averages. The laboratory bars for each device are in order of circulation.

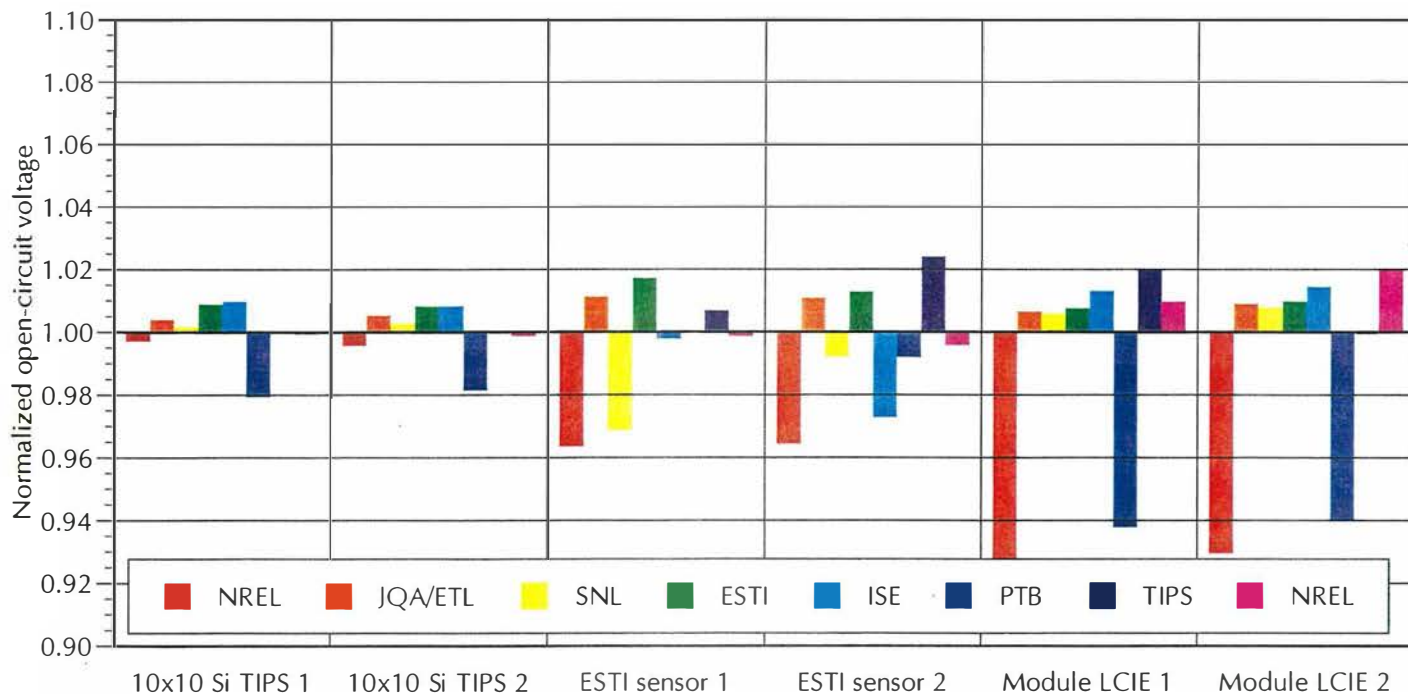


Figure 3-24. Reported open-circuit voltage data for the NT series large-area devices normalized by the device averages. The laboratory bars for each device are in order of circulation.

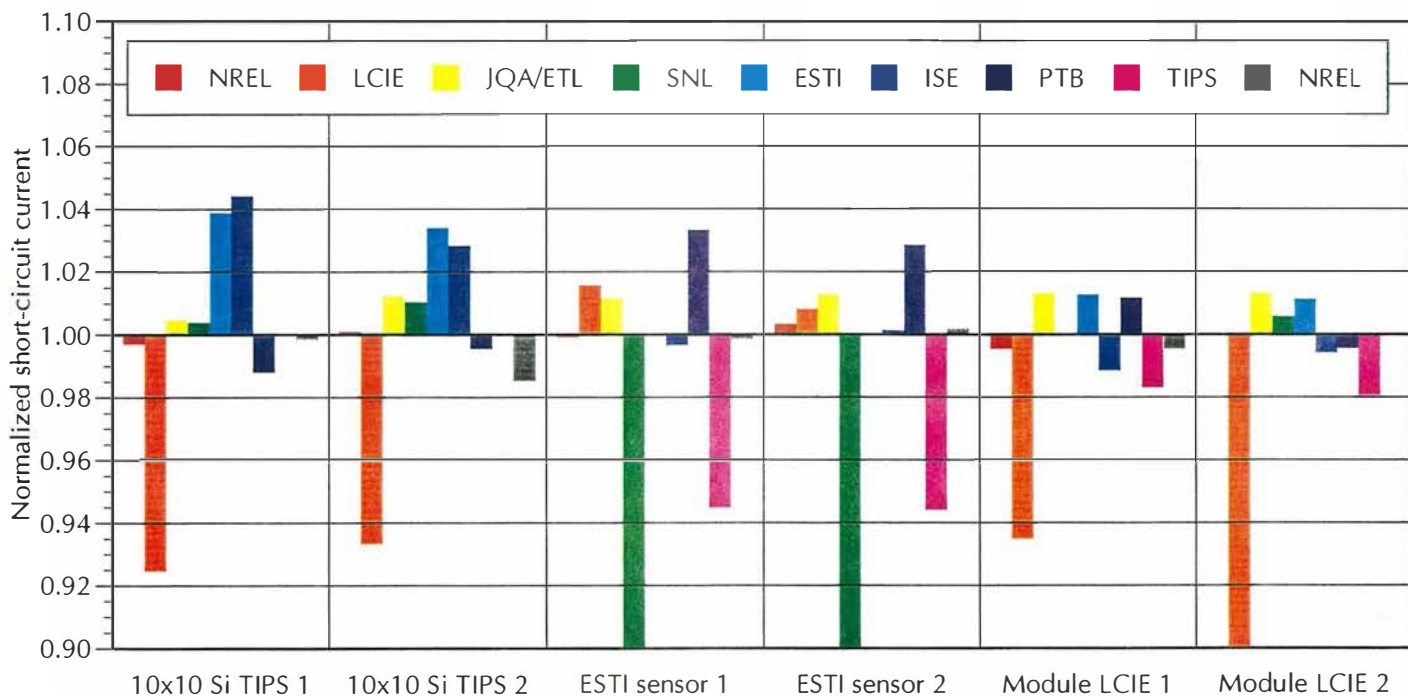


Figure 3-25. Reported short-circuit current data for the NT series large-area devices normalized by the device averages. The laboratory bars for each device are in order of circulation.

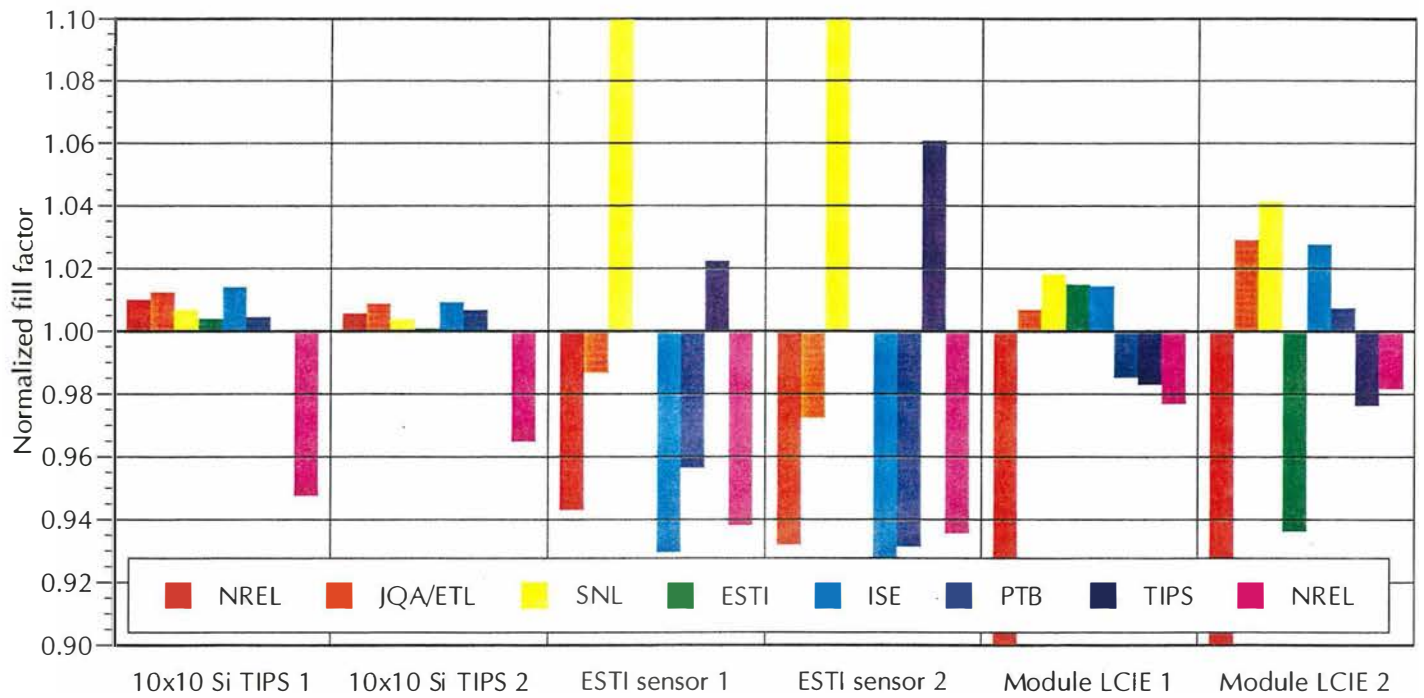


Figure 3-26. Reported FF data for the NT series large-area devices normalized by the device averages. The laboratory bars for each device are in order of circulation.

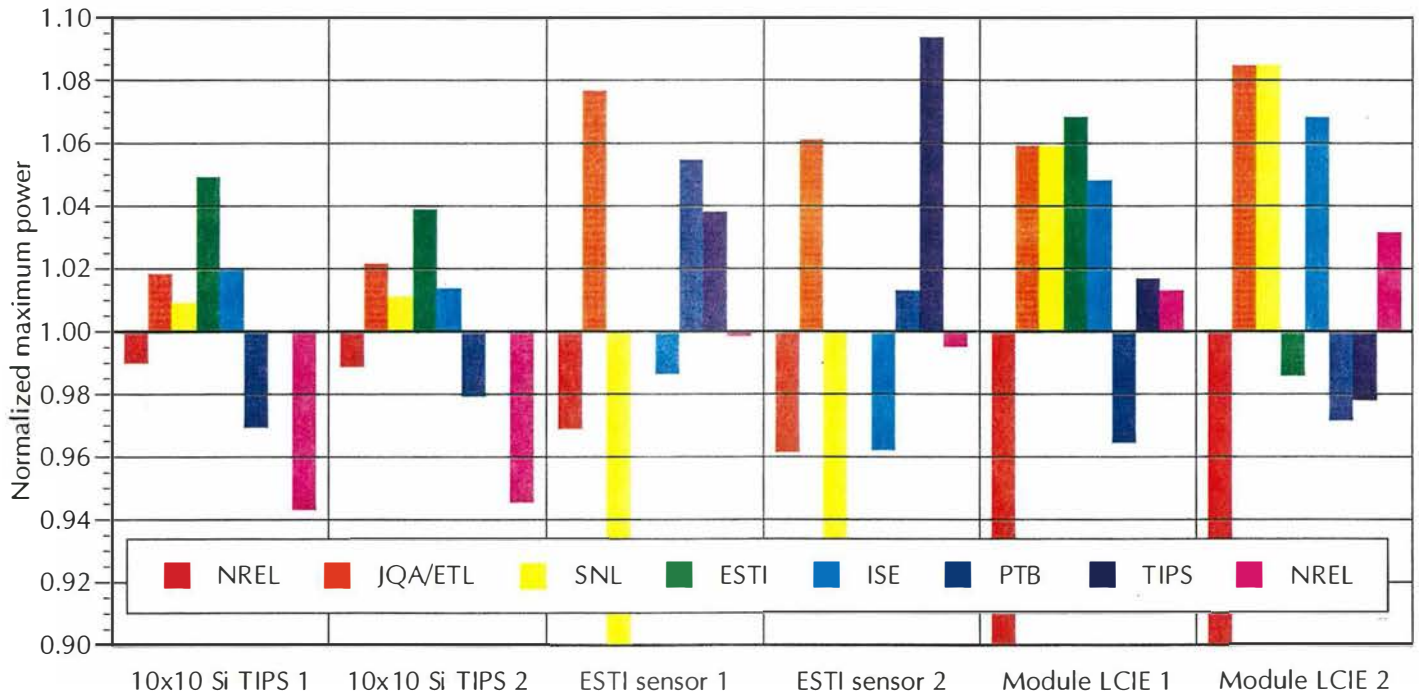


Figure 3-27. Reported maximum power data for the NT series large-area devices normalized by the device averages. The laboratory bars for each device are in order of circulation.

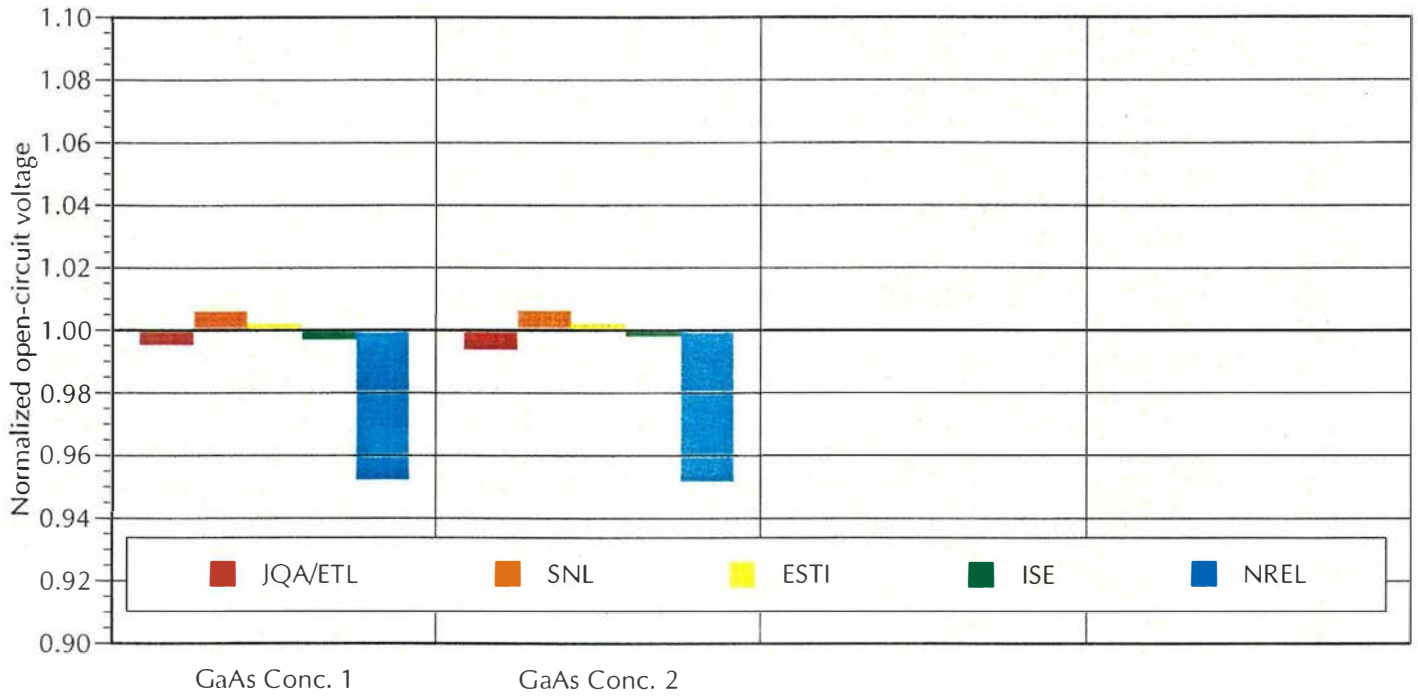


Figure 3-28. Reported open-circuit voltage data for the NT series GaAs concentrator module normalized by the device averages. The laboratory bars for each cell are in order of circulation.

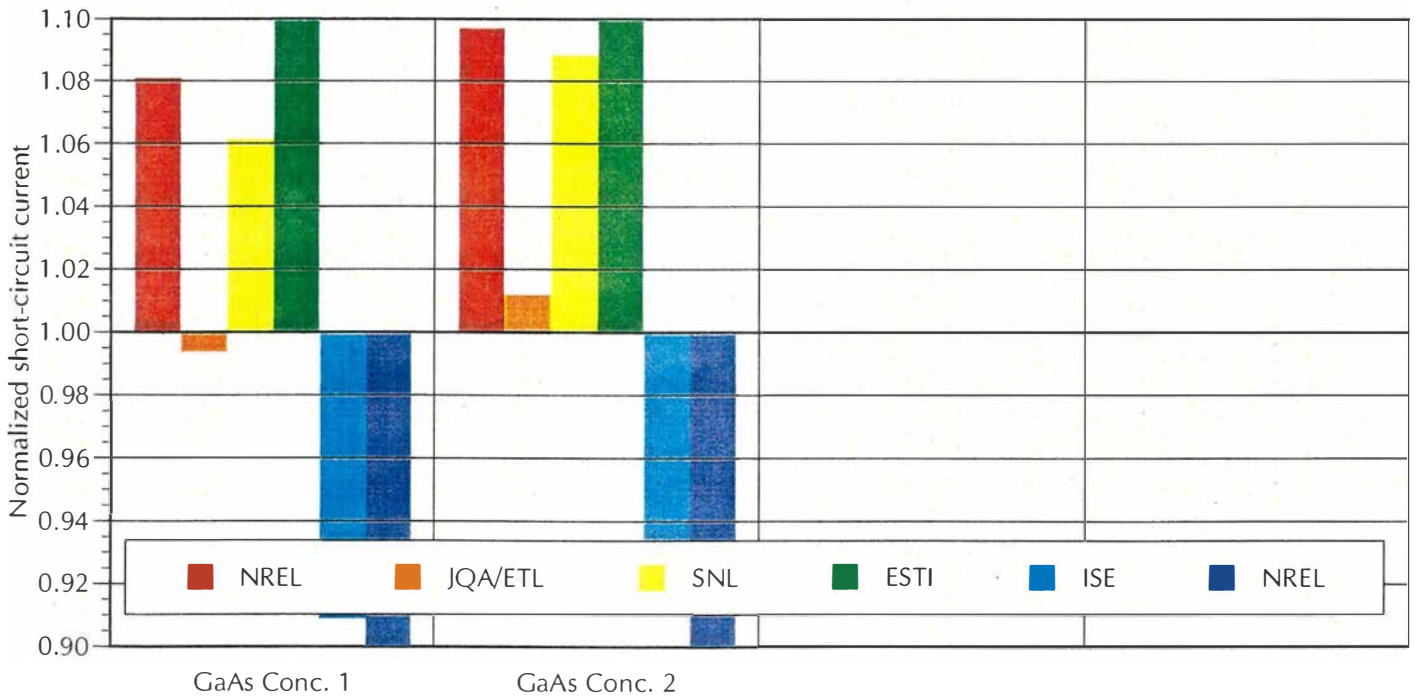


Figure 3-29. Reported short-circuit current data for the NT series GaAs concentrator module normalized by the device averages. The laboratory bars for each cell are in order of circulation.

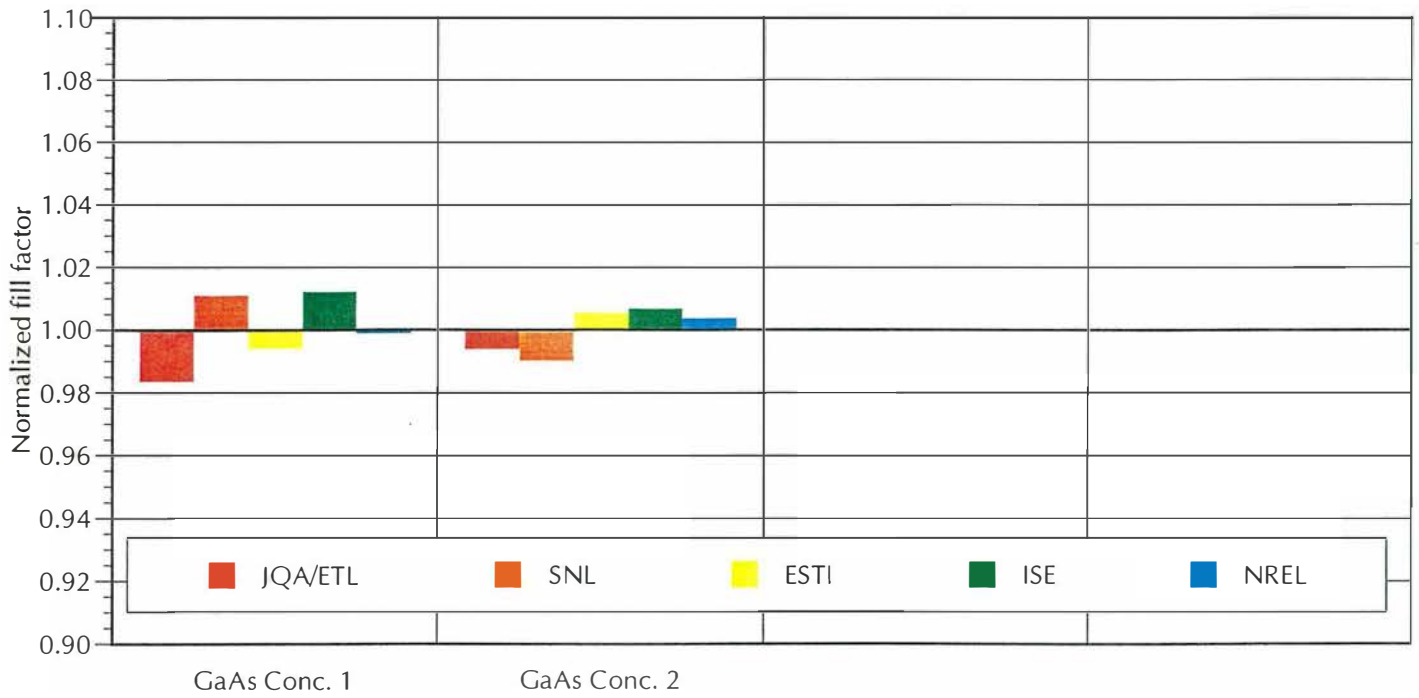


Figure 3-30. Reported FF data for the NT series GaAs concentrator module normalized by the device averages. The laboratory bars for each cell are in order of circulation.

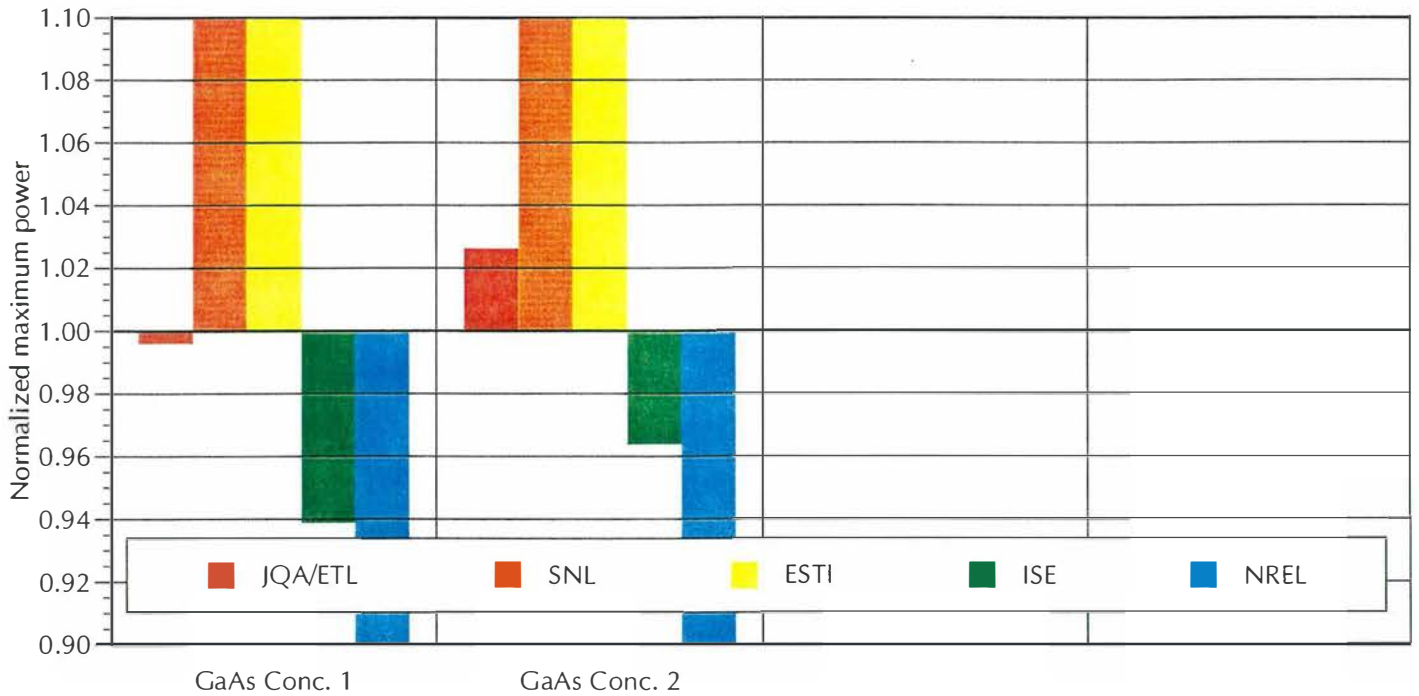


Figure 3-31. Reported maximum power data for the NT series GaAs concentrator module normalized by the device averages. The laboratory bars for each cell are in order of circulation.

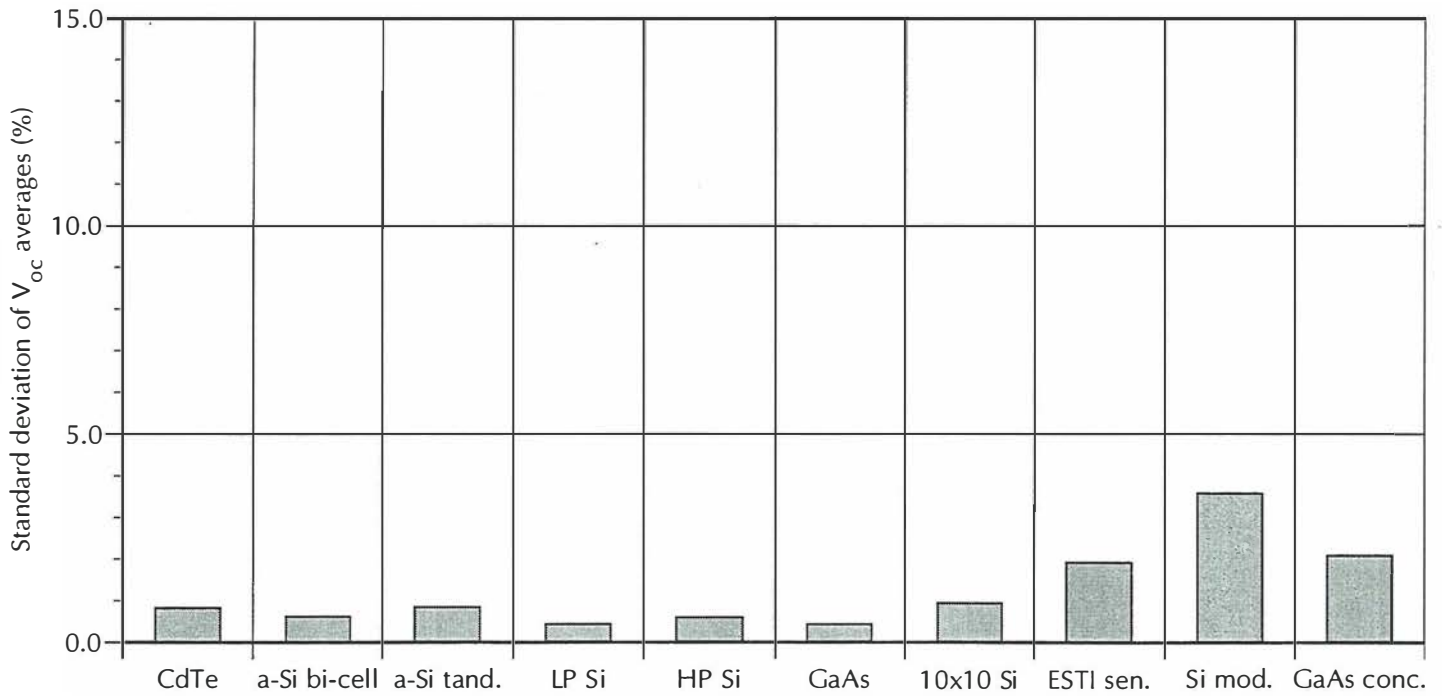


Figure 3-32. Standard deviation (%) of the reported open-circuit voltage data normalized by the device averages, for each device type in the NT series sample set.

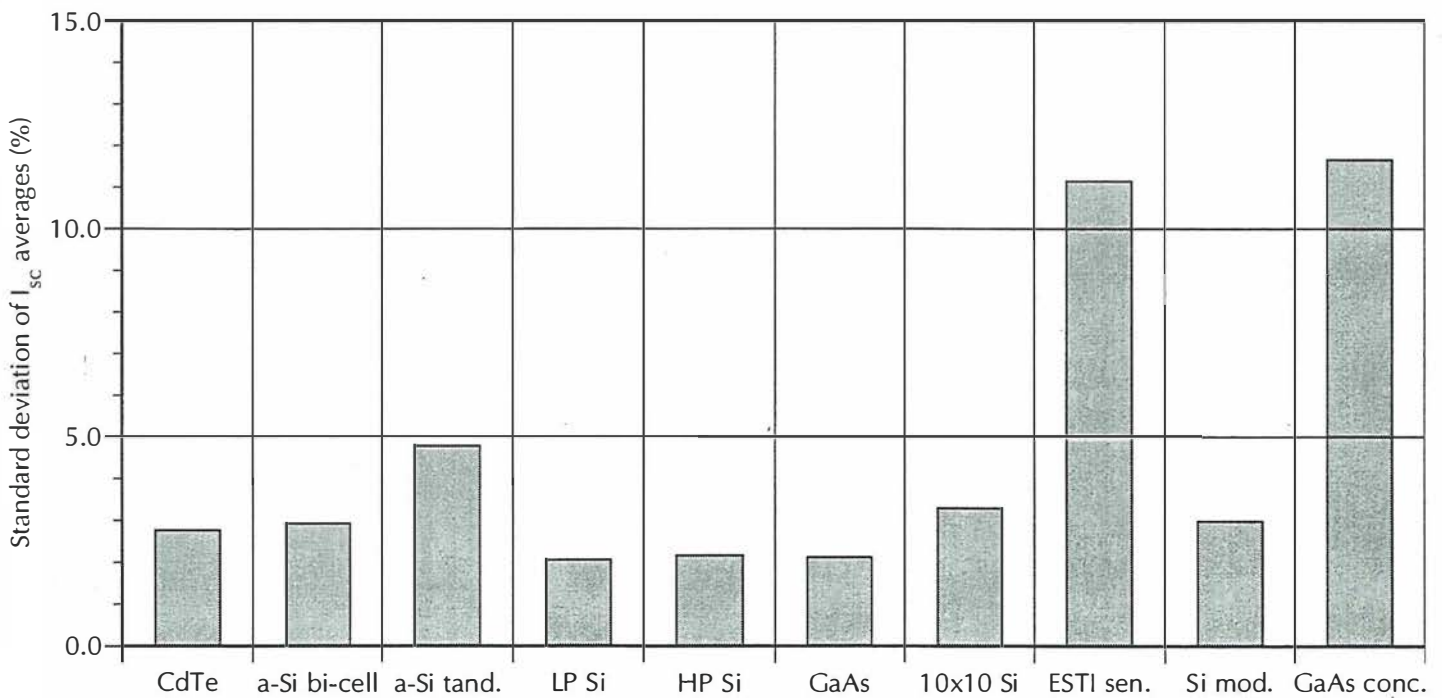


Figure 3-33. Standard deviation (%) of the reported short-circuit current data normalized by the device averages, for each device type in the NT series sample set.

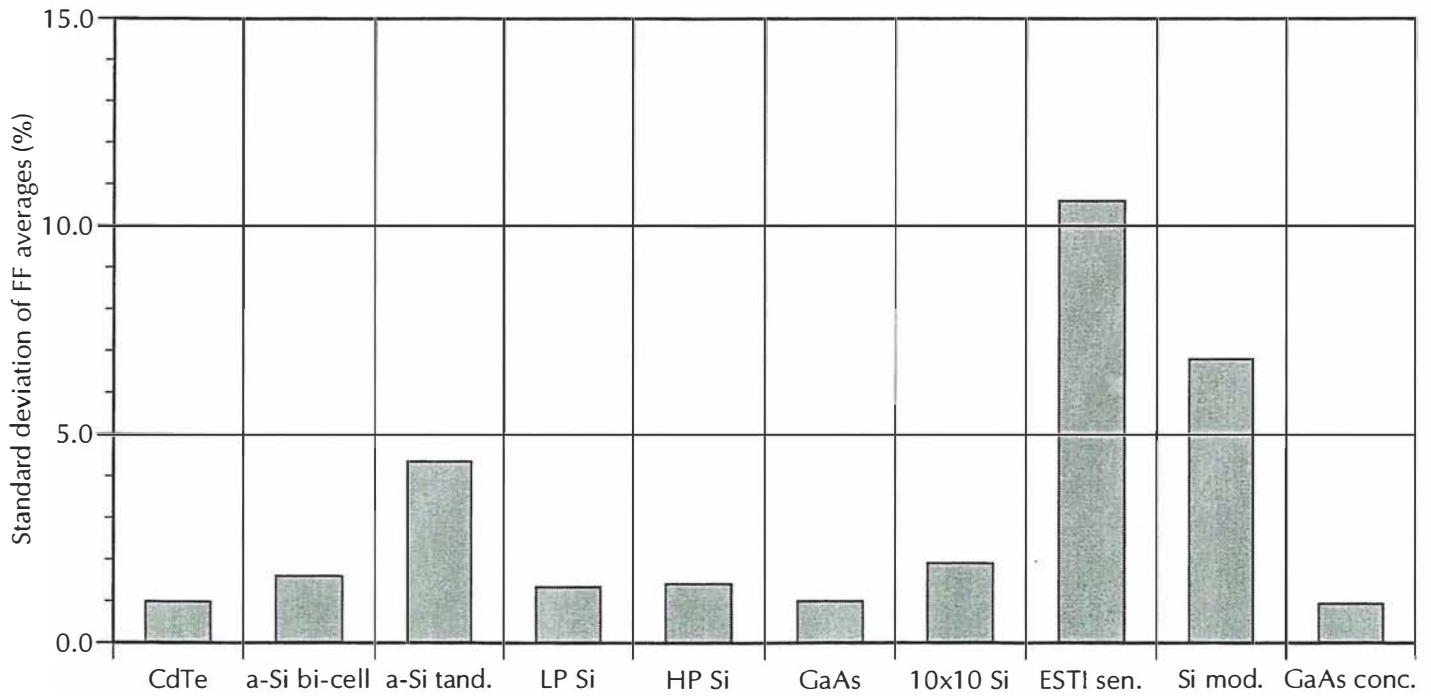


Figure 3-34. Standard deviation (%) of the reported FF data normalized by the device averages, for each device type in the NT series sample set.

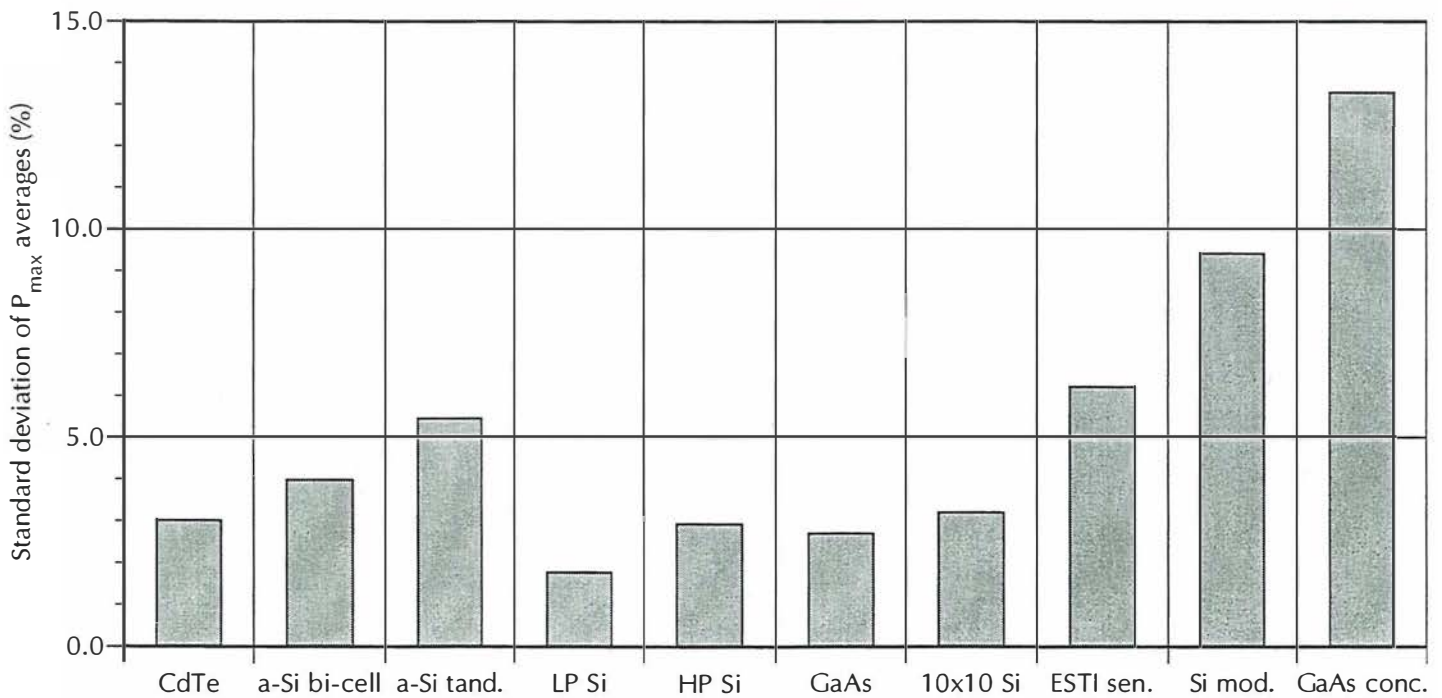


Figure 3-35. Standard deviation (%) of the reported maximum power data normalized by the device averages, for each device type in the NT series sample set.

large degradation of the I_{sc} , while the I_{sc} for S11 shows good agreement. Examination of the actual NREL I-V curves showed S11 with a decreased shunt resistance that reduced the FF from 0.590 to 0.504. Cell S31 appeared to be completely shorted because the I-V curve was a straight line. It is not possible to draw any further conclusions from these results.

Examination of the normalized results for the CdTe devices shows very close agreement for V_{oc} and FF with about 1% standard deviation, and significantly higher variation for I_{sc} and P_{max} (about 3% standard deviation). ISE noted that I_{sc} decreased with time under illumination, so the variations may be due to the well-known inherent instabilities in CdTe devices

With the exception of the IACS data, the SR results show reasonable agreement (see Figs. 3-36 through 3-39). The possible problems with the IACS measurements were discussed above (see Section 2.8.3). The largest variations are seen in the long wavelength cutoffs where the SR is changing rapidly because of the direct bandgap of these devices. Spectral bandwidth differences between measurement systems cause differences in the slope of the cutoff in this region. Figs. 3-37 and 3-38 indicate that the NREL SR measurement system was improved during the time between the initial and final NT measurements.

3.7.2 Amorphous Silicon Thin-Film Devices

The normalized I-V parameter results are shown in Figs. 3-16 through 3-19, and the area normalized SR results are in Figs. 3-40 through 3-45. Note again that LCIE did not measure these devices. The V_{oc} has good agreement, but the other parameters show much less agreement. Also, the single junction bi-cells (9306 and 9307) have better agreement than the dual junction tandem cells (9312 and 9313). This should be expected because both the I_{sc} and FF of multijunction devices are functions of the incident spectral irradiance and only NREL, ISE, JQA/ETL, and SNL used multisource simulator techniques to measure the tandem cells. The IACS I_{sc} data appear to be anomalously high in Fig. 3-17.

Results of the spectral responsivity analysis are plotted in Figs. 3-40 through 3-45. Although ESTI and PTB both reported SR data for the a-Si tandem cells, they did not measure the top and bottom junctions independently. Measuring both junctions at the same time results in a convolution of the response over the range where both junctions respond (about 500 to 700 nm). For this reason, the ESTI and PTB SR data were not analyzed and do not appear in Figs. 3-42 through 3-45.

The SR results on the a-Si bi-cells (Figs. 3-40 and 3-41) show good agreement, with the exception of the ESTI data, which show problems below 400 nm. For the tandem cells, the agreement is poorer, especially for the top cell of 9312 (Fig. 3-42). A comparison of Figs. 3-42 and

3-44 suggests that the SNL data for the 9312 top cell may have problems. The bottom cell measurements also have significant variations, with some structure at 650 nm near the peak response that was not detected by JQA/ETL.

3.7.3 Non-Silicon Spectral Responsivity Devices

Figs. 3-20 through 3-23 present the normalized I-V parameters for the filtered Si and GaAs devices. The V_{oc} measurements agree with standard deviations of less than 1%, the I_{sc} standard deviations are 3 times larger. Fill factor results are somewhat better, with the exception of ESTI, IACS, and TIPS, which appear to be outliers. NREL's initial I_{sc} measurements of the filtered Si cells appear in Fig. 3-21 to be outliers with the low-pass Si higher, and the high-pass lower. The NREL final measurements do not show this bias. The cracked windows on PTB RS-41 and PTB RS-44 do not appear to have affected the results for these cells.

Even though these three types of devices have very dissimilar spectral responses, Figs. 3-32 through 3-35 do not show any great differences in the standard deviations between them. The standard deviations for these devices as a group are the lowest in the NT series.

With the exception of the IACS data, the spectral responsivity results (Figs. 3-46 through 3-51) are reasonably close. The LCIE data for PTB RS-44 (low-pass Si) are significantly different, which most probably caused the LCIE I_{sc} result for this cell to be anomalously low (Fig. 3-21). In general, there is more SR scatter for the GaAs devices compared to the filtered Si.

3.7.4 Large-Area Devices

The normalized I-V parameters for the large area devices (Figs. 3-24 through 3-27) show large differences between the TIPS 10×10 cm cells, the ESTI sensors, and the LCIE 10×10 cm cells in the module packages. As described in Section 3-1, the TIPS cells had 4-pin connectors for Kelvin I-V measurements, the LCIE packages had two banana jacks, and the ESTI sensors contained two cells side by side, with one cell wired across an internal resistor.

Some of these differences are seen in the V_{oc} data, especially the NREL initial data. The NREL data for the ESTI sensors and the LCIE modules are low because the device temperatures during illumination were allowed to rise well above 25°C without cooling. Several other measurements are low, including ISE, SNL, and PTB. Because temperature control of the TIPS cells was easier, these two cells show the lowest differences while the LCIE modules show the highest.

Short-circuit current results show a number of outliers (see Fig. 3-25), including the LCIE data for the TIPS cells and the LCIE modules, the SNL and TIPS data for the ESTI sensors. The standard deviation for the ESTI sensors is very high at 11% (see Fig. 3-33).

Several conclusions can be drawn from the FF results for the large-area devices (Fig. 3-26). NREL reported that the TIPS cells were damaged prior to the final measurement, and this is seen in the reduced fill factors for these cells. NREL's initial measurements of the LCIE modules are quite low, and examination of the reported I-V curves showed an increased series resistance as compared to the final measurements. This eliminates damage as the problem, so the results were caused by a systematic error of some kind, which was probably the connections to the devices. ESTI's results for LCIE 2 also appear to be low. Even without considering outliers, the scatter for the LCIE modules is still high. The FF scatter for the ESTI sensors is even higher and is probably caused by the long two-wire contacts to these cells.

The maximum power results also show large variations (Fig. 3-27).

The spectral responsivity results (Figs. 3-52 through 3-57) show a number of individual measurements with wavelength dependent differences, especially the NREL and ESTI curves. LCIE's data for the LCIE modules seem to have a shape error that is particularly evident in module #2.

3.7.5 GaAs Concentrator Module

Normalized I-V parameter results for the GaAs concentrator modules are presented in Figs. 3-28 through 3-31. Except for the NREL final measurements, which were not temperature corrected, the V_{oc} results are very close (Fig. 3-28). In Fig. 3-29, the ISE and NREL data are seen to be significantly lower than the previous measurements, including the NREL initial results. Although no damage to the module was visible, it is apparent that some change occurred during circulation. No changes of FF can be seen in Fig. 3-30, which indicates that misalignment of the optical elements is a strong possibility. The differences in maximum power (Fig. 3-31) are due to the losses of short-circuit current.

With only three or four data sets available for the spectral responsivity analysis (Figs. 3-58 and 3-59), it is difficult to form any conclusions about the results. Note that the SNL data in Fig. 3-58 have significant shape differences compared to the other three curves.

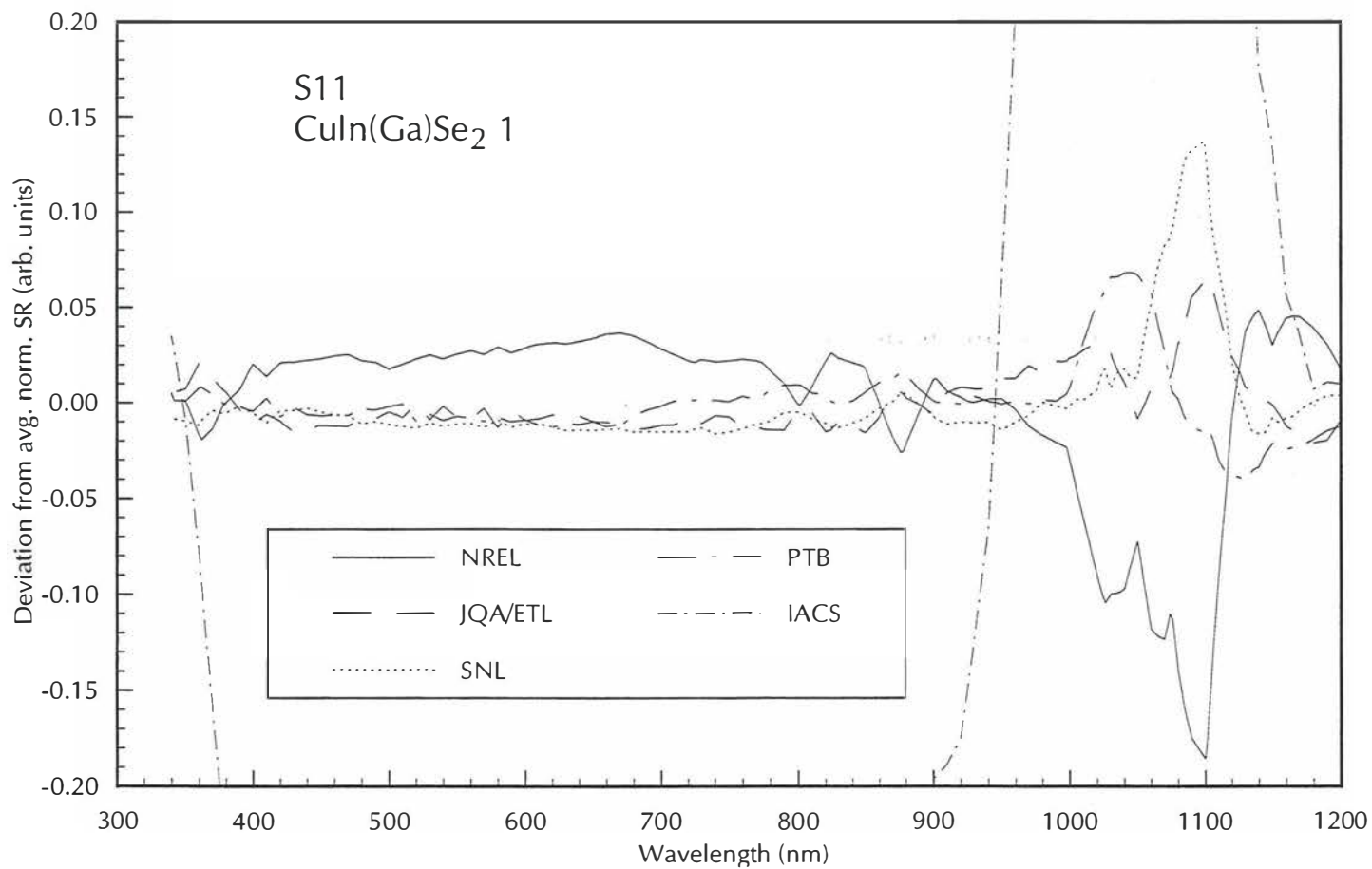
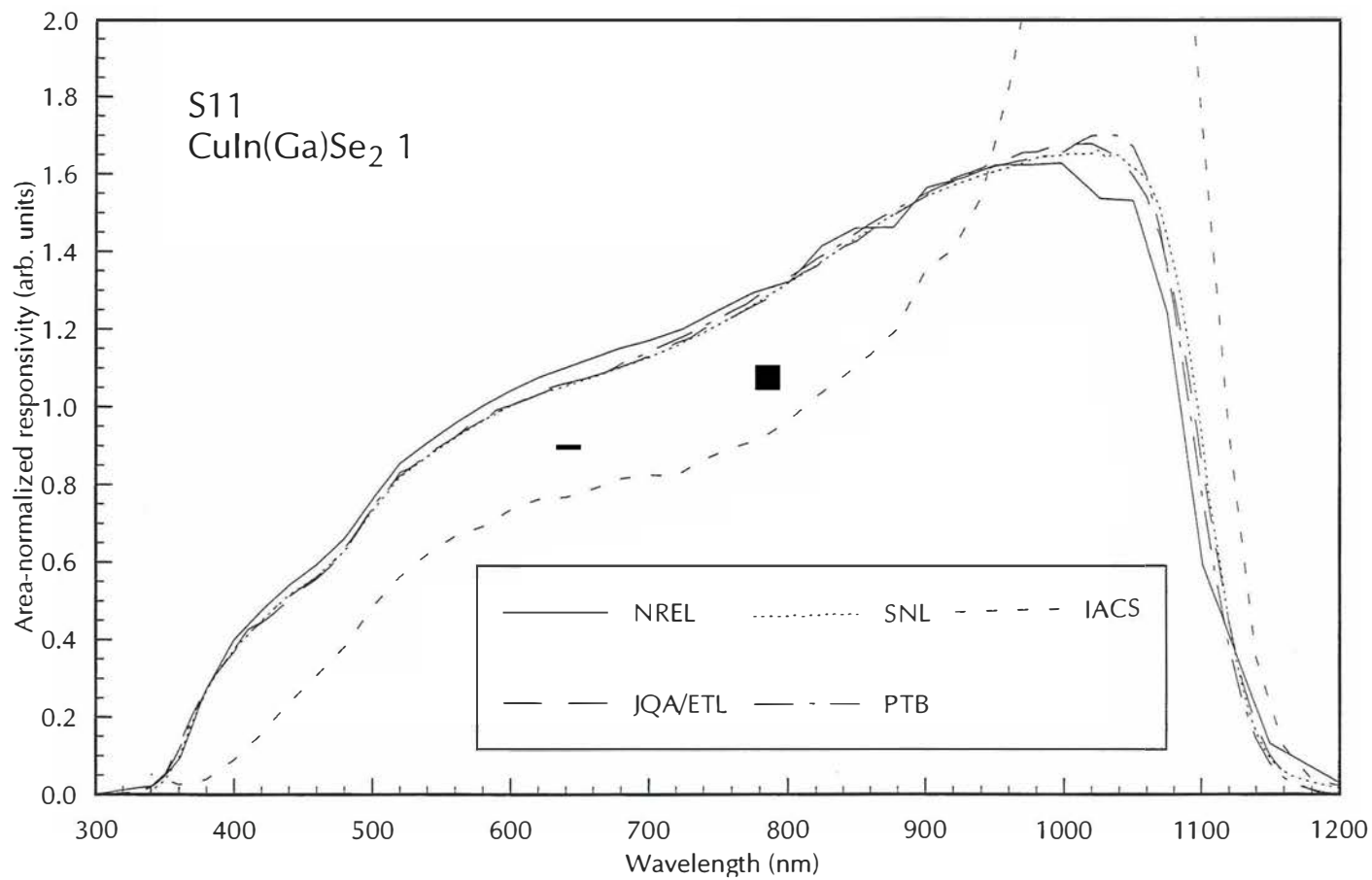


Figure 3-36. Area-normalized SR and deviation from average SR for CuIn(Ga)Se₂ S11

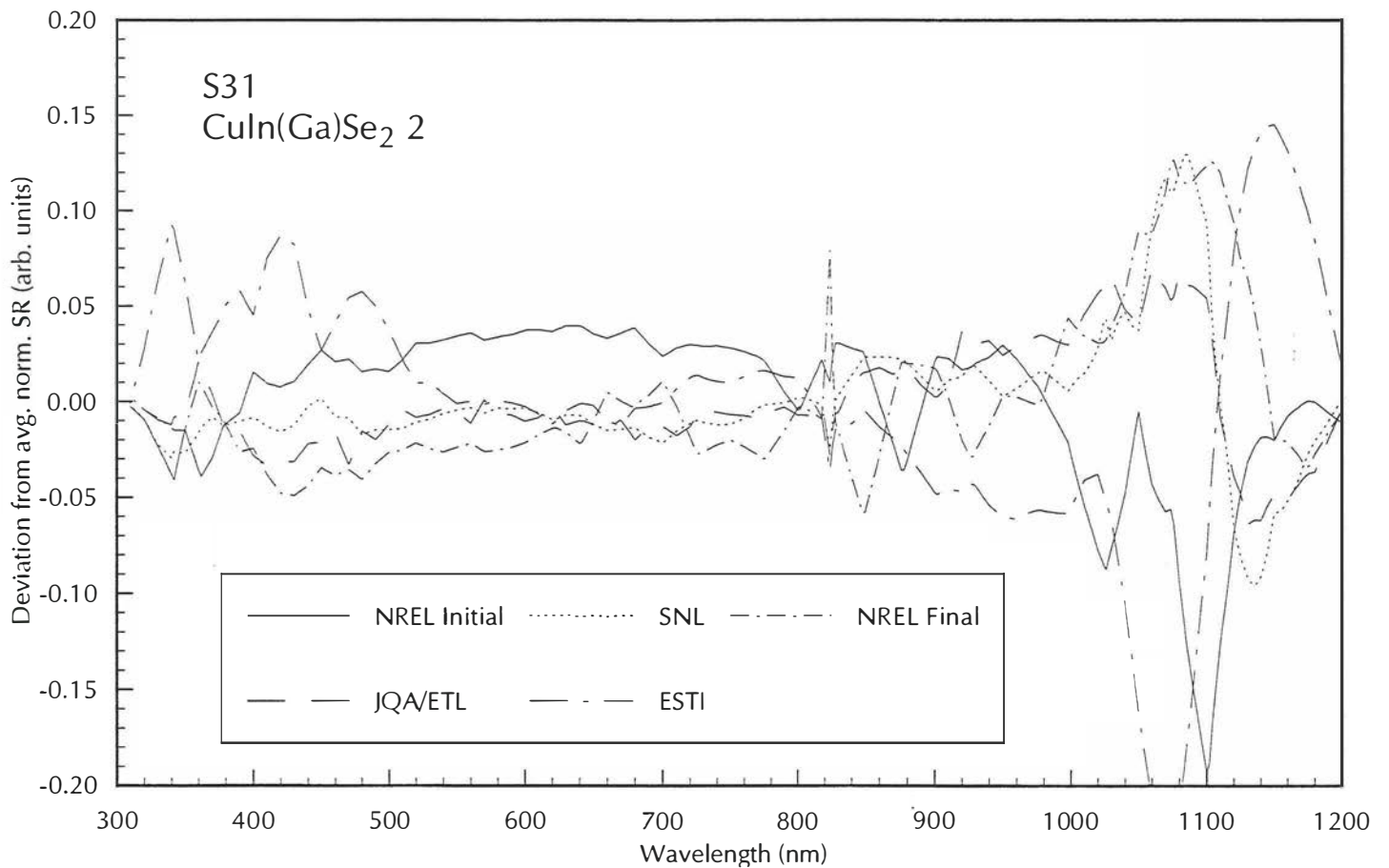
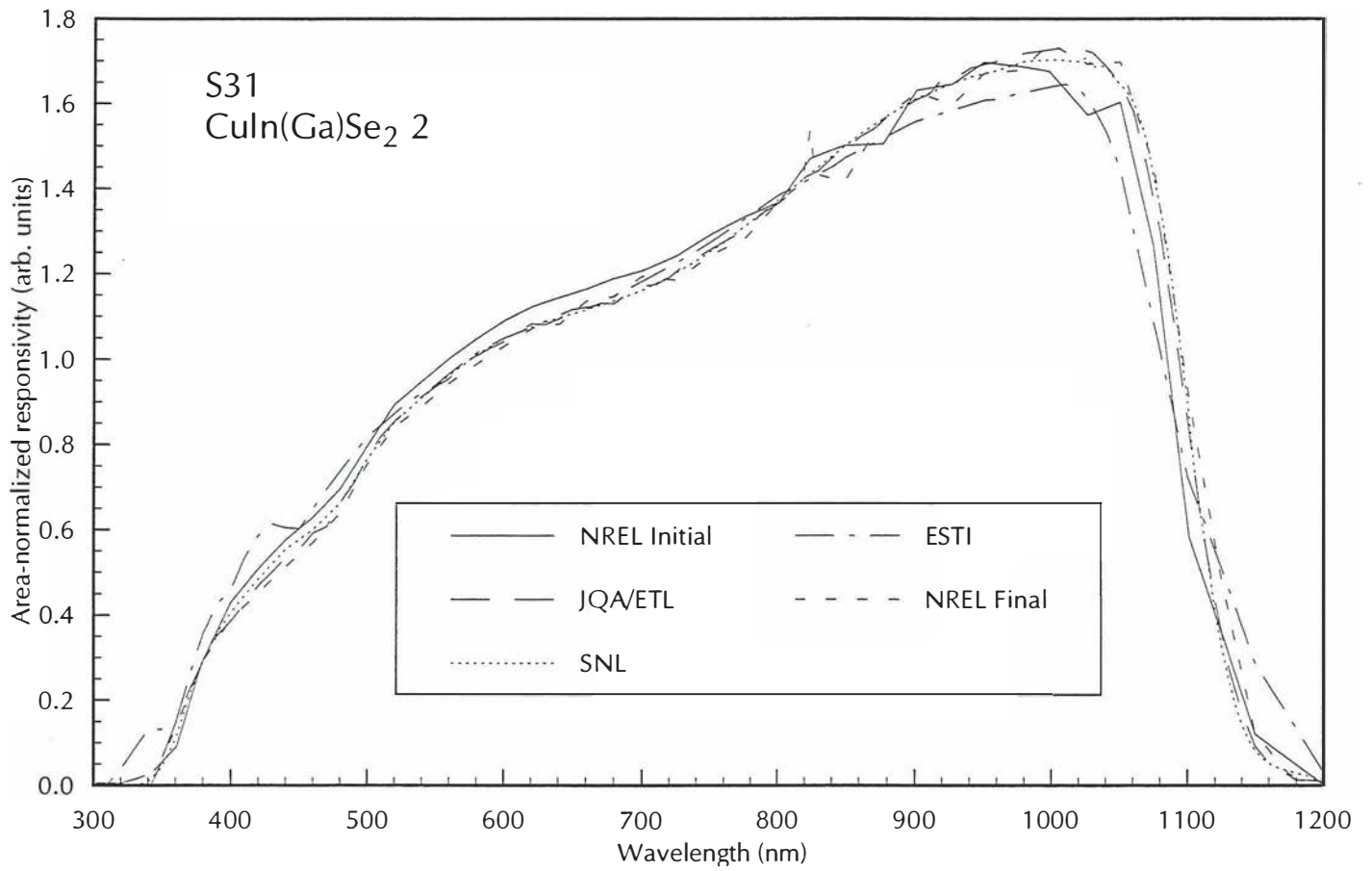


Figure 3-37. Area-normalized SR and deviation from average SR for CuIn(Ga)Se₂ S31

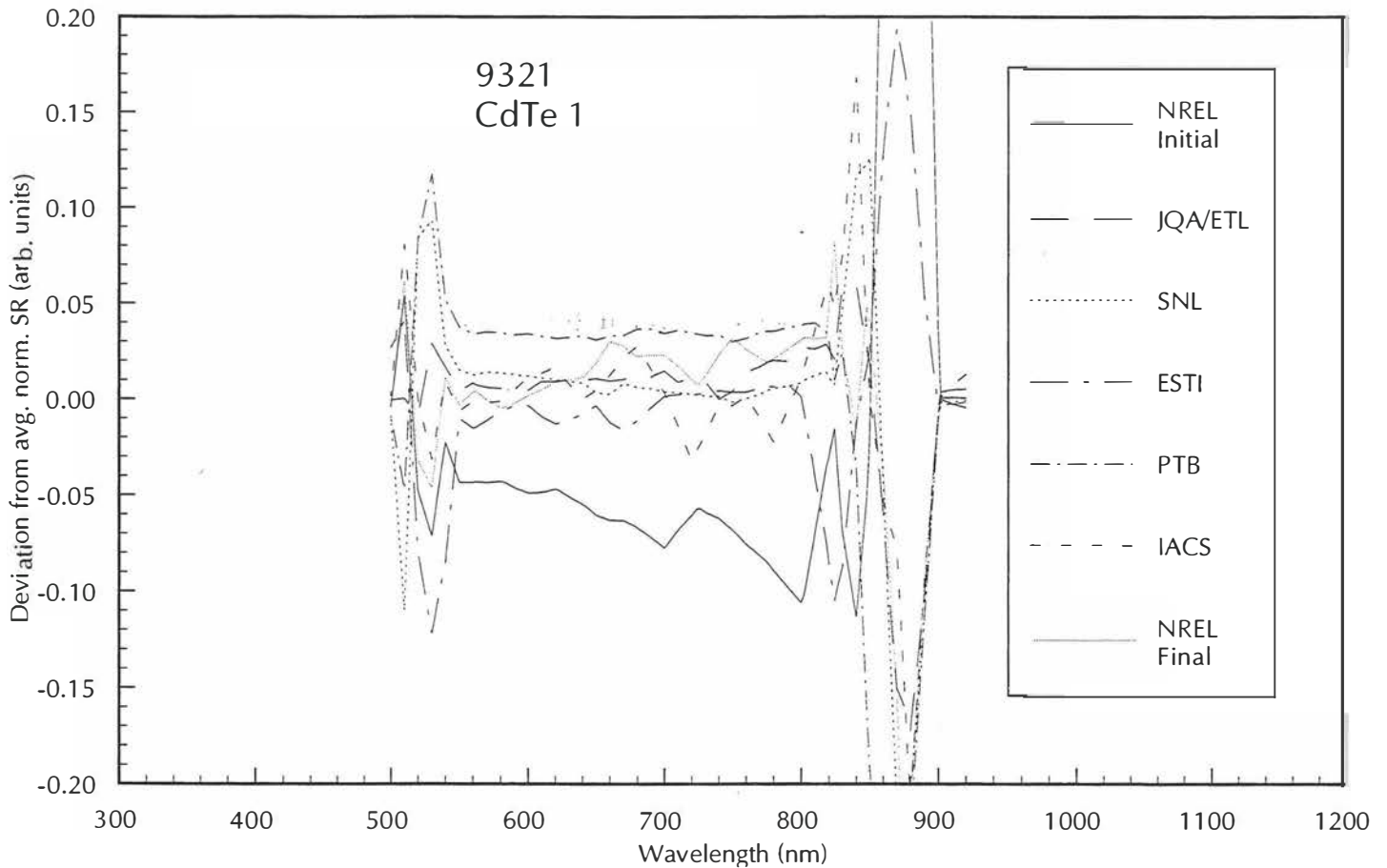
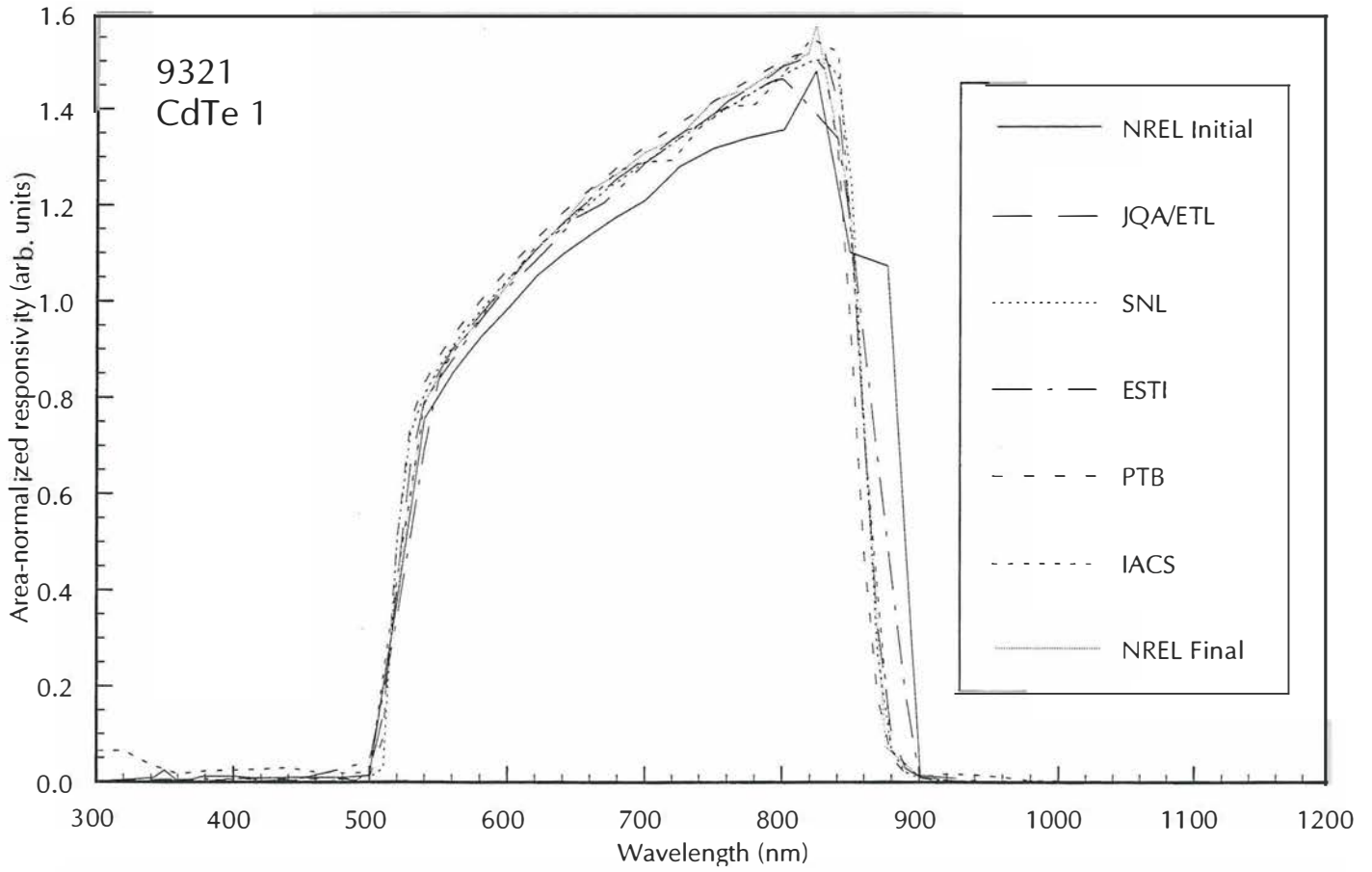


Figure 3-38. Area-normalized SR and deviation from average SR for CdTe 9321

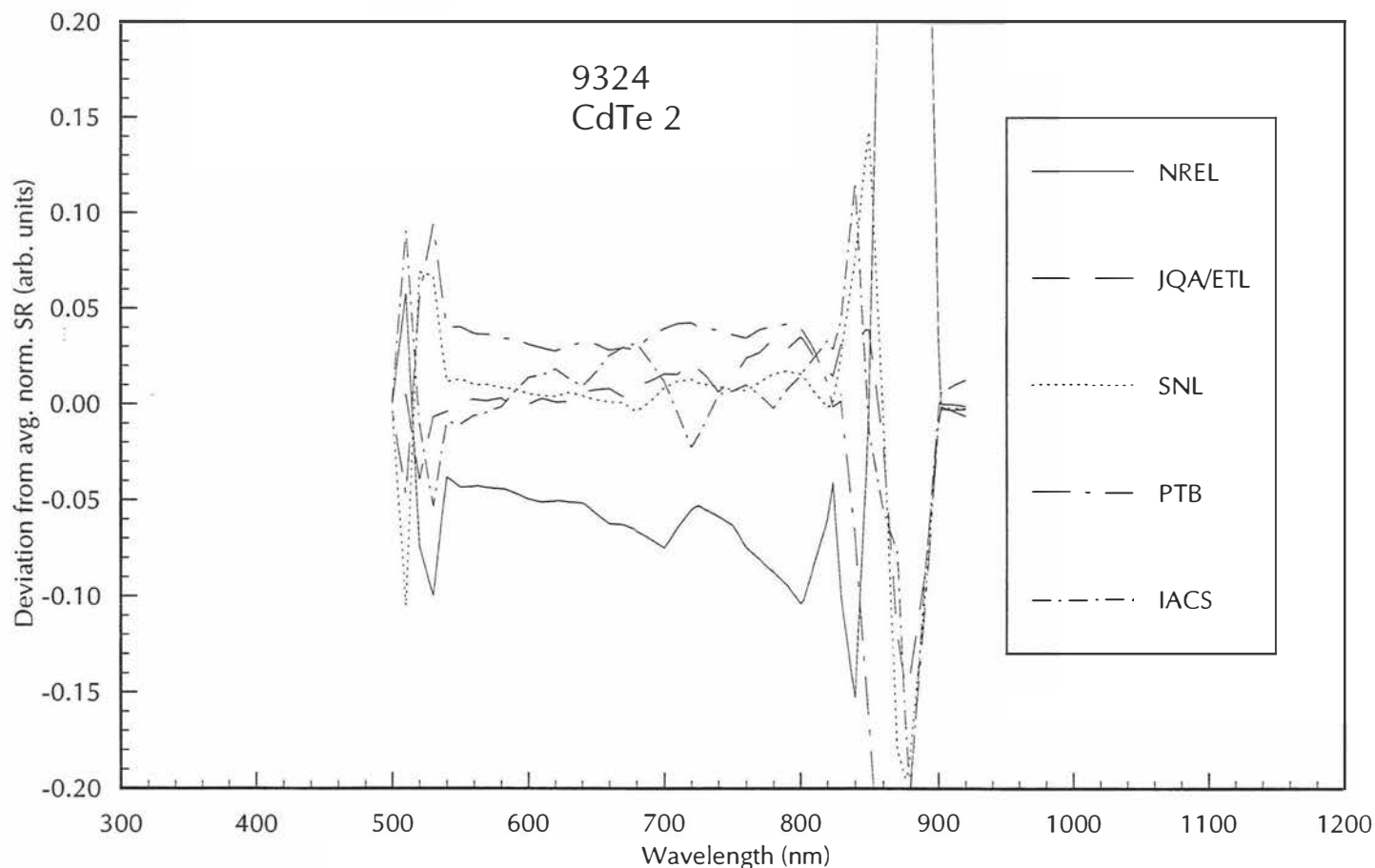
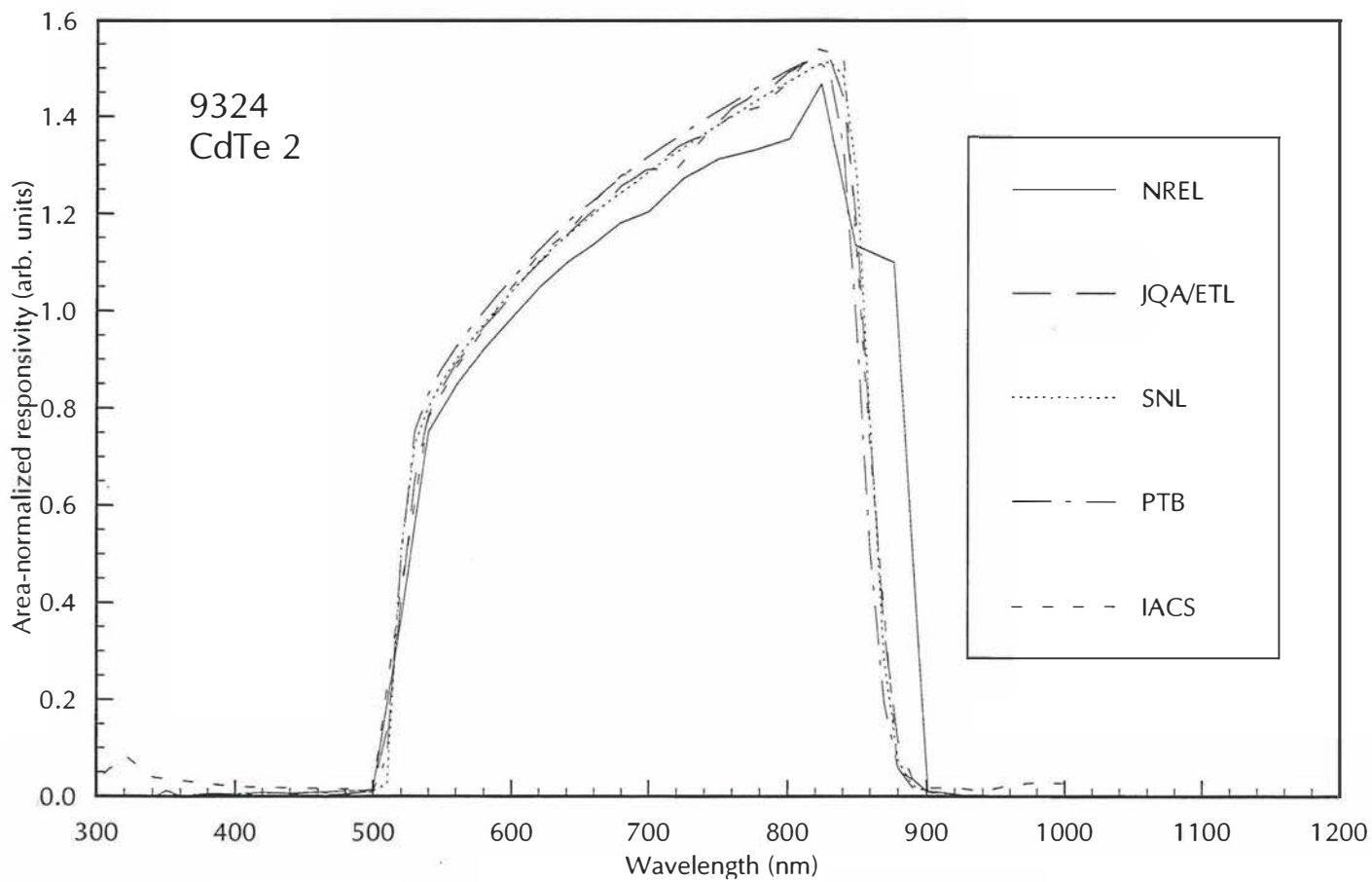


Figure 3-39. Area-normalized SR and deviation from average SR for CdTe 9324

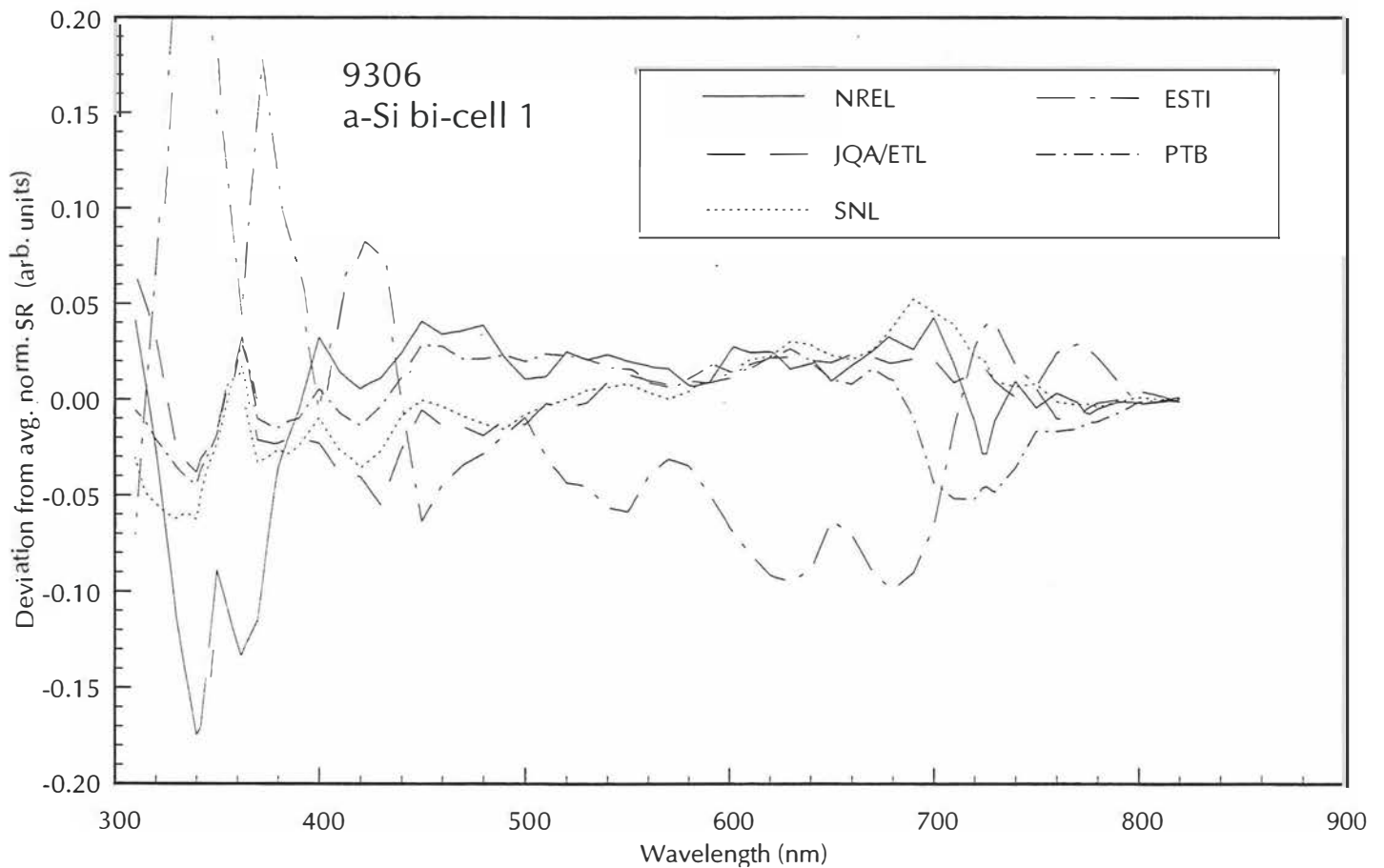
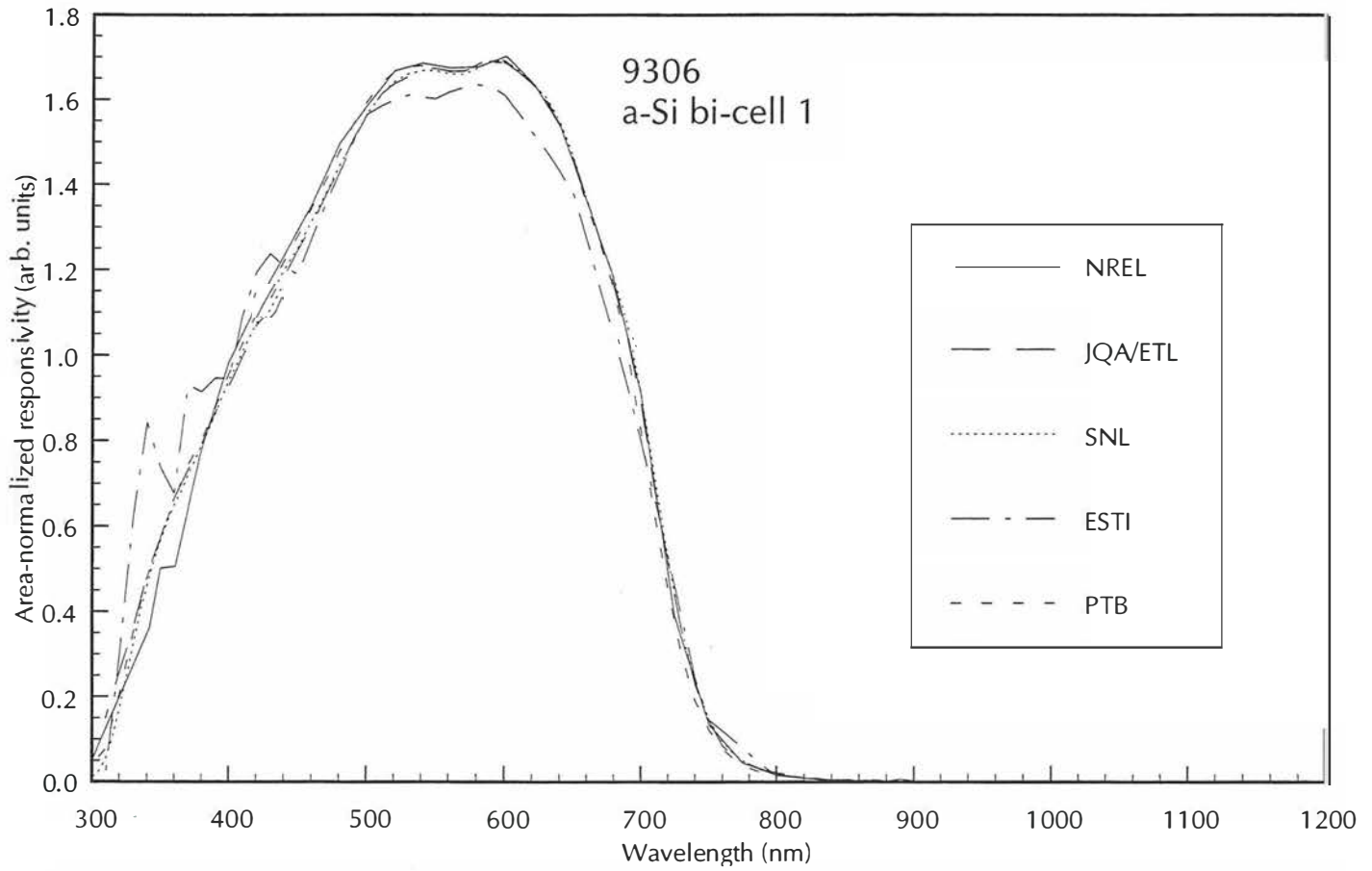


Figure 3-40. Area-normalized SR and deviation from average SR for a-Si bi-cell 9306

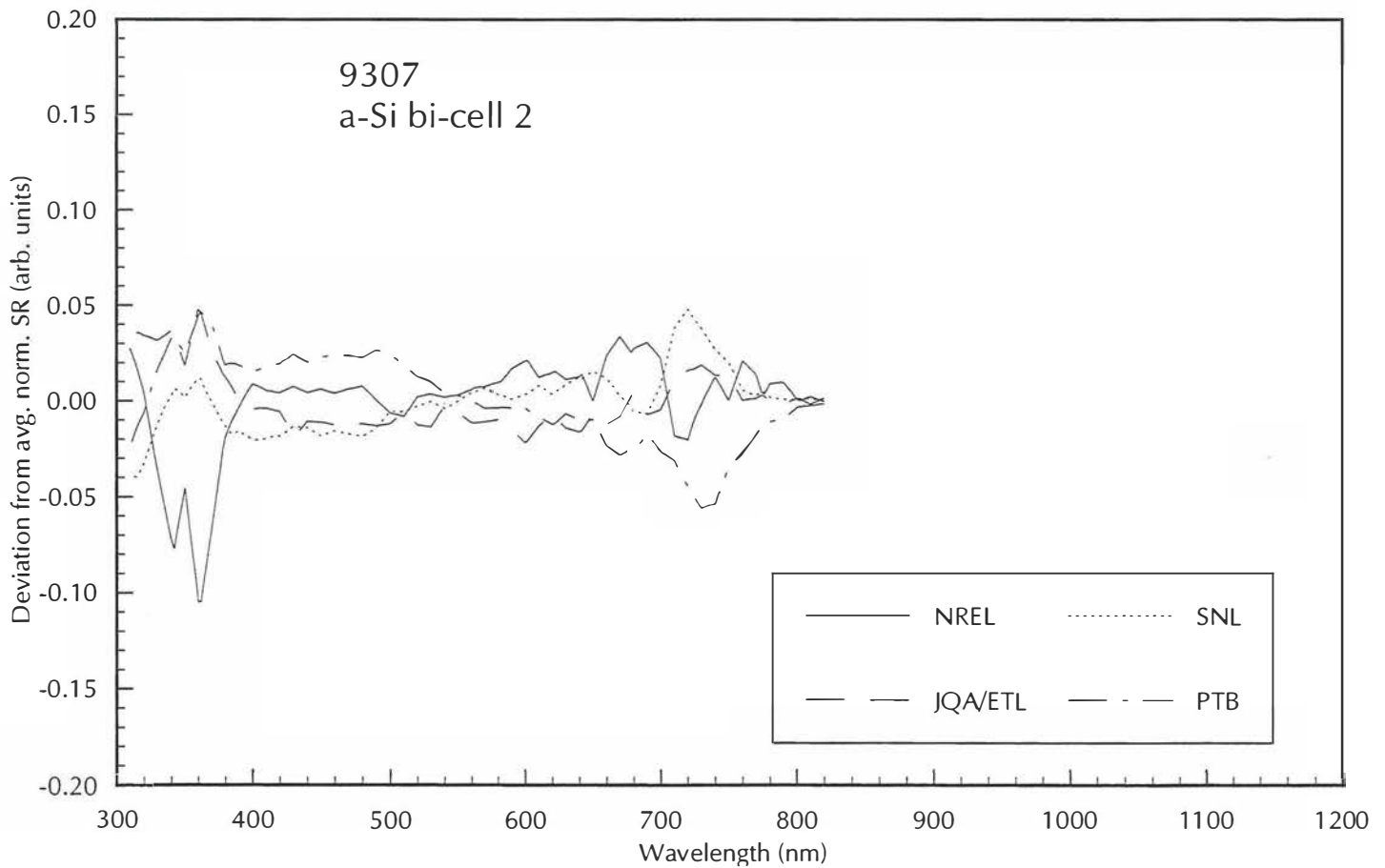
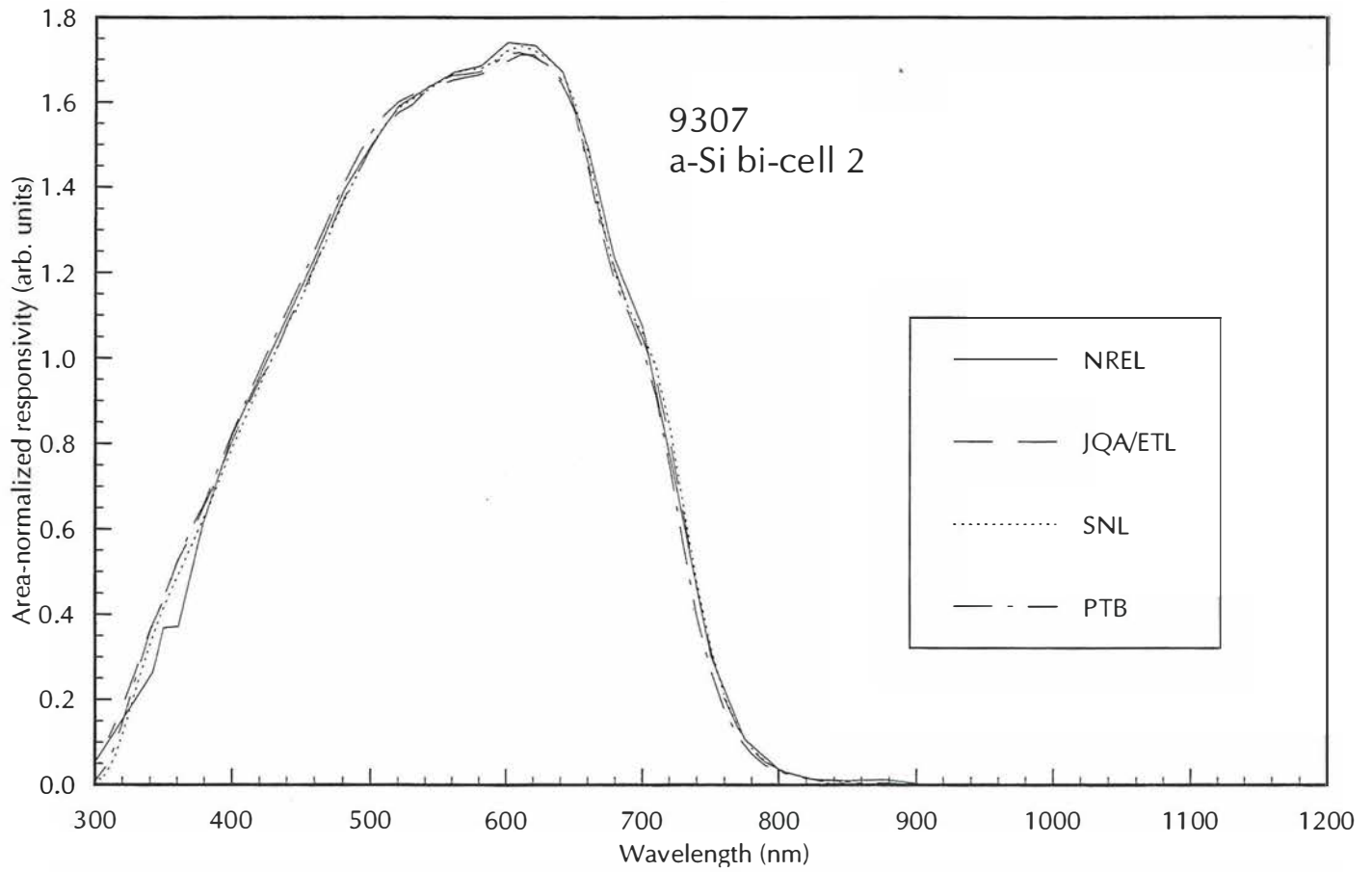


Figure 3-41. Area-normalized SR and deviation from average SR for a-Si bi-cell 9307

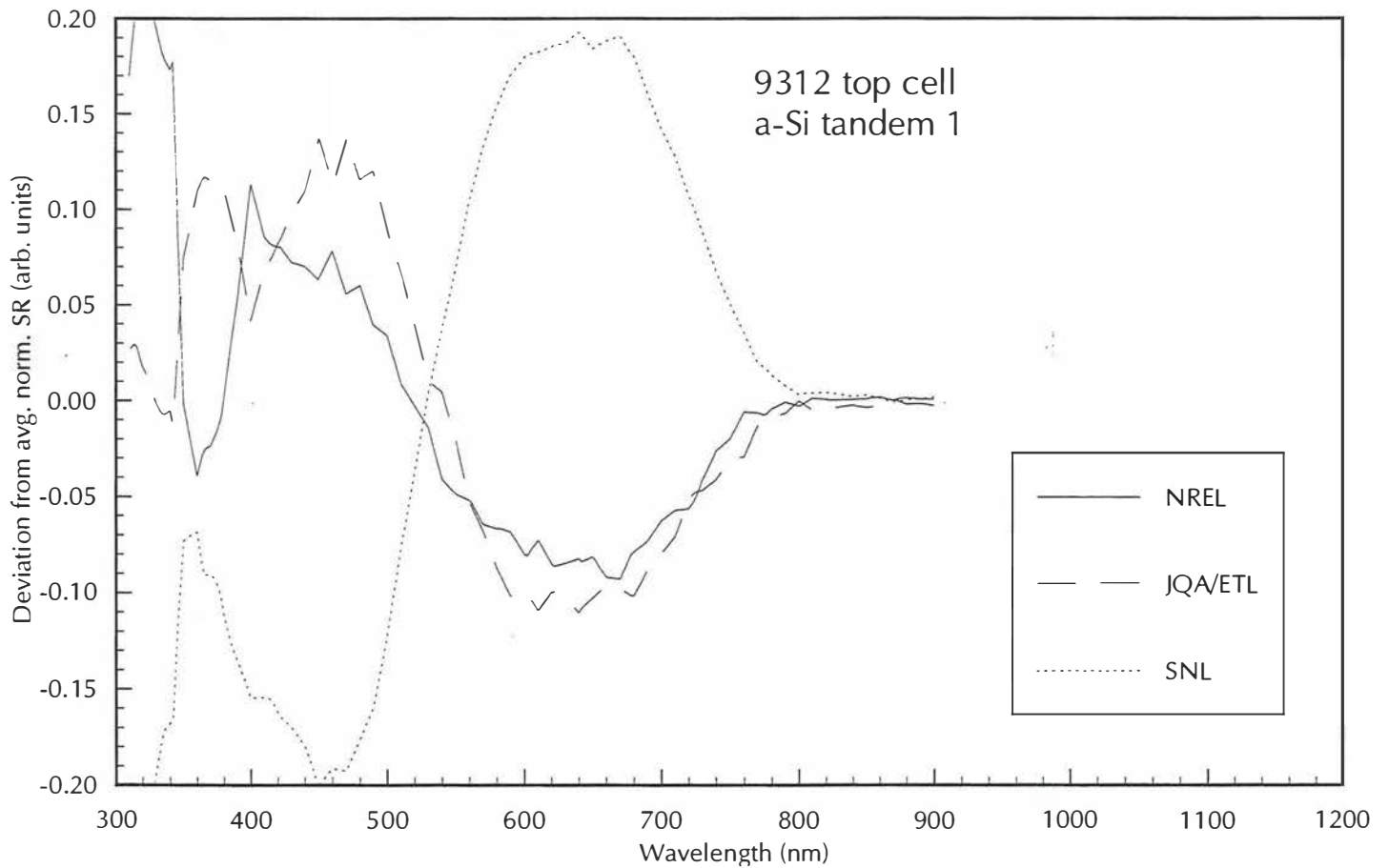
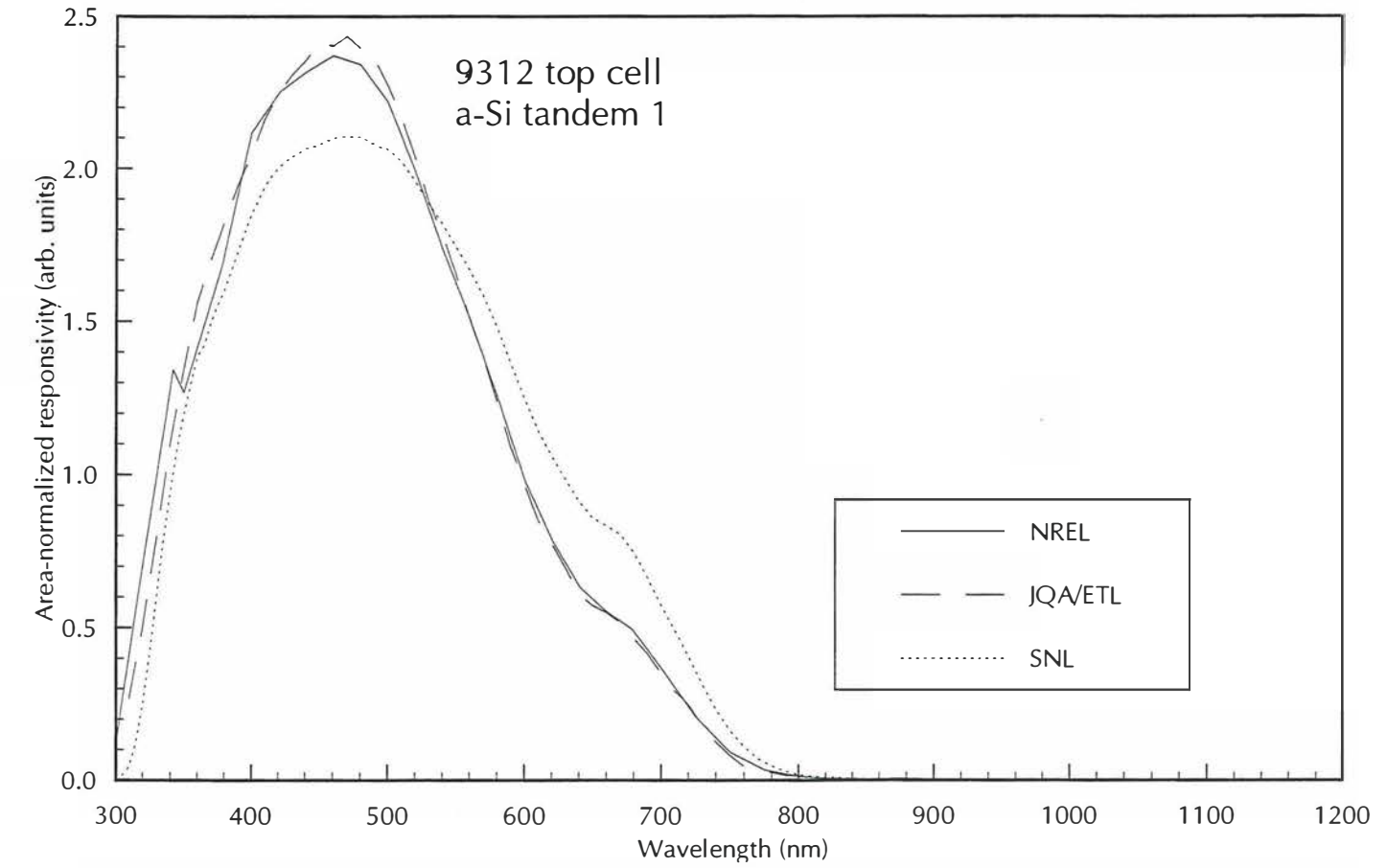


Figure 3-42. Area-normalized SR and deviation from average SR for a-Si 9312 top cell

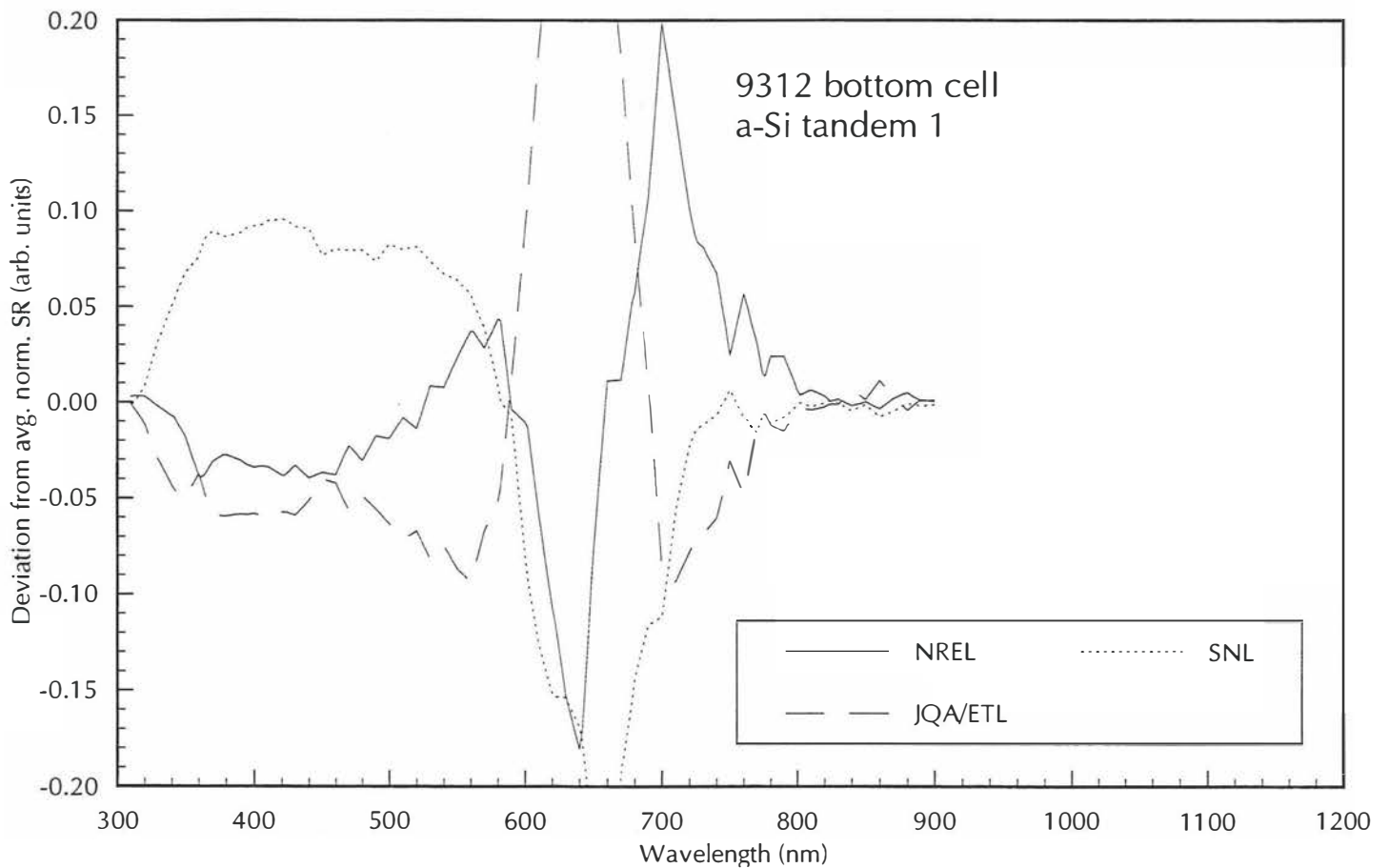
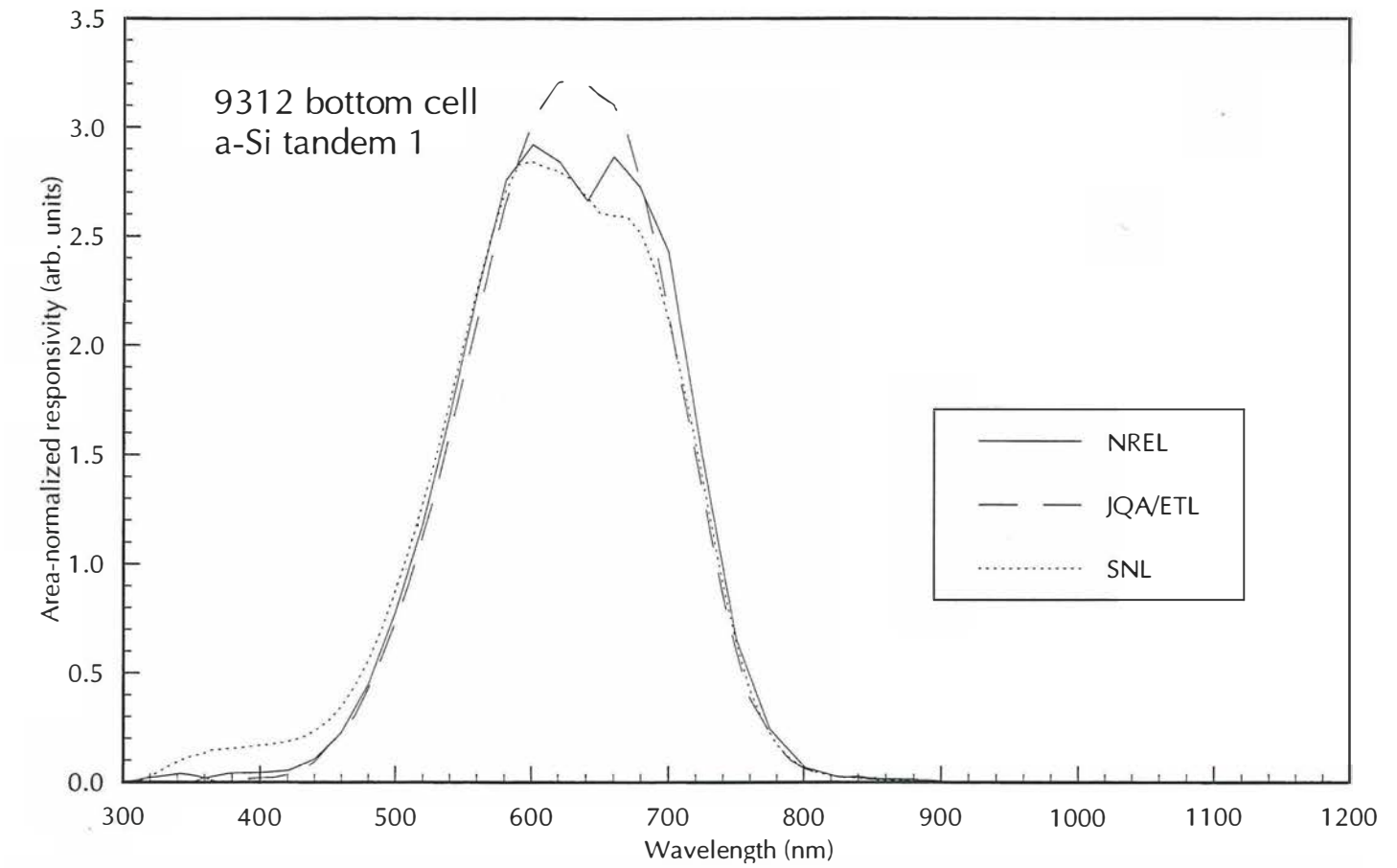


Figure 3-43. Area-normalized SR and deviation from average SR for a-Si 9312 bottom cell

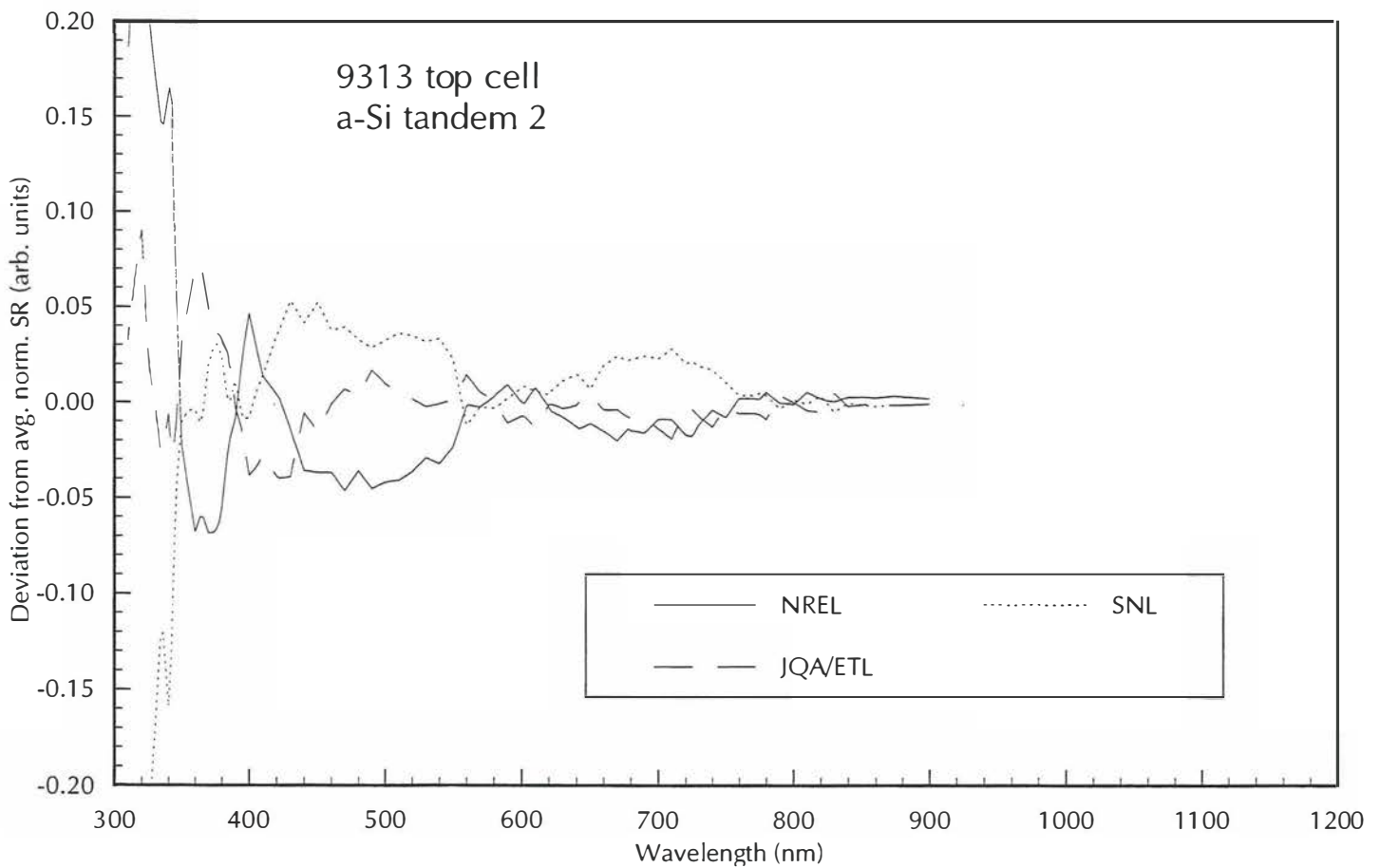
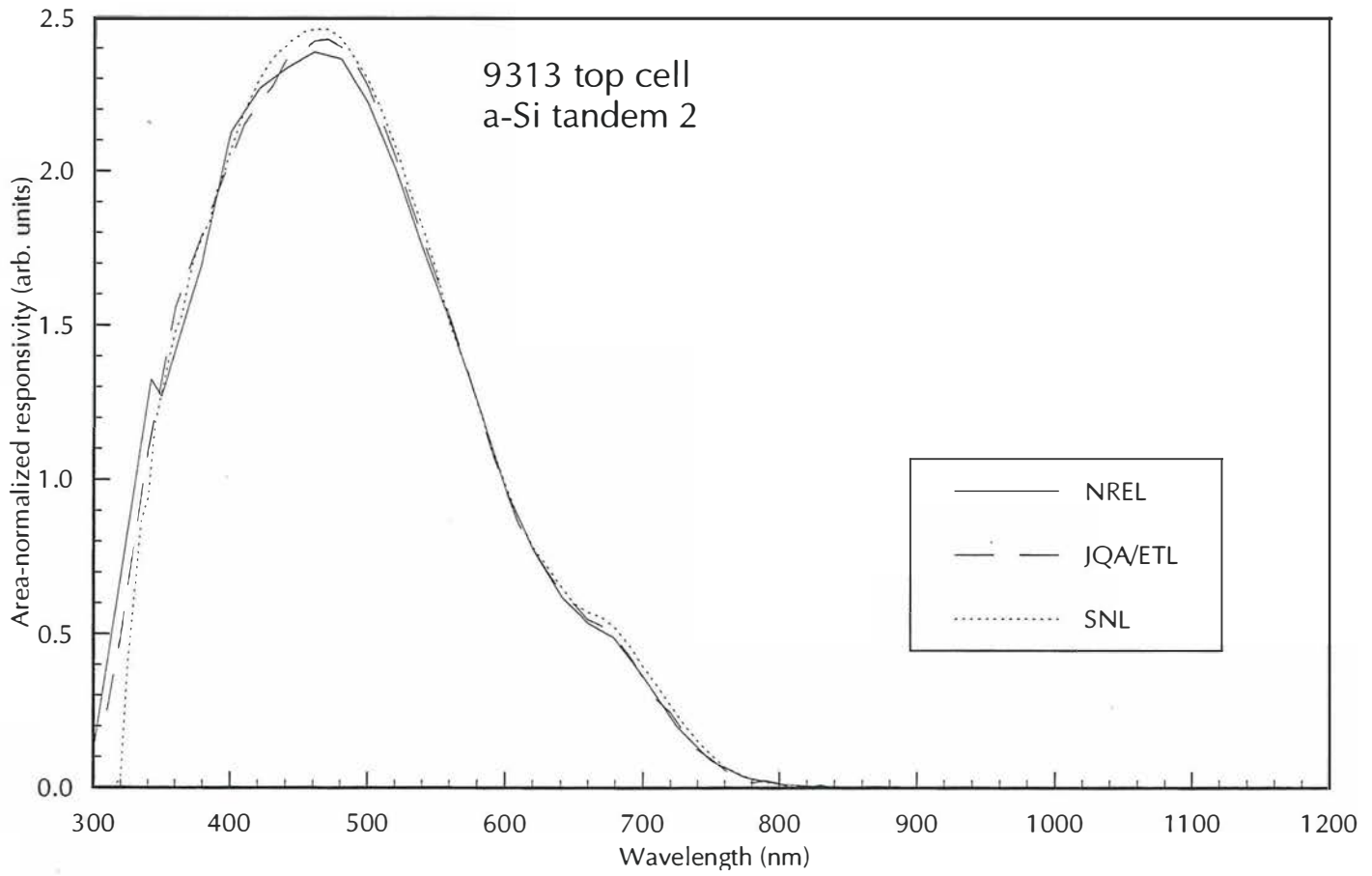


Figure 3-44. Area-normalized SR and deviation from average SR for a-Si 9313 top cell

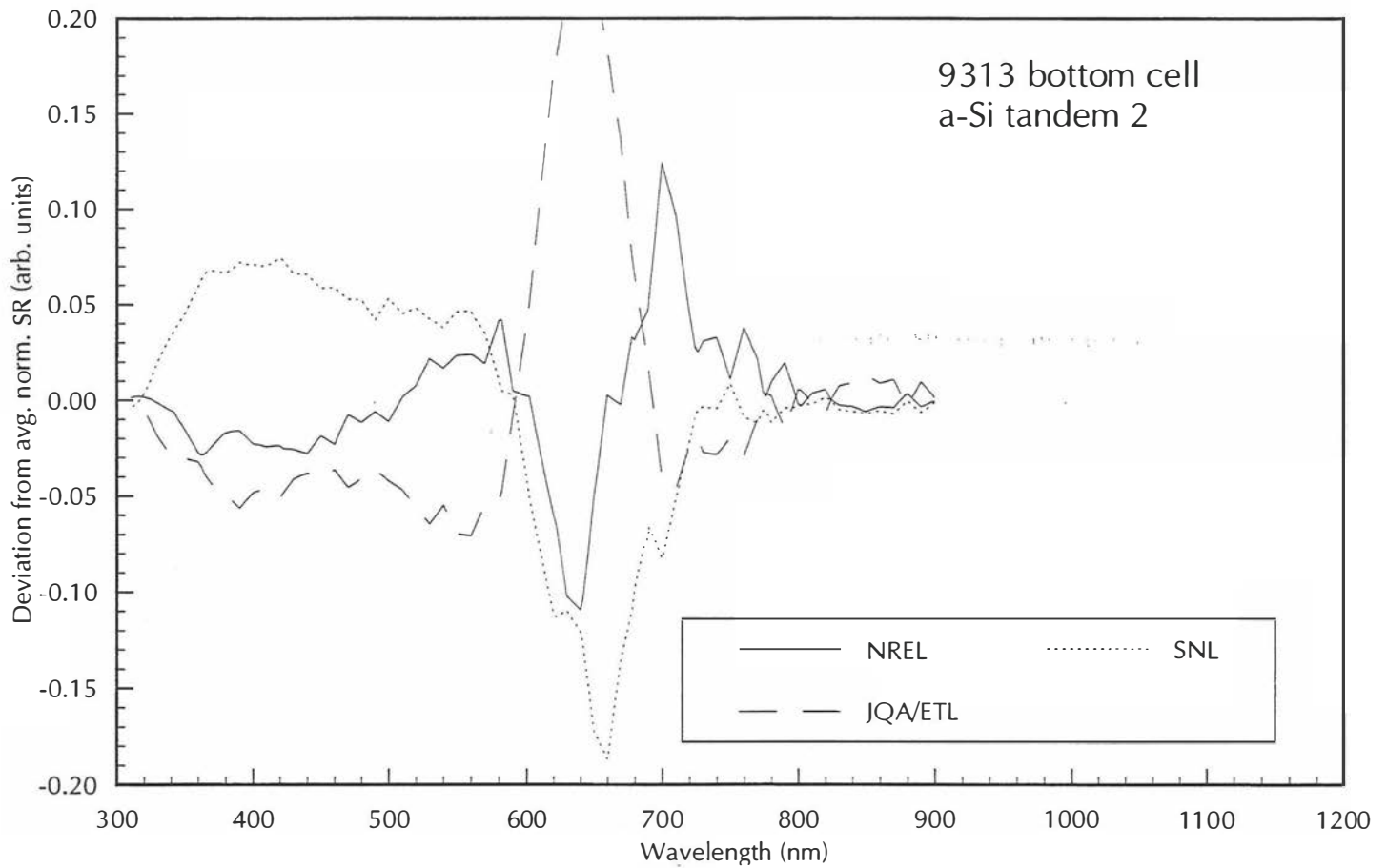
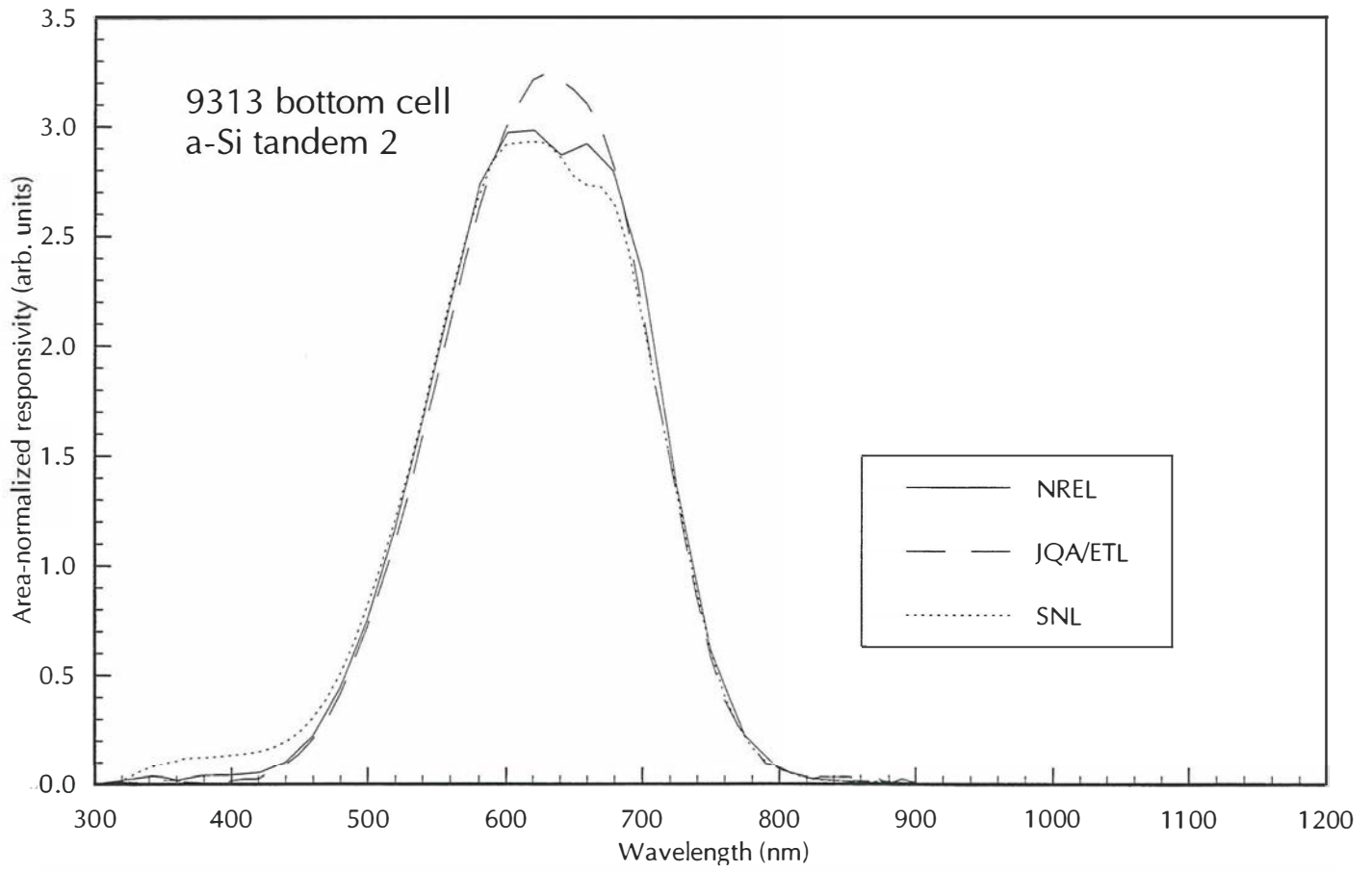


Figure 3-45. Area-normalized SR and deviation from average SR for a-Si 9313 bottom cell

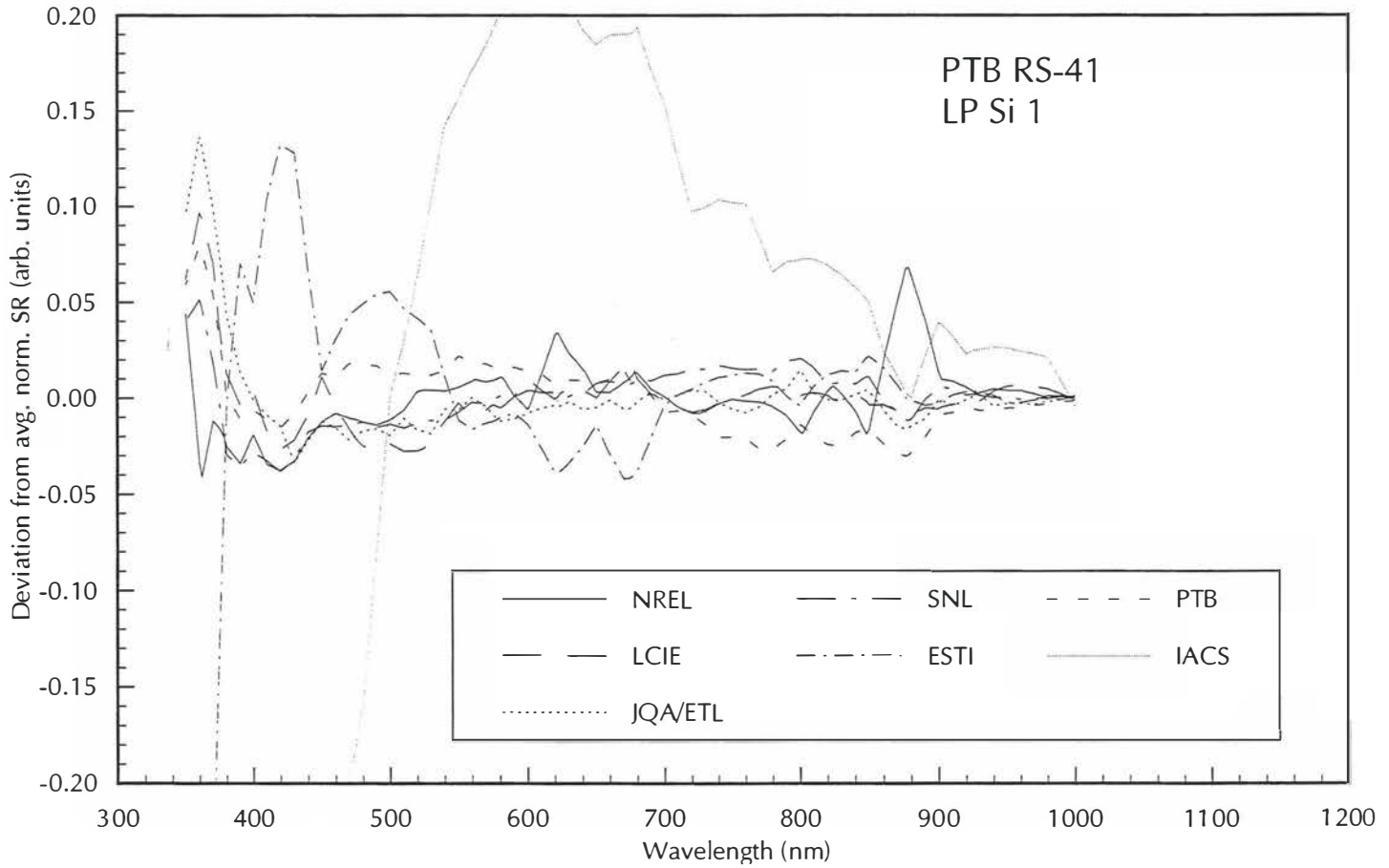
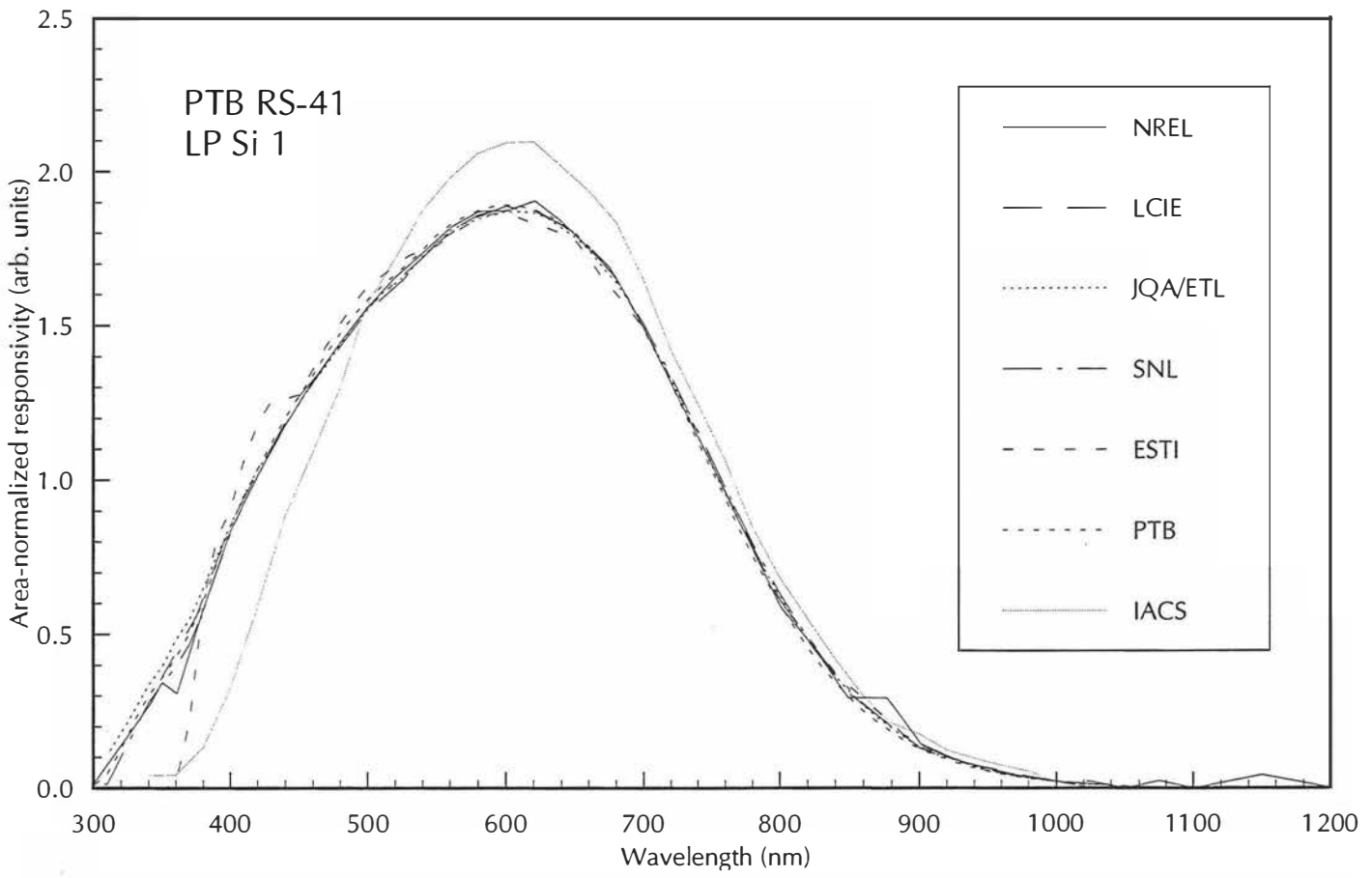


Figure 3-46. Area-normalized SR and deviation from average SR for low-pass Si PTB RS-41

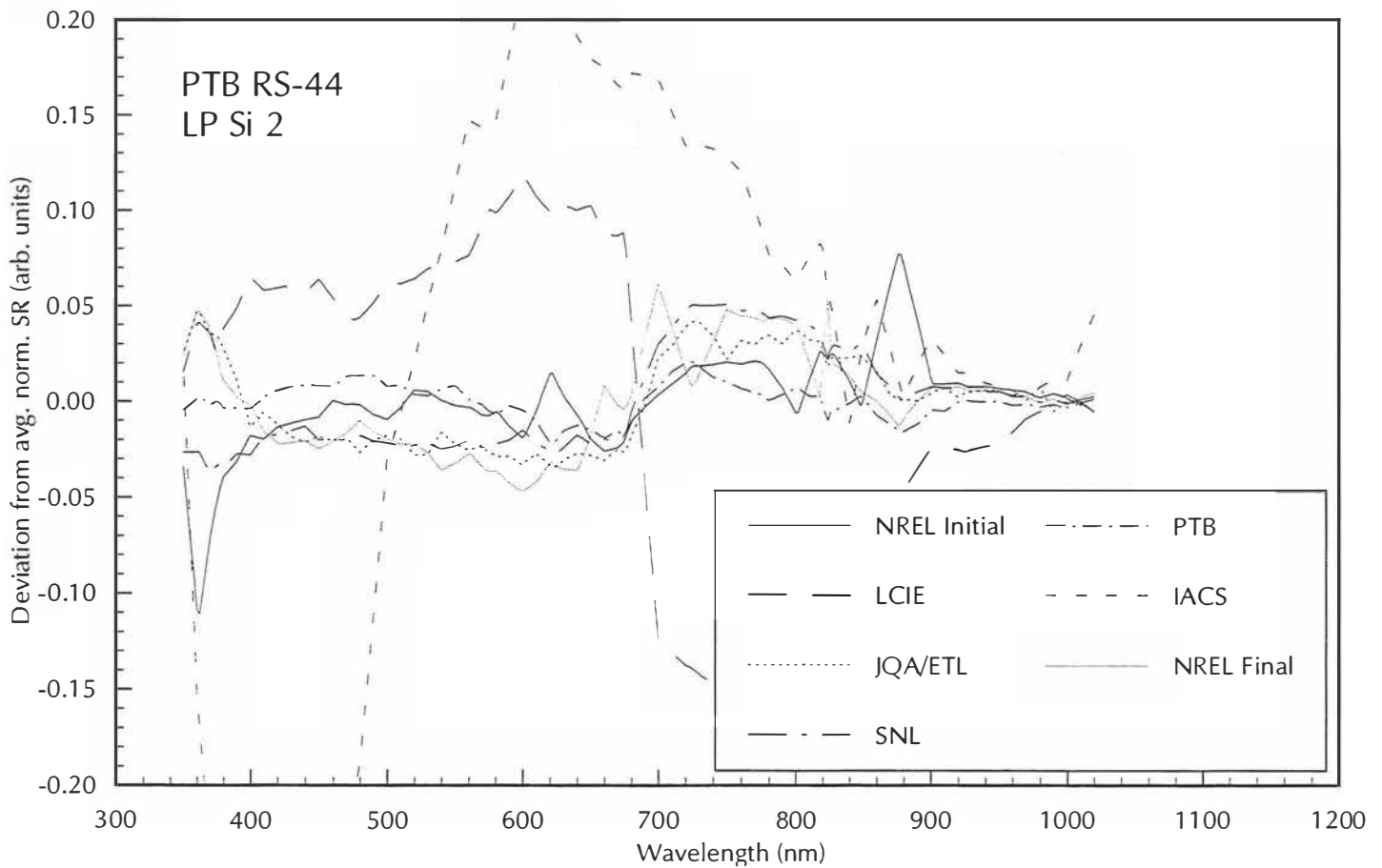
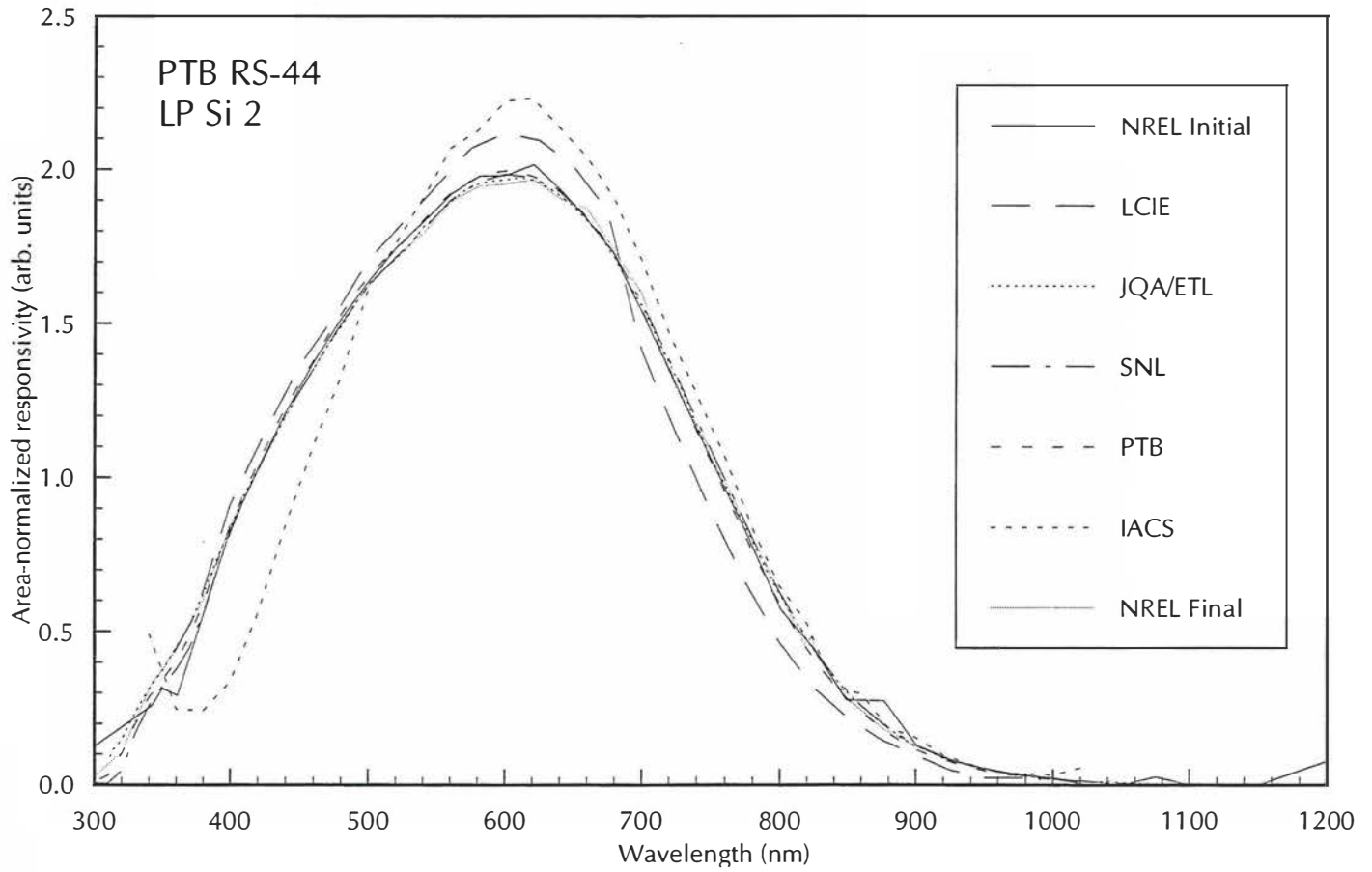


Figure 3-47. Area-normalized SR and deviation from average SR for low-pass Si PTB RS-44

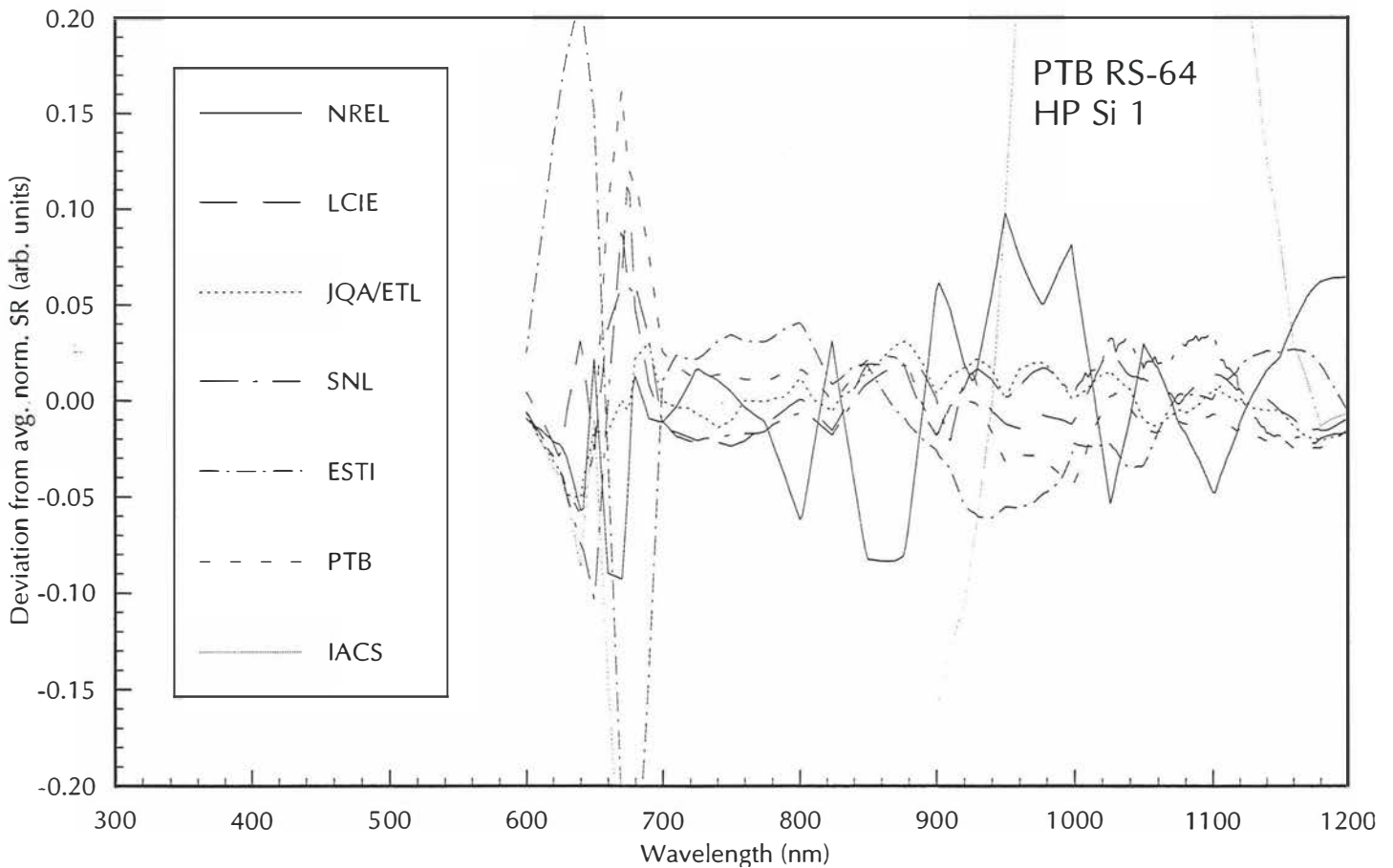
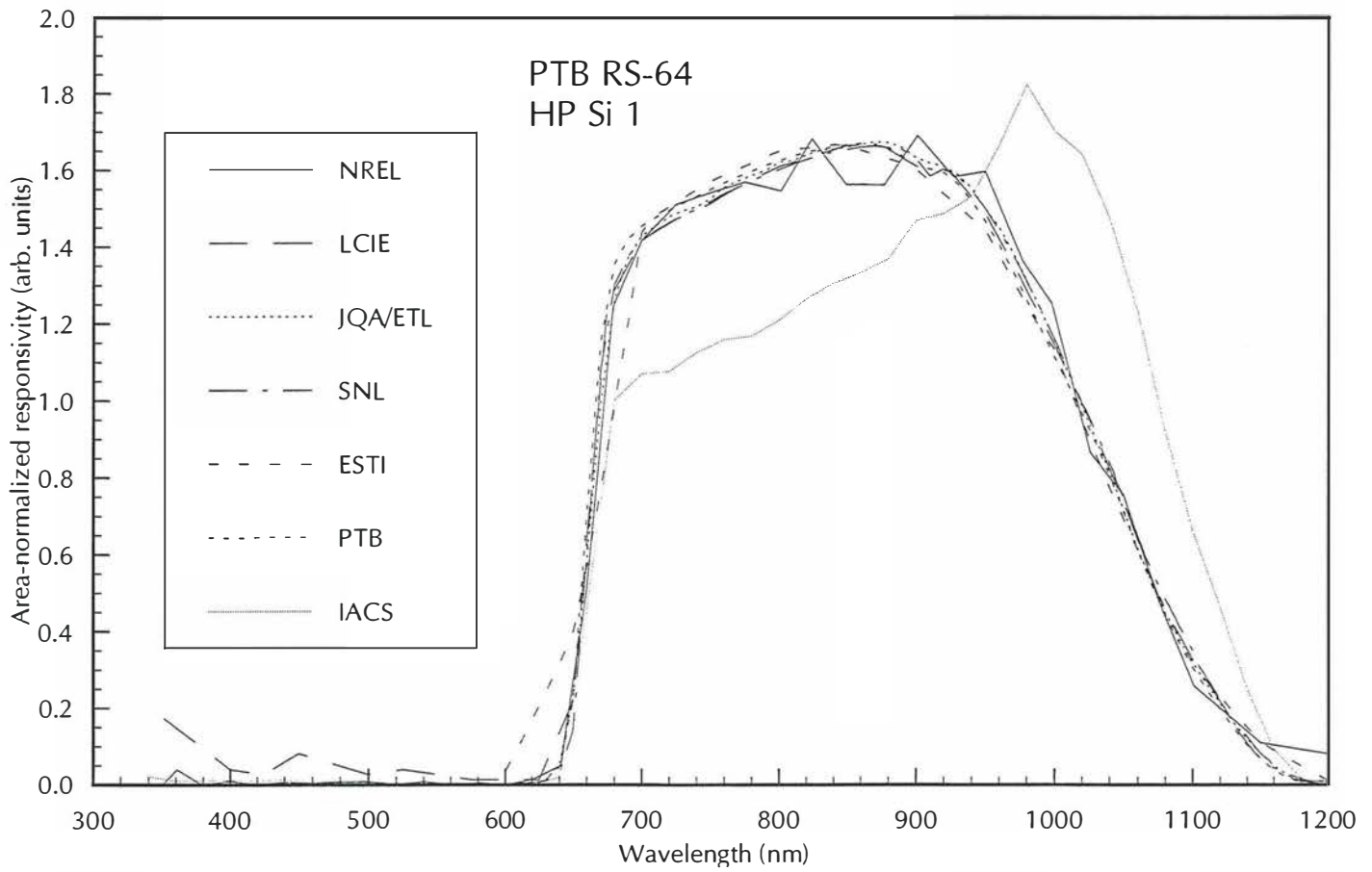


Figure 3-48. Area-normalized SR and deviation from average SR for high-pass Si PTB RS-64

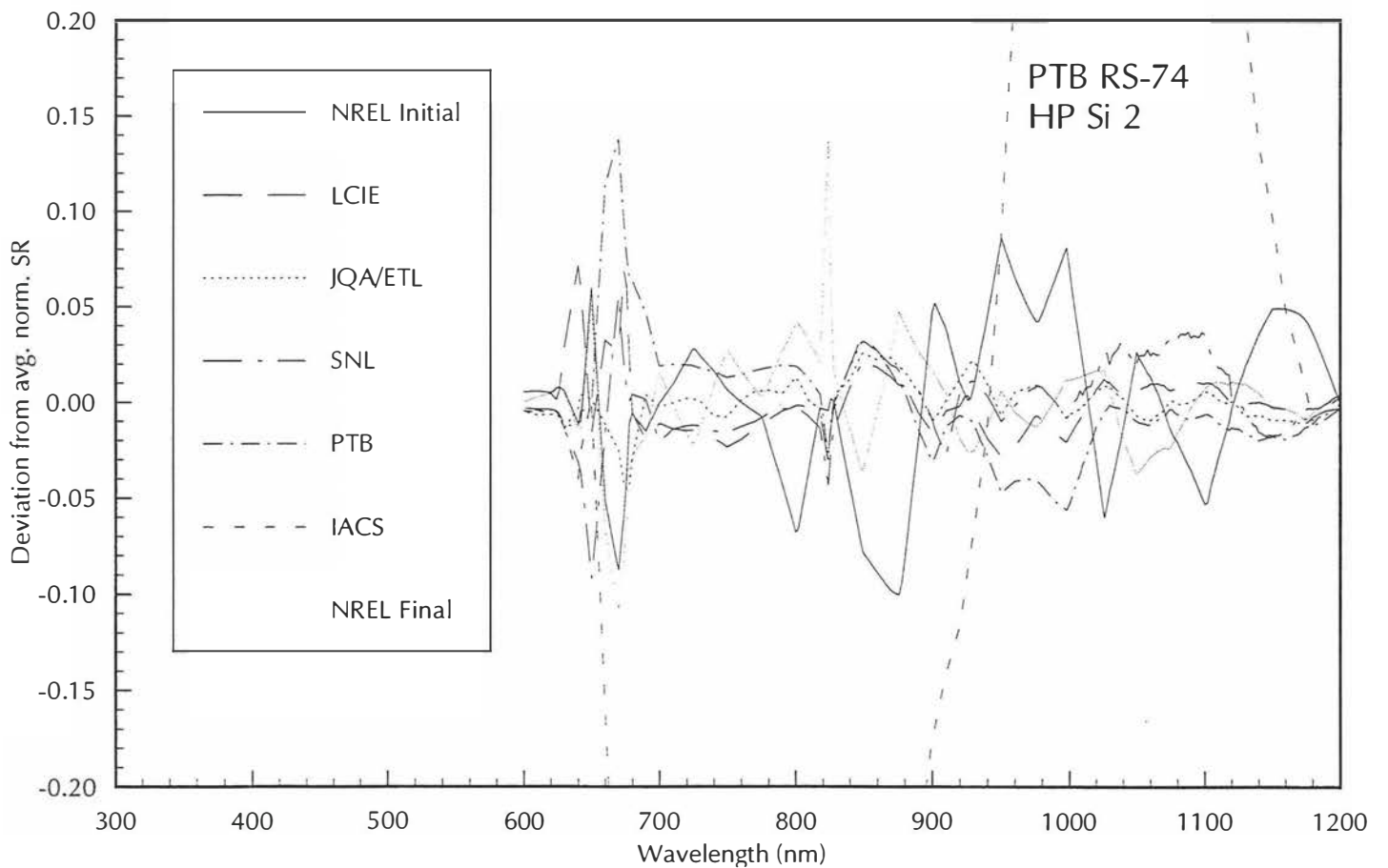
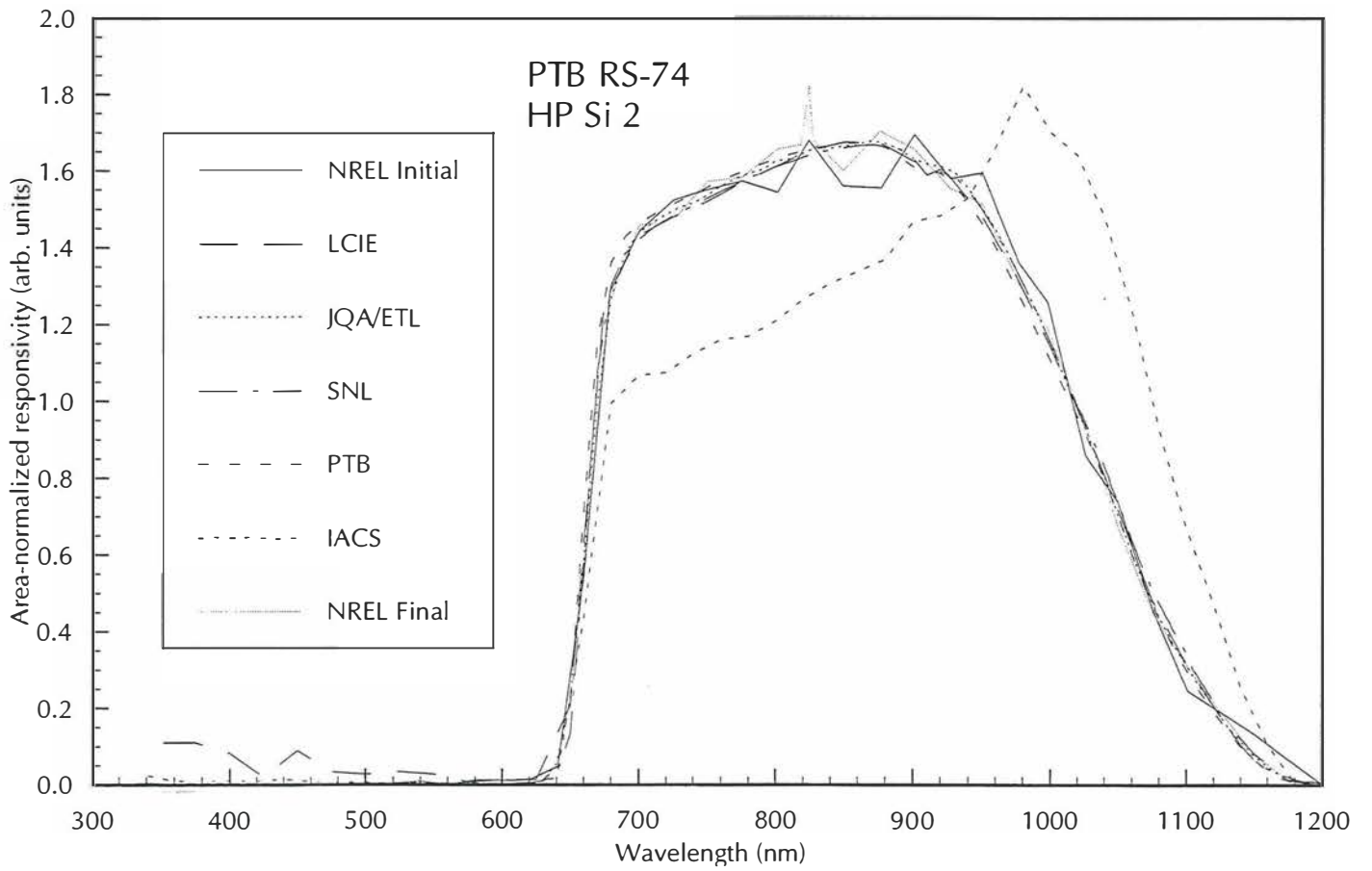


Figure 3-49. Area-normalized SR and deviation from average SR for high-pass Si PTB RS-74

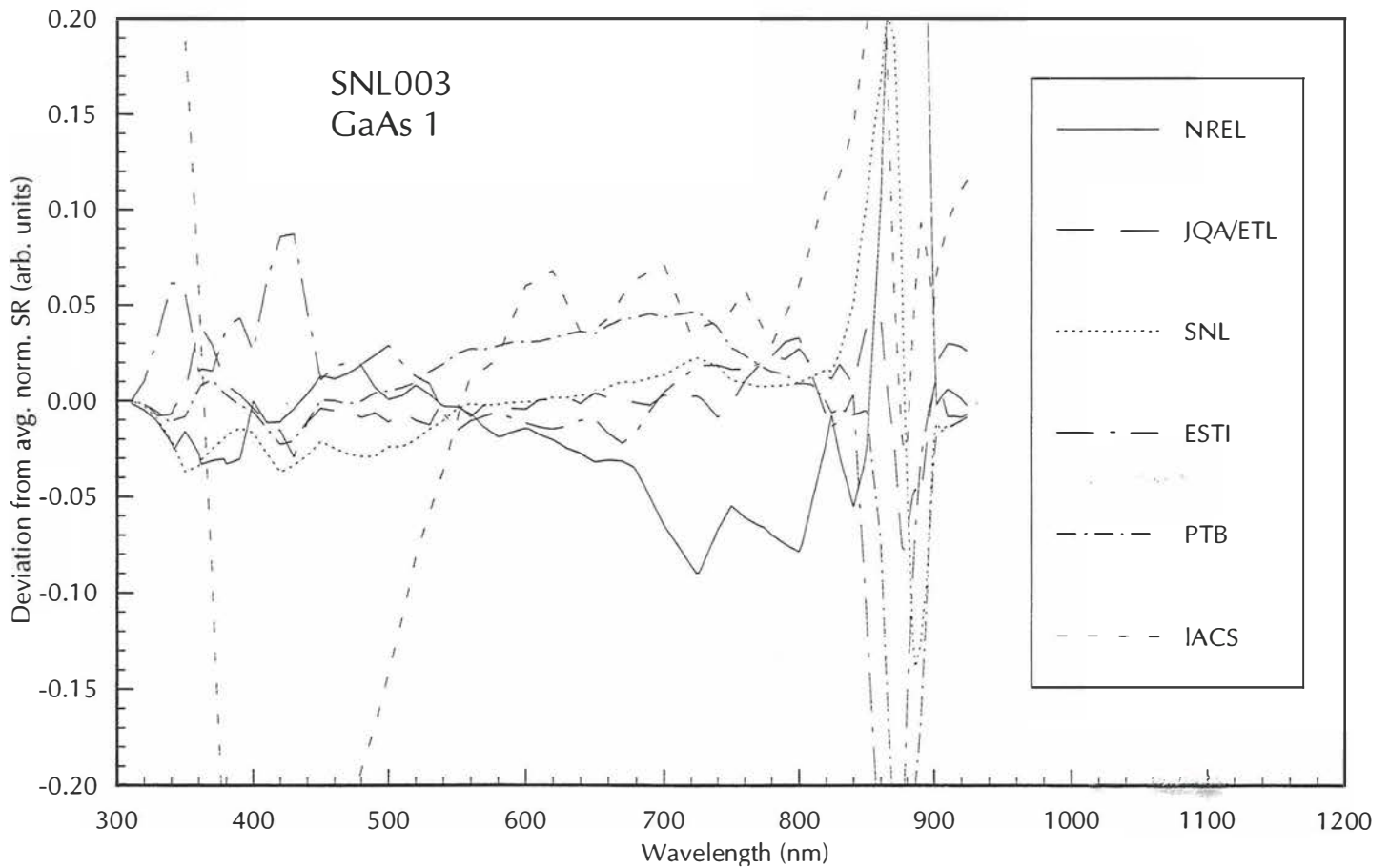
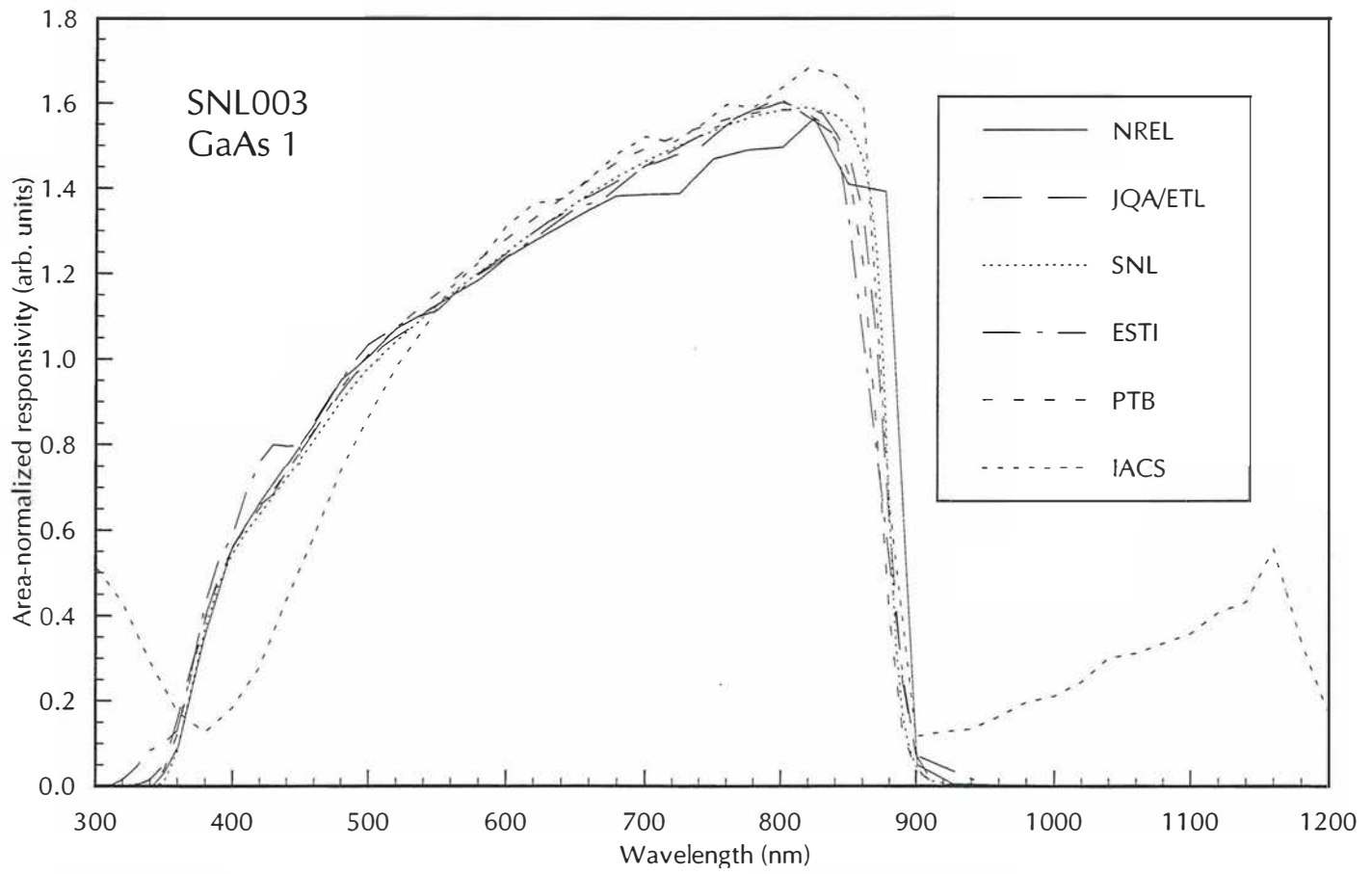


Figure 3-50. Area-normalized SR and deviation from average SR for GaAs SNL003

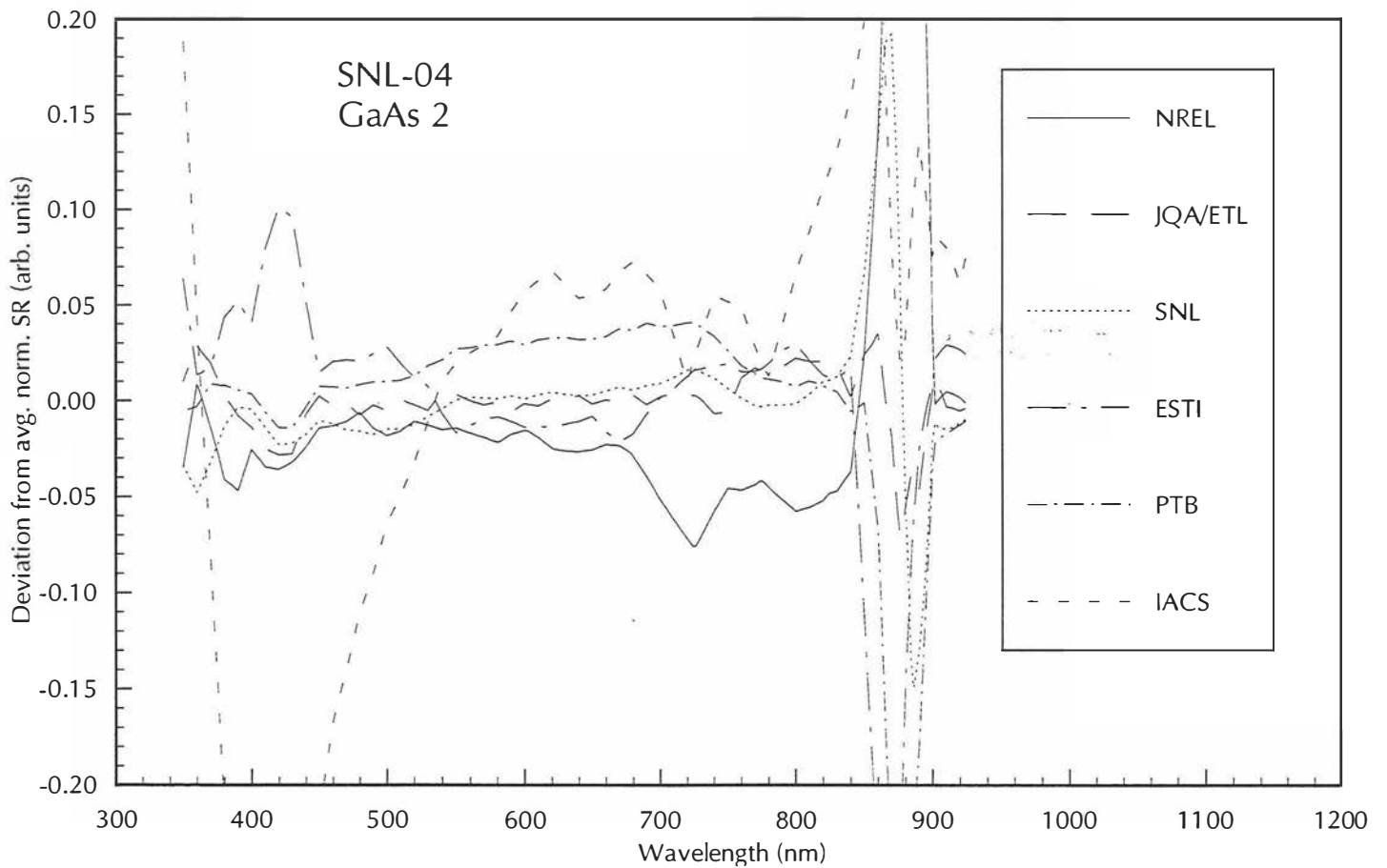
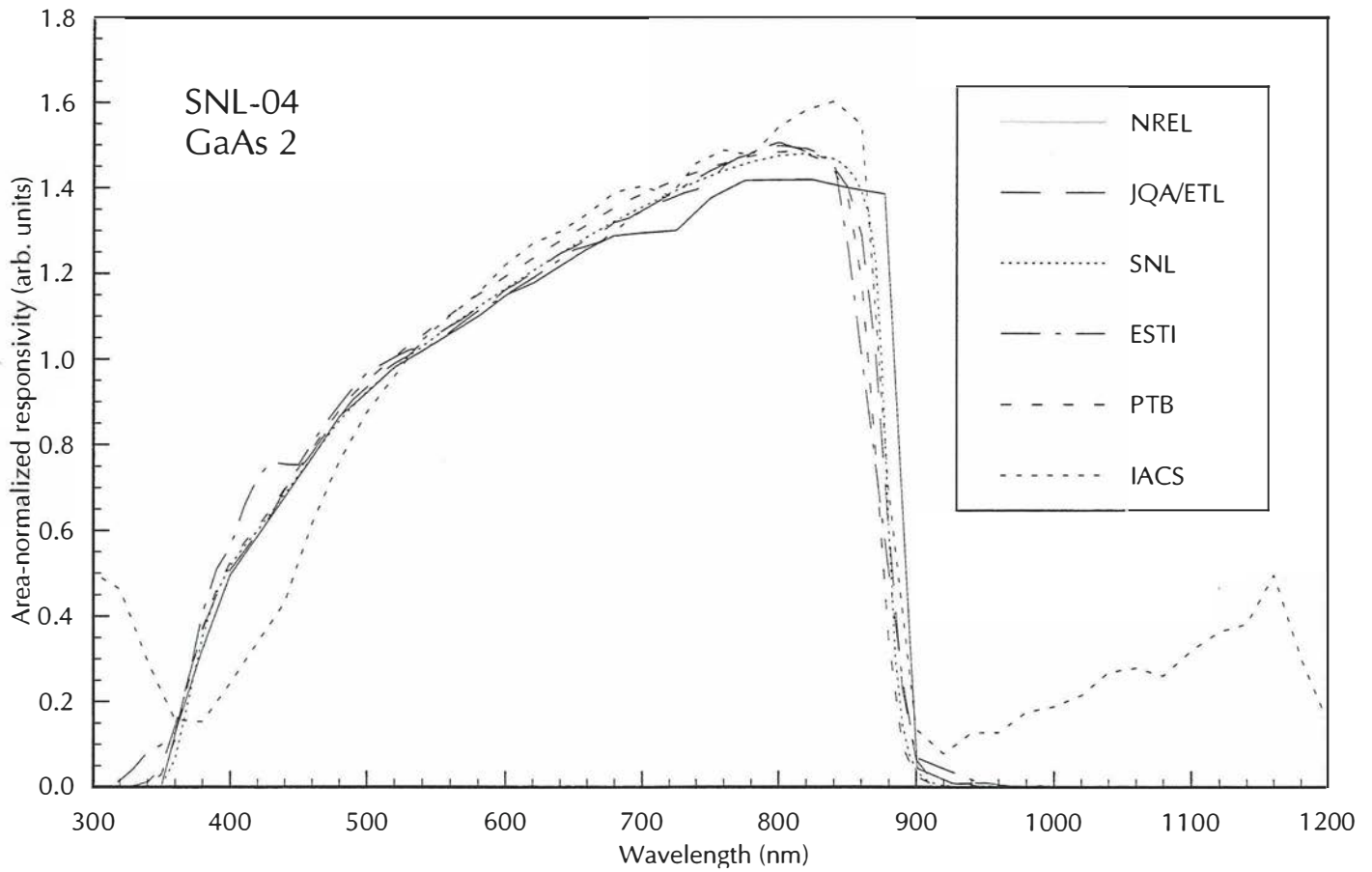


Figure 3-51. Area-normalized SR and deviation from average SR for GaAs SNL-04

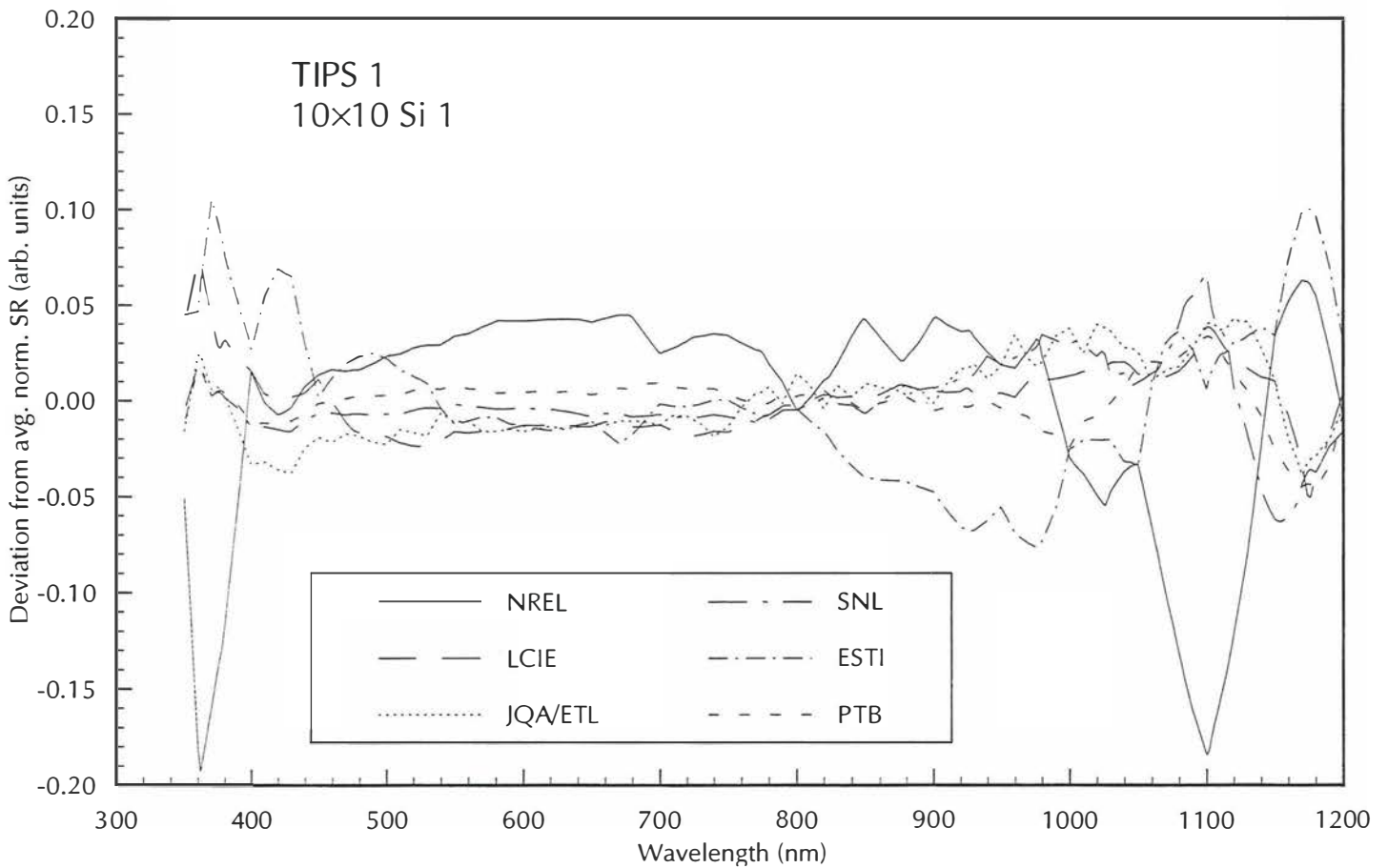
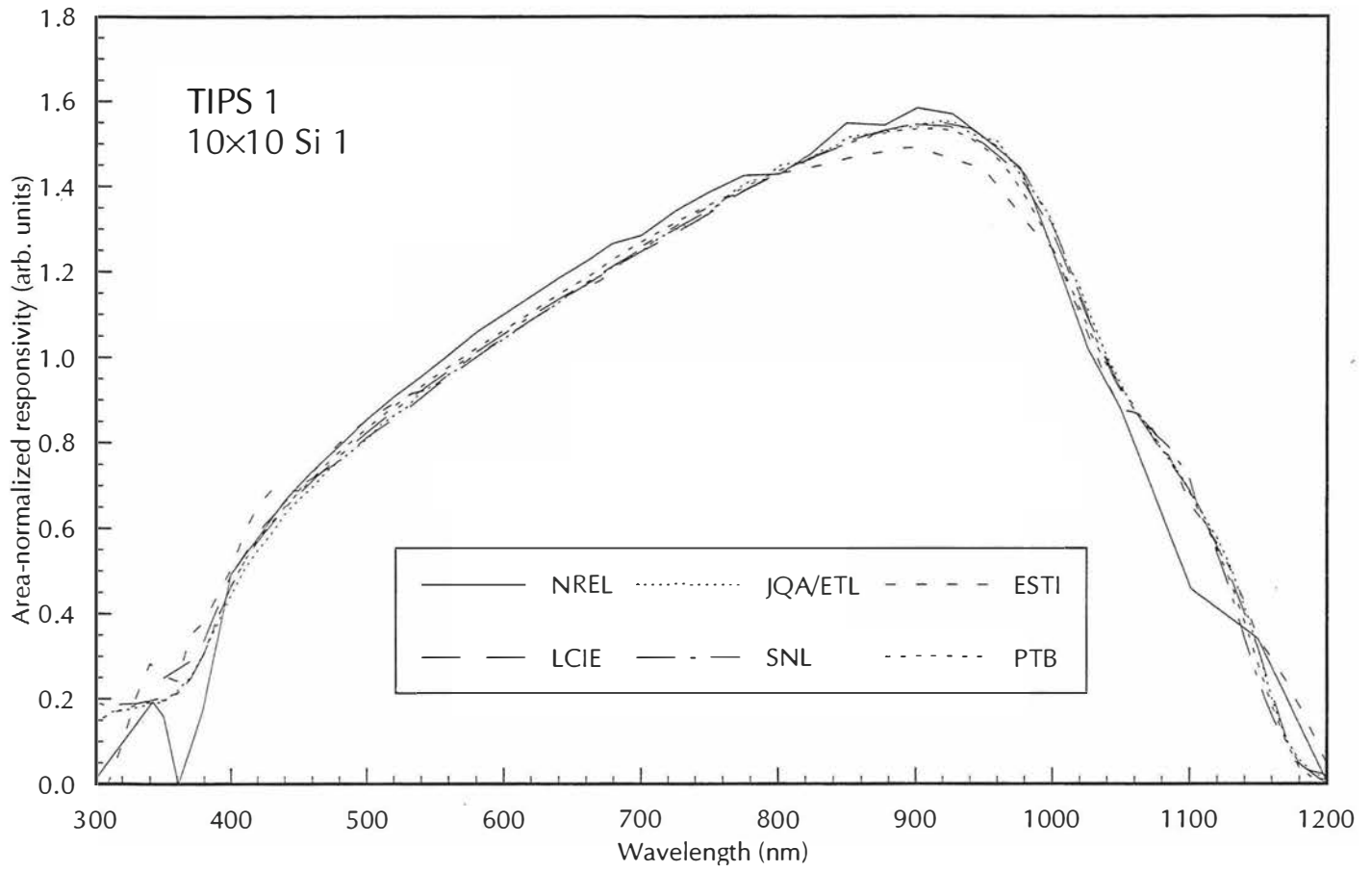


Figure 3-52. Area-normalized SR and deviation from average SR for 10×10 cm Si TIPS 1

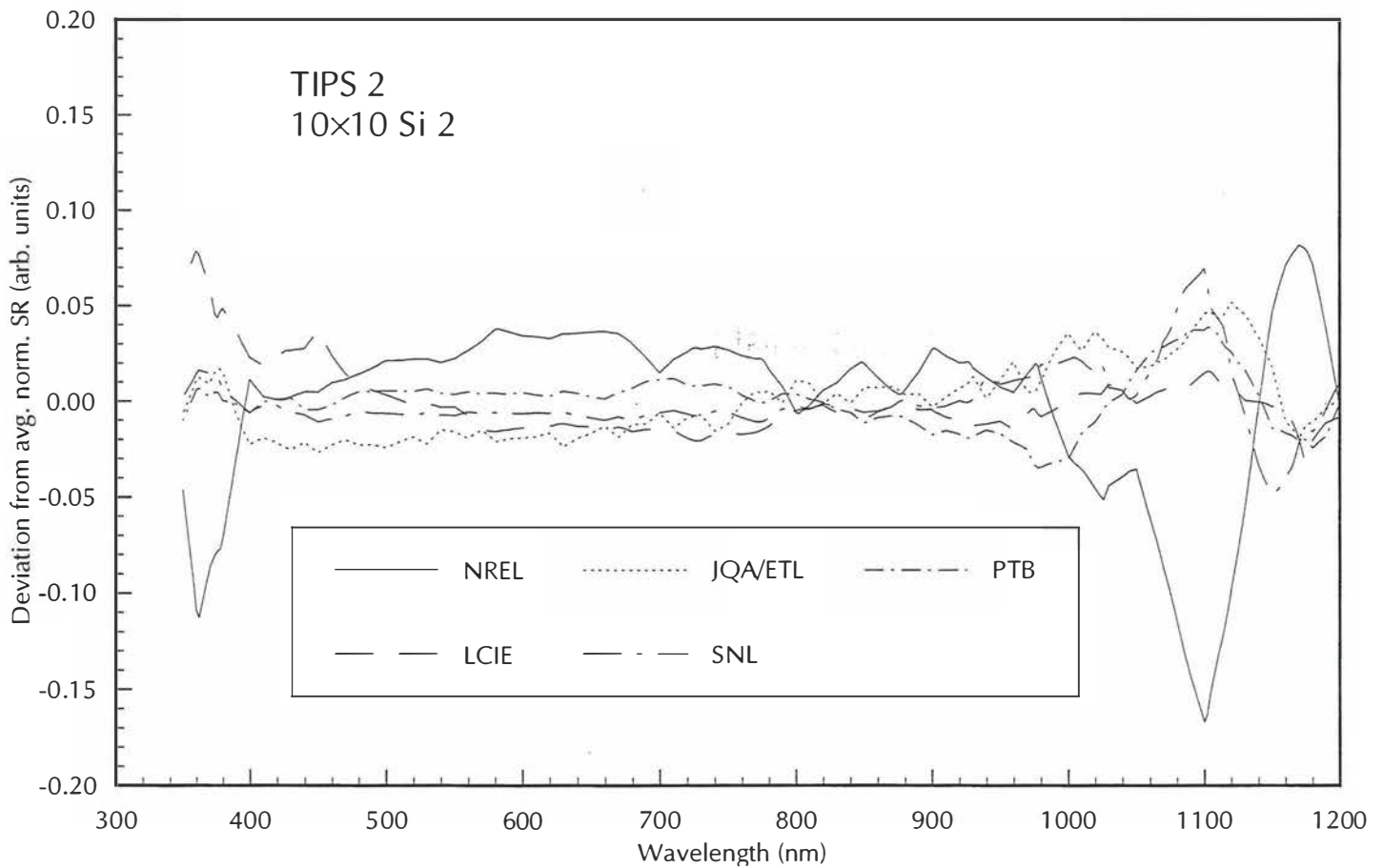
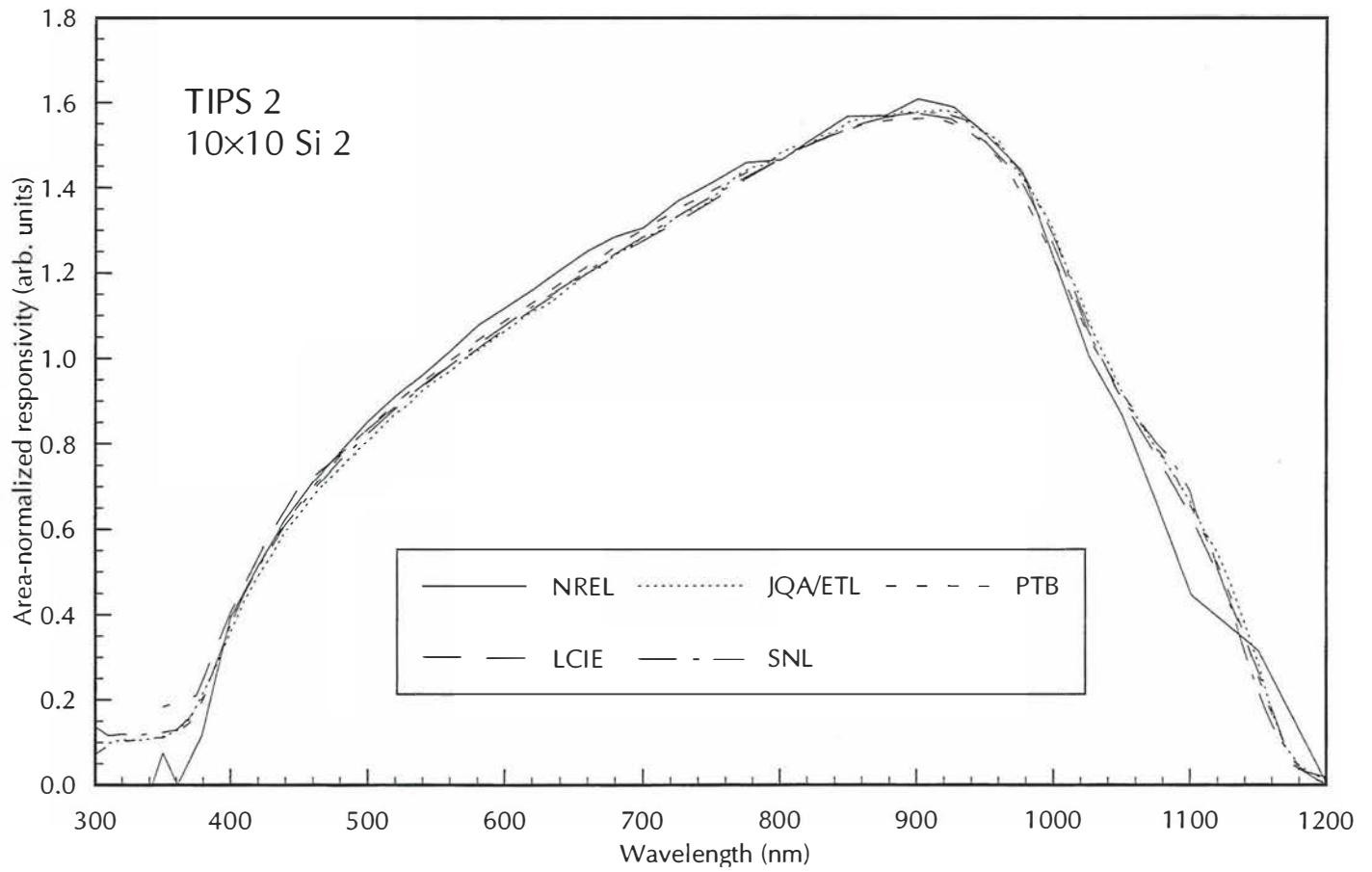


Figure 3-53. Area-normalized SR and deviation from average SR for 10×10 cm Si TIPS 2

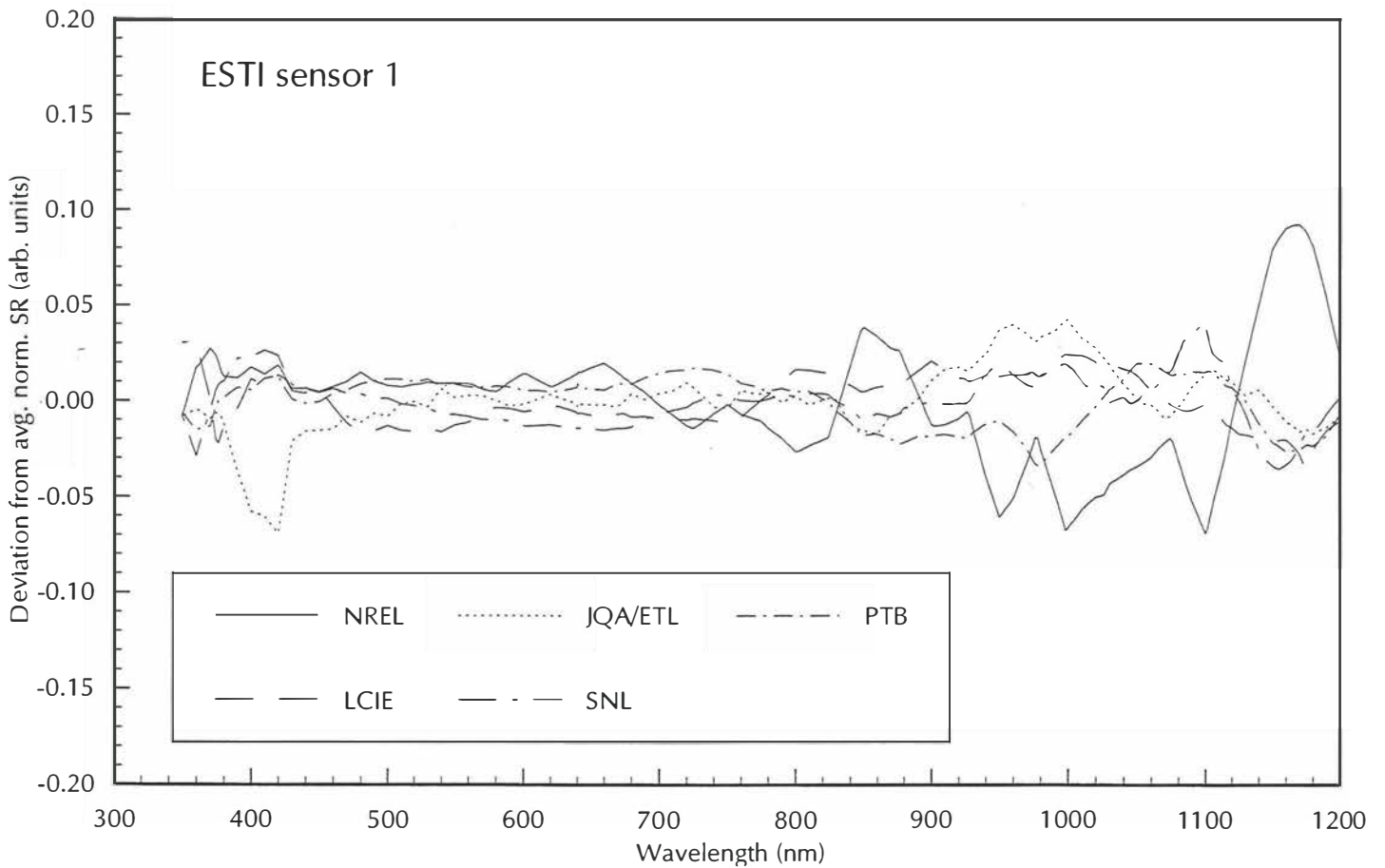
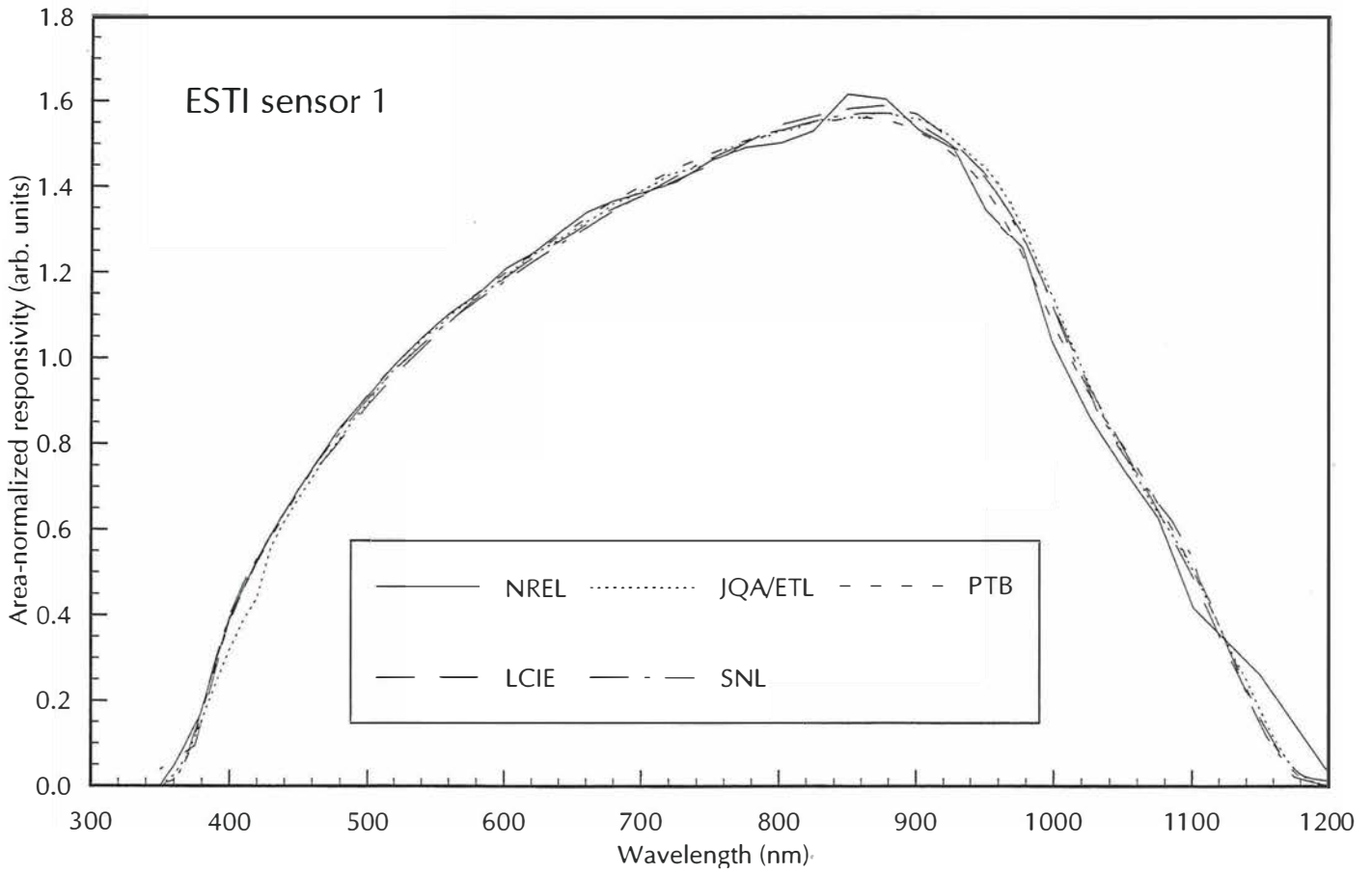


Figure 3-54. Area-normalized SR and deviation from average SR for ESTI sensor 1

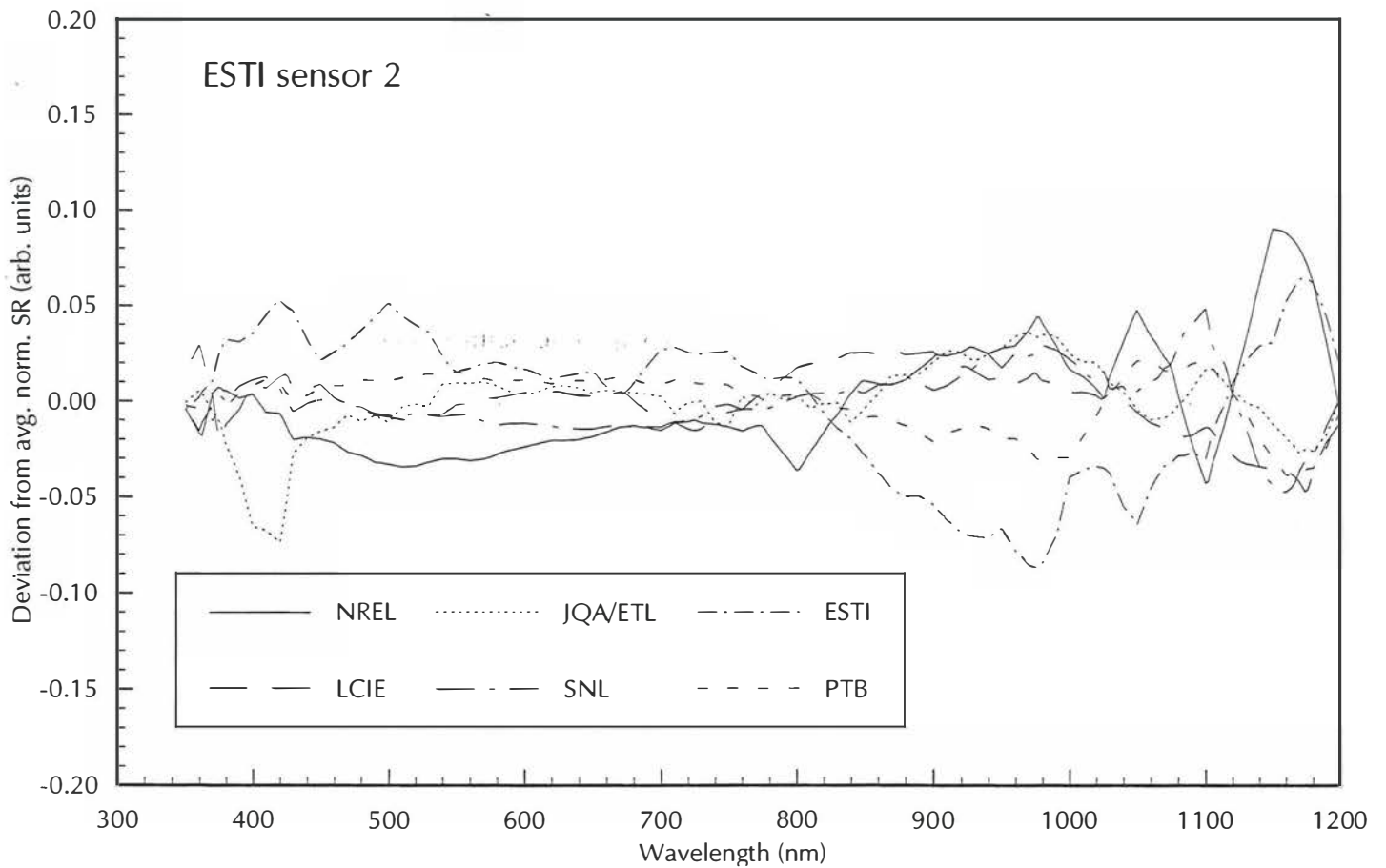
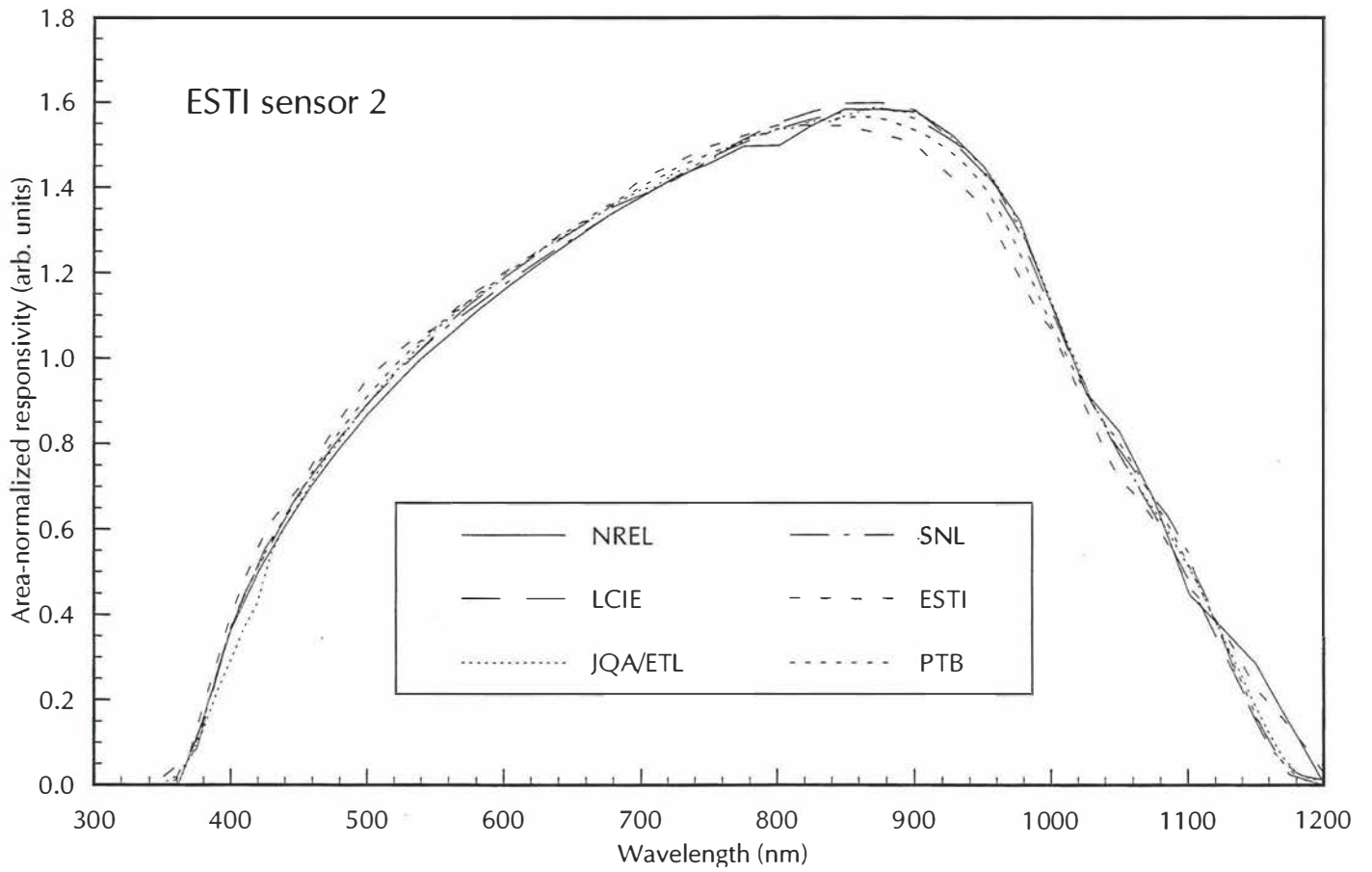


Figure 3-55. Area-normalized SR and deviation from average SR for ESTI sensor 2

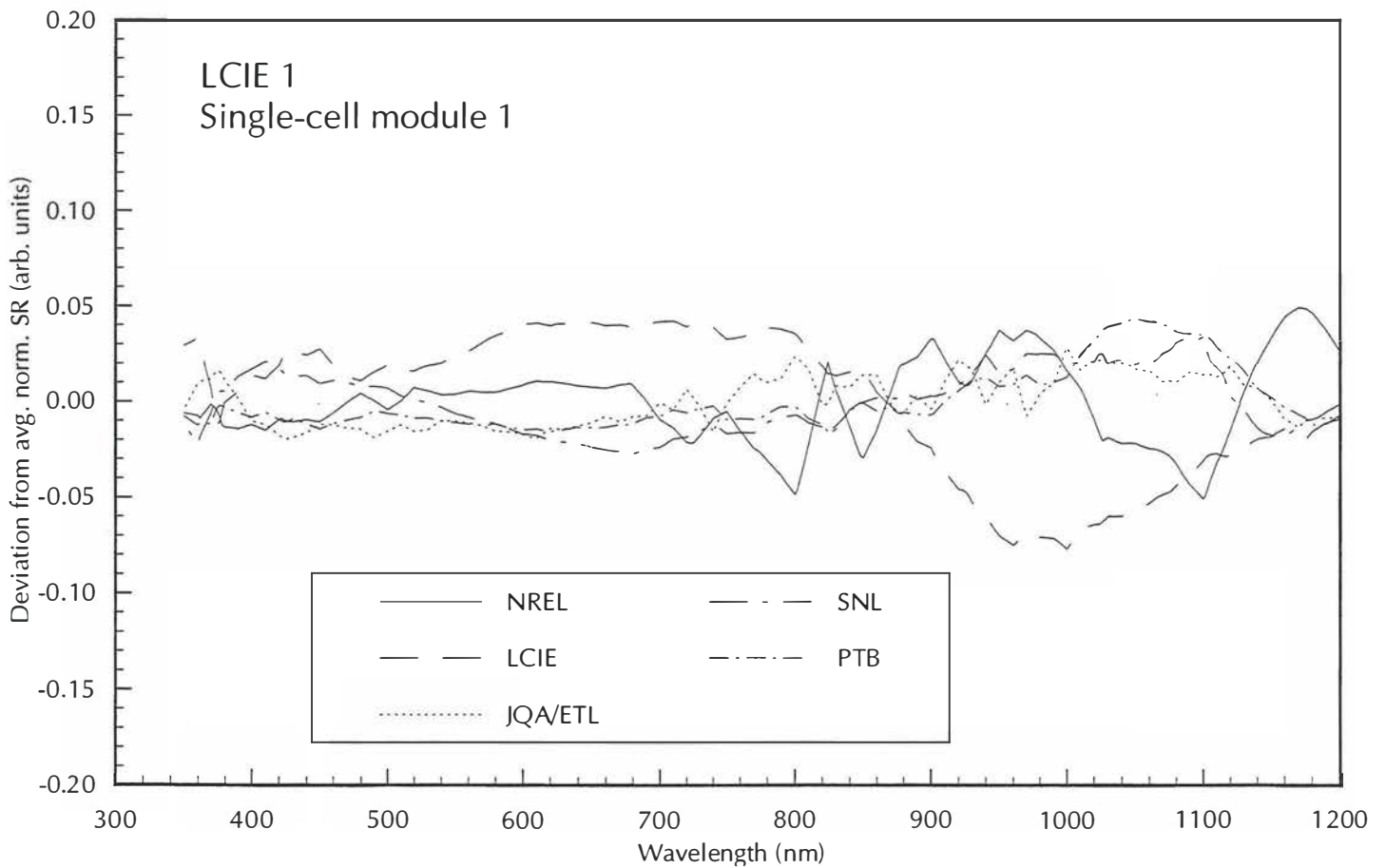
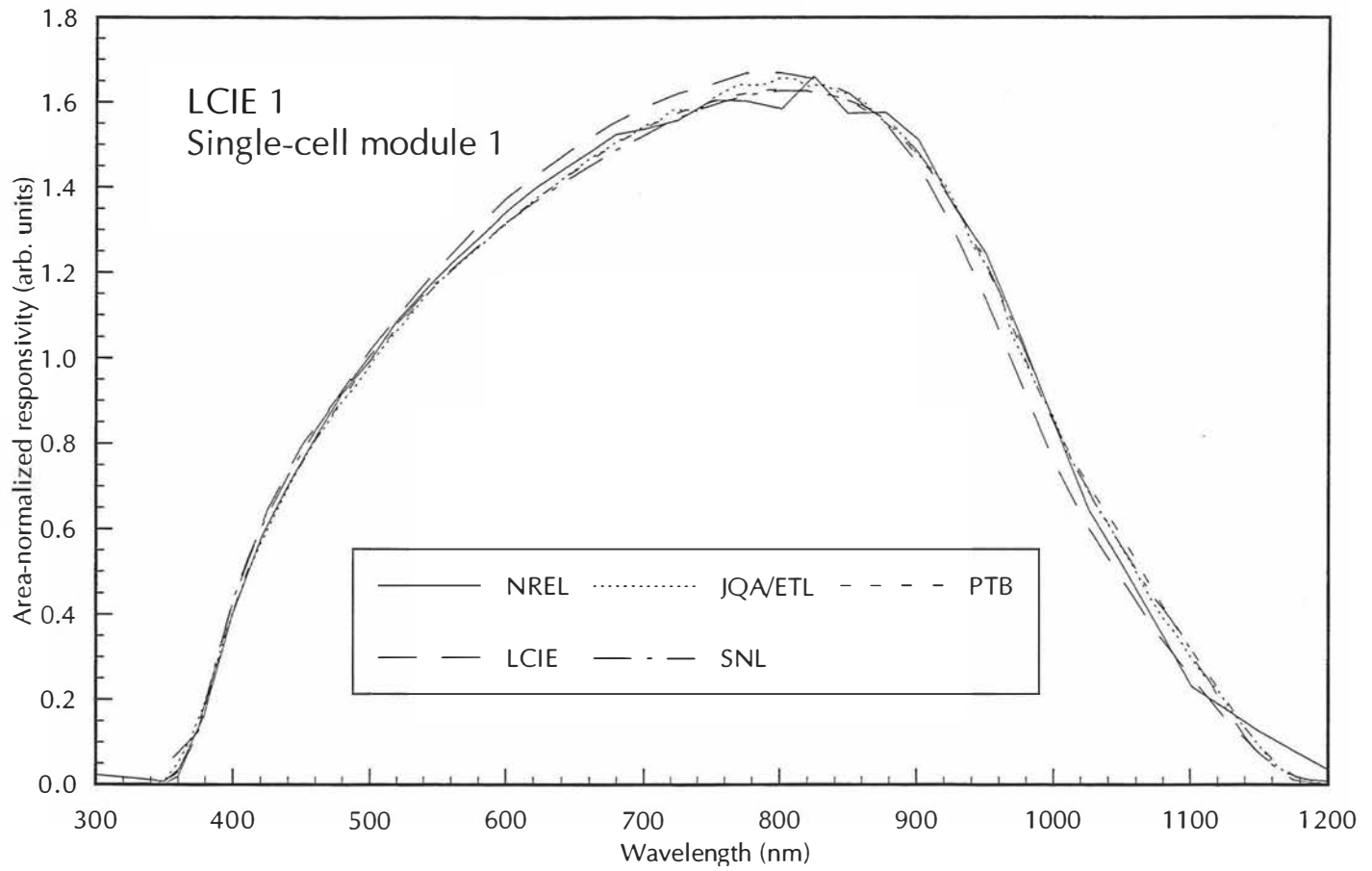


Figure 3-56. Area-normalized SR and deviation from average SR for single-cell module LCIE 1

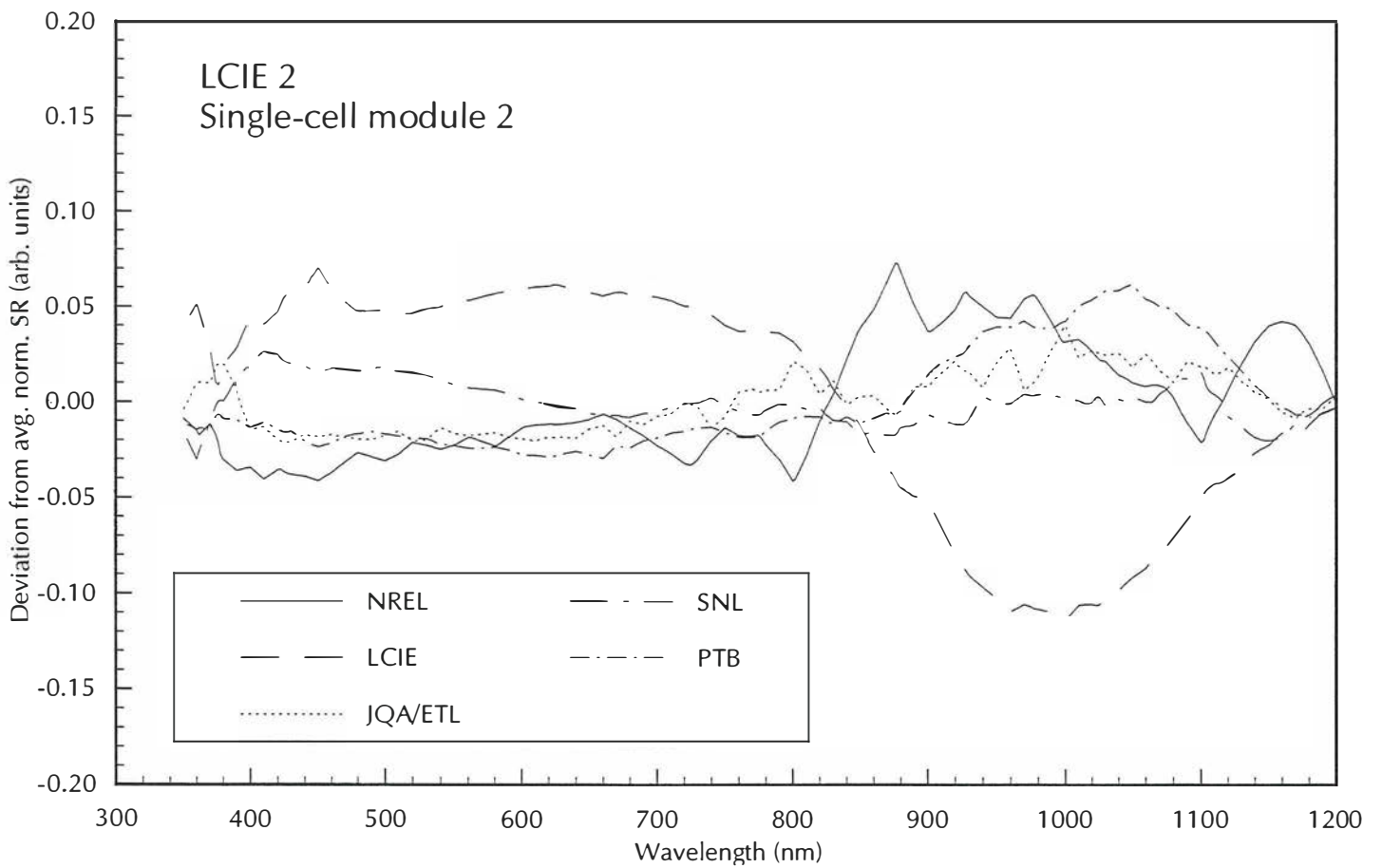
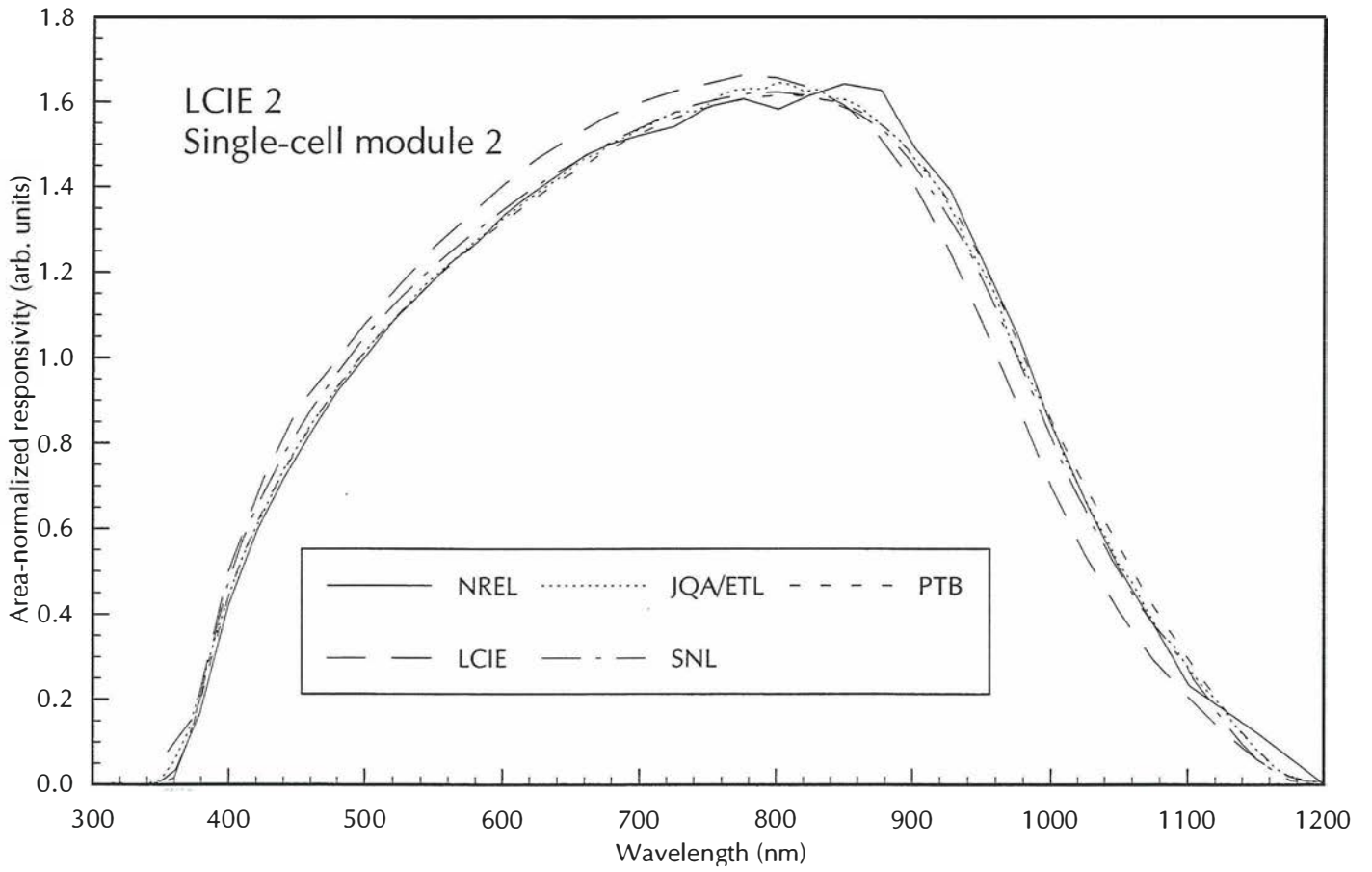


Figure 3-57. Area-normalized SR and deviation from average SR for single-cell module LCIE 2

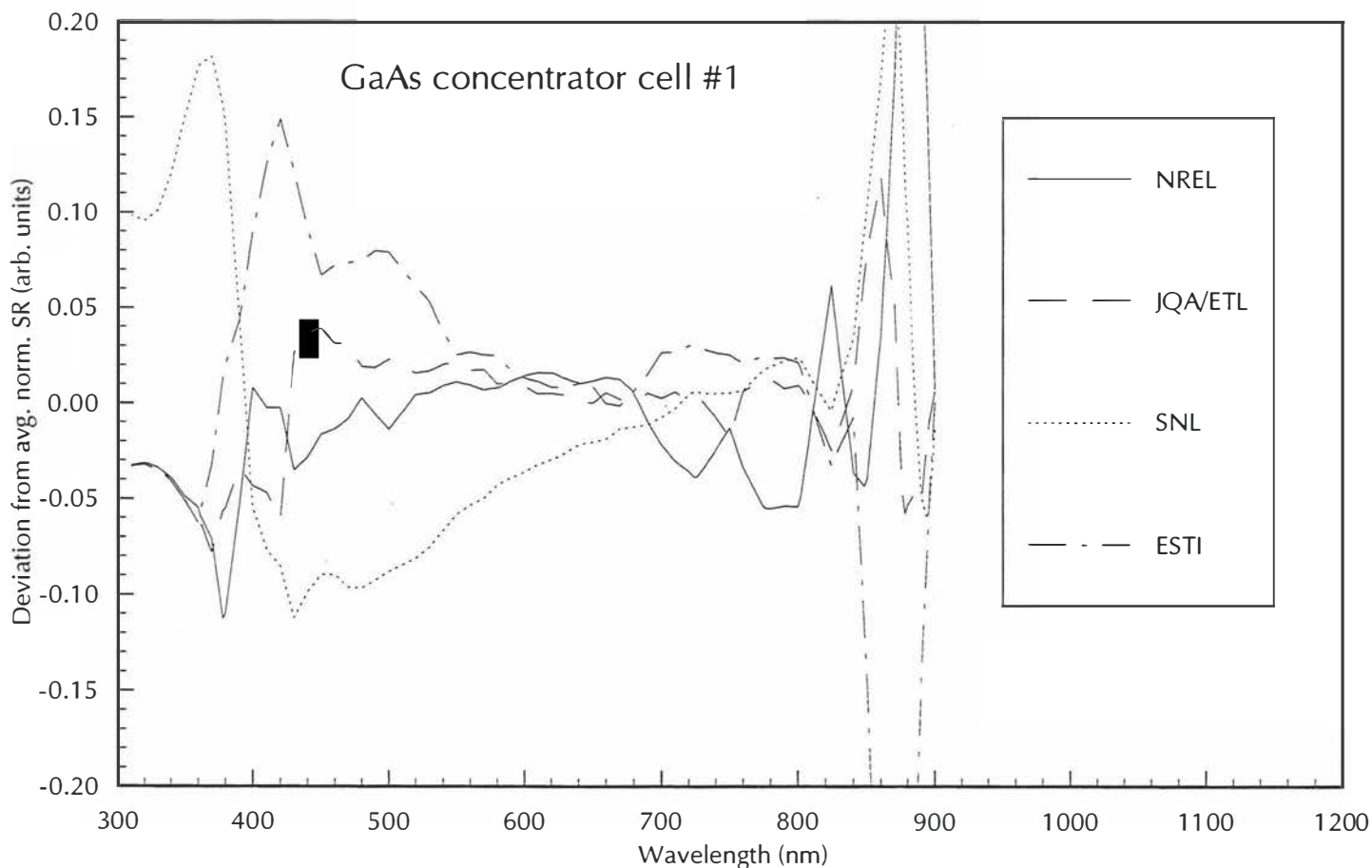
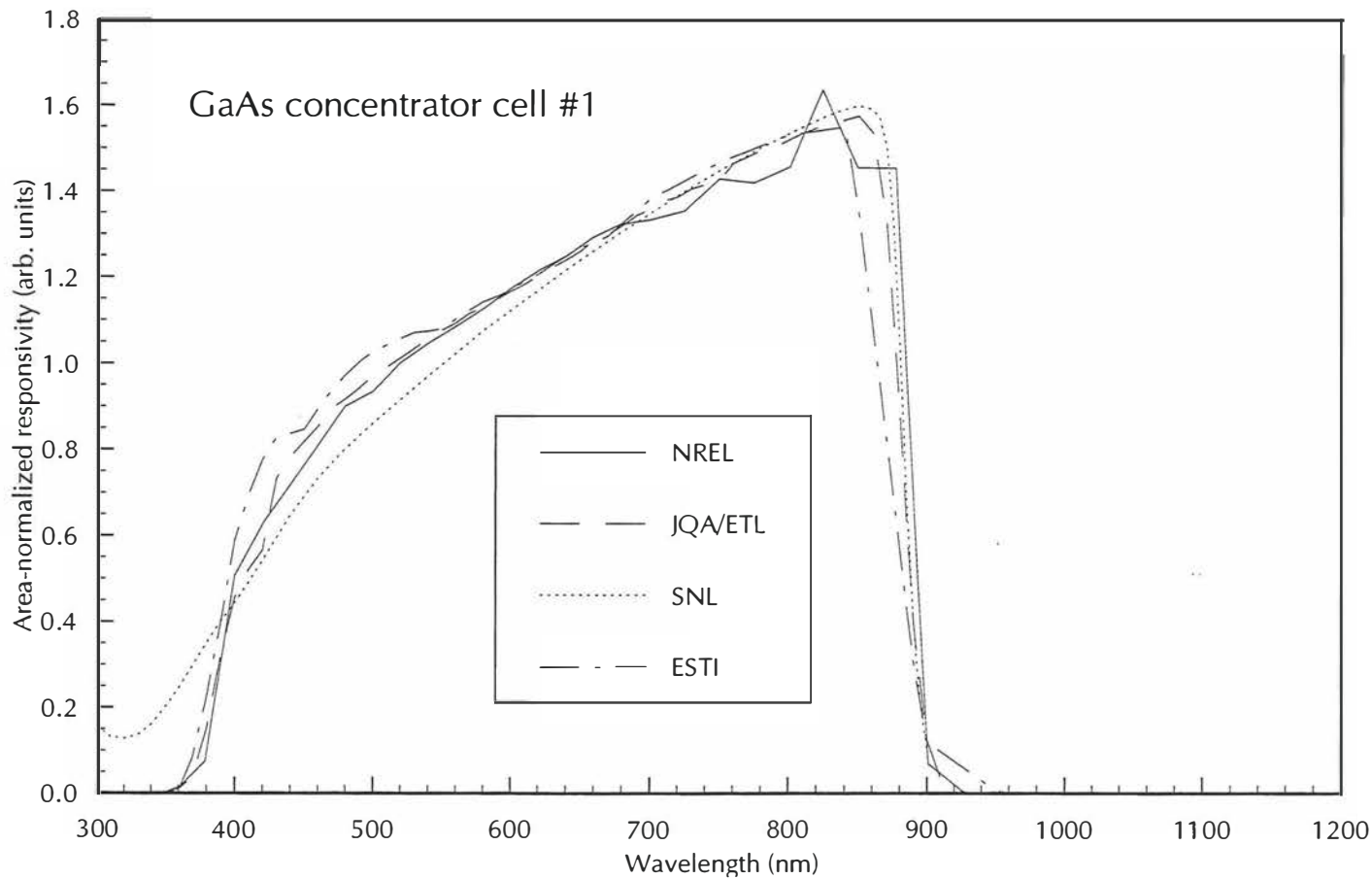


Figure 3-58. Area-normalized SR and deviation from average SR for GaAs concentrator cell #1

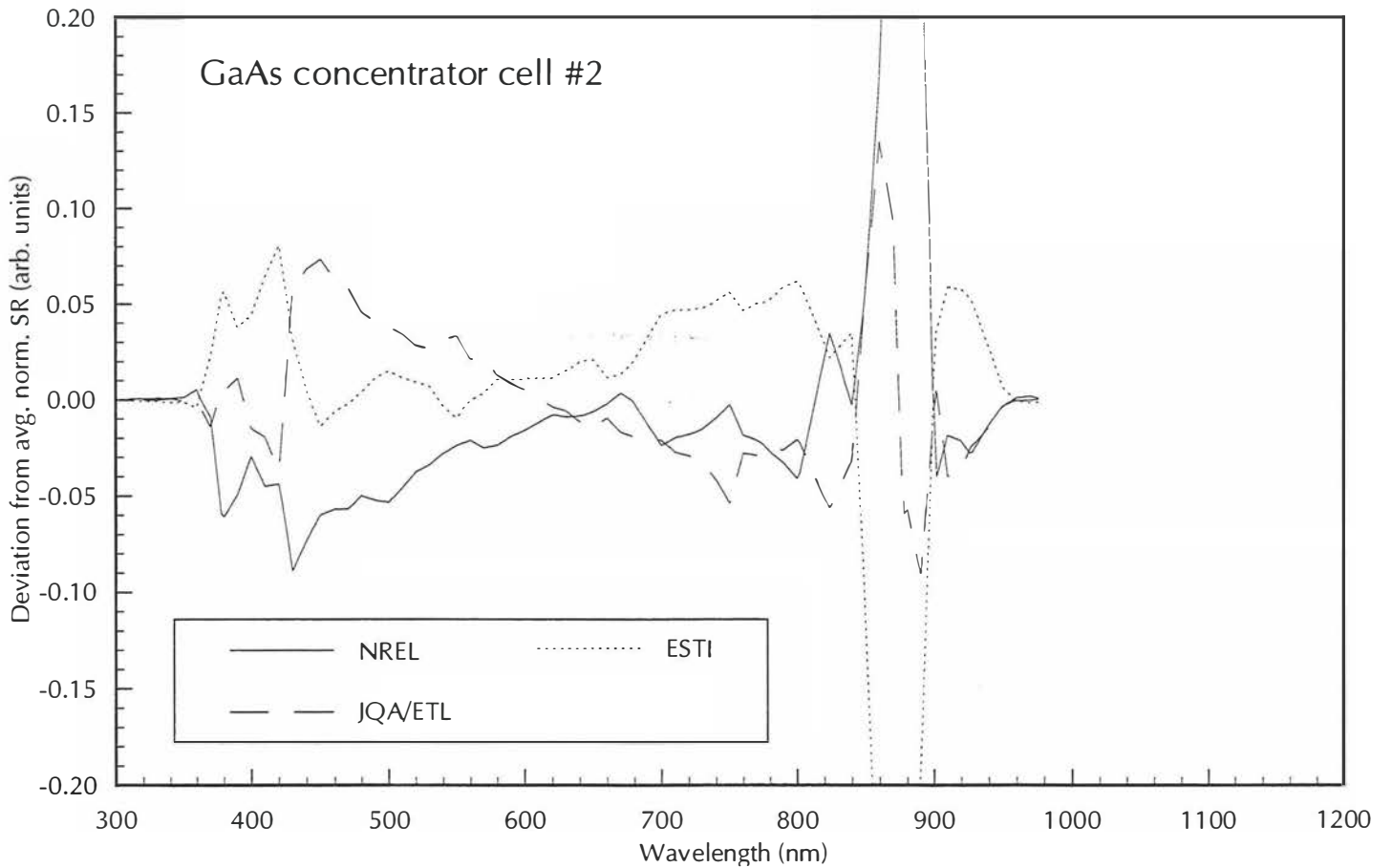
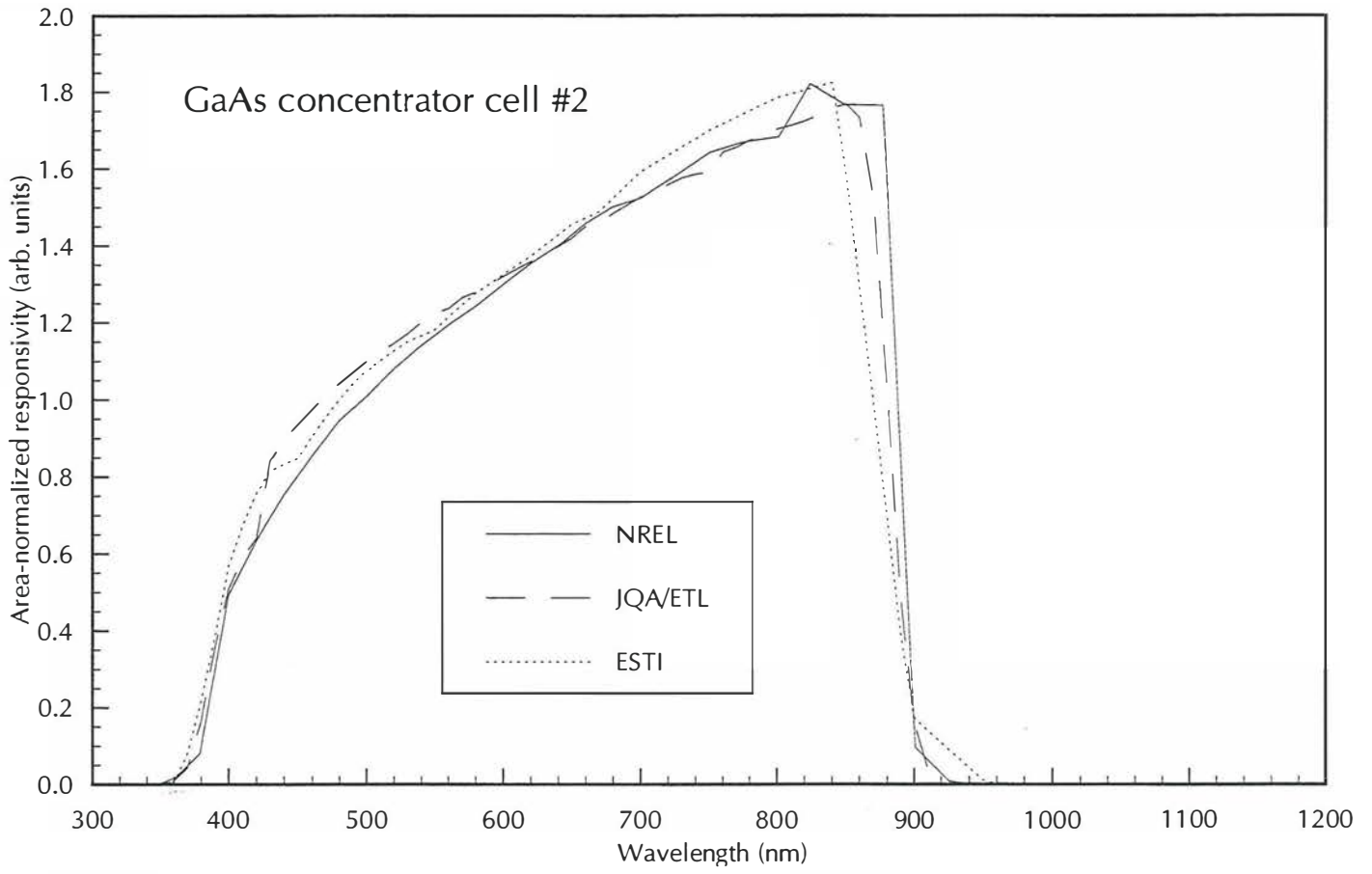


Figure 3-59. Area-normalized SR and deviation from average SR for GaAs concentrator cell #2

3.8 Conclusions

Although a great deal of data and analyses were generated by the NT series of the PEP'93, the intercomparison was marred by two serious problems: (1) the extremely long time period for sample circulation, caused by the ambitious schedule and shipping delays; and (2) unstable, damaged, and degraded samples. Two laboratories had the samples for periods much longer than the scheduled two months, and 33% of the original 24 devices in the sample set developed problems that limited their value to the project. In spite of these problems, the following conclusions can be made.

Open-circuit voltage agreement on all devices is excellent if the device temperature is controlled to the standard value (25°C). Fig. 3-32 shows that standard deviations of less than 1% are attainable when temperature control is used.

Agreement for short-circuit current measurements is 2–3 times worse than the V_{oc} results, and differences in I_{sc} cannot be attributed solely to spectral responsivity measurement differences. Therefore, I_{sc} differences must be caused by reference cells or radiometric calibrations. It is hoped that the WPVS can help reduce these differences.

The low- and high-pass filtered Si and the GaAs cells have nearly identical standard deviations of I_{sc} , so there do not appear to be any wavelength dependent biases associated with non-silicon performance measurements.

Light soaking effects in the CdTe cells may have increased the scatter of the I_{sc} results for these devices.

From Fig. 3-34 it can be seen that FF agreement is better than the short-circuit current agreement, but not as good as the V_{oc} results. An exception is the a-Si tandem cells, which showed a FF standard deviation comparable to the I_{sc} standard deviation. This is caused by the sensitivity of the FF of multijunction devices to the incident spectral irradiance.

For large area devices, FF agreement is good if repeatable four-wire contacts are available (as was true for the TIPS cells) and much worse for devices with two-wire contacts.

Although spectral responsivity results showed some significant shape differences, these differences apparently did not cause a large amount of scatter in the I_{sc} results. This is probably due to the use of solar simulators that are well matched to the reference spectral irradiance. Several laboratories did submit simulator spectral irradiance measurements; however, these were not analyzed for this report.

The spectral responsivity results have the poorest agreement in spectral regions where the signal-to-noise ratios are probably low and where the responsivity is changing rapidly. This is especially true of the bandgap cutoff region of devices using direct bandgap semiconductors.

Large differences, 10% and greater, were observed in the device areas (Table 3-8). For devices with well-defined geometries, such as the a-Si tandem cells and the LCIE single-cell modules, the differences were much less and typically less than 1%. Because area measurement errors contribute directly to errors in device efficiency, it is desirable to minimize such differences.

Spectral responsivity of multijunction devices is difficult to measure, and few laboratories have the facilities to perform these measurements.

3.9 Recommendations

After considering the objectives, results, and conclusions for the NT series, the following recommendations can be stated.

Laboratories need to carefully consider the following potential problems when making performance measurements of devices similar to those of the NT series sample set:

- Temperature measurement and control
- Wiring and contacting test devices
- Test device instabilities to light and voltage
- Spectral responsivity measurement
- Test device area measurement and definition
- Pulsed versus steady-state simulation
- Sweep speed of I-V curve tracing
- Larger area test devices
- Device area determination
- What is the correct method for measuring a newer technology device?

Multijunction devices require multijunction measurement techniques.

Short-circuit current measurements should be traceable to the World PV Scale.

4. General Recommendations

Beyond the recommendations already made for the WPVS and the NT series (see Sections 2.9.4 and 3.9), the following recommendations for future intercomparisons are made.

4.1 Objectives

Future intercomparisons are needed to continue monitoring differences on the following types of devices: multijunction, large-area, and thin-film. Judging by the results from the large-area cells, module measurements should also be included.

Results from the WPVS short-circuit current temperature coefficients show that this is a particularly difficult measurement. Temperature coefficients should be included in the future to study these problems.

Dark I-V should be considered for inclusion in the required measurements.

The PEP'93 did not address objective (3) in Section 1.2 above; i.e., to recommend methods of qualifying data in publications. Although this is a noble objective, it is not possible to use a round-robin program to accomplish it. One possible method for qualifying PV performance data could be an accreditation program for measurement laboratories, but considerations for such a program are beyond the scope of this report.

4.2 Organization

A new title should be selected for the next intercomparison because the Photovoltaic Energy Project has been officially terminated. It is not clear that a new sponsoring organization is needed because the PEP'93 was successfully concluded without the oversight of a sponsor. However, if a suitable organization is located or formed and can offer advantages beyond those of a voluntary grouping of laboratories, such a sponsor should be utilized.

4.3 Pitfalls

The PEP'93 has shown several organizational pitfalls that future intercomparisons should strive to avoid.

First, a qualification or acceptance of some kind is needed to screen out samples that will not survive the stresses of circulation. The WPVS proposal has an acceptance test for new admittance for

new cells, but non-WPVS intercomparisons also should have a way of eliminating poor samples before to the start of circulation.

Second, the selected samples should match the objectives of the intercomparison. For the NT series, the original intent for the large-area samples was to study FF differences on 10×10 cm cells that lacked attached contacts. The call for samples did not state this objective clearly, and the large-area devices in the final sample set all had attached wiring.

Finally, it is important to strictly adhere to the schedule established by the organizing agent. Extra time at one laboratory can cause extreme problems for the laboratories that follow. When this happens, participants cannot know, and thus cannot schedule internally, when they will need to perform the difficult measurements for a round robin. This is especially difficult for laboratories that use outdoor measurements. In the case of the NT series, shipping delays added two full years to the intercomparison. This is clearly unacceptable for the timely dissemination of results. Laboratories that have problems shipping sample sets in a timely fashion should not agree to participate.

4.4 Data Submission

Electronic data submission of results was very successful during the PEP'93, especially via electronic mail. It is highly recommended for future intercomparisons. Hard copy submission is prone to transcription errors and increases the work load of the coordinator. Also, I-V and spectral responsivity curves on paper have very limited value for analysis purposes. These are much easier to use if submitted in tabular electronic format.

5. References

- [1] H. Ossenbrink, R. Van Steenwinkel, K. Krebs, "The Results of the 1984/1985 Round-Robin Calibration of Reference Solar Cells for the Summit Working Group on Technology, Growth, and Employment," Joint Research Centre, Ispra Establishment, PREPRINT EUR 10613 EN, April 1986.
- [2] J. Metzdorf, T. Wittchen, K. Heidler, K. Dehne, R. Shimokawa, F. Nagamine, H Ossenbrink, L. Fornarini, C. Goodbody, M. Davies, K. Emery, R. DeBlasio, "Objectives and Results of the PEP'87 Round-Robin Calibration of Reference Solar Cells and Modules," *Proc. 21st IEEE PV Spec. Conf.*, Kissiminee, FL, 1990, pp. 952-959. See also "The Results of the PEP'87 Round Robin Calibration of Reference Solar Cells and Modules -Final Report-," PTB report PTB-Opt-31, ISBN 3-89429-067-6, Braunschweig, 1990, 174 p.
- [3] "Fluid Flow Measurement Uncertainty," *International Standards Organization Standard 5168*, Geneva, Switzerland, 1990.
- [4] "Guide to the Expression of Uncertainty in Measurement," *International Organization for Standardization and International Bureau of Weights and Measures*, ISBN 92-67-10188-9, 1st ed., Geneva, Switzerland, 1995, 101 p.
- [5] C.R. Osterwald, S. Anevsky, A.K. Barua, J. Dubard, K. Emery, D. King, J. Metzdorf, F. Nagamine, R. Shimokawa, N. Udayakumar, Y.X. Wang, T. Wittchen, W. Zaaïman, A. Zastrow, J. Zhang, "Results of the PEP'93 Intercomparison of Reference Cell Calibrations and Newer Technology Performance Measurements," *Proc. 25th IEEE PV Spec. Conf.*, Washington, DC, 1996, pp. 1263-1266.
- [6] C.R. Osterwald, S. Anevsky, A.K. Barua, P. Chaudhuri, J. Dubard, K. Emery, B. Hansen, D. King, J. Metzdorf, F. Nagamine, R. Shimokawa, Y.X. Wang, T. Wittchen, W. Zaaïman, A. Zastrow, and J. Zhang, "The World Photovoltaic Scale: an International Reference Cell Calibration Program," *Proc. 26th IEEE PV Spec. Conf.*, Anaheim, CA, 1997, pp. 1209-1212.
- [7] "Photovoltaic Devices—Part 2: Requirements for Reference Solar Cells," *International Electrotechnical Commission Standard 60904-2*, Geneva, Switzerland, 1989.
- [8] Product literature from PRC Krochmann GmbH, Geneststrasse 6, 10829 Berlin, Germany, telephone (0 30) 751 70 07, fax (0 30) 751 01 27. PRC stands for Photometry, Radiometry, and Colorimetry.
- [9] J. Metzdorf, W. Möller (eds.), "Meßtechnik in der Photovoltaik," PTB report PTB-Opt-32, ISBN 3-89429-099-4, Braunschweig, Germany, 1991, 188 p.
- [10] "Standard Specification for Physical Characteristics of Nonconcentrator Terrestrial Photovoltaic Reference Cells," *American Society for Testing and Materials Standard E 1040-93*, West Conshohocken, PA, 1993.
- [11] "Secondary Reference Crystalline Solar Cells," *Japanese Industrial Standard JIS C 8911-1989*, Japanese Standards Association, Japan, 1989.

- [12] “Photovoltaic Devices—Part 3: Measurement Principles for Terrestrial Photovoltaic (PV) Solar Devices with Reference Spectral Irradiance Data,” *International Electrotechnical Commission Standard 60904-3*, Geneva, Switzerland, 1989.
- [13] C.R. Osterwald, K.A. Emery, D.R. Myers, and R.E. Hart, “Primary Reference Cell Calibrations at SERI: History and Methods,” *Proc. 21st IEEE PV Spec. Conf.*, Kissimmee, FL, 1990, pp. 1062-1067. Also see “Standard Test Method for Calibration of Primary Non-Concentrator Terrestrial Photovoltaic Reference Cells Using a Tabular Spectrum,” *American Society for Testing and Materials Standard E 1125-94*, West Conshohocken, PA, 1994.
- [14] R. Shimokawa, F. Nagamine, Y. Miyake, K. Fujisawa, and Y. Hamakawa, “Japanese Indoor Calibration Method for the Reference Solar Cell and Comparison with Outdoor Calibration,” *Jpn. J. of Appl. Phys.* v. 26, pp. 86-91.
- [15] J. Metzdorf, “Calibration of Solar Cells 1: The Differential Spectral Responsivity Method,” *Appl. Optics* v. 6, 1987, pp. 1701-1708. Also see J. Metzdorf, T. Wittchen, B. Nawo, and W. Möller, “The Primary Reference Solar Cell Calibration Facility at PTB,” *Tech. Digest of the 5th International PV Solar Energy Conf. (PVSEC-5)*, Kyoto, Japan, 1990, pp. 705-708.
- [16] M. Wolf and H. Rauschenbach, “Series Resistance Effects on Solar Cell Measurements,” *Advanced Energy Conversion* v. 3, 1963, pp. 455-479.
- [17] Product literature from Omega Engineering, Inc., PO Box 4047, Stamford, CT 06907-0047, USA, telephone 203-359-1660, fax 203-359-7700.
- [18] J. Romero, N.P. Fox, and C. Fröhlich, “Improved Comparison of the World Radiometric Reference and the SI Radiometric Scale,” *Metrologia* v. 32, 1995/96, pp. 523-524.
- [19] F. Nagamine, R. Shimokawa, M. Suzuki, and T. Abe, “New Solar Simulator for Multi-Junction Solar Cell Measurements,” *Proc. 23th IEEE PV Spec. Conf.*, Louisville, KY, 1993, pp. 686-690.
- [20] G. Friesen, H.A. Ossenbrink, and W.J. Zaiman, “Investigation of Capacity Effects in BSF-Cells under Pulsed Illumination,” *Proc. 13th European PV Solar Energy Conf. and Exhibition*, Nice, France, 1995, pp. 2395-2397.
- [21] Product literature from Lemo USA Inc., PO Box 11488, Santa Rosa CA 95406, USA, telephone 800-444-5366, fax 707-578-0869.

Appendix 1 WPVS Reference Cell Package Design

The new WPVS reference cell design meets the goals outlined in Section 2.9.2, and can be broken down into 6 components: the physical package, the solar cell, encapsulation, the window, electrical connections, and temperature sensors. Each of these is presented below.

It should be emphasized that most of the requirements that are specified in the package design and the acceptance test (see Appendix 2) are intended to prevent or minimize the problems found among the individual cells that were circulated for the PEP'93. These include broken windows, encapsulation bubbles, internal reflections, high thermal masses, degradation of labels, and incompatible connections (see Section 2-1).

A1.1 Physical Reference Cell Package

Fig. A1-1 is the physical package (designed by JQA) that was developed from earlier Japanese designs (see Ref. [11] for an example). It differs from these designs by lacking an integral cooling stage and permanent cables. This reduces the thermal mass and the total thickness, and allows different laboratories to use whatever electrical connections are most convenient. Note that the thickness is 17 mm, which is slightly higher than the goal of 15 mm (see Section 2.9.2). The extra thickness was needed to accommodate the mating connectors at the package side. Using the definition in Ref. [10], the field of view for this package is approximately 164° , which meets the IEC 60904-2 specification [7]. Fig. A1-2 is an optional detachable water cooling stage.

Although Fig. A1-1 is complete and meets all the necessary requirements, it is noted that the features that should be considered standard are the outside dimensions, the window size and location, the solar cell location, the location and size of the four mounting holes at the corners, and the connector location. The other internal details were designed to be compatible with the manufacturing processes currently used by JQA. In any event, the package must have:

- An electrically and thermally conductive case
- Black exterior surfaces
- Black interior
- A field of view of at least 160°
- Permanent identification markings
- A flat rear surface without protrusions

Additionally, if a cooling system is provided (such as water or thermoelectric), it must be detachable from the main package.

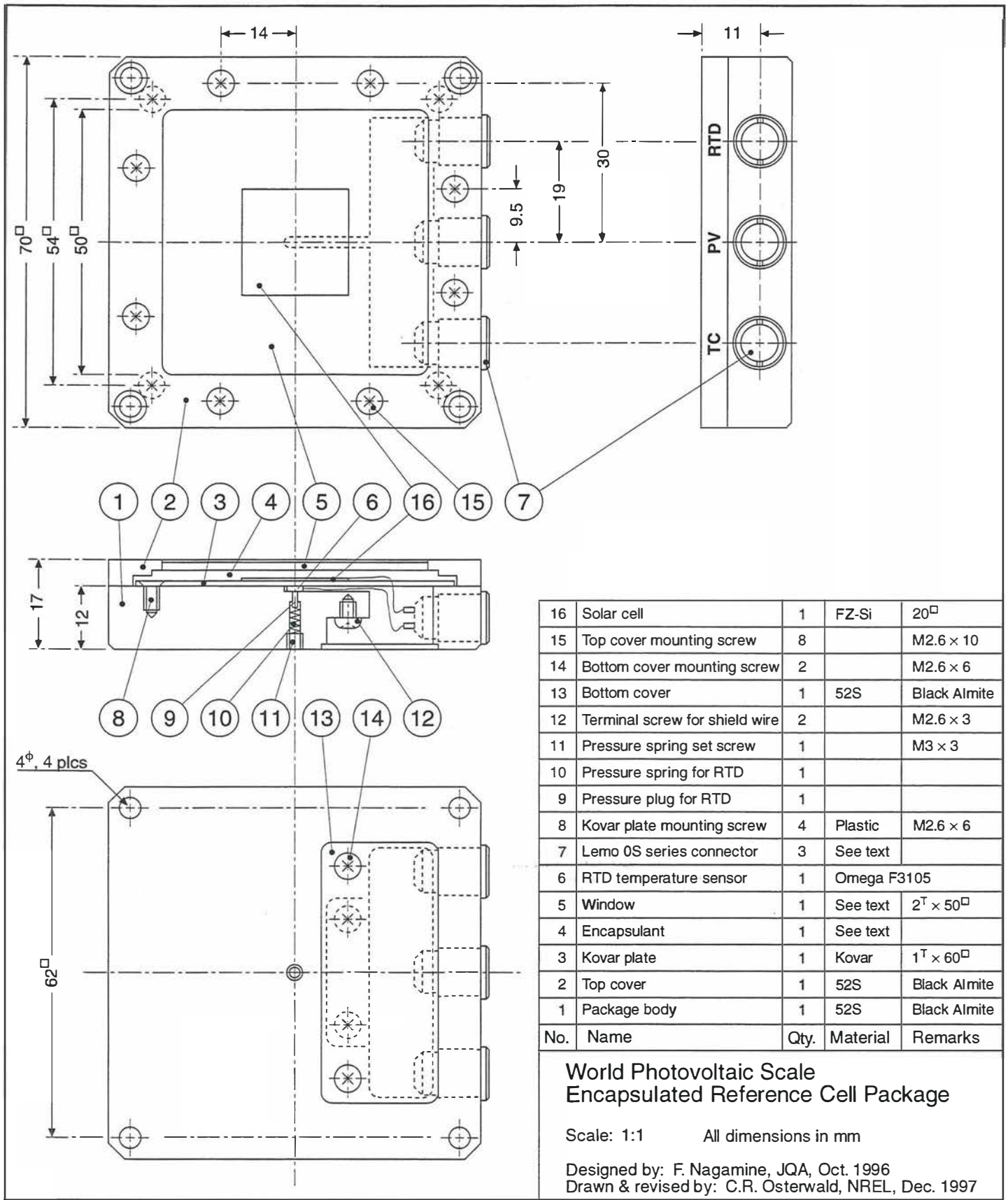


Figure A1-1. WPVS reference cell package design

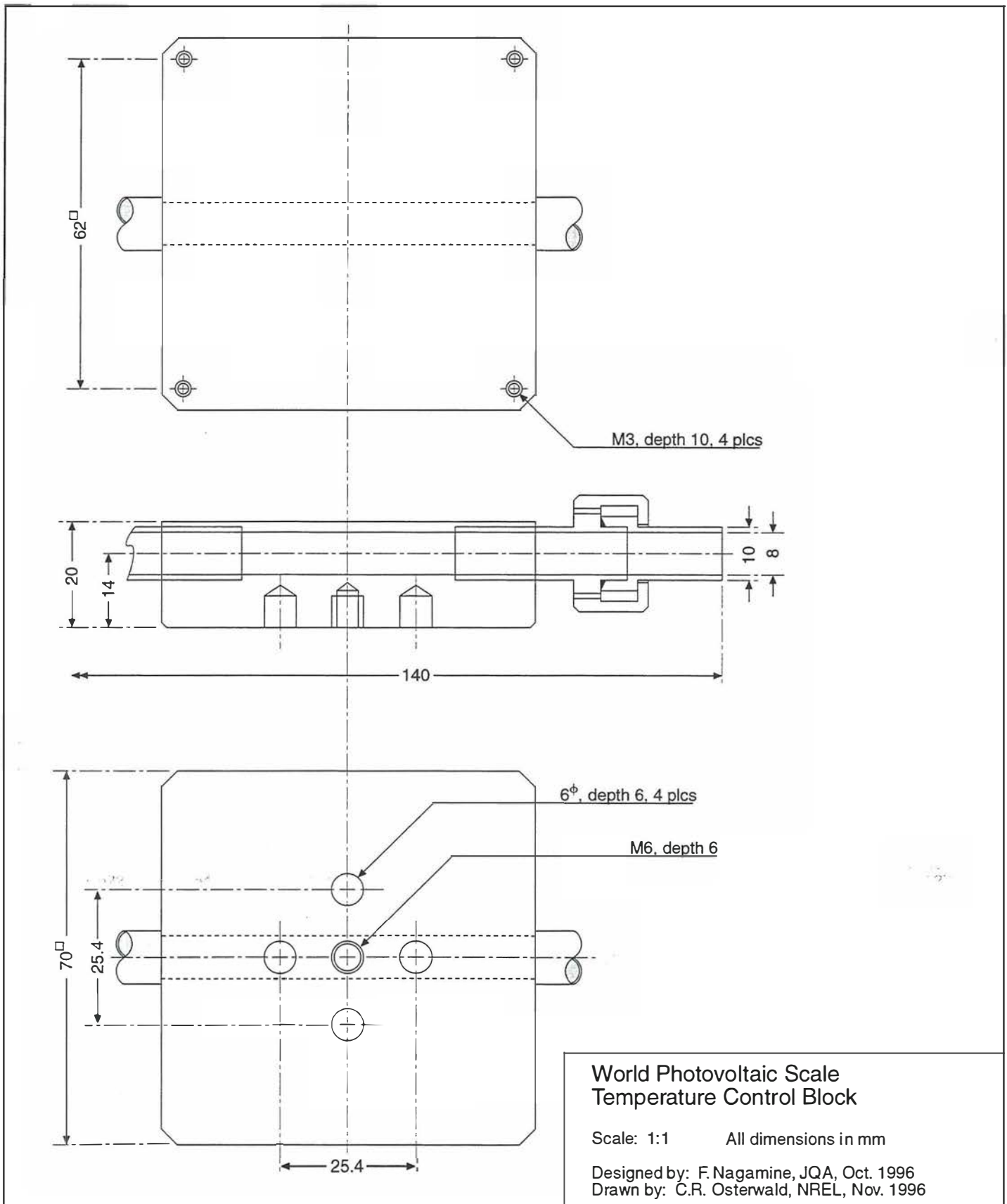


Figure A1-2. Optional temperature control block for the WPVS reference cell package design

A1.2 Solar Cell

The solar cell inside the package must meet several requirements. The cell must be

- Monocrystalline float zone (FZ) silicon
- 20×20 mm square, with a tolerance of ± 0.1 mm (equivalent to an area tolerance of $\pm 1\%$)
- Mounted parallel to the case rear surface within ± 0.1 mm or $\pm 0.25^\circ$
- Positioned laterally within ± 0.5 mm of the package center
- Electrically isolated from the package case.

Electrically, the cell must have a FF greater than 65% and a slope of the I-V curve at short-circuit current no greater than 5 mS.

No requirements are placed on the fabrication of the cell, but the cells used by PRC Krochmann are recommended because they have been found to be more than adequate for WPVS cells. These are monocrystalline FZ-Si cells made by Telefunken-Systemtechnik of Germany.

Several physical measurements of the solar cell are required at the time the package is manufactured and assembled. The solar cell area and the distance from the top of the solar cell to the front side of the window must be measured and provided as part of the calibration data. Also, the positional requirements above must be measured and verified.

A1.3 Window

A window that has a smooth front surface and is optically stable is required. The window can be quartz, an ultraviolet (UV) cutoff filter, or tempered glass of the type commonly used for module construction. Window durability is a primary design goal for WPVS cells—of the 20 cells circulated during the PEP'93, 3 sustained cracked or broken windows. For durability, it must be a minimum of 2 mm thick. The window should be mounted parallel to rear surface of the case within ± 0.1 mm or $\pm 0.25^\circ$.

A1.4 Encapsulation

An encapsulation material that provides index of refraction matching to the window material is required; an air gap between the solar cell and the window is not allowed. Recommended encapsulants that have been found to be suitable for reference cells include silicone and ethylene vinyl acetate (EVA). After encapsulation, no visible bubbles are allowed within 10 mm of the solar cell edges.

Note that because uncured silicone is a liquid, the design of Fig. A1-1 will need a barrier to prevent liquid silicone from flowing into the connector wiring area in the rear if access to the wiring area is needed at a later time. Another possible problem with silicone is the formation of bubbles during or after curing. One formulation in particular (Silgel 612, see Section 2.1) has a sensitivity to pressure that can cause bubbles to form after curing, especially with the lower atmospheric pressures encountered during air transportation.

A1.5 Temperature Sensors

Two independent temperature sensors are required—a T-type copper-constantan thermocouple and a four-wire Pt resistance temperature detector (RTD). The thermocouple is soldered to the front bus bar of the solar cell, and the RTD is in thermal contact with the rear surface of the cell. Fine gauge wire, 0.1 mm diameter or smaller, should be used for the thermocouple to minimize response time. The RTD should be a thin-film Pt RTD, 100 Ω , with $\alpha = 0.00385$ (temperature coefficient at 0°C), and must be electrically isolated from the solar cell. A suitable RTD, 2×2.3×1.3 mm, is Omega part number F3105 [17].

A1.6 Electrical Connections

Figure A1-3 is the wiring diagram for the WPVS package. The connectors are Lemo series 0S 10 mm round sockets [21]. A four-pin socket, Lemo part number ERA 0S 304 CLL, is used for the solar cell and RTD connections, and a three-pin socket with T-type thermocouple alloy contacts for the thermocouple connection (part number ERA 0S 304 CLT). The Lemo connectors are guaranteed for 5000 connect-disconnect cycles.

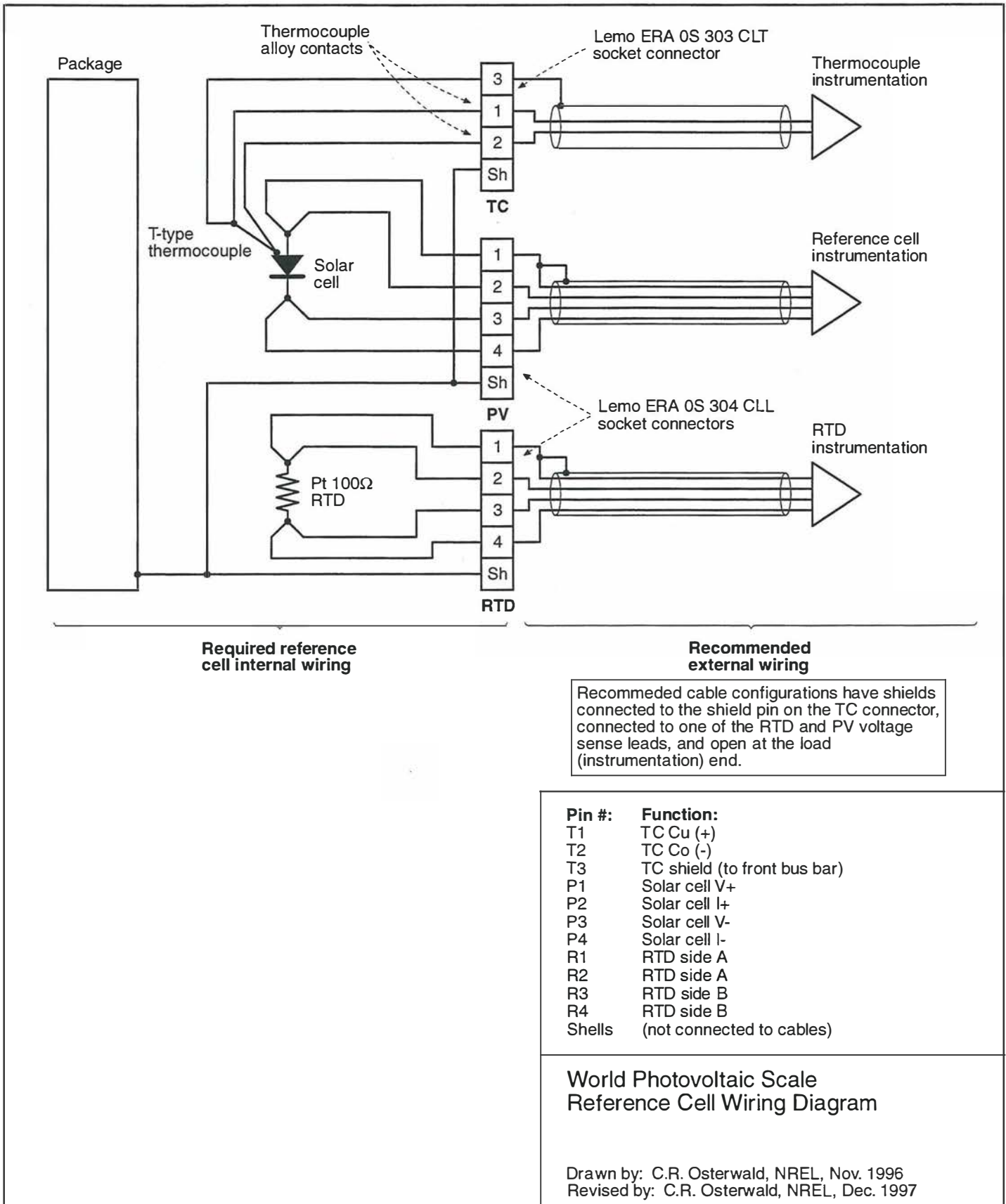


Figure A1-3. Wiring diagram for the WPVS reference cell package design

Appendix 2 WPVS Reference Cell Acceptance Test Procedure

In order to prevent or minimize problems with reference cells that will become part of the WPVS group, new reference cells must pass a comprehensive acceptance test procedure before beginning the calibration process. Fig. A2-1 shows the sequence of the acceptance test procedure, and the individual tests are specified below.

The results of the acceptance test become part of the cell's calibration documentation and must be available with the cell for future reference. After acceptance, the calibration process may begin.

A2.1 Physical and Dimensional Verification

This verification certifies that the new reference cell meets the physical and dimensional requirements of A1.1 and A1.2. Because the verification may involve measurements that are needed prior to the encapsulation of the cell, it is performed during manufacturing and before the actual acceptance tests. Note that A1.2 requires the solar cell area and the distance from the top of the solar cell to the front side of the window to be measured and kept as part of the calibration data.

A2.2 Visual Inspection

Visually verify that a new reference cell meets the requirements of A1.1, A1.3, and A1.4, and does not have obvious flaws that will limit its usefulness. Problems that should be identified include: internal reflections from non-black surfaces, encapsulant flaws such as bubbles or delamination, illegible or degraded identification markings, and a broken or scratched window. Following the light soak (see Section A2.7), the inspection must be repeated.

A2.3 Light I-V at STC Measurement

Obtain an I-V curve at STC [12] before and after the light soak (see Sec. A2.7). Determine the slope of the I-V curve at short-circuit current by performing a linear least-squares fit of the I-V data points near I_{sc} . The slope of the I-V curve must be less than 5 mS. Determine the FF, which must be greater than 65%.

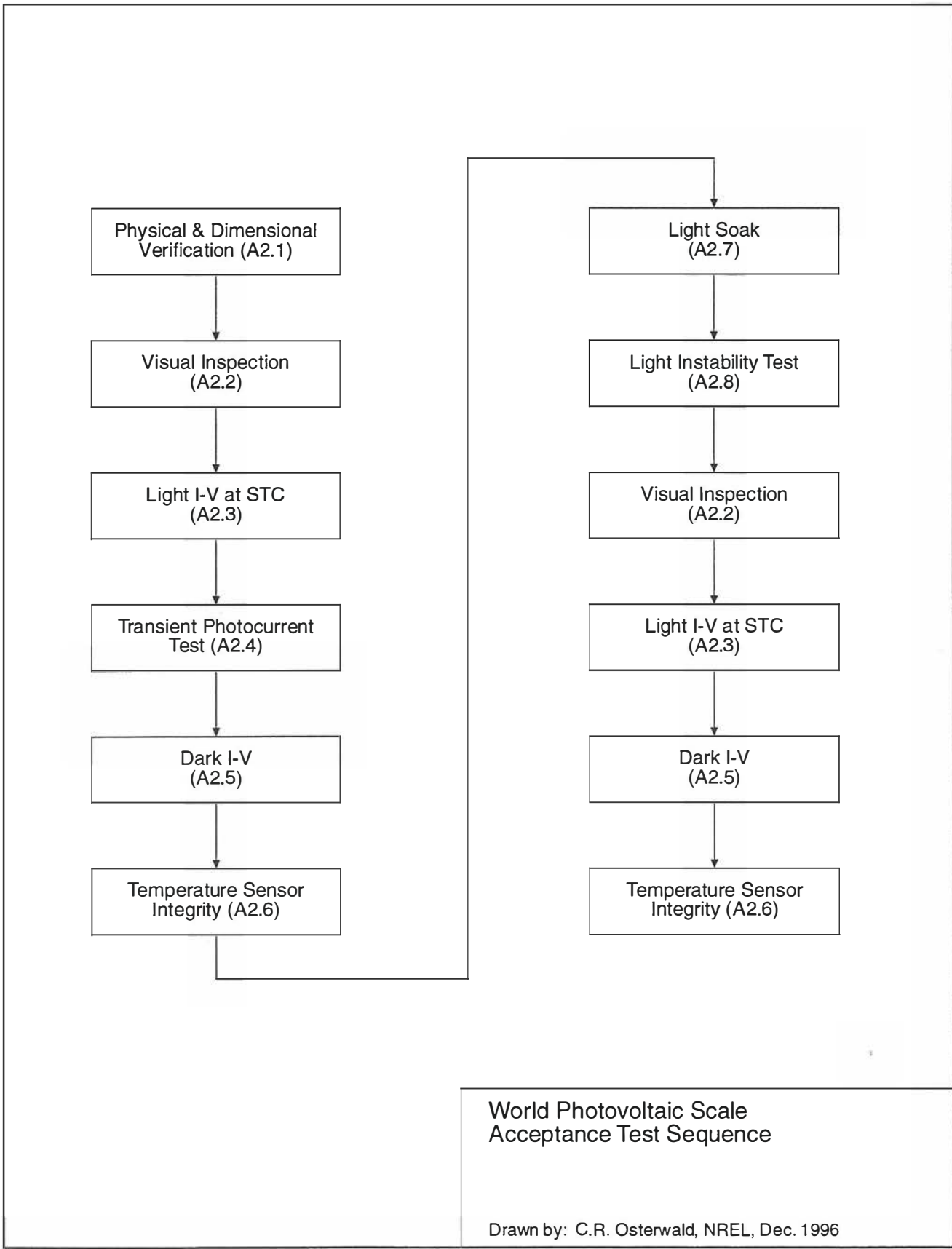


Figure A2-1. Flow diagram of WPVS acceptance test procedure

A2.4 Transient Photocurrent Test

WPVS cells are used in high-speed measurement systems such as pulsed solar simulators, and a transient photocurrent test using pulsed light emitting diodes (LEDs) is used to uncover reference cells that may not be appropriate for these applications.

Reference [20] contains a description of the instrumentation needed to perform the transient photocurrent test. Briefly, an array of high-efficiency red (630–700 nm) LEDs, operated by a fast-switching function generator, is used to illuminate the test cell to at least $0.5 \cdot I_{sc}$. The rise and fall times of the current through the LEDs must be verified to be less than 10 μ s, and the test cell voltage while illuminated must be less than 20 mV. Record the waveform of the I_{sc} vs. time.

A2.5 Dark I-V Measurement

A dark I-V measurement is used to document several solar cell parameters that may be used as a baseline to determine later if any degradation has occurred.

Measure the I-V curve of the reference cell in the dark between $0.5 \cdot V_{oc}$ in reverse bias and $1.1 \cdot V_{oc}$ in forward bias. Calculate the diode shunt resistance from the inverse of the average slope of the dark I-V curve near $0.4 \cdot V_{oc}$ in reverse bias. Calculate the diode series resistance from the inverse of the average slope of the dark I-V curve near V_{oc} in forward bias. Take the natural logarithm of the dark current and perform a linear least squares fit of the forward $\ln(I)$ -V curve in the upper linear (diffusion current) region. This region is normally just below the open-circuit voltage. Calculate the saturation current, I_0 , from the 0 V intercept of the fit. Calculate the diode quality factor, n, from the slope of the linear fit, m, using:

$$n = q / kT / m = 38.92 / m, \text{ for } T = 25^\circ\text{C}.$$

A2.6 Temperature Sensor Integrity Test

This test is intended to verify that both temperature sensors within the reference cell are functional.

With the reference cell in the dark and mounted on an adjustable temperature plate, vary the temperature between 10° and 50°C. Hold the temperature at a minimum of 5 different temperatures in this range and record the output of the two temperature sensors. The RTD must read within $\pm 0.5^\circ\text{C}$ and the T-type thermocouple within $\pm 1^\circ\text{C}$ at each temperature.

A2.7 Light Soak

A light soak is used to stabilize any light-induced degradation (a reduction of several percent in the short-circuit current within a few hours upon initial illumination is a known factor in silicon solar cells) and to verify the integrity of the solar cell electrical contacts.

Light soak the reference cell with greater than 850 W/m^2 Xe or natural sunlight illumination for 24 h. Do not cool the cell. During the soak, bias the cell to approximately V_{mp} and record current and voltage versus time. Contact integrity is verified if there are no current or voltage discontinuities.

For the 2×2 cm cells used in the WPVS, a $\sim 5\Omega$ resistive load is a convenient way to bias the cell during the light soak (the exact value of the load is the ratio of V_{mp} to I_{mp}).

A2.8 Light Instability Test

An instability test is performed to screen out cells that have I-V characteristics with long time constants under illumination. The test consists of measuring current versus time under illumination as the cell is switched between open- and short-circuit conditions.

Precondition the cell by keeping it shorted and in the dark for a minimum of 8 h prior to the test. While still shorted, place the cell in a 1-sun solar simulator, but do not expose the cell to light yet. Hold the cell in this condition for 5 min and begin recording the cell current at intervals of at most 50 ms. Expose the cell to 1000 W/m^2 and keep it shorted for 1 min. Open-circuit the cell and hold for 1 min. Short and again hold for 1 min. To pass the test, the steady-state values of the current must be attained within 100 ms following each transition.

A convenient way to switch the cell between open and shorted is to use a computer-controlled relay. To minimize contact bouncing, a mercury-wetted relay is recommended. Note that the spectrum of the simulator is irrelevant; a tungsten-halogen lamp is probably more appropriate because it is much more stable than an arc lamp.

Appendix 3 Individual WPVS Calibration Reports

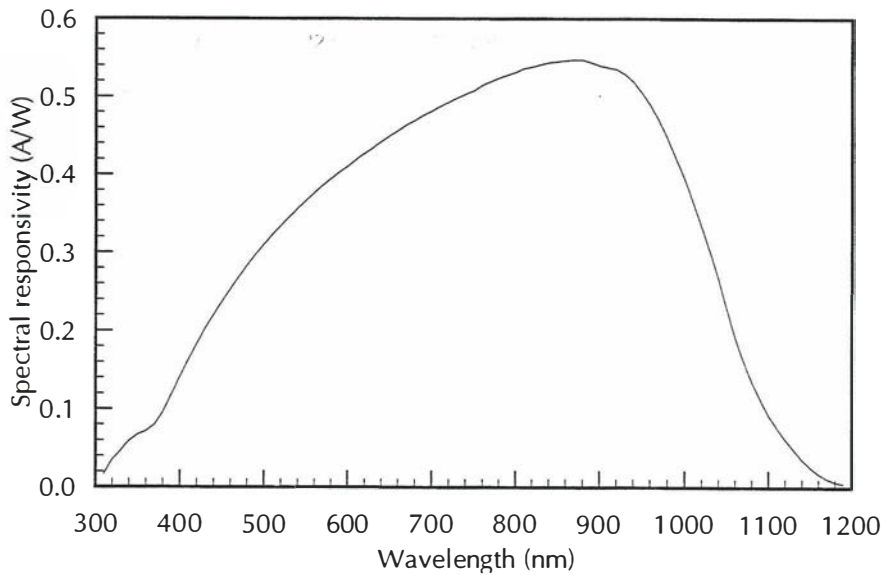
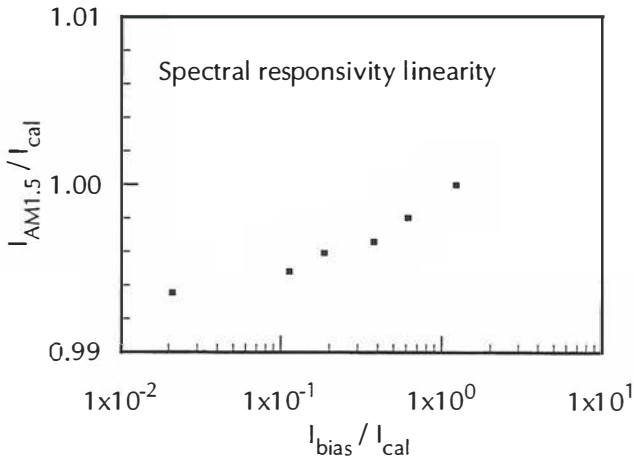
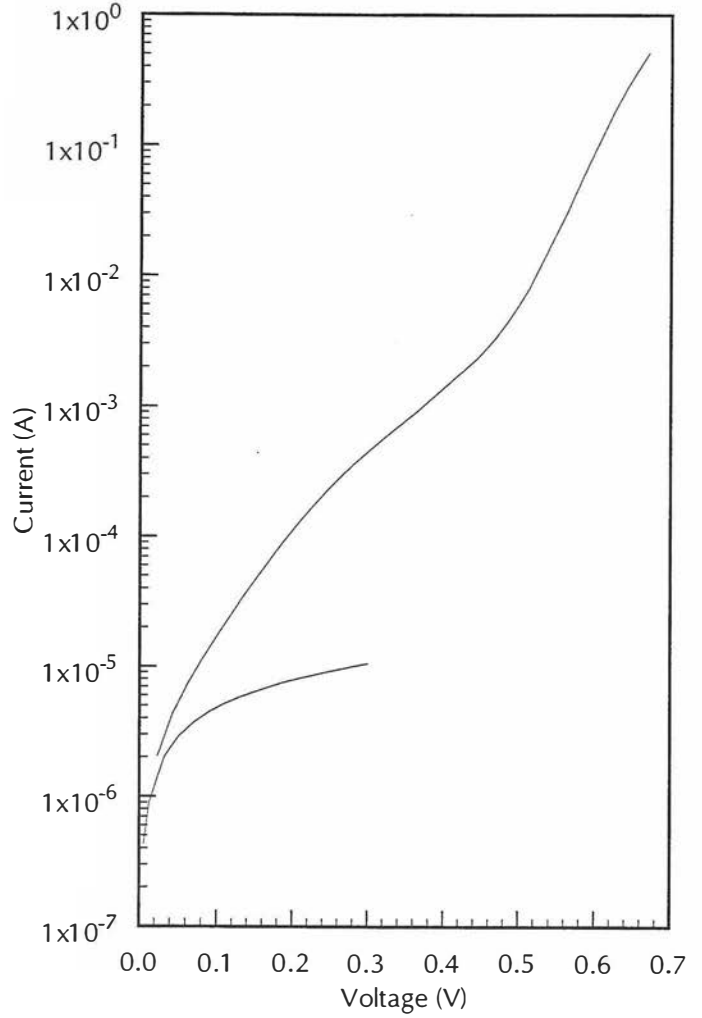
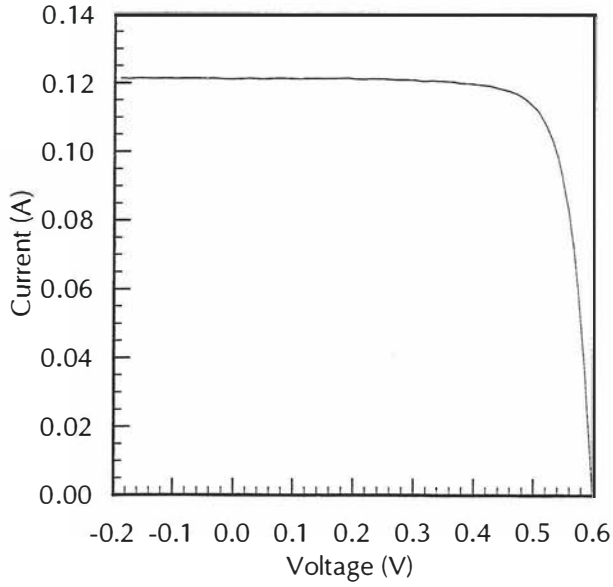
World Photovoltaic Scale Calibration Report 930216-1

Date:	October 17, 1996
Calibration temperature:	25°C
Short-circuit current:	123.29 mA
I_{sc} standard deviation:	0.85 %
I_{sc} temperature coefficient:	456 ppm / °C
Area:	399 mm ²
Open-circuit voltage:	599 mV
Fill factor:	0.779
$dI/dV _{V=0}$:	-0.45 mS
Series resistance:	0.15 Ω
Shunt resistance:	36.3 kΩ
n_1 :	1.39
I_{o1} :	4.38×10 ⁻⁹ A
n_2 :	3.40
I_{o2} :	1.44×10 ⁻⁵ A

Spectral responsivity (nm, A/W):

310	0.0163	490	0.2976	670	0.4635	850	0.5449	1030	0.3004
315	0.0257	495	0.3039	675	0.4664	855	0.5456	1035	0.2835
320	0.0350	500	0.3103	680	0.4694	860	0.5461	1040	0.2666
325	0.0408	505	0.3164	685	0.4727	865	0.5468	1045	0.2475
330	0.0464	510	0.3227	690	0.4762	870	0.5473	1050	0.2285
335	0.0528	515	0.3285	695	0.4788	875	0.5473	1055	0.2100
340	0.0593	520	0.3344	700	0.4815	880	0.5473	1060	0.1916
345	0.0633	525	0.3400	705	0.4846	885	0.5456	1065	0.1764
350	0.0674	530	0.3455	710	0.4876	890	0.5438	1070	0.1613
355	0.0694	535	0.3511	715	0.4903	895	0.5418	1075	0.1483
360	0.0714	540	0.3565	720	0.4928	900	0.5398	1080	0.1352
365	0.0757	545	0.3616	725	0.4956	905	0.5385	1085	0.1242
370	0.0799	550	0.3668	730	0.4984	910	0.5373	1090	0.1131
375	0.0879	555	0.3717	735	0.5007	915	0.5364	1095	0.1030
380	0.0961	560	0.3766	740	0.5031	920	0.5353	1100	0.0927
385	0.1070	565	0.3813	745	0.5055	925	0.5320	1105	0.0846
390	0.1180	570	0.3861	750	0.5077	930	0.5287	1110	0.0765
395	0.1294	575	0.3904	755	0.5113	935	0.5241	1115	0.0691
400	0.1408	580	0.3946	760	0.5148	940	0.5196	1120	0.0618
405	0.1517	585	0.3988	765	0.5171	945	0.5127	1125	0.0552
410	0.1625	590	0.4029	770	0.5193	950	0.5057	1130	0.0485
415	0.1727	595	0.4065	775	0.5217	955	0.4979	1135	0.0421
420	0.1828	600	0.4102	780	0.5240	960	0.4902	1140	0.0357
425	0.1928	605	0.4146	785	0.5259	965	0.4799	1145	0.0309
430	0.2028	610	0.4189	790	0.5276	970	0.4698	1150	0.0262
435	0.2114	615	0.4231	795	0.5296	975	0.4584	1155	0.0221
440	0.2202	620	0.4273	800	0.5315	980	0.4471	1160	0.0180
445	0.2286	625	0.4307	805	0.5337	985	0.4339	1165	0.0149
450	0.2370	630	0.4342	810	0.5361	990	0.4209	1170	0.0119
455	0.2451	635	0.4383	815	0.5372	995	0.4073	1175	0.0096
460	0.2533	640	0.4423	820	0.5382	1000	0.3937	1180	0.0073
465	0.2609	645	0.4459	825	0.5397	1005	0.3789	1185	0.0063
470	0.2685	650	0.4495	830	0.5412	1010	0.3641	1190	0.0052
475	0.2759	655	0.4528	835	0.5424	1015	0.3484		
480	0.2834	660	0.4563	840	0.5437	1020	0.3327		
485	0.2904	665	0.4599	845	0.5444	1025	0.3166		

Notes:



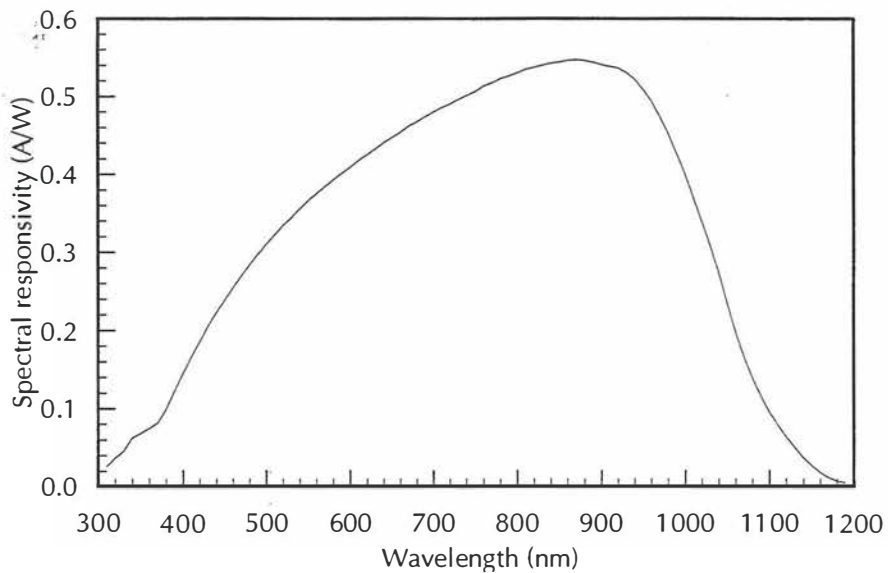
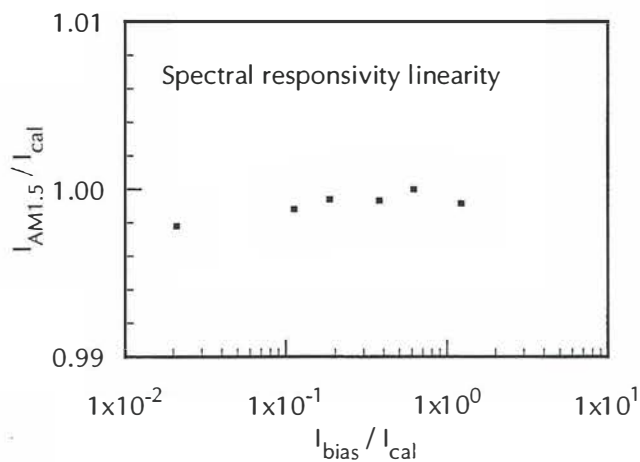
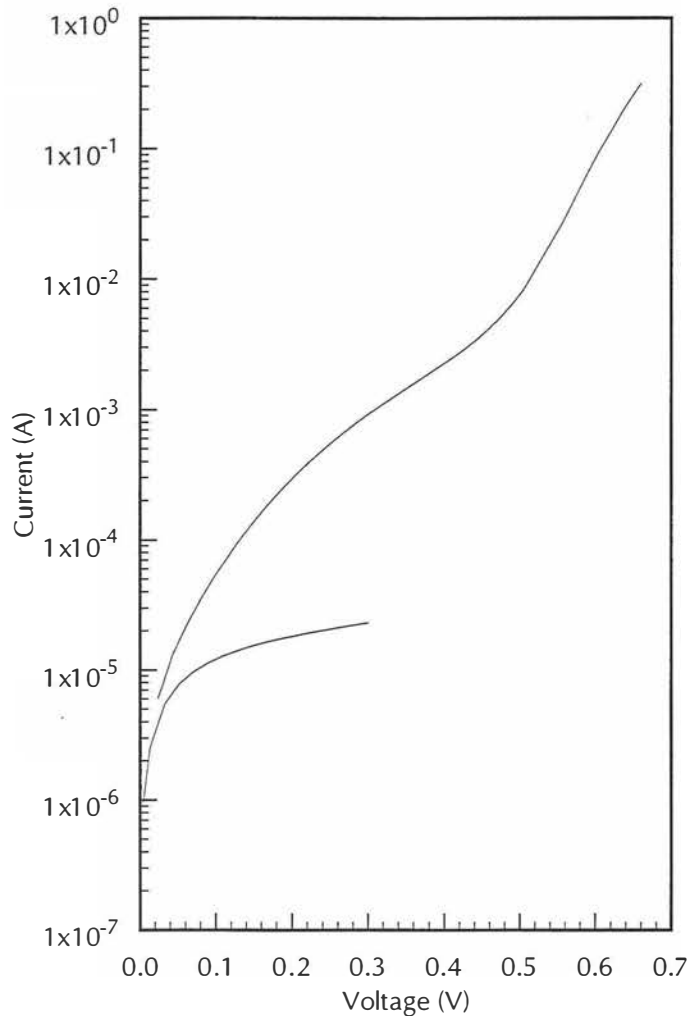
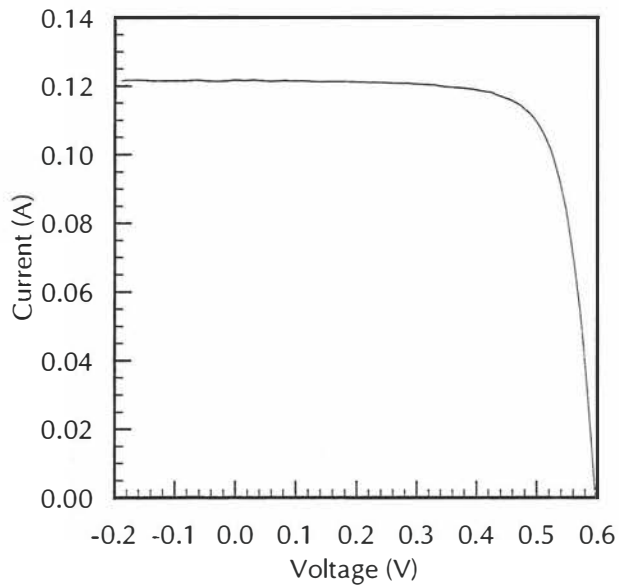
World Photovoltaic Scale Calibration Report 930216-2

Date:	October 17, 1996
Calibration temperature:	25°C
Short-circuit current:	123.47 mA
I_{sc} standard deviation:	0.91 %
I_{sc} temperature coefficient:	475 ppm / °C
Area:	399 mm ²
Open-circuit voltage:	598 mV
Fill factor:	0.753
$dI/dV _{V=0}$:	-0.50 mS
Series resistance:	0.20 Ω
Shunt resistance:	19.8 kΩ
n_1 :	1.61
I_{o1} :	3.92×10 ⁻⁸ A
n_2 :	4.24
I_{o2} :	5.73×10 ⁻⁵ A

Spectral responsivity (nm, A/W):

310	0.0262	490	0.2976	670	0.4622	850	0.5443	1030	0.3075
315	0.0317	495	0.3039	675	0.4650	855	0.5454	1035	0.2907
320	0.0371	500	0.3103	680	0.4678	860	0.5465	1040	0.2738
325	0.0415	505	0.3163	685	0.4710	865	0.5469	1045	0.2543
330	0.0459	510	0.3223	690	0.4742	870	0.5474	1050	0.2350
335	0.0545	515	0.3283	695	0.4770	875	0.5470	1055	0.2164
340	0.0629	520	0.3342	700	0.4799	880	0.5467	1060	0.1977
345	0.0659	525	0.3394	705	0.4829	885	0.5454	1065	0.1822
350	0.0688	530	0.3445	710	0.4858	890	0.5442	1070	0.1667
355	0.0717	535	0.3500	715	0.4881	895	0.5427	1075	0.1532
360	0.0747	540	0.3554	720	0.4902	900	0.5412	1080	0.1396
365	0.0784	545	0.3608	725	0.4933	905	0.5399	1085	0.1282
370	0.0821	550	0.3660	730	0.4964	910	0.5386	1090	0.1167
375	0.0910	555	0.3707	735	0.4988	915	0.5378	1095	0.1063
380	0.0998	560	0.3752	740	0.5013	920	0.5370	1100	0.0959
385	0.1114	565	0.3798	745	0.5038	925	0.5339	1105	0.0876
390	0.1229	570	0.3843	750	0.5065	930	0.5310	1110	0.0793
395	0.1341	575	0.3886	755	0.5100	935	0.5268	1115	0.0717
400	0.1455	580	0.3928	760	0.5135	940	0.5227	1120	0.0641
405	0.1559	585	0.3971	765	0.5156	945	0.5161	1125	0.0572
410	0.1663	590	0.4013	770	0.5177	950	0.5095	1130	0.0504
415	0.1762	595	0.4051	775	0.5203	955	0.5020	1135	0.0438
420	0.1859	600	0.4090	780	0.5228	960	0.4944	1140	0.0374
425	0.1958	605	0.4133	785	0.5245	965	0.4845	1145	0.0325
430	0.2057	610	0.4177	790	0.5263	970	0.4746	1150	0.0275
435	0.2144	615	0.4214	795	0.5283	975	0.4638	1155	0.0231
440	0.2229	620	0.4253	800	0.5304	980	0.4528	1160	0.0187
445	0.2310	625	0.4292	805	0.5327	985	0.4400	1165	0.0155
450	0.2390	630	0.4331	810	0.5348	990	0.4272	1170	0.0122
455	0.2467	635	0.4369	815	0.5362	995	0.4137	1175	0.0099
460	0.2546	640	0.4408	820	0.5374	1000	0.4001	1180	0.0075
465	0.2621	645	0.4441	825	0.5388	1005	0.3852	1185	0.0065
470	0.2696	650	0.4473	830	0.5402	1010	0.3703	1190	0.0055
475	0.2768	655	0.4507	835	0.5416	1015	0.3549		
480	0.2838	660	0.4540	840	0.5430	1020	0.3395		
485	0.2907	665	0.4580	845	0.5437	1025	0.3235		

Notes:



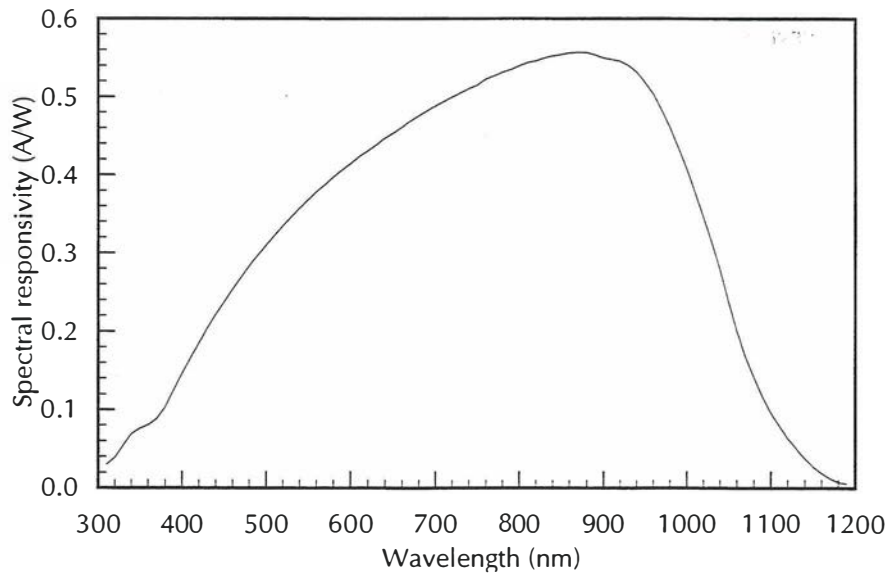
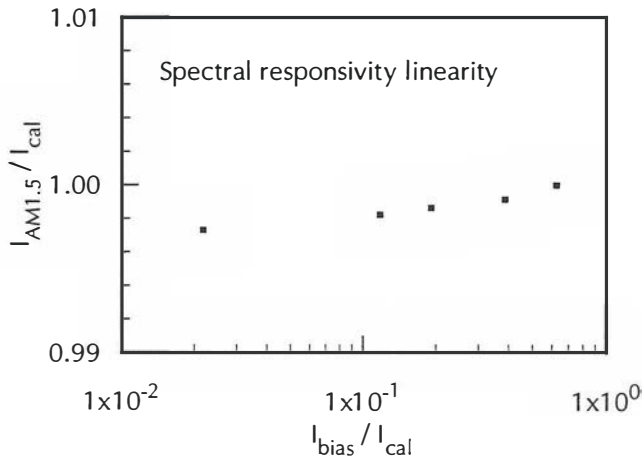
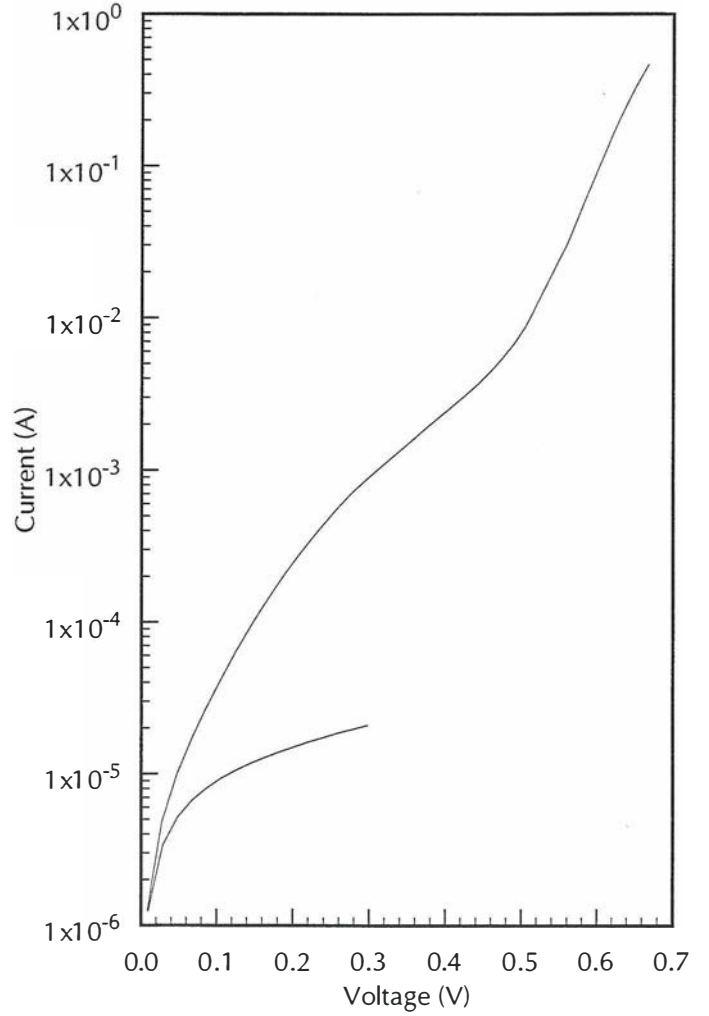
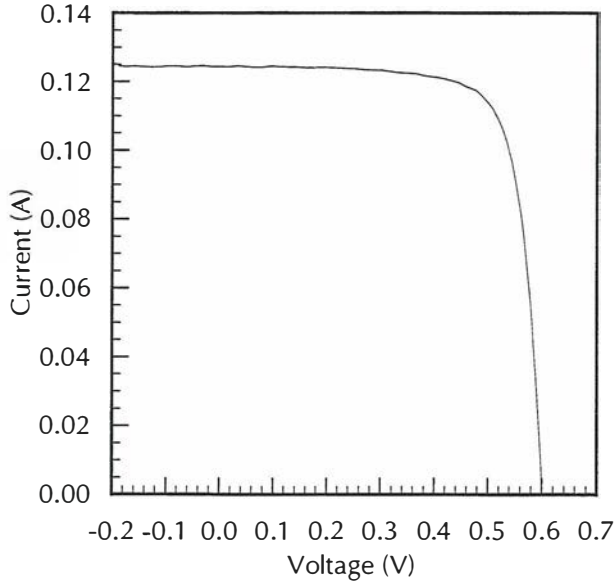
World Photovoltaic Scale Calibration Report 930417-1

Date:	October 17, 1996
Calibration temperature:	25°C
Short-circuit current:	124.99 mA
I_{sc} standard deviation:	1.08 %
I_{sc} temperature coefficient:	376 ppm / °C
Area:	399 mm ²
Open-circuit voltage:	602 mV
Fill factor:	0.761
$dI/dV _{V=0}$:	-0.57 mS
Series resistance:	0.05 Ω
Shunt resistance:	16.7 kΩ
n_1 :	1.52
I_{o1} :	1.94×10 ⁻⁸ A
n_2 :	3.92
I_{o2} :	4.59×10 ⁻⁵ A

Spectral responsivity (nm, A/W):

310	0.0296	490	0.2971	670	0.4691	850	0.5541	1030	0.3128
315	0.0344	495	0.3036	675	0.4723	855	0.5550	1035	0.2955
320	0.0391	500	0.3101	680	0.4754	860	0.5558	1040	0.2782
325	0.0467	505	0.3164	685	0.4787	865	0.5562	1045	0.2586
330	0.0543	510	0.3226	690	0.4819	870	0.5566	1050	0.2389
335	0.0617	515	0.3288	695	0.4849	875	0.5566	1055	0.2198
340	0.0690	520	0.3349	700	0.4879	880	0.5566	1060	0.2006
345	0.0726	525	0.3407	705	0.4909	885	0.5550	1065	0.1844
350	0.0761	530	0.3465	710	0.4937	890	0.5534	1070	0.1681
355	0.0782	535	0.3520	715	0.4965	895	0.5516	1075	0.1547
360	0.0804	540	0.3574	720	0.4994	900	0.5497	1080	0.1412
365	0.0843	545	0.3629	725	0.5021	905	0.5487	1085	0.1293
370	0.0883	550	0.3683	730	0.5048	910	0.5476	1090	0.1174
375	0.0957	555	0.3734	735	0.5075	915	0.5466	1095	0.1068
380	0.1032	560	0.3784	740	0.5103	920	0.5458	1100	0.0964
385	0.1140	565	0.3828	745	0.5126	925	0.5430	1105	0.0880
390	0.1247	570	0.3873	750	0.5148	930	0.5400	1110	0.0796
395	0.1352	575	0.3923	755	0.5187	935	0.5359	1115	0.0717
400	0.1457	580	0.3973	760	0.5225	940	0.5319	1120	0.0638
405	0.1558	585	0.4015	765	0.5246	945	0.5250	1125	0.0571
410	0.1658	590	0.4057	770	0.5266	950	0.5181	1130	0.0504
415	0.1753	595	0.4099	775	0.5289	955	0.5108	1135	0.0440
420	0.1848	600	0.4141	780	0.5313	960	0.5034	1140	0.0378
425	0.1944	605	0.4186	785	0.5330	965	0.4933	1145	0.0326
430	0.2039	610	0.4232	790	0.5347	970	0.4831	1150	0.0275
435	0.2125	615	0.4270	795	0.5370	975	0.4719	1155	0.0233
440	0.2212	620	0.4307	800	0.5394	980	0.4608	1160	0.0192
445	0.2293	625	0.4347	805	0.5415	985	0.4478	1165	0.0158
450	0.2374	630	0.4386	810	0.5436	990	0.4349	1170	0.0126
455	0.2454	635	0.4428	815	0.5447	995	0.4213	1175	0.0100
460	0.2534	640	0.4471	820	0.5458	1000	0.4075	1180	0.0076
465	0.2610	645	0.4502	825	0.5477	1005	0.3924	1185	0.0066
470	0.2684	650	0.4535	830	0.5495	1010	0.3774	1190	0.0058
475	0.2759	655	0.4573	835	0.5510	1015	0.3616		
480	0.2833	660	0.4611	840	0.5523	1020	0.3459		
485	0.2902	665	0.4651	845	0.5531	1025	0.3294		

Notes:



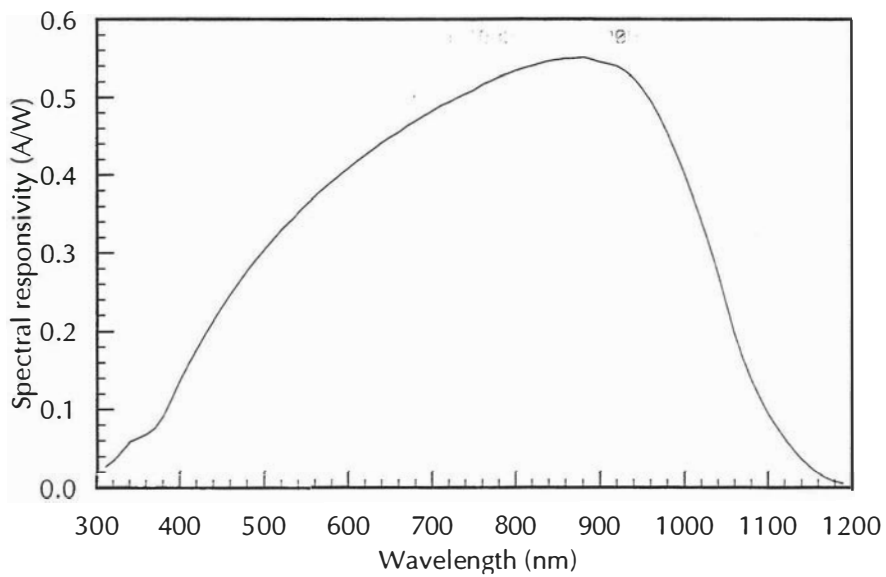
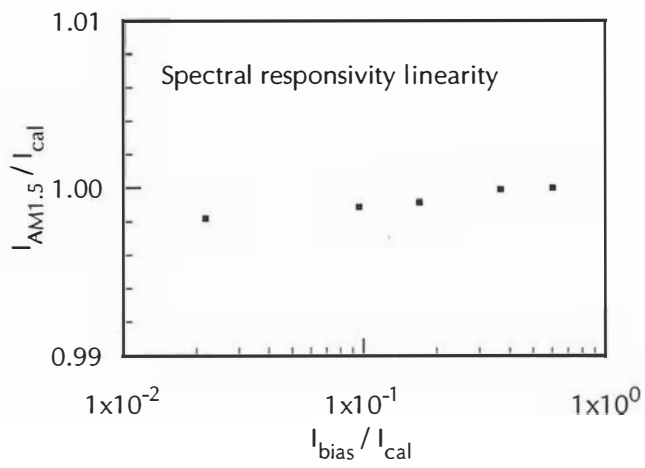
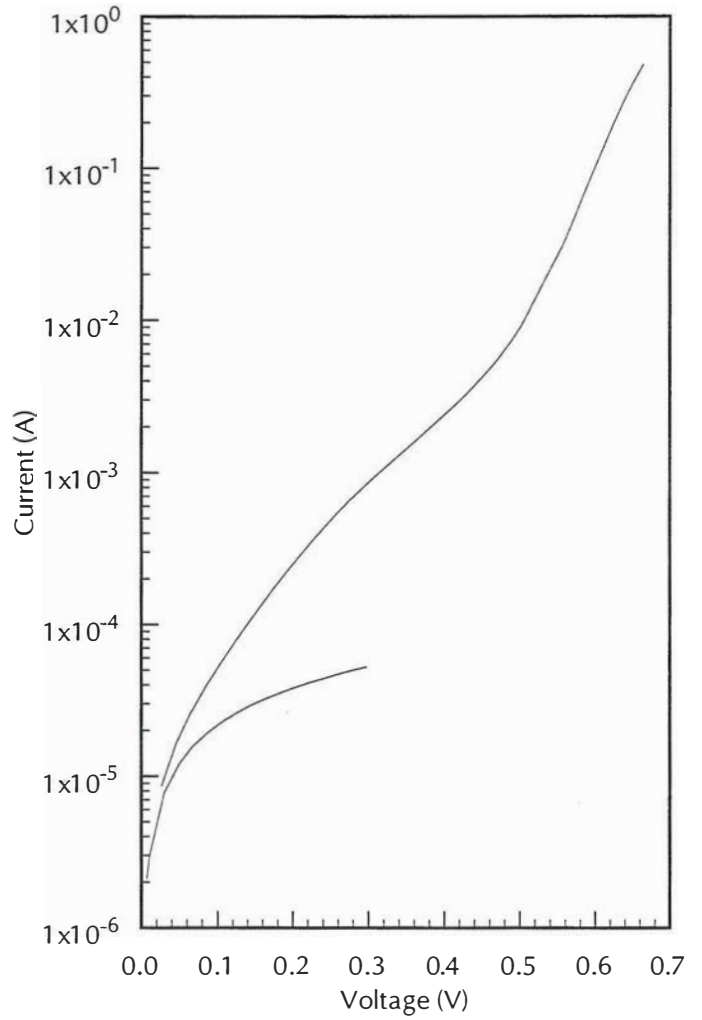
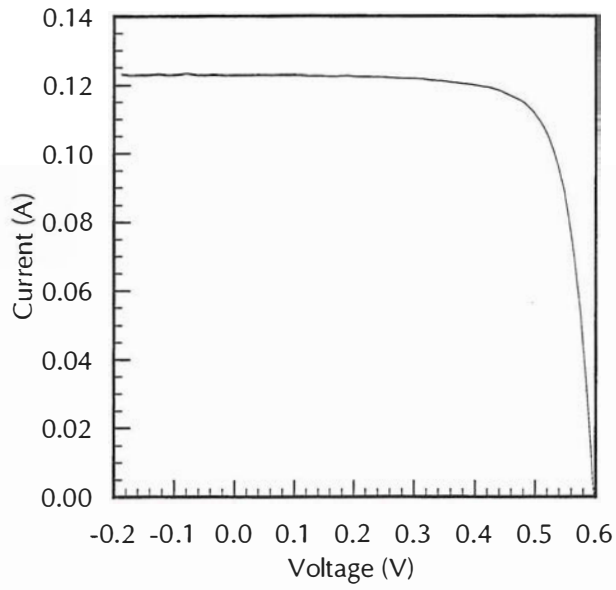
World Photovoltaic Scale Calibration Report 930417-2

Date:	October 17, 1996
Calibration temperature:	25°C
Short-circuit current:	123.11 mA
I_{sc} standard deviation:	1.27 %
I_{sc} temperature coefficient:	404 ppm / °C
Area:	399 mm ²
Open-circuit voltage:	598 mV
Fill factor:	0.759
$dI/dV _{V=0}$:	-0.30 mS
Series resistance:	0.07 Ω
Shunt resistance:	6.6 kΩ
n_1 :	1.53
I_{o1} :	2.48×10 ⁻⁸ A
n_2 :	3.72
I_{o2} :	3.69×10 ⁻⁵ A

Spectral responsivity (nm, A/W):

310	0.0270	490	0.2917	670	0.4637	850	0.5478	1030	0.3070
315	0.0311	495	0.2981	675	0.4666	855	0.5486	1035	0.2898
320	0.0352	500	0.3046	680	0.4697	860	0.5495	1040	0.2725
325	0.0410	505	0.3110	685	0.4732	865	0.5495	1045	0.2533
330	0.0467	510	0.3175	690	0.4765	870	0.5496	1050	0.2341
335	0.0527	515	0.3239	695	0.4795	875	0.5504	1055	0.2151
340	0.0587	520	0.3301	700	0.4824	880	0.5511	1060	0.1962
345	0.0610	525	0.3355	705	0.4857	885	0.5498	1065	0.1808
350	0.0633	530	0.3408	710	0.4891	890	0.5483	1070	0.1653
355	0.0657	535	0.3465	715	0.4915	895	0.5466	1075	0.1519
360	0.0681	540	0.3524	720	0.4939	900	0.5448	1080	0.1382
365	0.0721	545	0.3579	725	0.4967	905	0.5435	1085	0.1270
370	0.0761	550	0.3635	730	0.4995	910	0.5423	1090	0.1158
375	0.0838	555	0.3684	735	0.5020	915	0.5411	1095	0.1053
380	0.0914	560	0.3734	740	0.5045	920	0.5400	1100	0.0947
385	0.1026	565	0.3780	745	0.5069	925	0.5367	1105	0.0865
390	0.1137	570	0.3827	750	0.5093	930	0.5335	1110	0.0782
395	0.1253	575	0.3872	755	0.5129	935	0.5290	1115	0.0706
400	0.1369	580	0.3918	760	0.5164	940	0.5246	1120	0.0630
405	0.1473	585	0.3959	765	0.5187	945	0.5179	1125	0.0563
410	0.1577	590	0.4001	770	0.5208	950	0.5112	1130	0.0495
415	0.1675	595	0.4045	775	0.5234	955	0.5033	1135	0.0432
420	0.1773	600	0.4089	780	0.5258	960	0.4956	1140	0.0368
425	0.1868	605	0.4131	785	0.5278	965	0.4859	1145	0.0322
430	0.1963	610	0.4173	790	0.5298	970	0.4761	1150	0.0274
435	0.2050	615	0.4215	795	0.5316	975	0.4649	1155	0.0230
440	0.2136	620	0.4257	800	0.5336	980	0.4536	1160	0.0185
445	0.2222	625	0.4295	805	0.5354	985	0.4408	1165	0.0155
450	0.2307	630	0.4334	810	0.5372	990	0.4279	1170	0.0124
455	0.2387	635	0.4377	815	0.5386	995	0.4145	1175	0.0100
460	0.2467	640	0.4420	820	0.5399	1000	0.4009	1180	0.0075
465	0.2545	645	0.4456	825	0.5416	1005	0.3859	1185	0.0065
470	0.2621	650	0.4490	830	0.5432	1010	0.3710	1190	0.0056
475	0.2697	655	0.4521	835	0.5447	1015	0.3556		
480	0.2773	660	0.4552	840	0.5462	1020	0.3403		
485	0.2845	665	0.4594	845	0.5470	1025	0.3236		

Notes:



World Photovoltaic Scale Calibration Report 93308

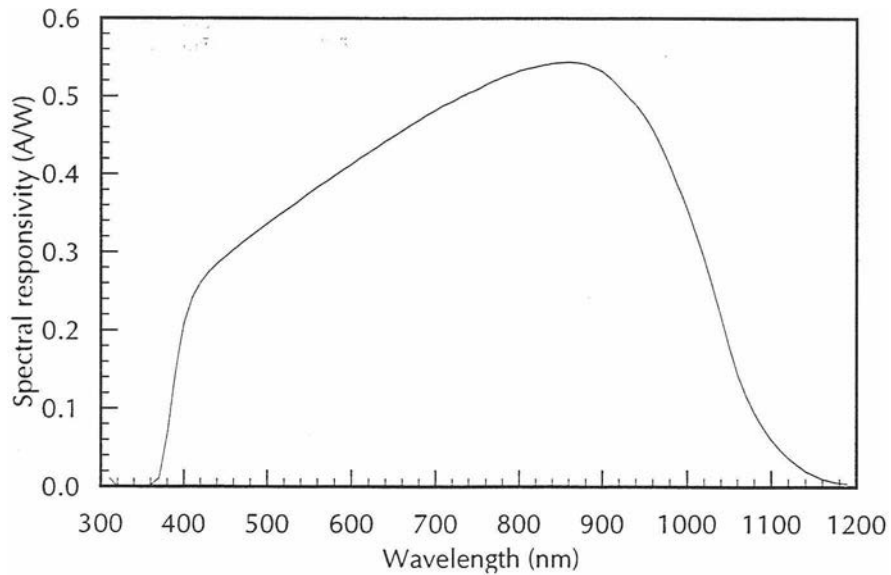
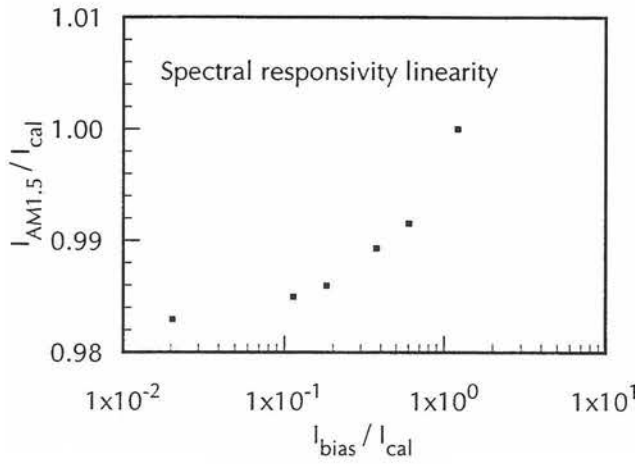
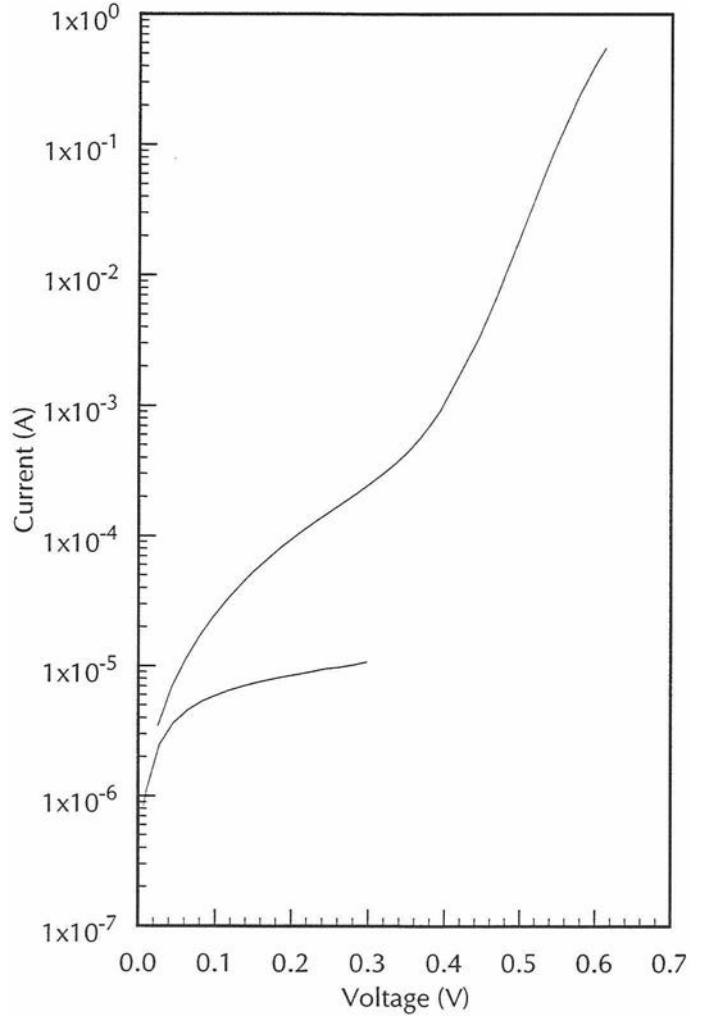
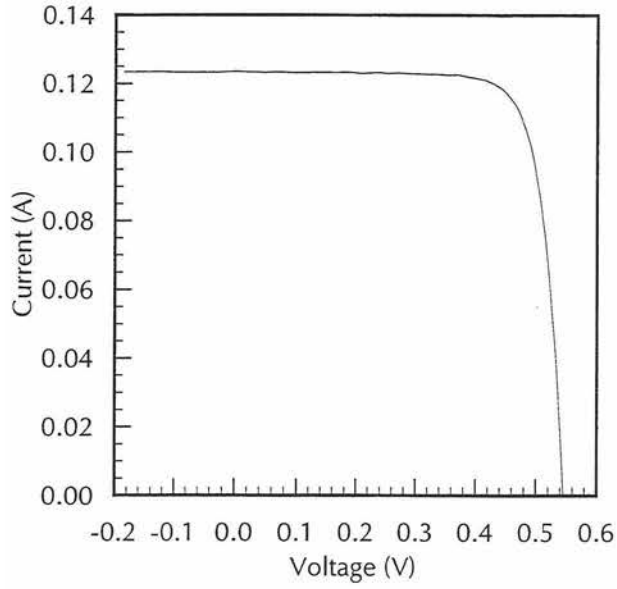
Date:	October 17, 1996
Calibration temperature:	25°C
Short-circuit current:	126.36 mA
I_{sc} standard deviation:	0.72 %
I_{sc} temperature coefficient:	559 ppm / °C
Area:	405 mm ²
Open-circuit voltage:	546 mV
Fill factor:	0.788
$dI/dV _{V=0}$:	-0.12 mS
Series resistance:	0.22 Ω
Shunt resistance:	45 kΩ
n_1 :	1.20
I_{o1} :	1.69×10^{-9} A
n_2 :	3.87
I_{o2} :	1.25×10^{-5} A

Spectral responsivity (nm, A/W):

310	0.0117	490	0.3282	670	0.4630	850	0.5433	1030	0.2556
315	0.0060	495	0.3323	675	0.4662	855	0.5437	1035	0.2368
320	0.0003	500	0.3365	680	0.4694	860	0.5441	1040	0.2181
325	0.0001	505	0.3404	685	0.4729	865	0.5436	1045	0.1992
330	0.0000	510	0.3443	690	0.4762	870	0.5432	1050	0.1803
335	0.0000	515	0.3483	695	0.4793	875	0.5424	1055	0.1624
340	0.0001	520	0.3523	700	0.4823	880	0.5414	1060	0.1446
345	0.0000	525	0.3560	705	0.4855	885	0.5392	1065	0.1310
350	0.0000	530	0.3597	710	0.4887	890	0.5368	1070	0.1174
355	0.0009	535	0.3637	715	0.4908	895	0.5345	1075	0.1062
360	0.0019	540	0.3677	720	0.4931	900	0.5322	1080	0.0949
365	0.0063	545	0.3718	725	0.4962	905	0.5276	1085	0.0857
370	0.0108	550	0.3760	730	0.4994	910	0.5231	1090	0.0767
375	0.0387	555	0.3799	735	0.5019	915	0.5176	1095	0.0687
380	0.0668	560	0.3839	740	0.5043	920	0.5121	1100	0.0608
385	0.1072	565	0.3873	745	0.5067	925	0.5060	1105	0.0544
390	0.1474	570	0.3906	750	0.5090	930	0.4999	1110	0.0482
395	0.1777	575	0.3945	755	0.5120	935	0.4946	1115	0.0427
400	0.2081	580	0.3983	760	0.5151	940	0.4892	1120	0.0371
405	0.2249	585	0.4020	765	0.5175	945	0.4818	1125	0.0327
410	0.2416	590	0.4058	770	0.5200	950	0.4743	1130	0.0284
415	0.2513	595	0.4091	775	0.5223	955	0.4656	1135	0.0244
420	0.2611	600	0.4124	780	0.5245	960	0.4569	1140	0.0205
425	0.2677	605	0.4166	785	0.5265	965	0.4458	1145	0.0180
430	0.2744	610	0.4207	790	0.5284	970	0.4347	1150	0.0153
435	0.2796	615	0.4241	795	0.5305	975	0.4224	1155	0.0130
440	0.2848	620	0.4275	800	0.5328	980	0.4102	1160	0.0107
445	0.2893	625	0.4312	805	0.5342	985	0.3967	1165	0.0091
450	0.2938	630	0.4348	810	0.5358	990	0.3833	1170	0.0075
455	0.2985	635	0.4387	815	0.5368	995	0.3694	1175	0.0065
460	0.3030	640	0.4424	820	0.5378	1000	0.3555	1180	0.0056
465	0.3073	645	0.4457	825	0.5390	1005	0.3401	1185	0.0049
470	0.3115	650	0.4490	830	0.5402	1010	0.3247	1190	0.0043
475	0.3158	655	0.4524	835	0.5413	1015	0.3085		
480	0.3200	660	0.4558	840	0.5425	1020	0.2921		
485	0.3242	665	0.4594	845	0.5429	1025	0.2738		

Notes:

One contact to solar cell shorted to metal package.



World Photovoltaic Scale Calibration Report 93309

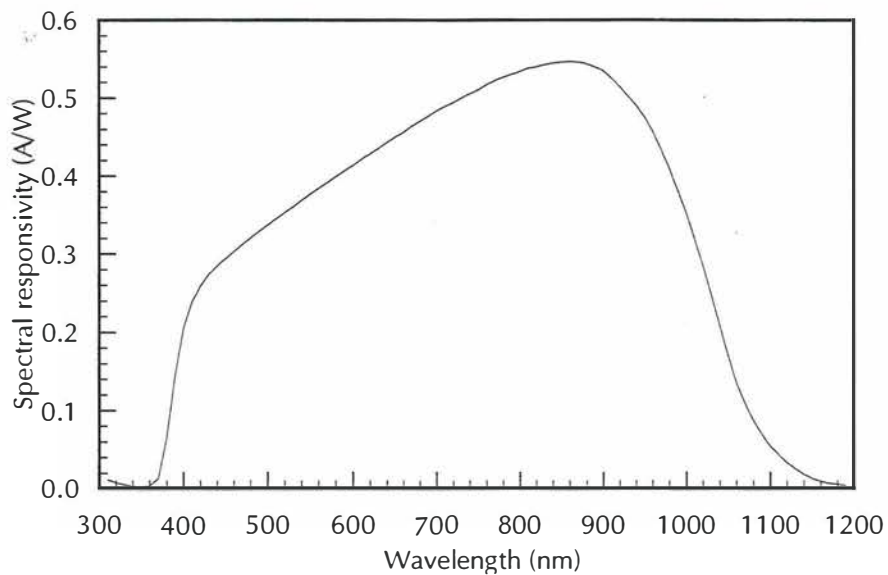
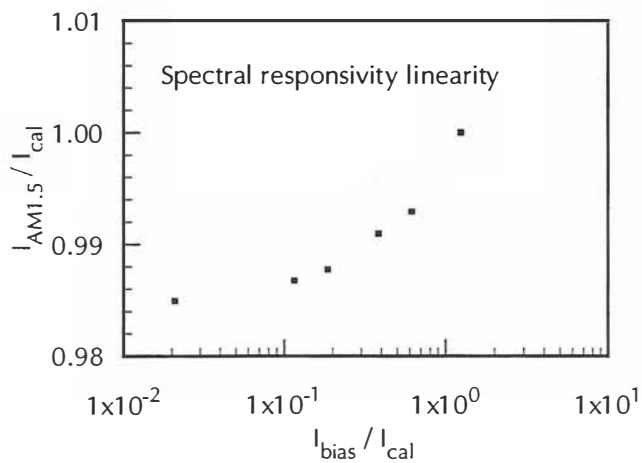
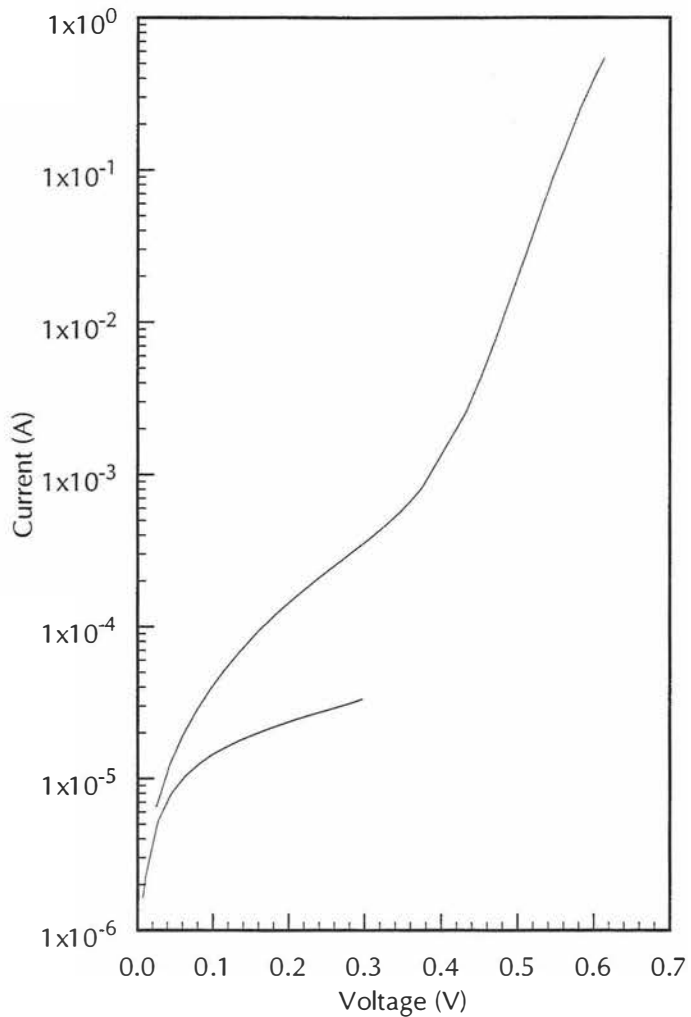
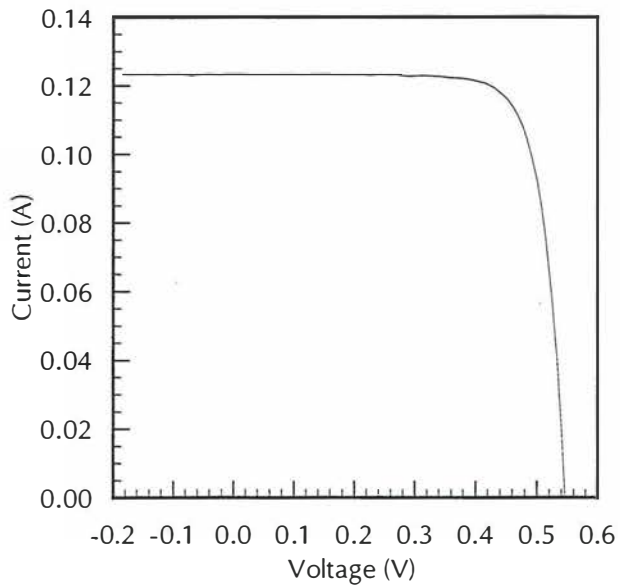
Date:	October 17, 1996
Calibration temperature:	25°C
Short-circuit current:	126.38 mA
I_{sc} standard deviation:	0.89 %
I_{sc} temperature coefficient:	528 ppm / °C
Area:	405 mm ²
Open-circuit voltage:	547 mV
Fill factor:	0.778
$dI/dV _{V=0}$:	-0.22 mS
Series resistance:	0.12 Ω
Shunt resistance:	10 kΩ
n_1 :	1.24
I_{o1} :	2.98×10 ⁻⁹ A
n_2 :	4.09
I_{o2} :	2.08×10 ⁻⁵ A

Spectral responsivity (nm, A/W):

310	0.0117	490	0.3290	670	0.4637	850	0.5462	1030	0.2469
315	0.0098	495	0.3330	675	0.4671	855	0.5465	1035	0.2279
320	0.0081	500	0.3368	680	0.4703	860	0.5469	1040	0.2087
325	0.0068	505	0.3410	685	0.4736	865	0.5466	1045	0.1897
330	0.0056	510	0.3451	690	0.4769	870	0.5462	1050	0.1707
335	0.0044	515	0.3489	695	0.4801	875	0.5452	1055	0.1530
340	0.0033	520	0.3528	700	0.4833	880	0.5441	1060	0.1353
345	0.0029	525	0.3567	705	0.4862	885	0.5421	1065	0.1224
350	0.0027	530	0.3604	710	0.4891	890	0.5401	1070	0.1095
355	0.0032	535	0.3645	715	0.4917	895	0.5377	1075	0.0986
360	0.0039	540	0.3685	720	0.4942	900	0.5353	1080	0.0875
365	0.0085	545	0.3725	725	0.4971	905	0.5307	1085	0.0789
370	0.0133	550	0.3765	730	0.5001	910	0.5259	1090	0.0702
375	0.0394	555	0.3802	735	0.5026	915	0.5205	1095	0.0625
380	0.0655	560	0.3839	740	0.5052	920	0.5151	1100	0.0548
385	0.1050	565	0.3876	745	0.5076	925	0.5088	1105	0.0495
390	0.1446	570	0.3912	750	0.5100	930	0.5026	1110	0.0440
395	0.1747	575	0.3950	755	0.5136	935	0.4970	1115	0.0387
400	0.2049	580	0.3987	760	0.5172	940	0.4913	1120	0.0334
405	0.2218	585	0.4025	765	0.5197	945	0.4837	1125	0.0294
410	0.2387	590	0.4064	770	0.5223	950	0.4762	1130	0.0254
415	0.2488	595	0.4097	775	0.5245	955	0.4672	1135	0.0219
420	0.2587	600	0.4131	780	0.5268	960	0.4582	1140	0.0185
425	0.2663	605	0.4170	785	0.5285	965	0.4467	1145	0.0157
430	0.2740	610	0.4210	790	0.5303	970	0.4351	1150	0.0130
435	0.2792	615	0.4246	795	0.5323	975	0.4228	1155	0.0114
440	0.2844	620	0.4282	800	0.5342	980	0.4103	1160	0.0097
445	0.2893	625	0.4318	805	0.5362	985	0.3960	1165	0.0085
450	0.2941	630	0.4353	810	0.5382	990	0.3818	1170	0.0073
455	0.2987	635	0.4391	815	0.5392	995	0.3668	1175	0.0065
460	0.3032	640	0.4429	820	0.5401	1000	0.3516	1180	0.0057
465	0.3076	645	0.4463	825	0.5414	1005	0.3354	1185	0.0051
470	0.3120	650	0.4498	830	0.5428	1010	0.3191	1190	0.0044
475	0.3162	655	0.4528	835	0.5438	1015	0.3018		
480	0.3205	660	0.4559	840	0.5448	1020	0.2845		
485	0.3247	665	0.4599	845	0.5454	1025	0.2658		

Notes:

One contact to solar cell shorted to metal package.



World Photovoltaic Scale Calibration Report NIM 9351

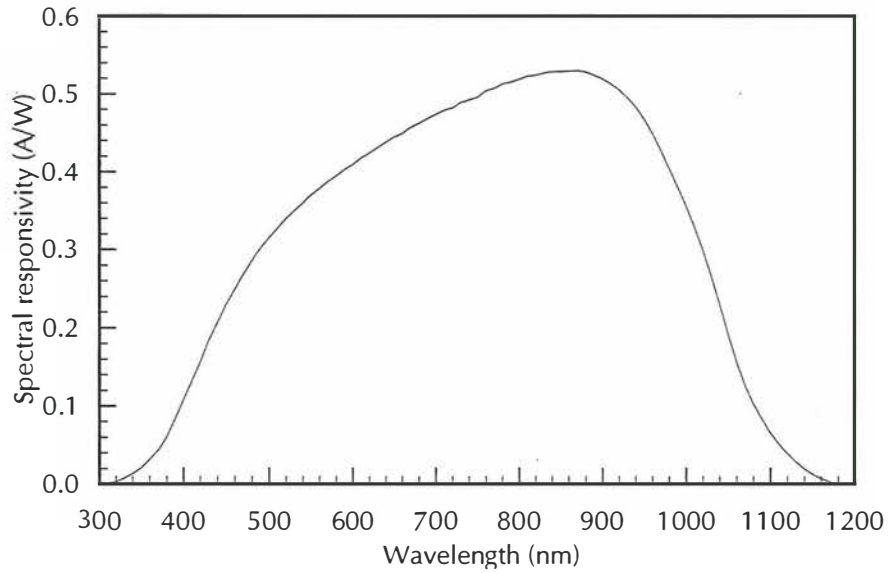
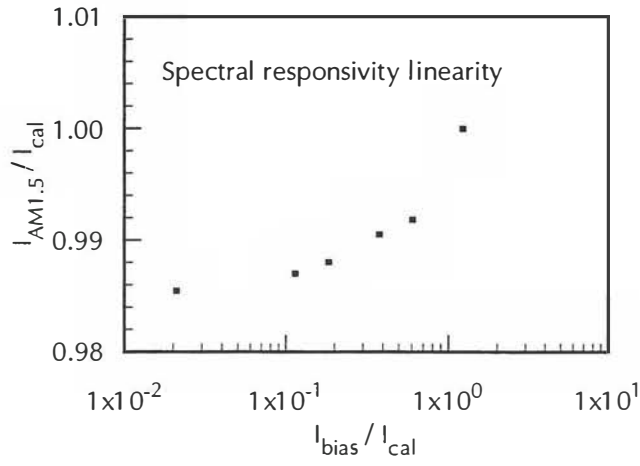
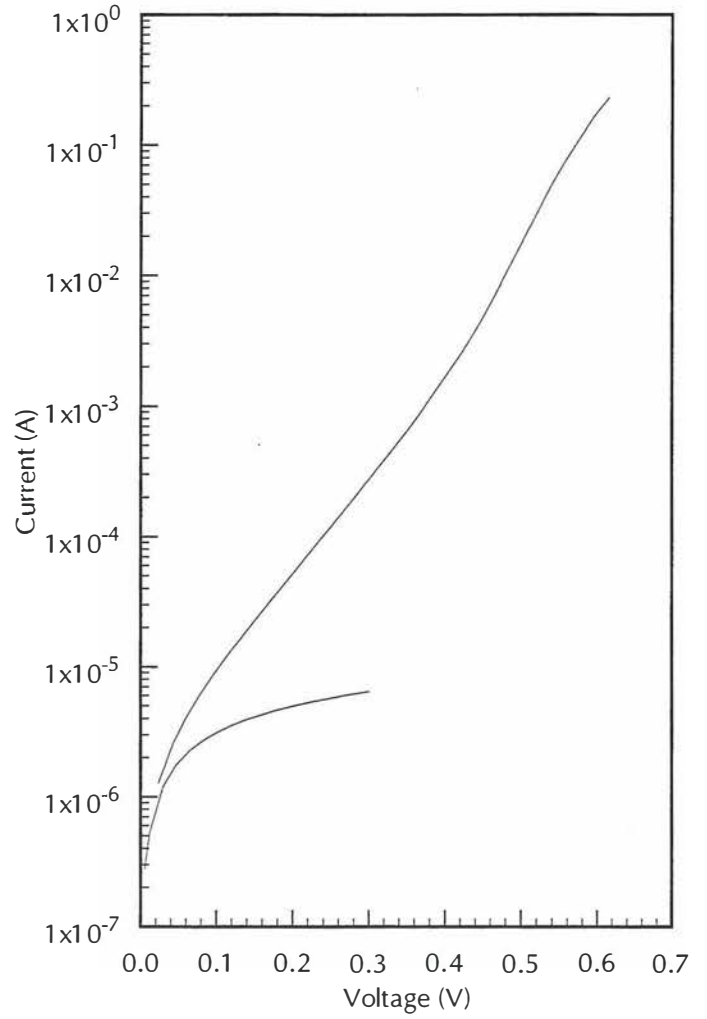
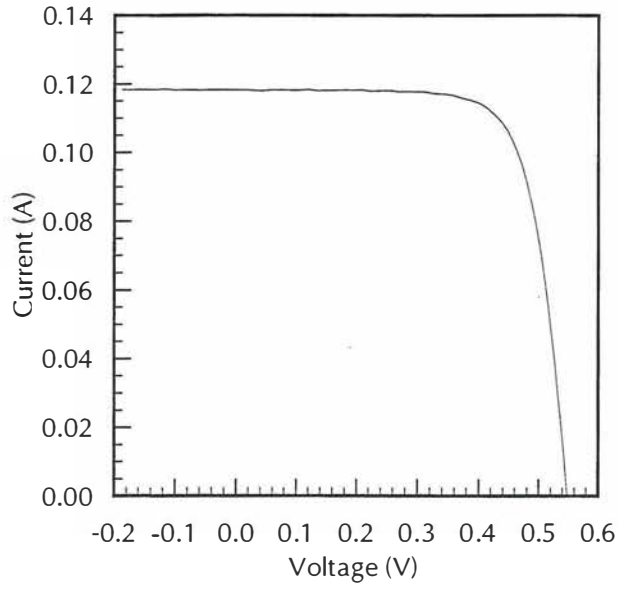
Date:	October 17, 1996
Calibration temperature:	25°C
Short-circuit current:	121.05 mA
I_{sc} standard deviation:	0.90 %
I_{sc} temperature coefficient:	496 ppm / °C
Area:	405 mm ²
Open-circuit voltage:	549 mV
Fill factor:	0.735
$dI/dV _{V=0}$:	-0.29 mS
Series resistance:	0.13 Ω
Shunt resistance:	66 kΩ
n_1 :	1.48
I_{o1} :	3.50×10^{-8} A
n_2 :	2.32
I_{o2} :	1.82×10^{-6} A

Spectral responsivity (nm, A/W):

310	0.0012	490	0.3028	670	0.4574	850	0.5294	1030	0.2665
315	0.0021	495	0.3093	675	0.4601	855	0.5294	1035	0.2487
320	0.0033	500	0.3159	680	0.4627	860	0.5296	1040	0.2306
325	0.0056	505	0.3222	685	0.4656	865	0.5298	1045	0.2116
330	0.0079	510	0.3283	690	0.4687	870	0.5301	1050	0.1926
335	0.0108	515	0.3345	695	0.4714	875	0.5294	1055	0.1745
340	0.0136	520	0.3406	700	0.4741	880	0.5284	1060	0.1567
345	0.0175	525	0.3456	705	0.4768	885	0.5263	1065	0.1417
350	0.0213	530	0.3508	710	0.4794	890	0.5242	1070	0.1267
355	0.0267	535	0.3556	715	0.4810	895	0.5219	1075	0.1150
360	0.0319	540	0.3606	720	0.4827	900	0.5196	1080	0.1033
365	0.0378	545	0.3658	725	0.4860	905	0.5163	1085	0.0935
370	0.0438	550	0.3708	730	0.4894	910	0.5130	1090	0.0837
375	0.0522	555	0.3748	735	0.4910	915	0.5094	1095	0.0751
380	0.0609	560	0.3790	740	0.4927	920	0.5058	1100	0.0662
385	0.0722	565	0.3834	745	0.4944	925	0.5006	1105	0.0591
390	0.0837	570	0.3880	750	0.4962	930	0.4954	1110	0.0520
395	0.0958	575	0.3915	755	0.5004	935	0.4894	1115	0.0461
400	0.1081	580	0.3952	760	0.5044	940	0.4835	1120	0.0401
405	0.1202	585	0.3992	765	0.5059	945	0.4758	1125	0.0348
410	0.1321	590	0.4034	770	0.5073	950	0.4679	1130	0.0296
415	0.1442	595	0.4065	775	0.5102	955	0.4587	1135	0.0248
420	0.1563	600	0.4096	780	0.5130	960	0.4495	1140	0.0202
425	0.1703	605	0.4138	785	0.5142	965	0.4387	1145	0.0167
430	0.1841	610	0.4180	790	0.5154	970	0.4282	1150	0.0132
435	0.1957	615	0.4213	795	0.5173	975	0.4163	1155	0.0106
440	0.2070	620	0.4243	800	0.5190	980	0.4046	1160	0.0079
445	0.2185	625	0.4280	805	0.5209	985	0.3928	1165	0.0058
450	0.2298	630	0.4314	810	0.5228	990	0.3811	1170	0.0038
455	0.2398	635	0.4349	815	0.5236	995	0.3687	1175	0.0021
460	0.2498	640	0.4385	820	0.5242	1000	0.3562	1180	0.0006
465	0.2592	645	0.4416	825	0.5255	1005	0.3427	1185	0.0004
470	0.2686	650	0.4449	830	0.5269	1010	0.3295	1190	0.0002
475	0.2776	655	0.4472	835	0.5278	1015	0.3147		
480	0.2867	660	0.4497	840	0.5288	1020	0.3001		
485	0.2947	665	0.4535	845	0.5290	1025	0.2832		

Notes:

NIM 9351



World Photovoltaic Scale Calibration Report NIM 9352

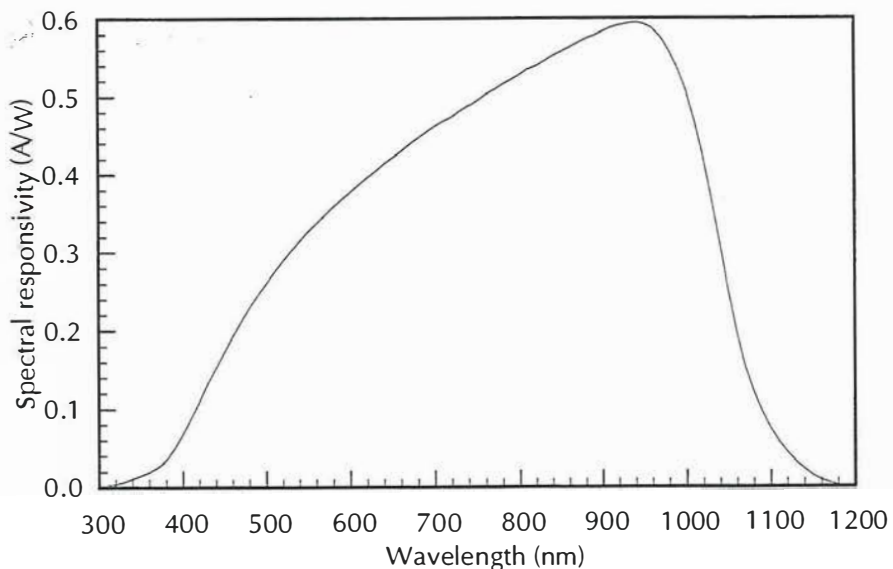
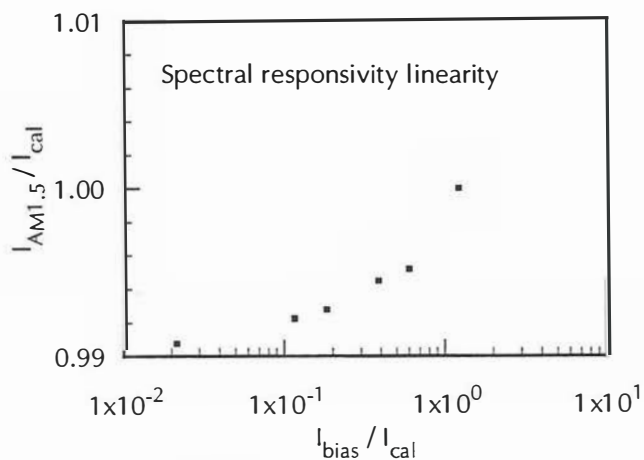
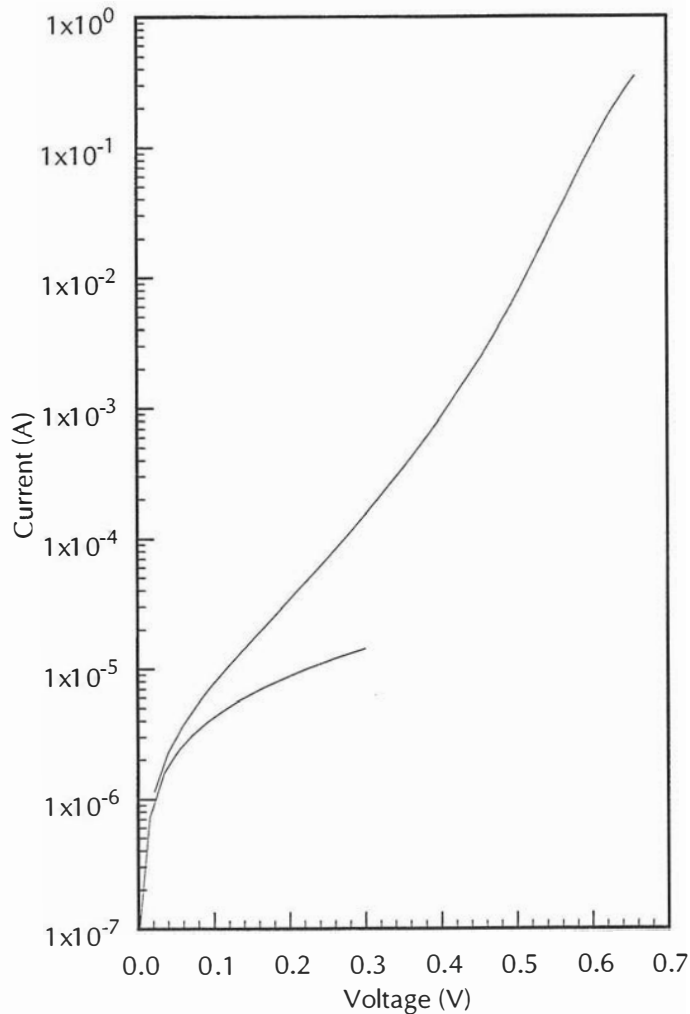
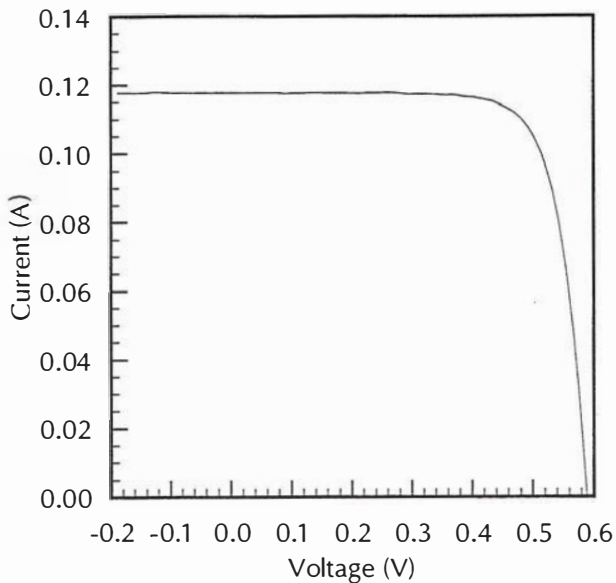
Date:	October 17, 1996
Calibration temperature:	25°C
Short-circuit current:	120.17 mA
I_{sc} standard deviation:	0.98 %
I_{sc} temperature coefficient:	404 ppm / °C
Area:	408 mm ²
Open-circuit voltage:	591 mV
Fill factor:	0.763
$dI/dV _{V=0}$:	-0.46 mS
Series resistance:	0.15 Ω
Shunt resistance:	19 kΩ
n_1 :	1.50
I_{o1} :	1.64×10^{-8} A
n_2 :	2.52
I_{o2} :	1.56×10^{-6} A

Spectral responsivity (nm, A/W):

310	0.0038	490	0.2455	670	0.4382	850	0.5568	1030	0.3669
315	0.0040	495	0.2528	675	0.4424	855	0.5596	1035	0.3375
320	0.0044	500	0.2602	680	0.4464	860	0.5624	1040	0.3084
325	0.0058	505	0.2677	685	0.4503	865	0.5654	1045	0.2788
330	0.0071	510	0.2752	690	0.4541	870	0.5683	1050	0.2493
335	0.0093	515	0.2822	695	0.4579	875	0.5711	1055	0.2223
340	0.0115	520	0.2891	700	0.4616	880	0.5739	1060	0.1955
345	0.0133	525	0.2955	705	0.4648	885	0.5761	1065	0.1739
350	0.0153	530	0.3020	710	0.4680	890	0.5781	1070	0.1525
355	0.0175	535	0.3082	715	0.4708	895	0.5804	1075	0.1366
360	0.0198	540	0.3145	720	0.4733	900	0.5828	1080	0.1210
365	0.0228	545	0.3207	725	0.4773	905	0.5854	1085	0.1085
370	0.0260	550	0.3268	730	0.4815	910	0.5880	1090	0.0958
375	0.0303	555	0.3322	735	0.4847	915	0.5896	1095	0.0853
380	0.0347	560	0.3373	740	0.4878	920	0.5909	1100	0.0746
385	0.0424	565	0.3425	745	0.4908	925	0.5919	1105	0.0660
390	0.0500	570	0.3476	750	0.4940	930	0.5931	1110	0.0575
395	0.0589	575	0.3530	755	0.4983	935	0.5939	1115	0.0508
400	0.0680	580	0.3583	760	0.5025	940	0.5949	1120	0.0438
405	0.0783	585	0.3629	765	0.5053	945	0.5939	1125	0.0379
410	0.0884	590	0.3677	770	0.5081	950	0.5927	1130	0.0319
415	0.0992	595	0.3722	775	0.5116	955	0.5903	1135	0.0274
420	0.1097	600	0.3770	780	0.5152	960	0.5878	1140	0.0228
425	0.1210	605	0.3817	785	0.5182	965	0.5822	1145	0.0186
430	0.1325	610	0.3863	790	0.5211	970	0.5767	1150	0.0145
435	0.1426	615	0.3911	795	0.5241	975	0.5679	1155	0.0117
440	0.1525	620	0.3958	800	0.5271	980	0.5592	1160	0.0089
445	0.1624	625	0.4002	805	0.5309	985	0.5477	1165	0.0069
450	0.1725	630	0.4043	810	0.5344	990	0.5362	1170	0.0050
455	0.1824	635	0.4089	815	0.5366	995	0.5215	1175	0.0034
460	0.1924	640	0.4137	820	0.5388	1000	0.5069	1180	0.0020
465	0.2015	645	0.4174	825	0.5418	1005	0.4874	1185	0.0012
470	0.2108	650	0.4214	830	0.5447	1010	0.4680	1190	0.0004
475	0.2197	655	0.4254	835	0.5481	1015	0.4450		
480	0.2286	660	0.4293	840	0.5517	1020	0.4220		
485	0.2372	665	0.4337	845	0.5543	1025	0.3944		

Notes:

Green wire/brown wire temperature sensor contacts unstable.



World Photovoltaic Scale Calibration Report PX102C

Date:	October 17, 1996
Calibration temperature:	25°C
Short-circuit current:	117.05 mA
I_{sc} standard deviation:	0.94 %
I_{sc} temperature coefficient:	504 ppm / °C
Area:	398 mm ²
Open-circuit voltage:	581 mV
Fill factor:	0.674
$dI/dV _{V=0}$:	-3.2 mS
Series resistance:	0.14 Ω
Shunt resistance:	1.8 kΩ
n_1 :	1.94
I_{o1} :	7.61×10^{-7} A
n_2 :	4.62
I_{o2} :	3.30×10^{-4} A

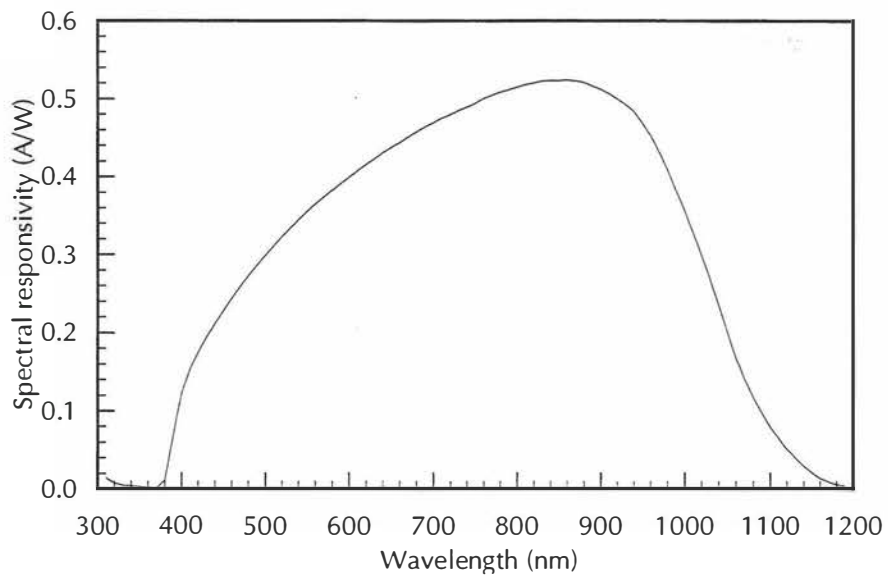
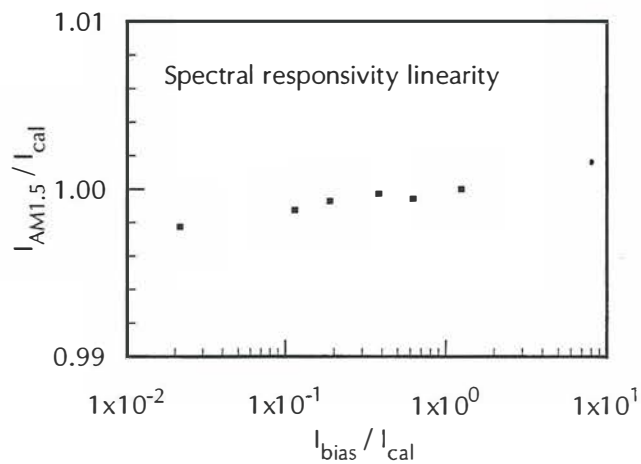
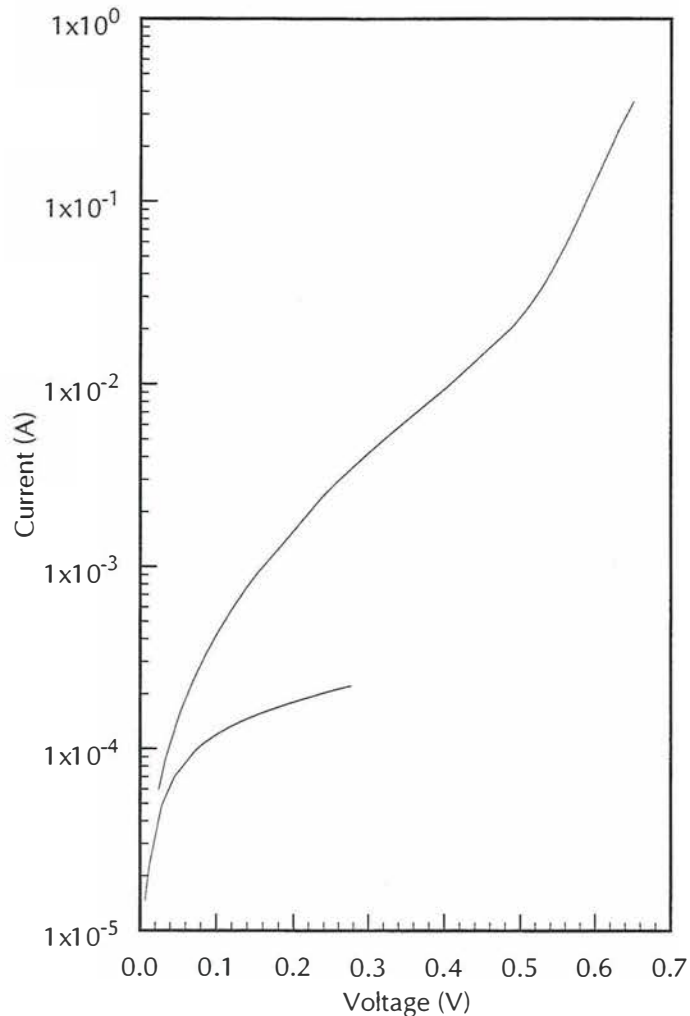
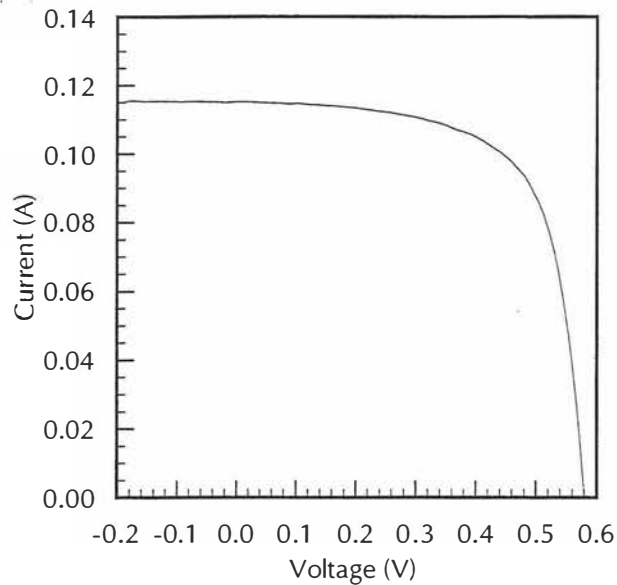
Spectral responsivity (nm, A/W):

310	0.0145	490	0.2862	670	0.4509	850	0.5234	1030	0.2680
315	0.0113	495	0.2926	675	0.4542	855	0.5237	1035	0.2519
320	0.0081	500	0.2991	680	0.4573	860	0.5241	1040	0.2358
325	0.0066	505	0.3050	685	0.4605	865	0.5235	1045	0.2187
330	0.0049	510	0.3110	690	0.4636	870	0.5230	1050	0.2014
335	0.0048	515	0.3169	695	0.4663	875	0.5220	1055	0.1847
340	0.0047	520	0.3230	700	0.4691	880	0.5209	1060	0.1680
345	0.0041	525	0.3284	705	0.4721	885	0.5187	1065	0.1546
350	0.0034	530	0.3338	710	0.4750	890	0.5164	1070	0.1410
355	0.0029	535	0.3391	715	0.4773	895	0.5143	1075	0.1295
360	0.0025	540	0.3446	720	0.4795	900	0.5121	1080	0.1178
365	0.0020	545	0.3498	725	0.4823	905	0.5093	1085	0.1078
370	0.0015	550	0.3551	730	0.4851	910	0.5065	1090	0.0978
375	0.0066	555	0.3598	735	0.4871	915	0.5033	1095	0.0889
380	0.0117	560	0.3644	740	0.4893	920	0.4998	1100	0.0800
385	0.0403	565	0.3691	745	0.4917	925	0.4963	1105	0.0728
390	0.0690	570	0.3736	750	0.4940	930	0.4926	1110	0.0656
395	0.0954	575	0.3779	755	0.4973	935	0.4882	1115	0.0587
400	0.1219	580	0.3824	760	0.5005	940	0.4838	1120	0.0519
405	0.1374	585	0.3866	765	0.5024	945	0.4765	1125	0.0462
410	0.1528	590	0.3908	770	0.5043	950	0.4691	1130	0.0403
415	0.1635	595	0.3947	775	0.5064	955	0.4609	1135	0.0351
420	0.1741	600	0.3987	780	0.5086	960	0.4526	1140	0.0298
425	0.1840	605	0.4029	785	0.5100	965	0.4425	1145	0.0257
430	0.1940	610	0.4071	790	0.5114	970	0.4322	1150	0.0217
435	0.2025	615	0.4112	795	0.5130	975	0.4207	1155	0.0180
440	0.2110	620	0.4154	800	0.5147	980	0.4091	1160	0.0143
445	0.2193	625	0.4190	805	0.5164	985	0.3961	1165	0.0119
450	0.2274	630	0.4226	810	0.5182	990	0.3829	1170	0.0095
455	0.2356	635	0.4266	815	0.5191	995	0.3696	1175	0.0079
460	0.2438	640	0.4307	820	0.5201	1000	0.3561	1180	0.0062
465	0.2510	645	0.4339	825	0.5213	1005	0.3422	1185	0.0053
470	0.2583	650	0.4372	830	0.5224	1010	0.3282	1190	0.0044
475	0.2654	655	0.4403	835	0.5229	1015	0.3136		
480	0.2726	660	0.4435	840	0.5235	1020	0.2991		
485	0.2794	665	0.4472	845	0.5234	1025	0.2836		

Notes:

One contact to solar cell shorted to metal package.

PX102C



World Photovoltaic Scale Calibration Report PX201C

Date:	October 17, 1996
Calibration temperature:	25°C
Short-circuit current:	123.29 mA
I_{sc} standard deviation:	1.00 %
I_{sc} temperature coefficient:	423 ppm / °C
Area:	399 mm ²
Open-circuit voltage:	600 mV
Fill factor:	0.794
$dI/dV _{V=0}$:	-0.13 mS
Series resistance:	0.12 Ω
Shunt resistance:	420 kΩ
n_1 :	1.23
I_{o1} :	5.51×10^{-10} A
n_2 :	2.64
I_{o2} :	1.29×10^{-6} A

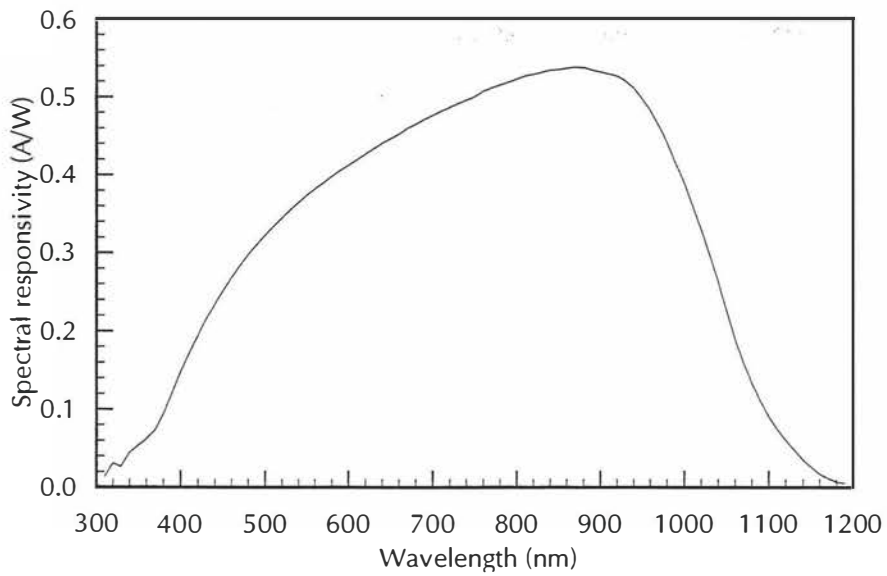
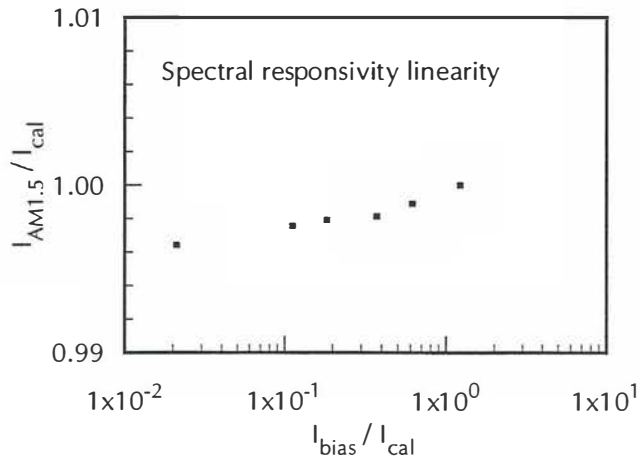
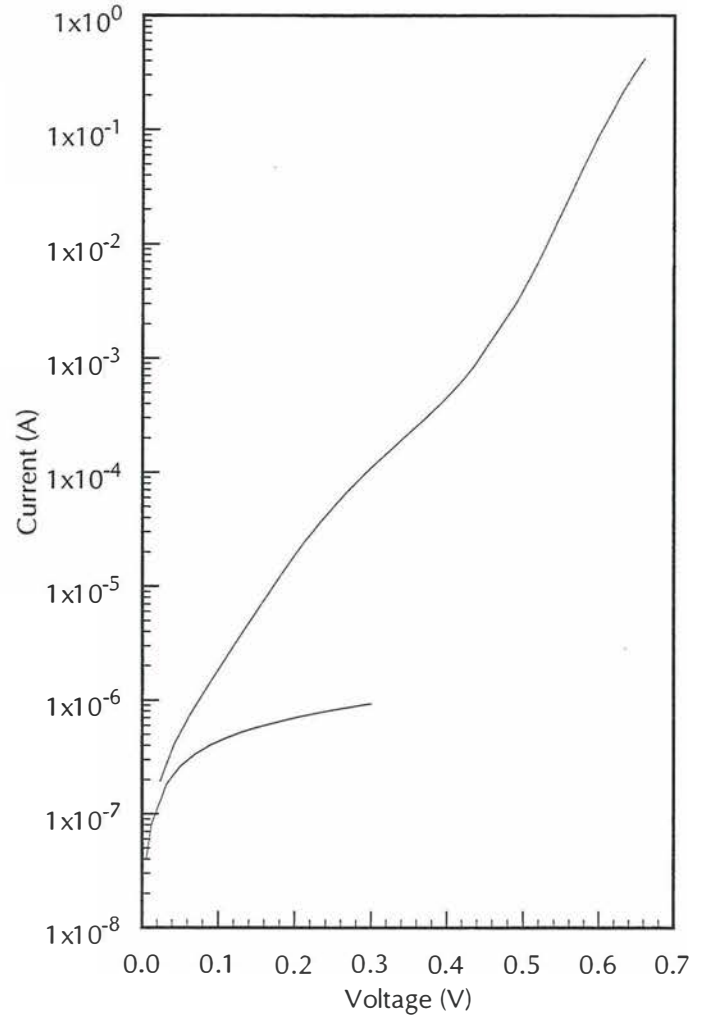
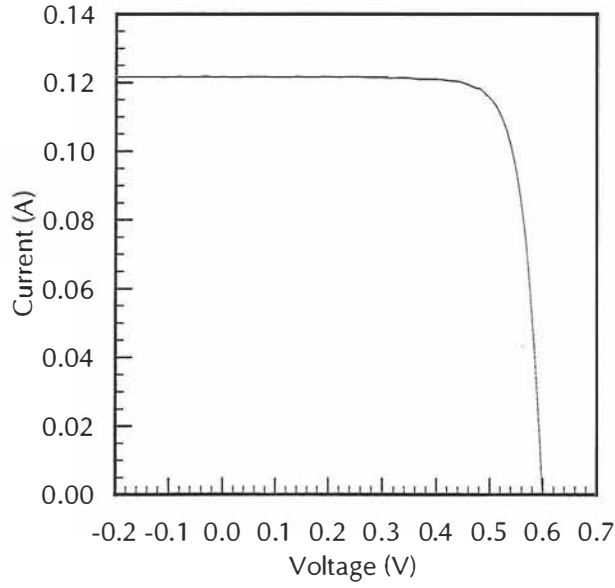
Spectral responsivity (nm, A/W):

310	0.0137	490	0.3105	670	0.4594	850	0.5351	1030	0.2974
315	0.0224	495	0.3165	675	0.4620	855	0.5359	1035	0.2805
320	0.0311	500	0.3225	680	0.4647	860	0.5368	1040	0.2636
325	0.0288	505	0.3283	685	0.4679	865	0.5375	1045	0.2450
330	0.0264	510	0.3341	690	0.4709	870	0.5381	1050	0.2263
335	0.0356	515	0.3395	695	0.4736	875	0.5379	1055	0.2080
340	0.0448	520	0.3449	700	0.4764	880	0.5377	1060	0.1896
345	0.0490	525	0.3499	705	0.4789	885	0.5363	1065	0.1746
350	0.0534	530	0.3550	710	0.4816	890	0.5347	1070	0.1595
355	0.0576	535	0.3599	715	0.4838	895	0.5333	1075	0.1465
360	0.0619	540	0.3647	720	0.4861	900	0.5319	1080	0.1335
365	0.0675	545	0.3692	725	0.4886	905	0.5307	1085	0.1223
370	0.0730	550	0.3736	730	0.4912	910	0.5294	1090	0.1112
375	0.0834	555	0.3778	735	0.4934	915	0.5282	1095	0.1011
380	0.0938	560	0.3820	740	0.4956	920	0.5268	1100	0.0911
385	0.1070	565	0.3859	745	0.4980	925	0.5238	1105	0.0830
390	0.1203	570	0.3899	750	0.5004	930	0.5206	1110	0.0749
395	0.1337	575	0.3940	755	0.5037	935	0.5161	1115	0.0677
400	0.1470	580	0.3982	760	0.5072	940	0.5114	1120	0.0607
405	0.1594	585	0.4017	765	0.5092	945	0.5047	1125	0.0543
410	0.1716	590	0.4053	770	0.5113	950	0.4980	1130	0.0479
415	0.1827	595	0.4088	775	0.5133	955	0.4905	1135	0.0417
420	0.1938	600	0.4121	780	0.5153	960	0.4829	1140	0.0355
425	0.2047	605	0.4156	785	0.5170	965	0.4731	1145	0.0308
430	0.2154	610	0.4190	790	0.5187	970	0.4632	1150	0.0262
435	0.2248	615	0.4229	795	0.5207	975	0.4523	1155	0.0218
440	0.2343	620	0.4266	800	0.5226	980	0.4414	1160	0.0174
445	0.2430	625	0.4300	805	0.5246	985	0.4284	1165	0.0145
450	0.2518	630	0.4333	810	0.5266	990	0.4154	1170	0.0117
455	0.2602	635	0.4369	815	0.5278	995	0.4024	1175	0.0094
460	0.2684	640	0.4407	820	0.5288	1000	0.3895	1180	0.0073
465	0.2760	645	0.4434	825	0.5302	1005	0.3748	1185	0.0064
470	0.2835	650	0.4464	830	0.5315	1010	0.3600	1190	0.0053
475	0.2907	655	0.4492	835	0.5328	1015	0.3448		
480	0.2979	660	0.4519	840	0.5340	1020	0.3295		
485	0.3041	665	0.4557	845	0.5345	1025	0.3134		

Notes:

One contact to solar cell shorted to metal package.

PX201C



World Photovoltaic Scale Calibration Report PTB RS-58

Date:	October 17, 1996
Calibration temperature:	25°C
Short-circuit current:	126.61 mA
I_{sc} standard deviation:	1.32 %
I_{sc} temperature coefficient:	559 ppm / °C
Area:	400 mm ²
Open-circuit voltage:	596 mV
Fill factor:	0.731
$dI/dV _{V=0}$:	0.0 mS
Series resistance:	0.33 Ω
Shunt resistance:	24 kΩ
n_1 :	1.86
I_{o1} :	3.47×10^{-7} A
n_2 :	2.36
I_{o2} :	3.85×10^{-6} A

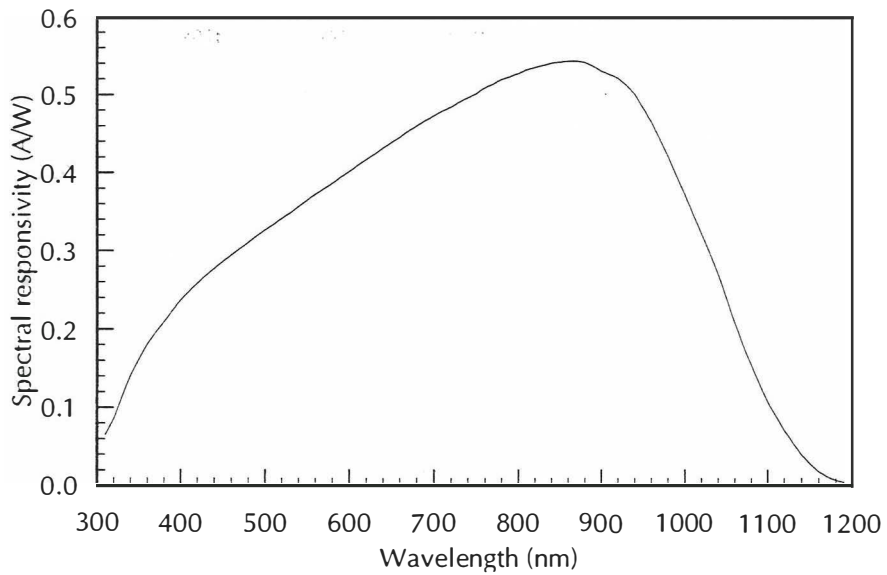
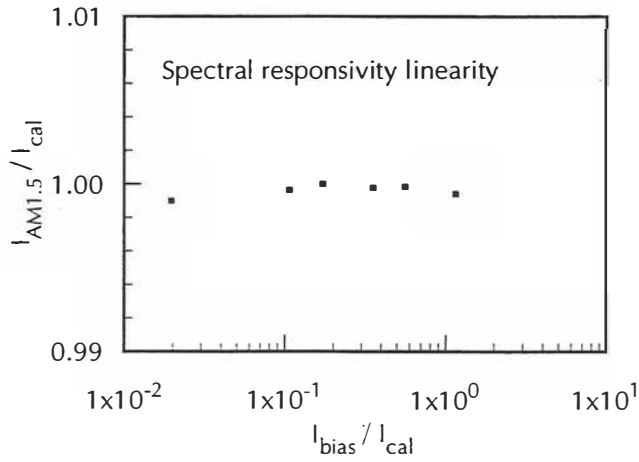
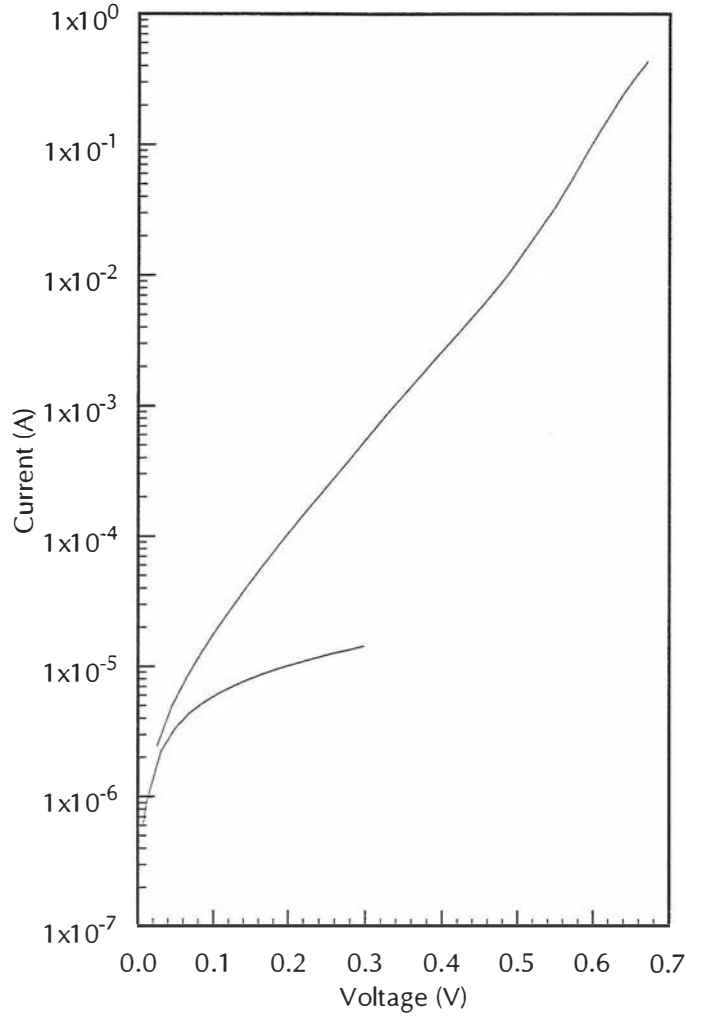
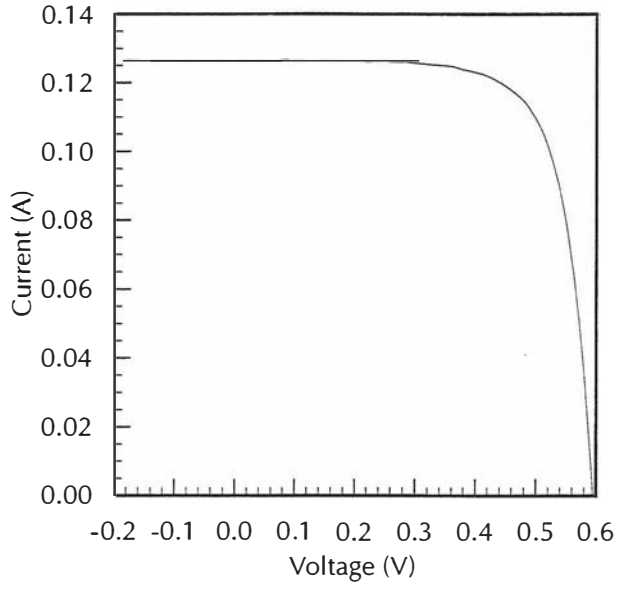
Spectral responsivity (nm, A/W):

310	0.0647	490	0.3194	670	0.4534	850	0.5420	1030	0.2978
315	0.0750	495	0.3231	675	0.4567	855	0.5427	1035	0.2847
320	0.0852	500	0.3269	680	0.4599	860	0.5433	1040	0.2715
325	0.0992	505	0.3306	685	0.4634	865	0.5436	1045	0.2560
330	0.1131	510	0.3341	690	0.4668	870	0.5437	1050	0.2406
335	0.1268	515	0.3381	695	0.4699	875	0.5429	1055	0.2250
340	0.1405	520	0.3420	700	0.4729	880	0.5421	1060	0.2093
345	0.1510	525	0.3455	705	0.4762	885	0.5397	1065	0.1952
350	0.1614	530	0.3490	710	0.4794	890	0.5371	1070	0.1809
355	0.1711	535	0.3530	715	0.4818	895	0.5341	1075	0.1681
360	0.1808	540	0.3571	720	0.4843	900	0.5310	1080	0.1553
365	0.1884	545	0.3610	725	0.4876	905	0.5287	1085	0.1432
370	0.1962	550	0.3650	730	0.4910	910	0.5264	1090	0.1312
375	0.2030	555	0.3689	735	0.4935	915	0.5241	1095	0.1199
380	0.2096	560	0.3728	740	0.4961	920	0.5219	1100	0.1087
385	0.2166	565	0.3762	745	0.4989	925	0.5172	1105	0.0993
390	0.2236	570	0.3797	750	0.5017	930	0.5125	1110	0.0899
395	0.2303	575	0.3833	755	0.5055	935	0.5070	1115	0.0810
400	0.2370	580	0.3869	760	0.5092	940	0.5013	1120	0.0720
405	0.2427	585	0.3907	765	0.5114	945	0.4926	1125	0.0638
410	0.2482	590	0.3946	770	0.5137	950	0.4838	1130	0.0556
415	0.2534	595	0.3980	775	0.5167	955	0.4747	1135	0.0480
420	0.2585	600	0.4015	780	0.5195	960	0.4655	1140	0.0405
425	0.2637	605	0.4054	785	0.5214	965	0.4548	1145	0.0349
430	0.2688	610	0.4094	790	0.5231	970	0.4440	1150	0.0292
435	0.2731	615	0.4132	795	0.5253	975	0.4328	1155	0.0241
440	0.2774	620	0.4168	800	0.5273	980	0.4218	1160	0.0190
445	0.2820	625	0.4205	805	0.5297	985	0.4096	1165	0.0157
450	0.2867	630	0.4240	810	0.5320	990	0.3972	1170	0.0125
455	0.2908	635	0.4279	815	0.5336	995	0.3849	1175	0.0102
460	0.2949	640	0.4316	820	0.5351	1000	0.3728	1180	0.0078
465	0.2989	645	0.4351	825	0.5365	1005	0.3602	1185	0.0066
470	0.3031	650	0.4386	830	0.5380	1010	0.3475	1190	0.0054
475	0.3069	655	0.4421	835	0.5393	1015	0.3351		
480	0.3108	660	0.4456	840	0.5408	1020	0.3229		
485	0.3151	665	0.4495	845	0.5415	1025	0.3104		

Notes:

One contact to solar cell shorted to metal package.
Bubbles in encapsulation.

PTB RS-58



World Photovoltaic Scale

Calibration Report

PTB RS-67

Date:	October 17, 1996
Calibration temperature:	25°C
Short-circuit current:	125.65 mA
I_{sc} standard deviation:	1.08 %
I_{sc} temperature coefficient:	422 ppm / °C
Area:	401 mm ²
Open-circuit voltage:	602 mV
Fill factor:	0.745
$dI/dV _{V=0}$:	-0.47 mS
Series resistance:	0.23 Ω
Shunt resistance:	13 kΩ
n_1 :	1.58
I_{o1} :	3.18×10^{-8} A
n_2 :	4.44
I_{o2} :	1.07×10^{-4} A

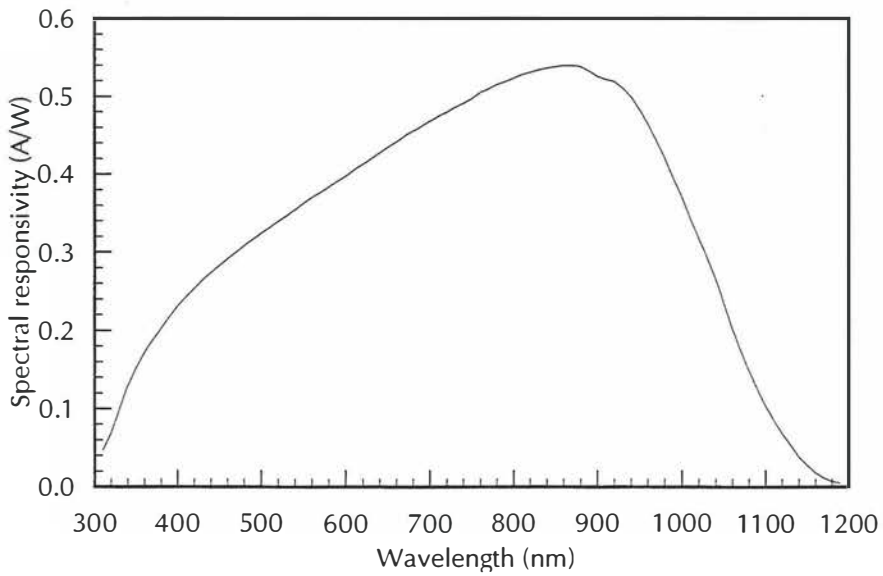
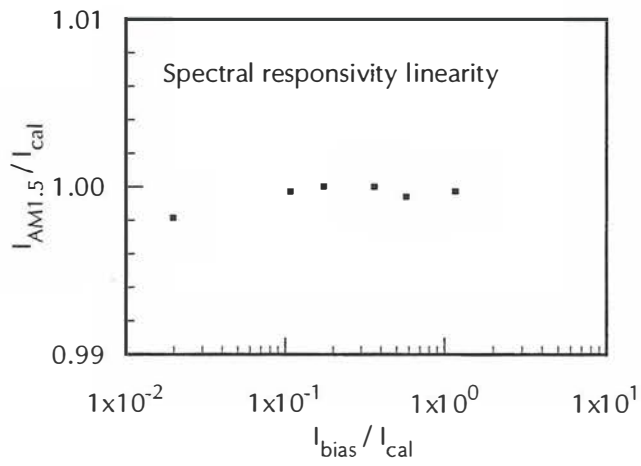
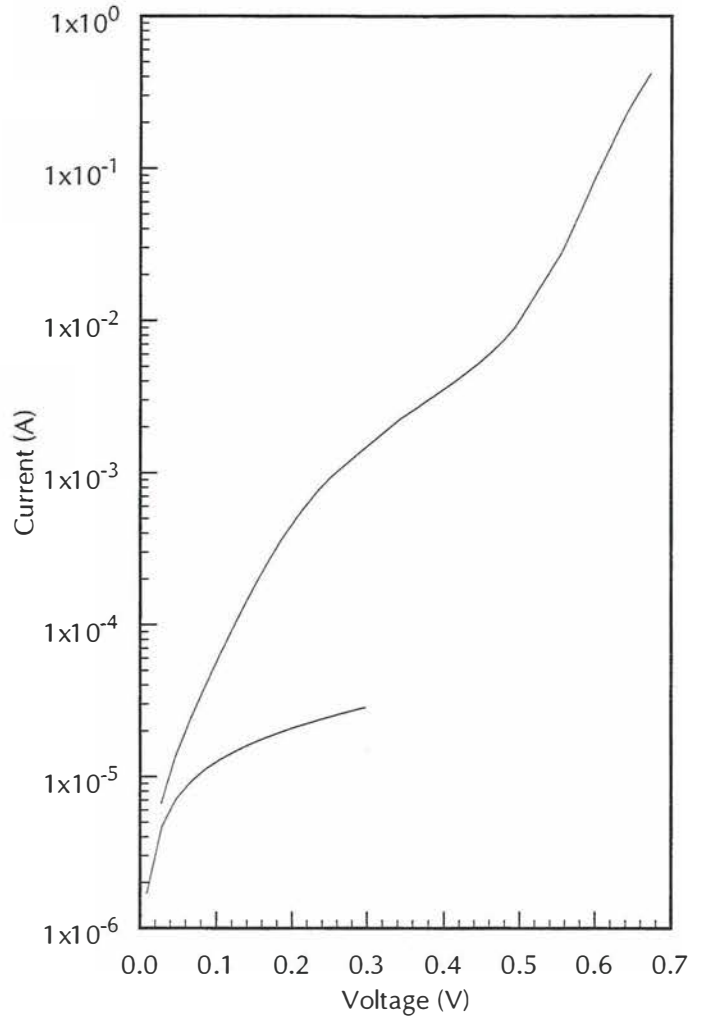
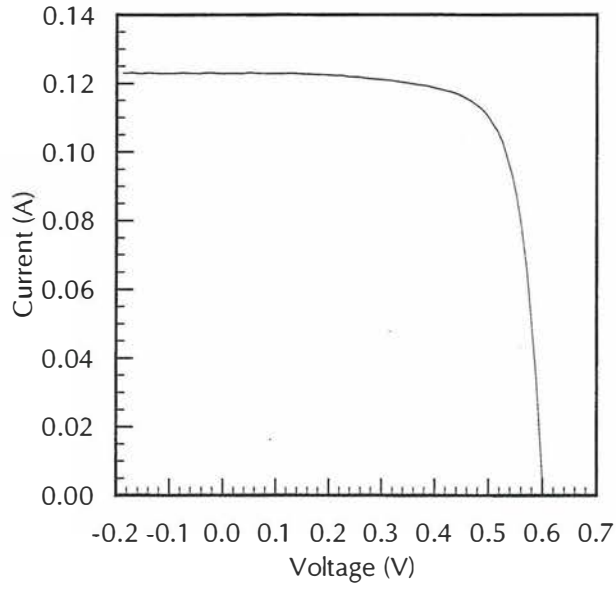
Spectral responsivity (nm, A/W):

310	0.0467	490	0.3165	670	0.4497	850	0.5381	1030	0.2921
315	0.0579	495	0.3205	675	0.4527	855	0.5391	1035	0.2785
320	0.0691	500	0.3244	680	0.4556	860	0.5399	1040	0.2651
325	0.0844	505	0.3283	685	0.4588	865	0.5399	1045	0.2493
330	0.0996	510	0.3321	690	0.4620	870	0.5400	1050	0.2337
335	0.1148	515	0.3359	695	0.4652	875	0.5393	1055	0.2179
340	0.1299	520	0.3396	700	0.4684	880	0.5388	1060	0.2021
345	0.1409	525	0.3433	705	0.4716	885	0.5359	1065	0.1883
350	0.1520	530	0.3469	710	0.4747	890	0.5329	1070	0.1744
355	0.1620	535	0.3508	715	0.4775	895	0.5296	1075	0.1616
360	0.1720	540	0.3547	720	0.4803	900	0.5263	1080	0.1488
365	0.1801	545	0.3588	725	0.4833	905	0.5243	1085	0.1372
370	0.1883	550	0.3628	730	0.4864	910	0.5221	1090	0.1257
375	0.1955	555	0.3665	735	0.4889	915	0.5209	1095	0.1147
380	0.2028	560	0.3701	740	0.4913	920	0.5196	1100	0.1036
385	0.2101	565	0.3735	745	0.4944	925	0.5153	1105	0.0945
390	0.2175	570	0.3769	750	0.4973	930	0.5111	1110	0.0853
395	0.2243	575	0.3804	755	0.5012	935	0.5055	1115	0.0769
400	0.2311	580	0.3840	760	0.5052	940	0.4999	1120	0.0685
405	0.2369	585	0.3875	765	0.5075	945	0.4916	1125	0.0608
410	0.2429	590	0.3909	770	0.5099	950	0.4833	1130	0.0532
415	0.2481	595	0.3943	775	0.5125	955	0.4743	1135	0.0457
420	0.2533	600	0.3976	780	0.5151	960	0.4652	1140	0.0384
425	0.2591	605	0.4017	785	0.5171	965	0.4544	1145	0.0329
430	0.2648	610	0.4057	790	0.5191	970	0.4436	1150	0.0276
435	0.2692	615	0.4095	795	0.5212	975	0.4327	1155	0.0229
440	0.2736	620	0.4131	800	0.5233	980	0.4216	1160	0.0183
445	0.2781	625	0.4167	805	0.5257	985	0.4087	1165	0.0151
450	0.2827	630	0.4203	810	0.5281	990	0.3957	1170	0.0117
455	0.2871	635	0.4240	815	0.5295	995	0.3831	1175	0.0095
460	0.2913	640	0.4276	820	0.5309	1000	0.3705	1180	0.0072
465	0.2956	645	0.4313	825	0.5325	1005	0.3571	1185	0.0063
470	0.2997	650	0.4349	830	0.5343	1010	0.3436	1190	0.0053
475	0.3040	655	0.4383	835	0.5355	1015	0.3307		
480	0.3084	660	0.4416	840	0.5367	1020	0.3176		
485	0.3124	665	0.4456	845	0.5375	1025	0.3049		

Notes:

One contact to solar cell shorted to metal package.
 Bubbles in encapsulation, including several over solar cell.

PTB RS-67



World Photovoltaic Scale Calibration Report PTB RS-68

Date:	October 17, 1996
Calibration temperature:	25°C
Short-circuit current:	125.59 mA
I_{sc} standard deviation:	1.37 %
I_{sc} temperature coefficient:	485 ppm / °C
Area:	400 mm ²
Open-circuit voltage:	603 mV
Fill factor:	0.769
$dI/dV _{V=0}$:	-0.23 mS
Series resistance:	0.14 Ω
Shunt resistance:	41 kΩ
n_1 :	1.51
I_{o1} :	1.49×10 ⁻⁸ A
n_2 :	2.92
I_{o2} :	6.54×10 ⁻⁶ A

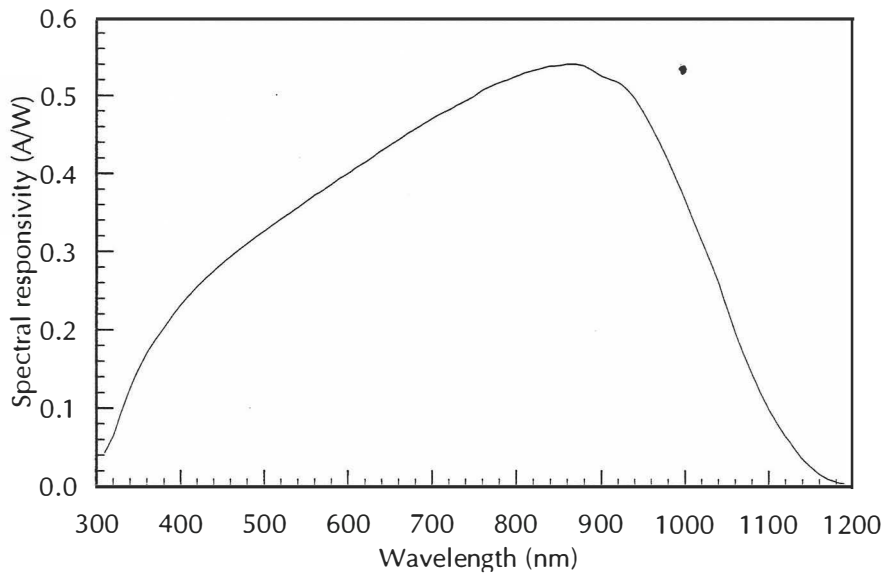
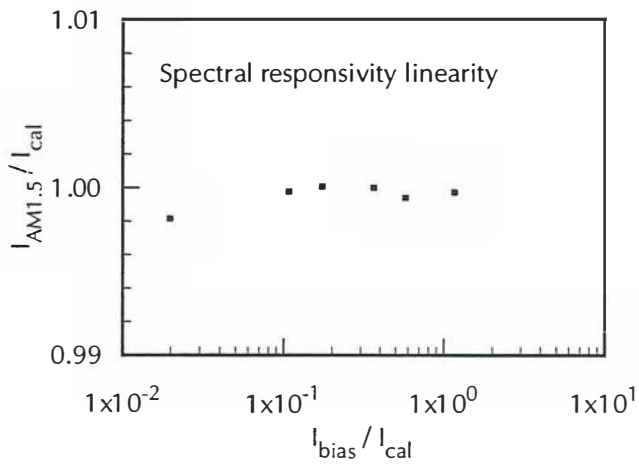
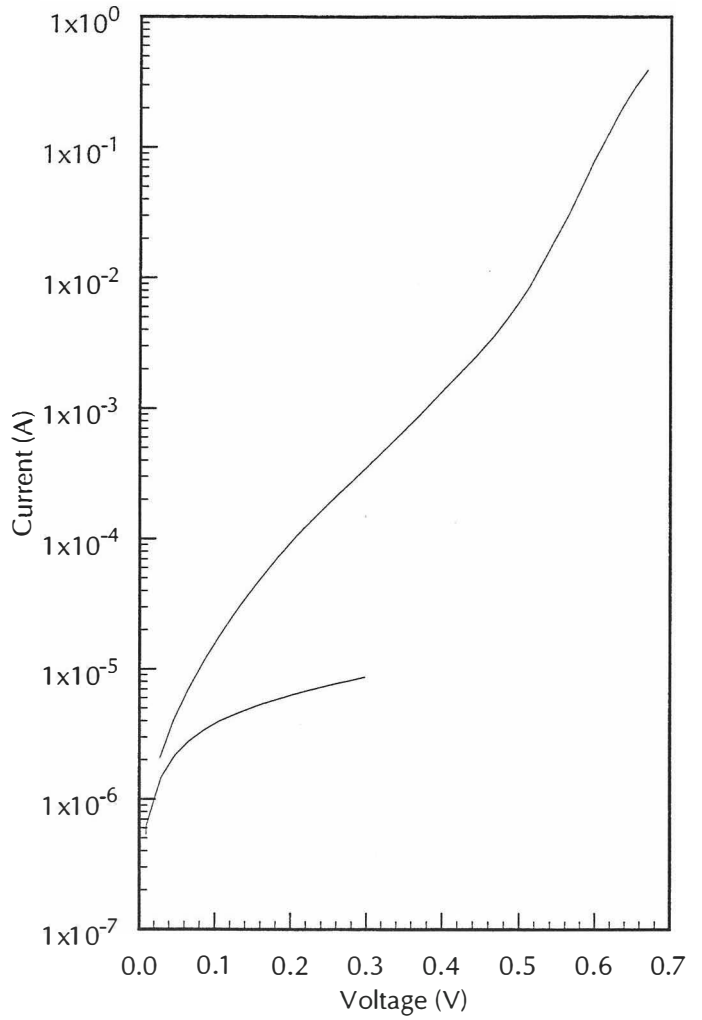
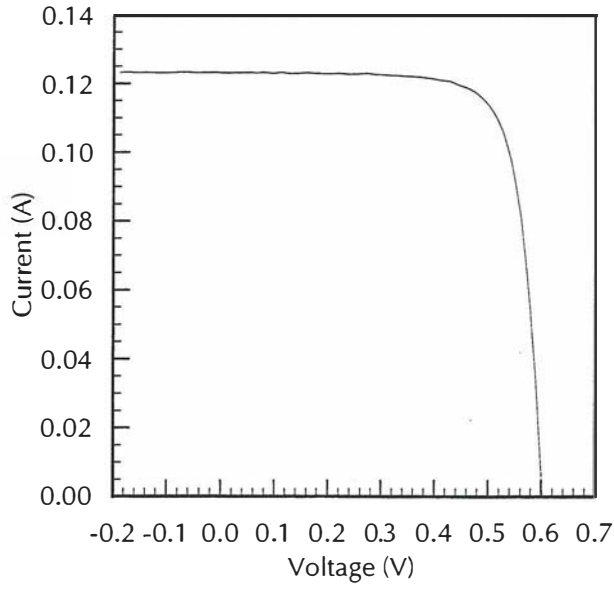
Spectral responsivity (nm, A/W):

310	0.0432	490	0.3190	670	0.4515	850	0.5386	1030	0.2882
315	0.0535	495	0.3227	675	0.4547	855	0.5397	1035	0.2748
320	0.0639	500	0.3265	680	0.4579	860	0.5407	1040	0.2614
325	0.0794	505	0.3303	685	0.4612	865	0.5407	1045	0.2454
330	0.0949	510	0.3343	690	0.4644	870	0.5406	1050	0.2293
335	0.1101	515	0.3382	695	0.4678	875	0.5394	1055	0.2133
340	0.1253	520	0.3422	700	0.4711	880	0.5382	1060	0.1975
345	0.1374	525	0.3457	705	0.4742	885	0.5351	1065	0.1837
350	0.1496	530	0.3492	710	0.4772	890	0.5321	1070	0.1698
355	0.1600	535	0.3530	715	0.4796	895	0.5285	1075	0.1574
360	0.1705	540	0.3568	720	0.4822	900	0.5249	1080	0.1449
365	0.1793	545	0.3609	725	0.4851	905	0.5229	1085	0.1332
370	0.1881	550	0.3649	730	0.4882	910	0.5209	1090	0.1214
375	0.1955	555	0.3688	735	0.4908	915	0.5191	1095	0.1106
380	0.2028	560	0.3726	740	0.4936	920	0.5173	1100	0.0998
385	0.2107	565	0.3758	745	0.4966	925	0.5130	1105	0.0909
390	0.2185	570	0.3792	750	0.4995	930	0.5086	1110	0.0819
395	0.2252	575	0.3826	755	0.5035	935	0.5026	1115	0.0736
400	0.2320	580	0.3862	760	0.5074	940	0.4964	1120	0.0655
405	0.2382	585	0.3901	765	0.5099	945	0.4876	1125	0.0579
410	0.2442	590	0.3941	770	0.5125	950	0.4790	1130	0.0502
415	0.2499	595	0.3973	775	0.5147	955	0.4698	1135	0.0431
420	0.2555	600	0.4005	780	0.5170	960	0.4604	1140	0.0360
425	0.2607	605	0.4043	785	0.5189	965	0.4498	1145	0.0311
430	0.2659	610	0.4081	790	0.5207	970	0.4389	1150	0.0261
435	0.2706	615	0.4116	795	0.5229	975	0.4276	1155	0.0216
440	0.2752	620	0.4151	800	0.5250	980	0.4164	1160	0.0171
445	0.2802	625	0.4188	805	0.5273	985	0.4040	1165	0.0140
450	0.2850	630	0.4224	810	0.5295	990	0.3916	1170	0.0109
455	0.2893	635	0.4263	815	0.5310	995	0.3789	1175	0.0091
460	0.2935	640	0.4301	820	0.5323	1000	0.3662	1180	0.0071
465	0.2979	645	0.4336	825	0.5339	1005	0.3532	1185	0.0060
470	0.3022	650	0.4371	830	0.5355	1010	0.3399	1190	0.0049
475	0.3063	655	0.4403	835	0.5369	1015	0.3267		
480	0.3105	660	0.4436	840	0.5382	1020	0.3137		
485	0.3147	665	0.4476	845	0.5385	1025	0.3010		

Notes:

One contact to solar cell shorted to metal package.
Bubbles in encapsulation, including several over solar cell.

PTB RS-68



World Photovoltaic Scale Calibration Report PTB RS-69

Date:	October 17, 1996
Calibration temperature:	25°C
Short-circuit current:	125.69 mA
I_{sc} standard deviation:	1.37 %
I_{sc} temperature coefficient:	530 ppm / °C
Area:	400 mm ²
Open-circuit voltage:	601 mV
Fill factor:	0.742
$dI/dV _{V=0}$:	-0.79 mS
Series resistance:	0.17 Ω
Shunt resistance:	6.1 kΩ
n_1 :	1.59
I_{o1} :	3.60×10^{-8} A
n_2 :	4.06
I_{o2} :	7.38×10^{-5} A

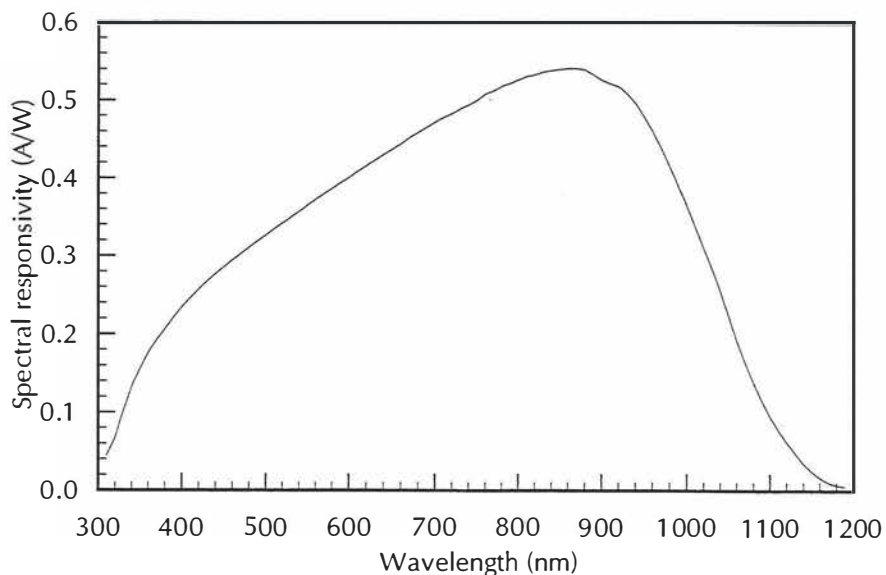
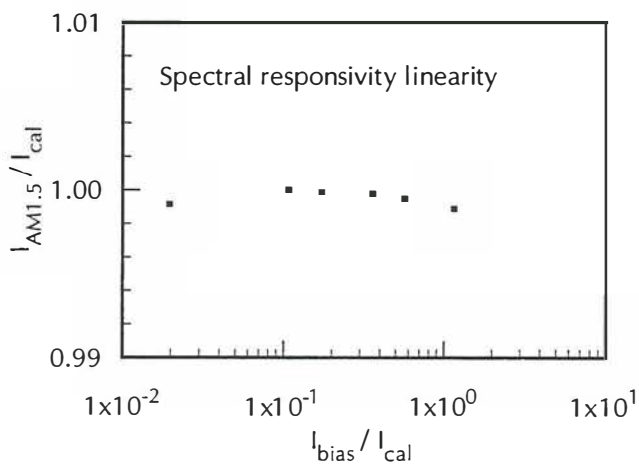
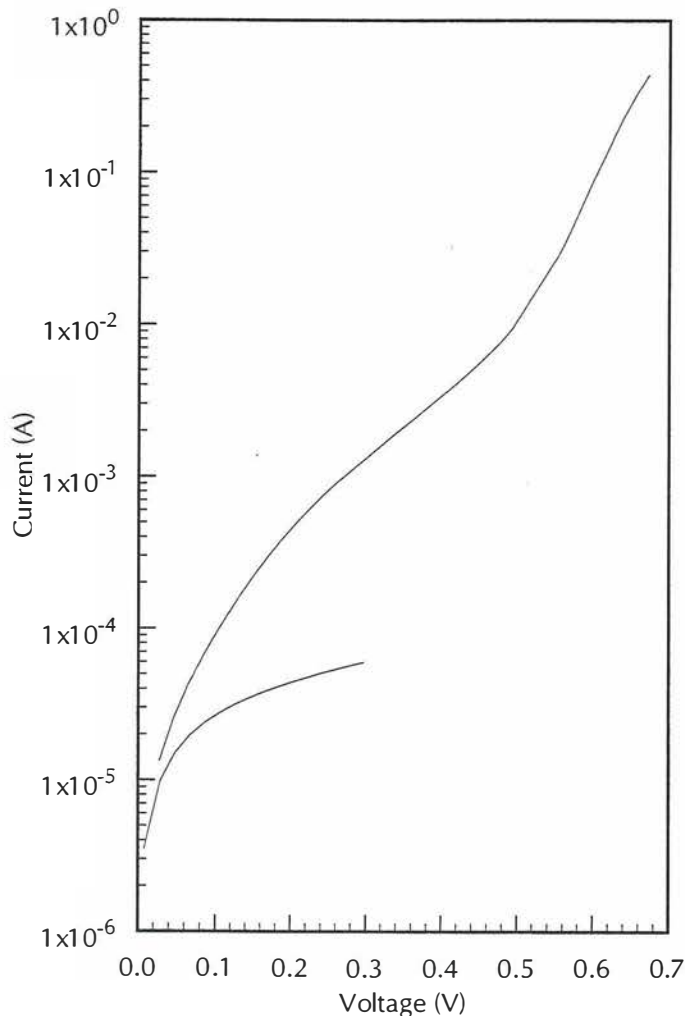
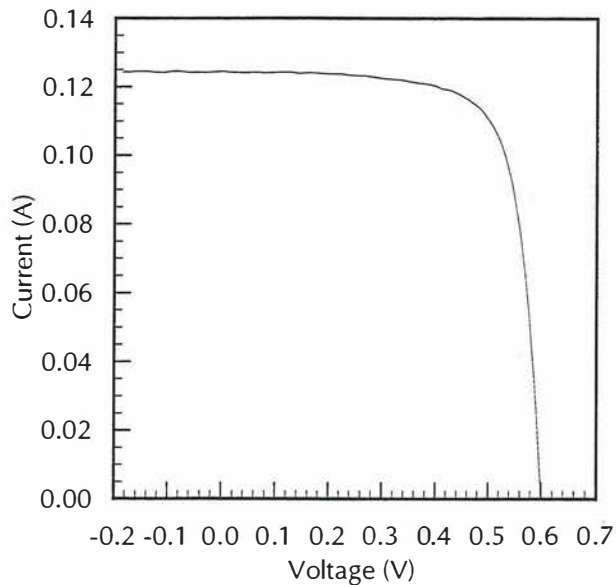
Spectral responsivity (nm, A/W):

310	0.0443	490	0.3192	670	0.4519	850	0.5398	1030	0.2835
315	0.0557	495	0.3230	675	0.4552	855	0.5404	1035	0.2695
320	0.0671	500	0.3267	680	0.4584	860	0.5411	1040	0.2556
325	0.0840	505	0.3307	685	0.4619	865	0.5411	1045	0.2396
330	0.1008	510	0.3347	690	0.4652	870	0.5411	1050	0.2236
335	0.1165	515	0.3384	695	0.4686	875	0.5402	1055	0.2078
340	0.1323	520	0.3422	700	0.4718	880	0.5394	1060	0.1919
345	0.1437	525	0.3458	705	0.4750	885	0.5363	1065	0.1779
350	0.1551	530	0.3495	710	0.4780	890	0.5332	1070	0.1639
355	0.1655	535	0.3532	715	0.4806	895	0.5298	1075	0.1511
360	0.1759	540	0.3571	720	0.4830	900	0.5263	1080	0.1383
365	0.1841	545	0.3610	725	0.4860	905	0.5239	1085	0.1272
370	0.1923	550	0.3648	730	0.4890	910	0.5216	1090	0.1163
375	0.1994	555	0.3687	735	0.4916	915	0.5198	1095	0.1057
380	0.2064	560	0.3724	740	0.4942	920	0.5179	1100	0.0952
385	0.2138	565	0.3760	745	0.4971	925	0.5134	1105	0.0867
390	0.2211	570	0.3795	750	0.5000	930	0.5090	1110	0.0783
395	0.2279	575	0.3830	755	0.5040	935	0.5028	1115	0.0703
400	0.2346	580	0.3864	760	0.5080	940	0.4967	1120	0.0623
405	0.2403	585	0.3902	765	0.5102	945	0.4880	1125	0.0552
410	0.2462	590	0.3939	770	0.5123	950	0.4792	1130	0.0481
415	0.2518	595	0.3972	775	0.5152	955	0.4700	1135	0.0415
420	0.2574	600	0.4006	780	0.5182	960	0.4607	1140	0.0347
425	0.2626	605	0.4046	785	0.5199	965	0.4498	1145	0.0297
430	0.2676	610	0.4084	790	0.5218	970	0.4388	1150	0.0248
435	0.2724	615	0.4120	795	0.5239	975	0.4271	1155	0.0207
440	0.2771	620	0.4158	800	0.5262	980	0.4154	1160	0.0167
445	0.2815	625	0.4192	805	0.5284	985	0.4028	1165	0.0136
450	0.2859	630	0.4227	810	0.5307	990	0.3902	1170	0.0107
455	0.2903	635	0.4264	815	0.5318	995	0.3772	1175	0.0089
460	0.2947	640	0.4300	820	0.5328	1000	0.3643	1180	0.0072
465	0.2986	645	0.4335	825	0.5346	1005	0.3508	1185	0.0063
470	0.3026	650	0.4368	830	0.5364	1010	0.3374	1190	0.0053
475	0.3067	655	0.4404	835	0.5374	1015	0.3236		
480	0.3108	660	0.4439	840	0.5383	1020	0.3098		
485	0.3150	665	0.4479	845	0.5390	1025	0.2967		

Notes:

One contact to solar cell shorted to metal package.

PTB RS-69



World Photovoltaic Scale Calibration Report PTB RS-78

Date:	October 17, 1996
Calibration temperature:	25°C
Short-circuit current:	117.50 mA
I_{sc} standard deviation:	1.19 %
I_{sc} temperature coefficient:	499 ppm / °C
Area:	400 mm ²
Open-circuit voltage:	597 mV
Fill factor:	0.759
$dI/dV _{V=0}$:	-0.42 mS
Series resistance:	0.33 Ω
Shunt resistance:	21 kΩ
n_1 :	1.56
I_{o1} :	2.87×10 ⁻⁸ A
n_2 :	3.46
I_{o2} :	2.02×10 ⁻⁵ A

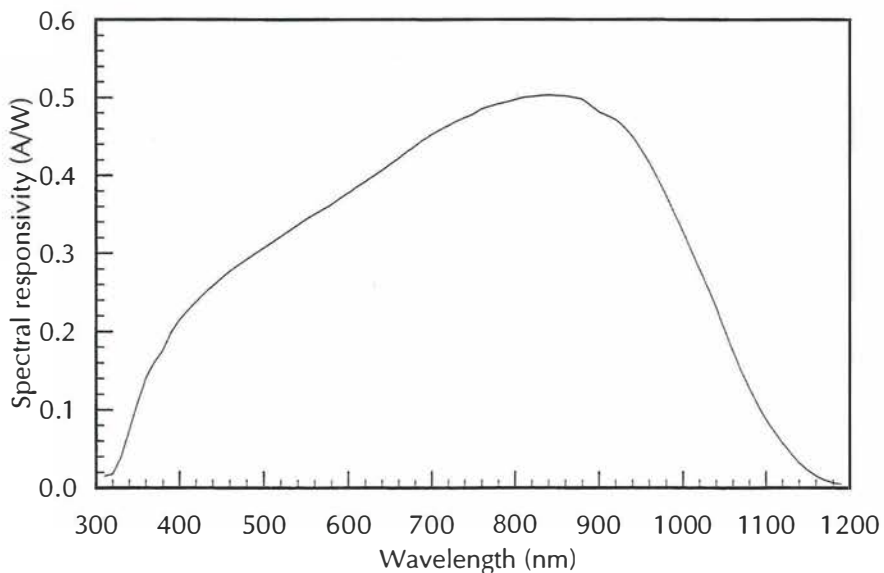
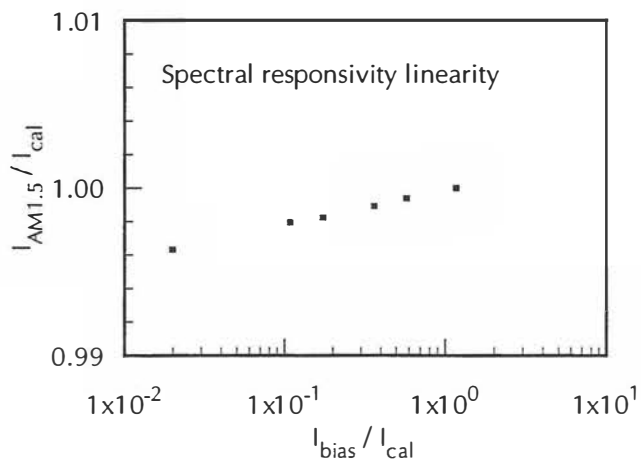
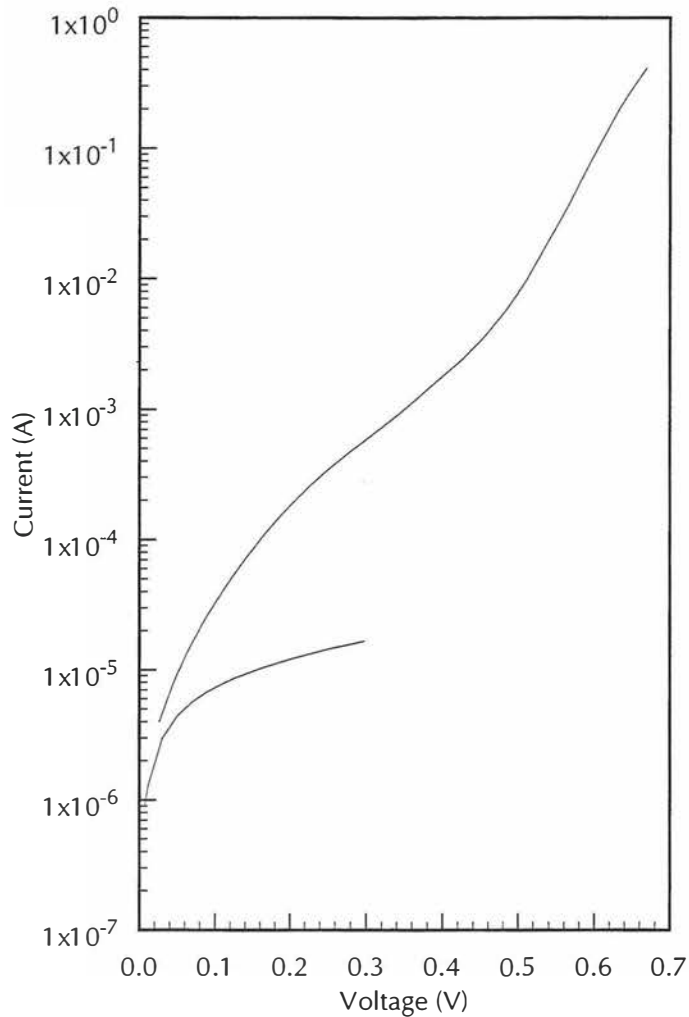
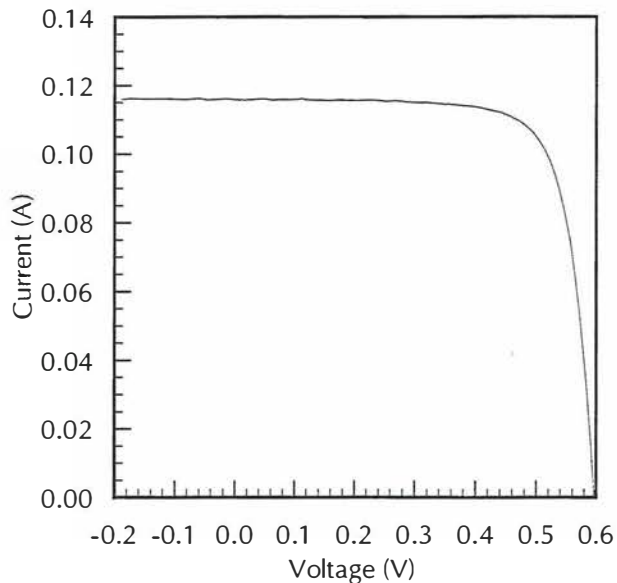
Spectral responsivity (nm, A/W):

310	0.0154	490	0.3001	670	0.4302	850	0.5025	1030	0.2566
315	0.0167	495	0.3036	675	0.4339	855	0.5023	1035	0.2440
320	0.0180	500	0.3070	680	0.4377	860	0.5022	1040	0.2315
325	0.0283	505	0.3106	685	0.4415	865	0.5012	1045	0.2173
330	0.0383	510	0.3143	690	0.4454	870	0.5002	1050	0.2033
335	0.0559	515	0.3179	695	0.4489	875	0.4989	1055	0.1893
340	0.0733	520	0.3217	700	0.4522	880	0.4977	1060	0.1754
345	0.0909	525	0.3253	705	0.4552	885	0.4939	1065	0.1628
350	0.1084	530	0.3290	710	0.4582	890	0.4901	1070	0.1501
355	0.1244	535	0.3327	715	0.4610	895	0.4860	1075	0.1390
360	0.1403	540	0.3366	720	0.4636	900	0.4819	1080	0.1278
365	0.1506	545	0.3402	725	0.4663	905	0.4794	1085	0.1175
370	0.1611	550	0.3438	730	0.4692	910	0.4768	1090	0.1072
375	0.1687	555	0.3472	735	0.4714	915	0.4744	1095	0.0976
380	0.1761	560	0.3504	740	0.4738	920	0.4720	1100	0.0880
385	0.1875	565	0.3535	745	0.4760	925	0.4672	1105	0.0803
390	0.1987	570	0.3566	750	0.4784	930	0.4623	1110	0.0727
395	0.2070	575	0.3596	755	0.4817	935	0.4562	1115	0.0652
400	0.2152	580	0.3627	760	0.4851	940	0.4501	1120	0.0578
405	0.2211	585	0.3666	765	0.4866	945	0.4420	1125	0.0513
410	0.2268	590	0.3703	770	0.4882	950	0.4341	1130	0.0447
415	0.2323	595	0.3739	775	0.4900	955	0.4254	1135	0.0386
420	0.2376	600	0.3774	780	0.4917	960	0.4166	1140	0.0325
425	0.2431	605	0.3812	785	0.4928	965	0.4063	1145	0.0279
430	0.2486	610	0.3850	790	0.4939	970	0.3961	1150	0.0232
435	0.2534	615	0.3886	795	0.4956	975	0.3851	1155	0.0194
440	0.2582	620	0.3924	800	0.4972	980	0.3743	1160	0.0157
445	0.2630	625	0.3958	805	0.4985	985	0.3629	1165	0.0131
450	0.2680	630	0.3993	810	0.4999	990	0.3513	1170	0.0105
455	0.2725	635	0.4031	815	0.5007	995	0.3397	1175	0.0087
460	0.2770	640	0.4068	820	0.5013	1000	0.3280	1180	0.0068
465	0.2811	645	0.4105	825	0.5019	1005	0.3162	1185	0.0060
470	0.2851	650	0.4143	830	0.5024	1010	0.3042	1190	0.0050
475	0.2887	655	0.4181	835	0.5028	1015	0.2920		
480	0.2922	660	0.4220	840	0.5032	1020	0.2800		
485	0.2961	665	0.4261	845	0.5029	1025	0.2683		

Notes:

One contact to solar cell shorted to metal package.

PTB RS-78



World Photovoltaic Scale Calibration Report TDB 9303

Date:	October 17, 1996
Calibration temperature:	25°C
Short-circuit current:	135.18 mA
I_{sc} standard deviation:	1.44 %
I_{sc} temperature coefficient:	482 ppm / °C
Area:	403 mm ²
Open-circuit voltage:	592 mV
Fill factor:	0.776
$dI/dV _{V=0}$:	0.0 mS
Series resistance:	0.12 Ω
Shunt resistance:	55 kΩ
n_1 :	1.39
I_{o1} :	6.58×10 ⁻⁹ A
n_2 :	2.75
I_{o2} :	2.26×10 ⁻⁶ A

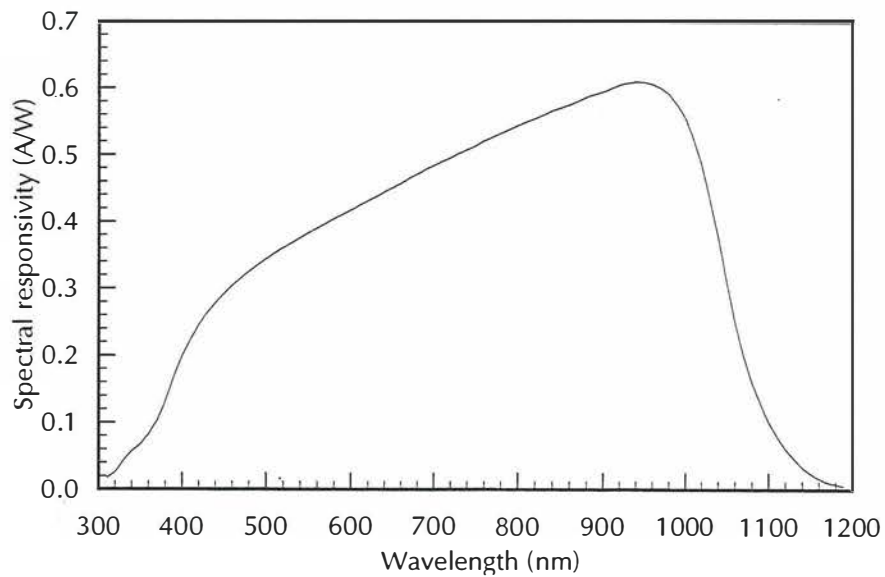
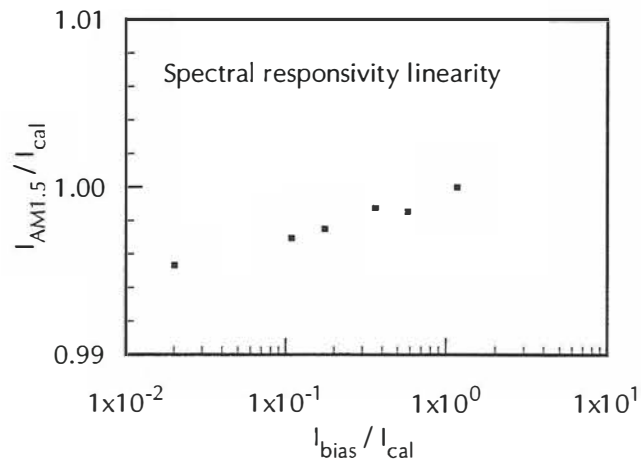
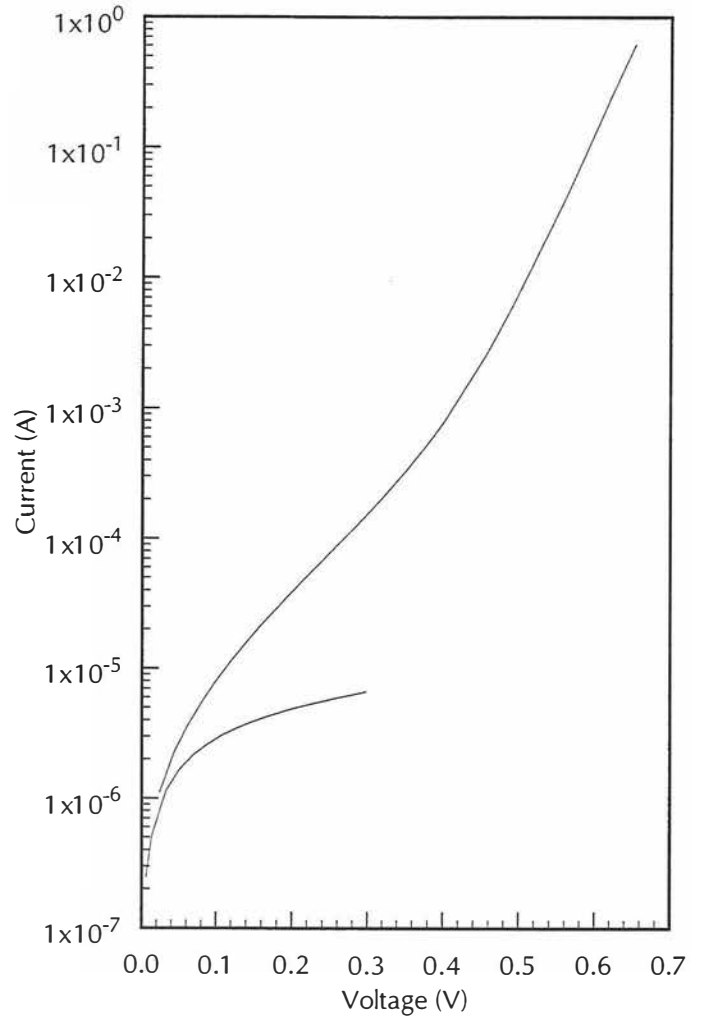
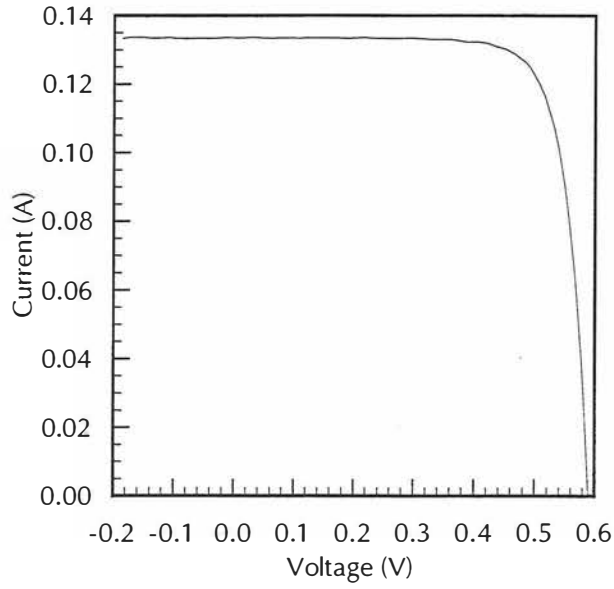
Spectral responsivity (nm, A/W):

310	0.0170	490	0.3350	670	0.4649	850	0.5707	1030	0.4323
315	0.0214	495	0.3396	675	0.4680	855	0.5729	1035	0.4042
320	0.0258	500	0.3440	680	0.4710	860	0.5751	1040	0.3760
325	0.0344	505	0.3483	685	0.4745	865	0.5779	1045	0.3432
330	0.0428	510	0.3525	690	0.4781	870	0.5807	1050	0.3105
335	0.0500	515	0.3567	695	0.4810	875	0.5837	1055	0.2797
340	0.0572	520	0.3607	700	0.4838	880	0.5865	1060	0.2488
345	0.0622	525	0.3642	705	0.4868	885	0.5888	1065	0.2247
350	0.0673	530	0.3679	710	0.4899	890	0.5911	1070	0.2006
355	0.0748	535	0.3719	715	0.4927	895	0.5928	1075	0.1807
360	0.0822	540	0.3758	720	0.4956	900	0.5946	1080	0.1606
365	0.0895	545	0.3795	725	0.4990	905	0.5974	1085	0.1449
370	0.1027	550	0.3834	730	0.5024	910	0.6001	1090	0.1291
375	0.1173	555	0.3868	735	0.5049	915	0.6026	1095	0.1151
380	0.1319	560	0.3903	740	0.5076	920	0.6051	1100	0.1010
385	0.1503	565	0.3935	745	0.5104	925	0.6065	1105	0.0906
390	0.1687	570	0.3968	750	0.5133	930	0.6079	1110	0.0801
395	0.1841	575	0.4005	755	0.5170	935	0.6089	1115	0.0705
400	0.1996	580	0.4042	760	0.5208	940	0.6099	1120	0.0611
405	0.2118	585	0.4073	765	0.5236	945	0.6095	1125	0.0535
410	0.2241	590	0.4104	770	0.5265	950	0.6092	1130	0.0462
415	0.2348	595	0.4136	775	0.5294	955	0.6077	1135	0.0397
420	0.2456	600	0.4170	780	0.5324	960	0.6063	1140	0.0333
425	0.2546	605	0.4207	785	0.5352	965	0.6034	1145	0.0288
430	0.2634	610	0.4242	790	0.5380	970	0.6005	1150	0.0242
435	0.2710	615	0.4278	795	0.5408	975	0.5964	1155	0.0205
440	0.2783	620	0.4312	800	0.5436	980	0.5921	1160	0.0170
445	0.2851	625	0.4343	805	0.5465	985	0.5838	1165	0.0142
450	0.2919	630	0.4372	810	0.5495	990	0.5756	1170	0.0112
455	0.2981	635	0.4409	815	0.5520	995	0.5654	1175	0.0097
460	0.3045	640	0.4446	820	0.5543	1000	0.5551	1180	0.0083
465	0.3098	645	0.4477	825	0.5573	1005	0.5394	1185	0.0071
470	0.3152	650	0.4508	830	0.5602	1010	0.5238	1190	0.0060
475	0.3201	655	0.4540	835	0.5632	1015	0.5046		
480	0.3251	660	0.4573	840	0.5661	1020	0.4856		
485	0.3300	665	0.4611	845	0.5685	1025	0.4590		

Notes:

Cable connector extends below back of package; can cause poor thermal contact to package.
Cell discovered to be shorted on 961029.

TDB 9303



World Photovoltaic Scale Calibration Report TDC 9305

Date:	October 17, 1996
Calibration temperature:	25°C
Short-circuit current:	125.10 mA
I_{sc} standard deviation:	1.15 %
I_{sc} temperature coefficient:	488 ppm / °C
Area:	402 mm ²
Open-circuit voltage:	547 mV
Fill factor:	0.785
$dI/dV _{V=0}$:	-0.24 mS
Series resistance:	0.07 Ω
Shunt resistance:	110 kΩ
n_1 :	1.20
I_{o1} :	1.63×10 ⁻⁹ A
n_2 :	2.48
I_{o2} :	1.53×10 ⁻⁶ A

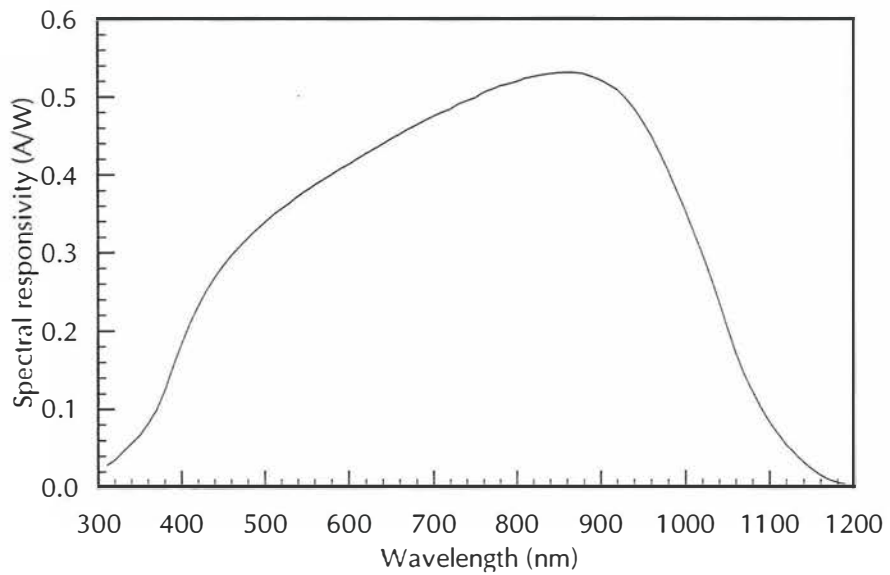
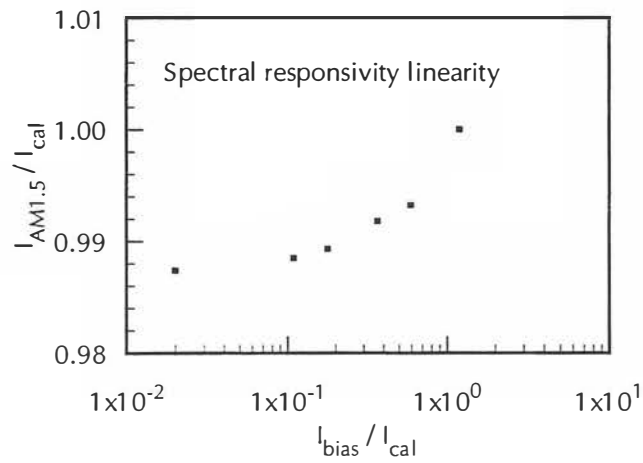
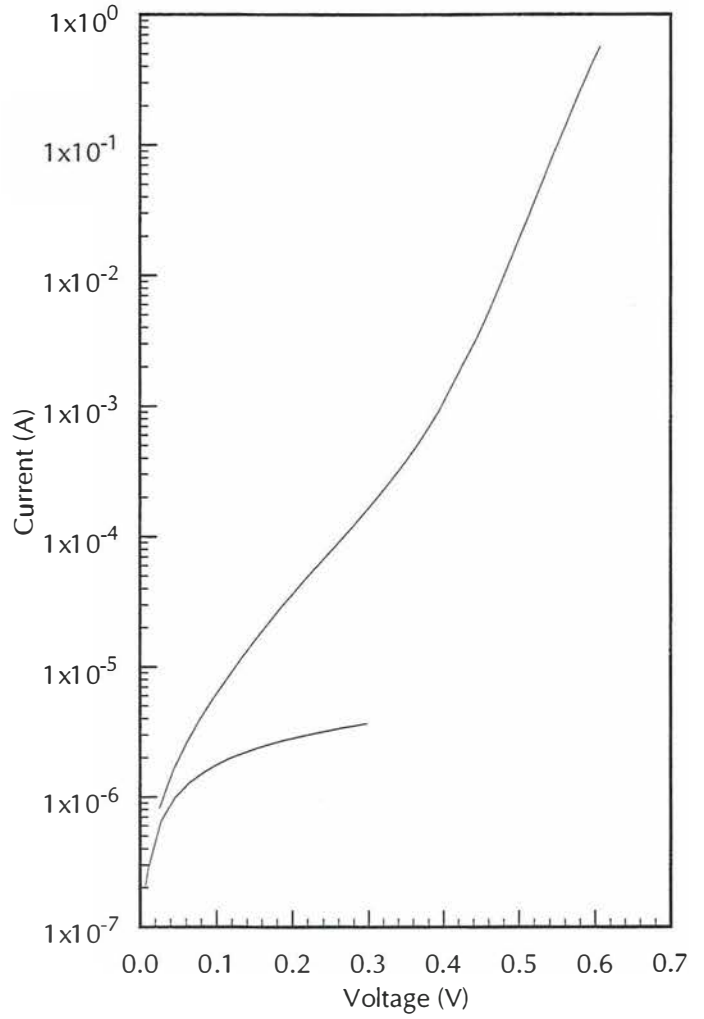
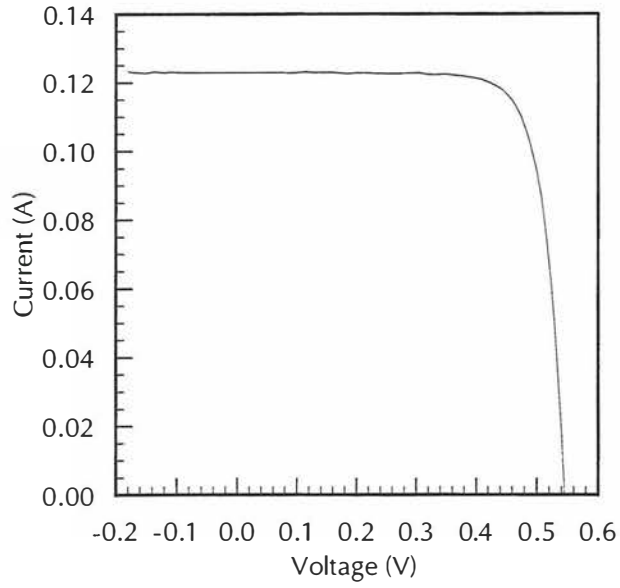
Spectral responsivity (nm, A/W):

310	0.0283	490	0.3293	670	0.4584	850	0.5307	1030	0.2689
315	0.0317	495	0.3341	675	0.4611	855	0.5309	1035	0.2532
320	0.0353	500	0.3390	680	0.4638	860	0.5312	1040	0.2375
325	0.0407	505	0.3436	685	0.4667	865	0.5311	1045	0.2207
330	0.0461	510	0.3483	690	0.4698	870	0.5309	1050	0.2039
335	0.0514	515	0.3524	695	0.4724	875	0.5303	1055	0.1878
340	0.0565	520	0.3565	700	0.4752	880	0.5296	1060	0.1717
345	0.0615	525	0.3602	705	0.4777	885	0.5276	1065	0.1585
350	0.0667	530	0.3637	710	0.4802	890	0.5258	1070	0.1451
355	0.0740	535	0.3681	715	0.4822	895	0.5238	1075	0.1339
360	0.0812	540	0.3723	720	0.4843	900	0.5218	1080	0.1227
365	0.0902	545	0.3760	725	0.4875	905	0.5188	1085	0.1127
370	0.0992	550	0.3797	730	0.4906	910	0.5157	1090	0.1025
375	0.1116	555	0.3833	735	0.4928	915	0.5126	1095	0.0932
380	0.1240	560	0.3868	740	0.4950	920	0.5093	1100	0.0840
385	0.1393	565	0.3903	745	0.4969	925	0.5039	1105	0.0766
390	0.1547	570	0.3936	750	0.4987	930	0.4984	1110	0.0692
395	0.1689	575	0.3969	755	0.5023	935	0.4921	1115	0.0619
400	0.1831	580	0.4002	760	0.5057	940	0.4856	1120	0.0548
405	0.1960	585	0.4036	765	0.5076	945	0.4772	1125	0.0489
410	0.2088	590	0.4069	770	0.5093	950	0.4687	1130	0.0431
415	0.2199	595	0.4102	775	0.5116	955	0.4597	1135	0.0378
420	0.2311	600	0.4134	780	0.5139	960	0.4506	1140	0.0324
425	0.2410	605	0.4167	785	0.5152	965	0.4397	1145	0.0279
430	0.2509	610	0.4201	790	0.5165	970	0.4286	1150	0.0234
435	0.2594	615	0.4237	795	0.5180	975	0.4169	1155	0.0195
440	0.2678	620	0.4271	800	0.5193	980	0.4053	1160	0.0157
445	0.2754	625	0.4303	805	0.5216	985	0.3926	1165	0.0129
450	0.2828	630	0.4333	810	0.5239	990	0.3800	1170	0.0102
455	0.2894	635	0.4365	815	0.5249	995	0.3672	1175	0.0083
460	0.2960	640	0.4398	820	0.5258	1000	0.3543	1180	0.0063
465	0.3018	645	0.4430	825	0.5268	1005	0.3406	1185	0.0055
470	0.3076	650	0.4461	830	0.5280	1010	0.3269	1190	0.0046
475	0.3133	655	0.4490	835	0.5288	1015	0.3129		
480	0.3188	660	0.4519	840	0.5297	1020	0.2987		
485	0.3241	665	0.4551	845	0.5301	1025	0.2838		

Notes:

Cable connector extends below back of package; can cause poor thermal contact to package.
Cover window cracked.

TDC 9305



World Photovoltaic Scale Calibration Report Y09

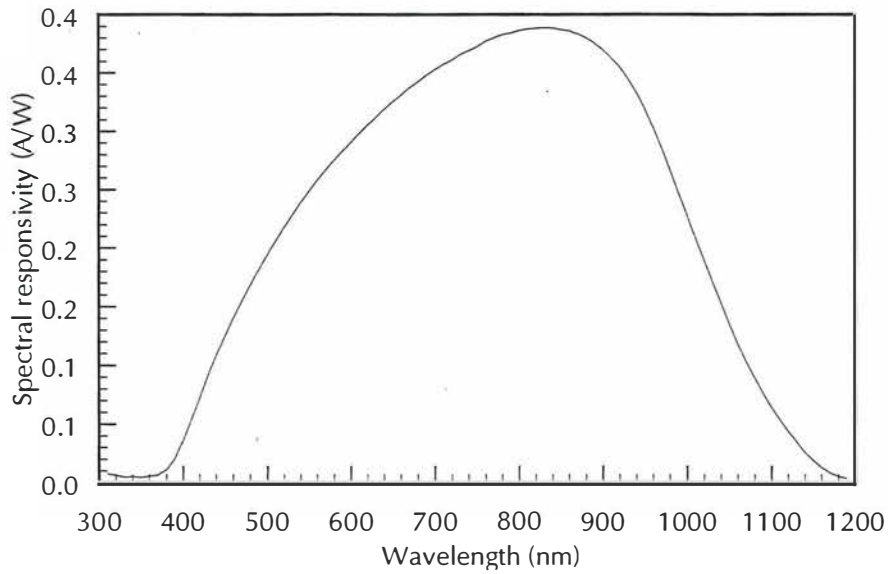
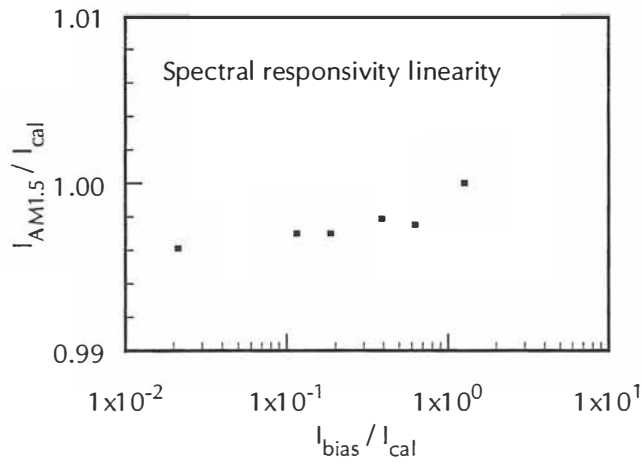
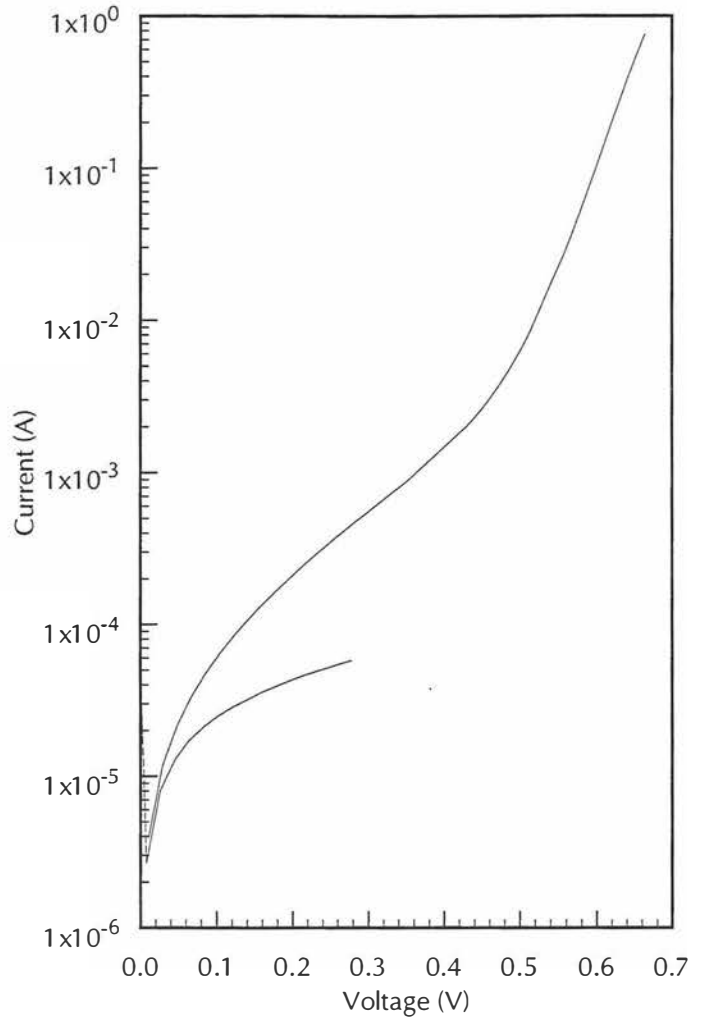
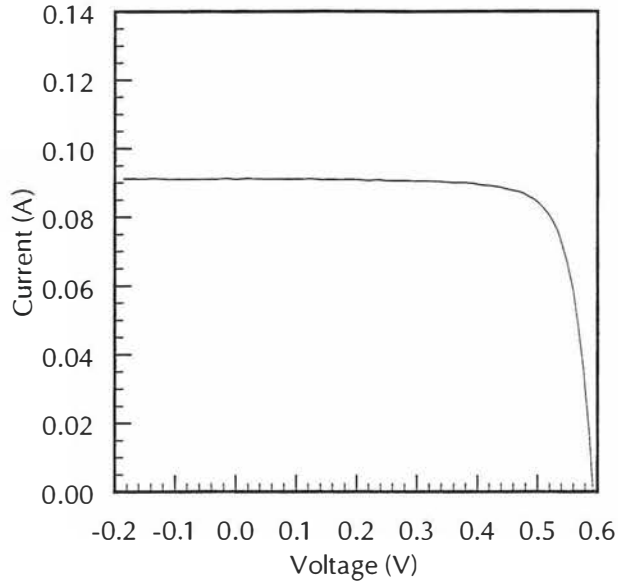
Date:	October 17, 1996
Calibration temperature:	25°C
Short-circuit current:	93.77 mA
I_{sc} standard deviation:	0.56 %
I_{sc} temperature coefficient:	571 ppm / °C
Area:	452 mm ²
Open-circuit voltage:	594 mV
Fill factor:	0.782
$dI/dV _{V=0}$:	0.0 mS
Series resistance:	0.08 Ω
Shunt resistance:	5.4 kΩ
n_1 :	1.28
I_{o1} :	1.25×10 ⁻⁹ A
n_2 :	4.01
I_{o2} :	3.02×10 ⁻⁵ A

Spectral responsivity (nm, A/W):

310	0.0078	490	0.1822	670	0.3371	850	0.3871	1030	0.1710
315	0.0071	495	0.1886	675	0.3397	855	0.3867	1035	0.1622
320	0.0064	500	0.1949	680	0.3422	860	0.3862	1040	0.1535
325	0.0056	505	0.2008	685	0.3450	865	0.3848	1045	0.1443
330	0.0049	510	0.2067	690	0.3478	870	0.3835	1050	0.1352
335	0.0051	515	0.2123	695	0.3502	875	0.3820	1055	0.1268
340	0.0053	520	0.2180	700	0.3527	880	0.3804	1060	0.1182
345	0.0049	525	0.2233	705	0.3551	885	0.3780	1065	0.1107
350	0.0046	530	0.2287	710	0.3574	890	0.3756	1070	0.1033
355	0.0050	535	0.2339	715	0.3592	895	0.3728	1075	0.0964
360	0.0054	540	0.2391	720	0.3610	900	0.3701	1080	0.0895
365	0.0061	545	0.2439	725	0.3633	905	0.3666	1085	0.0829
370	0.0066	550	0.2488	730	0.3657	910	0.3630	1090	0.0764
375	0.0088	555	0.2535	735	0.3674	915	0.3593	1095	0.0702
380	0.0110	560	0.2582	740	0.3691	920	0.3555	1100	0.0641
385	0.0158	565	0.2625	745	0.3708	925	0.3503	1105	0.0589
390	0.0207	570	0.2668	750	0.3725	930	0.3452	1110	0.0536
395	0.0283	575	0.2710	755	0.3749	935	0.3394	1115	0.0488
400	0.0359	580	0.2752	760	0.3773	940	0.3336	1120	0.0439
405	0.0448	585	0.2790	765	0.3786	945	0.3264	1125	0.0393
410	0.0536	590	0.2829	770	0.3800	950	0.3192	1130	0.0347
415	0.0628	595	0.2866	775	0.3814	955	0.3113	1135	0.0303
420	0.0719	600	0.2903	780	0.3828	960	0.3034	1140	0.0259
425	0.0816	605	0.2941	785	0.3835	965	0.2947	1145	0.0224
430	0.0913	610	0.2980	790	0.3842	970	0.2859	1150	0.0189
435	0.0999	615	0.3016	795	0.3853	975	0.2765	1155	0.0160
440	0.1084	620	0.3054	800	0.3864	980	0.2671	1160	0.0130
445	0.1164	625	0.3086	805	0.3871	985	0.2572	1165	0.0107
450	0.1243	630	0.3119	810	0.3878	990	0.2472	1170	0.0084
455	0.1323	635	0.3153	815	0.3880	995	0.2374	1175	0.0068
460	0.1401	640	0.3186	820	0.3883	1000	0.2276	1180	0.0052
465	0.1473	645	0.3217	825	0.3886	1005	0.2178	1185	0.0045
470	0.1545	650	0.3249	830	0.3889	1010	0.2080	1190	0.0037
475	0.1616	655	0.3278	835	0.3888	1015	0.1987		
480	0.1687	660	0.3308	840	0.3886	1020	0.1893		
485	0.1754	665	0.3340	845	0.3879	1025	0.1801		

Notes:

One contact to solar cell shorted to metal package.



World Photovoltaic Scale Calibration Report Y45

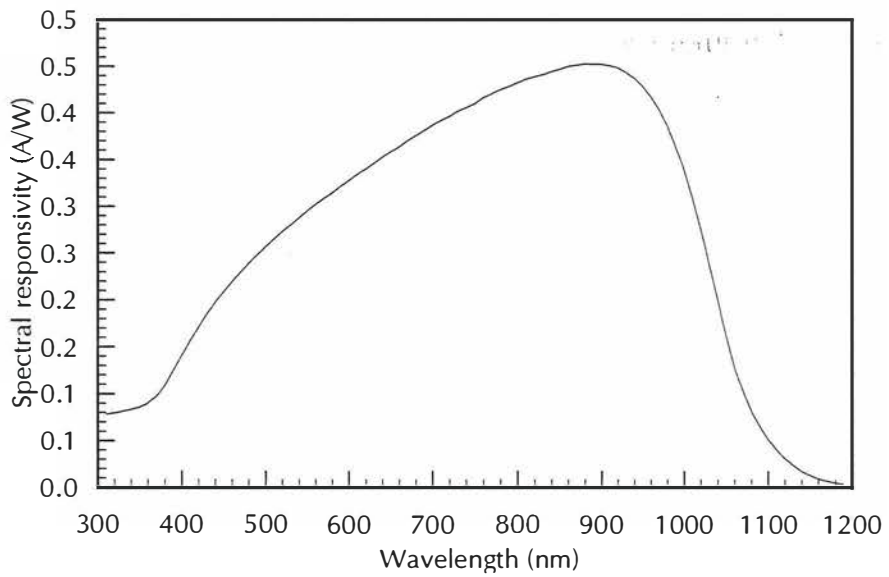
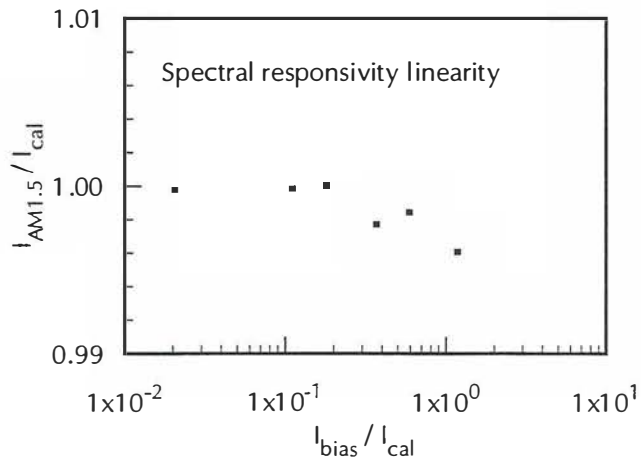
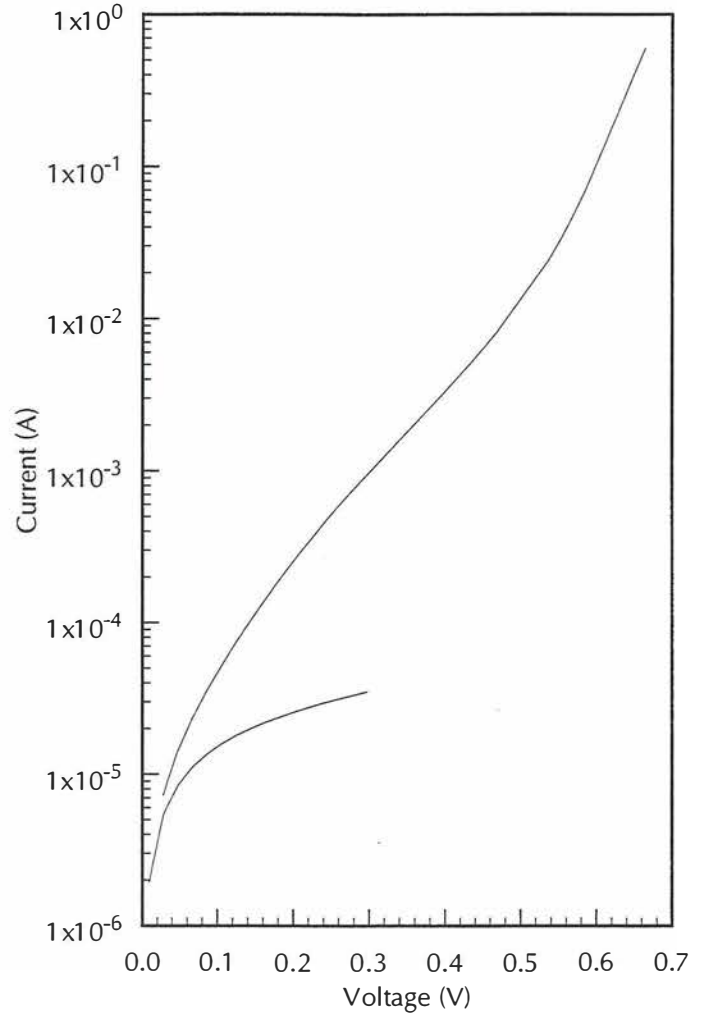
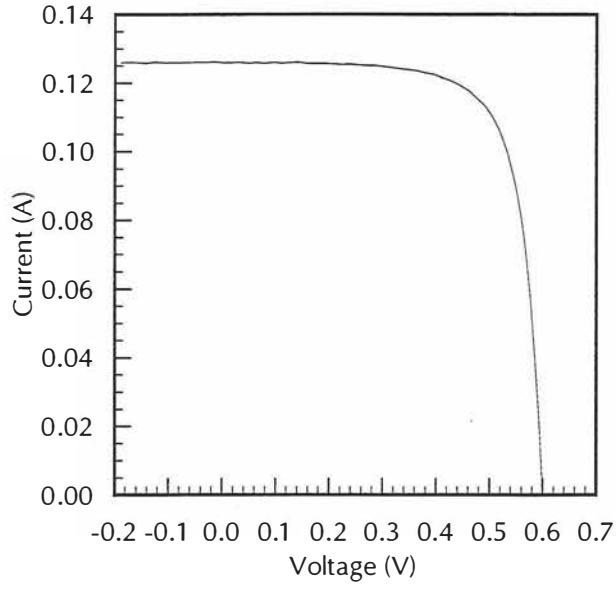
Date:	October 17, 1996
Calibration temperature:	25°C
Short-circuit current:	127.52 mA
I_{sc} standard deviation:	0.80 %
I_{sc} temperature coefficient:	626 ppm / °C
Area:	503 mm ²
Open-circuit voltage:	602 mV
Fill factor:	0.735
$dI/dV _{V=0}$:	-0.31 mS
Series resistance:	0.16 Ω
Shunt resistance:	10 kΩ
n_1 :	1.56
I_{o1} :	3.28×10 ⁻⁸ A
n_2 :	3.10
I_{o2} :	2.22×10 ⁻⁵ A

Spectral responsivity (nm, A/W):

310	0.0783	490	0.2483	670	0.3703	850	0.4472	1030	0.2379
315	0.0789	495	0.2526	675	0.3729	855	0.4487	1035	0.2189
320	0.0794	500	0.2570	680	0.3756	860	0.4502	1040	0.1999
325	0.0804	505	0.2611	685	0.3783	865	0.4509	1045	0.1812
330	0.0815	510	0.2652	690	0.3811	870	0.4515	1050	0.1624
335	0.0825	515	0.2693	695	0.3839	875	0.4523	1055	0.1452
340	0.0834	520	0.2733	700	0.3869	880	0.4529	1060	0.1280
345	0.0845	525	0.2768	705	0.3894	885	0.4528	1065	0.1157
350	0.0856	530	0.2803	710	0.3919	890	0.4528	1070	0.1035
355	0.0879	535	0.2841	715	0.3941	895	0.4526	1075	0.0928
360	0.0902	540	0.2879	720	0.3963	900	0.4525	1080	0.0822
365	0.0939	545	0.2916	725	0.3990	905	0.4517	1085	0.0742
370	0.0975	550	0.2955	730	0.4017	910	0.4510	1090	0.0661
375	0.1034	555	0.2988	735	0.4038	915	0.4499	1095	0.0589
380	0.1093	560	0.3022	740	0.4059	920	0.4488	1100	0.0516
385	0.1170	565	0.3055	745	0.4080	925	0.4462	1105	0.0464
390	0.1249	570	0.3088	750	0.4101	930	0.4436	1110	0.0410
395	0.1330	575	0.3118	755	0.4134	935	0.4406	1115	0.0362
400	0.1410	580	0.3149	760	0.4165	940	0.4378	1120	0.0313
405	0.1488	585	0.3183	765	0.4187	945	0.4333	1125	0.0278
410	0.1565	590	0.3216	770	0.4208	950	0.4288	1130	0.0242
415	0.1637	595	0.3247	775	0.4230	955	0.4235	1135	0.0209
420	0.1709	600	0.3277	780	0.4250	960	0.4180	1140	0.0178
425	0.1780	605	0.3311	785	0.4269	965	0.4110	1145	0.0157
430	0.1851	610	0.3345	790	0.4287	970	0.4038	1150	0.0135
435	0.1914	615	0.3374	795	0.4307	975	0.3951	1155	0.0119
440	0.1977	620	0.3403	800	0.4327	980	0.3865	1160	0.0101
445	0.2034	625	0.3433	805	0.4345	985	0.3752	1165	0.0088
450	0.2090	630	0.3464	810	0.4365	990	0.3638	1170	0.0075
455	0.2143	635	0.3497	815	0.4378	995	0.3515	1175	0.0065
460	0.2195	640	0.3529	820	0.4391	1000	0.3393	1180	0.0055
465	0.2246	645	0.3557	825	0.4403	1005	0.3240	1185	0.0049
470	0.2296	650	0.3584	830	0.4415	1010	0.3088	1190	0.0043
475	0.2344	655	0.3610	835	0.4431	1015	0.2921		
480	0.2392	660	0.3636	840	0.4449	1020	0.2754		
485	0.2438	665	0.3669	845	0.4460	1025	0.2566		

Notes:

One contact to solar cell shorted to metal package.



World Photovoltaic Scale Calibration Report Y124

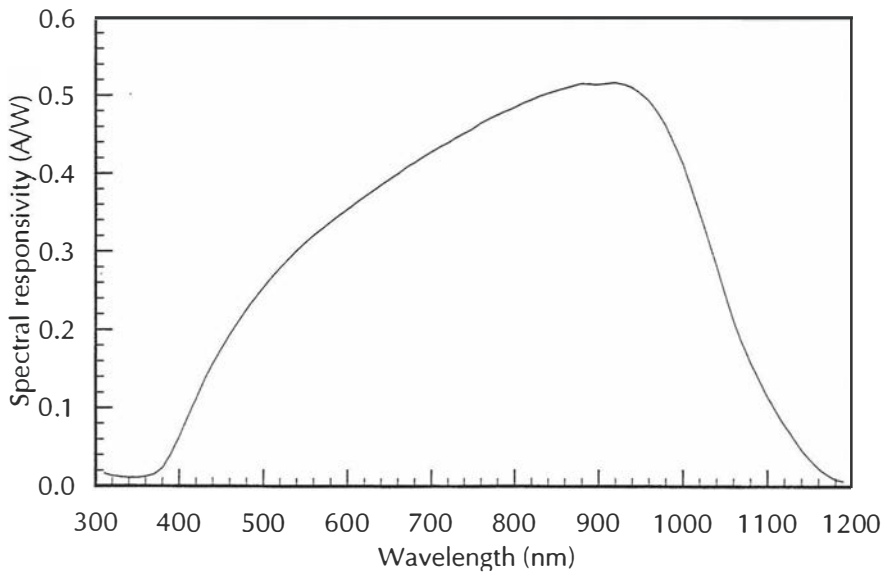
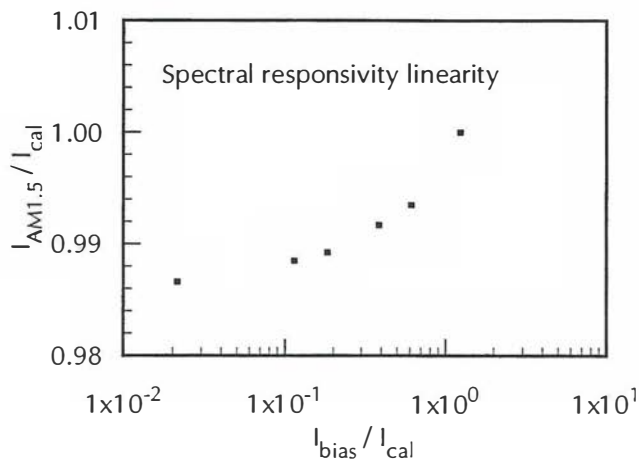
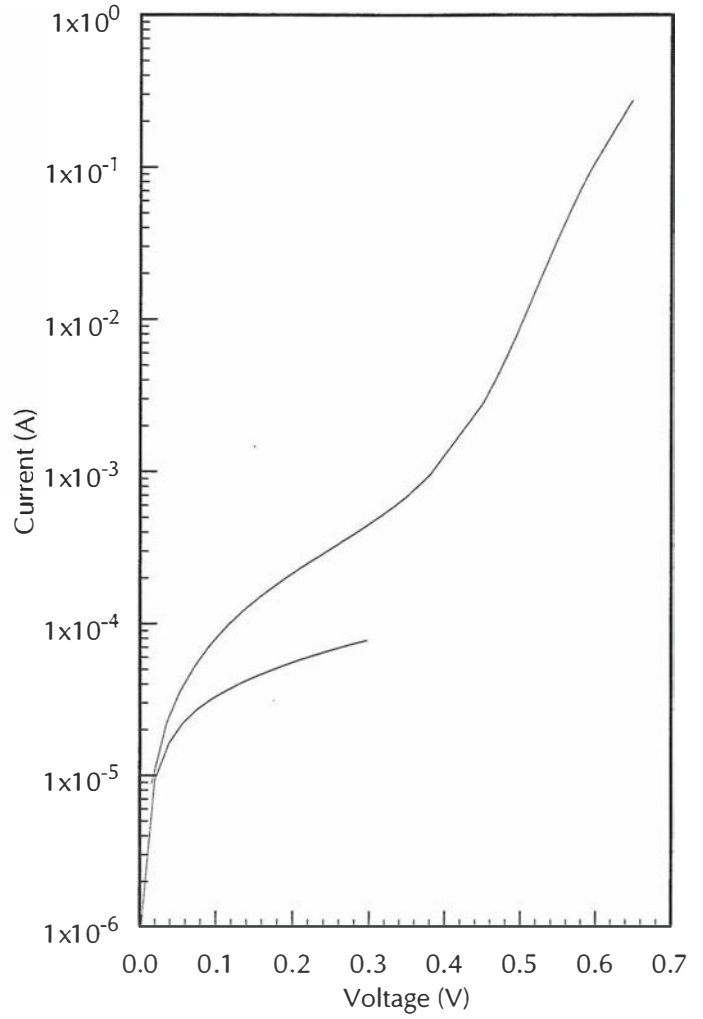
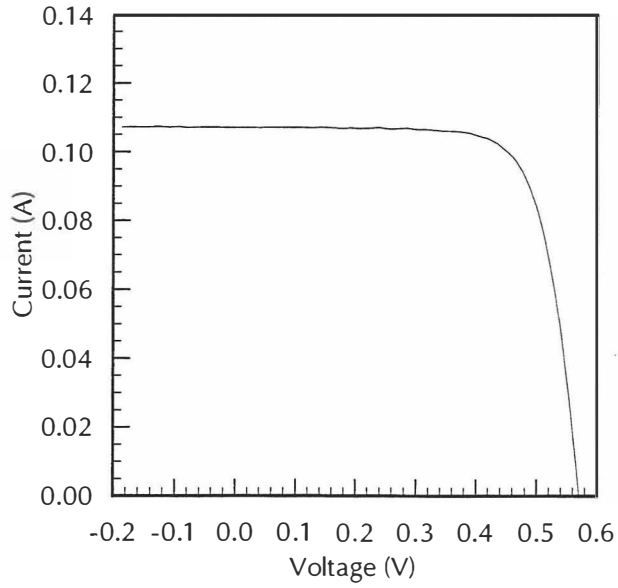
Date:	October 17, 1996
Calibration temperature:	25°C
Short-circuit current:	108.51 mA
I_{sc} standard deviation:	0.80 %
I_{sc} temperature coefficient:	412 ppm / °C
Area:	3.97 mm ²
Open-circuit voltage:	602 mV
Fill factor:	0.735
$dI/dV _{V=0}$:	-0.31 mS
Series resistance:	0.01 Ω
Shunt resistance:	4.4 kΩ
n_j :	1.50
I_{o1} :	2.22×10^{-8} A
n_2 :	5.03
I_{o2} :	4.52×10^{-5} A

Spectral responsivity (nm, A/W):

310	0.0166	490	0.2405	670	0.4077	850	0.5064	1030	0.3162
315	0.0149	495	0.2472	675	0.4110	855	0.5080	1035	0.2991
320	0.0133	500	0.2537	680	0.4142	860	0.5095	1040	0.2821
325	0.0127	505	0.2604	685	0.4176	865	0.5111	1045	0.2643
330	0.0121	510	0.2671	690	0.4209	870	0.5127	1050	0.2465
335	0.0118	515	0.2730	695	0.4243	875	0.5141	1055	0.2294
340	0.0114	520	0.2789	700	0.4277	880	0.5156	1060	0.2123
345	0.0113	525	0.2845	705	0.4307	885	0.5152	1065	0.1982
350	0.0110	530	0.2902	710	0.4339	890	0.5150	1070	0.1840
355	0.0118	535	0.2957	715	0.4367	895	0.5145	1075	0.1717
360	0.0124	540	0.3010	720	0.4393	900	0.5141	1080	0.1592
365	0.0138	545	0.3061	725	0.4427	905	0.5150	1085	0.1479
370	0.0154	550	0.3112	730	0.4460	910	0.5157	1090	0.1366
375	0.0193	555	0.3159	735	0.4488	915	0.5163	1095	0.1258
380	0.0233	560	0.3208	740	0.4516	920	0.5169	1100	0.1150
385	0.0319	565	0.3250	745	0.4545	925	0.5157	1105	0.1056
390	0.0404	570	0.3294	750	0.4574	930	0.5146	1110	0.0963
395	0.0515	575	0.3336	755	0.4610	935	0.5127	1115	0.0874
400	0.0626	580	0.3380	760	0.4647	940	0.5106	1120	0.0786
405	0.0750	585	0.3421	765	0.4675	945	0.5067	1125	0.0706
410	0.0875	590	0.3462	770	0.4701	950	0.5029	1130	0.0626
415	0.0994	595	0.3501	775	0.4727	955	0.4984	1135	0.0548
420	0.1112	600	0.3541	780	0.4752	960	0.4938	1140	0.0469
425	0.1234	605	0.3580	785	0.4775	965	0.4866	1145	0.0406
430	0.1357	610	0.3620	790	0.4799	970	0.4795	1150	0.0344
435	0.1461	615	0.3662	795	0.4823	975	0.4706	1155	0.0289
440	0.1565	620	0.3705	800	0.4844	980	0.4618	1160	0.0233
445	0.1660	625	0.3741	805	0.4873	985	0.4501	1165	0.0193
450	0.1754	630	0.3778	810	0.4903	990	0.4385	1170	0.0153
455	0.1846	635	0.3816	815	0.4924	995	0.4258	1175	0.0122
460	0.1938	640	0.3856	820	0.4945	1000	0.4130	1180	0.0092
465	0.2020	645	0.3891	825	0.4969	1005	0.3976	1185	0.0080
470	0.2102	650	0.3928	830	0.4993	1010	0.3824	1190	0.0068
475	0.2180	655	0.3963	835	0.5013	1015	0.3664		
480	0.2257	660	0.3997	840	0.5032	1020	0.3502		
485	0.2331	665	0.4037	845	0.5048	1025	0.3333		

Notes:

Package has internal light reflections; I_{sc} is lower if only the solar cell is illuminated.
One contact to solar cell shorted to metal package.



Appendix 4 Minutes of the PEP'93 Participants Meetings

A4.1 Minutes of the First Participants Meeting, October 1992

**PEP '93 Intercomparison
First Participants' Meeting Minutes
Montreux 12-15 October 1992**

Attendees:

Osterwald	NREL
Ossenbrink	ESTI
Nagamine	JMI
Shimokawa	ETL
Kazmerski	NREL
Metzdorf	PTB
Heidler	ISE
Imamura	WIP (guest)

Agenda:

1. Objectives
2. Participants
3. Sample Set
4. Calibration and Measurement Methods
5. Data Reporting
6. Schedule
7. Customs
8. Expected Results

1. Objectives

1. Establishment of World PV Scale (WPVS) through comparison of reference cells traceable to national metrology programs. Each participant will supply at least one silicon reference cell that will be calibrated by all participants and returned to the providing laboratory. The qualified average calibration value of these cells will constitute the WPVS.
2. Identification of problems with emerging technology and proposals/recommendations for suitable measurement procedures to be considered by standardization organizations.
3. Recommendations of how to qualify calibration data in publications.

2. Participants

1. Organizations that have already agreed to participate:
PTB, Germany
ISE, Germany
LCIE, France
RAE, UK
JMI/ETL, Japan
SNL, USA
NREL, USA
ESTI, CEC
VNIIOFI, Russia (will be contacted by PTB)
ENEA, Italy
2. Suggestions made for additional participants:
India (will be contacted by NREL)
China (NIM will be contacted by PTB)
ETSI, Spain (will be contacted by ESTI)

3. Sample Set

The sample set will be in two groups:

1. Approximately 15 packaged mono-crystalline silicon 2x2 cm reference cells meeting IEC 904-2 single cell package description that will constitute the WPVS.
2. Two cells from each of the following categories:
 - Concentrator with fixed optics
 - a-Si bi-cell
 - GaAs
 - high-pass (wavelength) filtered Si
 - low-pass (wavelength) filtered Si
 - CuInSe₂
 - 10x10 cm encapsulated Si
 - ESTI sensor
 - Two-terminal series-connected tandem
 - 10x10 cm bare Si
3. Sample sets 1 and 2 will be circulated separately.

4. Calibration and Measurement Methods

1. Participants will use their best method(s) that are traceable to national standards to calibrate the WPVS cells. For the newer technology devices as described in 3.2, the participants are free to use whatever techniques are available to obtain the efficiency values.

5. Data Reporting

1. All data must be submitted in electronic format to the organizing agent (NREL). All measurements must be with respect to SRC. Calibration data must be submitted to NREL within one month after completion of calibration.
2. WPVS — I_{sc} , temperature coefficient of I_{sc} if measured, U_{95} , relative spectral response, description of calibration method(s).
3. Newer technologies — I-V parameters, efficiency, area, description of measurement method(s), how area was measured.

6. Schedule

- 31 Dec 1992 — Deadline for response to questionnaire concerning agreement to participate, contribution of samples, and other technical details
- 31 Jan 1993 — Call for samples issued to all participants
- 31 Mar 1993 — Deadline for response to 2nd questionnaire concerning final technical details and schedule preferences
- 9-14 May 1993 Second Participants' Meeting during IEEE PVSC, Louisville KY USA
- 31 May 1993 — Deadline for submittal of samples to NREL
- 30 Jun 1993 — Pre-calibration check of all samples at NREL completed
- 1 Jul - 31 Aug 1993 Sample sets shipped to and calibrated by first two participants, followed by two months at each additional participant, including shipping time
- n End of calibrations
- n+1 month Post-calibration check of all samples at NREL completed
- n+3 months — Compilation by organizing agent (without analysis) completed, and sent to all participants
- n+5 months — Deadline for receipt of comments on analysis of results
- n+8~10 months Draft of final report sent to participants
- To be determined Third Participants' Meeting held during convenient PV conference
- Probable date for publication of final report — 1996

7. Customs

1. Organizing agent will become nominal owner of samples during intercomparison for customs purposes. Each participant should make sure the organizing agent can receive and return samples without customs problems. This can be done, for example, with a pro forma invoice and declaration "test materials, to be returned after test."

8. Expected Results

1. (see objectives)
2. Publication of final results

Montreux, 15 Oct 1992

C.R. Osterwald

A4.2 Minutes of the Second Participants Meeting, May 1993

**PEP '93 Intercomparison
Second Participants Meeting Minutes
Louisville 12 May 1993**

Attendees:

Osterwald	NREL
Ossenbrink	ESTI
Nagamine	JMI
Prince	US DOE
Kazmerski	NREL
Emery	NREL
Heidler	ISE
Zaaiman	ESTI
Bishop	ESTI
Claverie	LCIE
Chen	TIPS
King	SNL
Hansen	SNL

Agenda:

1. Schedules
2. Participants
3. Sample Set
4. Data Reporting
5. Next Meeting

1. Schedules

1. JMI announced that their assigned time slot for the Newer Technology Series is not acceptable. Following discussions with ISE, JMI, and NREL, JMI and NREL will trade time slots. The final schedule is attached to these minutes.

2. Participants

1. Organizations that have agreed to participate:
 - PTB, Germany
 - ISE, Germany
 - LCIE, France
 - JMI/ETL, Japan
 - SNL, USA
 - NREL, USA
 - ESTI, CEC
 - VNIIOFI, Russia
 - IACS, India
 - USPL, India
 - NIM, China
 - TIPS, China

3. Sample Set

1. Deadline for receipt of samples at NREL is 31 May, 1993. Organizations that have submitted samples (as of 12 May 1993):
 - NIM, China
 - TIPS, China
 - IACS, India

ESTI, CEC
JMI/ETL, Japan

2. The participants discussed the concentrator samples for the Newer Technology Series at length. The discussion focused on whether the samples should be modules with fixed optics, or concentrator cells (in this case the participants would measure efficiency vs. concentration ratio). It was decided to have modules with fixed optics. Reporting of data was also discussed, and it was determined that the participants should measure direct and total plane-of-array irradiance, and data should be corrected to SRC. Sandia agreed to supply correction coefficients for this purpose.

4. Data Reporting

The data reporting requirements were amended as follows (changes underlined):

1. All data must be submitted in electronic format in ASCII text to the organizing agent (NREL). A minimum of 4 digits should reported for the numerical data. All measurements must be with respect to SRC. Calibration data must be submitted to NREL within one month (plus 1 week shipping) after completion of calibration by individual laboratories.
2. WPVS — I_{sc} , temperature coefficient of I_{sc} if measured, U_{95} , relative spectral response (in units of nm for wavelength and A/W for responsivity), description of calibration method(s).
3. Newer technologies — I-V parameters, efficiency, area, description of measurement method(s), how area was measured.

5. Next Meeting

1. The Third Participants Meeting has been scheduled for December 1994 during the joint IEEE PVSC – PVSEC conference in Hawaii. Results from the first round of the Newer Technology Series will be discussed.

Louisville, 12 May 1993
C.R. Osterwald

A4.3 Minutes of the Third Participants Meeting, December 1994

Minutes of the 3rd Participant's Meeting, December 8, 1994, Waikoloa, Hawaii:

Agenda:

- Introductions
- Status of PEP'93
- Presentation of results from 1st round, NT Series samples
- Open discussion
- Next meeting

The meeting was opened at 2 pm by the Coordinator. The attendees were:

A. Barua: IACS
Abe, M. Suzuki: JQA/ETL
P. Basore: SNL
K. Bücher: ISE
W. Zaiman: ESTI
C. Osterwald, H. Field, K. Emery: NREL
A. Claverie: LCIE

The current known status and the remaining schedule of the intercomparison is attached. The Coordinator stated that at the present time, the exact locations of both sample sets is unknown because participating laboratories have not been informing him of shipping and arrival dates. K. Bücher stated that the NT Series samples were shipped from PTB on Nov. 27, 1994, and the WPVS samples were shipped to NIM from ISE in July 1994. (note—WPVS data from NIM were delivered to NREL on Feb. 21, 1995).

The Coordinator presented an overview of the results from the 1st round of the NT Series samples. This overview consisted of data from the following organizations: ISE, ESTI, SNL, JQA, LCIE, and NREL. Overall, the efficiency data showed about $\pm 5\%$ variation among the six laboratories with some samples showing much higher variations (greater than $\pm 10\%$). The DT1 and DT2 a-Si tandem cells apparently have degraded. It was decided at the meeting that the data from the 1st round participants should not be circulated among the remaining laboratories to avoid "coloring" the results. Several suggestions were concerning the analysis and display of the data; these will be incorporated into the final report. Overall, the attendees felt the agreement between laboratories for NT Series was "disappointing."

During the open discussion, it was recommended that the final report should contain a strong statement of the importance of the international round-robin efforts along with a recommendation for continuing the work in the future. Two questions that need to be answered in the final report were how laboratories measured the ESTI sensors and how cell areas were determined.

The next participants' meeting was set for March 4-8, 1996 at NREL in Golden, Colorado, USA. The objective of this meeting will be to discuss the results from both sample sets prior to the publication of the final report, which will be prepared by NREL (the organizing agent). A paper containing the results will be submitted for presentation at the 24th IEEE Photovoltaic Specialists Conference in May, 1996 (to be held near Washington, DC, USA). The authors of both the final report and the PVSC publication will be the persons identified by the participating laboratories as the primary contacts.

Respectfully submitted,

Carl Osterwald
Coordinator, PEP '93 Intercomparison

A4.4 Minutes of the Final Participants Meeting, March 1996

**PEP'93 Intercomparison
Final Participants' Meeting Minutes
Golden, Colorado 4-8 March 1996**

Attendees:

C. Osterwald	NREL (coordinator)
F. Nagamine	JQA
W. Zaaïman	ESTI
J. Dubard	LCIE
B. Hansen	SNL
K. Emery	NREL
L. Kazmerski	NREL (guest)
H. Field	NREL (guest)

Agenda:

- Introductions and opening
- Status of PEP'93
- Presentation of results from NT series
- Discussion of NT series results
- Presentation of results from WPVS
- Discussion of WPVS results
- Content of 25th IEEE PVSC poster paper
- Recommendations and final report
- Tour of NREL facilities

The Final Participants meeting was opened at 8:30 am, 4 March, by the Coordinator. The work of the NREL conferences group, which coordinated the amenities for the meeting and was led by J. Harty, was acknowledged and appreciated. Following introductions of all persons present, the Coordinator detailed the status of the PEP'93 Intercomparison. The Photovoltaic Energy Project, comprised of representatives from the seven PEP member nations, has disbanded officially, leaving the Expert Group of the PEP'93 Intercomparison operating alone. Thus, the results of this meeting and of the intercomparison will not be reported to the former PEP Coordination Committee.

The circulation history as of 1 March 1996 was reported. Delays in circulation were encountered in Russia and in India and the samples have not yet returned to NREL for the final post-circulation inspections and measurements. Thus, samples owned by participating laboratories could not be returned during the meeting as originally planned. Also, the actual condition of the samples is not known, beyond the information in the measurements reports that have been received by NREL. A copy of the circulation history of both sample sets is attached. Because of infrastructure problems within Russia, it was necessary for F. Nagamine to travel to VNIIOFI and carry the WPVS samples to Japan. Export/customs problems in India prevented shipment of the WPVS samples to ISE in Germany for an extended period of time. Thus, ISE has not had the opportunity to calibrate the WPVS reference cells yet. At the meeting, it was decided to not forward any of the data presented at this meeting to ISE in order to not compromise ISE's blindness for the intercomparison. The NT series samples remained at USPL for over one year, and the coordinator reported extreme difficulties communicating with this laboratory. Because of these factors, and the lateness of the intercomparison, the coordinator decided in September 1995 to exclude USPL from the WPVS. NIM and VNIIOFI both decided to exclude themselves from the NT series intercomparison.

The coordinator then detailed the procedures that were used to perform the initial analysis of the intercomparison data. Bar charts of reported data normalized by cell averages were generated, followed by an area normalization of the reported spectral response data which permitted a graphical display of laboratories' deviation from the average normalized spectral responsivity. This procedure was identical to the procedure reported at the 2nd Participants' meeting in Hawaii. A single numeric result for each spectral response curve was produced from an artificial reference spectral mismatch calculation. Scatter diagrams of the results from each laboratory were generated by taking every combination of the cell average-normalized data two at a time as X and Y data points. These plots provided a visual indication of the repeatability of each laboratories data along with clues to possible outliers.

Following a tour of the NREL PV research facilities, W. Zaaiman of ESTI presented a short position paper concerning the WPVS. This statement is attached.

Results from the NT series were then presented by the coordinator. Measurement methods used by the participating laboratories were outlined by each attendee, and the coordinator repeated the methods used by laboratories not present from the information submitted to NREL. The results will not be attached these minutes because the measurement data from IACS has not yet arrived at NREL.

During the subsequent discussion, it was noted that most laboratories did not use the ESTI sensors properly, which have two cells side-by-side. One cell is intended to operate at V_{oc} as a temperature sensor, and the other has an integral 20 m Ω shunt for use as an irradiance monitor. Most labs simply performed an I-V curve of the V_{oc} cell, which produced a poor fill-factor because of the length of the leads. Some labs did not attempt to measure the large area devices at 25°C, which resulted in many differences.

The data reported by ESTI were not corrected for spectral mismatch, thus these errors are present in the data presented at the meeting. ESTI was allowed resubmit their data corrected for spectral mismatch because this data was reported originally (but not used). Several laboratories reported two or more measurements of each sample (using different measurement systems) which were shown independently. It was decided to restrict the final results to a single measurement from each laboratory.

Only SNL, JQA/ETL, and NREL attempted true multijunction measurements of the a-Si series tandem devices, so these showed the highest deviations of any type of device. ESTI withdrew their data of the a-Si tandems after learning that their measurement system is not suitable for these types of devices. The experts agreed, and the experts also agreed to drop the DT 1 and DT 2 samples from further consideration because of apparent problems with intermittent contacts in these cells. Other potential degradation problems were noted, including the fill factor of the CuInGaSe cells and the appearance of bubbles in the encapsulation of the high- and low-pass filtered Si cells. Light soaking time also probably caused differences seen in both the CdTe and the CuInGaSe devices.

The GaAs concentrator module had differences caused by how laboratories treated the two cells that were part of the module. SNL measured the spectral response with the lens removed, which caused differences in the blue response. SNL measured the module as a whole with the two cells in series; all other labs each cell separately.

The spectral response deviation plots showed differences caused by bandwidths of spectral measurements for the direct bandgap devices. Reference spectral mismatch calculations showed that differences observed in I_{sc} are not caused by the spectral measurements. The

expert therefore concluded that I_{sc} differences are caused by total irradiance measurements. It is hoped that the WPVS will help reduce these errors.

Discussion of the NT series was concluded by agreeing to the content of the PVSC paper and the final report. Potential problem areas with newer technology devices were listed, and the question of what is the one right way to measure a cell was discussed, but a final answer could not be provided. Several recommendations for suitable measurement procedures to be considered by standardization organizations as follows:

- Use multijunction procedures for series tandem devices
- Don't use probe contacts to large area cells
- Temperature coefficients are important, but difficult to measure
- Every laboratory has different problems
- Extra care is needed when testing thin-film PV devices in flash simulators

An identical procedure was used to introduce the results of the WPVS calibrations, the initial data analysis, and the methods employed by the participants. Following a detailed examination of the available data, a procedure for determining the final qualified calibrated short-circuit currents was developed and agreed to by the participants. It was agreed that only primary calibration methods would be used to determine the final average calibrations. Therefore data from SNL, ESTI, and IACS will not be included. After removing these data, the normalized calibration data will be filtered by excluding any laboratories with 50% or more of data points that are outside of $\pm 2\%$ of the overall average. With these additional laboratories excluded, the normalized calibration data will be recalculated and any individual data points outside of $\pm 2\%$ of the overall average will be removed and the final calibrated short-circuit currents produced by averaging the remaining data. A qualified average spectral response table, scaled to equal the calibrated current, will be generated for each cell. All temperature coefficient data for each cell will also be averaged to obtain a WPVS temperature coefficient.

During the discussions the physical condition of several cells came into question. Bubbles in the encapsulation of RS-58, RS-67, RS-68, and RS-69 during the circulation, and the window of RS-69 was replaced after calibration by four laboratories. Cracks in the windows of RS-68 and TDC 9305 were also reported. Linearity of the cells was questioned because LCIE calibrated from absolute spectral response with low light bias. NREL volunteered to perform laser spot scans of the cells after they return, and it is hoped that PTB can provide spectral responsivity linearity data.

Temperature coefficient measurements were discussed at length, and recommendations were made for future calibrations, as follows:

- Light source should be class A Xenon solar simulator
- 1000 W/m²
- Temperature range should not exceed 10 to 50°C
- Cell should be in thermal equilibrium
- Always use internal sensor for temperature measurements
- Data at each temperature should be corrected for spectral mismatch using spectral response data for that temperature
- Data normalized to 25°C and reported as ppm/°C
- Perform linear regression of I_{sc} versus T data
- Report correlation coefficient and sample standard deviation from regression

The subject of how future WPVS calibrations should be done was a major topic of discussion, including allowances for new cells to become part of the WPVS group. All participants

agreed that recirculation of the WPVS cells should not be used because of the possibility of loss of all cells at once and because of the long periods of time needed for circulation, during which the cells cannot be used as reference cells. A proposal was developed during the meeting as follows:

- Laboratories traceable to WPVS will have exactly two WPVS cells
- Future calibrations would be done at a single laboratory every 1.5 – 2 years
- Calibration laboratory would be one whose data was part of the final average
- Traceable laboratories will perform best calibration on both WPVS cells
- One of two cells (alternating) will be hand-carried to calibration laboratory
- Calibration performed by host laboratory
- Representatives not required to be present during entire calibration
- Following calibration, a laboratory meeting will determine new WPVS
- Laboratories that do not provide calibration data and cell will no longer be considered traceable to WPVS
- A qualified running average will be used to maintain calibration values
- If possible, WPVS cells returned to owning laboratories by hand

Because of the wide variety of different reference cell designs currently in the WPVS, a significant amount of time was spent considering requirements for new cells to be allowed into the WPVS, along with how this can be accomplished. The diverse cells design causes problems during calibrations because of the large amount of time required to handle each cell differently. A physical design for new WPVS cells and an acceptance test that new cells must pass before any calibrations are done were developed, the details of which are attached to these minutes. Participants that were not able to attend the meeting are encouraged to send any comments or corrections to the coordinator prior to inclusion in the final report.

To be included in the WPVS, new cells would have to be calibrated by at least three of the laboratories whose data was included in the final WPVS, after which the new cells could be taken to the next available calibration event. The calibration value of the new cells and their acceptance into the WPVS group would be determined at the post calibration meeting.

The meeting was concluded by a discussion of the content of the WPVS portion of the PVSC paper and the final report. The coordinator thanked all the participants for their attendance and their hard work during the week. Minutes were produced during the final day of the meeting following the conclusion.

Golden, Colorado, 8 March 1996
C.R. Osterwald

Appendix 5 Acronyms, abbreviations, and symbols

A	Area
ASTM	American Society for Testing and Materials
B	Bias index
BIPM	International Bureau of Weights and Measures
CD-ROM	Compact Disc–Read-only memory
CIE	Commision Internationale de l’Eclairage
DSR	Differential spectral responsivity
E	Irradiance
E_{λ}	Spectral irradiance
ESTI	European Solar Test Installation
ETL	Electrotechnical Laboratory
EVA	Ethelene vinyl acetate
F	Normalization factor
FF	Fill factor
FWHM	Full width at half maximum
FZ	Float zone
IACS	Indian Association of the Cultivation of Science
IEC	International Electrotechnical Commission
IEEE	Institute for Electrical and Electronic Engineers
	Sampled quantity (only as a subscript)
I	Current
I_o	Dark saturation current
I_{mp}	Current at maximum power point
I_{sc}	Short-circuit current
ISE	Fraunhofer-Institut für Solare Energiesysteme
I-V	Current-voltage
JMI	Japan Machinery and Metals Inspection Institute (now called JQA)
JQA	Japan Quality Assurance Organization
LCIE	Laboratoire Central des Industries Electriques
LED	Light emitting diode
m	Slope of dark I-V curve fit
n	Diode quality factor or total number of points
NIM	National Institute of Metrology
NIST	National Institute for Standards and Technology
NMI	National Metrology Institute of Australia
NREL	National Renewable Energy Laboratory
NT	Newer Technology
P	Precision index
PEP	Photovoltaic Energy Project
	Power at maximum power point

PTB	Physikalisch-Technische Bundesanstalt
PV	Photovoltaic
PVSC	Photovoltaic Specialists Conference
R_{λ}	Spectral responsivity
R_s	Series resistance
R_{sh}	Shunt resistance
RTD	Resistance temperature detector
s	Responsivity (short-circuit current to total irradiance ratio)
s_{λ}	Sampled spectral responsivity
SI	Système International
SNL	Sandia National Laboratories
SR	Spectral responsivity
SRC	Standard reporting conditions
STC	Standard test conditions
T	Temperature
t_{95}	Student's t value for 95% confidence
TC-82	Technical Committee 82 of the International Electrotechnical Commission, for photovoltaic standards
TIPS	Tianjin Institute of Power Sources
U_{95}	Total uncertainty limit
USPL	Udhaya Semiconductors (P) Ltd.
VNIIOFI	All-Union Research Institute for Optophysical Measurements
V	Voltage
V_{mp}	Voltage at maximum power point
V_{oc}	Open-circuit voltage
WPVS	World Photovoltaic Scale
WRR	World Radiometric Reference
X-V	Cartesian coordinates
α	Temperature coefficient of short-circuit current
β	Temperature coefficient of open-circuit voltage
Δ_{λ}	Deviation from average spectral responsivity
λ	Wavelength

REPORT DOCUMENTATION PAGE

Form Approved
OMB NO. 0704-0188

Public reporting burden for this collection of information is estimated to average 1 hour per response, including the time for reviewing instructions, searching existing data sources, gathering and maintaining the data needed, and completing and reviewing the collection of information. Send comments regarding this burden estimate or any other aspect of this collection of information, including suggestions for reducing this burden, to Washington Headquarters Services, Directorate for Information Operations and Reports, 1215 Jefferson Davis Highway, Suite 1204, Arlington, VA 22202-4302, and to the Office of Management and Budget, Paperwork Reduction Project (0704-0188), Washington, DC 20503.

1. AGENCY USE ONLY (Leave blank)		2. REPORT DATE March 1998	3. REPORT TYPE AND DATES COVERED Technical Report	
4. TITLE AND SUBTITLE The Results of the PEP'93 Intercomparison of Reference Cell Calibrations and Newer Technology Performance Measurements: Final Report			5. FUNDING NUMBERS C: TA: PV706101	
6. AUTHOR(S) C.R. Osterwald, S. Anevsky, A.K. Barua, K. Bücher, P. Chauduri, J. Dubard, K. Emery, D. King, B. Hansen, J. Metzdorf, F. Nagamine, R. Shimokawa, Y.X.Wang, T. Wittchen, W. Zaيمان, A. Zastrow and J. Zhang				
7. PERFORMING ORGANIZATION NAME(S) AND ADDRESS(ES) National Renewable Energy Laboratory, Golden, Colorado; All-Union Research Institute for Optophysical Measurements, Moscow, Russia; Indian Association for the Cultivation of Science, Calcutta, India; Laboratoire Central des Industries Electriques, Fontenay-aux-Roses, France; Sandia National Laboratories, Albuquerque, New Mexico; Japan Quality Assurance Organization, Tokyo, Japan; Electrotechnical Laboratory, Ibaraki, Japan; Tianjin Institute of Power Sources, Tianjin, China; Physikalisch-Technische Bundesanstalt, Braunschweig, Germany; European Solar Test Installation, Ispra, Italy; Fraunhofer-Institut für Solare Energiesysteme, Freiburg, Germany; and National Institute of Metrology, Beijing, China			8. PERFORMING ORGANIZATION REPORT NUMBER	
9. SPONSORING/MONITORING AGENCY NAME(S) AND ADDRESS(ES) National Renewable Energy Laboratory 1617 Cole Blvd. Golden, CO 80401-3393			10. SPONSORING/MONITORING AGENCY REPORT NUMBER TP-520-23477	
11. SUPPLEMENTARY NOTES NREL Technical Monitor: NA				
12a. DISTRIBUTION/AVAILABILITY STATEMENT			12b. DISTRIBUTION CODE UC-1250	
13. ABSTRACT (Maximum 200 words) This report presents the results of an international intercomparison of photovoltaic (PV) performance measurements and calibrations that took place from 1993 to 1997. The intercomparison, which was organized and operated by a group of representatives from national PV measurements laboratories, was accomplished by circulating two sample sets. One set, consisting of 20 silicon reference cells, was intended to form the basis of an international PV reference scale. A qualification procedure applied to the calibration results gave average calibration numbers with an overall standard deviation of less than 2% for the entire set. The second sample set was assembled from a wide range of newer technologies that present unique problems for PV measurements. As might be expected, these results showed much greater differences among the laboratories. Methods were then identified that should be used to measure such devices, along with problems to avoid. The report concludes with recommendations for future intercomparisons.				
14. SUBJECT TERMS photovoltaics ; reference cell calibrations ; performance measurements ; PEP ; intercomparison			15. NUMBER OF PAGES 4 209	
			16. PRICE CODE	
17. SECURITY CLASSIFICATION OF REPORT Unclassified	18. SECURITY CLASSIFICATION OF THIS PAGE Unclassified	19. SECURITY CLASSIFICATION OF ABSTRACT Unclassified	20. LIMITATION OF ABSTRACT UL	